Argonne NATIONAL LABORATORY

ANL-06/23

APS SCIENCE

The annual report of the Advanced Photon Source at Argonne National Laboratory

2006

May 2007

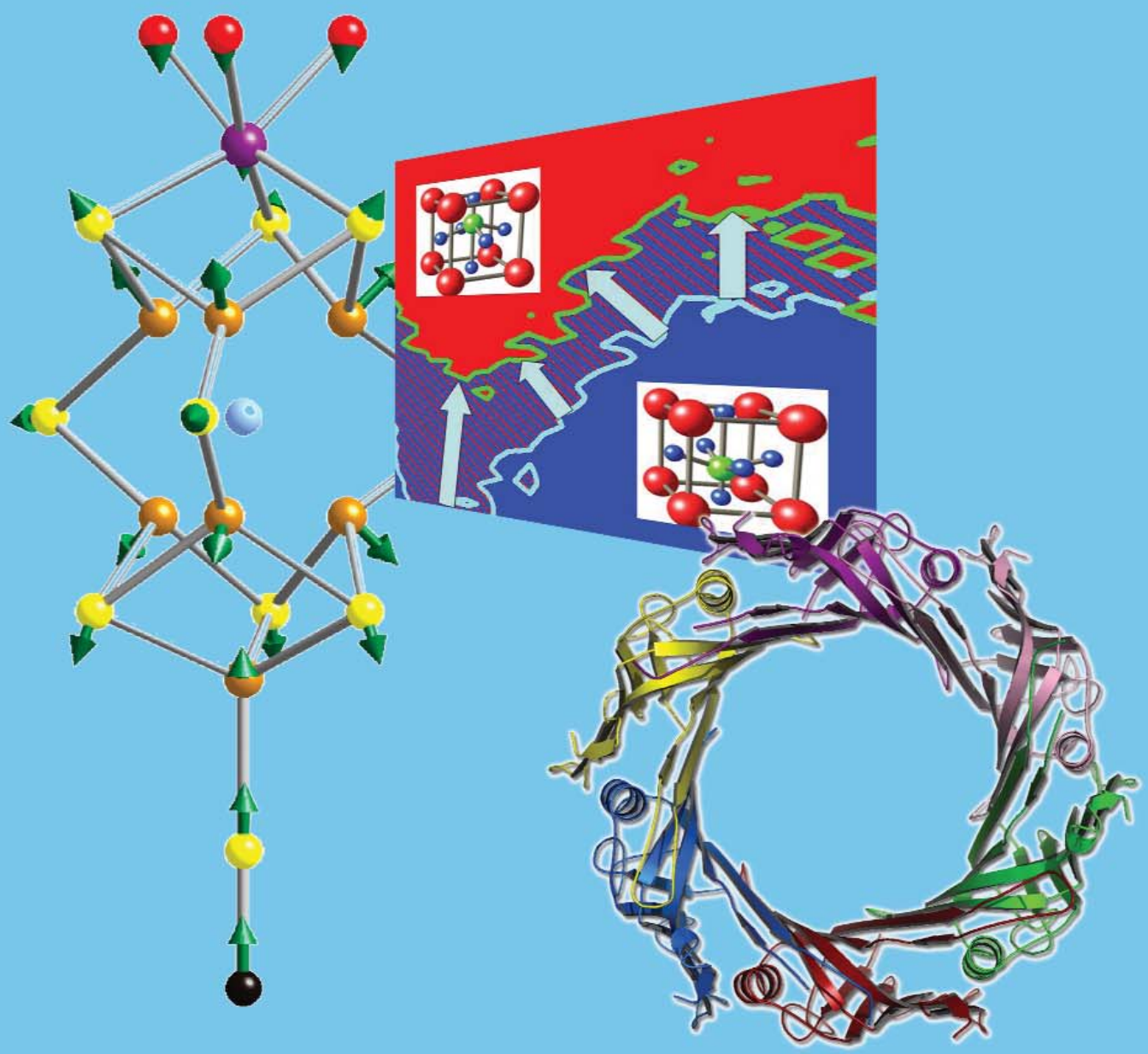

UChicago Argonne LLC

Office of Science
U.S. DEPARTMENT OF ENERGY

ANL-06/23 ISSN 1931-5015

Argonne is managed by UChicago Argonne, LLC, for the U.S. Department of Energy under contract DE-AC02-06CH11357. The Laboratory's main facility is outside Chicago, at 9700 South Cass Avenue, Argonne, Illinois 60439. For information about Argonne and its pioneering science and technology programs, see www.anl.gov.

The Advanced Photon Source at Argonne National Laboratory is supported by the U. S. Department of Energy, Office of Science, Office of Basic Energy Sciences, under Contract No. DE-AC02-06CH11357.

Availability of This Report:
This report is available at no cost, at http://www.osti.gov/bridge. It is also available on paper to the U.S. Department of Energy and its contractors, for a processing fee, from:
U.S. Department of Energy
Office of Scientific and Technical Information
P.O. Box 62
Oak Ridge, TN 37831-0062
phone (865) 576-8401
fax (865) 576-5728
reports@adonis.osti.gov

DISCLAIMER
This report was prepared as an account of work sponsored by an agency of the United States Government. Neither the United States Government nor any agency thereof, nor UChicago Argonne, LLC, nor any of their employees or officers, makes any warranty, express or implied, or assumes any legal liability or responsibility for the accuracy, completeness, or usefulness of any information, apparatus, product, or process disclosed, or represents that its use would not infringe privately owned rights. Reference herein to any specific commercial product, process, or service by trade name, trademark, manufacturer, or otherwise, does not necessarily constitute or imply its endorsement, recommendation, or favoring by the United States Government or any agency thereof. The views and opinions of document authors expressed herein do not necessarily state or reflect those of the United States Government or any agency thereof, Argonne National Laboratory, or UChicago Argonne, LLC.

Argonne NATIONAL LABORATORY

ANL-06/23

APS SCIENCE 2006

The annual report of the Advanced Photon Source at Argonne National Laboratory

In July of 1996, the camera recording APS construction captured this image of lightning on the early-morning horizon. Laboratory/office module 434 is in the foreground; the Argonne central campus and the APS central laboratory office building are beneath the lightning strike.

The Advanced Photon Source is funded by the U.S. Department of Energy, Office of Science, Office of Basic Energy Sciences

Welcome

by J. Murray Gibson...

... Associate Laboratory Director for Scientific User Facilities at Argonne National Laboratory and Director of the Advanced Photon Source.

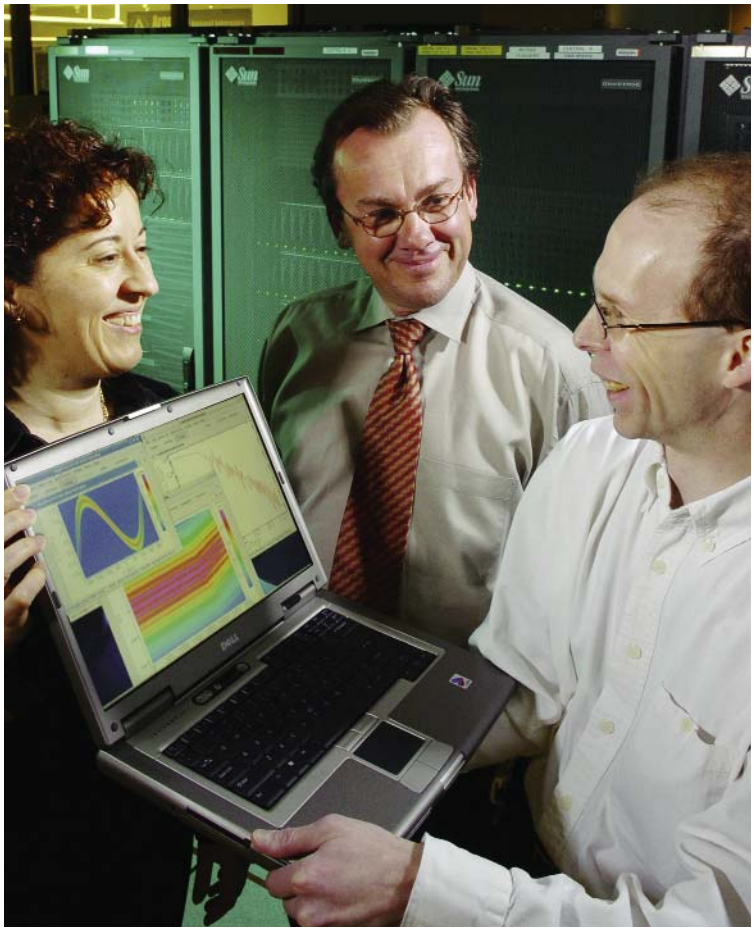

Katherine Harkay (left, ASD), Murray Gibson, and Michael Borland (ASD) in the APS computing room. On the laptop screen are images showing results of simulations for several APS upgrade options. The simulations were performed in this room on a Linux cluster dedicated to accelerator research, using the code ELEGANT (developed at Argonne by Borland et al.).

In my five years as Director of the Advanced Photon Source (APS), I have been fortunate to see major growth in the scientific impact from our facility. This year I am particularly enthusiastic about prospects for the long-term future. Every scientific instrument must remain at the cutting edge to flourish. Our plans for the next generation of the APS—an APS upgrade—got seriously in gear this year with strong encouragement from our users and sponsors. Although we are looking at several options, the most promising seeming to emerge is the energy-recovery linac (ERL), and we plan to carry out R&D on this and related options in the next few years. An ERL@APS would offer revolutionary performance, especially for x-ray imaging and ultrafast science, while not seriously disrupting the existing user base. I am very proud of our accelerator physics and engineering staff, who not only keep the current APS at the forefront, but were able to greatly impress our international Machine Advisory Committee with the quality of their work on the possible upgrade options (see page 10).

As we prepare for long-term major upgrades, our plans to develop and optimize all the sectors at the APS in the near future are advancing. Several new beamlines saw first light this year, including a dedicated powder diffraction beamline (11-BM), two instruments for inelastic x-ray scattering at sector 30, and the Center for Nanoscale Materials (CNM) Nanoprobe beamline at sector 26. Our partnership in the Linac Coherent Light Source —the first x-ray free-electron laser, now being built at the Stanford Linear Accelerator Center—contributes to revolutionary growth in ultrafast science (see page 163), and we are developing a pulse chirping scheme to get ~ps pulses at sector 7 of the APS within a year or so.

In this report, you will find selected highlights of scientific research at the APS from calendar year 2006. The highlighted

Continued on next page

work covers diverse disciplines, from fundamental to applied science. In the article on page 129 you can see the direct impact of APS research on technology. Several new products have emerged from work at the APS, to complement the tremendous output of work in basic science, which often has payoff in technology but over decades rather than years. Highlights in this report also reflect the relevance of APS work to U.S. Department of Energy (DOE) missions: for example, a route to more efficient fuel cells (page 22) that addresses the energy challenge, and natural approaches to cleaning up the environment (page 104).

"Every scientific instrument must remain at the cutting edge to flourish. Our plans for the next generation of the APS—an APS upgrade—got seriously in gear this year with strong encouragement from our users and sponsors."

The APS X-ray Operations and Research (XOR) organization increased its responsibility for beamline operations in 2006, taking sectors 33 and 34 (the former University-National Laboratory-Industry Collaborative Access Team [CAT]) under its wing. This brings the number of XOR beamlines to 27, the majority of the non-protein-crystallography stations at the APS. We have been working to optimize these beamlines in accordance with our developing strategic plan. In 2006 we dedicated beamline 1-ID entirely to high-energy scattering (see page 149), and developed a dedicated imaging capability at beamline 32-ID. We also work closely with our external partners and collaborative access teams to improve the capabilities for users. For example, we have recently installed two new specialized undulators—a 2.3-cm-period device and a 2.7-cm-period device—at BioCARS (sector 14). In partnership with the National Institutes of Health (NIH) intramural program of Phil Anfinrud, and the NIH National Center for Research Resources facility at BioCARS run by Keith Moffat (The University of Chicago), new state-of-the-art fast-laser equipment and optics have been installed, and we believe that this sector will have a photon flux in a single pulse second-to-none of any beamline around the world. It is thus ideally suited for ultrafast single-pulse diffraction experiments. We are instituting "HP-SynC," a centralized suite of facilities and expertise for high-pressure experiments around the ring, initiated by the High Pressure CAT (sector 16) and supported by DOE funding. Plans for enhanced capabilities for catalysis research are also in progress.

User support is a major focus for APS employees. We recognize that a barrier to usage of the APS, and other synchrotrons, is the lack of well-supported, user-friendly scientific software for analyzing data from experiments. There is a need for both faster real-time analysis to assist in more efficient use of beam time, and for access to data and software after the experiment. We have created a scientific software section in the Beamline Controls and Data Acquisition Group in the APS Engineering Support Division, and are seeking to grow this in the near future. We are also working with the Intense Pulsed Neutron Source at Argonne to build such capabilities for both x-ray and neutron science. Many of our employees work behind the scenes in supporting user operations, from mechanical and electrical infrastructure, to computer networks and cyber security. I thank all of these people for their hard work, which makes science not only possible, but better, for APS users.

The safety of our employees and our users is paramount, and this year we instituted an extensive testing and certification system for all electrical equipment brought by users (see page 173). We have a team of nine APS personnel trained in the Nationally Recognized Testing Laboratories (NRTL) requirements, who can inspect equipment that has not been NRTL-certified, in order to ensure that it is safe. If there are simple problems, we often fix them immediately at no charge to the user, or provide the service at cost to those users who need more extensive repairs.

Despite the fact that our sponsors, the U.S. DOE Office of Basic Energy Sciences and the U.S. Congress, have strongly supported the importance of adequate funding for productive large facilities such as the APS, the year 2006 was also a difficult one for us. Financial problems arose due to a number of political problems on a larger scale, and happily, it appears that the coming years will be better for us. I particularly would like to thank our users and employees for their patience during these challenging times, and for our users' advocacy of the importance of the APS to their research. Challenges notwithstanding, the future is bright, and as a team—our sponsors at DOE, our employees at APS and colleagues at Argonne, our users, and our advisory and review committees—we can bring about new and greater things. Thank you!

The APS Scientific Advisory Committee

by **Pierre E. Wiltzius...**

... Chair, APS Scientific Advisory Committee; Director of the Beckman Institute and Professor of Materials Science, Engineering, and Physics at the University of Illinois at Urbana-Champaign.

The APS Scientific Advisory Committee photographed during their meeting in January 2007. Seated, left to right: Denis McWhan (Brookhaven National Laboratory, retired) • Pierre Wiltzius, Chair, (Univ. of Illinois at Urbana-Champaign) • J. Murray Gibson (Argonne) • J. Michael Rowe (National Institute for Standards and Technology [NIST] Center for Neutron Research; retired), Standing, left to right: Patrick Gallagher (NIST Center for Neutron Research) • Wei Yang (National Institutes of Health) • Miles Klein (Univ. of Illinois at Urbana-Champaign) • Piero Pianetta (Stanford Linear Accelerator Center) • Richard Leapman (National Institutes of Health) • John Helliwell (Univ. of Manchester) • Donald Weidner (State Univ. of New York at Stony Brook) • Gene Ice (Oak Ridge National Laboratory) • Slade Cargill (Lehigh Univ.) • Paul Bertsch (Univ. of Georgia) • Howard Einspahr (Bristol-Myers Squibb; retired) • Bruce Bunker (Univ. of Notre Dame).

The Scientific Advisory Committee (SAC) of the APS held its annual meeting on January 23-25, 2007. The meeting included two days of informational updates and discussions of APS strategic and tactical planning, as well as formulation of specific recommendations to the APS for the 10 sector/beamline reviews conducted during 2006, the 8 current partner user programs, 2 collaborative access team proposals for new undulators, and issues raised during the 2006 SAC meeting. In addition, there was a day-long cross-cut review of structural biology; presentations from the review are available at: http://aps.anl.gov/News/Meetings/APS_Cross_ Cut_Reviews/2007/index.html.

Murray Gibson, Associate Laboratory Director for Scientific User Facilities at Argonne and Director of the APS, conveyed the good news that the building momentum at the Department of Energy's Office of Basic Energy Sciences (DOE-BES) has led the APS to explore a number of options for a future upgrade, the most

Continued on next page

promising of which, at this time, seems to be a fourth-generation source such as an energy-recovery linac. Options were guided by advice from a November 2006 high-level Machine Advisory Committee (page 10). It is likely that there will be funding from DOE-BES for the build-out of the remaining four original APS sectors. Gibson continued with scientific highlights, followed by information on new developments in APS R&D. He then described the APS reorganization, funding picture, spending profiles, and user status.

Discussion during and following Gibson's presentation focused on several main issues, primarily those associated with the APS organizational structure. The current configuration of both APS-managed and collaborative access team (CAT)-managed beamlines leaves CATs, primarily those in the life-science community, without a strong voice in APS management decisions. Scientific Advisory Committee members offered suggestions for ways to incorporate biologists into the APS decision-making process. Also raised were the issues of in-house science and the need for adequate beamline support to enable beamline scientists to establish their own research programs. Some progress has been made during the past year, but many APS beamlines still urgently need staff.

The SAC discussed the 10 sector reviews conducted during 2006 and formulated specific recommendations to the APS Director. Many of the beamlines are highly successful and productive, while a few have some organizational or funding challenges. It should also be noted that the transition from CATs to X-ray Operations and Research (XOR) sectors continues in a positive fashion. These sector reviews by external Sector Review Panels are well-established by now and are viewed as a useful evaluation tool, leading to greater coordination and better efficiencies around the ring. On behalf of the SAC, I would like to thank all the panel members who participate in these reviews.

Given that 8 of the 10 sectors scheduled for review in 2007 are operated by XOR, the SAC concurred with the APS proposal to review the science done at the XOR sectors in a cross-cut exercise, followed by a single management review shortly before the next SAC meeting.

The SAC learned that the X-ray Science Division is currently responsible for 27 beamlines on the APS floor. This provides significant opportunities for upgrades to create more effective and dedicated facilities. Decisions will be made after consideration of a number of factors: partner users on the beamline, transition time of sectors newly added to XOR, productivity, overall availability of techniques, and scientific talent.

The exciting plans for the build-out of the remaining four sectors and the redevelopment of existing lines were discussed, as well. Six new beamlines could result: Intermediate Energy X-ray Spectroscopy and Scattering, Intermediate Energy X-ray Magnetism, BioNanoprobe, Diffraction in High Magnetic Field, In situ Surface and Interface Science, and Advanced X-ray Imaging.

The SAC addressed the issues related to industrial, proprietary usage of the APS, specifically the results and status of an audit by the DOE Inspector General's Office requiring "full cost recovery." The APS has proposed several paths to compliance with a three-year phase-in. A final decision is in the hands of the DOE Chief Financial Officer.

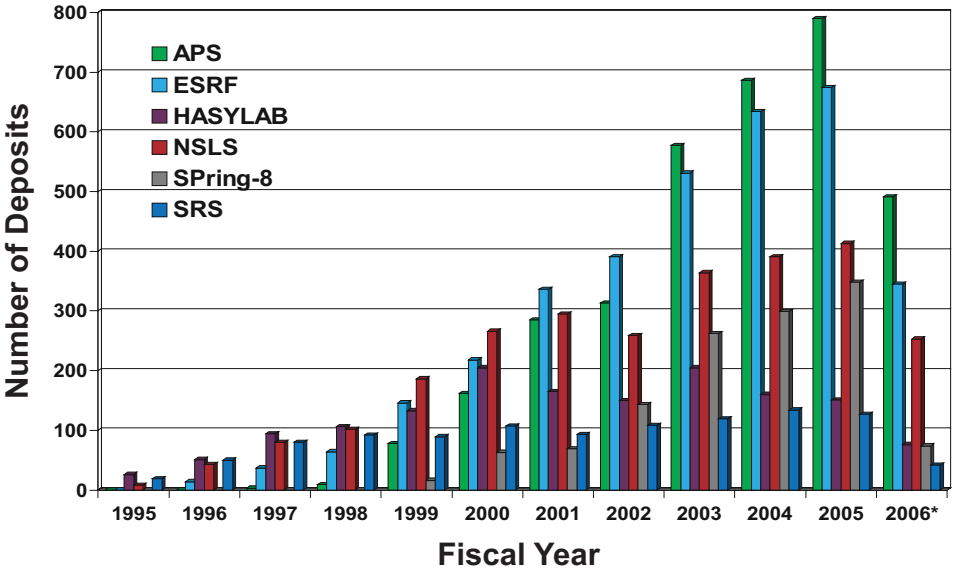

Fig. 1. Deposits in Protein Data Bank by high-deposit light sources as of 10.06. (Source: BioSync, http://biosync.rcsb.org/BiosyncStat.html.)

The status of the APS user program, with its three principal access modes (CAT member, partner user, general user) was discussed, as well. For fiscal year 2006, the APS had 3,274 on-site unique users and approximately 2,000 requests for beam time through the General User Program.

Lastly, the SAC reviewed a number of undulator upgrades, and several XOR and CAT plans and proposals. The members concurred with the proposed changes on beamlines 11-ID, 1-ID, and 4-ID, as well as the proposals from GSECARS and High Pressure CAT for new undulators.

Overall, the SAC found the APS will continue to operate at high capacity and productivity. The transition from CATs to XORs seems to progress with minimal disruption, leading to greater efficiencies and coherence around the ring. In the name of the SAC, I would like to congratulate the APS community for the great scientific progress that has been made. This year's cross-cut review highlighted, in particular, the enormous impact that the APS has had on the biological community as demonstrated by the large numbers of entries into the Protein Data Base (Fig. 1) resulting from experiments at highly productive APS beamlines. ❍

The APS Users Organization

by Gene Ice...
... Chair, APSUO Steering Committee; Oak Ridge National Laboratory Corporate Fellow/Group Leader for the X-ray Research and Applications Group, Metals and Ceramics Division.

The 2006 APS Users Organization Steering Committee, photographed at Argonne on November 26, 2006. Seated, left to right: Larry Lurio (Northern Illinois Univ.) • Tim Graber (The Univ. of Chicago, APSUO Vice-Chair) • Barbara Golden (Purdue Univ.) • Gene Ice (Oak Ridge National Laboratory, APSUO Chair) • Anne Mulichak (The Univ. of Chicago) • Carol Thompson (Northern Illinois Univ., *Ex Officio*) • Millicent Firestone (Argonne). Standing, left to right: Murray Gibson (Argonne) • Ward Smith (Argonne) • Thomas Gog (Argonne) • Simon Billinge (Michigan State Univ.) • Keith Brister (Northwestern Univ.) • Paul Evans (Univ. of Wisconsin-Madison) • David Reis (Univ. of Michigan). Not pictured: Simon Mochrie (Yale Univ.)

Fiscal year 2006 marked the 10th anniversary of user science at the APS. The APS user's meeting—jointly held with Argonne's Center for Nanoscale Materials, Intense Pulsed Neutron Source, and Center for Electron Microscopy—provided a forum for the celebration of the accomplishments of the last decade and for envisioning ways to expand the APS leadership position in critical scientific areas.

Enthusiasm for new research opportunities was captured by an overview talk on an energy-recovery linac proposed upgrade option to improve the APS performance by orders of magnitude. Another highlight of the meeting was the presentation of the Franklin Award to Wendy Mao (Los Alamos National Laboratory) for her elegant studies of novel high-pressure phenomena using synchrotron radiation. Plenary talks covered emerging scientific grand challenges in biology and energy research, and recognized pioneering research carried out at the APS. For example, presentations on "Biological Methane Oxidation" by Amy Rosenzweig (Northwestern University), "Using X-ray Speckle to Test Dynamical Scaling" by Mark Sutton (McGill University), "Synchrotron-Based Measurements of Magnetically Doped Transition Metal Oxides" by Scott Chambers (Pacific Northwest National Laboratory) and "From X-rays to Biogeochemistry to Beethoven" by Ken Kemner (Argonne) all were made possible by unique APS capabilities.

In addition to the plenary talks, there were a record number of workshops and two additional, large auxiliary workshops. A special emphasis was placed on providing resources to support invited speakers for the plenary sessions and for the workshops. This allowed organizers to invite experts from around the world and made the APS meeting both a celebration of science at the APS and a global forum for new ideas. Part of the user enthusiasm was driven by the prospect for a significant upgrade to the APS. (For more on the 2006 user meeting, see page 152.)

Of course, the primary role of the APS Users Organization (APSUO) is to represent the interests of the APS users community and to provide user perspective to APS management. In addition to quarterly APSUO meetings that form the main contact with APS management, the APSUO executive committee represents the users at beamline and other scientific reviews, attends the APS Operations Directorate Meetings, provides user input to the Partner User Council, attends the Scientific Advisory Committee meetings, and serves as an advocate for users who have specific concerns or grievances. Issues raised this year include the role of Partner User Proposals and the overlap with transition beam time as Department of Energy-funded beamlines move to X-ray Operations and Research management. Other issues included emergency user access during holidays; and a strong user priority for beamline upgrades, including software, x-ray optics, and detectors.

Advocacy is an ongoing focus for the APSUO and other user groups as they express to the public the value of initiatives that will help maximize the productivity of the APS and other federally-supported user facilities. Keith Brister (Northwestern University), of the Life Science Collaborative Access Team at APS sector 21, has been particularly helpful to our advocacy efforts by organizing the user community to efficiently contact their local representatives. We will continue to work with our sister user organizations from synchrotron, neutron, and high-energy facilities to educate our representatives about the importance of major user facilities for global competitiveness and for energy, medical, defense, education, and other national priorities. ❍

The APS Partner User Council

by **Bruce A. Bunker...**

... Chair, 2005-2006, APS Partner User Council; Professor of Physics, University of Notre Dame; Director of MR-CAT at the APS.

The 2006 APS Partner User Council Executive Committee photographed at Argonne on November 27, 2006. Front row, left to right: Murray Gibson (Argonne) • Randy Alkire (sector 19, Argonne) • Bruce Bunker (sector 10, Univ. of Notre Dame, Chair)• Lisa Keefe (sector 17, The Univ. of Chicago). Second row, left to right: • Kevin D'Amico (sector 31, SGX Pharmaceuticals, Inc.) • Malcolm Capel (sector 24, Cornell Univ.) • Robert Gordon (sector 20, Simon Frasier Univ.) • Robert F. Fischetti (sector 23, Argonne) • G. Brian Stephenson (sector 26, Argonne). Third row (standing), left to right: Vukica Srajer (sector 14, The Univ. of Chicago) • Keith Brister (sector 21, Northwestern Univ.) • Denis T. Keane (sector 5, Northwestern Univ.) • Thomas C. Irving (sector 18, Illinois Institute of Technology). Not pictured: Douglas Robinson (sector 6, Iowa State Univ.) • Kent Blasie (sector 9, Univ. of Pennsylvania) • Mark Rivers (sector 13, The Univ. of Chicago) • Jim Viccaro (sector 15, The Univ. of Chicago) • David Mao (sector 16, Carnegie Institution of Washington) • B.-C. Wang (sector 22, Univ. of Georgia) • John Hill (sector 30, Brookhaven National Laboratory).

The Partner User Council (PUC) represents users who have contributed to the APS by developing beamlines or other new capabilities. The PUC includes representatives from groups submitting partner user proposals, collaborative development teams (CDTs), and collaborative access teams (CATs). To facilitate communication, the Chairs of X-ray Operations and Research (XOR) advisory committees are also PUC members, as is the Chair of the APS Users Organization (APSUO) Executive Committee, and a representative of the APS. The PUC complements the APSUO in that those who build and operate beamlines and large instrumentation at the APS may have somewhat different interests and concerns than general users.

The PUC has an annual full meeting (scheduled to coincide with the annual APSUO meeting) and quarterly meetings of its Executive Committee. Additionally, a representative of the PUC attends the yearly meeting of the Scientific Advisory Committee and all sector reviews. the PUC representatives are also involved in the rating of Partner User Proposals and collaborative development team proposals, attending weekly APS operations meetings, and participating in setting the agenda for the monthly APS meetings that bring together facility personnel and beamline staff.

The quarterly PUC meetings combine both an Executive Session (usually with no APS staff attending) and a larger meeting with APS representatives. Meetings generally begin with an APS update from Murray Gibson—who describes budgetary and operational issues—and then move into discussions of particular items of concern.

The dominant issue this year has been the APS upgrade plan. Initially, this involved an increase in beam current to 300 mA and a major change in the storage ring lattice. Most PUC members were quite concerned by this plan, because the improvement in capabilities did not seem worth the 12-to-18-months shutdown necessary to implement the new lattice. The group is much more supportive of the energy-recovery linac (ERL) approach currently being explored. The PUC members are eager to be involved in the formulation of proposals to the Department of Energy (DOE) for R&D on ERLs and other serious options for the APS upgrade. The group is also very interested in working with the APS to coordinate future CAT beamline development and APS plans.

Another major issue for PUC members has been the coordination of XOR beamline development, plans of existing CATs, and both existing and proposed CDT and Partner User Proposals. With the APS moving toward single-technique beamlines, it is important to consider CAT capabilities and plans in a comprehensive strategy for future development of the entire facility.

An issue affecting some PUC members (and also some general users) is related to the DOE Inspector General's (IG's) audit of the APS. In this audit, the IG claimed that industrial users were underpaying for proprietary beam time and proposed significant increases. The APS and local DOE management did not fully agree with the IG, but proposed new algorithms to partially redress a perceived inequity, but corporate users who have made large contributions to beamline construction and operations are still very concerned about the large increase. As of this writing, these issues are still in discussion with the IG, the DOE, the APS, and industrial users.

Other topics addressed by the PUC this year have included changes to the general user program (e.g., modifications of program proposals), proposed tests or changes to the APS storage ring lattice, new operational modes, and topics for the APSUO annual meeting.

Meetings of the PUC and APS management have proven to be very successful in fostering communication in both directions, and we presume this will continue. ❍

The Advanced Photon Source (APS) facility at Argonne National Laboratory.
The APS occupies an 80-acre site on the Argonne campus, about 25 miles from downtown Chicago, Illinois.
For directions to Argonne, see www.anl.gov/Visiting/anlil.html.

Access to Beam Time at the APS

Beam time at the APS can be obtained either as a general user (a researcher not associated with a particular beamline) or as a partner user (e.g., a member of a collaborative access team [CAT], a partner user proposer, or a member of a collaborative development team [CDT]). If you are a CAT or CDT member, contact your CAT or CDT for instructions on applying for CAT/CDT beam time. At minimum, 25% of the time at all operating beamlines is available to general users, but many offer considerably more general user time, up to 80%.

How general users can apply for beam time at the APS:
1) First-time users should read the information for new users found on our Web site at http://www.aps.anl.gov/user/ new_users.html before applying for beam time. Also, certain administrative requirements must be completed. In particular, a user agreement between the APS and each research-sponsoring institution must be in place.

2) To choose the appropriate technique(s) and beamline(s), see the beamlines directory in the “Data” section of this volume or at http://beam.aps.anl.gov/pls/apsweb/beamline_display_pkg.beamline_dir.

3) Submit a proposal via the Web-based system. Proposals are evaluated before each user run. For more information and the current proposal schedule, see the proposal system overview at http://www.aps.anl.gov/user/beam time/prop_submission.html.

Table of Contents

Welcome 2
The APS Scientific Advisory Committee 4
The APS Users Organization 6
The APS Partner User Council 7
The Energy-recovery Linac:
A Promising Option for an APS Upgrade 10
APS Research Highlights 14
Structural Studies 16
Electronic & Magnetic Materials 21
First Light × 3 35
Engineering Materials & Applications 36
Soft Materials & Liquids 46
Chemical Science 57
Life Science 59
Structural Biology 70
Environmental, Geological, & Planetary Science 100
Atomic, Optical, & Molecular Physics 117
Nanoscience 120
Research at the APS and U.S. Economic Competitiveness 129
APS Beams Probe the Nanoscale 130
The Hard X-ray Nanoprobe 132
Novel X-ray Techniques & Instrumentation 134
APS Users 150
Exploring the Art of Materials Science at SRMS-5 158
The APS Light Source 160
APS Data 176
APS Publications 2006 186
Acknowledgments 220

Contact us

For more information about the Advanced Photon Source or to order additional copies of this, or previous, issues of *APS Science*, send an e-mail to apsinfo@aps.anl.gov, or write to APSinfo, Bldg. 401, Rm. A4115, Argonne National Laboratory, 9700 S. Cass Ave., Argonne, IL 60439.

APS Science is also available on line in PDF format at www.aps.anl.gov/News/Annual_Report/index.htm.

lightsources.org

For news from, and information about, light sources worldwide, see www.lightsources.org

The Energy-recovery Linac: A Promising Option for an APS Upgrade

The past year has been busy, but stimulating, for APS accelerator physicists. Although work on potential APS upgrades had progressed since 2003, when the Department of Energy's (DOE's) Office of Science released their report on *Facilities for the Future of Science – A Twenty-Year Outlook*, (http://www.sc.doe.gov/Scientific_User_Facilities/History/20-Year-Outlook-screen.pdf), an APS upgrade had not been center stage. Encouraged by the DOE to reconsider upgrade plans, a number of options were identified in 2006, including lattice upgrades for the storage ring and an energy-recovery linac (ERL) injector into the APS storage ring. Workshops were held in that year to evaluate the new science that could be made possible by an APS upgrade. It became clear that an ERL is one of the most serious options to consider for an APS upgrade, as it offers more revolutionary performance than storage ring upgrades with the least disruption to existing users. While R&D on the ERL is expanding, we will continue to evaluate other possible options. In this article, the ERL option is described in some detail.

The ERL option would allow the APS to leapfrog the nominal gains believed possible via a storage ring upgrade, while at the same time reducing the dark time (construction time with no x-ray production)—a serious concern voiced by the user community. From that point on, efforts focused on the possibility of integrating an ERL injector with the existing APS storage ring. This integration would allow existing beamlines, with the appropriate upgrades, to be utilized with the radiation generated by the ERL beam while achieving the mantra of revolutionary enhancements with minimal disruption to the existing scientific programs.

A Herculean effort by APS accelerator-physics personnel—including Michael Borland, John Carwardine, Yong-Chul Chae, Glenn Decker, Roger Dejus, Louis Emery, Katherine Harkay, Yuelin Li, Elizabeth Moog, Ali Nassiri, Vadim Sajaev, Nick Sereno, Yin-E Sun, Aimin Xiao, and Chih-Yuan Yao (all ASD); John Noonan (AST); and George Goeppner (AES)—allowed management to convene, on November 15-16, 2006, a Machine Advisory Committee (MAC) to critique selections of possible upgrades. The charge to the committee was to evaluate the various accelerator upgrade options that had been proposed and to determine if:

Continued on next page

The APS Machine Advisory Committee, photographed at Argonne on November 15, 2006, during their meeting to consider presentations on upgrade options made by APS accelerator staff. Left to right: Sam Krinsky (Natonal Synchrotron Light Source), Klaus Balewski (Deutsches Elektronen Synchrotron), Annick Ropert (European Synchrotron Radiation Facility), Vic Suller, Chair (Center for Advanced Microstructures and Devices), Georg Hoffstaetter (Cornell Univ.), Andrew Hutton (Jefferson Lab), Elaine Seddon (Daresbury Laboratory), and Max Cornacchia (Stanford Linear Accelerator Center [SLAC], retired). Not pictured: John Galayda (SLAC).

- the proposals will deliver claimed technical performance,
- the claimed performance was technically revolutionary,
- there were technical R&D challenges to successful delivery of the upgrade,
- estimates of expected disruption to users associated with implementing this option were correct and how to mitigate risks associated with the implementation, and
- other proposals should be considered.

In the executive summary of their report, the MAC stated:

"The proposed Outfield ERL is considered to be an extremely exciting light source which builds on the investment in beam lines and infrastructure already at the APS. It would provide a factor of about 150 increase in brightness compared to the existing APS in addition to increasing the coherent fraction of the x-ray beam and significantly reducing the bunch length. The claimed performance is not demonstrated at the present time and would rely on significant improvements to both the current and emittance delivered by high brightness electron guns. The committee is not able to guarantee that these improvements will be delivered, but is optimistic in the light of ongoing R&D at several institutes."

The full report of the MAC is on the APS Website at: www.aps.anl.gov/News/Conferences/2006/APS_Upgrade/apmac/Committee_Report.pdf.

Buoyed by the MAC's enthusiasm for the APS to pursue an ERL as part of the APS upgrade, work continues along these lines. Below is a brief summary of plans that have been developed to date and where the planning will go from here.

Accelerator Enhancements

While the purpose of the upgrade is to enable dramatically improved experiments, a premium is placed on preserving existing experimental capabilities with minimal disruption. This could well be achieved by augmenting the present injection systems with an energy-recovery linac that would then utilize the existing storage ring in a single-pass mode.

While the upgrade will deliver revolutionary capabilities, it will take time for the user community to take full advantage of these new specifications. To minimize disruption, a primary objective is preserving at all times the present APS capabilities.

The following will be maintained to the extent possible for either approach:

1) The existing APS storage ring tunnel will be utilized.
2) Beam energy will be at least 6 GeV, but with a goal of 7 GeV.
3) Existing beamlines will be preserved.
4) Existing beam stability will be maintained.
5) Delivered flux will be maintained (in high-flux mode).
6) The storage ring will be able to run in its present "storage ring mode" for as long as is necessary after the ERL has been commissioned.

An Energy-recovery Linac

In a storage ring, the particle beam's transverse and longitudinal dimensions are determined by the competing forces of radiation damping and the quantum nature of radiation emission. An equilibrium emittance is reached a few milliseconds (i.e., after a few thousand turns) after the particle bunch

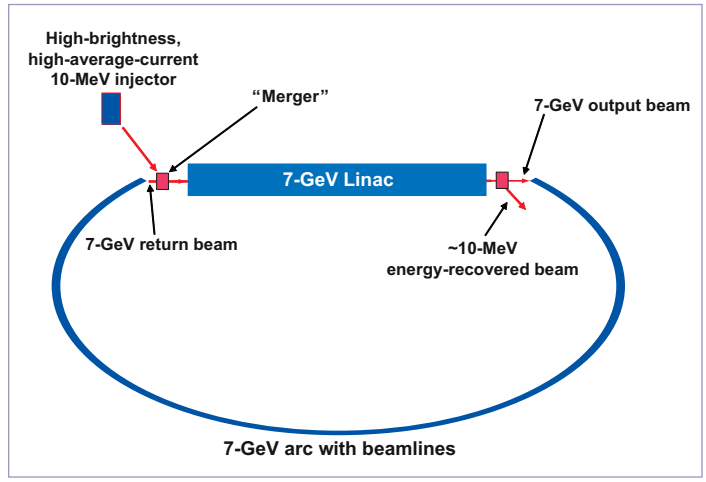

Fig. 1. Schematic of the energy-recovery linac concept.

is injected into the storage ring. For a given particle beam energy, linacs can produce a beam of much lower emittance than can storage rings, and can be used to generate x-rays with very low transverse emittance and short bunch length. However, because the particle beam will not retain this low emittance and short pulse length if stored, it must be thrown away after being used (as opposed to a storage ring, which recycles the electrons). Although, in principle, low-emittance, short-pulse linacs could be used to generate beams with energies of 7 GeV and currents of 100 mA if the electrons were used once and thrown away, the required wall-plug power to do this would be 700 MW (7 GeV × 0.1 A). By extracting the energy (i.e., energy recovery) from the "used" electron beam before it is thrown way (dumped), the power problem can be mitigated while retaining the desired traits (low transverse emittance and short pulse duration) of the linac-accelerated electrons. The energy extraction is accomplished by passing the 7-GeV beam through a superconducting linac, the same linac that originally accelerated the beam to 7 GeV, but now 180º out of phase from the acceleration mode [1]. The energy deposited back into the cavity by the returning beam can now be used to accelerate the next bunch(es) of electrons, and so forth. Figure 1 shows the conceptual layout of an ERL.

Energy-recovery linac layouts associated with the APS fall into two categories: placement of the linac inside the storage ring enclosure, and placement of the linac outside (Fig. 2, next page). The primary difference is that the ERL layouts outside the storage ring allow for a straight (i.e., not folded or recirculating) linac, and provide space for long undulators, additional beamlines in the turnaround arc, and the potential for a free-electron laser upgrade. The ERL layouts all produce comparable beam for injection into the existing storage ring. Because of the potential for additional beamlines in the turn-around arc (the arc from the linac that turns the beam back towards the APS storage ring) and the increased flexibility for future developments (for example, using the linac for subpicosecond x-ray pulse production), the outfield option appears to be the most attractive.

Continued on page 12

Table 1. Expected performance for three ERL operations modes.

Mode	High Flux	High Coherence	Ultrashort Pulse
Average current (mA)	100	25	1
Rep. rate (MHz)	1300	1300	1
Bunch charge (pC)	77	19	1000
Emittance (pm)	22	6	365
RMS bunch length (ps)	2	2	0.1
RMS momentum spread (%)	0.02	0.02	0.4

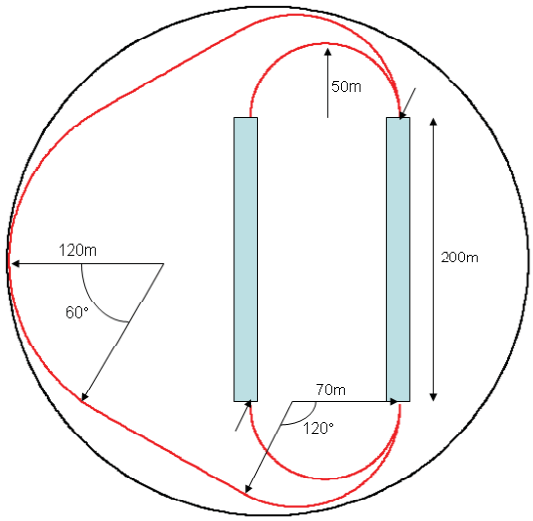

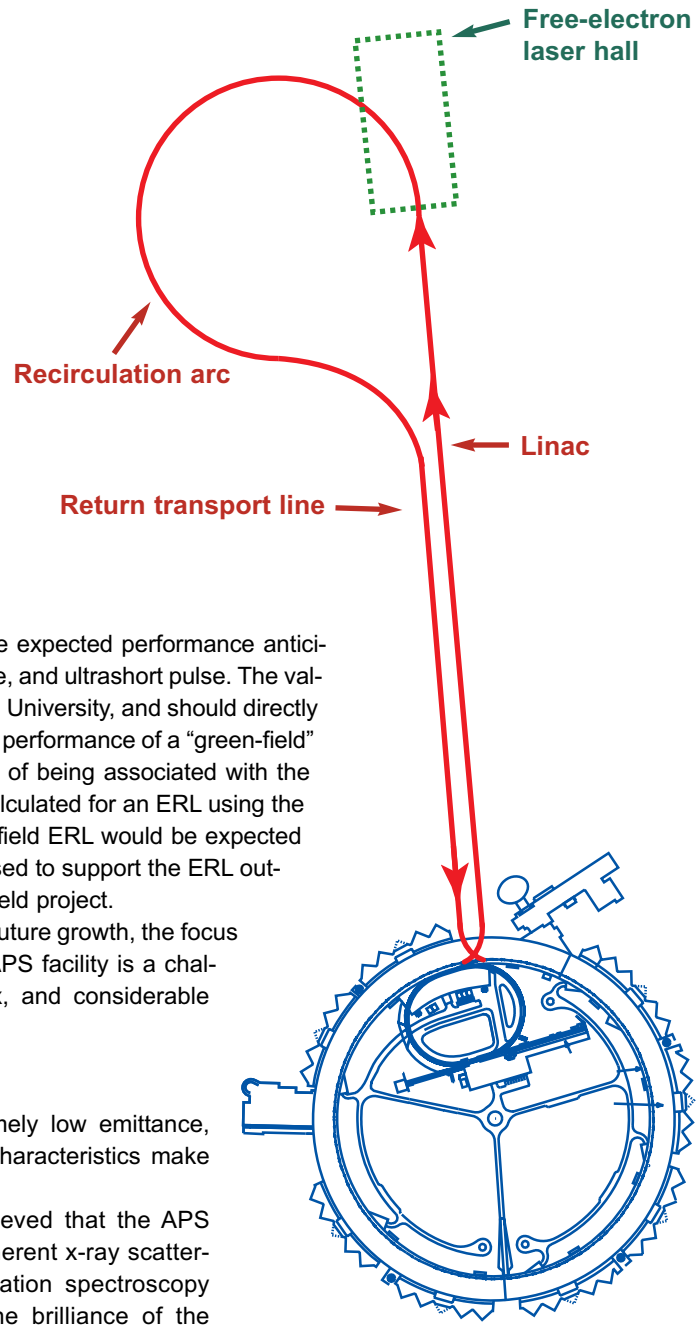

Fig. 2. Two proposed basic layouts for an APS ERL. The infield geometry is shown above; the outfield geometry is at right.

"A Promising Option" *continued from page 11*

An ERL can have a variety of operational modes. Table I shows the expected performance anticipated for three different modes of ERL operation: high flux, high coherence, and ultrashort pulse. The values (from G. Hoffstaetter, FLS2006) were developed for an ERL at Cornell University, and should directly apply to the APS ERL. Calculations have also been made of the expected performance of a "green-field" ERL, i.e., an ERL not constrained by the geometry and available space of being associated with the present APS storage ring. From Fig. 3 one can see that the brightness calculated for an ERL using the APS storage ring is well within a factor of 2 of what an optimized green-field ERL would be expected to generate. The fact that much of the infrastructure of the APS can be used to support the ERL outweighs the small increase in brightness one might realize from a green-field project.

Because the outfield option provides a much greater opportunity for future growth, the focus has been on this option. However, incorporating either option into the APS facility is a challenging task, requiring extensive changes to the accelerator complex, and considerable research and development.

Science with an ERL

Energy-recovery linacs promise very high brightness (i.e., extremely low emittance, equal in both planes) and options for short (<1 psec) pulses. These characteristics make ERLs extremely attractive to the scientific community.

Given the expected properties of the ERL x-ray beam, it is believed that the APS upgrade will have its greatest impact in the fields of x-ray imaging, coherent x-ray scattering, and time-resolved studies. For instance, in x-ray photon correlation spectroscopy (XPCS) experiments, the available flux is directly proportional to the brilliance of the source. Because the accessible time scales in XPCS increase with the square of the source brilliance, one can expect to go from the present time scales of about 1 msec to less than 1 μsec with the APS ERL. This will facilitate, for example, the study of non-equilibrium

Continued on next page

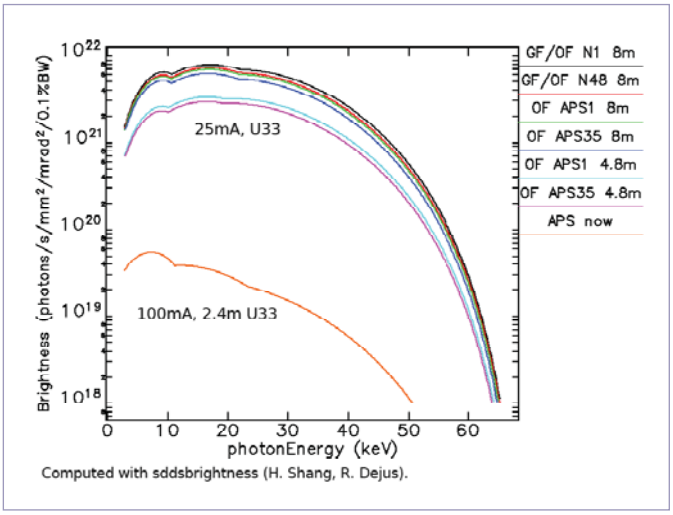

Fig. 3. Spectral brightness of the present APS compared to results for an outfield ("OF") and greenfield ("GF") ERL with different undulator lengths. The APS1 and APS35 locations are sectors 1 and 35 in the APS ring, whereas the N1 and N48 locations are sectors 1 and 48 in the turnaround arc or in the green-field ERL.

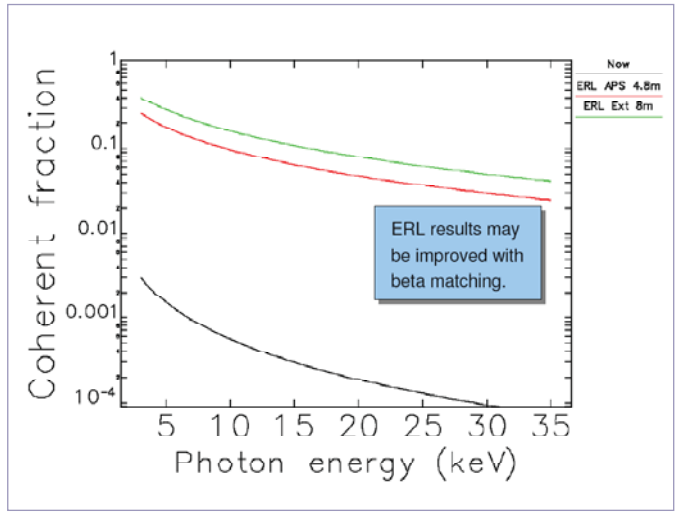

Fig. 4. Coherent fraction (i.e., fraction of the beam that is fully cohrerent) as a function of x-ray energy for the present APS (black line) and an APS ERL (colored lines).

dynamics during structural evolution of domain boundaries, grain boundaries, and defects in hard materials, as well as the dynamics of concentrated proteins in aqueous solution and dynamics of membranes and constituents within membranes in soft/biological materials.

In the field of x-ray imaging, the APS ERL option will allow for the most efficient usage of nanometer-focusing x-ray optics and advanced state-of-the-art scanning x-ray microscopy to <5 nm spatial resolution. Nanometer-sized beams, coupled with improved detectors, will provide unprecedented elemental sensitivity to sub-zepto ($<10^{-21}$) grams for trace metals (e.g., Zn, Fe, Mn) in biological cells, with the potential to locate single-metal atoms at <5-nm resolution. Such capabilities will enable molecular imaging of metal-containing proteins, functional contrast agents, and novel therapeutic drugs at organelle level, and aid in the development of new approaches to diagnose and treat diseases. For materials science, nanometer-size beams will offer a non-destructive, penetrating probe for impurity/ defects, grain boundaries, and nanodomain engineering of functional electronic and engineered materials such as solar cells and metal alloys. The ERL's high coherence (see Fig. 4) will permit advances in coherent diffraction imaging, which is much like crystallography but applied to noncrystalline materials. Emerging applications include the structure and strain in nanoparticles, atomic structure of amorphous materials, two-dimensional crystallography (e.g., membrane proteins), few-unit-cell crystals, and subcellular organelle structures in cells, to name a few.

Finally, shorter pulses from an ERL or a linac-based short-pulse source (such as a free-electron laser [FEL]) mean better temporal resolution for all time-resolved experiments for pump-probe studies in hard-condensed-matter physics, atomic physics, chemistry, and biology.

Toward an ERL Upgrade

Although it is believed that there are no technical "show-stoppers" to the construction of an ERL at the APS, there are accelerator issues that will require further R&D to ensure success. The key areas of R&D include:

- Injector design: gun and low-energy beam transport
- Cathode lifetime
- Superconducting linac cavity design and fabrication
- Radio frequency choice
- Multipass vs. single-pass linac
- Instability issues/beam break-up
- X-ray beam stability.

In addition, there is the need to explore possible problems associated with beam loss and how to reduce the "halo" that will accompany the main beam due to space charge effects, scattered drive-laser light, field emission from the gun and linac, intrabeam scattering, etc.

In parallel with accelerator work, R&D in support of beamline components (optics, detectors, etc.) will be required. To take full advantage of a highly coherent beam, improvements in optics (that can only be made with improvements to the present metrology capabilities) will be required, along with a robust program of detector development for high-speed area detectors, most likely integrating pixel array detectors. At present, APS personnel are developing a plan for the necessary R&D activities in support of an ERL and related linac-based light source options such as an FEL, with the goal of submitting that plan to DOE in 2007. This R&D should place us well to propose firmer plans for the APS upgrade around the beginning of the next decade.

Contact: Rod Gerig (rod@aps.anl.gov)
Dennis Mills (dmm@aps.anl.gov)

Reference

[1] M. Tigner, Nuovo Cimento **37**, 1228, (1965).

APS sectors:

Sectors 1-4: XOR
X-ray Operations and Research (XOR)

Sector 5: DND-CAT
DuPont-Northwestern-Dow Collaborative Access Team (CAT)

Sector 6: MU-CAT
Midwest Universities CAT

Sector 7: XOR

Sector 8: XOR (8-ID); NE-CAT (8-BM)

Sector 9: XOR/CMC
XOR/Complex Materials Consortium

Sector 10: MR-CAT
Materials Research CAT

Sectors 11 and 12: XOR/BESSRC
XOR/Basic Energy Sciences Synchrotron Radiation Center

Sectors 13 through 15: CARS
Center for Advanced Radiation Sources
- GeoSoilEnviroCARS—sector 13
- BioCARS—sector 14
- ChemMatCARS—sector 15

Sector 16: HP-CAT
High Pressure CAT

Sector 17: IMCA-CAT
Industrial Macromolecular Crystallography Association CAT

Sector 18: Bio-CAT
Biophysics CAT

Sector 19: SBC-CAT
Structural Biology Center CAT

Sector 20: XOR/PNC
XOR/Pacific Northwest Consortium

Sector 21: LS-CAT
Life Sciences CAT

Sector 22: SER-CAT
South East Regional CAT

Sector 23: GM/CA-CAT
General Medicine and Cancer Institutes CAT

Sector 24: NE-CAT (plus 8-BM)
Northeastern CAT

Sector 26: XOR/CNM
Center for Nanoscale Materials

Sector 30: XOR/IXS
XOR/Inelastic X-ray Scattering

Sector 31: SGX-CAT
SGX CAT

Sector 32: XOR

Sectors 33 and 34: XOR/UNI
XOR/University-National Laboratory-Industry

X-ray Operations and Research sectors comprise those beamlines operated by the APS.

Collaborative access team sectors comprise beamlines operated by independent groups made up of scientists from universities, industry, and/or research laboratories.

To access the APS as **general users** (GUs), researchers submit proposals that can be active for up to two years. These proposals are reviewed and rated by one of nine proposal review panels comprising scientific peers, generally not affiliated with the APS. Beam time is then allocated by either of two APS Beam Time Allocation Committees.

Those users who propose to carry out research programs beyond the scope of the GU program may apply to become **partner users** on any beamline operated by the APS. Prospective Partner User Proposals are peer reviewed by a subset of the APS Scientific Advisory Committee. Final decisions on the appointment of partner users are made by APS management.

Advanced Photon Source sector allocations and disciplines, and x-ray source configuration

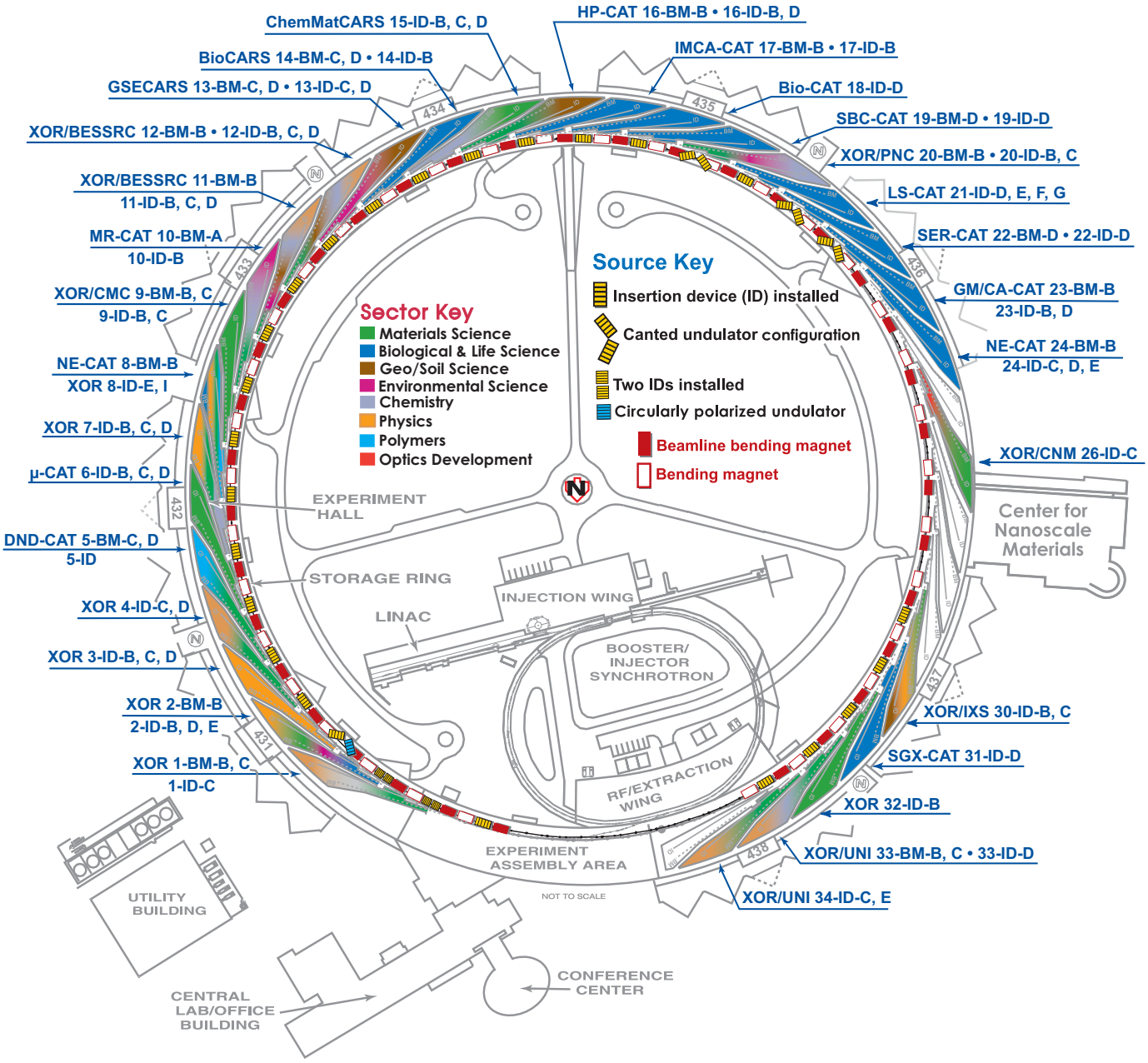

Source: http://beam.aps.anl.gov/pls/apsweb/beamline_display_pkg.beamline_dir

Measuring Elastic Strains in Deformed Single-crystal Copper

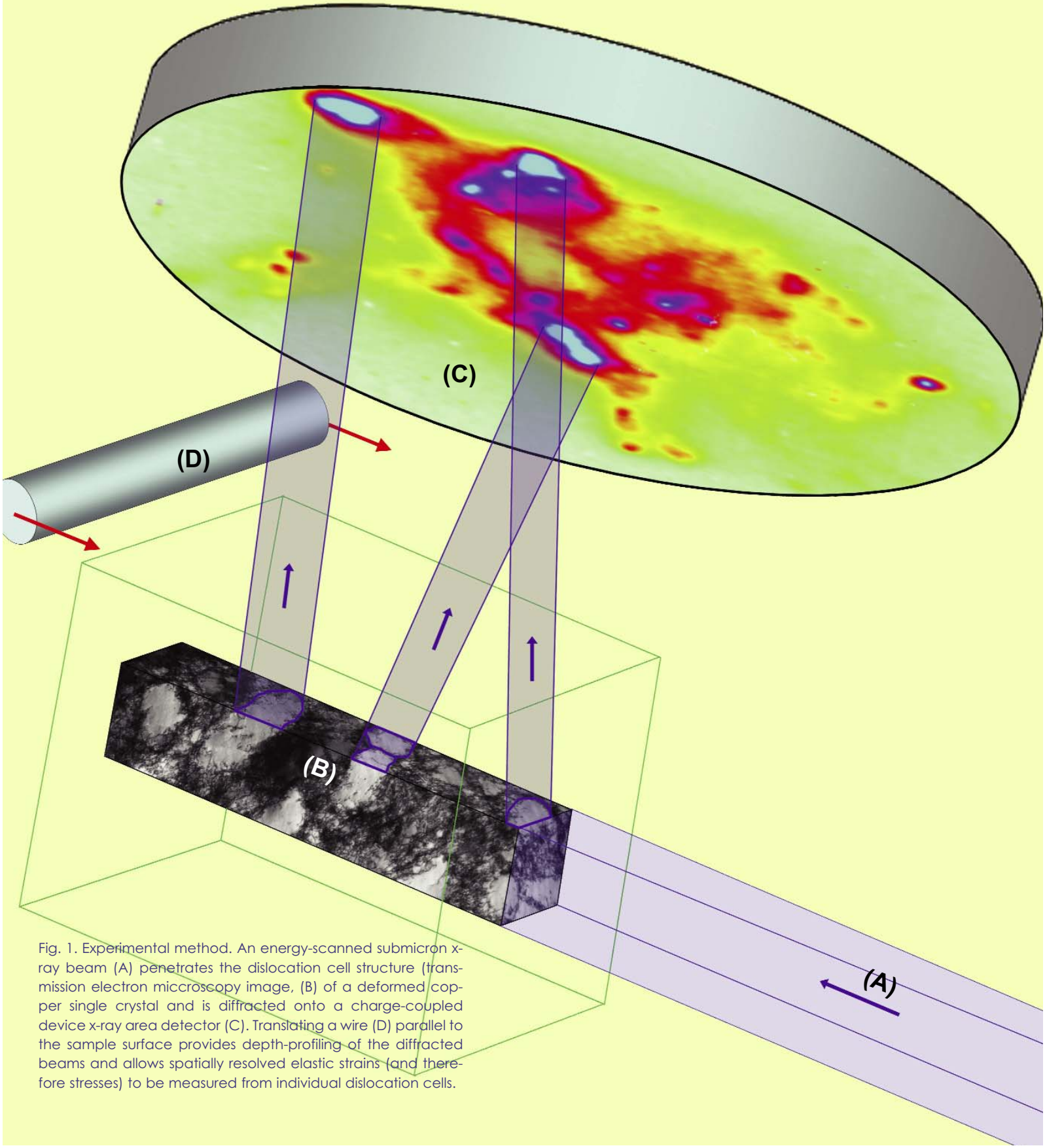

Fig. 1. Experimental method. An energy-scanned submicron x-ray beam (A) penetrates the dislocation cell structure (transmission electron miccroscopy image, (B) of a deformed copper single crystal and is diffracted onto a charge-coupled device x-ray area detector (C). Translating a wire (D) parallel to the sample surface provides depth-profiling of the diffracted beams and allows spatially resolved elastic strains (and therefore stresses) to be measured from individual dislocation cells.

Knowing how submicrometer elastic strains distribute themselves within deformed metal single crystals is key to an understanding of numerous important physical phenomena, including the evolution of complex dislocation structures governing mechanical properties within individual grains, the transport of dislocations through such structures, changes in mechanical properties that occur during reverse loading, and analyses of diffraction line profiles for microstructural studies of these phenomena. Researchers from the National Institute of Standards and Technology, Oak Ridge National Laboratory, the Carnegie Institution of Washington, the University of Southern California, and Argonne demonstrated the importance of this type of information by taking the first direct, spatially resolved measurements of elastic strains within individual dislocation cells in deformed copper single crystals. Broad distributions of elastic strains were found, which have important implications for theories of dislocation structure evolution, dislocation transport, and the extraction of dislocation parameters from x-ray line profiles.

When single crystals of ductile metals are deformed, atomic dislocations propagate throughout the structure, giving rise to high and low dislocation-density regions that are spoken of as dislocation cell walls and interiors, respectively. The formation and evolution of these dislocation cell structures is one of the most important aspects of the deformation process in ductile metals. While it is generally appreciated that patterning arises from the collective interactions of dislocations, it is not yet possible to predict the evolution of dislocation distributions and the resulting local stresses. The existence, magnitude, and spatial distribution of these stresses with respect to the dislocation microstructure have been long debated, and a definitive resolution of this issue is needed to validate and guide the ongoing development of recent dislocation-patterning and dislocation-transport theories.

The researchers used scanning-monochromatic differential-aperture x-ray microscopy (DAXM) to probe the local elastic lattice strains (and thus the stresses) within individual dislocation cells in copper single crystals deformed uniaxially in tension and compression. The spatially resolved scanning monochromatic DAXM measurements were conducted at XOR/UNI beamline 34-ID at the APS using an x-ray microbeam focused to ≈ 0.5 μm. The diffracted beams were detected using a charge-coupled device area x-ray detector, and depth resolution was provided by a diffracted-beam profiler (Fig. 1). The compression and tensile samples were deformed to relatively large final true flow stresses of ≈ 200 MPa at true strains of ≈ 30%.

These spatially resolved elastic strain measurements provide the first direct, quantitative test of Mughrabi's well-known two-component composite model that is commonly used to extract average cell-interior and cell-wall stresses from broadened x-ray line profiles, affording crucial quantitative validation of the composite model predictions.

A key finding of the study, however, is the dramatic variation of these strains from cell to cell within the sample, which contribute significantly to the shape and width of the diffraction line profiles. Quantitative analyses of extracted cell-wall and cell-interior subpeaks frequently use theoretical descriptions of dislocation broadened line profiles to extract dislocation structure parameters from plastically deformed samples. Such analyses often tacitly assume that all of the subpeak broadening comes from the dislocations, and therefore that cell-to-cell strain variations are negligible. This assumption must now be reevaluated in view of these measurements.

The existence of a broad distribution of dislocation cell elastic strains also has important implications for theoretical models of dislocation patterning and dislocation transport. At the dislocation level, critically important phenomena such as dislocation bowing, dislocation pinning and unpinning, unzipping of locks, and cross slip are highly sensitive to the local stress field experienced by the dislocations. Thus, theoretical models of dislocation patterning and transport must frequently make assumptions about the distributions of such stresses within a specimen. The researchers found that the stresses range from essentially 0 up to 50% of the macroscopic flow stress, an effect that is not included in existing dislocation transport models based on dislocation bowing and percolation theory. These theories will also have to be revisited in light of the current findings.

On the other hand, the dislocation patterning model developed by Hähner et al. [1] bases the entire evolution process on the presence of stress variations such as those reported by the researchers. The model associates dislocation cell formation with a noise-induced structural transition in a system far from equilibrium, where the noise term reflects fluctuations in the stress experienced by mobile dislocations traversing a sample. Extensions of this model relate the stress fluctuations to variations in the local dislocation density and generalize the two-component composite model to account for a continuous spectrum of local dislocation densities and cell stresses. The dislocation cell elastic strain measurements provide striking experimental support for the underlying assumptions of this model. — *Vic Comello*

Reference

[1] P. Hähner et al., Phys. Rev. Lett. **81**(12), 2470 (1998).

See: L.E. Levine[1]*, B.C. Larson[2], W. Yang[3], M.E. Kassner[4], J.Z. Tischler[2], M.A. Delos-Reyes[4], R.J. Fields[1], and W. Liu[5], "X-ray microbeam measurements of individual dislocation cell elastic strains in deformed single-crystal copper," Nat. Mater. **5**, 619 (2006). DOI: 10.1038/nmat1698

Author affiliations: [1]National Institute of Standards and Technology, [2]Oak Ridge National Laboratory, [3]Carnegie Institution of Washington, [4]University of Southern California, [5]Argonne National Laboratory

Correspondence: *Lyle.Levine@nist.gov

M.E.K. and M.D.R. acknowledge support from the DOE Office of Basic Energy Sciences (BES) and thank the National Center for Electron Microscopy at LBNL for access to the TEM. Research at ORNL is supported by DOE BES, Division of Materials Sciences, under contract with UT-Battelle, LLC. The XOR/UNI facilities on sectors 33 and 34 at the APS are supported by the DOE Office of Science. Use of the Advanced Photon Source was supported by the U.S. Department of Energy, Office of Science, Office of Basic Energy Sciences, under Contract No. W-31-109-ENG-38.

A Gold and Silicon Get-Together

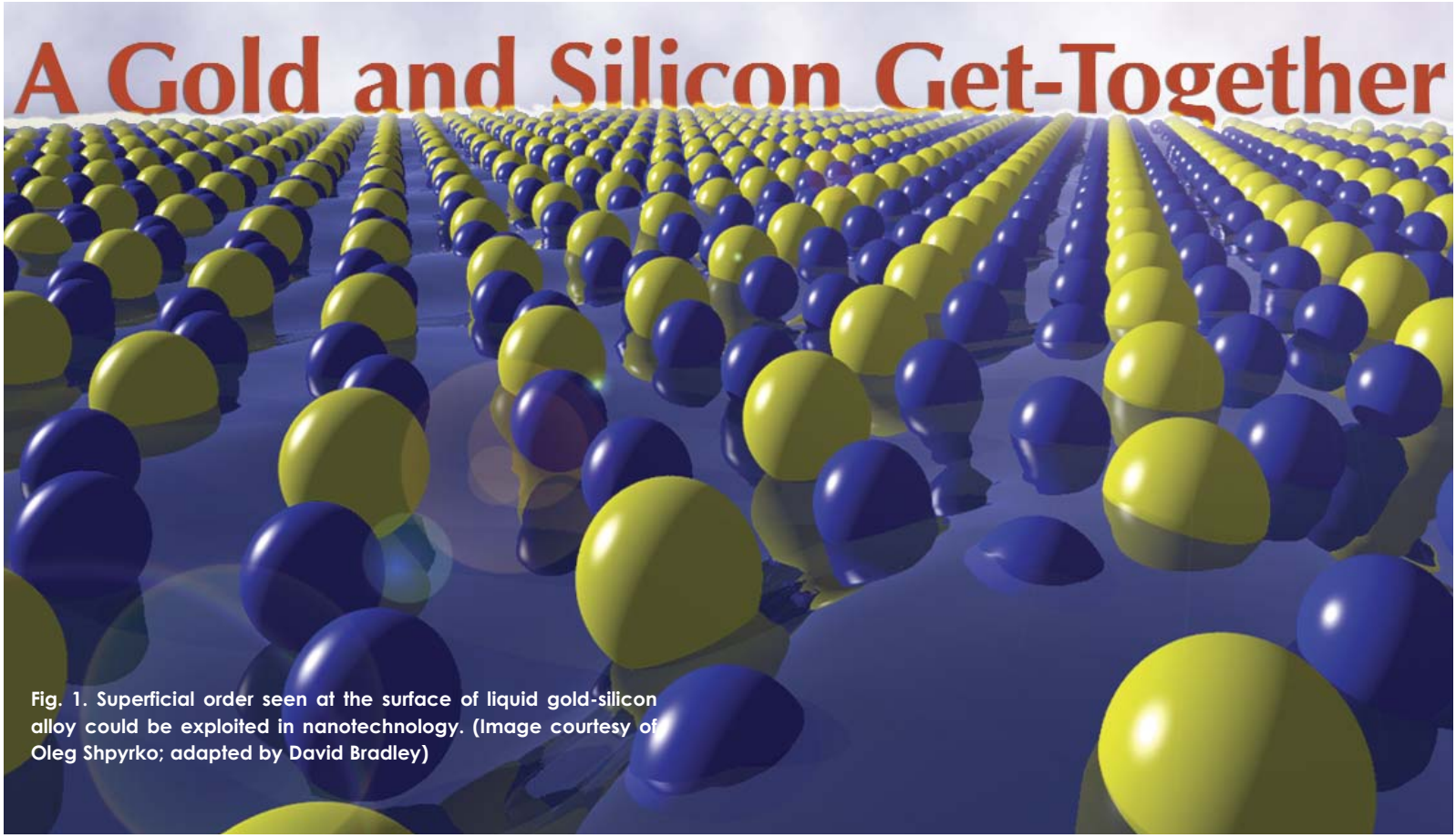

Fig. 1. Superficial order seen at the surface of liquid gold-silicon alloy could be exploited in nanotechnology. (Image courtesy of Oleg Shpyrko; adapted by David Bradley)

By definition, there is no crystalline order in a liquid. But researchers from Harvard University, Brookhaven National Laboratory, The University of Chicago, and Bar-Ilan University in Israel, using the ChemMatCARS beamline 15-ID at the APS, discovered something rather unusual when they melted an alloy of gold and silicon: the surface of this material proved to be ordered and formed a crystal-like monolayer and a structure seven or eight layers deep (Fig. 1). Such surface features might be exploited in fabricating nanoscale devices from this novel alloy and could play a role in new theories of matter that explain some of the bizarre properties of this and other composites.

Alloys often have very different properties than their constituent metals. Bronze, for instance, an alloy of copper and tin, is much tougher than either metal alone. Alloys of other metals made with semiconductor elements (such as silicon), however, have become a focus of attention for materials scientists hoping to create new designer materials for nanotechnological applications, such as gold-silicon systems for the self-assembly of silicon nanowires. Because of the low melting point of this material, it might also be useful for tightly bonding nanoscopic components that will not melt at the operating temperature of the device.

One of the reasons these new alloys are so intriguing is because of their structure and physical properties. Gold is used to make microscopic connections between components in integrated circuits, while silicon is well known as the stock in trade of the computer chip industry.

Gold melts at about 1,063º C, and silicon at 1,412º C. Mix 82 parts of gold with 18 parts of silicon to make a new type of alloy ($Au_{82}Si_{18}$), and the melting point of the composite plummets so that $Au_{82}Si_{18}$ melts at just 359º C. This in itself is not particularly unusual. Other alloys have a eutectic melting point well below the melting points of their constituent materials. However, just *how* this material melts is enabling new insights into the nature of matter.

This study shows that the behavior of $Au_{82}Si_{18}$ is different from other alloys in a critical way. The group focused on the surface of the molten alloy and found that unlike most liquids, there is some long-range order among its constituent atoms. It is as if the surface is frozen, but the bulk of the liquid remains molten, forming a monolayer-thick crust on the surface. While a liquid-like layer on a solid surface just below the melting point is common, this inverse situation is much more unusual.

The researchers used a raft of x-ray techniques on the beamline, including specular reflectivity, grazing incidence diffraction, and diffuse scattering. Each technique exploited the intense beams available at the APS and allowed the team to extract key information about the positions of the gold and silicon atoms close to the surface of the molten alloy. The layering they observed in the alloy's surface

Continued on page 20

Synthesis and Characterization of the Nitrides of Platinum and Iridium

It has long been assumed that noble metals such as gold and platinum were too unreactive to bond to nitrogen atoms and form nitrides. However, in 2004, the first platinum nitrides were synthesized, offering hope that if such strong, hard metals could be made in bulk they could form longer lasting electronic, magnetic, or optical devices. Researchers from Lawrence Livermore National Laboratory (LLNL), the Carnegie Institution of Washington, and the Atomic Weapons Establishment, Aldermaston, using the HP-CAT 16-ID-B beamline at the APS, determined the structure of platinum nitrides devised from first principles. This work provides a structural theory that jibes with experimental evidence, unlike earlier theories that predicted a zinc-blende structure or a fluorite structure. This work also describes the first synthesis of iridium nitride.

Theoretically determined structures for metal nitrides showed many failings. The zinc-blende structure, looking like a diamond structure, was shown not to be able to exist under ambient conditions—it was not elastically stable, and the bulk modulus was a factor of two less than the bulk modulus of platinum. The fluorite structure was stable, but these researchers show that it did not have the correct Raman spectra or bulk modulus.

Recently, the researchers have synthesized the nitrides at LLNL by squeezing the metal and the nitrogen in a diamond anvil up to 500,000 atmospheres and heating it to a synthesis temperature of at least 1600K for the iridium and 2000K for the platinum.

Raman spectra of the synthesized platinum compound showed two intense and two weaker modes, which did not correspond to modes that would be expected if the platinum nitride had a fluorite structure. Instead, the Raman spectra corresponded more closely to a pyrite structure. The iridium nitride, in contrast, had at least 11 modes, suggesting it has more atoms in the unit cell and/or a less symmetric structure than the platinum nitride.

Angle dispersive x-ray diffraction was performed on the nitrides at the HP-CAT beamline. The data acquired were vital to correctly determine the respective structures. X-ray photoelectron spectroscopy was performed at LLNL and yielded a stoichiometry for both nitrides of 2 ± 0.5, i.e., a ratio of two nitrogen atoms to every metal atom in the compound. Previous structures hypothesized just one nitrogen atom per metal atom.

Based on both the Raman spectra and the stoichiometry information, the authors assumed a pyrite structure for platinum nitride and explored its behavior. This structure is cubic, with metal atoms arranged in a face-centered cubic lattice in which there is a metal atom at each corner of the cube with another metal atom at the center of the face of each cube. Four pairs of nitrogen atoms fill in each face.

Calculating the Raman spectra of this theoretical structure showed four of the five modes with the calculated frequencies all within 10% or better of the experimental values. The pyrite structure also is in equilibrium for a lattice constant of 4.79 Å, which is in better agreement with the experimental value of 4.8 Å than the fluorite structure's 4.866 Å. In addition, the bulk modulus for the new structure was calculated to be 347 GPa, significantly higher than the values calculated for the fluorite structure, and also significantly higher than the bulk modulus of platinum by itself; 276 GPa. This constitutes further evidence that the theoretically predicted pyrite structure coincides well with experiment. Preliminary results from iridium nitride suggest that its bulk modulus, too, is very large. With such a close correlation between the theoretical and experimental Raman spectra and bulk modulus, the researchers concluded that the pyrite struc-

Continued on page 20

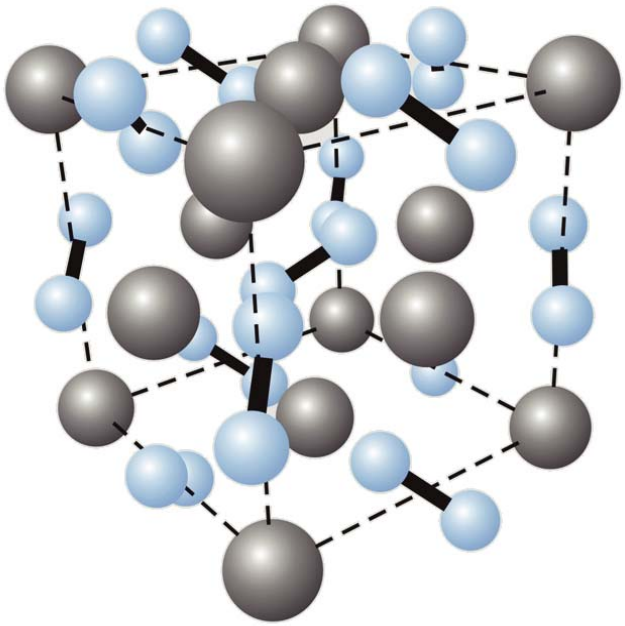

Fig. 1. Diagram of the proposed pyrite structure of PtN_2. Gray and blue spheres represent platinum and nitrogen, respectively.

"Nitrides" continued from page 19

ture is a far more accurate picture of the newly created compound platinum nitride. As for the iridium nitride, while it has the same stoichiometry, it appears to exhibit much lower symmetry.

— Karen Fox

See: Jonathan C. Crowhurst[1]*, Alexander F. Goncharov[1,2], Babak Sadigh[1], Cheryl L. Evans[1], Peter G. Morrall[1,3], James L. Ferreira[1], and A. J. Nelson[1], "Synthesis and Characterization of the Nitrides of Platinum and Iridium," Science **311**, 1275 (3 March 2006). DOI: 10.1126/science.1121813

Author affiliations: [1]Lawrence Livermore National Laboratory, [2]Carnegie Institution of Washington, [3]AWE, Aldermaston

Correspondence: *crowhurst1@llnl.gov

Use of the HP-CAT facility was supported by DOE Basic Energy Sciences, DOE National Nuclear Security Administration, NSF, Department of Defense Tank-Automotive and Armaments Command, and the W. M. Keck Foundation. This work was preformed under the auspices of the U.S. Department of Energy by the University of California, Lawrence Livermore National Laboratory (LLNL), under contract W-7405-ENG-48 and was supported by the Laboratory Directed Research and development office of the LLNL. Use of the Advanced Photon Source was supported by the U.S. Department of Energy, Office of Science, Office of Basic Energy Sciences, under Contract No. W-31-109-ENG-38.

"Gold and Silicon" continued from page 18

extends three times deeper than any previously observed surface freezing.

The researchers noted that at a temperature just above the eutectic point, the alloy forms a single ordered layer just one atom thick at its surface, beneath which the gold and silicon form ordered layer upon layer of atoms, down to a depth of seven or eight layers. The origin of this unusual behavior—not seen before in any metallic alloy—may lie in the fact that in the solid state, the gold-silicon alloy does not display any order. The alloy is a uniquely glassy structure in which the atoms cannot pack neatly together as they do in other metallic alloys to form a crystalline state. However, on melting, the atoms gain the necessary freedom to arrange themselves with some semblance of order, but only on the surface where bonding between atoms is limited to the sides and below.

— David Bradley

See: Oleg G. Shpyrko[1,2*], Reinhard Streitel[1], Venkatachalapathy S. K. Balagurusamy[1], Alexei Y. Grigoriev[1], Moshe Deutsch[3], Benjamin M. Ocko[4], Mati Meron[5], Binhua Lin[5], and Peter S. Pershan[1], Science **313**, 77 (7 July 2006). DOI: 10.1126/science.1128314

Author affiliations: [1]Harvard University, [2]Argonne National Laboratory, [3]Bar-Ilan University, [4]Brookhaven National Laboratory, [5]The University of Chicago

Correspondence: *oshpyrko@anl.gov

This work was supported by the U.S. Department of Energy grant DE-FG02-88-ER45379 and the U.S.-Israel Binational Science Foundation, Jerusalem. Brookhaven National Laboratory is supported by U.S. DOE contract DE-AC02-98CH10886. ChemMatCARS Sector 15 is principally supported by NSF/DOE grant CHE0087817. Use of the Advanced Photon Source was supported by the U.S. Department of Energy, Office of Science, Office of Basic Energy Sciences, under Contract No. W-31-109-ENG-38.

AROUND THE EXPERIMENT HALL

A DELEGATION FROM DOWN UNDER

A high-level Australian delegation, led by the State of Victoria's Treasurer and Innovation Minster John Brumby, visited the APS in April 2006 to enhance the delegation's understanding of the benefits of synchrotron science. The Australian Synchrotron Project, one of Australia's biggest investments in R&D architecture, will start operations in 2007. New Zealand, which is also investing in the Australian Synchrotron, was represented in the tour by New Zealand's ambassador to the United States and a federal minister. ● The APS and the Australian Synchrotron signed a Memorandum of Understanding on scientific collaboration in 2005 to enable researchers at both facilities to exchange ideas and explore new experimental technology. Brumby noted that he looks forward "to ongoing exchange between our two synchrotrons and to explore linkages with the Center for Nanoscale Materials." ● In the photo—taken at the Center for Advanced Radiation Sources (CARS) sectors (GSECARS, ChemMatCARS, and BioCARS) at the APS—are, from left, Minister John Hargreaves, ACT Government; Minister John Brumby, Treasurer and Minister for Innovation, Industry and Regional Development, Government of Victoria; Ambassador Roy Ferguson, New Zealand Ambassador to the United States, New Zealand Government; Minister Trevor Mallard, Minister for Economic Development and Minister for Industry and Regional Development, New Zealand Government; P. James Viccaro, CARS Executive Director and ChemMatCARS Principal Investigator; and Robert Rosner, Director, Argonne National Laboratory.

Explaining Thin-film Ferroelectricity in Strontium Titanate

Silicon, with well-established fabrication capabilities and excellent electromechanical properties, is a favorite of many industries. Not least of these are electronics manufacturers, who use silicon for large, high-quality, and relatively low-cost wafers for semiconductor devices such as solar cells and avalanche diodes; the list is a long one with connections to many industries. But on the occasions when another material is preferable to silicon, developers want to reap the benefits and experience of using silicon as the substrate. Researchers from the National institute of Standards and Technology, Motorola Labs, Argonne, Ames Laboratory, and the Naval Research Laboratory have uncovered surprising new information about how a potentially important material for electronics, strontium titanate ($SrTiO_3$), acts when it is grown as a thin film on silicon.

Strontium titanate is one of a group of promising metal oxide materials that could be used for computer memory or as a more complex material whose structure and electronic properties are engineered. Bulk $SrTiO_3$ is not ferroelectric (i.e., it is not electrically polarizable), but thin films of $SrTiO_3$ are ferroelectric at room temperature—hence their potential for electronic-memory devices. How and why the ferroelectric properties change are more complex questions. Previous research used transmission-electron microscopy to image films and interfaces, but questions still existed as to how perfectly the thin film had been grown on the substrate. $SrTiO_3$ films were meticulously grown at Motorola Labs; then both their in-plane and out-of-plane lattice constants were measured at the APS.

The Si substrate has a face-centered cubic crystal lattice, while the thin film has a cubic perovskite structure. The researchers grew the film using a kinetically controlled sequential deposition process so that at the interface there was an atom-by-atom registry between the substrate and thin film, with no detectable amorphous SiO_2, which would prevent coherent registry between the film and substrate.

X-ray diffraction data were collected at the XOR/UNI 33-BM beamline at the APS. The x-rays were 9.0-keV photons and the data were collected using a four-circle diffractometer and a Si(111) crystal analyzer.

The researchers found that at the interface in those films, the in-plane lattice constant of the $SrTiO_3$ is the same as that of the Si substrate, although it begins to relax back to its normal lattice constant after a few monolayers—about 20 Å (Fig. 1). The film had a higher in-plane compressive strain than had been previously attained with an enormous out-of-plane lattice constant exceeding the prediction of the bulk elastic constants of $SrTiO_3$ by nearly 100%.

The researchers explained these results via density functional theory calculations. Additionally, they concluded that oxygen vacancies at the interface and hydroxide (OH) adsorbates on the surface would be able to screen the electrostatic depolarization field and allow the ferroelectric distortion in these ultra-thin films. — *Yvonne Carts-Powell*

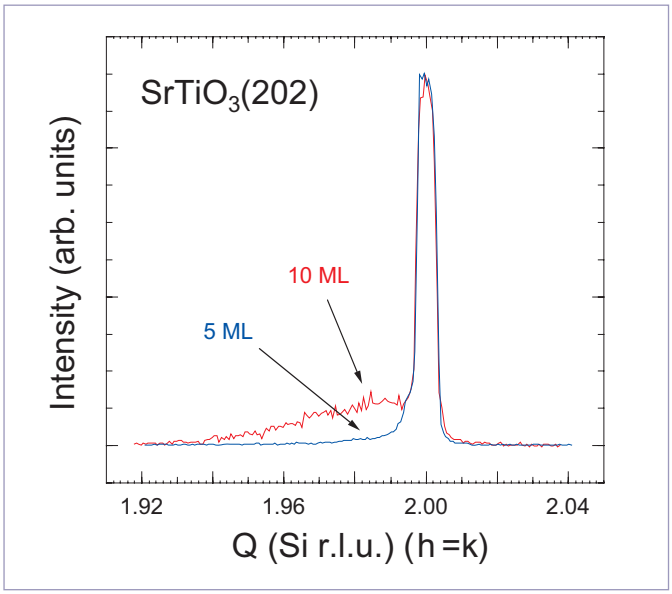

Fig. 1. *h=k* scans along the Si110 direction for the 5 ML and 10 ML films. The curves have been recorded at *l*~2.7 Si r.l.u. to isolate the $SrTiO_3$ diffraction from the Si substrate and have been scaled to equal peak height.

See: J.C. Woicik[1]*, H. Li[2], P. Zschack[3], E. Karapetrova[3], P. Ryan[4], C.R. Ashman[5], and C. S. Hellberg[5], "Anomalous lattice expansion of coherently strained $SrTiO_3$ thin films grown on Si(001) by kinetically controlled sequential deposition," Phys. Rev. B **73**, 024112, (2006).

Author affiliations: [1]National Institute of Standards and Technology, [2]Motorola Labs, [3]Argonne National Laboratory [4]Ames Laboratory, [5]Naval Research Laboratory
Correspondence: woicik@bnl.gov

Two of the authors (C.R.A and C.S.H.) acknowledge support from the DARPA QuIST MIPR 02 N699-00 program. Computations were performed at the ASC DoD Major Shared Resource Center. Use of the Advanced Photon Source was supported by the U.S. Department of Energy, Office of Science, Office of Basic Energy Sciences, under Contract No. W-31-109-ENG-38.

Is Carbon the Key to Improving the Efficiency of Fuel Cells?

Do not throw away your batteries yet, but researchers are getting closer to pinpointing catalytic systems that may improve the efficiency of direct methanol fuel cells. Using x-ray absorption fine structure spectroscopy (XAFS) at the MR-CAT (10-ID) and PNC-CAT (20-BM) beamlines, a team from the University of Notre Dame and Indiana University Northwest recently found that films produced by incorporating platinum (Pt) nanoparticles onto single-walled carbon nanotubes (CNTs) produced catalytic activity an order of magnitude greater than Pt particles fused onto spherical fullerenes (C60). Further exploration using XAFS revealed that it's the structure of the carbon support that accounts for this dramatic difference in the efficiency of the system.

The carbon support system itself, whether a sphere or a nanotube, has insignificant catalytic properties, but electrochemical deposition of platinum nanoparticles—a common technique to bind noble metals to carbon—changes the overall catalytic activity of the system. Previous XAFS probes of platinum on a carbon support confirmed the reducing potential and formation of platinum nanoparticles. The current study used XAFS and electrochemistry measurements to compare the structure and catalytic activity of platinum particles on two different carbon supports: the spherical C_{60} and the CNT.

Continued on next page

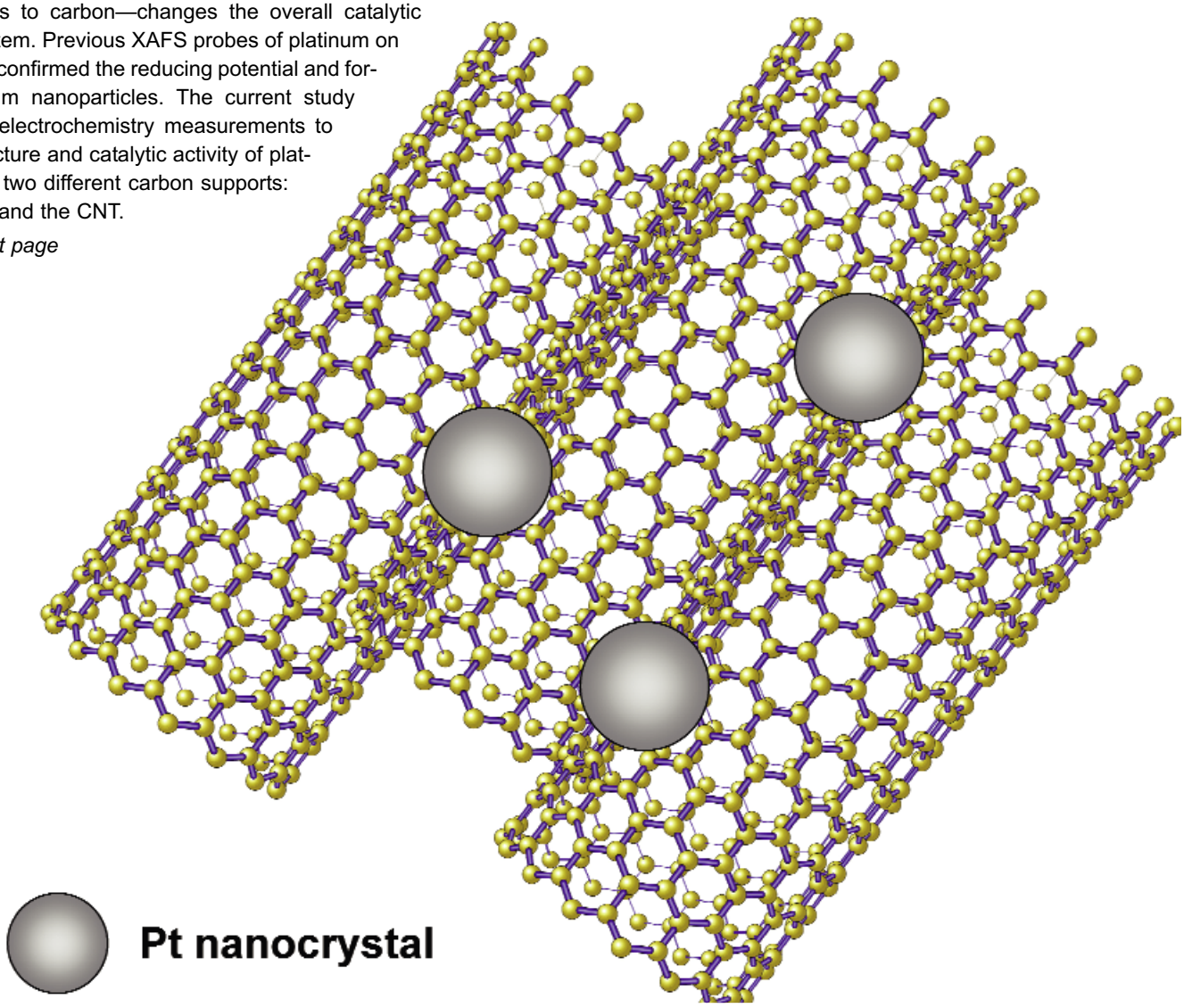

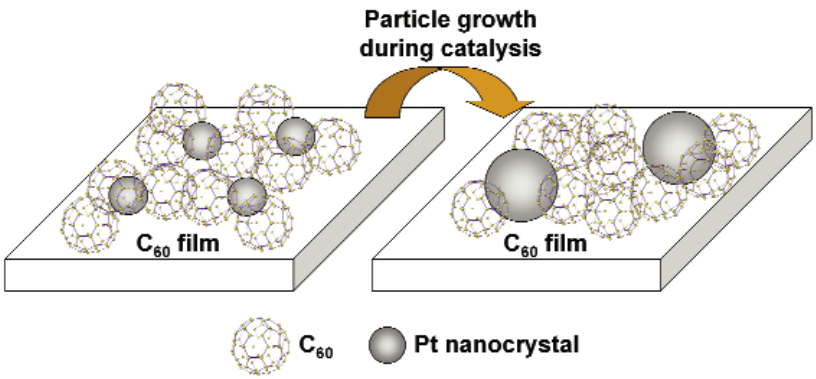

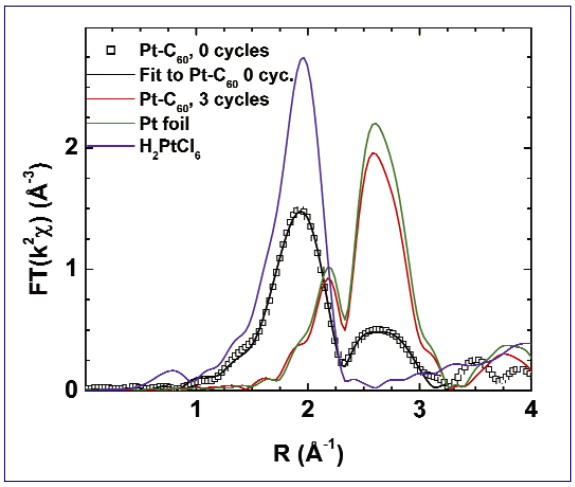

Fig. 2. Above: Pt nanocrystals deposited on C60 films undergo structural changes during the catalytic process. Right: Fourier-transformed EXAFS spectra of Pt–C60 as-prepared (black squares and fit) and after three cycles of methanol oxidation (red) compared to Pt metal (green) and H_2PtC_{l6} (blue) standards.

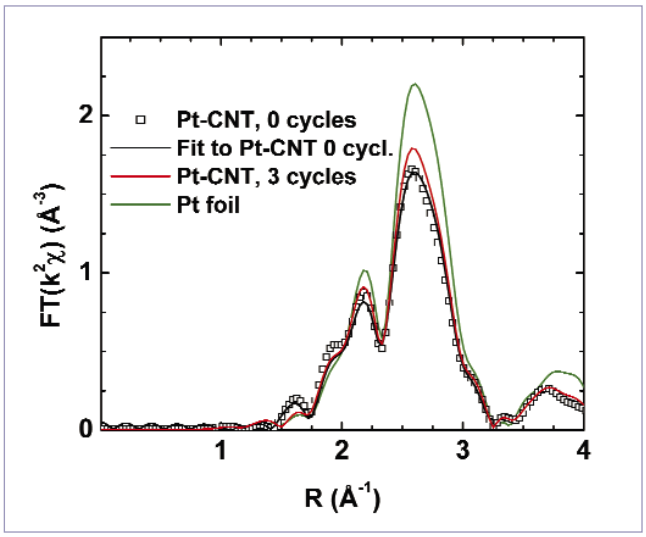

Fig. 1. Opposite page: Pt nanocrystals anchored on carbon nanotube films show a high degree of stability during the catalytic oxidation of methanol. Above: Fourier-transformed XAFS spectra of Pt-CNT as-prepared (black squares and fit) and after three cycles of methanol oxidation (red) compared to Pt metal standard (green).

C_{60} and CNT films were first deposited onto the surface of optically transparent electrodes followed by electrodeposition of Pt nanocrystals. The films were then subjected to multiple catalytic cycles of methanol oxidation in an electrochemical cell. Although both systems showed increased oxidation current during the first four cycles of methanol oxidation, values of the peak currents indicated that Pt-CNT films had much higher catalytic activity than the Pt-C_{60} films.

To determine the structural changes that might explain the large differences in catalytic activity, the team then observed the films before methanol oxidation, after three cycles of oxidation, and after 20 cycles followed by a 48-h period of aging in a mixture of methanol and sulfuric acid. The Fourier-transformed XAFS spectra (Fig. 1) showed no change in the structure of the Pt atoms in the CNT film, even after the 20 cycles and period of aging, indicating the superior stability of this construct. The platinum ions in the Pt-C_{60} catalyst, however, showed dramatic structural changes after exposure to the first three cycles of oxidation and reduced catalytic activity (Fig. 2). The peak in the Fourier-transformed XAFS spectra at 1.9 Å disappears, and the peak at 2.8 Å becomes more prominent, which suggests that a significant fraction of Pt atoms—still in the form of Pt chloride after electrodeposition—is reduced to metallic form after exposure to methanol oxidation.

Materials formed by fusing noble metals (such as platinum) onto carbon supports are promising candidates in the production of direct methanol fuel cells, which may soon power increasingly popular small hand-held devices. Given the expense of noble metals, however, we need to determine the most efficient and affordable systems. Techniques such as XAFS can help determine, before further testing, which materials are the best candidates for use in direct methanol fuel cells.

— Elise LeQuire

See: István Robel[1], G. Girishkumar[1], Bruce A. Bunker[1*], Prashant V. Kamat[1], and K. Vinodgopal[2], "Structural Changes and Catalytic Activity of Platinum Nanoparticles Supported on C_{60} and Carbon Nanotube Films During the Operation of Direct Methanol Fuel cells," Appl. Phys. Lett. **88**, 073113 (2006).
DOI: 10.1063/1.2177354

Author affiliations: [1]University of Notre Dame, [2]Indiana University Northwest
Correspondence: *bunker@nd.edu

Use of the Advanced Photon Source was supported by the U.S. Department of Energy, Office of Science, Office of Basic Energy Sciences, under Contract No. W-31-109-ENG-38.

The Flip-flops of Magnetite

Magnetite is one of the handiest substances humanity has ever discovered—it has been used for thousands of years because of its magnetic properties. Yet, some things about it are still mysterious. Formerly classified as a ferromagnetic material, in which all of the magnetic atoms are aligned with each other in perfect lockstep, it is actually ferrimagnetic: each iron magnetic ion is aligned in the opposite direction to the next, yet with the magnetic moment in one ion stronger than in the other, so that an overall net magnetic moment is maintained. Magnetite undergoes a reorientation of its magnetization at the relatively low-temperature metal-to-insulator transition it displays, known as the Verwey transition. But examining processes in detail at the specific magnetic sites could yield valuable clues as to what's happening. That is what a research team from Argonne, the University of Washington, and CSIC-Universidad de Zaragoza has done at the XOR 4-ID-D beamline at the APS.

In magnetite, the magnetic Fe ions are distributed both on octahedral and tetrahedral sites, with the magnetic moments at the octahedral sites antialigned with those at the tetrahedral sites. To determine whether the postulated charge ordering within octahedral sites is the mechanism behind reorientation of magnetization at the metal-to-insulator transition, site-specific observations are needed. The research team used a variation of the DANES (diffraction anomalous near-edge structure) technique called MDANES (magnetic DANES) that can identify the nonequivalent magnetic sites by using different Bragg reflections. By applying and reversing a magnetic field, the experimenters could observe the changes at the sites and how they behave during magnetization reversal.

Two magnetite single crystals were studied at their (022) and (222) Bragg reflections that separately probe the tetrahedral and octahedral sites, respectively. Measurements of the MDANES spectrum through the Fe K-edge resonance were made, with incident intensity detected by an ion chamber and diffracted intensity by an avalanche photodiode. By changing the helicity of the circularly polarized x-rays, the MDANES signal can provide an asymmetry ratio (AR) that gives information about the magnetic moments of the sample along both the incident and scattered wave vectors. The team measured the Fe K-edge resonance MDANES and how it changed with variations in the magnetic field. This provided the equivalent of hysteresis loops for the different sites (Fig. 1).

Above the Fe K-edge, DANES measurements are hard to interpret as a result of self absorption, but this effect is mitigated in the differential measurement of the AR signal. Measurements at the (222) and (022) Bragg reflections show quite different MDANES spectra, but because MDANES depends on both chemical and magnetic contributions, this difference may not be solely attributable to magnetic characteristics. To verify the different magnetic properties of the nonequivalent sites, the experimenters also considered the field reversal loops obtained at the different Bragg angles. These are undeniably different, with the tetrahedral (022) sites displaying significant magnetic-field-dependent hysteresis and the octahedral (222) sites showing far less hysteresis. The team also found a great difference in the remanence-to-saturation ratios, with values of ≈ 0.07 for the octahedral sites and ≈ 0.31 Oe for the tetrahedral sites.

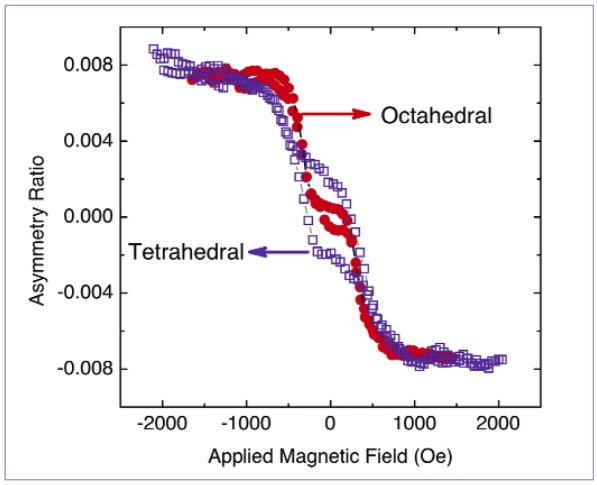

Fig. 1. Site-specific magnetic moment reversal loops for octahedral and tetrahedral iron sites in a magnetite single crystal.

Along with the hysteresis differences between the tetrahedral and octahedral sites, the remanence-to-saturation ratios indicate that the magnetization reversal mechanism in these crystals involves a combination of coherent rotation of the magnetic moments and domain nucleation and growth. The research team believes that further experiments along these lines, perhaps at low temperature rather than room temperature, might reveal further secrets about magnetite's magnetic reversal properties. — *Mark Wolverton*

See: A. Cady[1], D. Haskel[1*], J.C. Lang[1], Z. Islam[1], G. Srajer[1], A. Ankudinov[2], G. Subìas[3], and J. Garcìa[3], "Site-specific magnetization reversal studies of magnetite," Phys. Rev. B **73**, 144416 (2006). DOI: 10.1103/PhysRevB.73.144416
Author affiliations: [1]Argonne National Laboratory, [2]University of Washington, [3]CSIC-Universidad de Zaragoza
Correspondence: *haskel@aps.anl.gov

Use of the Advanced Photon Source was supported by the U.S. Department of Energy, Office of Science, Office of Basic Energy Sciences, under Contract No. W-31-109-ENG-38.

Probing Room-temperature Spintronics

Dilute magnetic semiconductors (DMS) have attracted intense interest as potentially useful materials for manufacturing spin-electronic (or spintronic) devices such as mass-storage hard drives for computers. To fabricate these materials, ions with unpaired d electrons are doped into semiconductors in an effort to induce spin polarization in the free carrier band. The availability of DMS materials that retain spin polarization at and above room temperature would make possible entirely new functionalities in microelectronics. Having gained considerable insight into the prototypical low-temperature DMS—Mn-doped GaAs (Mn:GaAs)—scientists now seek to understand how magnetism develops in doped oxide semiconductors. Certain magnetically doped transition metal oxides exhibit ferromagnetism at and above room temperature, but the physical cause(s) remains highly controversial. Recently, a team of researchers from the University of Washington, Pacific Northwest National Laboratory, and Argonne used the XOR/PNC 20-ID beamline at the APS to carry out spectroscopic measurements that help reveal the connections between structure, composition, and ferromagnetic ordering in Co-doped ZnO (Co:ZnO).

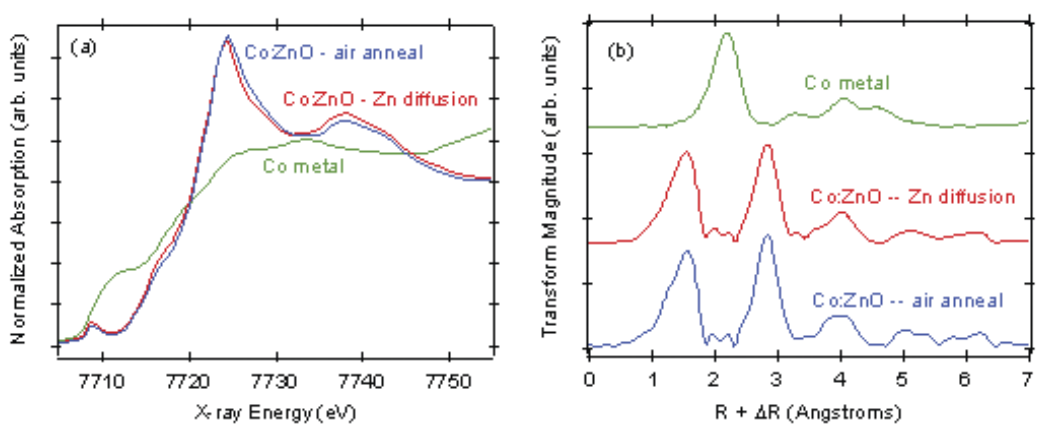

X-ray absorption data for 300-nm epitaxial $Co_{0.09}Zn_{0.92}O/\alpha\text{-}Al_2O_3(012)$: Co K-edge XANES (a) and EXAFS (b) radial distribuion after Zn diffusion and after air annealing, along with reference data for Co metal.

Previous experiments indicated the existence of ferromagnetism in Co-doped ZnO with high Curie points (the temperature below which magnetic ordering can occur), which is a prerequisite for practical device applications. In Mn:GaAs, the ferromagnetism has been shown to be controlled by charge carriers, introduced by the Mn, that in turn mediate exchange interaction between the Mn spins. The situation in the doped oxides is much less clear, however. By independently varying the magnetic and electronic dopant concentrations in ZnO epitaxial films, the research team sought to understand how high-Curie-point ferromagnetism depends on these quantities. The electronic dopant was interstitial Zn (Zn_i) that was diffused into the film after growth. Zn_i generates a shallow bound electron state in the gap, leading to partial *n*-type conductivity. A key tool in the analysis was x-ray absorption spectroscopy, performed at beamline 20-ID.

An epitaxial film of 9% Co-doped ZnO was grown on a sapphire substrate by chemical vapor deposition to a thickness of 300 nm. The sample was insulating and paramagnetic as grown. After exposure to Zn vapor, the film became *n*-type and ferromagnetic at room temperature. Heating in air resulted in a reversion to the insulating, paramagnetic state as Zn_i diffused out to the surface, oxidized, and formed new layers of ZnO. Significantly, the process was fully reversible over many cycles. The magnetization, conductivity, infrared absorbance (a measure of the Zn_i concentration), and Co^{2+} ligand field band absorbance (a measure of the paramagnetic Co^{2+} concentration) were measured as a function of treatment. Strong kinetic correlations were found between the Zn_i concentration and both conductivity and saturation magnetization. The Co K-shell near-edge structure (XANES) showed statistically insignificant changes after Zn diffusion, indicating no detectable change in

Continued on page 26

"Spintronics" continued from page 25

Co^{2+} speciation. Co K-shell extended x-ray absorption fine structure (EXAFS) showed identical scattering lengths before and after Zn diffusion, and the scattering lengths were indicative of Co at Zn sites (Co_{Zn}) in the ZnO lattice. Zn K-edge XANES showed an increase in intensity at 9665 eV after Zn diffusion, which may be characteristic of Zn_i.

Together, these data reveal a strong correlation between the presence of Zn_i and ferromagnetism in Co:ZnO, and suggest that shallow bound donor electrons from Zn_i are important in parallel alignment of the Co^{2+} spins. However, there are other possible explanations that are currently being explored as well. This work serves to highlight the utility of high-brightness synchrotron facilities in performing element-specific structural studies of materials in which subtle compositional changes may be very important. Through such experiments, the intriguing properties of candidate DMS materials such as Co:ZnO might be fully understood and harnessed for applications.

— David Voss and Scott Chambers

See: Kevin R. Kittilstved[1], Dana A. Schwartz[1], Allan C. Tuan[2], Steve M. Heald[2], Scott A. Chambers[2], and Daniel R. Gamelin[1],* "Direct Kinetic Correlation of Carriers and Ferromagnetism in Co^{2+}:ZnO," Phys. Rev. Lett. **97**, 037203 (2006).
DOI: 10.1103/PhysRevLett.97.037203

Author affiliations: [1]University of Washington, [2]Pacific Northwest National Laboratory
Correspondence: *Gamelin@chem.washington.edu

This work was funded by the U.S. National Science Foundation (DMR-0239325 to D. R. G.), the Research Corporation, the Dreyfus Foundation, and the Sloan Foundation. Work at the Environmental Molecular Sciences Laboratory (a national scientific user facility sponsored by the U.S. DOE's Office of Biological and Environmental Research and located at Pacific Northwest National Laboratory) was supported by the U.S. DOE Office of Science, Division of Materials Sciences and Engineering. Use of the Advanced Photon Source was supported by the U.S. Department of Energy, Office of Science, Office of Basic Energy Sciences, under Contract No. W-31-109-ENG-38.

Pinning Down the Depinning CDW

Charge density waves (CDWs) are an intriguing phenomenon that occurs in certain quasi-one-dimensional metals. The electron density and the positions of the atoms in the crystal are periodically modulated at half the Fermi wavelength. When an electric field is applied, these waves can slide through the crystal, producing collective charge transport via a mechanism originally proposed to explain superconductivity. But impurities can inhibit or "pin" the motion of the CDW, and the strength of this pinning varies with crystal thickness. Variations in thickness that occur in some crystals and manifest themselves as physical steps on their surface can cause the bulk CDW to tear or shear. Understanding how and when the CDW shears can provide insight into the elasticity and dynamics of these unusual electronic crystals. Researchers from the University of Wisconsin, Cornell University, and Argonne probed CDW shear behavior in $NbSe_3$ through the use of x-ray microbeam diffraction at XOR beamline 2-ID-D at the APS. This work points to new methods for gaining an understanding of the dynamics of electronic crystals.

The experimenters measured the CDW shear strain profile in two sample crystals of $NbSe_3$, one 15-μm wide and 1.2-μm thick, and one 12-μm wide and 1.4-μm thick. Each crystal featured a single large step running parallel to its b^* axis, along which CDW motion occurs. Because CDW shear is expected to occur at scales of about 1 μm, x-ray microdiffraction, with its submicron resolution, is especially well-suited for the study of this phenomenon.

Depinning the CDW requires the application of an electric field larger than a threshold field, E_T. Although pinning arises from bulk impurities, the pinning strength and depinning field grow with decreasing crystal thickness when crystals are thinner than a few microns. In a crystal with a step in thickness across its width, such as those used by the experimenters, the CDW in the thicker side can shear from the thinner, more strongly pinned side. This should produce a rotation of the CDW wave vector, with the vector tilted in the a^*-b^* plane by an angle φ. This angle varies across the width (and step) of the crystal, and if the crystal is rocked, the angle and angular broadening can be measured, quantifying CDW shear.

The research team coupled this handy phenomenon to submicron x-ray beams to examine how the CDW shears as the applied electric field is increased from zero to the depinning field E_T and beyond. Nothing happens until the CDW depins at E_T, but then the diffraction profiles near the crystal step show large changes. As the electric field increases above E_T, the center of the curves varies across the width of the crystal by up to 40 mdeg, with the largest variation observed just above the E_T threshold.

When the rotation of the CDW wave vector (represented as the φ angle peak position shift) is plotted as a function of position across the crystal width (along the c^* axis), the maxi-

Continued on next page

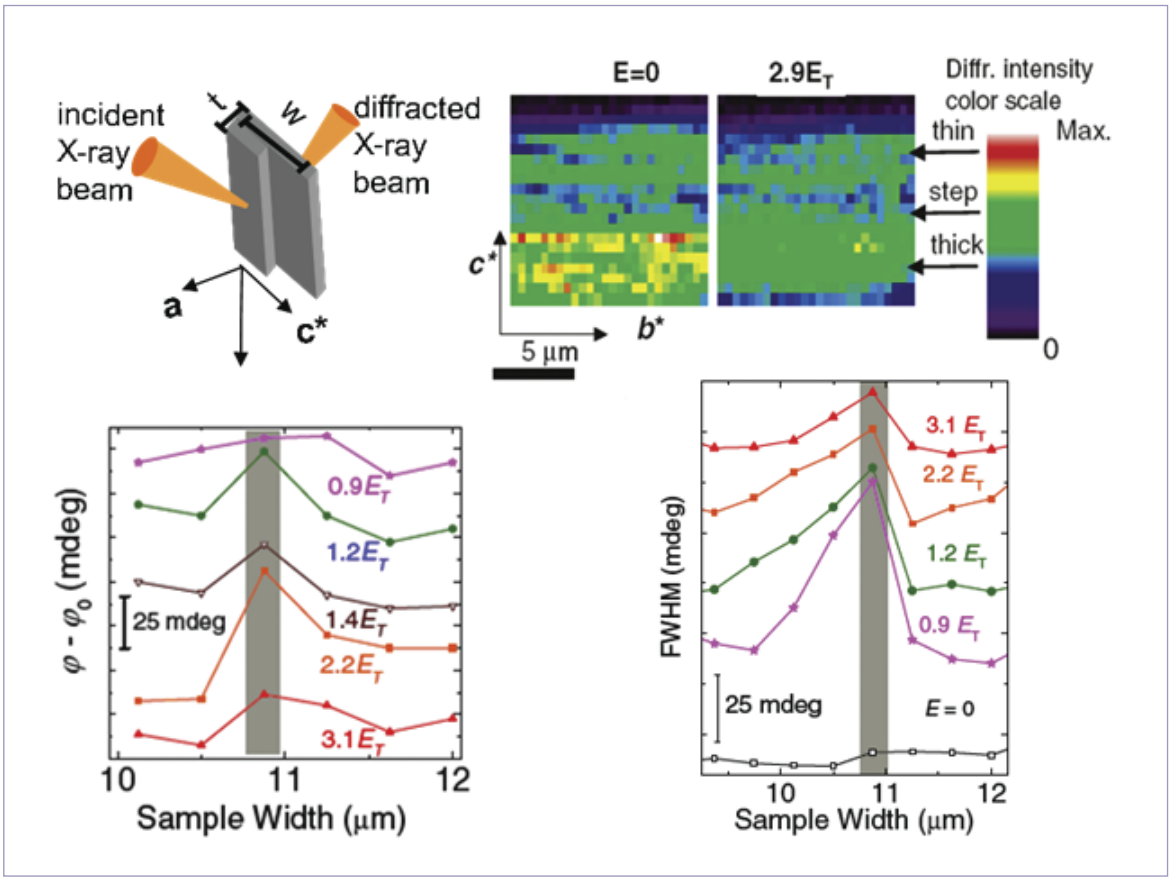

Fig. 1. Diagram upper left: X-ray microbeam setup for an $NbSe_3$ crystal with a stepped cross section, showing the relevant crystallographic directions. Momentum transfer is along the CDW transport direction (*b**). Images upper right: A decrease of the microdiffraction intensity, after depinning of the CDW and due to a loss of transverse coherence. The graphs show the measure of the rotation of the CDW wavevector for a variety of electric fields, and a variation of the microdiffraction intensity for the same set of electric field values. E_T is the field at which CDW depins.

mum φ angle rotation occurs near the crystal step. No wave vector rotations are seen near the crystal edges, thus ruling out CDW pinning by crystal surfaces. By fitting this data and comparing them with previous electric transport measurements of CDW shear, the research team was able to estimate the CDW's shear modulus as $G = 1.8 \times 10^7$ N/m^2, approximately 50 times smaller than the CDW's longitudinal modulus.

By performing direct measurements of CDW shear strain profiles, the research team has provided a unique demonstration of the capabilities and resolution of x-ray microbeam diffraction at the APS microdiffraction facility. Their work suggests applications of microbeam diffraction in other collective phenomena such as superconductivity and ferromagnetism.

— Mark Wolverton

See: A.F. Isakovic[1], P.G. Evans[2], J. Kmetko[1], K. Cicak[1], Z. Cai[3], B. Lai[3], and R.E. Thorne[1]*, "Shear Modulus and Plasticity of a Driven Charge Density Wave," Phys. Rev. Lett. **96**, 046101 (3 February 2006). DOI: 10.1103/PhysRevLett.96.257801

Author affiliations: [1]Cornell University, [2]University of Wisconsin, [3]Argonne National Laboratory
Correspondence: *ret6@cornell.edu

This work was supported by the NSF (DMR 04-05500). Sample mounts were prepared using the Cornell Nanoscale Facility, a member of the National Nanotechnology Infrastructure Network, which is supported by the National Science Foundation (Grant No. ECS 03-35765). Use of the Advanced Photon Source was supported by the U.S. Department of Energy, Office of Science, Office of Basic Energy Sciences, under Contract No. W-31-109-ENG-38.

Interface Effects in Magnetic Oxide Superlattices

Studies of the interface between two materials have a rich history of revealing new physics that is not present when either constituent material is studied by itself. The most ubiquitous application of this research is the transistor, which spearheaded the advent of the electronic revolution. On the other hand, magnetism is the basis for many present, near-term, and future technologies, including hard drives, next-generation memory systems such as magnetic RAM, giant magnetoresistance RAM, and spin-dependent tunneling memory. The drive for these new technologies, coupled to past success in interfacial physics, led scientists to look toward atomic-scale-precision methods for the manufacture of high-quality layers of different semiconducting magnetic oxide materials that can be stacked to form superlattices. Suitable candidates for stacking are cuprate and manganite oxides, whose valence electrons are subject to strong magnetic interactions, and whose interfacial magnetization coupling would naturally have a significant effect on the transport of currents. In recent years, high-quality cuprate-manganite superlattices have been prepared and their bulk magnetic characteristics recorded, but the microscopic mechanisms underlying these observations have remained largely unexplored. Now, researchers have used both x-ray magnetic circular dichroism (XMCD) and neutron reflectometry to obtain the first detailed microscopic picture of the magnetic landscape along the superlattice plane, revealing intriguing new insights into the subtle interplay between ferromagnetism and superconductivity at the interface.

The XMCD experiments were carried out at the XOR 4-ID-C beamline at the APS, and beamline ID08 of the European Synchrotron Radiation Facility. The resulting spectra are illustrated in Fig. 1(a). These spectra correspond to a superlattice of alternating, 100-Å-thick, c-axis oriented layers of $YBa_2Cu_3O_7$ (YBCO) and $La_{2/3}Ca_{1/3}MnO_3$ (LCMO), and were taken at the resonant 2p → 3d transition $L_{2,3}$ edges. They show a clear difference in absorption between right and left circularly polarized x-rays, and thus provide definitive evidence of a small, induced magnetic moment on Cu in the YBCO layer near the interface with the LCMO. This was surprising because, while manganite layers are known to undergo a ferromagnetic transition at a temperature of around 180K, cuprates never exhibit ferromagnetism.

To investigate the origin of the ferromagnetic polarization of Cu, additional XMCD measurements were made over a wide range of temperatures at both Cu and Mn edges, and as illustrated in Fig. 1(b), the striking similarities in the temperature dependence of both the Cu and Mn signals indicate the magnetic moment of the Cu is a result of the strong coupling

Continued on page 31

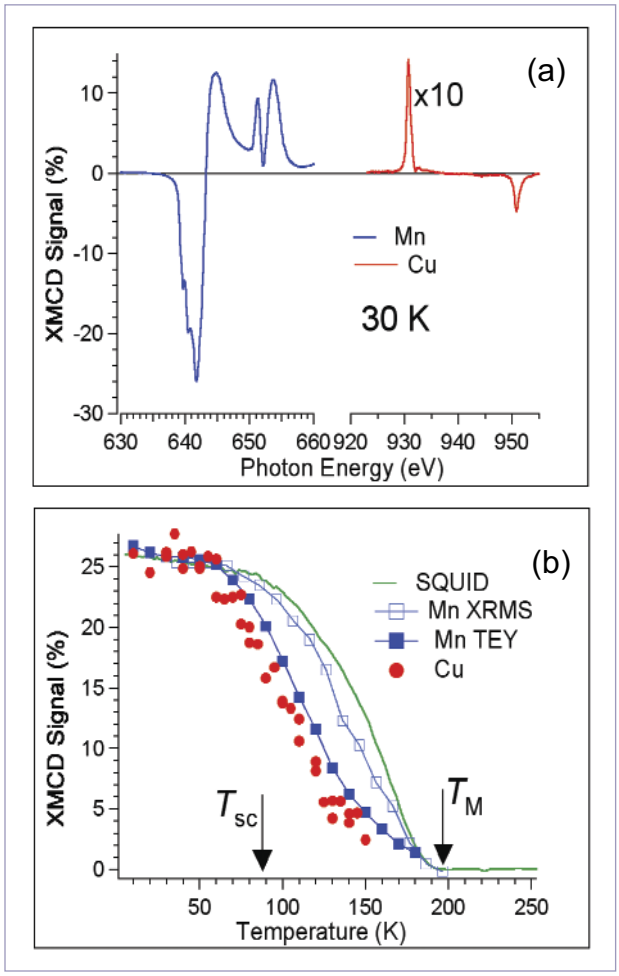

Fig. 1. X-ray magnetic circular dichroism spectra. (a) Core-level absorption XMCD signals for Cu (red) and Mn (blue). Note that the Cu signal has been magnified by a factor of 10 for the sake of comparison. (b) Temperature dependence of Cu and Mn XMCD signals compared to bulk magnetization (green), normalized to the value of the dichroism on Mn.

X-ray Analysis for Better Optical Storage Materials

Materials called "chalcogenide glasses" have been at the forefront of a revolution in optical data storage. Of special interest is the compound $Ge_2Sb_2Te_5$ (GST), which exhibits the very useful ability to switch reversibly between amorphous and crystalline phases on exposure to light or electrical pulses. Because the properties of these phases are different and can represent data bits, GST is being studied for data-storage-device applications. To engineer optimum switching performance, however, materials scientists seek a detailed understanding of the mechanism responsible for the amorphous-crystalline transition. Recently, a team of researchers from North Carolina State University and the Colorado School of Mines used the MR-CAT 10-ID beamline at the APS in conjunction with powerful theoretical tools to study the bonding mechanisms in the amorphous phase of GST. Their results underscore the ability of high-brilliance x-ray beams, such as those from the APS, to provide atomic-scale measurements for clarifying phase transition mechanisms of technological interest.

Samples of GST were fabricated by radio frequency sputtering 2.7-μm films onto aluminum foils. The foils were sectioned into 10 mm x 4 mm pieces and stacked to create layered specimens with a total thickness of 22 μm. Extended x-ray absorption fine structure (EXAFS) spectra were obtained at MR-CAT beamline 10-ID. Spectra near the K edges of Ge, Sb, and Te were collected in transmission moder. Fitting of the Fourier transformed spectra was carried out with standard analysis codes to yield atomic bond distances and coordination numbers consistent with tabulated values.

These measurements were analyzed in the context of bond constraint theory, which provides a framework for characterizing amorphous materials in much the same way that periodicity serves to characterize crystalline materials. In this theoretical picture, a material is good for forming glass if the average number of constraints (that is, stretching or bending motions) per atom is equal to the dimensionality of the amorphous network. Atoms are constrained to remain where they are unless energy is provided to stretch or bend the bonds that hold them in place, and bond constraint analysis quantifies this concept. Materials that are either too constrained (stressed and rigid) or not constrained enough (floppy) will not be good candidates for easily switched structural transitions. Structural probes such as EXAFS can be used to construct a detailed picture of the bonding arrangements for each of the atoms in GST. When the average constraint numbers for each of the constituent atoms are added together, the result is a total of 3.07, which is in good agreement with the dimensionality of the network D = 3.

Bond constraint analysis based on the EXAFS results shows that GST is an intermediate region of the ternary phase diagram where entropy effects in the amorphous phase and enthalpy effects in the crystalline phase balance out to allow reversible transitions. With this information, it should be possible to fine tune the GST composition for optimum switching.

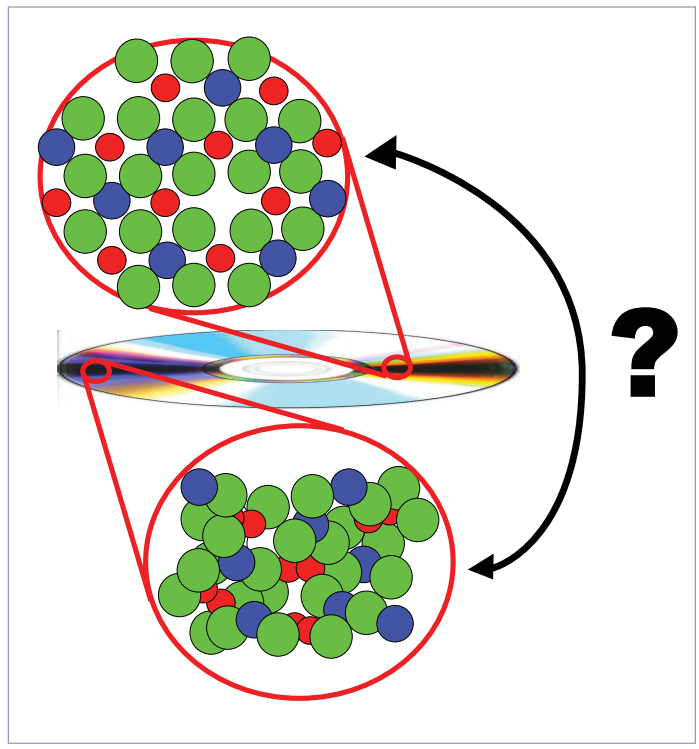

Fig. 1. The two phases of GST that are used for data storage. The lower, amorphous phase consists of Ge_2Te_3 units and Sb_2Te_3 units interconnected by an amorphous tissue of two- and three-fold coordinated Te. The upper diagram shows the well-characterized crystalline phase.

The findings show the value of detailed atomic-scale measurements in elucidating phase transition mechanisms of technological interest, especially when the measurements can be performed at high-brightness third-generation synchrotrons such as the APS. — *David Voss*

Continued on page 31

Nonequilibrium Processes in Pulsed Laser Deposition

Pulsed laser deposition (PLD) is a powerful and widely used method for growing thin films and multilayered materials. It offers simplicity of use and—because the chemical structure of the deposited thin film matches the chemical structure of the target material—the ability to preserve the stoichiometric relationship between deposited film and target material. Applications of PLD include production of superconducting and insulating circuit components, magneto-optic storage devices, multilayer x-ray optics devices, and protective and insulating coatings on vulnerable components. But even though PLD enjoys widespread use, the underlying processes are not well understood, making PLD a ripe subject for research. For example, collaborators from Oak Ridge National Laboratory and the University of Illinois performed surface x-ray diffraction (SXRD) measurements at the XOR/UNI 33-ID beamline at the APS in order to analyze the two-layer growth behavior in PLD of strontium titanate ($SrTiO_3$). Their results show that extremely fast nonequilibrium interlayer transport processes dominate the deposition process over much slower, thermally driven interlayer transport processes. The experiment performed by these researchers provides new insight into the growth processes associated with PLD.

Generally, the PLD technique deposits a thin film onto a substrate with the use of a high-power pulsed laser beam that is focused inside a vacuum chamber. The laser beam strikes a solid target whose material is quickly vaporized, forming an energetic plume. The ejected species are then deposited as a thin film onto a heated substrate that has been positioned to face the target. The deposition occurs from a mixture of neutral and ionized atoms, and molecular fragments with energies in the range from a few tenths to a few hundred electronvolts.

This study demonstrates that PLD film growth is dominated by fast, nonequilibrium processes that occur during the arrival of the laser plume on the growing surface. Further, the collaborators show that much slower, thermally driven processes that are dependent on the dwell time (pause) between consecutive laser shots play a negligible role in interlayer transport. In fact, the collaborators obtained quantitative data showing that nonequilibrium processes are at least three orders of magnitude faster than thermal processes, which can be relegated to an even lesser role with the use of shorter dwell times.

Prior to the experiment, the $SrTiO_3$ samples were etched in a buffered hydrofluoric acid solution (with a pH around 5) for about 1 min and then annealed at a temperature that can range from 950º to 1,050º C. Atomic force microscopy (AFM) was used to select samples with well-developed terraces for the growth experiments. These samples were then annealed at 850º C in a 2 mTorr oxygen atmosphere. The growth experiments were performed after the temperature had dropped to 650º C. At this temperature the intensity of the x-ray crystal truncation rods levels off to around 8 x 10^5 counts per second (cps).

The SXRD measurements were performed at the 33-ID beamline. A key advantage of SXRD is that it provides for the direct recovery of surface coverage from measured intensities of the reciprocal lattice rods. The collaborators used a monochromatic 10-keV x-ray beam for real-time measurements in a PLD chamber configured for SXRD. Measurements of the diffracted intensity, which were set at the specular (mirror-like) anti-Bragg reflection, were performed with an avalanche photodiode detector.

Continued on next page

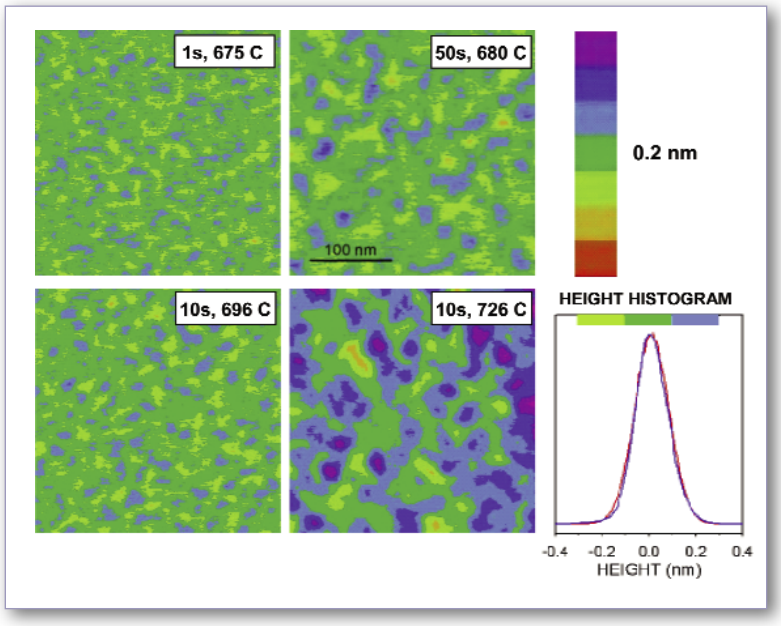

Fig. 1. The AFM images represent an attempt to visualize what the x-rays are "seeing." The labels designate the dwell time and the substrate temperature. The images clearly show that low substrate temperatures and short dwell times represent conditions conducive to layer-by-layer growth. The color height scale and the height histogram on the right side illustrate the distribution of material on the growing surface in term of half unit cell (0.2 nm) increments.

"Interface Effects" continued from page 28

between the spins in the Cu and the ferromagnetic moment of Mn across the superlattice interface.

In order to reconstruct the full magnetization profile, the XMCD data were compared to specular neutron reflectivity results previously obtained from the same samples: these measurements showed that there was a 10-Å region of LCMO with a suppressed magnetic moment that was anti-ferromagnetically coupled to an appoximately 1-cell-thick spin-polarized region of YBCO. By assuming that every Cu atom carries a localized magnetic moment on the order of a Bohr's magnetron, the investigators were further able to estimate that the magnitude of this antiferromagnetic interaction is about 0.2-0.4 times the size of the nearest neighbor Cu spin coupling within a copper oxide layer.

This detailed microscopic description of the magnetic and electronic structure at the interface is believed to be the first of its kind, and provides valuable information for the understanding of the magnetic characteristics at the interface between ferromagnetic and superconducting oxides. — *Luis Nasser*

See: J. Chakhalian[1,2]*, J.W. Freeland[3], G. Srajer[3], J. Strempfer[1], G. Khaliullin[1], J.C. Cezar[4], T. Charlton[5], R. Dalgliesh[5], C. Bernhard[1], G. Cristiani[1], H.-U. Habermeier[1], and B. Keimer[1], "Magnetism at the interface between ferromagnetic and superconducting oxides," Nat. Phys. **2**, 244 (April 2006).
DOI: 10.1038/nphys272
Author affiliations: [1]Max Planck Institute for Solid State Research, [2]University of Arkansas, [3]Argonne National Laboratory, [4]European Synchrotron Radiation Facility, [5]Rutherford Appleton Laboratory
Correspondence: *j.chakhalian@fkf.mpg.de

Use of the Advanced Photon Source was supported by the U.S. Department of Energy, Office of Science, Office of Basic Energy Sciences, under Contract No. W-31-109-ENG-38.

"Optical Storage" continued from page 29

See: D.A. Baker[1], M.A. Paesler[1]*, G. Lucovsky[1], S.C. Agrawal[1], and P.C. Taylor[2], "Application of Bond Constraint Theory to the Switchable Optical Memory Material $Ge_2Sb_2Te_5$," Phys. Rev. Lett. **96**, 255501 (30 June 2006).
DOI: 10.1103/PhysRevLett.96.255501
Author affiliations: [1]North Carolina State University, [2]Colorado School of Mines
Correspondence: *paesler@ncsu.edu

Work supported by the Air Force Research laboratory under Grant No. F29601-03-01-0229 and by the National Science Foundation under Grant No. DMR 0307594. MR-CAT operations are supported by the Department of Energy and the MR-CAT member institutions. Use of the Advanced Photon Source was supported by the U.S. Department of Energy, Office of Science, Office of Basic Energy Sciences, under Contract No. W-31-109-ENG-38.

"Nonequilibrium" continued from page 30

In order to compare the rate of nonequilibrium and thermal processes, the collaborators studied the SXRD transients using a time resolution of microseconds. Analysis of AFM images of films of different thickness (Fig. 1) grown under a variety of conditions showed that surface roughness is restricted to only two layers. Once this was identified, the collaborators found that, within the framework of the two-layer coverage model, the majority of the deposition occurs during the arrival of the plume and only a relatively minor fraction is transferred into the lower layer by slow thermal equilibrium processes. With a time frame for interlayer transfer on the order of microseconds or less, the collaborators could directly confirm that nonequilibrium processes dominate PLD growth.

Because PLD growth takes place primarily by extremely fast nonequilibrium processes, shorter dwell times can be used to suppress the slower thermal transport components. When shorter dwell times were used, the collaborators found that laser-driven completion of the layers dominated the growth process, resulting in smoother surfaces.

Guided by the detailed and quantitative results produced in these experiments, the collaborators are confident that theoretical studies can be used to generalize PLD growth kinetics in the form of new scaling relationships, along with the potential to customize film properties and surface morphology.

— *William Arthur Atkins*

See: J.Z. Tischler[1], Gyula Eres[1]*, B.C. Larson[1], Christopher M. Rouleau[1], P. Zschack[2], and Douglas H. Lowndes[1], "Nonequilibrium Interlayer Transport in Pulsed Laser Deposition," Phys. Rev. Lett. **96**, 226104 (2006).
Author affiliations: [1]Oak Ridge National Laboratory, [2]Argonne National Laboratory
Correspondence: *eresg@ornl.gov

Research sponsored by the Division of Materials Sciences and Engineering, Office of Basic Energy Sciences, US Department of Energy, under Contract No. DE-AC05-00OR22725 with Oak Ridge National Laboratory, managed and operated by UT-Battelle, LLC. The XOR/UNI facility is supported by the U.S. DOE through the Frederick Seitz Materials Research Laboratory at the University of Illinois at Urbana-Champaign, the Oak Ridge National Laboratory, the National Institute of Standards and Technology, and UOP LLC.Use of the Advanced Photon Source and of the Center for Nanoscale Materials was supported by the U.S. Department of Energy, Office of Science, Office of Basic Energy Sciences, under Contract No. W-31-109-ENG-38.

Probing the Promise of Artificial Manganese Films

Spinel ferrite materials, which hold great promise for electronics applications, have inspired considerable enthusiasm among engineers and designers in recent years. The handy ferri- and ferromagnetic properties of these materials stem from their unique atomic structure, particularly in the case of one of the most popular: manganese ferrite (MFO). Although MFO ($MnFe_2O_4$) shares the same structure as the spinel mineral, the distribution of manganese and iron ions in its unit cell can vary depending on how the MFO is formed, and these variations affect the particular magnetic characteristics of the sample. Although the advent of techniques such as laser ablation deposition offer ways to create ferrites customized for specific uses, the potential of such "artificial" ferrites is limited without some means to characterize and thus accurately control the fine atomic structure of the material. Without knowing what ions are going where—not to mention other vital information such as bond distances and cation valences—there's no way to "tune" artificial ferrite growth to obtain the desired qualities. Now a research team from Argonne, Northeastern University, the Institute of Metal Physics, and Nankai University has developed a means of probing site-specific structures in MFO films. Using DAFS (diffraction anomalous fine structure) spectroscopy at the XOR 4-ID-D beamline at the APS, the team was able to resolve local structure in inequivalent sites of the Mn unit cell.

While there are many ways to peek inside the local unit cell structure of ferrites, not all are very effective when dealing with spinel ferrites, in which absorbing atoms are found in different and inequivalent sites. Because of this quirk of spinel structure, even a versatile tool such as EXAFS (extended x-ray absorption fine structure) spectroscopy is of only limited use, because of the overlapping of EXAFS signals from the inequivalent sites. With DAFS spectroscopy, diffracted intensity can be measured from a carefully chosen set of Bragg peaks, avoiding the overlapping signals and allowing a clear picture of structure at the local site level. Although DAFS has been used previously to examine charge ordering in some spinel ferrites, these researchers are the first to use the technique to study fine atomic structure in MFO films. Because the proper methods of reliably reducing DAFS data are a controversial question, the experimenters verified their data by measuring at several different Bragg peaks for consistency and checking averaged DAFS data with EXAFS measurements.

The team created MFO films under nonequilibrium conditions to allow variations in site-occupancy ratios, with an alternating target laser ablation deposition technique, followed by DAFS measurements at the APS. A fast avalanche photodiode was used to measure diffracted peak intensity from the (111), (222), and (422) reflections in the 6,300-ev to 6,900-eV energy range, i.e., around the Mn K-absorption edge. The EXAFS spectra measured in fluorescence were used for absorption corrections and confirmation of the DAFS results.

In the mixed spinel structure of the MFO unit cell, Mn and Fe are arranged among 8 tetrahedral sites and 16 octahedral

Continued on page 34

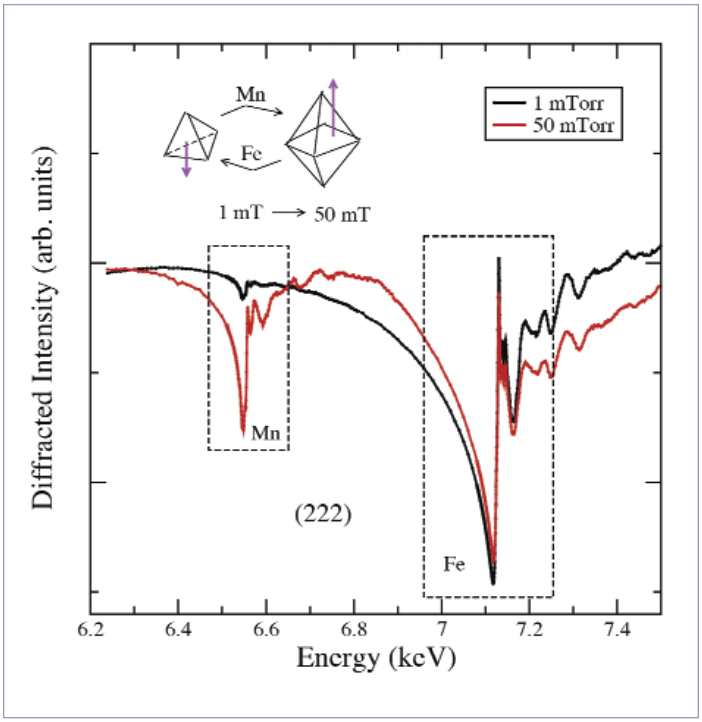

Fig. 1. Diffraction anomalous fine structure at the (222) reflection probing octahedral B sites. Increasing the oxygen pressure in the deposition chamber during sample growth enhances the presence of Mn ions at B sites. This results in increased DAFS intensity at the Mn K-edge resonance and a simultaneous decrease in intensity at the Fe K-edge resonance.

A Closer Look at the $CeTe_3$ Charge Density Wave

Charge density waves can be complicated. In their organized (or commensurate) form these waves are locked onto an underlying crystal lattice. But they can also be incommensurate, the wavelength of the charge density having no relationship to the underlying lattice. These incommensurate charge density waves (IC-CDWs) can provide a handy tool for understanding important properties—such as electron-lattice coupling—of one- and two-dimensional metals, but they're not necessarily the easiest phenomenon to pin down or quantify. They can show up either as uniform incommensurate modulations throughout a sample, or they can be divided into domains containing locally commensurate waves with distortions (the discommensurations) in the waves at the boundaries. Various experimental techniques (including photoemission spectroscopy and nuclear magnetic resonance) can help to distinguish between uniform and discommensurate IC-CDWs, but quantitative data are difficult to obtain with these modalities. A team of researchers from Michigan State University tried a different tactic: using an atomic pair distribution function (PDF) technique to determine atomic displacements in $CeTe_3$ through x-ray diffraction studies at the MU-CAT 6-ID-D beamline at the APS. Their work has afforded new information about the heretofore inaccessible commensurate domains of an IC-CDW, while proving that the CDW in $CeTe_3$ is discommensurated rather than uniformly incommensurate.

The key to the team's new approach is the difference between the atomic displacement data obtained through crystallographic techniques and that determined from the PDF technique. In discommensurated $CeTe_3$, the structure of local domains deviates from the overall average observed crystallographically, and PDF can give quantitative data on the local atomic displacements. The IC-CDW state of rare-earth Te materials is remarkably stable and simple, making these substances particularly well-suited for this sort of study.

The PDF of a system is simply defined as the probability of finding one atom or particle at a particular distance, *r*, from another atom or particle. In undistorted $CeTe_3$ at room temperature, the PDF curve peaks at about 3.1 Å, but shows a shoulder feature on the low-*r* side of the curve, which is also present on curves derived from distorted crystallographic and local structure models and results from Te-Te bond lengths in the square Te net of the crystal structure. By refining these Te-net distortions in the PDF calculations for $2.5 < r < 6.37$ Å (with $r_{max} = 6.37$ Å), the experimenters were better able to fit the calculated and experimental PDF data.

This refined picture of the local atomic structure reveals that Te-Te bond lengths are distributed into both short and long distances, unlike the

Continued on page 34

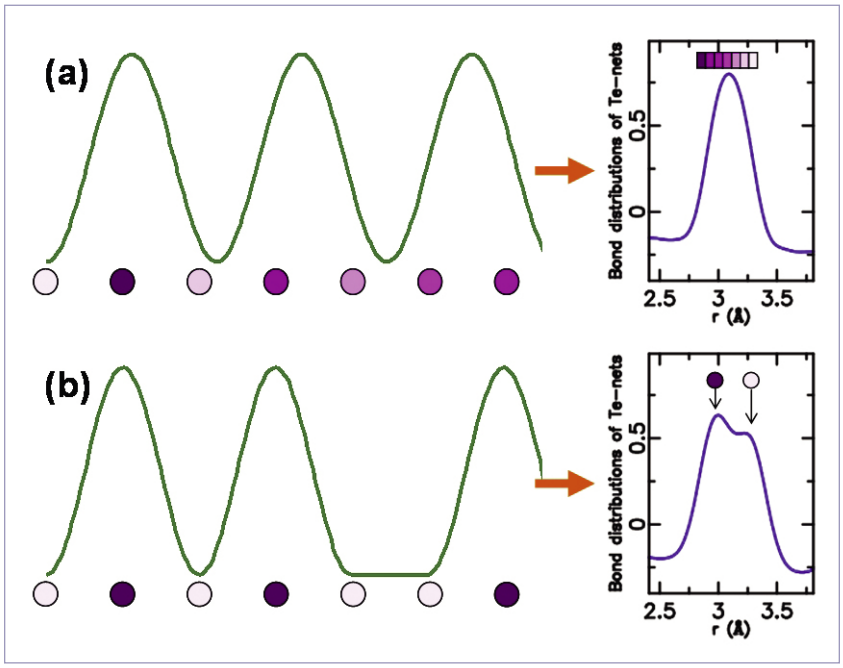

Fig. 1. (a) uniform vs. (b) discommensurated incommensurate charge density waves. The colored circles indicate schematically the position of bonds in the underlying lattice, and the sinusoidal waves the conduction-electron charge density distribution. The color of the circles indicates the length of the bond, with dark colors being shorter bonds and light colors, longer bonds. In the case of the uniform wave the phase of the CDW with respect to the lattice, which modulates the bond-length, varies continuously giving rise to a broad distribution of bond-lengths. In the discommensurated case, the wave is locally in-phase with the lattice, with "phase-slips" or discommensurations. In a PDF measurement, the former results in a broad Gaussian distributed peak and in the latter case a bimodal peak, as shown by the actual experiment.

"Manganese Films" continued from page 32

sites, which the experimenters refer to as A and B sites, respectively. The team used an iterative Kramers-Krönig algorithm to solve the local structure for the inequivalent A and B sites. They found that most of the Mn cations, approximately 80%, prefer the tetrahedral A sites, with the remaining 20% occupying B sites, demonstrating a strong preference on the part of the Mn cations for the tetrahedral sites. Also, the Mn-O first-shell bond distance is considerably greater than the corresponding Fe-O bond distance in the A sites, while almost no change in B-site bond distances is found. However, the effective coordination number in the first oxygen shell Mn octahedral B sites is greatly reduced. Because the ionic radius of Mn is larger than that of Fe, the expansion of the Mn-O bonds at A sites isn't unexpected, but curiously, a similar expansion of bond distances in the B sites is not seen. The researchers conclude that this is the result of two processes: expansion due to the larger Mn ionic radii and contraction because of the reduced coordination, creating a greater degree of covalency in the Mn-O bonds at B sites.

The research team's work demonstrates the usefulness of DAFS for resolving the local atomic structure of artificial manganese ferrite films grown under nonequilibrium conditions. While further experiments are necessary to determine whether the observed characteristics are due only to these growth conditions or are also present in bulk crystals, the team has shown that DAFS is a valuable addition to the arsenal of available techniques for examining fine atomic structure.

— *Mark Wolverton*

See: E. Kravtsov[1,2], D. Haskel[1]*, A. Cady[1], A. Yang[3], C. Vittoria[3], X. Zuo[4], and V.G. Harris[3], "Site-specific local structure of Mn in artificial manganese ferrite films," Phys. Rev. B **74**, 104114 (2006). DOI: 10.1103/PhysRevB.74.104114

Author affiliations: [1]Argonne National Laboratory, [2]Institute of Metal Physics, [3]Northeastern University, [4]Nankai University
Correspondence: *haskel@aps.anl.gov

This work was supported in part by National Science Foundation Project No. DMR-022654 and by Office of Naval Research Project No. N00014-01-1-0721. Use of the Advanced Photon Source was supported by the U.S. Department of Energy, Office of Science, Office of Basic Energy Sciences, under Contract No. W-31-109-ENG-38.

"Charge Density Wave" continued from page 33

symmetric, Gaussian bond-length distribution of the crystallographic model. Typically, this behavior would be seen as oligomerization within a commensurate structure, when Te forms bonds and nonbonded interactions with neighboring atoms. But because in this experiment the average CDW modulation is known to be definitely incommensurate, this observation provides compelling evidence that the structure of the incommensurate state of $CeTe_3$ is a combination of locally commensurate domains that are separated by discommensurations.

The researchers also studied the exposed Te net of a $CeTe_3$ crystal with scanning tunneling microscopy (STM), obtaining Fourier transforms of CDW images that display extra peaks around the fundamental peak. These results supported the discommensurated nature of the CDW.

Discommensurations have been observed before from other local probe experiments such as NMR and photoemission; however, this is the first time that the nature of the Peierls distortion—the local atomic displacements occurring as a result of the CDW—could be determined quantitatively. The team's work has opened a window into the previously inaccessible commensurate domains of an IC-CDW, while also proving that the CDW in $CeTe_3$ is, in fact, discommensurated rather than uniformly incommensurate. This more precise and quantitative technique promises to provide greater insight into the intricacies of incommensurate charge density wave systems and the secrets they hold about the underlying mechanisms in these interesting materials. — *Mark Wolverton*

See: H.J. Kim, C.D. Malliakas, A.T. Tomic, S.H. Tessmer, M.G. Kanatzidis, and S.J.L. Billinge*, "Local Atomic Structure and Discommensurations in the Charge Density Wave of CeT_3," Phys. Rev. Lett. **96**, 226401 (2006).
DOI: 10.1103/PhysRevLett.96.226401

Author affiliation: Michigan State University
Correspondence: *billinge@pa.msu.edu

This work was supported by the National Science Foundation through grants Nos. DMR-0304391, DMR-0443785, and DMR-0305461. MU-CAT is supported by the U.S. Department of Energy through Contract No. W-7405-ENG-82 Use of the Advanced Photon Source was supported by the U.S. Department of Energy, Office of Science, Office of Basic Energy Sciences, under Contract No. W-31-109-ENG-38.

First Light × 3

First Light for LS-CAT

At 10:24 a.m. on June 27, 2006, two x-ray beams from dual canted undulators drilled twin channels into a block of acrylic. The Life Sciences Collaborative Access Team (LS-CAT) marked its first step toward emerging as the newest structural biology sector at the APS.

The LS-CAT is a member-based collaborative access team that includes the University of Michigan, Michigan State University, the Van Andel Research Institute, Wayne State University, Northwestern University, the University of Wisconsin at Madison, Vanderbilt University Medical Center, and the University of Illinois at Urbana-Champaign.

The LS-CAT will operate four experiment stations for x-ray crystallography using two insertion devices (IDs). The first of the four will provide a highly tunable, focused beam using one of the IDs, while the remaining three stations will split the beam from the second ID to provide fixed-energy (or slightly tunable) capabilities.

Contact: Keith Brister (k-brister@northwestern.edu)

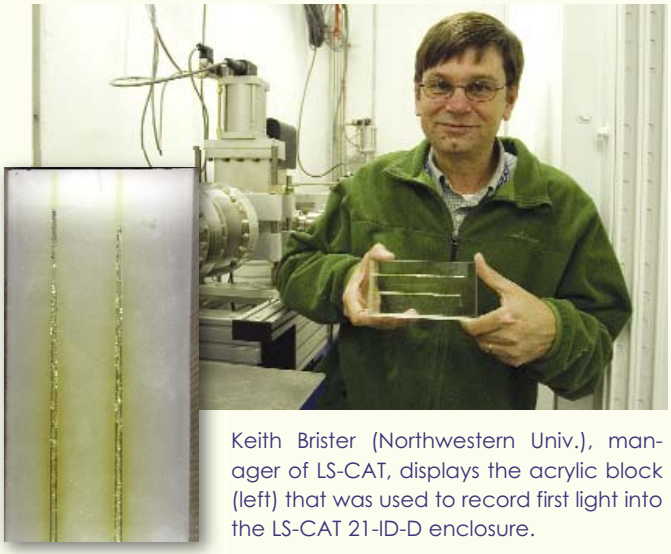

Keith Brister (Northwestern Univ.), manager of LS-CAT, displays the acrylic block (left) that was used to record first light into the LS-CAT 21-ID-D enclosure.

First Light for HERIX

The High Resolution Inelastic X-ray Spectrometer (HERIX, photo at right) at APS sector 30 recorded its first spectrum in October 2006 during the commissioning phase. The sample was honey, which, due to its high viscosity, produces a nearly delta-shaped peak (inset) that can be used to study the instrument resolution at different scattering angles. The broad wings on the sides are phonon excitations from the 20% residual water in the honey sample. HERIX, designed by an Argonne group, is now a user instrument with beam time allocated for general users. It works with up to nine analyzers in parallel with an energy resolution around 1.6 meV. The flux at the sample position will be 10^9 photons/sec in a spot of 30 x 10 μm.

Contact: Ercan Alp (eea@aps.anl.gov)

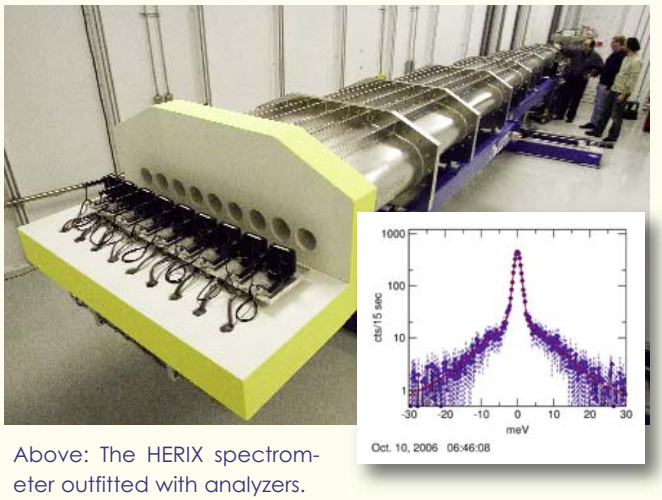

Above: The HERIX spectrometer outfitted with analyzers.

Below: Ayman Said (Western Michigan Univ.), Yuri Shvyd'ko, Harald Sinn, and Ercan Alp (all of the Inelastic X-ray and Nuclear Scattering Group in XSD) with the MERIX spectrometer. Not shown are group members Scott Coburn and John Hill of Brookhaven National Laboratory, and Clem Burns of Western Michigan University.

First Light for MERIX

The MERIX (Medium Resolution Inelastic X-ray Scattering) Spectrometer (photo at lower right) was commissioned in November-December 2006 at the sector 30 beamline of the APS. The spectrometer was developed by a collaborative design team comprising scientists and engineers from Argonne, Brookhaven National Laboratory, and Western Michigan University. The MERIX spectrometer will be used for the study of collective valence electron excitations in correlated electron systems, primarily of transition-metal oxides.

The x-ray photon energy range of MERIX is 5-12 keV and the targeted energy resolution is ~100 meV, covering the K-absorption of vanadium to zinc. A unique feature of the new MERIX spectrometer is its ability to scatter both vertically and horizontally, thus enabling study of polarization-dependent charge excitations.

The MERIX instrument is equipped with mirrors, providing microfocused beam on the sample—5 μm in the vertical direction and 40 μm in the horizontal direction—enabling studies of small samples and samples under high pressure. The MERIX monochromator delivers to the sample x-ray photons in the 70-meV- or 120-meV-energy bandwidths. The inset shows the first spectrum taken at the Cu K-edge of $CuGeO_3$.

MERIX is now a user instrument with beam time allocated for general users. *Contact: Yuri Shvyd'ko (shvydko@aps.anl.gov)*

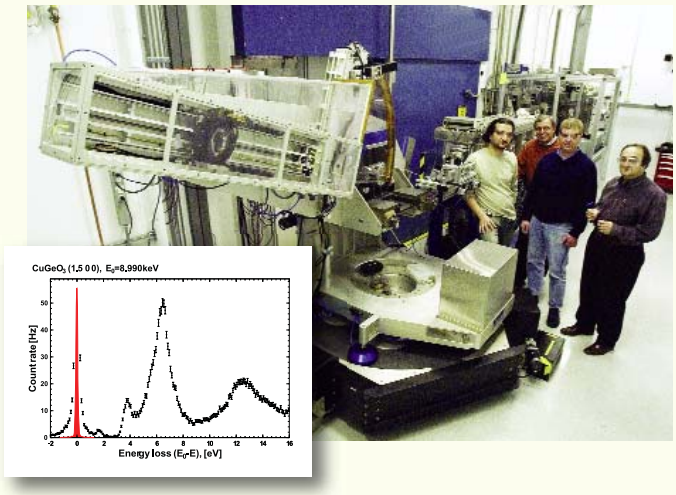

Concrete Clues to Halting Sulfate Attack on Cement Materials

The ability of Portland cement concrete—a mixture of cement, water, sand, and coarse aggregate—to resist degradation when in contact with sulfate-containing environments is determined, for the most part, by the composition of the cementitious materials and the water-to-cement (w/c) ratio. Although it is easy to manipulate these parameters during the mixing of cement-based products, it has been difficult to ascertain the best combination to resist long-term damage from sulfate attack. Nevertheless, identifying the appropriate mixture to ensure long-term sulfate durability has important economic, environmental, and safety considerations for a wide range of industrial applications. Collaborators from the Georgia Institute of Technology, Northwestern University, and Argonne National Laboratory used the XOR 1-ID beamline at the APS to assess the physical and chemical degradations of various combinations of cement mixtures. They affirmed that cement composition has a major impact on the ability to resist sulfate damage and isolated several compositions that appear to be resistant to sulfate. However, additional research is needed to better understand the internal mechanisms involved with sulfate attack on cement.

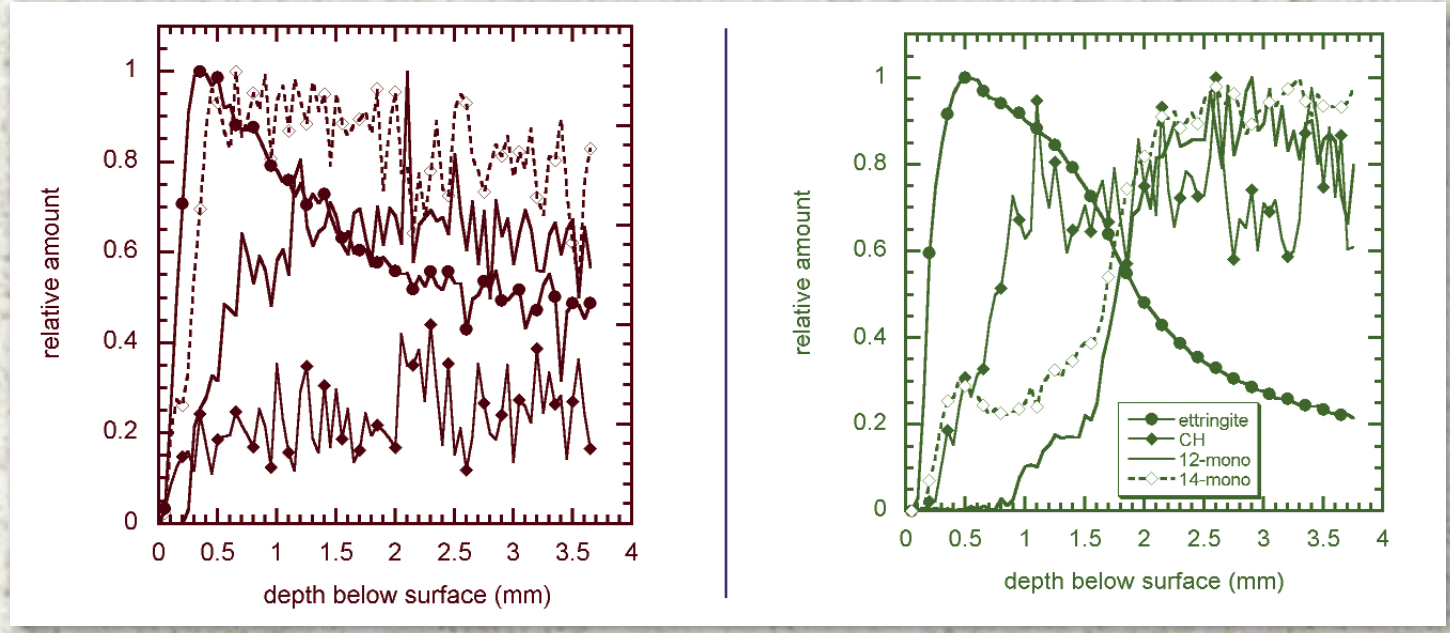

Fig. 1. EDXRD measurements, obtained at APS beamline 1-ID, show composition depth profiles for Type I cement paste samples with w/c ratio of 0.485. (left) Data are for an unexposed control sample. (right) Data are for a sodium-sulfate exposed sample after 52 weeks. The legend serves both measurements and indicates the presence of ettringite, calcium hydroxide (CH), and hydrous monosulfoaluminate (in both 12-water and 14-water forms). As the scaling of the lines in the two plots has been chosen to best illustrate the spatial relationships between the various phases, it is not possible to quantitatively compare the amounts of the different phases within a plot or between plots.

Because other techniques cannot give adequate information about the progression of sulfate attack, the collaborators used two emerging x-ray characterization methods—x-ray microtomography (microCT) and and depth-resolved energy dispersive x-ray diffraction (EDXRD)—to measure microstructural characteristics of cement paste and paste/aggregate samples. In addition, expansion and change in compressive strength were measured to complement the x-ray data.

To carry out their investigations, ASTM (American Society for Testing and Materials) pastes of ordinary Type I and sulfate-resistant Type V cements were prepared at w/c ratios of 0.435 and 0.485. They were cast as 1.2-cm-diameter cylinders for microCT and EDXRD, 1.27-cm cubes for compressive strength measurements, and mortar bars for expansion (according to ASTM C 1012). To assess the influence of aggregate on the damage propagation, single crystal quartz aggregate was introduced at a ratio of 0.20 by mass into the cylindrical samples. After demolding at one day, the cylinders, cubes, and bars were cured for two days in limewater at room temperature before being placed in sodium sulfate solutions at 10,000-ppm sulfate ion concentration. The solutions were changed weekly to maintain consistent concentration. Control (unexposed) samples remained in limewater. MicroCT measurements used a Scanco μCT 40 bench-top system with a 70-kVp x-ray tube, while EDXRD measurements came from beamline 1-ID.

Overall, the collaborators found that cement composition had a major impact on the ability of cement mixtures to resist sulfate damage. As expected, Type V cement was found to be better at resisting sulfate distress than Type I. Type V samples showed less cracking, less expansion, and better retention of compressive strength. Physical damage to Type V samples also showed up later and was slower to progress than with Type I. For Type I and V samples, an anticorrelation between potentially expansive ettringite (hydrous calcium aluminosulfate) and gypsum was observed by using EDXRD in the ~1 mm nearest the sample surface, suggesting the decomposition of ettringite into gypsum. Cracking was also observed in this near-surface region by microCT, although the cracks were typically detected *after* gypsum formation was noted. The observations were not entirely consistent with current understanding of the roles of ettringite and gypsum formation and the associated damage during sulfate attack. Thus, the researchers propose that further research is necessary to better understand better these damage patterns.

When examining the influence of w/c ratio, samples with the lower w/c ratio produced less expansion, as expected. Average expansion was similar for both w/c ratios at the beginning of the measurement period, but the average length change increased less rapidly for the lower w/c samples. Although expansion data generally agreed with expected behavior with changing w/c ratio, the physical damage measured in cylindrical cement paste samples by microCT did not agree with expected behavior. Although more severe damage—specifically, earlier cracking and more rapid damage—was expected from the higher w/c ratio, it actually occurred with the lower 0.435 ratio. The authors ascribe this unexpected result to changes in extensibility and pore structure—with the lack of aggregate—at the lower w/c ratio.

As expected, the introduction of sulfate to Type I samples containing quartz aggregate particles (w/c of 0.485) were initially and progressively more damaging than a compositionally similar sample without aggregate.

The integrated sulfate research program of the collaborators confirmed many currently held beliefs about the influence of certain internal parameters at the beginning and during the progression of sodium sulfate attacks on Portland cement-based materials. However, other results disproved the influence of certain parameters. Because of these discrepancies, the researchers feel that further fundamental research is needed to link the chemical, physical, and mechanical changes occurring in cement-based materials during reactions with sodium sulfate.

— *William Arthur Atkins*

See: N.N. Naik[1], A.C. Jupe[1], S.R. Stock[2], A.P. Wilkinson[1], P.L. Lee[3], and K.E. Kurtis[1*], "Sulfate Attack Monitored by microCT and EDXRD: Influence of Cement Type, Water-to-Cement Ratio, and Aggregate," Cement Concrete Res. **36**, 144 (2006). DOI: 10.1016/j.cemconres.2005.06.004

Author affiliations: [1]Georgia Institute of Technology, [2]Northwestern University, [3]Argonne National Laboratory

Correspondence: *kkurtis@ce.gatech.edu

This research was supported by National Science Foundation (NSF) CMS-0084824. The microtomography equipment was acquired under NSF OIA-9977551. Use of the Advanced Photon Source was supported by the U.S. Department of Energy, Office of Science, Office of Basic Energy Sciences, under Contract No. W-31-109-ENG-38.

When Superalloys Are Joined Together

A superalloy (high-performance alloy) has the characteristics of superior mechanical strength and creep resistance (the ability to resist permanent deformation under long-term stress) at high temperatures, good surface stability, and corrosion and oxidation resistance. These alloys are used in manufacturing for a wide range of industrial applications, including those in the aerospace and marine industries. When welding with nickel-based (Ni-based) single-crystal superalloys, complicated interactions occur, such as displacements caused by thermal stresses in different areas of the weld. Gaining a better understanding (and control) of these so-called "dislocation interactions" is important information for manufacturers. To that end, researchers from Oak Ridge National Laboratory used an XOR/UNI beamline at the APS to study the structural changes that occur in the welds of Ni-based, single-crystal alloys. Their study shows that it is possible to retain the quasi-single-crystalline structure of Ni-based, single-crystal superalloys under certain welding conditions.

The collaborators used polychromatic x-ray microdiffraction (PXM), along with orientation imaging microscopy, scanning electron microscopy, and optical microscopy in order to characterize structure formation in the superalloys. Data collection was performed using microbeam Laue diffraction on the XOR/ UNI 34-ID beamline at the APS. The welds of two Ni-based, single-crystal superalloys, RENE N5 and CMSX-4, were studied in order to research the resulting physical processes occurring within these weld joints. Because of the welds, a complicated thermomechanical environment is produced inside the weld joint during the heating and cooling processes.

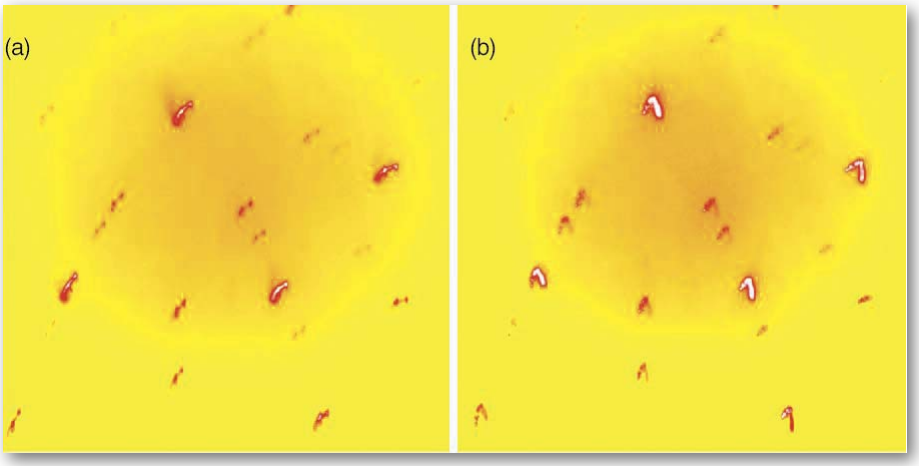

Fig. 1. Laue patterns demonstrate inhomogeneous plastic deformation in different locations of the thermomechanical zone of the weld. Regions with a one (a) and two (b) rotation axes are observed within each probed location.

The base metal structure and the initial weld process determine the properties of the weld. The base metal in both alloys has a quasi-single-crystal dendrite structure. The movement of the weld pool through the sample during welding creates a thermomechanical region that forms the quasi-single-crystalline weld structure.

Upon cooling at the fusion line, nucleation of the dendrites (in the melted weld pool) takes place, thereby separating the base metal within the heat-affected zone. The form of the fusion line, along with the direction of the nucleating dendrites, is determined by the direction of temperature gradient and the BM structure.

While dendrites are forming, the angle between the dendrite direction and the temperature gradient (at the solidification front) continuously increases. When the angular separation between them reaches 45˚, the dendrite growth direction abruptly changes and becomes perpendicular to the temperature gradient. The result is three different regions of dendrite growth direction within the weld.

Optical imaging microscopy analysis showed that in the thin, near-surface region, the overall orientation change is much smaller in the CMSX4 weld than in the RENE N5 weld. Synchrotron radiation PXM analysis revealed that in both superalloys, strong plastic deformation occurs in the fusion zone and heat-affected zone at relatively large distances (~1-2 mm) from the weld. As opposed to the near-surface orientation distribution, the plastic deformation was much greater in CMSX4 than in RENE N5 because the weld in RENE N5 retained a higher level of residual stress.

Geometrically necessary dislocations densities were nearly two times greater in the CMSX4 weld joint than in the

Continued on page 41

Exploring Shape Memory Alloys

Shape memory alloys (SMAs) are metals with a unique, almost magical capability: they "remember" their "original" shape. After a SMA is deformed, it regains its original geometry by itself when heated. This makes SMAs tremendously useful for military, medical, safety, and robotics applications, to name a few. Their amazing properties are due to a temperature-dependent transformation between two phases of the alloys. But development of SMAs has been hit-or-miss, and even the best SMAs suffer from three unfortunate features: they succumb to fatigue too quickly; their transition occurs only within a tight temperature range; and they are subject to hysteresis, which results in different transition temperatures when cooling or heating the material. A method for rapidly investigating properties of materials with "memory" (i.e., reversible structural phase transitions) has been developed by an international collaboration of researchers from six universities and research centers. With help from the XOR 2-BM beamline at the APS, the researchers discovered a promising area from which better shape memory alloys for medical, electronic, optical, and other applications may spring.

A recently developed theory explains how shape memory is related to the crystalline symmetry and geometric compatibility between two phases of the alloy: a Martensite and an Austenite. The theory offers an explanation for the hysteresis and suggests ways to reduce it. Also, because the energy responsible for the hysteresis is stored in the material—creating defects that are prone to cracking—reducing the hysteresis could reduce the material's tendency to fracture.

Generally, an Austenite has a face-centered cubic (FCC) structure, while a Martensite has a similar but slightly distorted crystalline structure. When an Austenite is cooled or stressed, it undergoes a diffusionless shearing deformation to transform to a Martensite; i.e., the bonds between atoms in the crystal lattice may change their lengths and direction but are not broken.

The researchers in this study performed a combinatorial experiment to verify the theory and search for SMAs with extremely small hysteresis widths. They discovered that a single parameter in the theory (specifically, the middle eigenvalue of the transformation stretch tensor) has direct correlation with the hysteresis width.

The theory can be used as a practical guide to develop superior SMAs because its only inputs are lattice parameters, which can be adjusted by changing the composition of alloys. The combinatorial approach allowed the researchers to rapidly map and track the lattice-parameter change across large compositional phase diagrams.

They developed a thin-film, composition-spread technique in order to screen the lattice parameters and the thermal hysteresis of a variety of alloys made from copper, nickel, and titanium. In a vacuum chamber equipped with three sputtering guns, they deposited thin films onto a wafer with a triangular configuration to create a gridded natural gradient of each metal. By adjusting the power applied to each gun and the distance between the guns and the wafer, they were able to adjust the amount of each metal in the resulting alloy.

Continued on page 40

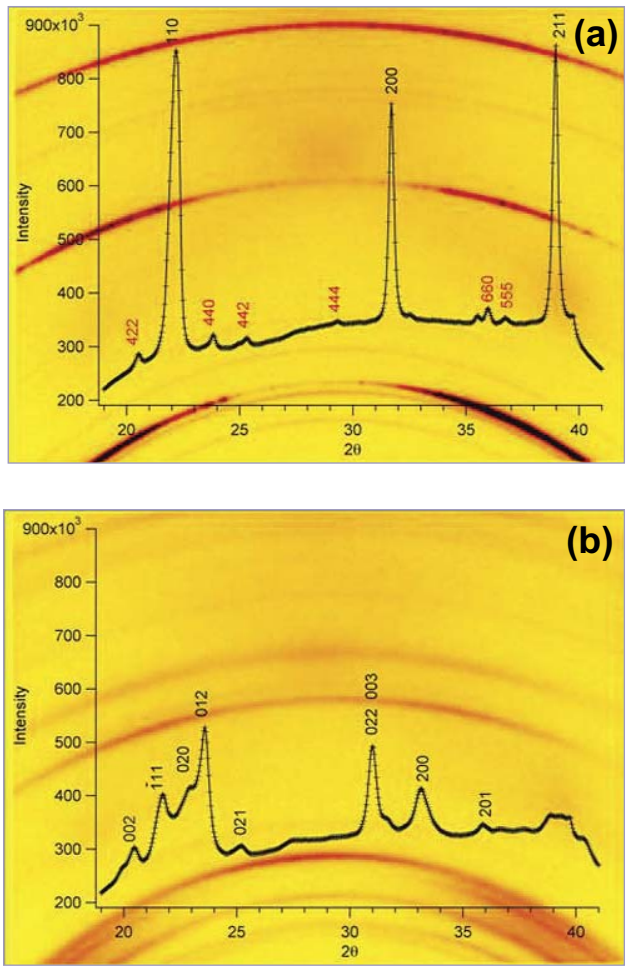

© 2006 Nature Publishing Group

Fig. 1. X-ray-diffraction images and integrated patterns of the spot with composition $Ni_{35.4}Ti_{62.9}Cu_{1.7}$. The images were taken at 135° C (a) and 0° C (b).

"Shape Memory" continued from page 39

Then, they used synchrotron x-ray microdiffraction at beamline 2-BM on the thin films to rapidly obtain diffraction data that allowed them to perform a complete lattice parameter analysis on all the different compositions in the samples. The work would have required a year to complete if a standard x-ray source were used.

Specifically, the researchers discovered a promising area from which better shape memory alloys may spring. The work also has broader implications in creating functional materials for medical, electronic, optical, and other applications.

— Yvonne Carts-Powell

See: Jun Cui[1,2*], Yong S. Chu[3], Olugbenga O. Famodu[1], Yasubumi Furuya[4], Jae. Hattrick-Simpers[1], Richard D. James[5], Alfred Ludwig[6,7], Sigurd Thienhaus[6,7], Manfred Wuttig[1], Zhiyong Zhang[5], and Ichiro Takeuchi[1,8], "Combinatorial search of thermoelastic shape-memory alloys with extremely small hysteresis width," Nat. Mater. **5**, 286 (1 April 2006).
DOI: 10.1038/nmat1593

Author affiliations: [1]University of Maryland, [2]GE Global Research Center, [3]Argonne National Laboratory, [4]Hirosaki University, [5]University of Minnesota, [6]Caesar Research Center, [7]Ruhr-Universitat Bochum, [8]University of Maryland
Correspondence: cuijun@umd.edu

This work was supported by ONR-N000140110761, ONR-N000140410085, NSF DMR-0231291, NSF DMS-0074043 and MRSEC DMR-0520471. Use of the Advanced Photon Source was supported by the U.S. Department of Energy, Office of Science, Office of Basic Energy Sciences, under Contract No. W-31-109-ENG-38.

Stress, Strain, and Creep in TGOs

Thermally grown oxides (TGOs) are essential to corrosion protection for structural materials operating at high temperatures, such as in turbine blades. A common TGO is aluminum oxide, Al_2O_3, which forms naturally on aluminum-containing alloys. However, strains can develop in TGOs, which can cause oxide cracking and, thus, reduce their ability to resist corrosion. The possibility that large tensile strains could develop during the growth process has not been appreciated in the past. Because of their importance for high-temperature materials applications and for general insights into oxidation behavior, many scientists have tried to measure the growth of stresses in TGOs formed on Fe-Cr-Al(Y) (iron-chromium-aluminum [yttrium]) alloys. Little success was reported until collaborators from Argonne National Laboratory and Lawrence Berkeley National Laboratory used synchrotron radiation from the XOR/BESSRC beamline 12-ID at the APS to confirm an earlier study that large tensile stresses develop spontaneously in α-Al_2O_3 when thermally grown on a Fe-Cr-Al(Y) alloy. The collaborators also found that creep (slow flow of the oxide under high temperature or pressure) in the oxide relaxes (reduces) stress. These discoveries provide a significant advance in the field of oxidation research.

The composition of the first-formed oxide, $(FeCrAl)_2O_3$, closely corresponds to the FeCrAl(Y) base material. Subsequently, aluminum oxide develops preferentially because it is more stable than chromium and iron oxides. Eventually, Al_2O_3 becomes a continuous layer, which forces a decrease in the oxygen pressure at the metal-oxide interface. When the oxidation of Fe and Cr has ended completely, the oxide forms Al_2O_3. The diluted $(Fe,Cr,Al)_2O_3$—at a sufficiently high temperature—converts to a relatively pure α-Al_2O_3. During the early growth process, tensile stress develops as $(Fe,Cr,Al)_2O_3$ converts to α-Al_2O_3. *Continued on next page*

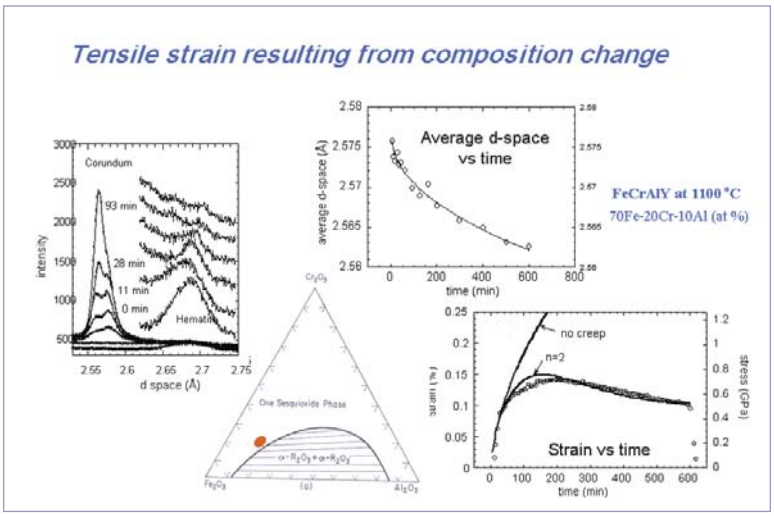

Fig. 1. Tensile strain resulting from composition change: Evolution of $(Fe,Cr,Al)_2O_3$ (hematite) to α-Al_2O_3 (corundum); d-spacing contracts with oxidation time, causing large tensile stress in constrained oxide.

"Superalloys" continued from page 38

RENE N5 weld. In both alloys, the most intense plastic deformation zones bordered the fusion line and the line of dendrite orientation change within the fusion zone (Fig. 1).

In summary, a dislocation structure is formed during steady melt zone movement in the thin Ni-based superalloy. The researchers observed oscillations in the formed dislocation structure, both at microscopic and macroscopic levels. While the dislocations were forming, a partial or complete dissolution of particles in the matrix also occurred, which was temperature dependent. Macroscopically, the distribution of the dislocation density is due to a symmetric temperature gradient that was perpendicular to the direction of melt zone movement. Maximal dislocation density correlates with the interface between the heat affected and fusion zones.

Microscopically, oscillations of dislocation density were also observed within the same macroscopic region. The average length of oscillations is related to local melting and solidifying conditions, and to dendrite size. The collaborators concluded that it is possible to improve weld quality by applying a special thermal treatment to the base material. They also agreed that there is a decrease in the probability of isolated grains forming in the fusion zones. — *William Arthur Atkins*

See: Oleg M. Barabash*, Rozaliya I. Barabash, Stan A. David, and Gene E. Ice, "Residual Stresses, Thermomechanical Behavior and Interfaces in the Weld Joint of Ni-based Superalloys," Adv. Eng. Mat. **8**(3) (2006).
DOI: 10.1002/adem.200500239
Author affiliation: Oak Ridge National Laboratory
Correspondence: *barabashom@ornl.gov

Research sponsored by the U.S. Department of Energy Division of Materials Sciences and Engineering, Office of Basic Energy Sciences, and the ORNL SHARE user facility, under Contract DE-AC05-00OR22725 with UT-Battelle, LLC. The XOR/UNi beamline 34-ID is supported by the University of Illinois at Urbana-Champaign, Materials Research Laboratory (U.S. DOE, the State of Illinois-IBHE-HECA, and the NSF), and by the Oak Ridge National Laboratory (U.S. DOE under contract with UT-Battelle LLC). Use of the Advanced Photon Source was supported by the U.S. Department of Energy, Office of Science, Office of Basic Energy Sciences, under Contract No. W-31-109-ENG-38.

"Stress, Strain, and Creep" continued from page 40

In fact, during oxidation at 1,100º C, the tensile stress increases until the oxide composition stabilizes at α-Al_2O_3. Creep then overtakes tensile stress generation, and the stress eventually decreases toward zero.

The collaborators based their study on a recent controversial x-ray diffraction (XRD) study by Peter F. Tortorelli et al. from Oak Ridge National Laboratory (ORNL). Tortorelli et al. found that very large tensile stresses—close to 1 GPa—developed in the alumina TGO formed on a Fe-Cr-Al(Y) alloy. Using materials provided by ORNL, the collaborators confirmed the Tortorelli results and identified the mechanism controlling this behavior.

The collaborators placed FeCrAl(Y) (a base material for commercial alloys) on a thin alumina shelf in an open-ended horizontal tube furnace. A 21.6-keV x-ray beam from beamline XOR/BESSRC 12-BM at the APS illuminated the sample while it oxidized as it approached 1,100° C, and the material was left for an additional 10 h at 1,100° C. An image plate detector recorded the Debye-Scherrer diffraction ring patterns from the growing oxide; from these patterns, strain measurements were obtained.

The collaborators charted (Fig. 1) the evolution of $(FeCrAl)_2O_3$ (hematite) to α-Al_2O_3 (corundum) via x-ray diffraction spectra, with d-spacing from the diffraction ring as a function of time. The average d-space contracts as the composition dilutes. The effect of dilution is shown to be large enough to cause a large tensile stress in the constrained oxide. However, when they compared their findings to theoretical levels, the collaborators concluded that creep should also be taken into consideration. The collaborators found that creep rates were reasonably close to those observed in Y-doped bulk ceramic, which is similar to the alumina TGO. Thus, tensile stress from a changing oxide composition and creep relaxation are the two main mechanisms controlling the level of strain.

The collaborators were the first to recognize this composition-change mechanism that causes large tensile stresses in TGO alumina and, then, to model the strain behavior, including the relationship between tensile stress and creep. This new information will play an important role in learning more about the formation of protective oxides on commercial structural alloys. A better understanding of the behaviors of growth strains in TGOs will allow for the development of improved protective oxides. In addition, the use of synchrotron radiation by these researchers increased the accuracy of the study of oxide growth processes that lead to strain generation. Further studies are recommended in order to distinguish among the mechanisms that result in strain generation or relaxation.

— *William Arthur Atkins*

See: Boyd W. Veal[1*], Arvydas P. Paulikas[1], and Peggy Y. Hou[2], "Tensile stress and creep in thermally grown oxide," Nat. Mater. **5**, 349 (May 2006). DOI: 10.1038/nmat1626
Author affiliations: [1]Argonne National Laboratory; [2]Lawrence Berkeley National Laboratory
Correspondence: *veal@anl.gov

This research was sponsored by the U.S. Department of Energy, Basic Energy Sciences, Materials Science, under contract Nos. W-31-109-ENG-38 and DE-AC03-76SF00098. Use of the Advanced Photon Source was supported by the U.S. Department of Energy, Office of Science, Office of Basic Energy Sciences, under Contract No. W-31-109-ENG-38.

Imaging the Interior of a High-speed Industrial Spray

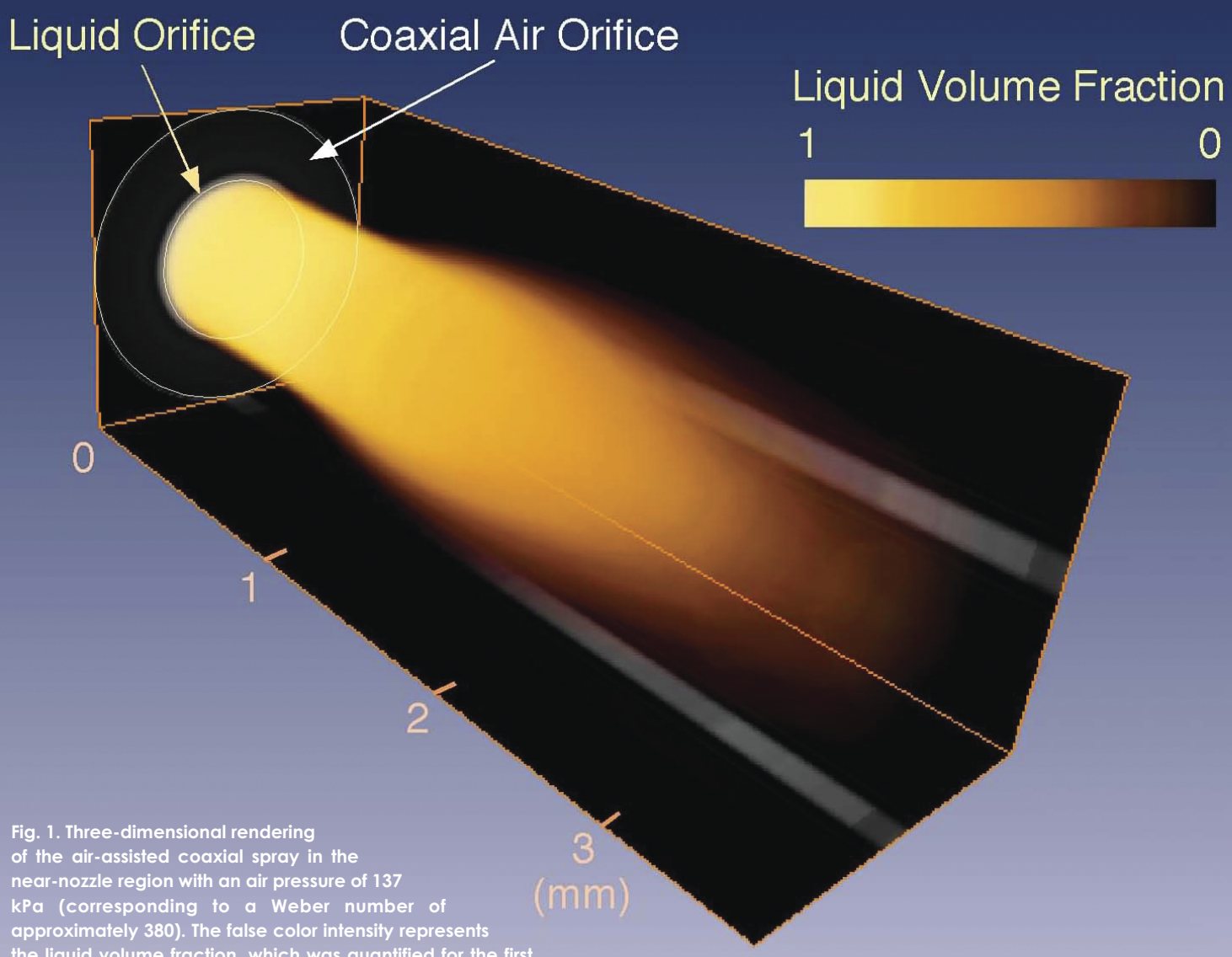

Fig. 1. Three-dimensional rendering of the air-assisted coaxial spray in the near-nozzle region with an air pressure of 137 kPa (corresponding to a Weber number of approximately 380). The false color intensity represents the liquid volume fraction, which was quantified for the first time with x-ray phase-contrast imaging. (Image courtesy of Francesco De Carlo [XSD]).

We use paint sprays to cover all manner of surfaces, but our ability to optimize the sprayers themselves has been quite limited. "Seeing" beneath the surface of the jet from a high-speed industrial paint sprayer can yield important new information. Researchers and engineers from Argonne National Laboratory and from Illinois Tool Works (ITW) Inc., of Glenview, Illinois, using extreme-brilliance x-ray beams from the XOR 7-ID beamline at the Advanced Photon Source (APS), have captured the first images of the highly transient multiphase spray flow just millimeters from a high-speed industrial spray nozzle, taking us one step down the road toward improved high-speed industrial sprays.

High-speed sprays have many industrial and consumer applications, such as surface finishing (paint and particle coating) and gas turbine combustion applications. These sprays comprise a jet of liquid surrounded by a high-speed coaxial air jacket that atomizes the liquid jet. For coating (or paint) applications, the liquid transfer efficiency of the spray materials has a direct effect on how economically they can be used, as well as a definite impact on the environment. In order to increase the efficiency of industrial sprays and make them more environmentally friendly, we must improve them at the source: the design of the spray nozzle.

Despite their multitude of uses, until now the fundamental physics that governs the spray flow patterns and the droplet deposition on the spray target have not been fully understood. This is due, in large part, to a lack of information about the morphology of spray plumes close to the nozzle, such as liquid breakup mechanism and spray mass distribution. Traditional visualization tools, like visible-light-based imaging, have not been effective, because light is scattered off the cloud of small liquid droplets the way the beam from car headlights diffuses in fog. Furthermore, most of the liquid materials in industrial applications (such as paint) are, by their nature, optically opaque. And to date, theoretical and computational studies of the sprays have proven to be extremely difficult, if not impossible, to carry out.

The initial and boundary conditions for the simulation model development of air-assisted sprays cannot be simply obtained from conventional optical measurements in part because these measurements do not normally yield quantitative information about the sprays. One has to know where the sprays are and how they are atomized before one can do a realistic transfer analysis to determine the effectiveness of spray nozzle designs.

As an essential step towards developing the primary breakup model in air-assisted sprays—and overcoming the difficulties in visible-light-based measurements—the Argonne-ITW research team imaged the complex and transient multiphase spray flow just millimeters from a spray nozzle by using a fast x-ray phase-contrast imaging technique made possible by the intense x-ray beams from the APS. Owing to their weak interaction with matter, x-rays can penetrate and image liquid jets surrounded by a large number of small liquid droplets. Intense x-ray beams from the APS made it possible to perform the measurement in real time.

An off-the-shelf commercial air-spray gun was used to generate continuous water sprays in air. The injection nozzle of this spray gun consists of a central circular orifice for the liquid and a ring-like air outlet. The high-pressure atomization air was propelled through the air opening with a speed that can be supersonic. The high relative velocity between the liquid jet and the air stream can generate a highly unsteady turbulent multiphase flow and induce the breakup of the liquid jet. In the x-ray images obtained at the APS the drastic effect of the high-speed, atomizing air and near-nozzle liquid mass density distribution was visualized for the first time (Fig. 1).

The x-ray experimentation at Argonne has already produced some intriguing discoveries. The research team found that, unlike the case of a low-speed jet (such as the water from a garden hose) where the breakup is mostly due to the surface tension at the air/liquid interface, the breakup of high-speed-spray jets can occur in the jet core, which causes sudden decreases in liquid volume fraction, even within 1 mm from the nozzle exit.

This first-ever visualization of near-nozzle high-speed coaxial flows can be used to develop and validate liquid breakup models and is indispensable for understanding downstream spray formation. The collaborative effort between Argonne and ITW at the APS promises to have a major impact on nozzle design, spray parameters, modeling, and simulation, holding out the promise of improved industrial spray systems.

— Jin Wang & Richard Fenner

See: Y.J. Wang[1], Kyoung-Su Im[1], K. Fezzaa[1], W.K. Lee[1], Jin Wang[1*], P. Micheli[2], and C. Laub[2], "Quantitative x-ray phase-contrast imaging of air-assisted water sprays with high Weber numbers," Appl. Phys. Lett. **89**, 151913 (2006).
DOI: 10.1063/1.2358322

Author affiliations: [1]Argonne National Laboratory, [2]Illinois Tool Works Inc.
Contact: *wangj@aps.anl.gov

This work and use of the APS are supported by the U.S. Department of Energy, Office of Science, Office of Basic Energy Sciences, under Contract No. W-31-109-ENG-38.

LOOKING INTO METALLIC GLASS

Metallic glass is an amorphous metal: it does not crystallize when cooled from liquid to solid. Since crystallization does not occur, the atomic-scale structure is highly disordered, much like a liquid. This structure gives metallic glasses the unique properties of high strength and elasticity that make them ideal for a wide range of applications, including military hardware and sporting equipment such as golf-club heads. Because they are true glasses, metallic glasses soften when heated, rather than melt abruptly, making it easy to form them into complex shapes. Scattering techniques have long been used to study the structure of amorphous materials and to measure elastic strain in crystalline alloys. However, the ability to measure accurately elastic strain in glasses was thought to be limited by the material's structural randomness, along with difficulties in collecting data and analyzing it. Recent studies have shown that it is indeed possible to measure elastic strain in bulk metallic glass. As a result, researchers from Johns Hopkins University and Argonne used the XOR 1-ID beamline at the APS to measure elastic strain on a bulk amorphous metallic alloy. This study shows that elastic strain in metallic glass can be measured accurately with high-energy x-ray scattering.

During uniaxial compression loading, the collaborators measured stresses of up to about 60% of the yield stress (the critical point at which a material does not return to its original shape when stress is removed). To determine elastic strain, they used two methods: direct measurements from normalized scattering data (in reciprocal space) and indirect measurements from the resulting pair correlation function.

To carry out their investigations, the researchers made homogeneous alloy ingots of $Zr_{57}Ti_5Cu_{20}Ni_8Al_{10}$ by melting repeatedly the pure elements with purified argon in an electric-arc furnace. The ingots were cast into uniform cylindrical rods. They were then cut and polished to make specimens for compression testing. The collaborators performed x-ray scattering *in situ* during loading in uniaxial compression using monochromatic high-energy x-rays at beamline 1-ID. A digital image plate recorded the ring patterns (Fig. 1), which were averaged from several x-ray exposures.

In scattering data, the elastic scattering intensity $I(q)$, a function of the magnitude of the scattering vector q, is part of the total structure factor:

$$S(q) = \frac{I(q)}{N\langle f(q)\rangle^2}$$

where N is the number of atoms and $\langle f(q)\rangle$ is the averaged atomic scattering factor for x-rays. For indirect measurements, the pair correlation function $g(r) = \rho(r)/\rho_o$—where $\rho(r)$ is the pair distribution function (r is the distance from an average atom to the origin) and ρ_o is the average atomic density—is obtained by Fourier transformation of $S(q)$.

When parallel to the loading direction, $S(q)$ shows a peak shift to larger q with increasing compressive stress (Fig. 2), while the opposite action is observed in the transverse direction: $S(q)$ shows a peak shift to smaller q with increasing compressive stress. Likewise, in the loading direction, the peak in $g(r)$ shifts to smaller r with increasing compressive stress, and

Continued on next page

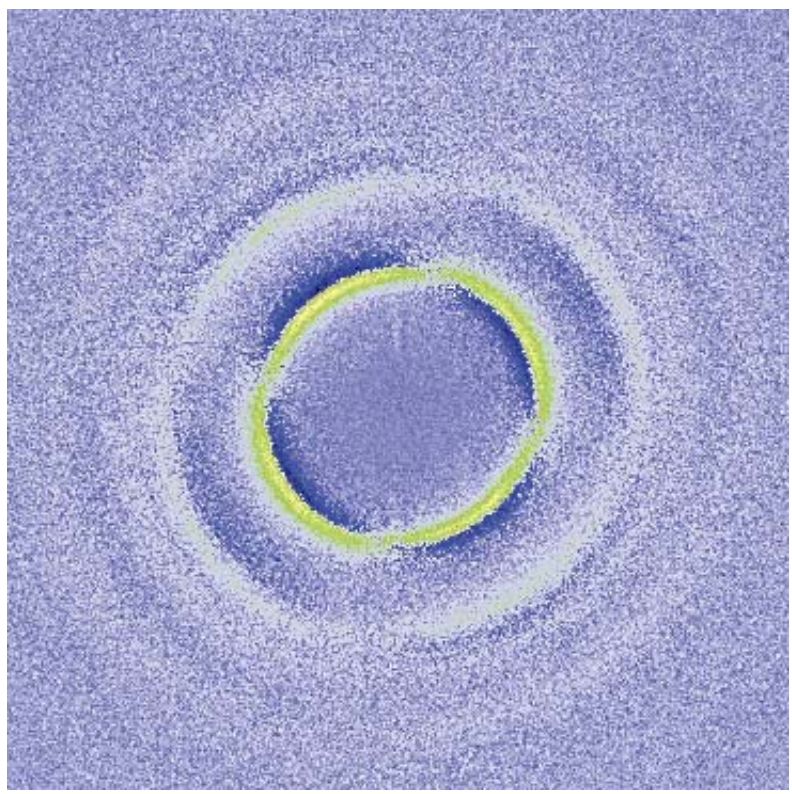

Fig. 1. Change in x-ray scattering between loading and unloading for a specimen tested in pure shear. The distortion of the scattering rings reflects the principal strains (which are oriented approximately ± 45° from vertical).

the transverse data show the opposite trend. When comparing the two measurements, the researchers found similar strain results for lengths (r) greater than 4 Å.

The elastic modulus (which indicates stiffness of atomic bonds) shows that the strain determined from the first peak in $g(r)$ is only slightly smaller in value than at higher r. The peak widths decrease in the compression direction, and they increase in the transverse direction but by a smaller amount. This result indicates that there is a reduction in peak width with increasing load. The elastic modulus was found to have values that were close to macroscopic measurements of similar metallic glasses.

The strain measured for atoms in the nearest-neighbor atomic shell, however, was found to be smaller than for the more distant shells. Therefore, the elastic modulus is larger. The effect was confined to the nearest-neighbor shell. The researchers suggest that the difference in strain is due to the effects of anelastic atomic rearrangements of atoms in topologically unstable regions of the glass. The majority of atoms experience ordinary bond-stretching events (explaining the strain in the first nearest-neighbor shell); the anelastic rearrangements occur for only a few atoms, but they allow the entire structure to relax (explaining the larger strain at larger distances).

The group also found a more uniform distribution of stresses in the metallic glass during loading, indicating that the entropy of the glass is reduced under loading. This finding suggests that the stiffness of metallic glasses has a contribution from entropic effects, analogous to the effect of entropy on the stiffness of elastomers.

The ability to measure elasticity will be important for further studies, such as accurate comparisons with computational models of deformation of metallic-glass-matrix composites.

— *William Arthur Atkins*

See: T.C. Hufnagel[1]*, R.T. Ott[1,2], and J. Almer[3], "Structural aspects of elastic deformation of a metallic glass," Phys. Rev. B **73**, 064204 (2006). DOI: 10.1103/PhysRevB.73.064204

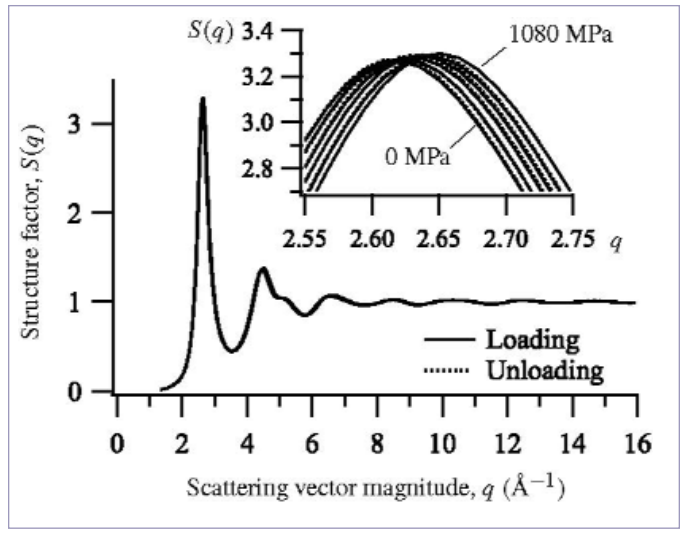

Fig. 2. Change in the structure factor $S(q)$ in the loading direction for a metallic glass under uniaxial compression. With increasing stress, the main peak in $S(q)$ (inset) shifts to a larger scattering vector, q.

Author affiliations: [1]Johns Hopkins University, [2]Ames Laboratory, [3]Argonne National Laboratory
Correspondence: *hufnagel@jhu.edu

T.C.H. and R.T.O. gratefully acknowledge financial support from U.S. Department of Energy Grant No. FEFG02-98ER45699 and Army Research Laboratory ARMAC-RTP Cooperative Agreement No. DAAD19-01-2-000315. T.C.H. additionally acknowledges financial support from National Science Foundation Grant No. DMR-0307009. Use of the Advanced Photon Source was supported by the U.S. Department of Energy, Office of Science, Office of Basic Energy Sciences, under Contract No. W-31-109-ENG-38.

AROUND THE APS

"Introduce a Girl to Engineering Day"

As part of Argonne's fifth annual "Introduce a Girl to Engineering Day" (IGED2006), a number of APS employees participated in the Lab-wide tours and demonstrations on February 26 that gave 40 sixth-, seventh-, and eighth-grade girls from U.S. public, private, and home schools a first-hand look at the possibilities of careers in engineering and science. ● The young women then toured Argonne, with stops at the Soil Analysis Laboratory, the Powertrain Facility, the Recycling Center, the Computer Access Grid, the Argonne Tandem Linear Accelerator System, and the APS. In addition, each girl spent the day with a personal Argonne mentor. ● While at the APS, the students heard about "Beethoven's Bones" from Francesco De Carlo (XSD) and "The World's Brightest X-rays" from Eric Landahl (XSD). Christa Benson, Anne Boron, Dana Capatina, Christy Dannenberg, and Oliver Schmidt (all AES) served as mentors, interacting directly with the students and answering a multitude of questions. Debby Quock (AES) and Mark Erdmann (AES) participated in the lunchtime career Q&A panel session, which featured Argonne Director Robert Rosner. ● Students' impressions of the day included: "The tours gave me a lot of information and I enjoyed them…, [Beethoven] was very cool…." "They were good and gave us tons of info [about Beethoven]…." "The x-ray was really interesting but I wish we could have ridden on the tricycles!...." And "I think the X ray is so cool!" The photo shows De Carlo and some of the IGED2006 students gathered around a hands-on educational exhibit in the APS atrium to learn about diffraction.

When Two Liquids Meet

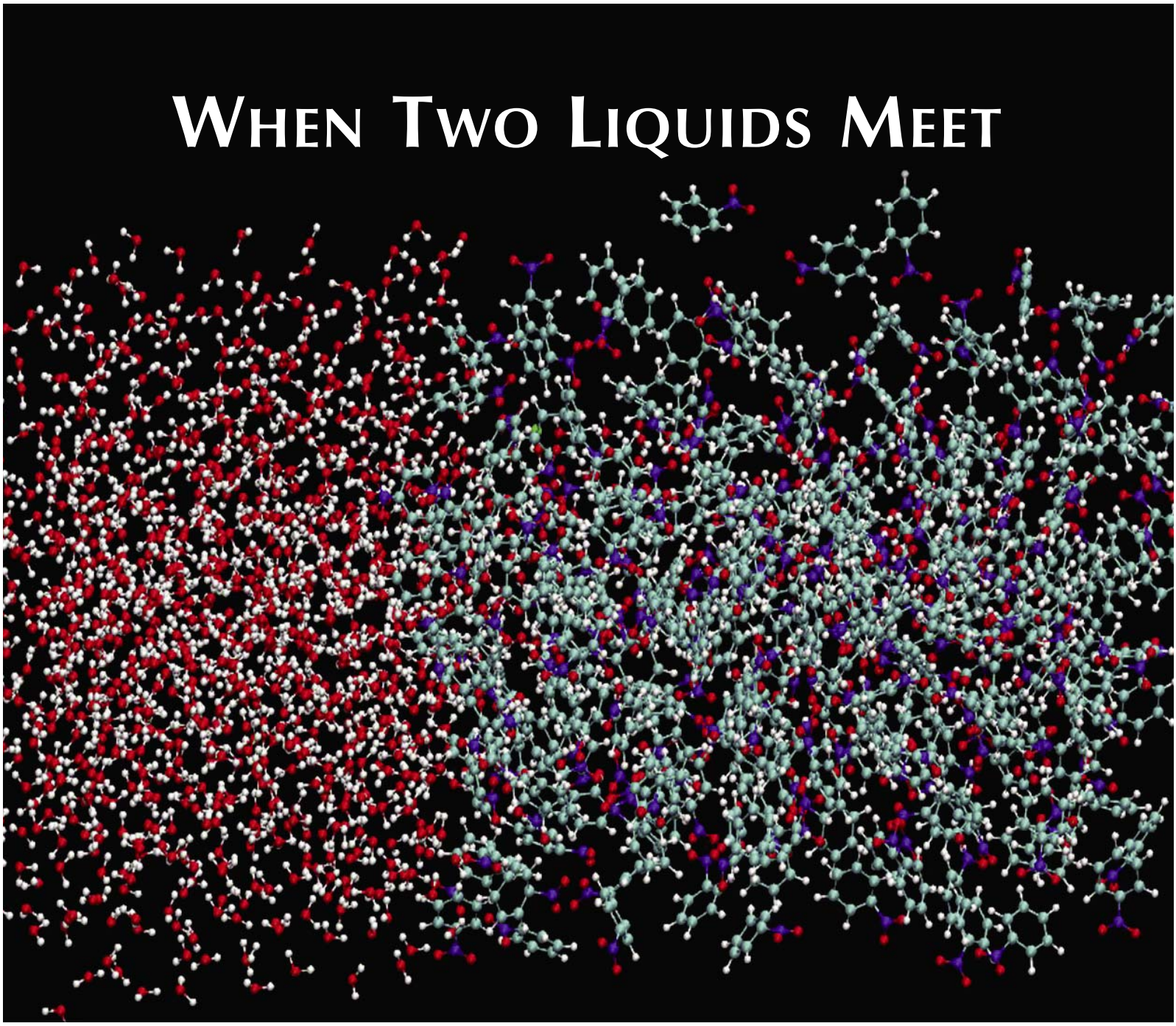

What happens when two liquids meet? Sometimes they mix, other times they remain quite distinct from one another. The question of what occurs at the interface between two liquids has vexed researchers for decades, because understanding the nature of this interaction could provide important new information in biology, as well as improve analytical chemistry. Researchers from the University of Illinois at Chicago; The University of Chicago; the University of California, Santa Cruz; and Northern Illinois University have used the ChemMatCARS beamline 15-ID at the APS to carry out x-ray reflectivity measurements from a liquid-liquid interface to obtain a clear view of exactly what occurs when two liquids meet. Their findings suggest that for two electrolyte solutions, the behavior of liquids does not follow the most well-known theory, on which earlier studies are based.

< Fig. 1. Simulating the interface between water and nitrobenzene can reveal the free energy of a single ion, depending on its distance from the interface. By combining this value with the Poisson-Boltzmann equation, the researchers could correctly predict the measured x-ray reflectivity due to the distribution of ions near the interface.

Ion transport across cell membranes is a key process in all living things and involves liquid-liquid interactions. Likewise, preparation and separation of dissolved compounds from medical or environmental samples for diagnostics and testing can always be improved as a result of new insights into how liquids behave in even the most dilute sample.

The Gouy-Chapman theory, developed in the early twentieth century by Georges Gouy and David Leonard Chapman, helps explain how charged particles (ions) behave near a flat surface that is also charged. The theory provides useful insights into how ions in solution interact with other charge carriers (such as colloidal particles) and so is important to electrochemists developing novel batteries, fuel cells, and electrochemical sensors. The extension of the theory to ions in solution interacting with the charged flat surface of an interface between two liquids, however, has not been proved beyond doubt.

Schlossman and his colleagues found that contrary to the conventional wisdom, the Gouy-Chapman theory does not necessarily apply to the liquid-liquid interface. Their x-ray reflectivity studies on the interface between an aqueous and an organic electrolyte solution deviate significantly from the predicted behavior of ions in such a system. Indeed, the findings corroborate the suspicions of scientists carrying out theoretical studies and discrepancies in electrochemical measurements made in the 1990s.

The Gouy-Chapman theory makes numerous assumptions. It suggests that (1) ions are effectively point charges, (2) there are only electrostatic interactions occurring between colliding particles, (3) the electrical permittivity of the double-layer interface seen between two interacting systems is uniform, and (4) the solvent remains the same at the atomic scale. Almost a century of research, while supporting Gouy-Chapman to a degree, has gradually led to a breakdown of these assumptions as sophisticated new experimental techniques, such as high-resolution x-ray reflectivity, have become available.

Fundamentally, the new study reveals what some scientists have suspected all along: the assumptions made in the Gouy-Chapman theory are only valid in the ideal case and that real solutions and interfaces do not behave that way. The researchers found that ion or solvent sizes do affect the behavior of two electrolyte solutions at their interface and there are various interactions between particles other than simple Coulombic electrostatic attractions and repulsions. The result is ordering of ions and solvents at the interface that is simply ignored in the Gouy-Chapman view.

The researchers also compare their findings with the predictions of several more modern theories of ions at interfaces. Because the predictions of these other theories disagree with their data, the researchers performed molecular dynamics simulations that charted the free energy of a single ion as it is passed through the interface. This ion-free energy was then used to modify the Poisson-Boltzmann equation, which underlies the Gouy-Chapman theory, to make predictions that agreed with their experiments.

The researchers suggest that their studies will be applicable to studies of ion distributions near charged solid surfaces (such as electrodes) and at the interface between a liquid and a vapor. The research is also applicable to molecular biology, where ions interact with the charged surface of biomolecules, such as protein ion channels and receptors. In all of these situations it is anticipated that correlations due to the finite sizes of ions and molecules will influence their arrangement and the resultant local electric fields.

An immediate impact of this work is the indication that several decades of electrochemical studies, which utilized the liquid-liquid interface as a model system for reaction kinetics and biomimetic phenomena, can be related directly to the underlying ionic ordering. Further studies of the sort undertaken by these researchers will be required to make this connection.

— David Bradley

See: Guangming Luo[1], Sarka Malkova[1], Jaesung Yoon[1], David G. Schultz[1], Binhua Lin[2], Mati Meron[2], Ilan Benjamin[3], Petr Vanýsek[4], and Mark L. Schlossman[1*], "Ion Distributions near a Liquid-Liquid Interface," Science **311**, 216 (2006).
DOI: 10.1126/science.1120392
Author affiliations: [1]University of Illinois at Chicago; [2]University of Chicago; [3]University of California, Santa Cruz; [4]Northern Illinois University,
Correspondence: *schloss@uic.edu

M.L.S. and P.V. acknowledge support from NSF-CHE0315691, and I.B. acknowledges support from NSF-CHE0345361. ChemMatCARS is supported by NSF-CHE, NSF-DMR, and the U.S. Department of Energy. Use of the Advanced Photon Source was supported by the U.S. Department of Energy, Office of Science, Office of Basic Energy Sciences, under Contract No. W-31-109-ENG-38.

Back to the Future: Rewriting the History of Brass Metallurgy

The astrolabe was the most sophisticated astronomical instrument prior to the invention of the telescope. Used to compute the movement of the stars and determine the time of day or night, astrolabes were fabricated from thin plates of brass. Using non-destructive synchrotron techniques at XOR beamline 1-ID at the APS, an interdisciplinary team of materials science researchers from Lehigh University and Argonne, and a historian at the Adler Planetarium & Astronomy Museum in Chicago, IL, explored brass components from a group of 17th-century astrolabes as part of a larger study of 40 Adler astrolabes. Their findings, considered in the context of the known history of metallurgy, allowed the team to push the date of a sophisticated brass-making technique back a couple of centuries, to give an astonishingly detailed glimpse of the craftsmanship of the time, and to gain insight into a significant technological breakthrough in brass metallurgy.

To determine the composition of the brass alloy and method of fabrication, the team used three synchrotron radiation techniques to study components from eight astrolabes manufactured in and near Lahore, an ancient city in today's Pakistan. For this study, the non-destructive nature of the experiments was of utmost importance. The Adler Planetarium collection contains rare, indeed invaluable, specimens from all regions where astrolabes were produced and from all ages when they were produced.

Since Roman times, brass alloys were created using the calamine—or cementation—process, in which metallic copper was heated in a crucible along with charcoal and zinc oxide/ore. The Lahore craftsmen were able to advance the technology to a higher level thanks in part to a nearby source of metallic zinc, which was much rarer than zinc ore.

The amount of zinc that can be absorbed by copper from zinc ore is only about 32% or less by weight. Low-zinc, or alpha-phase, brass is suitable for fabricating thin plates only with great labor. A repeated series of hammering and annealing steps is required to reduce a 10-mm cast plate to the desired thickness of about 1 mm, a common dimension of the thin plates used in making astrolabes.

The brass alloy found in the Lahore astrolabe components contains both alpha and beta phases. In the beta phase, the zinc content ranges from 33% to 46% by weight. A higher zinc content changes the crystalline microstructure and composition of the alloy. The rearrangement of atomic structure renders the dual-phase alloy more malleable at a lower temperature and allows hot forming, streamlining the process to one hammering step.

Transmission x-ray diffraction analysis confirmed a higher zinc content in the Lahore astrolabe components than is found in brass produced in Europe and other parts of the world in the 17th century and earlier.

X-ray radiography probed the thickness of the alloy. Slight variations in thickness support the hypothesis that the Lahore plates were pounded into thin sheets by hand rather than pressed in a (modern) rolling mill. X-ray fluorescence revealed the detailed, near-surface composition of the alloy.

By shifting the composition of brass to a dual-phase alloy, the Lahore craftsmen were able to improve the traditional technology and shorten the steps involved in fabricating thin brass plates as early as 1601, nearly two centuries before European metallurgists who, until this study on the Lahore astrolabes, had been credited with inventing the technique.

— Elise LeQuire

See: B.D. Newbury[1]*, M.R. Notis[1], B. Stephenson[2]**, G.S. Cargill III[1], and G.B. Stephenson[3], "The Astrolabe Craftsmen of Lahore and Early Brass Metallurgy," Ann. Sci. **63**(2), 201 (April 2006). DOI: 10. 1080/00033790600583162

Author affiliations: [1]Lehigh University, [2]Adler Planetarium & Astronomy Museum, [3]Argonne National Laboratory

Correspondence: *bdn2@lehigh.edu, **bstephenson@adlerplanetarium.org

The authors would like to thank the Adler Planetarium and Astronomy Museum for access to the astrolabes studied in this work. B.D.N. was supported by the Department of Energy Office of Science, Office of Basic Energy Sciences, under contract # W-31- 1O9-Eng-38 as well as by the Adler Planetarium and Astronomy Museum for travel funds. Use of the Advanced Photon Source was supported by the U.S. Department of Energy, Office of Science, Office of Basic Energy Sciences, under Contract No. W-31-109-ENG-38.

A New Compound Comes into View

It is known that ice formed under pressures higher than atmospheric pressure can assume one of at least a dozen different known phases, characterized by crystal structures, densities, and O-H bonding that differ from those of ordinary, hexagonal crystalline ice (I_h), but the precise details of the chemical bonding that characterize each of these exotic phases are still not fully understood. To expand our knowledge of the rich phase diagram of ice at high pressure, a team of scientists from Los Alamos National Laboratory, the Carnegie Institute of Washington, The University of Chicago, and the National Synchrotron Radiation Research Center investigated water at high pressure in a diamond anvil cell. By using an inelastic x-ray scattering technique—x-ray Raman spectroscopy—the compressed H_2O samples were bombarded with moderately hard (~10-keV) x-rays to probe their oxygen K-edge structure. Serendipitously, in the course of their investigation they discovered a previously unseen, stable compound of O_2 and H_2 molecules. This result may open the door to exciting new directions in radiation chemistry research and lead to a better understanding of water under extreme temperature and pressure conditions.

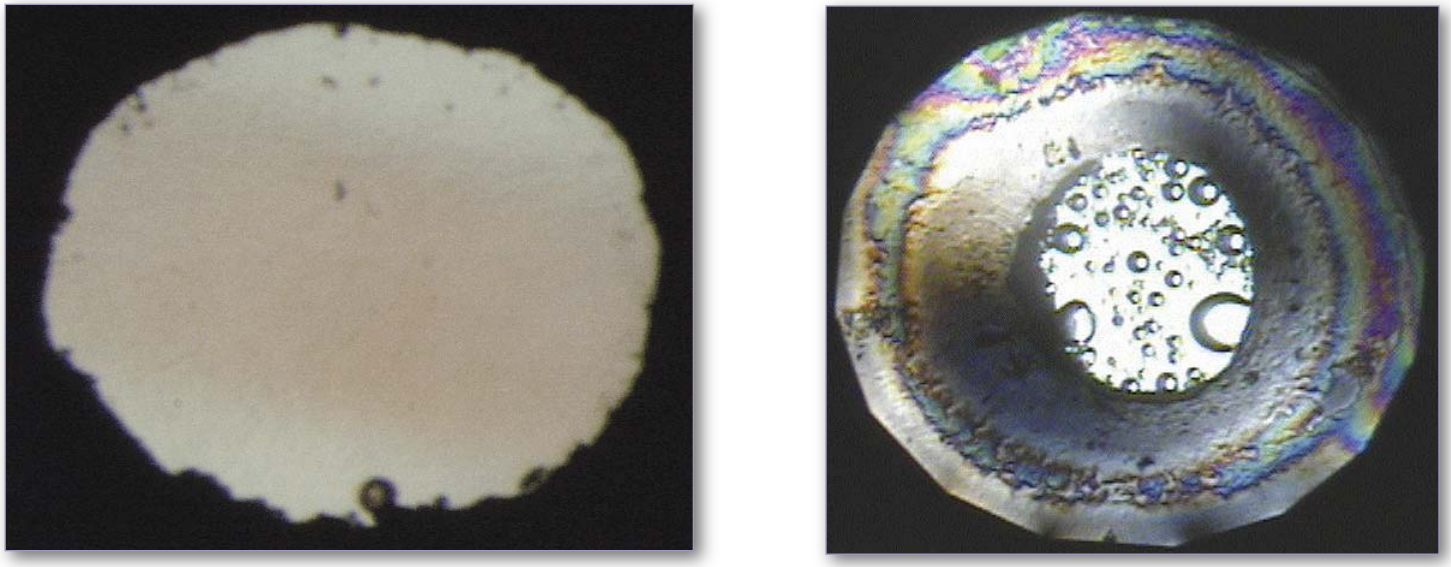

Fig. 1. Photomicrographs of two diamond anvil cell samples taken at the GSECARS 13-ID-C beamline at the APS. (A) Sample after XRS measurement at 8.8 GPa. The light brown streak through the middle of the sample shows the portion irradiated by the x-ray beam. A small ruby ball (bottom edge of the gasket) was used for pressure calibration. (B) After the release of pressure to below 1 GPa, bubbles of O_2 and H_2 formed. Sample is approximately 200 microns in diameter.

The researchers knew that for oxygen bonded with hydrogen in H_2O, the K-edge spectra peaked around 540 eV. For pressures between 1 and 2 GPa (10,000–20,000 atmospheric pressure), they were monitoring the subtle changes of the multiplicity, peak positions, and intensity of the 540-eV peak group that reveal the specific O-H bonding that characterizes different ice structures. However, at pressures above 2.5 GPa, they found that the x-rays induced cleaving of the H_2O molecule that radically altered the spectra. This was evidenced by the appearance of a 530-eV peak, characteristic of O-O bonding in O_2 molecules, which reached a maximum intensity after 6 h of exposure to the incident x-ray beam. This peak indicates the loss of O-H bonding, which is the basis of all ice and water structures, and the formation of a completely new material that still has the H_2O composition. At a pressure of 15.3 GPa, this peak was equal in height to the 540-eV multiplet; this effect was verified by the results of independent experiments performed at the APS and at SPring-8.

Well-documented, x-ray-induced phase transitions are rare, and the researchers were taken by surprise. The ice sample changed from the familiar colorless solid to light brown; at first, the group were puzzled by what was going on. Further optical Raman spectroscopy (ORS) measurements clearly fin-

Continued on page 50

"New Compound" continued from page 49

gerprinted the characteristic H_2 and O_2 peaks, which, coupled to a reduced H_2O signal, offered clear proof that the H_2O molecules had dissociated and a new material made of H_2 and O_2 molecules had been formed.

To gain a better understanding of the structure of this new material, the group performed a series of ORS and x-ray diffraction (XRD) experiments to study the effects of beam intensity and exposure times. The precise fingerprinting offered by their experimental technique ruled out the possibility that this material was an exotic mix of hexagonally close-packed (hcp)-H_2 and εO_2 and showed that the material was an alloy with approximate chemical formula $(O_2)(H_2)_2$. The XRD studies of the H_2-O_2 alloy, carried out at beamline 16-ID-B of the High Pressure Collaborative Access Team at the APS, revealed that the material is a well-crystallized solid and, apparently, a very stable one at ambient temperature and high pressures. The researchers' original interest in studying ice, beyond gaining a better understanding of the complete phase diagram, was to investigate the possibility of using ice to store hydrogen in fuel cells. But this discovery opens the door to many new and exciting directions in radiation chemistry. — *Luis Nasser*

See: Wendy L. Mao[1]*, Ho-kwang Mao[2], Yue Meng[2], Peter J. Eng[3], Michael Y. Hu[2], Paul Chow[2], Yong Q. Cai[4], Jinfu Shu[2], and Russell J. Hemley[2], "X-ray–Induced Dissociation of H_2O and Formation of an O_2–H_2 Alloy at High Pressure," Science **27**(5799), 636 (27 October 2006).
DOI: 10.1126/science.1132884

Author affiliations: [1]Los Alamos National Laboratory, [2]Carnegie Institute of Washington, [3]The University of Chicago, [4]National Synchrotron Radiation Research Center
Correspondence: *wmao@lanl.gov

The NSF–Division of Materials Research (DMR-0508988), NSF–Division of Earth Sciences (EAR) Petrology and Geochemistry, NSF-EAR Geophysics, and NSF-EAR Instrumentation and Facility Programs provided financial support, and HP-CAT provided synchrotron beam time. GeoSoilEnviro Consortium for Advanced Radiation Sources (GSECARS) is supported by the NSF-EAR (EAR-0217473), U.S. Department of Energy (DOE)–Geosciences (DE-FG02-94ER14466), and State of Illinois. HP-CAT is supported by the DOE–Office of Basic Energy Sciences (BES), DOE–National Nuclear Security Administration, Carnegie DOE Alliance Center, NSF, Department of Defense–Tank-Automotive and Armaments Command, and W. M. Keck Foundation. The work performed at BL12XU, SPring-8, is partly supported by the National Synchrotron Radiation Research Center and National Science Center of Taiwan. Use of the Advanced Photon Source was supported by the U.S. Department of Energy, Office of Science, Office of Basic Energy Sciences, under Contract No. W-31-109-ENG-38.

Around the Experiment Hall

Reaching for Answers to Questions about the Heart

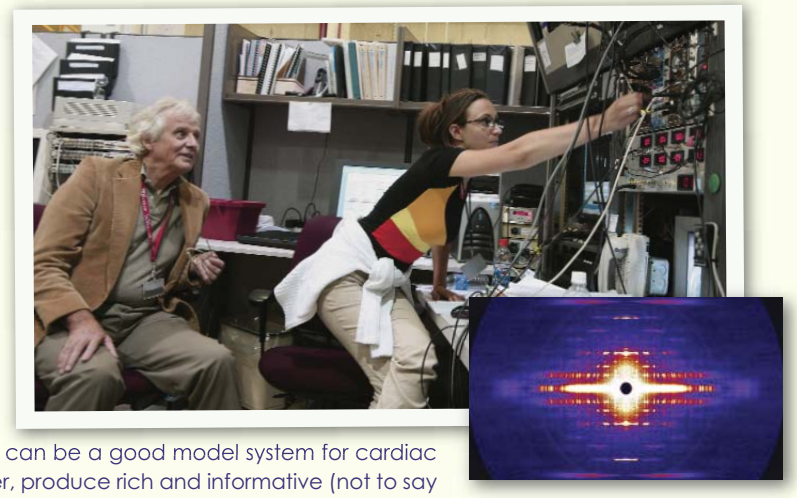

Michael Reedy (Duke University) and Tanya Bekyarova (Illinois Institute of Technology [IIT]) in action on the Bio-CAT beamline 18-ID at the APS. They are studying mechanisms of stretch activation in insect flight muscle. ● Stretch activation is very important in human heart muscle when contraction of one part of the heart stretches adjacent muscle tissue causing it to respond a moment later by generating more force, aiding cardiac "ejection," i.e., the amount of blood pumped per beat. Muscle structure and function can be studied using high-brilliance x-ray beams from the APS and the experimental technique, time-resolved small-angle fiber diffraction. ● Unfortunately, cardiac muscle is relatively poorly ordered and the diffraction patterns relatively uninformative. Fortunately, because of its physiological properties, the flight muscle of insects can be a good model system for cardiac muscle, and because of its high degree of structural order, produce rich and informative (not to say beautiful) diffraction patterns (right). Muscle contracts by the cyclical action of motor proteins called myosin that bind to particular sites on the actin protein. This interaction is normally prevented by tropomyosin, a large, rodlike protein that blocks the myosin binding site on actin turning the system "off." Reedy and Bekyarova are carrying out experiments aimed at determining the motion of tropomyosin and how it turns the muscle "on" and "off" during the process of stretch activation. *(Photo and contact: Tom Irving, IIT)*

Watching Gels Get the Stress Out

The macroscopic flow properties of a wide assortment of disordered soft materials—such as foams, concentrated emulsions, and colloidal suspensions—can change dramatically from fluid-like to solid-like with subtle changes in microscopic characteristics. This behavior bears strong resemblance to the liquid-glass transition that occurs in molecular fluids. The theoretical concept of jamming was developed to unify a range of fluid-solid transitions in disordered soft materials and to connect them to the glass transition. As part of the jamming phase diagram, solids can be made fluid by sufficiently large shear stress, a feature that is shared by many disordered soft materials. A central and challenging feature of liquids cooled into glass is the extremely slow subsequent evolution of their properties, a process known as "aging." An important question is whether other routes to creating disordered solids—e.g., changes in shear stress—lead to materials that evolve in the same way. Understanding the recovery-from-shear of disordered soft solids would provide important insights into the fundamental physics of these materials, give new insights into the reasons glass ages, and could also help improve technologies that exploit substances that are gel-like at rest and fluid after agitation, such as paints, foods, and personal-care products, to name a few. To investigate the microscopic mechanisms of recovery from shear in disordered soft solid materials and compare it with aging in glasses, researchers combined multispeckle x-ray photon correlation spectroscopy (XPCS)—carried out at the XOR 8-ID beamline at the APS—and diffusing wave spectroscopy (DWS) studies on concentrated colloidal gels subjected to strong shear. Their results call into question the connection between aging in glasses and the slow equilibration that various disordered soft solids display and should motivate a rethinking of models that seek to unify these phenomena.

The gels used in this experiment comprised solutions of nanometer-scale silica particles (~30% volume fraction) jammed by an entropically driven attractive force due to added polymer in the solution. These depletion gels can be transiently fluidized by the application of strong shear, as shown schematically in Fig. 1. The experiments carried out by the researchers—from Johns Hopkins University, the University of Ottawa, the University of Illinois at Urbana-Champaign, and Florida State University and Florida A&M University—monitored the particle-scale motions in the gels following the cessation of a fluidizing shear in order to search for an evolution in the dynamics that might be associated with aging. The use of both the XPCS and DWS techniques allowed for the study of dynamics over a wide range of length and time scales.

The XPCS experiments at the 8-ID beamline employed a silicon monochromator and precision slits to select a micron-scale cross section of the incident beam in order to produce a partially coherent source of x-rays incident on the sample. X-rays scattered from the concentrated gels were collected in a charge-coupled device (CCD) area detector configured for a range of wave vectors from 0.04 nm^{-1} to 0.39 nm^{-1}—a range tuned for the distance between nearest-neighbor spheres in the concentrated gel. Sequences of CCD images were analyzed to determine the intensity autocorrelation function for cor-

Continued on page 53

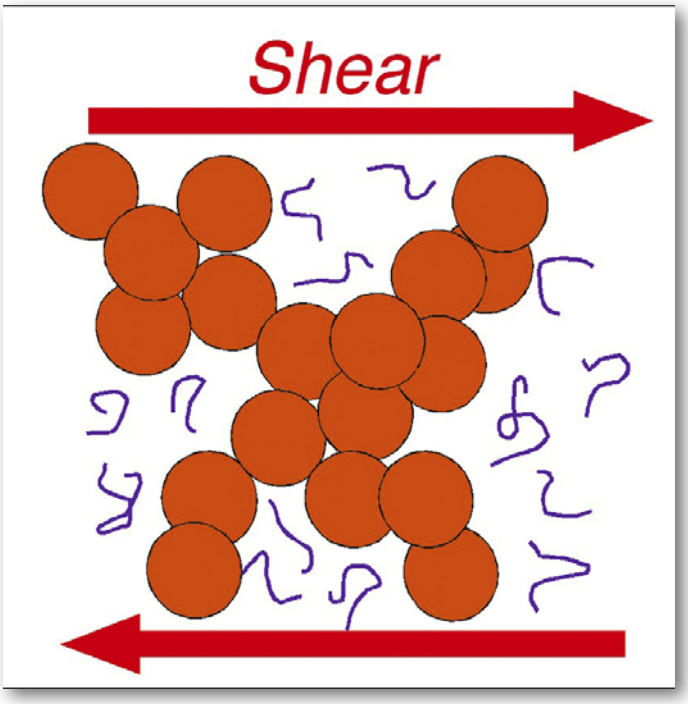

Fig. 1. Sketch of a sheared depletion gel of concentrated 45-nm-radius silica nanoparticles ($0.25 < \phi < 0.36$) in a decalin solution of R_g = 3.5-nm polystyrene coils.

The L_3 Phase of a Jammed Polymer Blend

The L_3 phase is a complicated isotropic fluid solution containing a multiply-connected, random, bi-layer membrane that extends throughout the three-dimensional space. Such a spatial arrangement divides space into two subvolumes, giving it a structure that appears similar to a sponge. Recently, the attention directed toward L_3 phases has dramatically increased, primarily because of their prevalence in systems containing amphiphilic molecules. In the past, researchers have found it difficult to experimentally determine the relaxation of equilibrium fluctuations at wave vectors around the peak of the static scattering, which corresponds to the characteristic length scales of the L_3 phase. Now, researchers from Yale University, the Massachusetts Institute of Technology, and Argonne used multispeckle x-ray photon correlation spectroscopy (XPCS) to study a triblock copolymer-homopolymer blend, revealing the dynamics of spontaneous thermal fluctuations in the L_3 (sponge) phase of the blend as a function of wave vector and temperature. A surprise result of these measurements, however, is the observation of a crossover from stretched- to compressed-exponential relaxation as temperatures decrease from 180° C to 120° C. They believe such behavior has not previously been observed. More importantly, such behavior indicates that the L_3 phase may thermally transition from high-temperature fluid states to low-temperature jammed states.

A polymer blend consisting of a symmetric poly(styrene-ethylene/butylene-styrene) tri-block copolymer (PSEBS) and a polystyrene homopolymer (PS) was used in this experiment. The blend was prepared from one part of PSEBS and four parts of PS, by volume. It was then annealed over several days under vacuum conditions at a constant temperature of 160° C. XPCS measurements of the intermediate scattering function from the samples were then taken at XOR beamline 8-ID at the APS.

The small-angle x-ray-scattering profiles show peaks at zero wave vector and non-zero wave vector that together are distinctive of the L_3 phase. The measured intermediate scattering functions (ISFs), which quantify the relaxation of fluctuations and are measured by XPCS, show a positive curvature at 180° C (Fig. 1), which indicates stretched-exponential behavior. However, at 120° C, the plot shows a negative curvature, which points to a compressed-exponential pattern.

The collaborators explain this change in behavior by suggesting that it is the result of "jamming," and suggest that in this case the origin of jamming (sometimes called dynamical arrest—when soft matter such as gels, foams, and emulsions go from a fluid to a solid-like state after many of the particles stop moving in unison) involves the arrest of topological relaxation.

Although the static structure of the samples is similar at the different temperatures studied, the collaborators hypothesize that a temperature change causes an alteration in the equilibrium topology, and that, for instance, such an alteration could result from a modest change in the equilibrium mean separation between membranes and the equilibrium thickness of the membrane.

Continued on next page

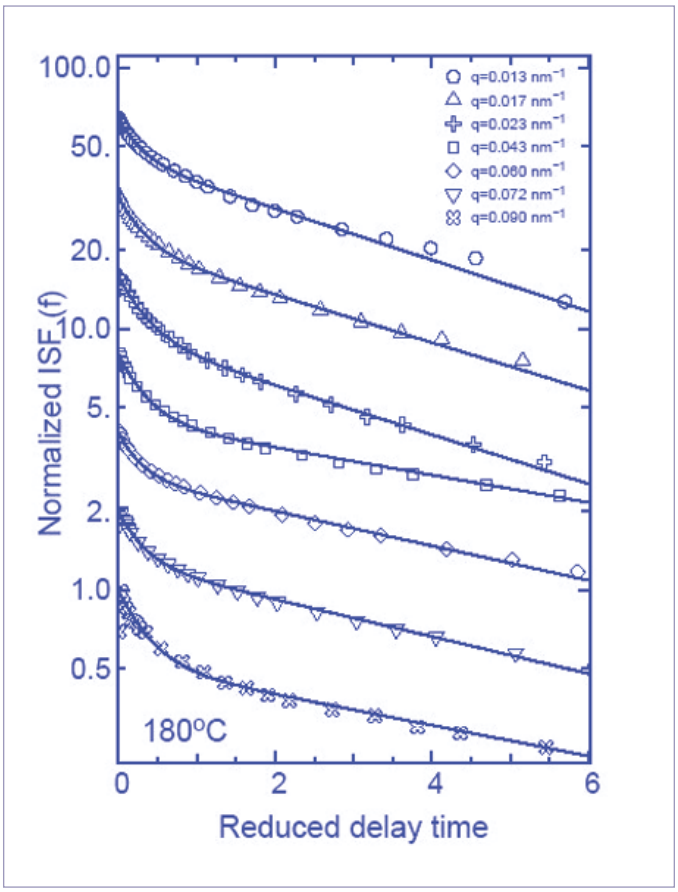

Fig. 1. Intermediate scattering functions obtained via XPCS at 180° C for several wave vectors (Q) for PSEBS-PS blends that realize an L_3 (sponge) phase.

"Gels" continued from page 51

relation delay times of 2.6 to 1,000 s at various stages following the cessation of shear, as illustrated in Fig. 2. Combined with the DWS experiments, these results provide a quantitatively coherent picture of the dynamics that, indeed, displayed a seemingly perpetual evolution strongly reminiscent of aging in glasses. However, analysis of the correlation functions demonstrates that these dynamics of recovery from shear are not directly related to traditional aging phenomena in glasses. Rather, they belong to a new type of slow, non-diffusive motion that is apparently universal to a range of disordered soft solids and that can be modeled as strain in response to heterogeneous local stress.

The conclusion arrived at by these researchers calls into question the connection between aging in glasses and the slow equilibration that various disordered soft solids display. Their conclusion should also motivate a rethinking of models that seek to unify these phenomena, and connect them with general paradigms for the behavior of soft and hard glassy materials.

— *William Arthur Atkins*

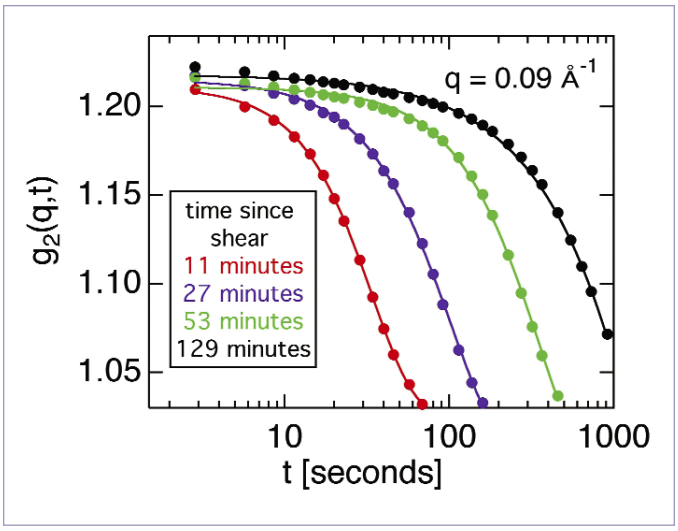

Fig. 2. XPCS intensity autocorrelation functions as a function of time since shearing for a silica-polystyrene depletion gel (silica volume fraction ϕ = 0.28 and polystyrene concentration c_p = 32 g/l) in decalin.

See: B. Chung[1], S. Ramakrishnan[2], R. Bandyopadhyay[1], D. Liang[1], C.F. Zukoski[3], J.L. Harden[1,4]*, and R.L. Leheny[1]**, "Microscopic Dynamics of Recovery in Sheared Depletion Gels," Phys. Rev. Lett. **96**, 228301 (2006).
DOI: 10.1103/PhysRevLett.96.228301
Author affiliations: [1]Johns Hopkins University, [2]Florida State University and Florida A&M University, [3]University of Illinois at Urbana-Champaign, [4]University of Ottawa

Correspondence: *jharden@uottawa.ca
**leheny@pha.jhu.edu

Funding was provided by the NSF (DMR-0134377). Use of the Advanced Photon Source was supported by the U.S. Department of Energy, Office of Science, Office of Basic Energy Sciences, under Contract No. W-31-109-ENG-38.

"Jammed Polymer" continued from page 52

In addition, the collaborators hypothesize that at temperatures of 140° C and above, the membrane topology is able to equilibrate during the experiment. However, at around 120° C, the membrane topology does not equilibrate because topological equilibration is activated—and, thus, is increasingly slow at lower temperatures—and collective diffusion is slowed due to larger viscosity within the PS. Consequently, the L_3 structure is subjected to increased internal stresses associated with its topological frustration. Specifically, the deformations that occur, due to these internal stresses, are the origin of the ISF relaxation recorded at 120° C. The collaborators also state that, at the three temperatures of 140, 160, and 180° C, the current data represent the initial ascertainment of the equilibrium dynamics of a polymer L_3 (sponge) phase. Finally, a crossover from stretched to compressed exponential relaxations is not unique to the sponge phase in polymer systems. Recently, Balsara and co-workers have observed similar behavior in a closely-related polymer microemulsion [1].

— *William Arthur Atkins*

Reference

[1] Megan L. Ruegg, Amish J. Patel, Suresh Narayanan, Alec R. Sandy, Simon G.J. Mochrie, Hiroshi Watanabe, and Nitash P. Balsara, "Condensed Exponential Correlation Functions in Multicomponent Polymer Blends Measured by X-ray Photon Correlation Spectroscopy," Macromolecules **39**, 8822 (2006).

See: P. Falus[1,2], M.A. Borthwick[2], A.R. Sandy[3], and S.G.J. Mochrie[1]*, "Crossover from Stretched to Compressed Exponential Relaxations in a Polymer-Based Sponge Phase," Phys. Rev. Lett. **99**, 066102 (2006).
DOI: 10.1103/PhysRevLett.97.066102
Author affiliations: [1]Yale University, [2]Massachusetts Institute of Technology, [3]Argonne National Laboratory
Correspondence: *simon.mochrie@yale.edu

This research was supported by the NSF via Grant No. DMR 0453856. Use of the Advanced Photon Source was supported by the U.S. Department of Energy, Office of Science, Office of Basic Energy Sciences, under Contract No. W-31-109-ENG-38.

Stress vs. Structure Relaxation: Which Comes First?

One can learn a lot about a person by observing how they react to stress and how they relax. The same principle holds true in materials science, where, for instance, studying the stress relaxation behavior of polymers can yield valuable information on molecular structure and organization, clues to the ways a material will perform in application. Relatively large-scale phenomena, such as structural and stress relaxation, provide a picture of what's happening at much smaller molecular-level scales. But the relaxation of stress in polymer structures does not necessarily happen all at once, nor is it always a simple process. In more complex structures, such as a disordered block-copolymer melt, factors such as differences in concentration and the transient formation of structures including micelles—small aggregates of polymeric molecules—can make it difficult to determine just when everything has finally settled into a peaceful equilibrium. Researchers from the University of California, Berkeley; Argonne; Yale University; Polytechnic University; Kyoto University; and Lawrence Berkeley National Laboratory investigated some of these complications, using the XOR 8-ID beamline at the APS to study the relationship between structural relaxation and stress relaxation in a block-copolymer melt and obtaining the first quantitative measurements of both processes. As it happens, the two are not necessarily the same.

The team subjected a polystyrene-block-polyisoprene copolymer, SI(7-27), to small-angle x-ray scattering (SAXS) and x-ray photon correlation spectroscopy (XPCS) static and dynamic measurements on the XOR 8-ID beamline at the APS. Previous work had demonstrated that at 70 ± 2° C, the block-copolymer melt transitioned from order to disorder with molecules in hexagonally-packed cylinders yielding to disordered micelles. These micelles show very strong x-ray scattering under SAXS.

The XPCS technique allows structural relaxation to be quantified not at the 500-nm scale limit of light photon correlation spectroscopy, but at the molecular scale of ~20 nm, providing better differentiation between terminal stress relaxation and molecular structural relaxation phenomena. The team also

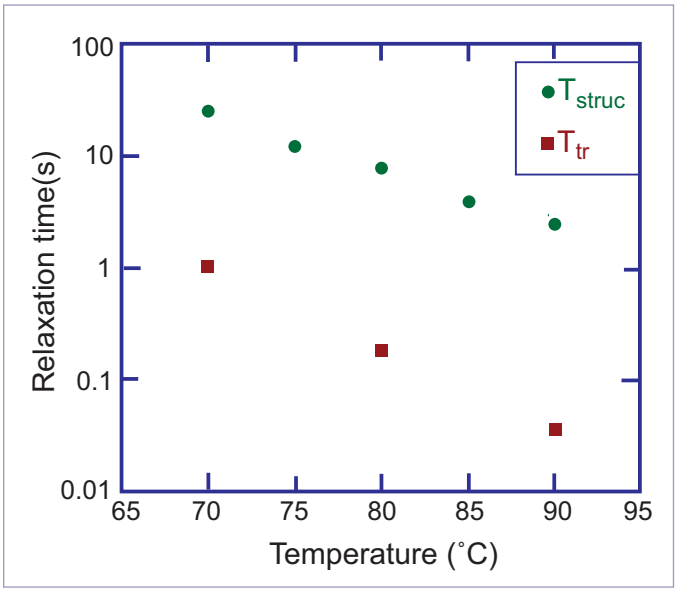

Fig. 1. Structural and terminal stress relaxation times, T_{struc} and T_{tr}, of the block copolymer melt measured by XPCS and rheology, respectively. Note that macroscopic stress relaxation occurs much more rapidly than microscopic structural relaxation.

used an ARES Rheometer for rheological measurements in a frequency range from 0.1 to 100 rad s^{-1}. The T_{struc}, or structural relaxation time, proved to be 1-2 orders of magnitude larger than T_{tr}, the rheological terminal relaxation time, with T_{tr} showing a greater dependence on decreasing temperature than T_{struc}. Frederick-Larson theory confirms this correlation between T_{struc} and T_{tr}.

The structure of a perturbed micelle-containing phase can relax in one of two ways: either the micelles themselves dissolve and reappear in arrangements that are closer to equilibrium, or intact micelles can migrate around and approach equilibrium. The research team's XPCS data demonstrate that in the SI(7-27) block-copolymer melt, it is the latter process—the diffusion of intact micelles—that dominates the structural relaxation. Meanwhile, rheological observations show that the stress relaxation occurs on much faster time scales because it is dominated by the dynamics of disordered fluctuations in concentration.

In achieving the first quantitative measurements of stress and structural relaxation in a block-copolymer melt, the researchers have demonstrated that there is a significant difference between the two, meaning that the common term "longest relaxation time" applied to these types of polymer structures is

Continued on next page

"Stress vs. Structure" continued from page 54

perhaps more than a little oversimplified. More than this, the team's experiment provides an effective example of how the study of equilibrium dynamics on the molecular scale can point the way to greater understanding of other processes that affect polymer structure. Sometimes there is more going on than one simple measurement technique (such as rheology) might indicate, so that a finer analytic technique (e.g., XPCS) might be needed. The team's use of XPCS adds another tool to the materials scientist's arsenal. — *Mark Wolverton*

See: Amish J. Pate[1], Suresh Narayanan[2], Alec Sandy[2], Simon G.J. Mochrie[3], Bruce A. Garetz[4], Hiroshi Watanabe[5], and Nitash P. Balsara[1,6]*, "Relationship between Structural and Stress Relaxation in a Block-Copolymer Melt," Phys. Rev. Lett. **96**, 257801 (2006). DOI: 10.1103/PhysRevLett.96.257801

Author affiliations: [1]University of California, Berkeley; [2]Argonne National Laboratory; [3]Yale University; [4]Polytechnic University; [5]Kyoto University; [6]Lawrence Berkeley National Laboratory

Correspondence: *nbalsara@berkeley.edu

Financial support was provided by the National Science Foundation (DECS 0103297 and DMR 0504122). A.J.P. gratefully acknowledges additional support from Tyco Electronics. S.G.J.M. was supported by NSF DMR 0453856. Use of the Advanced Photon Source was supported by the U.S. Department of Energy, Office of Science, Office of Basic Energy Sciences, under Contract No. W-31-109-ENG-38.

What's Flipping the Charges?

At its most fundamental level, most of the action taking place at cell membranes depends on ions: positive, negative, in various combinations and concentrations, controlling what goes in and out of a cell, the recognition of one cell by another, and other vital processes of molecular biology. Many of these phenomena are still poorly understood, among them charge inversion, which comes about when ions somehow attract so many of their oppositely-charged counterparts that the result is not neutralization but an effective reversal of the local charge density. A team of researchers from Carnegie Mellon University, Iowa State University, the NIST Center for Neutron Research, and Leipzig University peered into the process of charge inversion at charged interfaces in an electrolytic solution, using the Ames Laboratory Liquid Surface Diffractometer at the MU-CAT 6-ID-B beamline of the APS. What they found could lead to a better understanding of the basic physics of cell membranes and interfaces, which are essential to the integrity and functionality of the cells themselves.

The experimenters spread films of an acidic lipid (DMPA) on $LaCl_3$ solutions of varying concentrations on a Langmuir trough—an instrument that allows control of the area density of the lipid and thus the charge density at the interface—and performed isotherm and x-ray scattering studies. Utilizing the capability of the APS synchrotron to produce intense x-ray beams of precisely-selected photon energy, resonant x-ray spectra were obtained at 5.486 keV (the La L_{III} absorption edge) on the Ames Laboratory horizontal surface diffractometer and compared with spectra at other, off-resonance x-ray energies. The spectra contain information on the electron distribution near the surface, and hence the molecular organization of the 2-nm-thick organic surface film. The comparison of resonant and off-resonance spectra enabled the team to identify specifically the distribution of highly charged La^{3+} ions near the charge interface.

Isotherm studies show that multivalent ions condense the liquid/hexatic lipid monolayer into hexatic domains at exceedingly low salt concentrations, but the detailed role of the highly charged cations in that process remained unclear. The unique capabilities of the APS synchrotron radiation allowed these researchers to solve that puzzle. Between bulk $LaCl_3$ concentrations of 100 to 500 nM, off-resonance and on-resonance reflectivities were similar, but above 500-nM $LaCl_3$, the off-resonance reflectivities, in particular, were much higher, whereas the increase in resonant scattering remained modest. This is conclusive evidence that La^{3+} cations condense at the acidic interface; the surprise was the low concentration at which this condensation was observed. Off-resonance reflectivity measurements over a wider range of salt concentrations between 100 nM and 10 μM at higher pressures corroborated these findings.

A qualitative comparison between the resonant and off-resonant scattering length density profiles of the surface layer revealed what was happening in a 10-nm-thick layer at the surface. Because the experimenters tuned the resonant x-ray beam specifically to the La^{3+} cations, they were able to precisely relate the cation distribution to the area density of the anionic surface charges. When the number of La^{3+} ions per

Continued on page 56

"Flipping the Charges" continued from page 55

DMPA headgroup ($n_{La^{3+}}$) is plotted as a function of the salt content in the electrolytic subphase, the data fall into two distinct regimes of high and low bulk $LaCl_3$ concentrations separated by a transition regime. The first regime corresponds to ~1 La^{3+} that binds to 3 $DMPA^-$ at the interface. The sharp transition regime occurs when the accumulation of La^{3+} ions near the interface triggers the further deprotonation of phosphate groups, thereby doubling the interfacial charge density. This is an expected result in interface chemistry. However, the third regime—and specifically the amount of cation condensation in that regime—cannot be explained by standard surface chemistry. The team observed a binding stochiometry of 1:1 between anions and cations, indicating that ion-ion correlations must play an important role in the reorganization of the interface. Since thermal disorder, i.e., entropy, is the natural enemy of correlated states, other interfacial effects must be active to overcome the associated increase in surface free energy. The research team offers two possible explanations: (1) a "molten salt" state with La^{3+} ions intercalated between negative charges on the phosphate oxygens, and/or (2) enhanced nonelectrostatic interactions that help stabilize the correlated state.

The team's work demonstrates evidence of charge inversion in acidic DMPA monolayers at exceedingly small electrolyte concentrations, at least two orders of magnitude lower than expected from current theory. These experimental results suggest that correlations between mobile ions and interfacial charges (also known as interfacial Bjerrum pairing), which have so far been somewhat overlooked in theories of charged interfaces in biology, may play a major role in the charge inversion process. If this observation could be further substantiated in future work, it holds significant implications for the basic physics of cell membranes and interfaces. — *Mark Wolverton*

See: J. Pittler[1], W. Bu[2], D. Vaknin[2], A. Travesset[2], D.J. McGillivray[3], and M. Lösche[3,4*], "Charge Inversion at Minute Electrolyte Concentrations," Phys. Rev. Lett. **97**, 046102 (28 July 2006).
DOI: 10.1103/PhysRevLett.97.046102

Author affiliations: [1]University of Leipzig, [2]Iowa State University, [3]NIST, [4]Carnegie Mellon University
Correspondence: *quench@cmu.edu

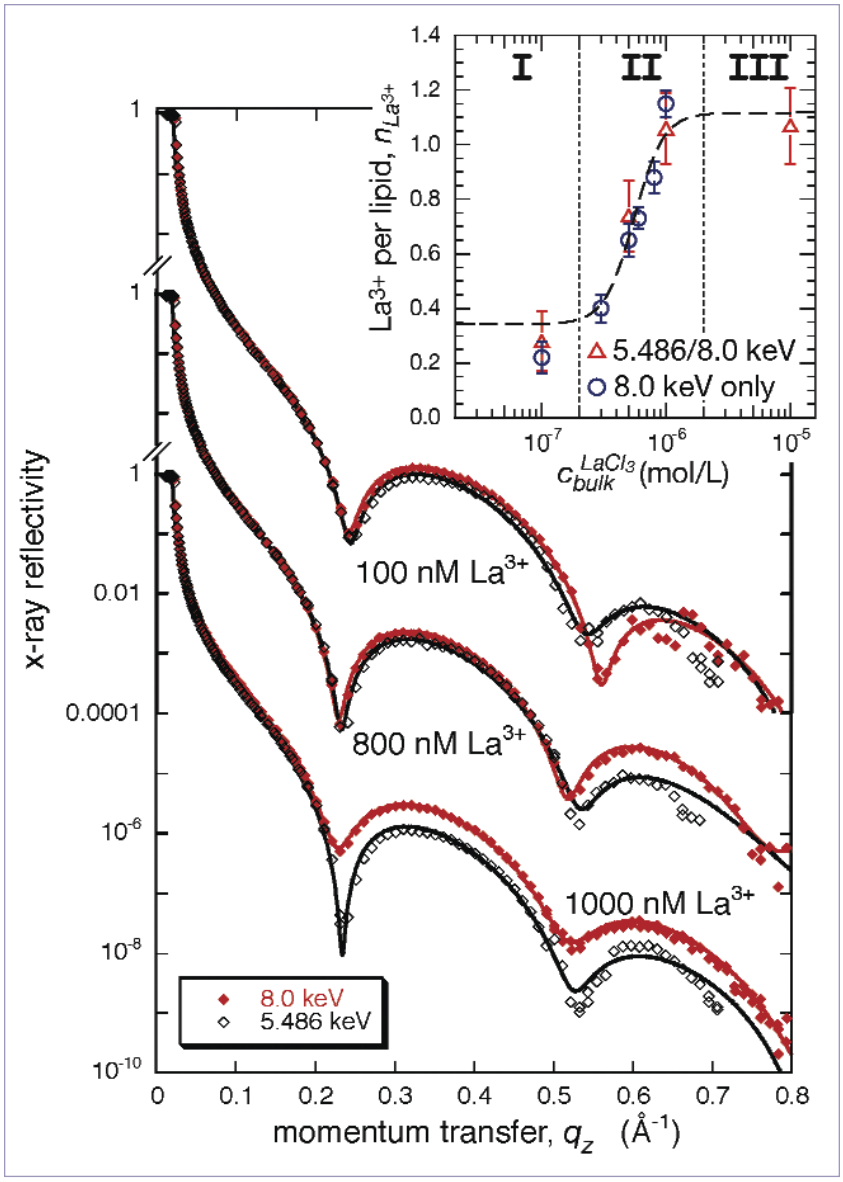

Fig. 1. Surface-sensitive x-ray scattering from acidic lipid surface layers on electrolytic solutions of highly charged cations. Main panel: The non-resonant reflection (red) of x-rays, sensitive to the top-most ~10-nm-thick layer on an aqueous subphase that is covered by an organic monolayer, which attracts La^{3+} cations, is compared with x-ray reflection (black) in which the photon energy is resonant with La. (Note that the scattering power of La at resonance is lower than off-resonance.) Clearly, a jump in the contribution of La to the scattering is observed at below 1 μm ion concentration in the subphase. A compilation of similar results at various salt concentrations (inset) reveals different regimes of ion condensation at the interface. The observed jump to charge overcompensation (~1 La^{3+} per $DMPA^{2-}$) at around 0.5 μm occurs at a concentration that is about 2–4 orders of magnitude lower than previously thought.

The MU-CAT sector at the APS is supported by the U.S. DOE, Office of Science, Office of Basic Energy Sciences under Contract No. W-7405-ENG-82. M.L. was supported by the NSF (Grant No. CTS-0555201), the NIH (Grant No. 1 RO1 RR14812), the Regents of the University of California, and the Volkswagen Foundation (Grant No. I/77709). A.T. is partially supported by NSF (Grant No. DMR-0426597). Use of the Advanced Photon Source was supported by the U.S. Department of Energy, Office of Science, Office of Basic Energy Sciences, under Contract No. W-31-109-ENG-38.

Red-hot and Prussian Blue

Novel materials that behave strangely by contracting when they are heated, instead of expanding as one would expect, could solve numerous problems in engineering. Mixed with a conventional material, these negative thermal expansion (NTE) materials could be used to make composites that neither expand nor contract when the temperature changes. Such designer NTE materials, which might be used in aeronautics, adhesives, and electronics are a step closer to application thanks to work by scientists from the University of Sydney and Argonne using XOR/BESSRC beamline 11-ID-B at the APS. The researchers used the light source to study in detail the structure of a range of NTE materials based on the compound Prussian blue.

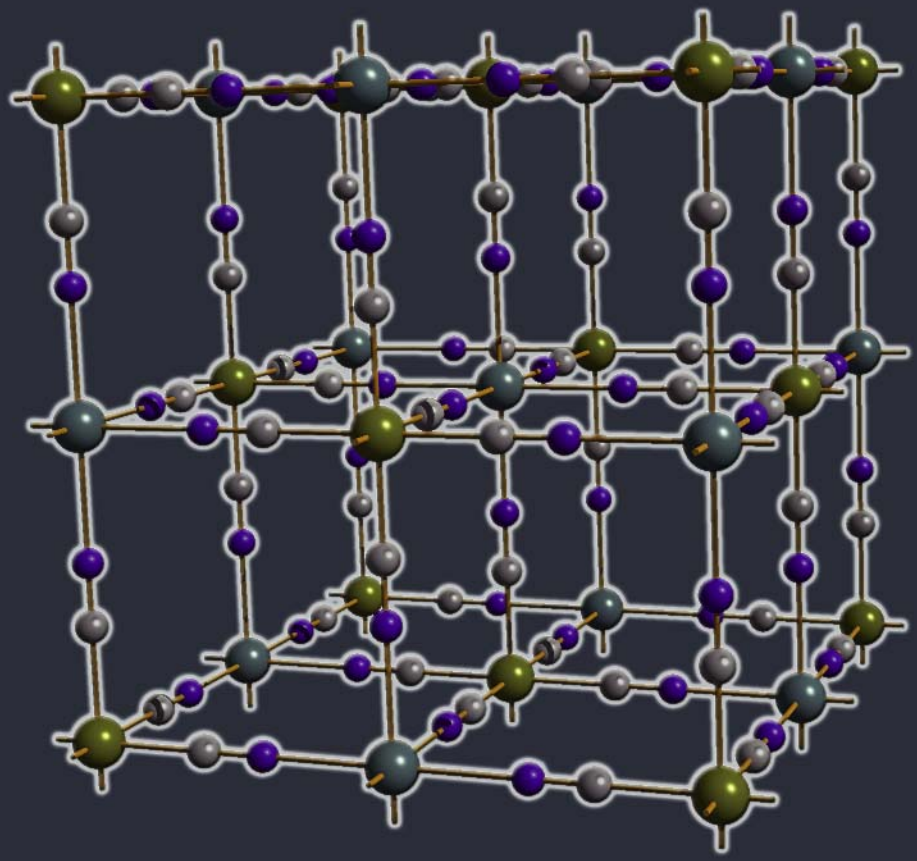

Fig. 1. Unlike most materials, Prussian blue and its analogs, including this cadmium-platinum material, contract on heating. (Three-dimensional rendering by David Bradley from a CIF data file supplied by Cameron Kepert.)

Most materials expand when heated; steel rails expand on hot days and buckle, while the effects of pouring a very hot drink into a cold glass are immediately apparent as the glass expands unevenly and shatters. There are, however, a few materials that do not follow the rules. Water, for instance, contracts when melted, which is why ice floats in a jug of water. There are a small number of other compounds that undergo this negative thermal expansion, too. Such materials might be used to compensate for the normal expansion of other materials when they get hot in engineering applications, such as aeronautics and space exploration, construction, and transport. Mixing an expanding with a contracting material would result in a zero-expansion composite. Such a composite would solve many engineering problems and could be used in dental fillings that do not expand or contract when hot or cold foods are chewed, thereby reducing the risk of tooth damage and pain.

The vivid blue pigment Prussian blue, discovered three centuries ago in boiling pig's blood, undergoes negative thermal expansion. It has been used in pharmaceuticals and as the blue in blueprints, and it was the pigment of choice during Picasso's “blue period.” Prussian blue, iron(III) hexacyanoferrate(II), contains two iron atoms linked by cyano (CN) bridges, while analogs can contain two different pairs of metals.

These researchers studied a new series of Prussian blue compounds in which one of the pair of metal atoms is platinum and the other manganese, iron, cobalt, nickel, copper, zinc, and cadmium. The researchers have investigated the structures of these materials to see whether they might correlate structure with expansion properties.

Previous work has led to a theory to explain how such materials might contract when they are heated rather than

Continued on page 58

"Prussian Blue" continued from page 57

expand like other materials. Normally, due to the fact that atoms vibrate more with heating, the atoms in a material are pushed farther apart at higher temperatures, with the net result that the substance as a whole expands. However, this simplistic view does not take into account complex bond linkages that might be present between the atoms in framework complexes, for instance.

In such materials, light elements (e.g., oxygen, carbon and nitrogen) commonly form bridges between the metal atoms. These lighter elements undergo transverse "skipping rope"-type movements that increase in amplitude as the temperature rises. Such vibrations actually pull the metal atoms closer together, resulting in a net contraction of the material.

Kepert and colleagues have found that by varying the second metal in their Prussian blue analogs, they could tune the materials' negative thermal expansion. Each second metal in the series alters the energy of the transverse vibrations by changing how tightly the cyanide units are bound, analogous to tightening a violin string and so increasing its vibrational energy.

This means that the degree to which the metal atoms are pulled together with increasing temperature differs. Stronger bonds between the cyano groups and the metals means less opportunity for contraction, with the most tightly bound material having almost zero thermal expansion properties.

— David Bradley

See: Karena W. Chapman[1], Peter J. Chupas[2], and Cameron J. Kepert[1]*, "Compositional Dependence of Negative Thermal Expansion in the Prussian Blue Analogues $M^{II}Pt^{IV}(CN)_6$ (M = Mn, Fe, Co, Ni, Cu, Zn, Cd)," J. Am. Chem. Soc. **128**, 7009 (2006). DOI: 10.1021/ja060916r

Author affiliations: [1]University of Sydney, [2]Argonne National Laboratory

Correspondence: *c.kepert@chem.usyd.edu.au

This work was supported by the Australian Research Council and the Australian Synchrotron Research Program, which is funded by the Commonwealth of Australia under the Major National Research Facilities. K.W.C. acknowledges a Joan R. Clark Research Scholarship. Use of the Advanced Photon Source was supported by the U.S. Department of Energy, Office of Science, Office of Basic Energy Sciences, under Contract No. W-31-109-ENG-38.

Around the Experiment Hall

The 2006 Sidhu Award to Peter Chupas

Peter Chupas of the X-ray Science Science Division (XSD) Chemistry, Environmental, and Polymer Science Group was named the 2006 recipient of the Sidhu Award, given each year by the Pittsburgh Diffraction Society "for the best contribution to crystallography or diffraction by an investigator within five years of the Ph.D." Chupas was recognized for his work on studies leading to the development of a new method for rapid collection of pair-distribution-function (PDF) data. This is now the method of choice for PDF measurements and forms the basis of the first and only dedicated pair distribution function beamline in the U.S., XOR 11-ID-B at the APS, for which Peter is the beamline scientist. • The Sidhu awardee receives $500 and a certificate. A condition of the Award requires the recipient to deliver the Sidhu Award Lecture at the Pittsburgh Diffraction Conference, held each year at Duquesne University in Pittsburgh, PA, which Chupas did in October 2006. • The Sidhu Award is made in memory of Professor Surhain Sidhu, who was a founding member of the Pittsburgh Diffraction Conference. At the time (1942), he was Professor of Physics and Director of the X-ray Laboratory at the University of Pittsburgh. Later, he moved to Argonne, where he pioneered the use of the null matrix in neutron diffraction. This involves choosing isotopes of an element in the proportion that gives a zero net coherent scattering factor. The procedure has been widely used for studying biological materials in which the isotopic ratio of H to D is appropriately adjusted. • Past winners of the Sidhu Award include Qun Shen (1988) and Jin Wang (1994). Both are now group leaders in XSD, Shen for the X-ray Microscopy and Imaging Group and Wang for the Time Resolved Research Group.

Giving Nitrogen the Shakes

Learning about the vibrations of an enzyme vital to life on Earth may reveal a chemical "X-factor" that has puzzled scientists for years. The identity of the mysterious X atom will improve our understanding of how bacteria extract nitrogen from the air and might lead to new catalysts for the chemical industry. Researchers from Lawrence Berkeley National Laboratory; the University of California, Davis; Virginia Polytechnic Institute and State University; the Scripps Research Institute; Argonne National Laboratory; and the Japan Synchrotron Radiation Research Institute have used XOR beamline 3-ID at the APS and beamline 9-XU at SPring-8 (Japan) to uncover new information about the behavior of atoms at the core of a critical nitrogen-fixing enzyme.

Nitrogenase is one of the most important enzymes on the planet. It is produced by microbes known as diazotrophs, some of which are free-living in the ground and oceans, while others reside in root nodules found in leguminous plants such as soybeans. Nitrogenase has the unique ability to pluck nitrogen (N_2) from the atmosphere and make it react. This process of nitrogen fixation is still something of a mystery, although we know that nitrogen molecules are split and hydrogen is added to make ammonia (NH_3). This fixed nitrogen is used by plants to make amino acids and proteins and so lies at the root of life's food chains.

At the core of most nitrogenase enzymes is an active site containing the so-called iron-molybdenum cofactor. This is a "biological nanoparticle" consisting of a cluster of atoms—1 molybdenum (Mo), 7 iron (Fe), and 9 sulfur (S) atoms—held in place by protein side-chains and homocitrate. Previous work by crystallographer Douglas Rees of the Howard Hughes Medical Institute and co-workers revealed a detailed map of the electron density in the nitrogenase found in the bacterium *Azotobacter vinelandii*, Av1. This particular nitrogen-fixing species is readily grown in laboratory culture and so provides an archetypal system for study. Rees and his colleagues revealed an unknown light atom "X" at the heart of this enzyme and pointed to the identity of the X-factor as a nitrogen, carbon, or oxygen atom.

The researchers used APS and SPring-8 beamlines to carry out an iron57 nuclear resonance vibrational spectroscopy (NRVS) study of this active center of nitrogenase. The study revealed the first spectroscopic evidence about how the atoms of the FeMo-cofactor vibrate, both when it sits in the protein or after extraction as "FeMoco" into organic solvents.

The NRVS technique is sensitive to the motion of the iron atoms; the more the atoms vibrate, the stronger the NRVS signal. The key discovery from the NRVS so far is that atom X acts

Continued on page 60

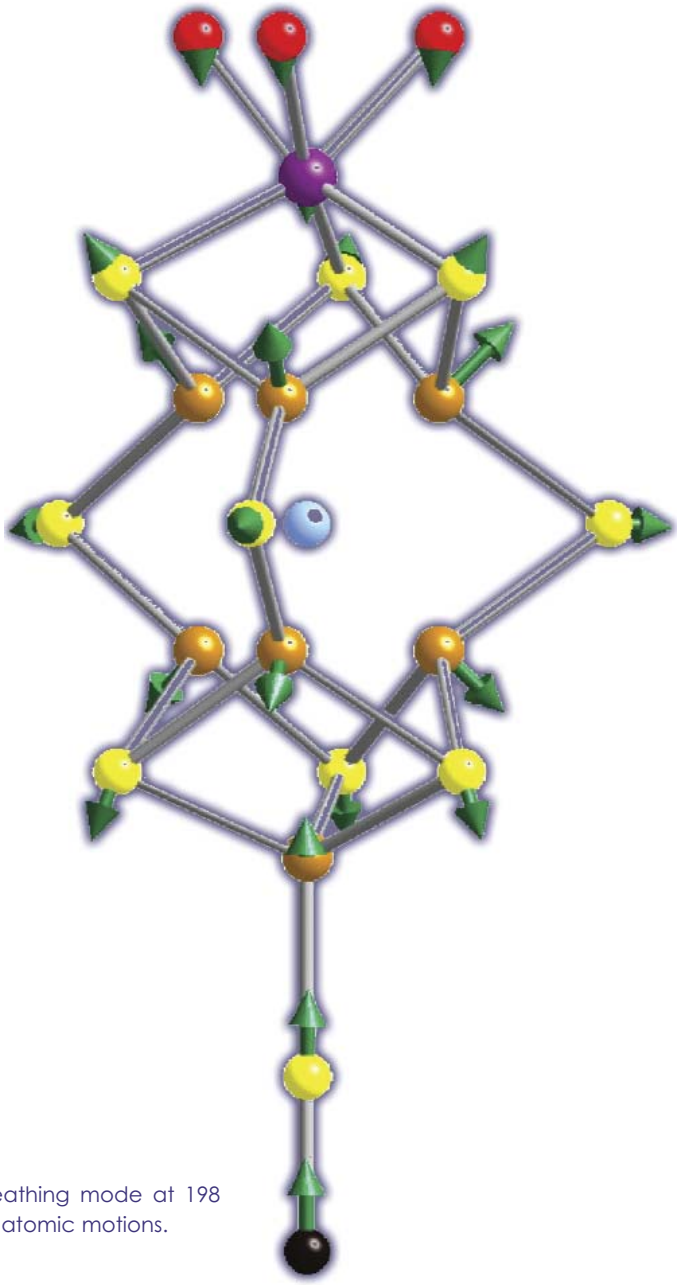

Fig. 1. Simplified FeMoco breathing mode at 198 cm^{-1}, arrows indicate relative atomic motions.

"Nitrogen" continued from page 59

as sort of a "glue" for the cluster. This has the effect of making the vibrational breathing modes that involve expansion of the central 6Fe core more rigid than expected. By comparing the observed vibrational frequencies with theoretical density functional theory (DFT) calculations, these researchers have shown that carbon and nitrogen were viable candidates for X, while oxygen or an empty core was not in good agreement with the DFT simulations.

In the future, the group hope to determine whether or not small changes in the spectra can be induced by substituting the X atom with an isotope of carbon or nitrogen, 13C or 15N. This would settle the identity of X once and for all. The team is also working with a Utah State University researcher to study the binding of N_2 and other small molecules in the active site. The researchers hope that NRVS will allow them to characterize the steps involved in nitrogen fixation in more detail.

Determining the identity of X in the nitrogenase enzymes would improve our understanding of the underlying mechanism of nitrogen fixation and how the cofactor is synthesized by the bacteria. Such understanding might help chemists create novel catalysts that mimic the co-factors and so make industrial nitrogen fixation much more efficient. — *David Bradley*

See: Yuming Xiao[1], Karl Fisher[3], Matt C. Smith[1], William E. Newton**[3], David A. Case***[4], Simon J. George[2], Hongxin Wang[1,2], Wolfgang Sturhahn[5], Ercan E. Alp[5], Jiyong Zhao[5], Yoshitaka Yoda[6], and Stephen P. Cramer*[1,2], "How Nitro-genase Shakes—Initial Information about P-Cluster and FeMo-cofactor Normal Modes from Nuclear Resonance Vibrational Spectroscopy (NRVS)," J. Am. Chem. Soc. **128**, 7608 (2006). DOI: 10.1021/ja0603655

Author affiliations: [1]University of California, Davis; [2]Lawrence Berkeley National Laboratory; [3]Virginia Polytechnic Institute and State University; [4]The Scripps Research Institute; [5]Argonne National Laboratory; [6]Japan Synchrotron Radiation Research Institute

Correspondence: *cramer@lbl.gov, **wenewton@vt.edu, ***case@scripps.edu

This work was funded by NIH grants GM-44380 (S.P.C.), GM-65440 (S.P.C.), GM-39914 (D.A.C.), and DK-37255 (W.E.N.) and the DOE Office of Biological and Environmental Research (S.P.C.). SPring-8 is supported by JASRI. Use of the Advanced Photon Source was supported by the U.S. Department of Energy, Office of Science, Office of Basic Energy Sciences, under Contract No. W-31-109-ENG-38.

AROUND THE EXPERIMENT HALL

Ten Years of Spectroscopy at APS Beamline 3-ID

The excitement expressed by a group of scientists at the APS on January 24, 1996, was the culmination of years of preparation and signaled an end to a nomadic existence at various synchrotron radiation centers around the world. "First beam" filled the station of APS sector 3-ID and within a few months, scientific experiments with sub-meV energy resolution were under way. A team from the then-Synchrotron Radiation Instrumentation group, with support from APS engineering personnel and management, created and perfected a novel x-ray spectroscopy, now known as nuclear resonant inelastic x-ray scattering (or nuclear resonant vibrational spectroscopy). ● Over the next decade, scientists working at XOR sector 3-ID discovered the Nuclear Lighthouse Effect, invented nuclear resonant magnetometry, designed the highest resolution x-ray monochromators (which still hold the world record), and pioneered inelastic spectroscopy at mega-bar pressures and thousands of Kelvin. More than a dozen students have prepared doctoral dissertations based on their work at sector 3-ID. Today, the beamline is operated by the Inelastic X-ray and Nuclear Resonant Scattering Group. It serves the biophysics, inorganic biochemistry, geophysics, materials science, and condensed matter physics communities. ● Ten years later, on February 17, 2006, many of those original scientists, as well as new colleagues and users, gathered in the APS experiment hall to celebrate the past and future of sector 3-ID (and to have their picture taken). *Contact: Wolfgang Sturhahn (sturhahn@aps.anl.gov)*

Sarcomere Synchrony

Any time we move our arms, billions of protein molecules work in unison to contract one muscle while letting another muscle relax. The mechanical details of muscle contraction have been known for a long time, deduced from experiments with frog legs, reconstruction of the proteins involved in crystallographic studies, and many other kinds of research. But no one has ever taken such detailed time-lapse molecular pictures of the proteins at work within living muscle. Researchers from Brandeis University, the University of Florence, and Illinois Institute of Technology investigated whether the muscle-contracting proteins work the same way inside muscles as they do inside laboratories. But muscle cells are full of water and the proteins don't line up quite as regularly as they would purified in crystals. So rather than spend 30 to 40 hours collecting data with a typical x-ray tube, the researchers turned to the Bio-CAT beamline 18-ID at the APS. With a million times more intensity than a “home source” x-ray tube—and the ability to focus the x-ray beam into a narrow line—the team got a detailed view of the proteins at work (Fig. 1). Not only did they measure the degree of movement of the proteins, but they saw that the proteins synchronized themselves in living muscle much better than anticipated.

Although muscles look like a long single unit to the eye, they are actually made up of small segments called sarcomeres, linked together along the length of a single cell. Every sarcomere contracts at about the same time, shortening the overall length of the muscle. Proteins are the workhorses behind the contraction. One row of proteins—known as actin—forms a kind of stiff track along which other proteins—called myosin—attach. Myosin molecules have long handles that wrap around each other to form a connected, rigid backbone. From this backbone rise lever arms, which are topped by flexible heads that grab onto the actin track. As the lever arm swings on its pivot, the heads pull the actin filaments, shortening the sarcomere.

To view this activity in a living muscle, the team first stimulated the thigh muscle of a *Rana pipiens* (commonly known as the Northern Leopard Frog) to make the muscle contract, and then kept the muscle tense. They then released the muscle quickly and briefly—within a millisecond—so that it shortened by about 1% of its length. At the same time, the extreme brilliance of APS x-ray beams allowed the researchers to take “snapshots” of the proteins. From the scattering of x-rays by the actin and myosin, the team could reconstruct the positions of the different parts of the proteins: the track, the heads, the handles and lever arms.

The myosin heads start out almost perpendicular to the actin track: about 10º to 15º off, with a group of myosin heads every 14 nm. Then, when the muscle shortens, the arms swing a full 60º through the perpendicular axis, moving the heads a total distance of 10 nm.

In addition, the more in-sync the myosin proteins moved with each other, the clearer the data were that the team collected. The researchers expected the myosin heads to be at a variety of angles. But the lever arms only differed by a few tens of degrees from each other. Because most other data on actin and myosin have been collected from purified muscle proteins, this work reveals a more accurate image of what's going on in active, intact muscles. — *Mary Beckman*

See: Hugh Huxley[1]*, Massimo Reconditi[2], Alex Stewart[1]**, and Tom Irving[3], "X-ray interference studies of crossbridge action in muscle contraction: evidence from quick releases," J. Mol. Biol. **363**, 743 (May 2006). DOI: 10.1016/j.jmb.2006.08.075
Author affiliations: [1]Brandeis University, [2]University of Florence, [3]Illinois Institute of Technology
Correspondence: *huxley@brandeis.edu; **alex@brandeis.edu

Bio-CAT is a National Institutes of Health-supported Research Center RR- 08630. H.E.H. received support during part of this work from NIH Grant no. AR43733. Use of the Advanced Photon Source was supported by the U.S. Department of Energy, Office of Science, Office of Basic Energy Sciences, under Contract No. W-31-109-ENG-38.

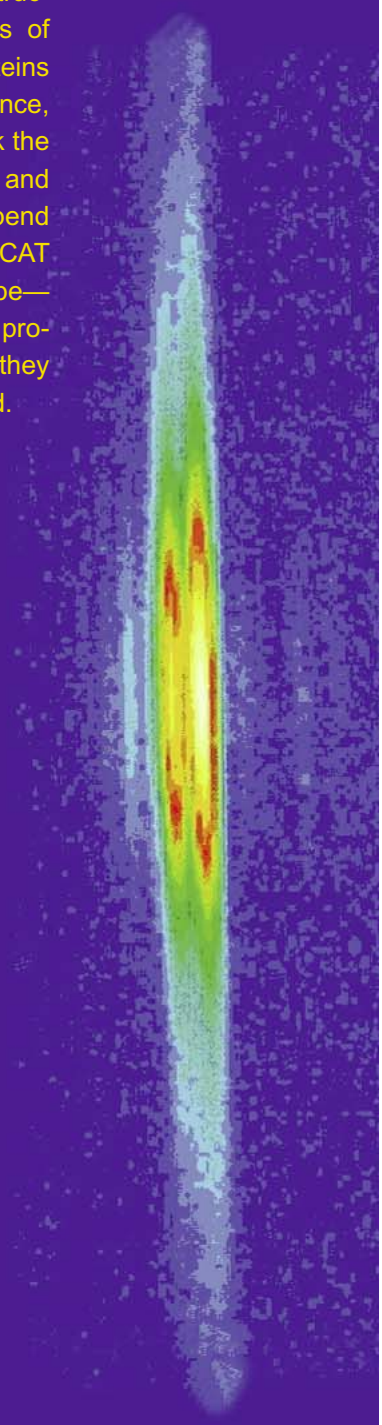

Fig. 1. Reflection (shown in false color) from an intact contracting frog thigh muscle.

THE CORRECT SIGNALS TO REGULATE ASSEMBLY IN BACTERIA

You are what you eat is just another way of saying that input determines output, after some metabolic messing around in between. It's the "in between" that interests biologists, because that is where the difference between healthy and diseased cells can originate. If the normal sequence of intermediate steps between the beginning and end of a biochemical pathway is disrupted, the disruption can lead to major changes in cellular functioning. A better understanding of the input-output relationships is critical to medical progress. The steps necessary for producing the right output can be numerous and complex, and some pathways have taken decades to unravel. In one of the identified mechanisms, called "two-component signal transduction," the input causes a receiver domain to be phosphorylated, a step that governs what happens to the output modules. By employing x-ray scattering and electron microscopy researchers from Pennsylvania State University; the University of California, Berkeley; Lawrence Berkeley National Laboratory; The University of Georgia; and the Illinois Institute of Technology using the BioCAT 18-ID beamline at the APS were able to describe—in stunning detail—a novel two-component mechanism for assembling a protein associated with bacterial transcription. This work greatly advances our understanding of what happens in normal and, by inference, diseased cells.

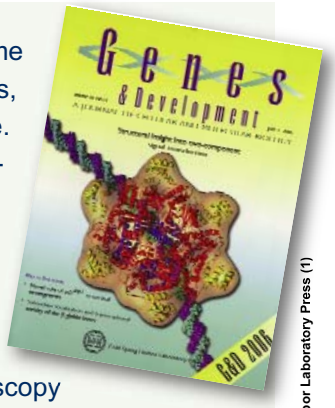

© 2006 Cold Spring Harbor Laboratory Press (1)

Transcription is the process by which the cell's DNA is read to make RNA, which is in turn translated into protein. The DNA-to-RNA transition is, naturally, quite complex and intricately regulated, because the cell can only function normally if DNA is translated to protein at the exact right moment. RNA polymerases—those enzymes responsible for creating RNA from DNA—are many and varied. One RNA polymerase will function normally only with the help of enhancer-binding proteins, such as the nitrogen-regulatory protein C of enteric bacteria (NtrC). NtrC is believed to be involved in regulating transcription for up to 2% of the genome, so determining its structure is of great importance.

The structures of the enhancer-binding proteins like NtrC are quite complex—in addition to their ATPase and DNA-binding domains, they have a regulatory domain, which (in half the cases) has been found to be a receiver domain for a two-component signal transduction system. Until now, available structural data on NtrC-like proteins, while suggestive of how the "in between" steps could occur, did not provide a complete model. The researchers in this study, with the help of beamline 18-ID,

Continued on next page

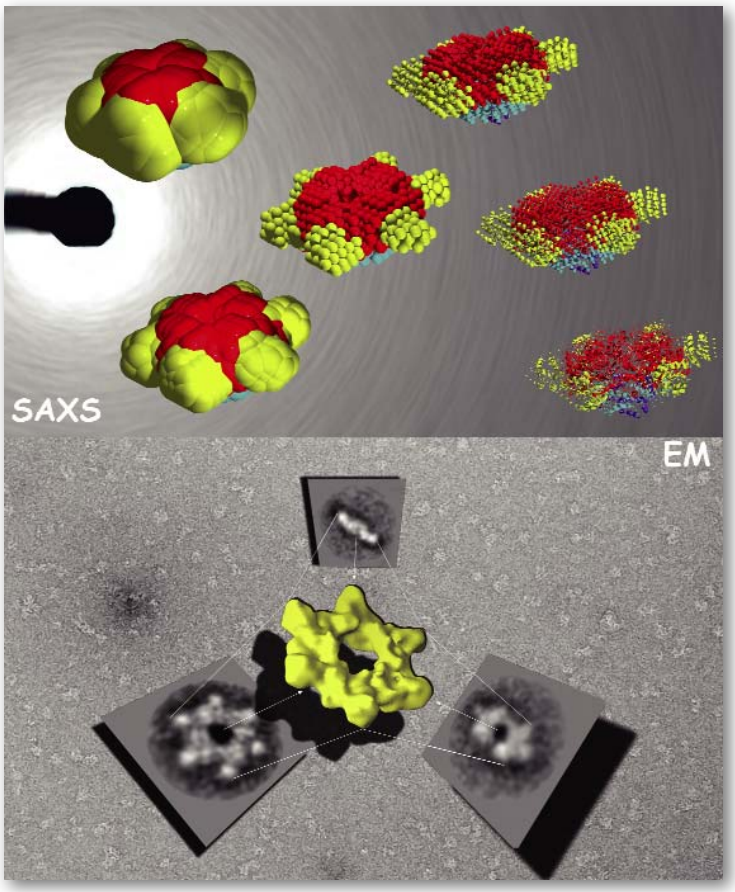

Fig. 1. Top: NtrC structure by SAXS, showing juxtaposition of the receiver (yellow), ATPase (red), and DNA binding (blue) domains. Bottom: Image reconstructions of EM, revealing nucleotide-directed order-disorder transitions in the DNA-binding and GAFTGA loop regions of the protein.

used small- and wide-angle x-ray scattering (SAXS/WAXS) and electron microscopy (EM) to develop structures for the full-length NtrC from *Salmonella typhimurium*. These new data not only provide a complete picture of how the individual domains of the protein fit into the activated enzyme, but they also reveal a new mechanism for using two-component signal transduction in regulating AAA+ ATPase domains. The group was also able to identify additional structural features—the ordering of the DNA binding domain and an outward extension of a GAFTGA loop region—that could be important in the hydrolysis-activation process and may suggest avenues for further study.

The new mechanism discovered by the research group involves juxtaposition of the receiver domains and the ATPase ring. The beautiful structure of the NtrC revealed by this study shows a central ATPase domain, with six receiver domains packed tightly around it (Fig. 1). Three dimers of DNA-binding domains lie underneath the main ring—these domains become flexible and are believed to detach from the central ring when inorganic phosphate is released. In addition, by using the NtrC structure and previous biochemical data, the researchers were able to postulate contact between the activated receiver domain of one subunit and the ATPase domain of another, thus explaining how the NtrC receiver domains play a positive role in regulating assembly of the ATPase domains into their functional ring form (Fig. 2). This configuration of receiver and ATPase domains differs markedly from previous models proposed for how two-component signal transduction "negatively" regulates assembly of AAA+ ATPase rings in a related protein called NtrC1. By using the new model, researchers can identify structural differences underlying positive versus negative regulation for this family of enhancer-binding proteins. The structure also allows hypotheses about how specific changes in NtrC amino acids and in order-disorder of the GAFTGA loop and DNA-binding domains could affect assembly, thereby suggesting explanations for disease states, drug-design possibilities, and, in the broad view, how input affects output.

— *Mona Mort*

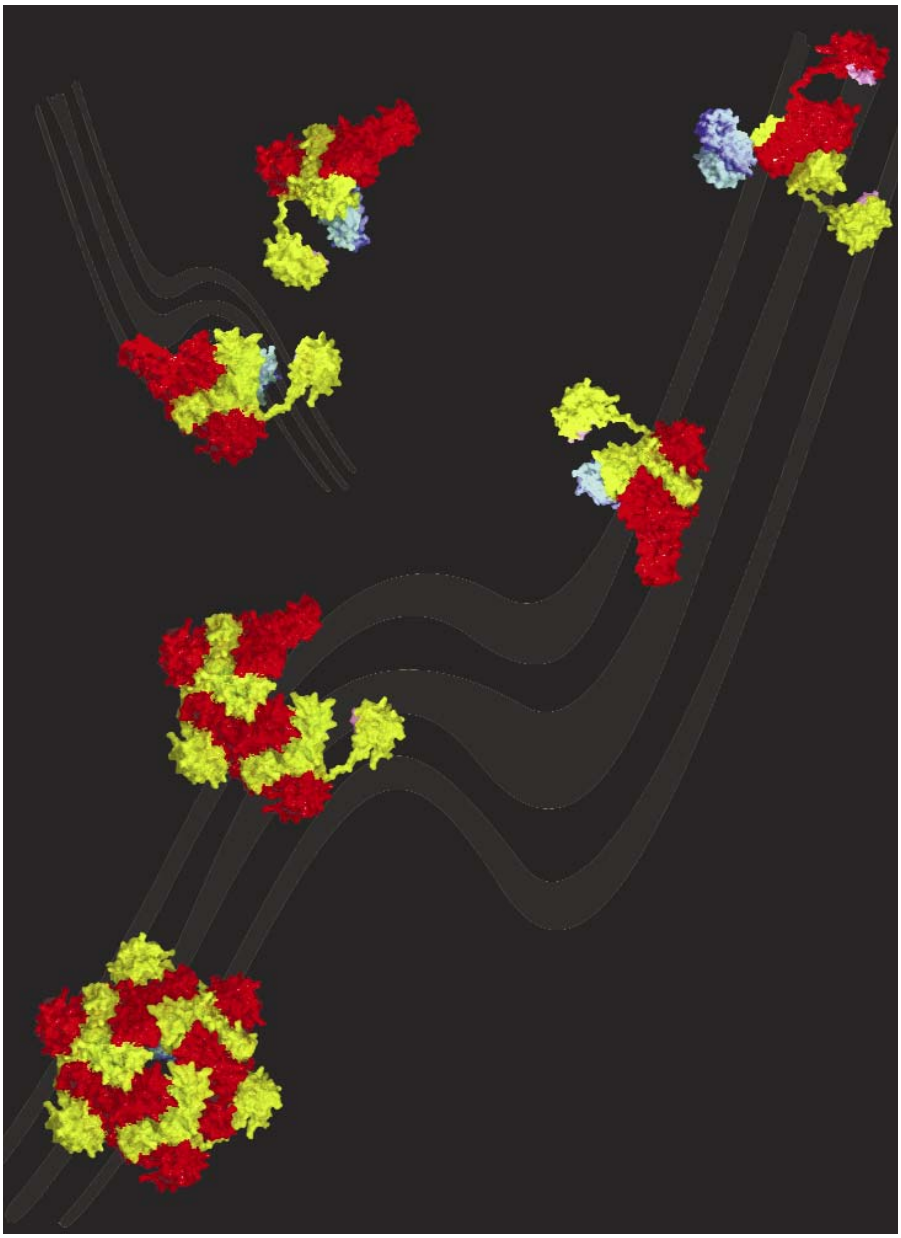

Fig. 2. A model for the "positive" mechanism of ring assembly by the NtrC AAA+ ATPase, showing surface representations of NtrC changing from its inactive dimer (upper right) to active oligomer (lower left) form; receiver and ATPase domains of partners (yellow or red); DNA binding domains (blue).

See: S. De Carlo[1], B. Chen[3], T.R. Hoover[4], E. Kondrashkina[5], E. Nogales[1,2]**, and B.T. Nixon[3]*, "The Structural Basis for Regulated Assembly and Function of the Transcriptional Activator NtrC," Gene. Dev. **20**, 1485 (2006).
DOI: 10.1101/gad.1418306

Author affiliations: [1]University of California, Berkeley; [2]Lawrence Berkeley National Laboratory; [3]The Pennsylvania State University; [4]University of Georgia; [5]Illinois Institute of Technology
Correspondence: *btn1@psu.edu for SAXS/WAXS, **enogales@lbl.gov for EM

This work was funded by a Genomes to Life grant from the U.S. Department of Energy to E.N. and B.T.N. E.N. is a Howard Hughes Medical Institute Investigator. Bio-CAT is a National Institutes of Health-supported Research Center grant (No. RR-08630). Use of the Advanced Photon Source was supported by the U.S. Department of Energy, Office of Science, Office of Basic Energy Sciences, under Contract No. W-31-109-ENG-38.

Understanding Protein Behavior

Many biological phenomena, both normal and pathological, involve protein molecules that trigger key events by attaching themselves to the outer membranes of cells. Understanding the functioning of cells, as well as developing new drugs and biomaterials, depends on a deep understanding of the changes that take place when proteins associate with these lipid membranes. Proteins may link to membranes by a variety of binding mechanisms and important conformational changes may occur during the attachment, but the full details of such processes are not clear. Recently, researchers from Sandia National Laboratories, the University of Delaware, Los Alamos National Laboratory (LANL), and the National Institute of Standards and Technology (NIST) revealed key structural aspects of lipid membrane changes during protein binding using the x-ray facilities at the APS and at HASYLAB in Germany. The cellular processes involved in such diseases as botulism, cholera, and tetanus involve multiple binding sites, so understanding the role of binding site multiplicity on cell membrane structure is crucial and studies such as this promise to help in understanding the nature of these interactions.

When proteins interact with natural cell membranes that consist of lipid layers, the membrane organization can undergo structural rearrangements. These alterations can depend on the complexity of the protein binding, and in particular whether the binding is via multiple or single sites. To study this process under controlled conditions requires use of a suitable model system to mimic the cell membrane. Real cell membranes expand and contract, so a realistic artificial system with similar properties must be employed. Langmuir monolayers, in which carefully chosen lipid molecules are floated on an aqueous substrate, offer a system in which surface area and pressure can be controlled and monitored during protein adsorption.

The research team studied structural changes in the metal-chelating lipid 1,2-distearyl-rac-glycero-3-triethyleneoxide iminodiacetatic acid (DSIDA) during interactions with myoglobin and egg-white lysozyme proteins. When the chelating sites of the lipid are loaded with copper or nickel ions, they will bind to the histidine residues on the protein molecules with known binding energies, depending on the ion. Myoglobin has five exposed histidines, whereas lysozyme has only one, making it possible to observe differences between single and multiple site binding.

X-ray reflection (XR) and grazing incidence x-ray diffraction (GIXD) studies were carried out at the XOR/CMC 9-ID beamline at the APS and at HASYLAB (Germany) beamline BW1. X-ray reflection measurements are useful for providing information about the amount of adsorbed protein and electron density profile within the monolayer normal to the interface, while GIXD can probe the structural changes in the plane of the membrane caused by protein binding. Neutron reflection studies at NIST and LANL provided data to complement the XR results. To create the lipid membrane samples, DSIDA was floated on a phosphate buffer solution in a Teflon© trough equipped with a moveable barrier to establish constant surface pressure. Protein was introduced behind the barrier and flowed into the buffer solution underneath the lipid monolayer.

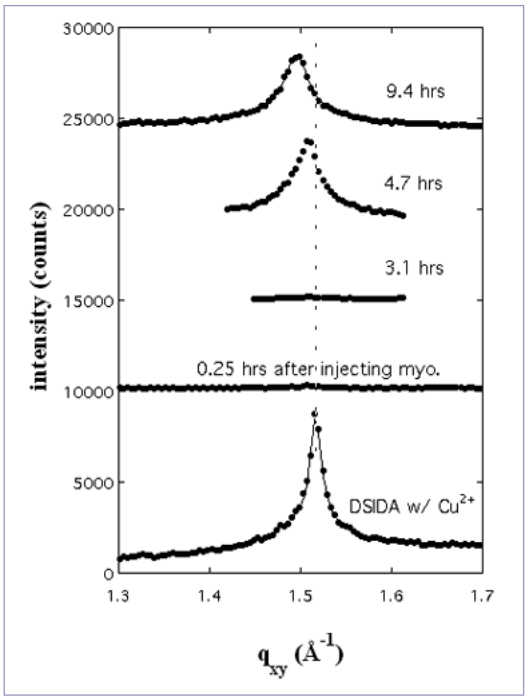

Fig. 1. Bragg peaks from GIXD data for DSIDA/Cu^{2+} films prior to injecting myoglobin and at various times after injection. Before injection, the sharp peak shows the ordering of the lipid membrane. Upon injection, the peak disappears, signaling breakup of the ordering. Several hours later an ordering, with a different hexagonal packing of the lipid molecules, appears.

The GIXD data show the rapid breakup of the ordered DSIDA packing after introduction of myoglobin onto a copper-loaded lipid membrane. After several hours a modified ordering emerged that indicated an increase in the size of the hexagonal unit cell of the lipid (Fig. 1). Nickel-loaded DSIDA showed a similar behavior, but over a longer time scale consistent with the weaker binding between the lipid system and the histidines.

Continued on page 66

FILLING THE GAPS IN COLLAGEN STRUCTURE

Collagens—we might take them for granted, but without them there would be no way to build tissues of the heart, skin, cornea, or bones. In much the same way that wood is used to frame a house and form a structure for the overlying construction materials, collagens are proteins used in the framing of mammalian tissues, but gaining an accurate picture of their three-dimensional structure in the body has proven more difficult. Knowing more about the structure of collagens could help biochemists improve their understanding of heart disease and cancer. Thanks to work by a research group based at the Illinois Institute of Technology and using the BioCAT 18-ID beamline at the APS, a complete structure for a collagen molecule—as it actually appears in the extracellular matrix (ECM)—is now available. This new knowledge of collagen structure provides important insights about several molecules involved in human disease.

The research group was able to determine a three-dimensional structure for a collagen (Type I from intact rat-tail tendons) as it would actually appear in the ECM. The structure is breathtakingly complex. The entire super-unit of collagen contains collagen segments packed together such that neighboring molecules, known as microfibrils, are super-twisted and then interdigitated with each other (Fig. 1). The interdigitation appears to be responsible for the super-lattice, which is constructed of quasi-hexagonally packed collagen molecules. The researchers constructed a new electron density map that, for the first time, clearly shows how all of the molecular segments, including the previously unresolved gap region, are situated (Fig. 1C). Also for the first time, the complete path of each collagen molecule can be visualized, including how the interdigitated microfibrils are arranged. And, perhaps most importantly, these data (Fig. 2) all pertain to the native structure of the collagen—how it would actually appear in living tissue.

The term "microfibril" has been used to name the basic units, or boards, of the frame created by the collagen molecules. The exact structure of the microfibril itself has been elusive—until now. By tracing the path of a single collagen molecule through several unit cells, the researchers solved this mystery. What their analysis reveals is that the microfibril is constructed of five one-dimensional, pleated collagen molecules, with a right-handed super-twist. This microfibril unit then packs with its neighbor to form the observed interdigitation. This intricate packing explains why individual microfibrils could not be isolated—it is not possible to remove them from the superstructure without destroying their own structure.

This new information about how the collagen molecules are stacked and connected makes it possible to develop hypotheses about how two molecules related to human disease—decorin and the Matrix Metallo-Proteinase (MMP)—behave. Decorin appears to be important in proper tissue construction via microfibrillar and fibrillar packing; when the gene for decorin is disrupted, fragile skin and connective tissue diseases, such as Ehlers-Danlos syndrome, can ensue. The new collagen structure provided by the research group shows sharp turns in a gap region, freeing up molecular space that could be used for decorin binding, especially on the surface of the struc-

Continued on page 66

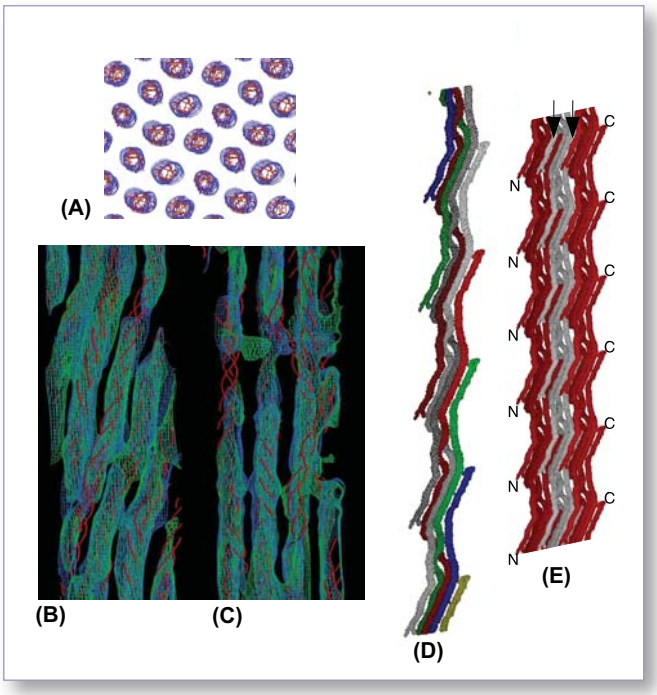

Fig. 1. (A) Cross-section of multiple unit cells of the crystalline lattice. (B) Overlap region of the 1-D repeat, with the triple helical backbone of the pre-refined model (red). (C) Same as B, except for the gap region where the super-twist occurs. (D) Two microfibrils, colored differently to easily identify the helical nature of the microfibril twist. (E) Same as D, except three microfibrillar structures are shown, packed together to reveal the interdigitation.

"Protein Behavior" continued from page 64

Upon injection of lysozyme, no change in the Bragg peak was observed, indicating the strong effect of binding site multiplicity on membrane reorganization. Synthetic peptides with two histidines also resulted in breakup of the membrane order, adding further weight to the picture of multiple site binding.

Several important disease processes, such as the binding of botulinum, cholera, and tetanus toxins, involve multiple binding sites, so the stakes are high for understanding the role of binding site multiplicity on cell membrane structure. Studies such as this may help elucidate the nature of these interactions. Moreover, the results show the key role that third-generation x-ray sources can play in providing high-brightness-input beams for precision structural analysis of biomembranes.

— *David Voss*

See: H. Yim[1], M.S. Kent[1]*, D.Y. Sasaki[1], B.D. Polizzotti[2], K.L. Kiick[2], J. Majewski[3], and S. Satjia[4], "Rearrangement of Lipid Ordered Phases Upon Protein Adsorption Due to Multiple Site Binding," Phys. Rev. Lett. **96**, 198101 (2006).
DOI: 10.1103/PhysRevLett.96.198101

Author affiliations: [1]Sandia National Laboratories, [2]University of Delaware, [3]Los Alamos National Laboratory, [4]National Institute of Standards and Technology
Correspondence: *mskent@sandia.gov

Sandia is a multiprogram laboratory operated by Sandia Corporation, a Lockheed Martin Company, for the United States Department of Energy under Contract No. DEAC04-94AL85000. Use of the Advanced Photon Source was supported by the U.S. Department of Energy, Office of Science, Office of Basic Energy Sciences, under Contract No. W-31-109-ENG-38.

"Collagen" continued from page 65

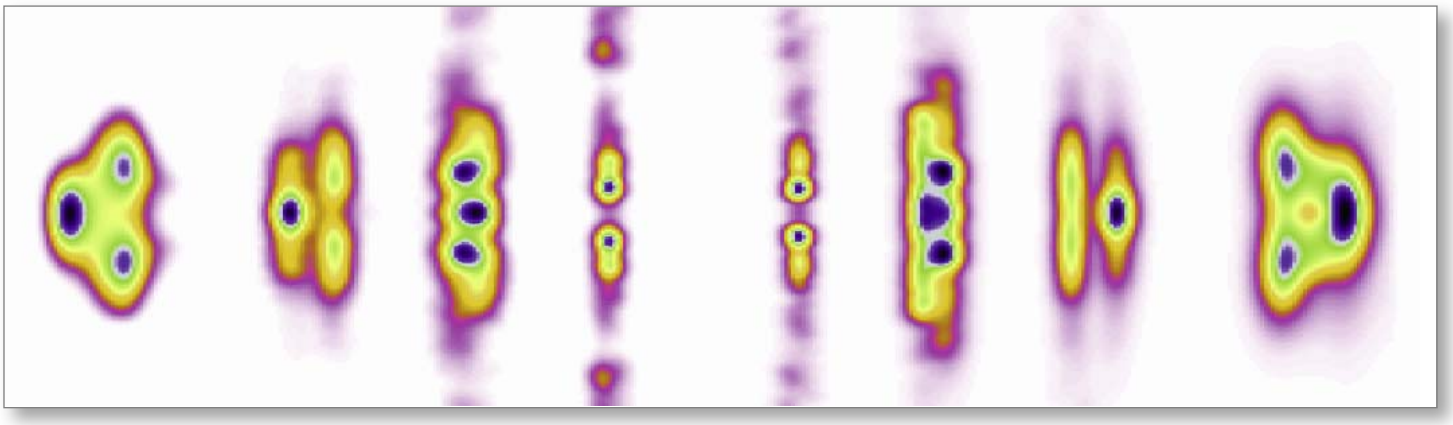

Fig. 2. Background subtracted off-meridian diffraction pattern of rat-tail tendon (left) and simulated diffraction pattern from model-derived intensities (right); the similarity between patterns shows the accuracy of the final model.

ture. Collagenase (MMP1), which is active in the extra-cellular matrix (and, when malfunctioning, is implicated in heart disease and cancer), is thought to rely on the superstructure of the collagen molecule for normal binding and activation. Now that this three-dimensional collagen structure can be clearly envisioned, exactly what happens when MMP functioning goes awry can be postulated.

The newly published collagen structure is especially important because it is specific with respect to the microfibrillar substructure, as well as the overall superstructure, which leads to important insights into the way collagen binds other extra-cellular matrix molecules. These data will fill in several gaps for researchers studying the biology of the extracellular matrix and related tissue disease, where framing is all-important in enduring stability. — *Mona Mort*

See: J.P.R.O. Orgel[1,2*], T.C. Irving[1], A. Miller[3], T.J. Wess[4], "Microfibrillar Structure of Type I Collagen *in situ*," PNAS **103**, 9001 (2006). DOI: 10.1073pnas.0502718103

Author affiliations: [1]Illinois Institute of Technology, [2]Rosalind Franklin University of Medicine and Science, [3]University of Stirling, [4]Cardiff University
Correspondence: *orgel@iit.edu

Thanks to the staffs of the Biophysical Collaborative Access Team, a National Institutes of Health-supported Research Center RR08630; the Structural Biology Center Collaborative Access Team, which is supported by U.S. Department of Energy Grant W-31-109-ENG-38; and the Southeast Regional Collaborative Access Team (supporting institutions may be found at www.ser-cat.orgmembers.html) for their assistance in the development of this project. This work was supported by American Heart Association Greater Midwest Affiliate Grant 0435339Z (to J.P.R.O.O.). A.M was supported by a Leverhulme Emeritus Research Fellowship. T.J.W. was supported by Biotechnology and Biological Sciences Research Council Grant BBS_B_09643. Use of the Advanced Photon Source was supported by the U.S. Department of Energy, Office of Science, Office of Basic Energy Sciences, under Contract No. W-31-109-ENG-38.

Pump Those Drugs Right Out of the Cell

Melanoma skin cancer cells are notorious for warding off anti-cancer drugs, especially those that head straight for the chromosomes or architectural scaffolding in cells. These drugs break up the DNA or demolish the internal support structures, thereby destroying dangerous cells. But melanoma cells are trained for destructive forces. After all, the healthy skin cells from which they arise have to deal with the harmful effects of radiation or nasty chemicals in their day-to-day task of protecting the body. Researchers from the National Cancer Institute, the National Institutes of Health, and Argonne decided to take advantage of XOR beamline 2-ID-D at the APS to probe the inner environment of skin cancer cells and determine where they hide a metal-containing drug that kills other kinds of cancer cells. The researchers found the drug compartmentalized in a spot where the drug would not have access to chromosomes and could be exported from the cell. Disrupting this system might disable melanoma's ability to deflect anti-cancer therapies.

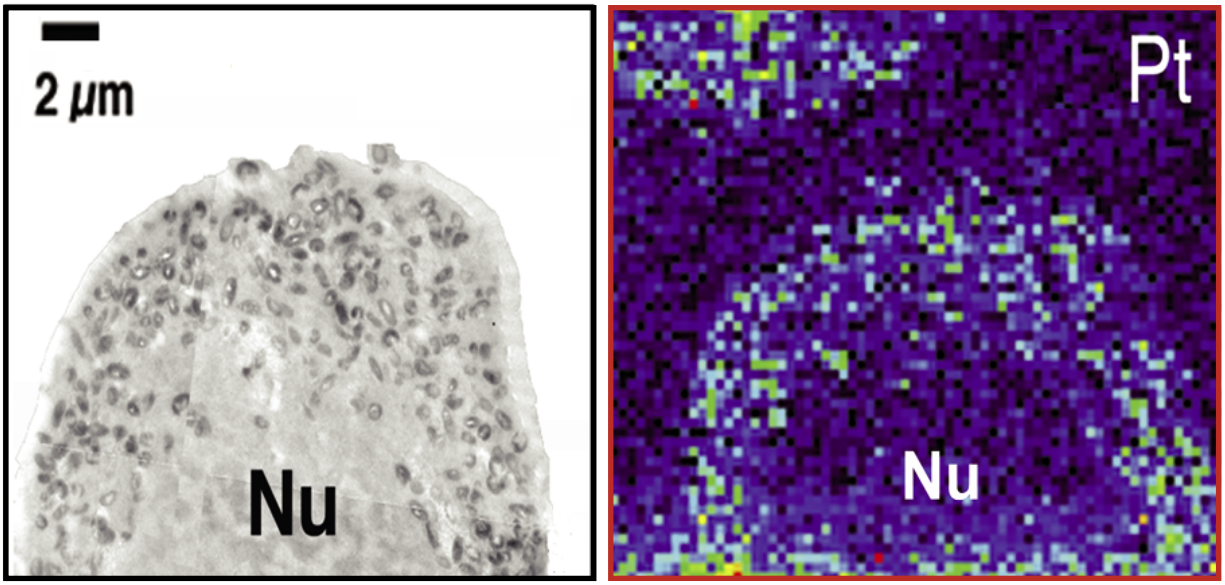

Fig. 1. A melanoma cell (electron micrograph, left) accumulates cisplatin (green and light blue dots, right) outside of the nucleus (Nu) in melanosomes.

The drug cisplatin destroys many kinds of cancer cells. But skin cancers called melanomas can withstand the drug's attack. Previous research at the National Cancer Institute suggested that cisplatin hides out in tiny structures in cells, called organelles. Some skin cells contain organelles called melanosomes, which under normal conditions make pigment. Because melanosomes are unique to cells that cause melanomas, the researchers decided to look in the melanosomes. Cisplatin contains a bit of the metal platinum, so the team could take advantage of Argonne's expertise with x-rays on biological systems to probe in cells and light up metal atoms.

To find out what the skin cancer cells are doing differently from other malignancies, the team compared where cisplatin settled in cultured melanoma cells to cultured non-melanoma, lung cancer cells, which are susceptible to the drug. The team added high concentrations of the drug to the growth medium of the two types of cells and determined the drug's location. Within cervical cancer cells, the drug moved into the nucleus, where the chromosomes reside. But far less cisplatin found its way into the skin cancer cells' nuclei. To get a less cluttered look, the team added a much lower concentration of cisplatin to

Continued on page 69

VERIFYING THE ACCURACY OF MOLECULAR TOOLS

Many cellular processes—from reproduction of our chromosomes to the ability of cells to respond to the environment—rely on the shape of DNA. Drugs that work by contacting DNA may not be effective on DNA molecules of unexpected shape. But when researchers study DNA, their conclusions are only as good as the tools they use. Because many such tools have been developed from rigid DNA molecules, researchers from Argonne, the University of Florida, and Northwestern University wanted to see how well such tools determined the form of the same molecules floating in solution, which can flex and more closely represent reality. But liquids add a lot of background noise to data collection in some kinds of experiments, so the researchers utilized the XOR/BESSRC 12-ID and 12-BM beamlines at the APS, where extremely stable x-ray beams and high-precision detectors let the researchers find their DNA molecules amid the fluidic cacophony.

DNA—the molecule that encodes genetic information in every living thing—is a relatively uncomplicated entity. Essentially the shape of a ladder whose stiles twist, packing the rungs to varying degrees of tightness, DNA molecules nevertheless take on several forms depending on which direction they turn and how tightly. Genes are encoded in so-called B form DNA. Some repetitious DNA sequences take up the slightly more tightly packed B′ form. Many tools that have been developed over the years to determine the form that DNA sequences take have been drawn from crystallized, immobilized DNA. This information is like a static photo. In reality, DNA molecules breathe and move, so researchers might be missing pieces of the puzzle. For example, experiments on fibrous DNA (which does not pack neatly into crystals nor float freely) indicated the B′ form exists, but researchers have never been able to crystallize B′ DNA. Therefore, the tools used to study DNA might lack representation of B′ form.

To determine how big a problem this might be, these researchers measured different sequences of DNA floating freely in solution, using the solution x-ray diffraction (SXD) technique. One sequence of DNA

Continued on next page

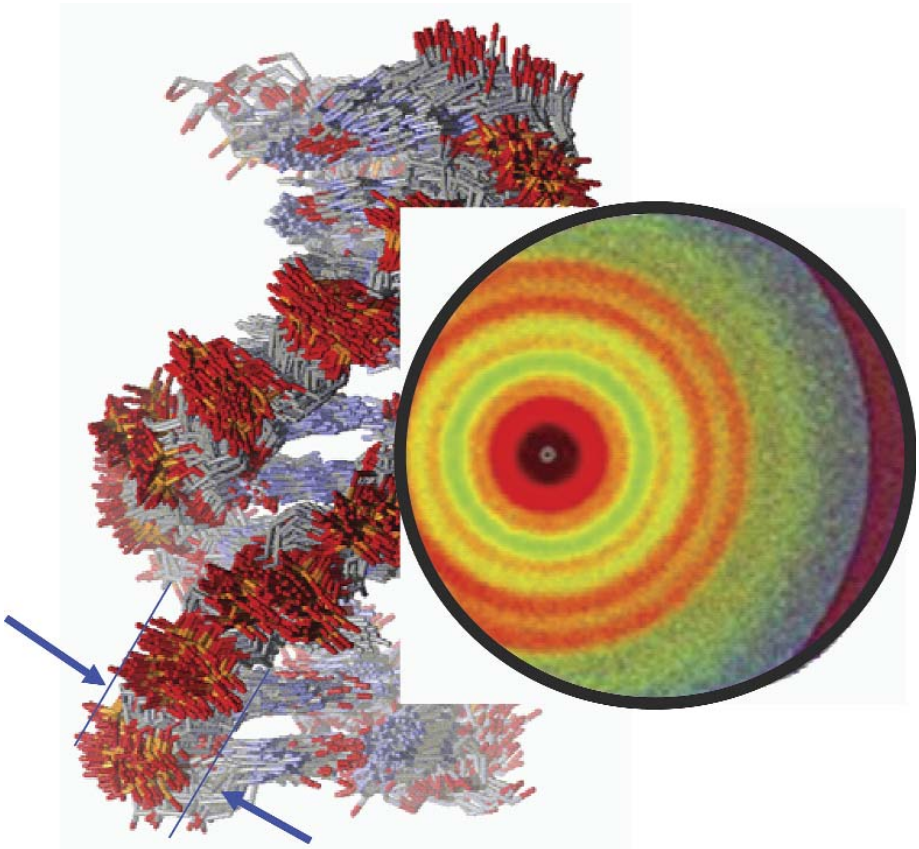

Simulated solution structure ensemble of a DNA molecule.

"Drugs" continued from page 67

the melanoma cells. Most of the drug within the cells was outside of the nucleus. Then the team marked the melanosomes with zinc. More than 50% of the cisplatin resided with the zinc in melanosomes, which remain outside of the nucleus.

Normally, pigment-producing skin cells send the pigment out to other skin cells, so the researchers wondered if the melanosomes dumped the cisplatin to prevent the accumulation of dangerous amounts. The researchers added the lower concentration of cisplatin to skin cancer cells. After two weeks, the team measured the amount of pigment the cells spit into the culture medium. The cells discharged seven times as much pigment in the presence of cisplatin than without, showing that the drug stimulated the melanosomes to work harder. Additional experiments showed that skin cancer cells with melanosomes already geared up to work overtime could withstand higher concentrations of the toxic drug. Lastly, the researchers determined that the pigment itself did not contribute to the drug resistance, as some data previously suggested. The work suggests that novel compounds that trip up the melanosomes might help drugs like cisplatin poison skin cancer cells. — *Mary Beckman*

See: Kevin G. Chen[1], Julio C. Valencia[1], Barry Lai[2], Guofeng Zhang[3], Jill K. Paterson[1], François Rouzaud[1], Werner Berens[1], Stephen M. Wincovitch[1], Susan H. Garfield[1], Richard D. Leapman[3], Vincent J. Hearing[1], and Michael M. Gottesman[1]*, "Melanosomal sequestration of cytotoxic drugs contributes to the intractability of malignant melanomas," Proc. Nat. Acad. Sci. USA **103**, 9903 (June 27, 2006).
DOI: 10.1073pnas.0600213103
Author affiliations: [1]National Cancer Institute, [2]Argonne National Laboratory, [3]National Institutes of Health
Correspondence: *mgottesman@nih.gov.

This work was supported by the Intramural Research Program of the National Institutes of Health, National Cancer Institute, Center for Cancer Research. Use of the Advanced Photon Source was supported by the U.S. Department of Energy, Office of Science, Office of Basic Energy Sciences, under Contract No. W-31-109-ENG-38.

"Molecular Tools" continued from page 68

was composed entirely of adenosine building blocks on one strand, which makes up one stile of the twisted ladder, and thymidine on the other (polyA). Another sequence of DNA consisted of alternating adenosine and thymidine building blocks along each strand (polyAT). Fibrous DNA experiments showed that polyA shapes up as B′ and polyAT settles comfortably as B form.

Analyzing the data using SXD showed that the polyA molecules are indeed of the B′ form, while the polyAT took B form. But when the team analyzed the data with a more common structural determination method—molecular dynamics (MD) simulations—they found MD identified both polyA and polyAT molecules as existing in B form DNA, indicating these computer programs can skew toward B form.

But these experiments are performed on a group of molecules, not just one. So the final result is a composite of the structures of the individual molecules. To determine whether MD completely missed the B′ forms of polyA, the team looked at more than 2,000 individual MD snapshots, each representing an individual molecule. They found that even though the overall MD picture of polyA was B form, about 20% of the individual snapshots were form B′. Having demonstrated the ability to discriminate the closely related duplex DNA B and B′ forms in solution, the researchers are working to extend SXD methods to more accurately determine the structure of pliant molecules. — *Mary Beckman*

See: Xiaobing Zuo[1], Guanglei Cui[2], Kenneth M. Merz, Jr.[2], Ligang Zhang[3], Frederick D. Lewis[3], and D. M. Tiede[1]*, "X-ray diffraction 'fingerprinting' of DNA structure in solution for quantitative evaluation of molecular dynamics simulation," Proc. Nat. Acad. Sci. U.S.A. **103**(10), 3534 (March 7, 2006).
DOI: 10.1073pnas.0600022103
Author affiliations: [1]Argonne National Laboratory, [2]University of Florida, [3]Northwestern University
Correspondence: *tiede@anl.gov

Simulations on the computing cluster, JAZZ, in the Laboratory Computing Resource Center at Argonne were supported by the Office of Basic Energy Sciences, U.S. Department of Energy, Contract W-31-109-ENG-38 (to Argonne National Laboratory). G.C. and K.M.M. were supported by National Institutes of Health Grant GM44974, and L.Z. and F.D.L. were supported by Department of Energy Contract DE-FG02-96ER14604. Use of the Advanced Photon Source was supported by the U.S. Department of Energy, Office of Science, Office of Basic Energy Sciences, under Contract No. W-31-109-ENG-38.

Secrets of a Secretion Apparatus in Bacterial Infection

A significant percentage of cystic fibrosis patients have lung infections caused by the bacterium *Pseudomonas aeruginosa*. The infections can be chronic or acute and are the main cause of death in patients afflicted with the disease. Figuring out just how the bacterium is able to wreak such havoc on lung tissue would be a major advance in fighting cystic fibrosis. Because disease-causing bacteria often use a secretion apparatus to invade the host, much recent work has focused on understanding the link between a virulence gene and a protein secretion apparatus in *P. aeruginosa*. The Midwest Center for Structural Genomics at Argonne—a program funded by the National Institutes of Health's Protein Structure Initiative—selected the protein called Hcp1 (a component of a secretion apparatus from *P. aeruginosa*) for structure determination. With the help of the SBC-CAT 19-ID beamline at the APS, fine details of this system have now been discovered by a research team from the Harvard Medical School, Argonne, and The University of Chicago. The group identified a protein important for proper functioning of the secretion apparatus, detected that protein in lung secretions from cystic fibrosis patients, and determined its three-dimensional structure. Not only is this finding of major importance in knowing how to treat cystic fibrosis, but it will also help in understanding how other disease-causing bacteria produce successful infections.

Continued on next page

The researchers focused on the known capacity for *P. aeruginosa* to create both acute and chronic infections, a feature that gives it some versatility as a pathogen. In an acute infection, the host can be debilitated and perhaps killed within a short period of time, whereas a chronic infection occurs at a lower level and would likely afflict the host over a longer period. Genes coding for factors known as "global virulence regulators" appear to govern whether the infection will be chronic or acute. In studying these virulence regulators, a previously undescribed virulence locus came to light. The investigators found that this gene was necessary for chronic *P. aeruginosa* infection of rat lung. In addition, they found the locus to be very similar to genes that mediate infection from other pathogenic bacteria by facilitating extracellular protein secretion.

Armed with these facts, the research group set out to test how making subtle changes in the gene complex would affect protein secretion. Using a series of analyses, the group identified the *P. aeruginosa* gene responsible for encoding the protein known as Hcp1. The gene is found within a locus regulated by the global virulence regulators, so the investigators have named it the "Hcp1 secretion island" within *P. aeruginosa*.

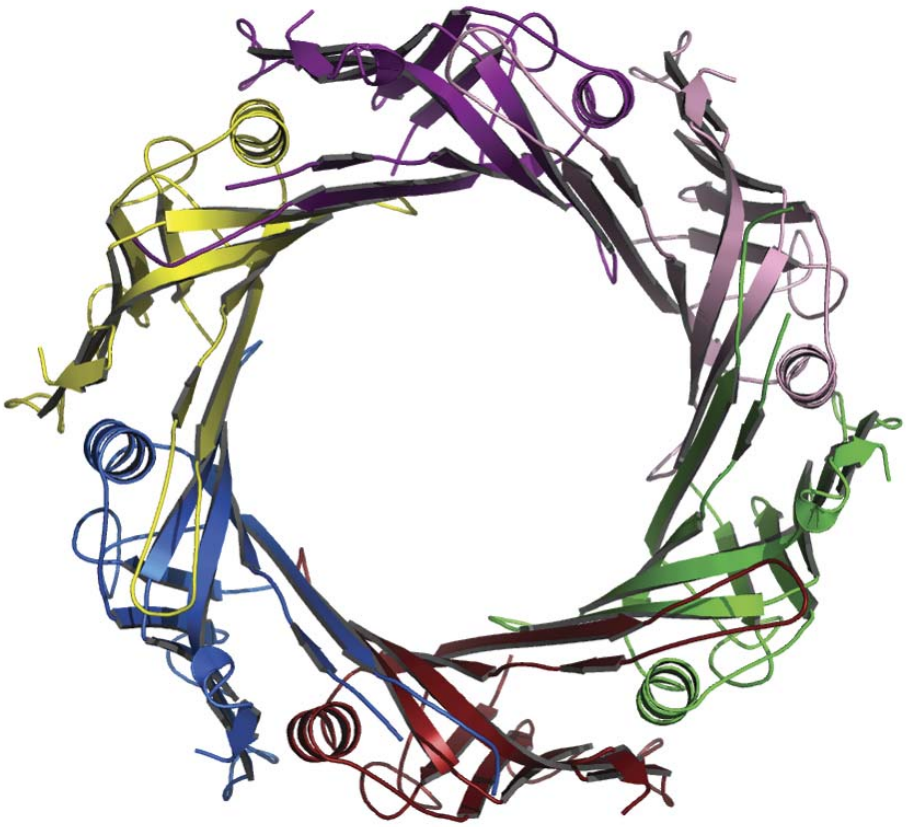

Fig. 1. Ribbon representation (top view) of the crystallographic Hcp1 hexamer, with individual subunits highlighted in different colors.

Through a series of careful analyses, including determination of the x-ray crystal structure of *P. aeruginosa* Hcp1, the experimenters definitively determined both the genetic locus and the protein essential for effective operation of the secretion apparatus. Interestingly, Hcp appears to be similar to the disease-causing organisms known as Gram-negative proteobacteria—including *P. aeruginosa*—but is very different from other proteins for which structures have been determined. The intriguing structure of Hcp1 is formed when six monomers assemble into hexameric rings with a pore-like structure (Fig. 1). The rings appear to be important physiologically and are the main form of the protein when it is in solution. Because the hexameric form of Hcp1 has a large diameter, the researchers propose that assembly of the intact particle most likely occurs after secretion.

The research group further refined the structural model by investigating which regions of Hcp1 would be important in making it biologically active. This analysis involved comparing the structure of 107 Hcp1 proteins from 43 bacterial species to find parts of the structure that were conserved. It appears that the top and bottom faces need to stay the same and are highly conserved, whereas those on the inner and outer circumferences are not conserved. This knowledge will be of particular importance in finding promising drug targets for foiling the bacterial secretion apparatus.

The extensive evidence—both biochemical and genetic—collected by the research group presents a very clear picture of how the HSI-I locus of *P. aeruginosa* encodes a protein secretion apparatus and plays an important role in chronic infections. These essential data will be used in developing vaccines and therapies for treatments of chronic *P. aeruginosa* infections in cystic fibrosis patients. The results of this work will also undoubtedly be applied to understanding the protein secretion apparatus of other related pathogenic bacteria, as well as to a general understanding of how disease-causing bacteria successfully invade their hosts. — *Mona Mort*

See: Joseph D. Mougous[1], Marianne E. Cuff[2], Stefan Raunser[1], Aimee Shen[1], Min Zhou[2], Casey A. Gifford[1], Andrew L. Goodman[1], Grazyna Joachimiak[2], Claudia L. Ordoñez[1], Stephen Lory[1], Thomas Walz[1], Andrzej Joachimiak[2,3]*, and John J. Mekalanos[1]**, "A Virulence Locus of *Pseudomonas aeruginosa* Encodes a Protein Secretion Apparatus," Science **312**, 1526 (9 June 2006). DOI: 10.1126/science.1128393

Author affiliations: [1]Harvard Medical School, [2]Argonne National Laboratory, [3]The University of Chicago

Correspondence: **John_Mekalanos@hms.harvard.edu; *andrzejj@anl.gov

This work was supported in part by grants to J.J.M. from the NIH (AI26289), to S.L. from the NIH (AI21451), and to A.J. from the NIH (GM62414 and GM074942) and the U.S. Department of Energy, Office of Biological and Environmental Research, under contract W-31-109-Eng-38. J.D.M. is a Damon Runyon Fellow supported by the Damon Runyon Cancer Research Foundation (DRG-1873-05). Use of the Advanced Photon Source was supported by the U.S. Department of Energy, Office of Science, Office of Basic Energy Sciences, under Contract No. W-31-109-ENG-38.

A Pac-Man-like Protein That Chews Up Insulin and Amyloid-Beta

The three-dimensional structure of insulin-degrading enzyme (IDE), a protein that breaks down insulin and amyloid-beta—the molecule implicated in Alzheimer's disease—has been determined by researchers from The University of Chicago and Argonne using beamlines 14-BM-C (BioCARS) and 19-ID (SBC-CAT) at the APS. The protein seems to alternate between two states—an open form that recognizes other proteins and a closed form that clamps shut around them and chops them up. The result may help in designing better drugs to treat diabetes and Alzheimer's.

Biologists have wondered how IDE recognizes and breaks down a wide variety of smaller proteins (called substrates) without molesting other proteins that have similar shapes. To find out, the University of Chicago-Argonne group made crystals of human IDE mixed with one of four substrates: insulin and amylin, hormones that lower blood sugar; glucagon, a hormone that raises blood sugar; and the brain protein amyloid-beta, a major component of protein plaques found in patients with Alzheimer's disease.

When the researchers determined IDE's structure from x-ray diffraction patterns obtained at 14-BM-C and 19-ID, they found that IDE consists of two large pieces—connected by a short loop—that close (Fig. 1) to form a chamber shaped like a prism.

The enclosed chamber prevents substrates from entering or leaving, meaning the two pieces of IDE must open to let in substrate. Once inside, the substrate must wedge itself into a cavity that breaks apart specific bonds holding the substrate together. The enzyme structure showed that the substrates twisted from their normal helix shape into a zigzag shape by the chamber, giving the enzyme better access to the bonds between substrate molecules.

The researchers identified several factors that allow IDE to recognize its substrates. Its bond-breaking cavity is relatively small—just large enough to accommodate insulin—and lined with positively charged molecules, which repel positively charged substrates. The precise shape of the substrate must also match up with those of the enclosed chamber and cavity.

The ability of IDE to break the bonds of its substrates seems to depend on the speed at which it can open and close. The researchers created mutant versions of the protein designed to loosen the connections between its two halves, or to solidify the link. The looser forms of the protein degraded substrate 30 to 40 times more rapidly, suggesting that the mutant protein is quicker to release chopped up substrates and accept new molecules. A stronger link between the two halves of IDE, in contrast, took away the enzyme's ability to degrade its substrates.

The researchers propose that certain chemicals could, in principle, change the rate at which IDE breaks down substrate. If so, they note, such compounds might help the body get rid of excess amyloid-beta, which seems to accumulate as plaque in the brains of people with Alzheimer's disease and may contribute to the memory loss that defines the condition. Similarly, the right compound might alter IDE's effect on insulin and help people with diabetes better regulate the concentration of sugar in their blood. — *JR Minkel*

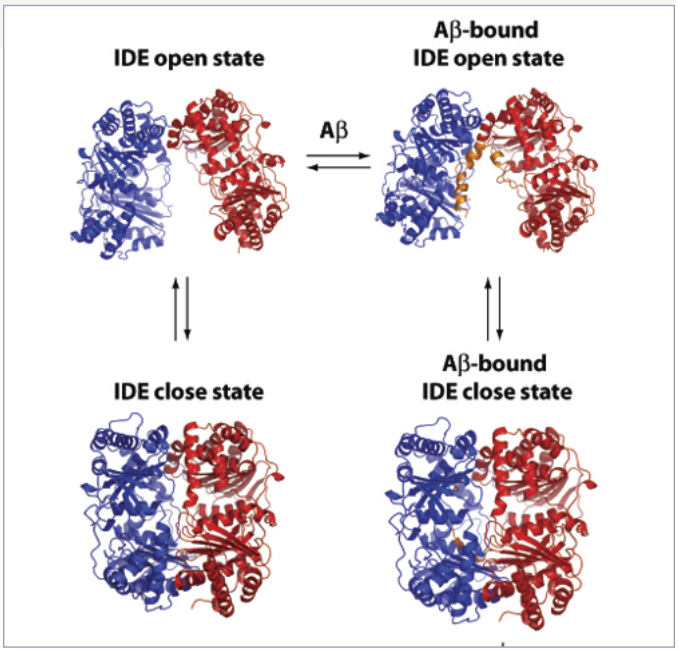

Fig. 1. The proposed degradation cycle of IDE, which has two domains (blue and red). Separation of these domains allows the capture of the brain protein fragment amyloid-beta (orange). The entrapment of amyloid-beta leads to its degradation.

See: Yuequan Shen[1], Andrzej Joachimiak[2], Marsha Rich Rosner[1], and Wei-Jen Tang[1]*, "Structures of human insulin-degrading enzyme reveal a new substrate recognition mechanism," Nature **443**, 870 (19 October 2006).
DOI:10.1038/nature05143
Author affiliations: [1]The University of Chicago, [2]Argonne National Laboratory
Correspondence: *wtang@uchicago.edu

This research supported by NIH and The University of Chicago Diabetes Center grants to W.T. Use of the Advanced Photon Source supported by the U.S. Department of Energy, Office of Science, Office of Basic Energy Sciences, under Contract No. W-31-109-ENG-38.

A Possible Parkinson's Protein Hinges Open and Shut

Degenerative brain disorders—such as Parkinson's and Alzheimer's—refuse to give up their secrets easily. To piece together the pathways that cause such conditions, one potentially informative method is to study the shapes of proteins involved in damaging or protecting brain cells. A team of researchers from Brandeis University and the Brigham and Women's Hospital and Harvard Medical School recently solved the three-dimensional (3-D) structure of a largely unstudied protein implicated in Parkinson's disease. Called ubiquitin C-terminal hydrolase (UCH-L1), it shows signs of being able to bend open and closed, and it is likely kept under tight control by a still mysterious partner protein, the team concluded. To begin shedding light on its exact biological role, the researchers reconstructed the structure of UCH-L1 on the basis of x-ray diffraction patterns obtained at GM/CA beamline 23-ID at the APS.

Parkinson's disease, like other progressive brain disorders, tends to leave deposits of unruly protein in the brain. UCH-L1 is an extremely abundant protein catalyst, or enzyme, in the brain, where it plays a role in removing proteins that have built up in cells and are no longer needed. Biologists believe it does so by severing a chemical bond between a protein called ubiquitin and another unknown protein, or substrate. Investigators have tied different forms of UCH-L1 to genetic propensities to develop or be resistant to Parkinson's, presumably because of the enzyme's ability to regulate protein buildup. UCH-L1 remains mysterious, however.

The researchers in this study found that UCH-L1 consists of two lobes. Between the lobes is a cleft containing several amino acids that are characteristic of an active site—the place on an enzyme that catalyzes a reaction. This study revealed that, by itself, UCH-L1 does not appear to be an active enzyme, because the key amino acids in its active site are too far apart to effectively work together, and the cleft is covered by a loop of protein.

Instead, this study shows that UCH-L1 is probably activated by its substrate. Viewed from one angle, the protein looks like a pie missing a single wedge where the substrate likely binds (Fig. 1). If any sizable protein inserted itself into this trough, its walls would bulge outward, disrupting some of the bonds that prevent the active site from adopting a more favorable shape, the researchers maintain. As a result, the loop covering the active site should get pushed out of the way. Consistent with this idea, the loop contains a hinge region in which two strands of protein seem to complement each other like a Velcro strap, suggesting that the hinge could unravel and become more flexible when jostled.

Although the structure suggests a mechanism of action for UCH-L1, it gives scant clue as to the protein's substrate and

Continued on page 75

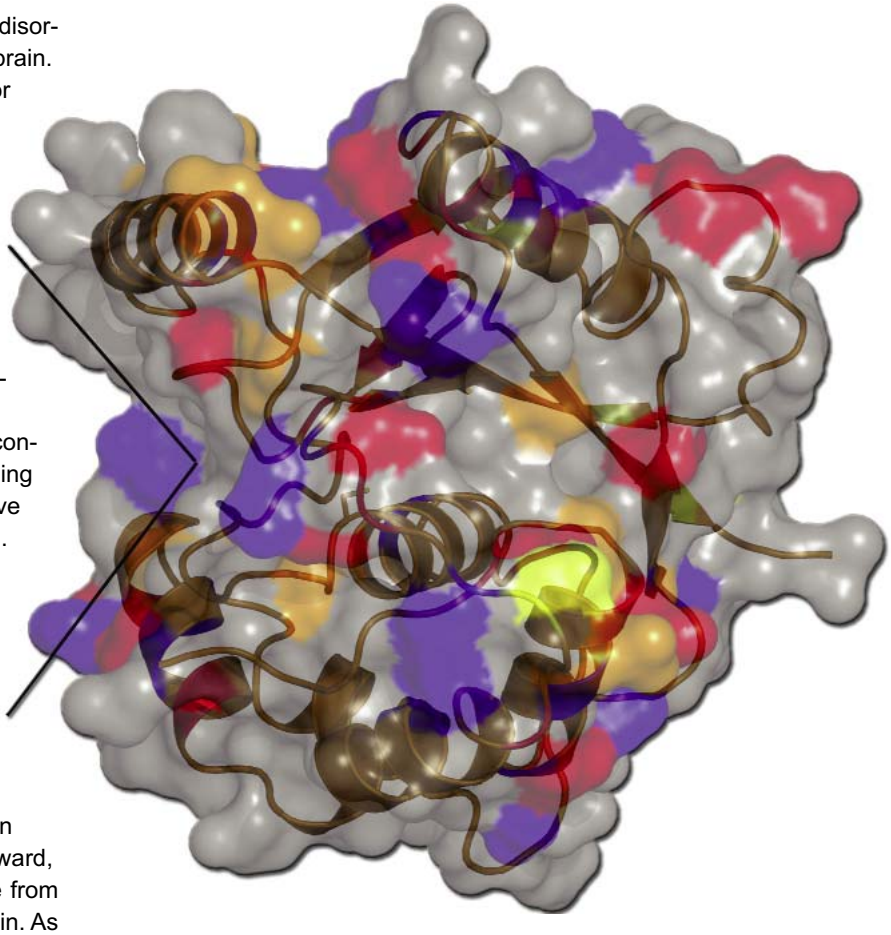

Fig. 1. The 3-D structure of UCH-L1 (brown ribbon diagram), a brain enzyme implicated in Parkinson's disease, overlaid with a schematic representation of the protein. UCH-L1 probably catalyzes a chemical reaction on another protein in a cleft between its two lobes (notch at left).

How An Amazing Hot-dog-fold Enzyme Smote the Aromatic

Bacteria are usually thought of in a negative, disease-causing context. But these simple microorganisms are playing a positive role in cleaning up environmental pollution. Employing naturally occurring biota to help clean up pollutants, a strategy known as bioremediation, is receiving increasing attention, mainly because it is a relatively safe approach and does not introduce chemicals that themselves need to be cleaned up. The bacteria used for eating aromatic compounds, which form carbon rings and are common in petroleum and many other sources of contamination, actually use the aromatics as sources of energy. In much the same way as wine makers use microorganisms to metabolize the sugars in crushed grapes and turn them into a desired by-product—alcohol—some bacteria have a biochemistry that allows them to use the aromatics as a source of nutrition and turn them into benign molecules. So, it makes sense to at least try to clean up an oil spill by inoculating it with bacteria that would naturally utilize the offending chemicals. But before bacteria can become bioremediation stars, we need to know more about how they metabolize pollutants. To that end, a research group from the University of New Mexico, Sloan-Kettering Institute, and Cornell University—employing the SGX-CAT beamline 31-ID at the APS—studied a bacterial enzyme used in degrading aromatics. Their work reveals important new details about the bacterias' structure and function, knowledge that not only provides much-needed basic biochemical details, but will also make it easier for researchers for researchers to predict how the bacteria will behave in the course of environmental cleanups.

The research group zeroed in on a particular enzyme system involved in degrading phenylacetate, which is important in pathways for breaking down a wide variety of natural and synthetic aromatics. Previous work had shown that, in the bacterium *Escherichia coli*, a gene cluster controlled 14 different proteins involved in the complex process of degrading phenylacetate. Within that group of 14, one gene—known as PaaI—had not been characterized with respect to its role in the degradation pathway. The product of the gene is a PaaI protein, which, because of characteristics including its final shape, belongs to the hot-dog-fold enzyme superfamily. Through careful analyses, the investigators were able to provide critical information about the structure and biochemical function of this enzyme (a thioesterase).

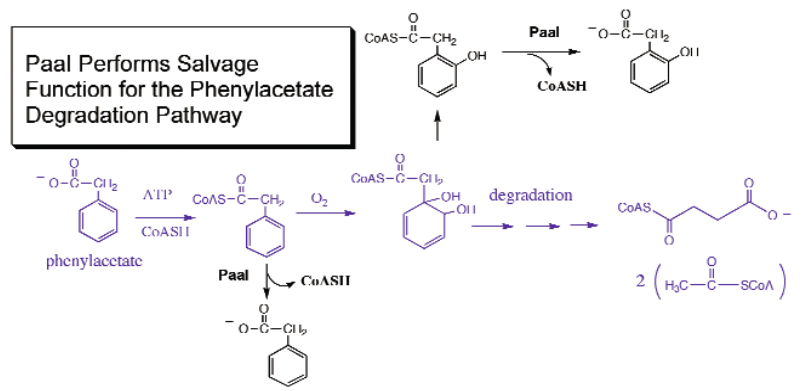

Fig. 1. PaaI catalyzed reactions (black) support the phenylacetate degradation pathway (blue) by releasing coenzyme A (CoASH) from the first intermediate of the pathway—when downstream pathway enzymes are lacking—and from the spontaneous dehydration (dead end) product of the second pathway intermediate.

First, the researchers used biochemical assays to show that PaaI was active in degrading phenylacetate in the bacteria *Arthrobacter evansii* and *E. coli*. Having shown that this enzyme plays an important role in this biochemical process, they were then able to pinpoint the role of PaaI by testing it on various intermediate products in the pathway. This work led them to rule out PaaI's role in the lower pathway and to find where in the upper pathway its presence is critical. Locating that step, which is associated with the ring-hydroxylated thioesters, meant that the researchers could, at last, definitively assign a role for PaaI in the degradation of phenylacetate (Fig. 1).

Next, the group went on to determine the x-ray crystal structure of the PaaI thioesterase from *E. coli*. Knowing the structure makes it much easier to understand chemical behavior and to predict the binding and mechanistic attributes of the enzyme (Fig. 2). Without a definitive structure, such predictions are mere guesses.

Once they had a structure, the researchers could then predict how the enzyme would facilitate the recognizing and binding necessary at that particular point in the phenylacetate degradation pathway. Using mutant proteins that were specifi-

Continued on next page

"Parkinson's Protein" continued from page 73

therefore its possible role in Parkinson's. The substrate's structure should fit with the binding site of the protein, the researchers noted. They also speculated that the mutant forms of the protein—thought to protect against or confer susceptibility to the disease—probably have the same overall structure. The mutation linked to disease susceptibility affects the active site of the amino acids and would slightly change the structure there, perhaps reducing or enhancing the protein's affinity for its unknown substrate. The protective mutation alters amino acids on the surface of the protein and perhaps changes its interaction with other proteins. — *JR Minkel*

See: Chittaranjan Das[1,2], Quyen Q. Hoang[1,2], Cheryl A. Kreinbring[1], Sarah J. Luchansky[2], Robin K. Meray[2], Soumya S. Ray[2], Peter T. Lansbury[2], Dagmar Ringe[1,2], and Gregory A. Petsko[1,2]*, "Structural basis for conformational plasticity of the Parkinson's disease-associated ubiquitin hydrolase UCH-L1," Proc. Nat. Acad. Sci. USA **103**, 4675 (March 21, 2006). DOI: 10.1073pnas.0510403103

Author affiliations: [1]Brandeis University, [2]Brigham and Women's Hospital and Harvard Medical School
Correspondence: *petsko@brandeis.edu

GM/CA-CAT is funded in whole or in part with federal funds from National Cancer Institute Grant Y1-CO-1020 and National Institute of General Medical Science Grant Y1-GM-1104. Portions of this research were carried out at the Stanford Synchrotron Radiation Laboratory, a national user facility operated by Stanford University on behalf of the U.S. Department of Energy, Office of Basic Energy Sciences. G.A.P. is a Duvoisin Fellow of the American Parkinson's Disease Association. G.A.P. and D.R. are recipients of an award from the McKnight Endowment Fund for Neuroscience. Parkinson's disease work at Brandeis University was initiated with generous support from the Ellison Medical Foundation. Use of the Advanced Photon Source was supported by the U.S. Department of Energy, Office of Science, Office of Basic Energy Sciences, under Contract No. W-31-109-ENG-38.

"Amazing Hot-dog-fold" continued from page 74

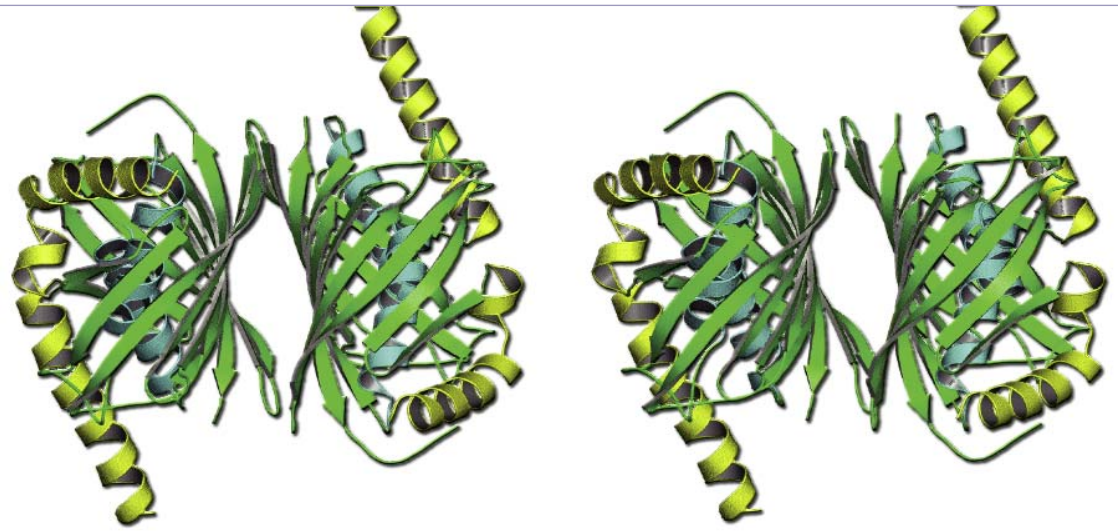

Fig. 2. A stereo picture of the PaaI tetrameric enzyme.

cally designed to answer questions about specifics, the investigators could provide beautiful detail about PaaI, where it is active in the pathway, and how it behaves.

The researchers performed further analyses to determine how PaaI fits into the evolutionary tree of the hot-dog-fold thioesterase superfamily. Interestingly, the structure of PaaI has diverged so that it specifically recognizes and is most active with certain intermediates and can liberate a molecule known as CoA. The present research reveals a function for PaaI to which it is well suited by its structure. The mystery of where PaaI acts in the phenylacetate degradation pathway has now been solved. In addition, these data provide critical information for the field of bioremediation, making it easier to use bacteria to smite aromatics before these pollutants can do significant environmental damage. — *Mona Mort*.

See: Feng Song[1], Zhihao Zhuang[1], Lorenzo Finci[1], Debra Dunaway-Mariano[1*], Ryan Kniewel[2], John A. Buglino[2], Veronica Solorzano[2], Jin Wu[3], and Christopher D. Lima[2], "Structure, Function, and Mechanism of the Phenylacetate Pathway Hot Dog-fold Thioesterase PaaI," J. Biol. Chem. **281**(16), 11028 (April 21, 2006). DOI: 10.1074/jbc.M513896200

Author affiliations: [1]University of New Mexico, [2]Sloan-Kettering Institute, [3]Weill Medical College of Cornell University
Correspondence: *dd39@unm.edu

Use of the SGX-CAT beamline facilities at sector 31 of the Advanced Photon Source was provided by SGX Pharmaceuticals, Inc., which constructed and operates the facility. Use of the Advanced Photon Source was supported by the U.S. Department of Energy, Office of Science, Office of Basic Energy Sciences, under Contract No. W-31-109-ENG-38.

A Vital Brain Receptor in 3-D

Throughout the brain and spinal cord, whenever one nerve cell wants to excite a neighboring nerve cell into sending an electrical signal, the molecule that kicks off that process is usually an amino acid called "glutamate." In the last five years researchers have made strides in understanding how glutamate causes receptor proteins on the surface of nerve cells to wink open and allow ions to flow inside the cell, a key step in creating that electrical signal pulse. Much of that progress has come from researchers solving the three-dimensional (3-D) structures of these glutamate receptors.

Glutamate receptors respond only to the amino acid glutamate and related molecules. Although one glutamate receptor-blocking drug exists for the treatment of dementia, so far the proteins are primarily a window into evolutionary history and basic biology. Evolution seems to have assembled the receptor from several pieces that can still be found in bacteria. The protein consists of three major domains, like scoops on an ice-cream cone. Within the cell membrane sits the ion channel domain, the component that opens to let ions through. The core domain contains a pocket for binding glutamate and is the engine that drives ion channel activation. The topmost domain controls assembly so that four subunits combine to form a functional dimer of dimers.

The most exciting recent advances have come from 3-D structures of the core domains bound to a large variety of different molecules, derived from studies at the SER-CAT 22-ID beamline at the APS and elsewhere [1]. These structures have allowed researchers to explore general models for how glutamate activates the receptor and how that activity is dialed up or down. In general, glutamate molecules wedge into two clamshell-like clefts on either side of the core domain (see Fig. 1). The core responds by pinching in the middle and thereby clamping down on glutamate. By inserting molecules of various sizes and shapes into the core and studying the resulting structure, groups have found that different molecules cause the core to pinch shut to varying degrees. The degree of clamping, in turn, determines how well the receptor is activated.

A broad-brush model for receptor activation has emerged based on these findings. When the core domain pinches in on itself, the dimers shorten and widen, pulling open the ion channel domain, somewhat like a pair of scissors. Researchers have identified crystal structures that correspond to this state. Chemicals that block the receptor jam the core domain in its resting position by physically obstructing the clefts and thereby preventing the core from pinching shut. The receptors can also become desensitized while still bound to glutamate. In this case, the pair of subunits in a dimer fall apart after briefly applying tension to the ion channel before closing the scissors again.

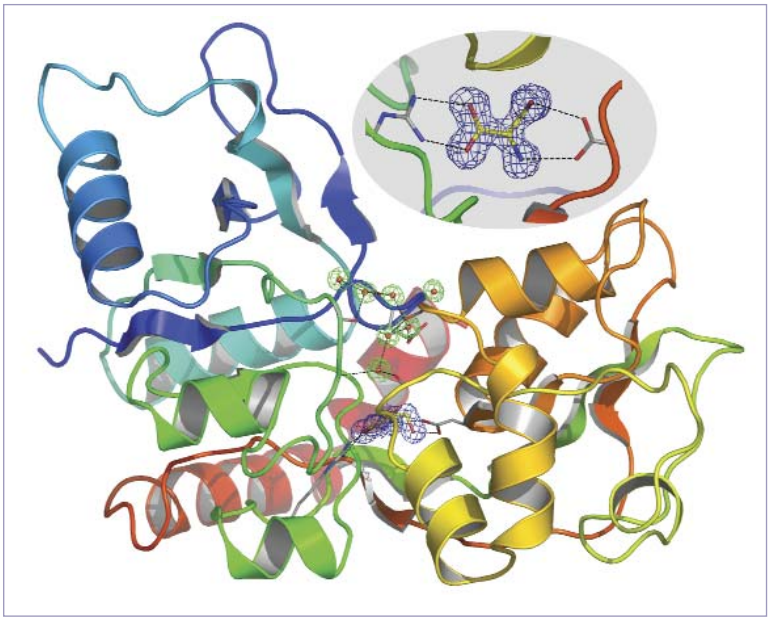

Fig. 1. The amino acid D-serine (inset) buries itself deep in a glutamate receptor called NR3A in this schematic representation of the receptor's 3-D structure. D-serine lodges in a clamshell-like structure formed from two opposing domains of NR3A. Hydrogen bonds between the receptor and water molecules (groups of green circles) stabilize the clamshell's closure.

Researchers have recently obtained 3-D structures for the desensitized state. The ongoing challenge is to determine the structure of the ion channel domain in an intact receptor.

— JR Minkel

See: [1] Mark L. Mayer, "Glutamate receptors at atomic resolution," Nature **440**, 456 (23 March 2006). DOI: 10.1038/nature04709

Author affiliation: National Institutes of Health
Correspondence: mayerm@mail.nih.gov

Work in the author's laboratory is supported by the intramural research program of NICHD, NIH, DHHS. Synchrotron diffraction data were collected at the SER-CAT facility, which is operated by the University of Georgia on behalf of 25 academic, industrial, state, and federal institutions. Use of the Advanced Photon Source was supported by the U.S. Department of Energy, Office of Science, Office of Basic Energy Sciences, under Contract No. W-31-109-ENG-38.

Cellular Machines for Breaking Down RNA

Genes are stored as DNA, but when a cell needs a certain gene, it copies the DNA sequence into a closely related molecule of RNA, which is usually translated into a protein molecule that plays some important function in the cell. To prevent RNA molecules from being active for too long and interfering with each other's functions, the cell must rapidly chew up or degrade RNA molecules. In organisms such as yeast and humans, one major system for degrading RNA is the exosome, a poorly understood cluster of proteins that can grab onto RNA molecules to chop them up. To gain a better understanding of these cellular machines, researchers using the GM/CA-CAT 23-ID and NE-CAT 24-ID beamlines at the APS have solved the structure of a cluster of human proteins that breaks down RNA. The study is aimed at understanding how exosomes maintain the cell's balance of RNA, which is crucial for almost every aspect of a cell's life, including its growth and its ability to respond to the outside world in a timely manner.

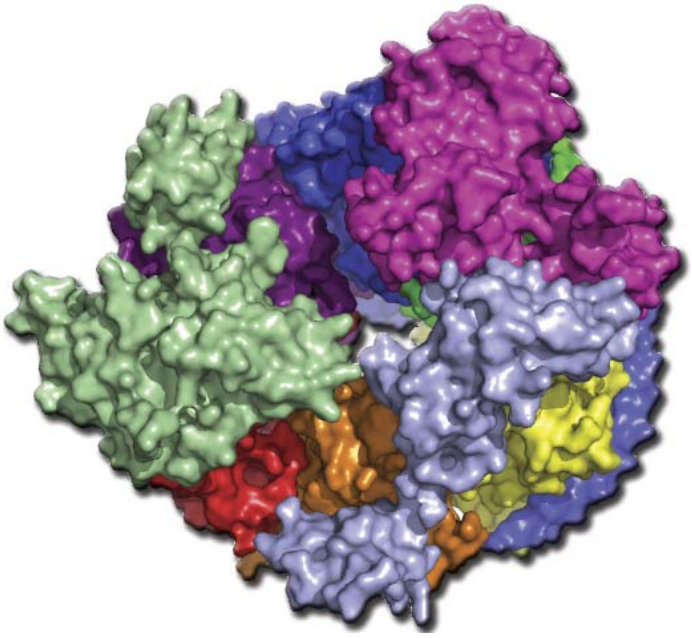

Fig. 1. Surface representation of the human RNA exosome using different colors for each of the nine protein subunits. Graphics prepared with PYMOL (DeLano Scientific, San Carlos, CA, USA. http://www.pymol.org).

The researchers, from the Sloan-Kettering Institute, reconstituted one human exosome and three exosomes from yeast. They were able to crystallize the human exosome, which consists of nine different proteins, and determine its structure by x-ray crystallography. Similar to related RNA-degrading bacterial proteins, the human exosome has a donut shape (Fig. 1) that may allow it to bring RNA molecules inside, where it can break their atomic bonds. The exosome's nine subunits fit together like a jigsaw puzzle, the team noted, which is consistent with the fact that all nine proteins were necessary to assemble a working exosome.

The researchers have been unable to determine the structure of the exosome when it is attached to RNA, so they cannot say exactly how the protein cluster performs that task. However, they did find that two of its subunits, when joined into a pair, were able to break down RNA. Combined with other experiments, the finding suggests that these two subunits were responsible for the exosome's RNA-degrading activity. The whole exosome was able to chew up RNA more rapidly than the pair of subunits alone, indicating that the other subunits may help hold RNA molecules in place or may stick to other proteins in the cell that help the exosome do its job.

The human and yeast exosomes contained different subunits and differed in their ability to break down RNA, which may help researchers identify roles for those subunits. One yeast exosome had nine subunits, like the human form, but was unable to degrade RNA. However, a yeast exosome with one additional protein was able to break down RNA, suggesting that yeast and human cells use different exosome subunits to break down RNA. The researchers also observed that an 11-subunit yeast exosome was able to chew up a different variety of RNA molecules. Taken together, these data suggest that yeast and human exosomes contain individual subunits with different activities, but that each set cooperates to target RNA molecules for destruction. — *JR Minkel*

See: Quansheng Liu, Jaclyn C. Greimann, and Christopher D. Lima*, "Reconstitution, Activities, and Structure of the Eukaryotic RNA Exosome," Cell **127**, 1223 (December 15, 2006).
DOI: 10.1016/j.cell.2006.10.037
Author affiliation: Sloan-Kettering Institute
Correspondence: *limac@mskcc.org

Use of the NE-CAT beamline is based upon research conducted at the Northeastern Collaborative Access Team beamlines of the APS, which is supported by award RR-15301 from the NCRR at the NIH. GM/CA-CAT has been funded in whole or in part with Federal funds from the NCI (Y1-CO-1020) and the NIGMS (Y1-GM-1104). C.D.L. is a Rita Allen Foundation Scholar. Use of the Advanced Photon Source was supported by the U.S. Department of Energy, Office of Science, Office of Basic Energy Sciences, under Contract No. W-31-109-ENG-38.

A Bump on the Road to Anonymity

Our immune system protects us from invading germs and microbes, but to do so it must be able to tell the difference between ourselves (the "self") and the outside world. Some viruses elude destruction by our immune systems by mimicking parts of the self. Researchers from Monash University, the University of Melbourne, Istituto Giannina Gaslini, and the University of Genova took a close look at how the immune system can distinguish between proteins that are of the self and those that are of foreign proteins. Using the BioCARS beamline 14-BM-C at the APS, the research team found that certain immune cells can distinguish a foreign protein from a self protein by identifying a single methyl group—a mere molecular bump on any protein.

While antibodies can efficiently mop up viruses before they infect cells, once a virus is inside a cell it is beyond the reach of antibodies. But the immune system has developed a way to recognize cells that harbor viruses. Almost all cells in the body express proteins on their surfaces that act as a flag for the immune system. Sometimes the flag denotes a healthy protein, and other times the flag calls attention to a virus that must be eradicated. Essentially, this flag is a bite off a larger protein from the cell, a small fragment called a peptide. Normally these peptides come from self proteins, but if a virus has invaded the cell, the cell displays a peptide from one of the virus's proteins instead. Immune cells (T cells) can recognize the viral peptide as foreign and kill the virus-carrying cell.

But cytomegalovirus—or CMV, a relatively harmless virus that infects most of the population but only causes problems in immune-suppressed people—fools the T cells by displaying a peptide that looks like self. In 90% of people, CMV gets away with this. But in the other 10%, CMV does not succeed and the CMV-carrying cells are killed off. Previous research suggests this is due to differences in the proteins (called the T cell receptor) on T cells that recognize the peptide.

To determine why the T cells from 10% of the population manage to stop CMV, the research team crystallized the proteins that negotiate the recognition. A protein called HLA-E holds the peptide like a sausage in a hot dog bun, showing off the peptide to T cells. The T cell receptor then feels the HLA-E and peptide combination. If the combination feels like self (whether it is self or CMV *pretending* to be self), the T cell goes on its merry way. But if the T cell receptor finds something odd, the T cell will destroy the cell.

The team made T cell receptors from a person (code named KK) in the 10% of the population that is not fooled by CMV's fake peptide, and used those T cell receptors in their crystals, together with HLA-E bound to the CMV mimic. With the high resolution afforded by the BioCARS beamline, the researchers could determine the features of the HLA-E/peptide combination the T cell receptor recognized.

The team found that certain finger-like projections of the T cell receptor contacted a methyl group at one particular spot on the CMV peptide (Fig. 1). Self peptides do not have this methyl group and so the T cell receptor does not recognize them. The results support the team's biochemical studies, which showed that KK's T cell receptors bind more tightly to the CMV peptide than to the self peptides, allowing the T cell to tell whether the peptide was foreign. — *Mary Beckman*

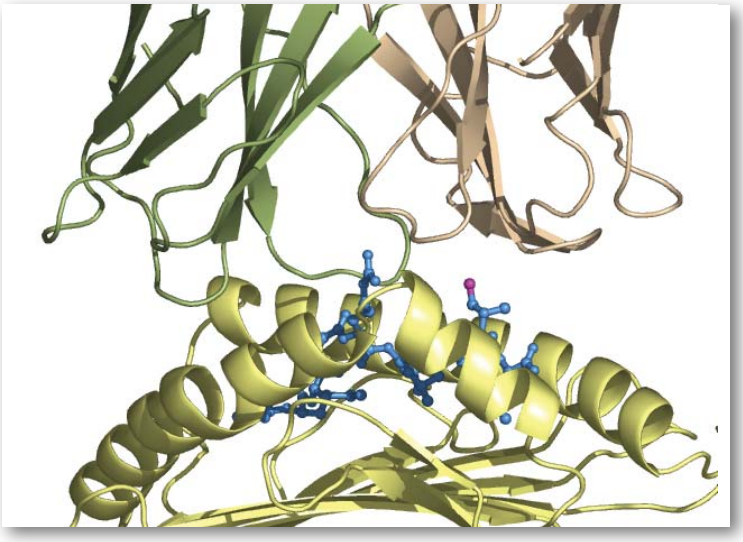

Fig. 1. A portion of the ribbon diagram of CMV. The methyl group (or "bump") is shown in pink.

See: Hilary L. Hoare[1], Lucy C. Sullivan[2], Gabriella Pietra[3,4], Craig S. Clements[1], Eleanor J. Lee[2], Lauren K. Ely[1], Travis Beddoe[1], Michela Falco[3], Lars Kjer-Nielsen[2], Hugh H. Reid[1], James McCluskey[2], Lorenzo Moretta[3,4], Jamie Rossjohn[1]*, and Andrew G. Brooks[2]**, "Structural basis for a major histocompatibility complex class Ib-restricted T cell response," Nat. Immunol. **7**(3), 256 (March 2006). DOI: 10.1038/ni1312

Author affiliations: [1]Monash University, [2]University of Melbourne, [3]Istituto Giannina Gaslini, [4]University of Genova
Correspondence: *jamie.rossjohn@med.monash.edu.au, **agbrooks@unimelb.edu.au

Financial support was provided by the National Science Foundation (DECS 0103297 and DMR 0504122). A.J.P. gratefully acknowledges additional support from Tyco Electronics. S.G.J.M. was supported by NSF DMR 0453856. Use of the Advanced Photon Source was supported by the U.S. Department of Energy, Office of Science, Office of Basic Energy Sciences, under Contract No. W-31-109-ENG-38.

Transporting Offenders on the Cellular Highway

Packaging matters. Just imagine being seduced by a beautiful label into buying a bottle of wine, even though you know you should not judge a wine by its label. Or moving a box of wine glasses to find half of them broken because they were not properly packed. In the world of the cell, just as in the macro-space inhabited by humans, packaging is critically important, especially when it comes to evicting foreign bodies such as viruses trying to establish and infect. In fact, one reason that the acquired immune deficiency syndrome-causing human immunodeficiency virus (HIV) is so successful is because it hijacks the cellular process that tries to isolate it and move it out of the cell, and then uses this system for its own reproductive cycle. Other viruses, including Ebola, are also known to operate in this manner. Knowing more about the packaging machinery—and the conveyor belt it creates in the cell—will help science in finding ways to combat viral infection and understand other metabolic defects caused by cellular packaging gone awry. A new study carried out by researchers from the National Institutes of Health with the help of the SER-CAT 22-ID beamline at the APS and beamline 9-2 at the Stanford Synchrotron Radiation Laboratory (SSRL), provides elegant details that bring a critical cellular trafficking step into clear focus, thereby advancing our understanding of certain viral infections, and how to combat them.

The researchers chose to study a middle section of the cellular conveyor belt called the endosomal sorting complex required for transport (ESCRT), which had already been shown to be critical for down-regulating receptors, creating lysosomes—the cellular trash baskets—and for proper budding of HIV. Focusing on ESCRT-I in yeast cells, the team studied three of the vacuolar protein sorting (Vps) proteins (Vps23, Vps28, and Vps37) that are involved in assembling the ESCRT-I core, a previously unsolved structure. Through a series of careful analyses, the research group determined the crystal structures of the Vps23:Vps28 subcomplex and of the Vps23:Vps28:Vps37 core.

The beautiful architecture of this section of the ESCRT-I complex arises from the dance between function and form. The core complex of ESCRT-I is a heterotrimer: it contains one unit each of Vps23, Vps28, and Vps37 (Fig. 1). Specific sections of the proteins, such as the C-terminal steadiness box of Vps23, the N-terminal half of Vps28, and the C-terminal half of Vps37, participate in assembly of the ESCRT-I complex. To correctly perform these functions, the underlying, or subunit, structure of each protein

Continued on page 81

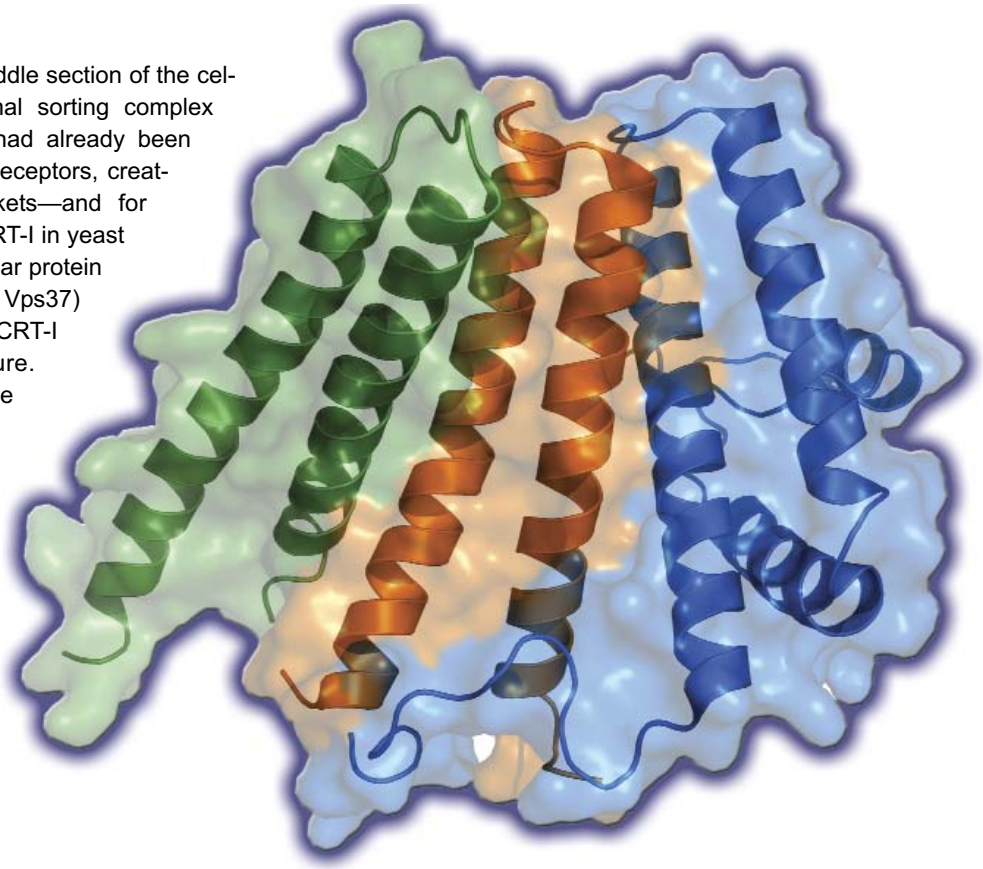

Fig. 1. Ribbon diagram of the ESCRT-I core complex, showing spatial relationships of the Vps37 (green), Vps23 (orange), and Vps28 (blue) helices.

Trying To Keep Herpes Viruses Out of Nerve Cells

Herpes simplex virus type 1, the scourge of kindergartens everywhere, is the culprit behind those ugly cold sores so many people grow up with. But it also represents a family of other herpes viruses that cause chickenpox, mononucleosis, and genital herpes, among other problems. Most people get infected with these kinds of viruses while quite young; afterwards, the viruses lie dormant in nerve cells for the rest of the person's life (some come back in adulthood, such as when chickenpox virus re-emerges as shingles). The viruses use a combination of proteins called glycoproteins to enter cells. Researchers from the Howard Hughes Harvard Medical Institute and the University of Pennsylvania used high-brilliance x-ray beams at the NE-CAT beamline 24-ID at the APS to probe the structure of HSV-1's glycoprotein B. Glycoprotein B surprised the researchers by looking quite a bit like the glycoprotein of an unrelated virus—a protein that can gets its virus inside cells without any help.

Herpes viruses are huge (by viral standards), and are coated in the same material that makes up cell membranes. This coat, a so-called "viral envelope," melts into cell membranes, creates a pore, and allows the virus to spill its contents—its genes and supporting proteins—into the cell, where it can cause disease while it reproduces itself. Embedded in that envelope are a variety of glycoproteins, some of which help the envelope fuse with cells. Scientists who want to develop drugs to keep these germs out are trying to understand the steps the glycoproteins take in molecular detail. Previous work has shown that all the viruses in the herpes virus family need at least three glycoproteins, gB, gH, and gL, to fuse. Of the three, gB has the most in common within the family.

To determine the physical structure of gB, the researchers first needed to coax the glycoprotein into crystallizing. However, the "glyco" portion of gB—sugar molecules attached to the protein—flop around and are of assorted sizes, making crystallization difficult. With only a handful of not-very-well-shaped crystals, the team turned to the 24-ID beamline, which provided a small-focus x-ray beam and required a short exposure time, allowing the team to collect significant amounts of data before the crystals were damaged beyond use.

Continued on next page

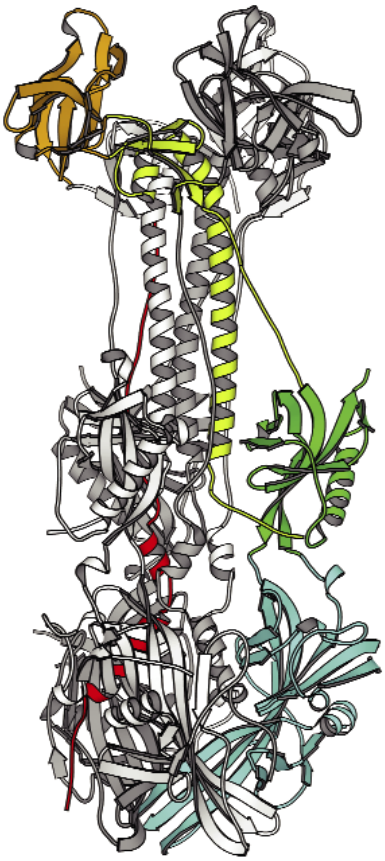

HSV-1 gB

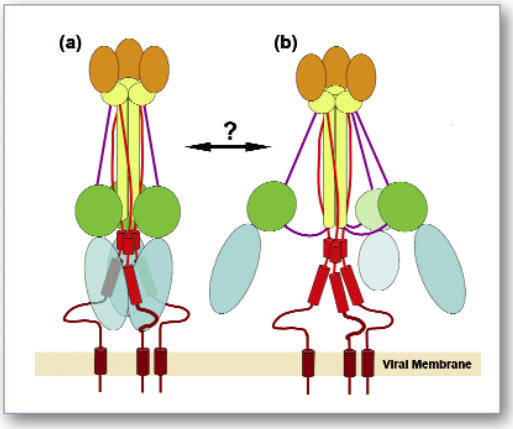

Fig. 1. Left: Ribbon diagram of the gB trimer. Bottom: Schematic model of gB, illustrating how it could refold in an umbrella-like fashion. (a) Structure determined in this work. Domains are shown schematically by using the color scheme in Fig. 1. The membraneproximal regions are shown as brown lines. Transmembrane regions are shown as brown cylinders. (b) The linkers leading into and out of the domain I-II module would permit a large-amplitude rotation. The structure described here might represent either the starting point or the endpoint of such a translocation, and thus it might have either a prefusion or a postfusion conformation (double-headed arrow).

© 2006 American Association for the Advancement of Science. All Rights Reserved.

"Herpes Viruses" continued from page 80

Often, crystallographers will be able to map the data they collect onto a previously determined structure of a related protein. But gB was the first of its kind, according to its sequence of amino acid building blocks, so the researchers had to start from scratch. After the painstaking work of translating the raw data into a physical structure, the researchers found that gB looked remarkably like an unrelated glycoprotein—glycoprotein G from vesicular stomatitis virus, a germ that causes fluid-filled blisters in animals and whose amino acid sequence differs radically from gB. And unlike gB, VSV G is all that's needed for the virus to get into cells. Comparing gB to VSV might help the researchers determine why gB needs the help of gH and gL.

The team also learned details about how gB might do its fusion job. To fuse viral envelopes with cell membranes, glycoproteins need to change shape, which enables the glycoprotein sitting on the virus to grab the cell and bring the virus and membrane together. The scientists found that gB looks like it could open like an umbrella does: fixed portions of gB are connected by flexible linkers. However, the team has yet to determine whether the gB they crystallized is the before-fusion shape or the post-fusion gB. They will need to determine that before using the structure to design anti-fusion drugs—drugs that might help with those ugly cold sores. — *Mary Beckman*

See: Ekaterino E. Heldwein[1,2]*, Huan Lou[4], Florent C. Bender[4], Gary H. Cohen[4], Roselyn J. Eisenberg[4], and Stephen C. Harrison[1,2,4], "Crystal Structure of Glycoprotein B from Herpes Simplex Virus 1," Science **313**, 217 (14 July 2006).
DOI: 10.1126/science.1126548
Author affiliations: [1]Harvard Medical School, [2]Laboratory of Molecular Medicine, [3]Howard Hughes Medical Institute, Children's Hospital; [4]University of Pennsylvania
Correspondence: *heldwein@crystal.harvard.edu

This work was supported by NIH grants AI065886 (to E.E.H.), AI049980 (to S.C.H.), and AI056045 and NS36731 (to R.J.E.). S.C.H. is an investigator in the Howard Hughes Medical Institute. Use of the Advanced Photon Source was supported by the U.S. Department of Energy, Office of Science, Office of Basic Energy Sciences, under Contract No. W-31-109-ENG-38.

"Transporting Offenders" continued from page 79

has a common element: a core consisting of two helices, while also exhibiting differences critical to their different duties. For example, a hydrophobic binding site on the surface of the N-terminal domain of Vps28 allows it to undergo critical changes in shape that permit correct assembly of the complex. In this same protein, Vps28, the C-terminal domain binds another endosomal sorting complex, ESCRT-II.

The research team then went on to use their detailed structure of ESCRT-I to produce a model for assembly of these very important trafficking molecules. From the compact core of ESCRT-I, domains from Vps23, Vps28—and from other proteins—project to bind additional components needed in this particular section of the cellular conveyor belt. To validate their model, the researchers demonstrated that the subunit interfaces evident in the crystal structure were essential for assembly and proper functioning of ESCRT-I in living yeast cells.

The discovery of essential structural details was critical to postulating how assembly actually occurs in yeast and, because of the similarities in protein structure, in humans. The human ESCRT-I complex is expected to have a similar architecture, including the hydrophobic hole on its surface. Since the human ESCRT-I complex is essential to HIV budding, the hydrophobic hole is an attractive target for anti-HIV therapies involving small molecule inhibitors that would prevent the domain's ability to undergo necessary conformational changes.

Having a model for how the ESCRT-I assembles and makes itself available for binding other partners in the trafficking process is essential to understanding how foreign bodies (such as viruses) are moved along in the cell toward the lysosome, where they are then treated as trash and degraded. Knowing how this process is supposed to work makes it much easier to understand how things can go wrong in both the normal metabolic cycle of the cell, and in allowing a virus to take over this cellular highway for its own purposes of procreating and eventually destroying its host. — *Mona Mort*

See: Michael S. Kostelansky[1], Ji Sun[2], Sangho Lee[1], Jaewon Kim[1], Rodolfo Ghirlando[1], Aitor Hierro[1], Scott D. Emr[2], and James H. Hurley[1]*, "Structural and Functional Organization of the ESCRT-I Trafficking Complex," Cell **125**, 113 (April 7, 2006).
DOI: 10.1016/j.cell.2006.01.049
Author affiliations: [1]National Institutes of Health; [2]University of California, San Diego
Correspondence: *hurley@helix.nih.gov

M.S.K. is a PRAT fellow of the NIGMS, NIH. This research was supported by NIH intramural support, NIDDK and IATAP, to J.H.H. and by the Howard Hughes Medical Institute to S.D.E. The SSRL, a national user facility operated by Stanford University on behalf of the U.S. DOE Office of Basic Energy Sciences, is supported by the DOE Office of Biological and Environmental Research and the NIH National Center for Research Resources Biomedical Technology Program and National Institute of General Medical Sciences. Use of the Advanced Photon Source was supported by the U.S. Department of Energy, Office of Science, Office of Basic Energy Sciences, under Contract No. W-31-109-ENG-38.

A Bird Flu Protein Link to Virulence

Smart viruses infect without killing the host, at least in the short term. In such low-level infections, the virus gains time to persist, reproduce, infect other individuals, and spread through the population. Some viruses persist in certain host populations without killing them, but in other hosts they have a rapid and deadly effect. The H5N1 virus strains responsible for recent lethal outbreaks of bird flu apparently existed for quite some time in wild goose populations without doing much harm. But when the same strains infected chickens, the results were disastrous, leading to high chicken mortality and a health risk for humans living in proximity. In fact, the risk of epidemic was considered high enough to lead China to institute large-scale killing of poultry to stop the spread of H5N1 influenza. Understanding just how this influenza virus succeeds in its virulent attack on chicken cells will not only help keep poultry healthy, but will also ultimately aid in combating the infection in humans. To that end, researchers from Baylor College of Medicine used the SBC-CAT 19-ID beamline at the APS to produce a detailed structure for an H5N1 protein linked to virulence. Their work—which was confirmed by a research group from the Chinese Academy of Agricultural Sciences—clearly links a section of the protein to increased virulence in chickens and represents great progress in understanding how to make the virus less effective in killing its hosts—including humans.

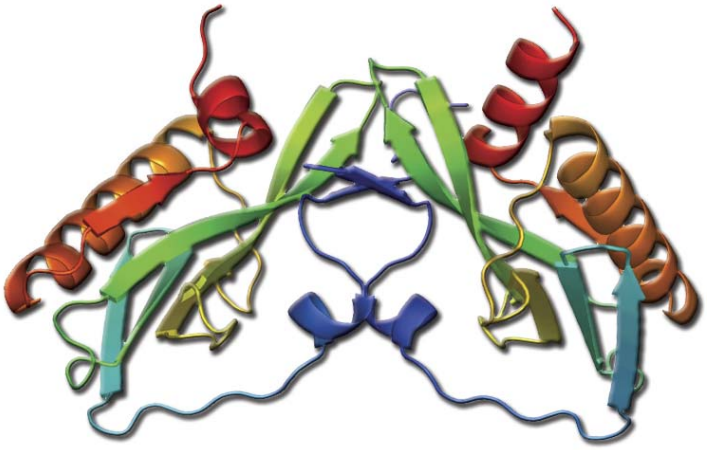

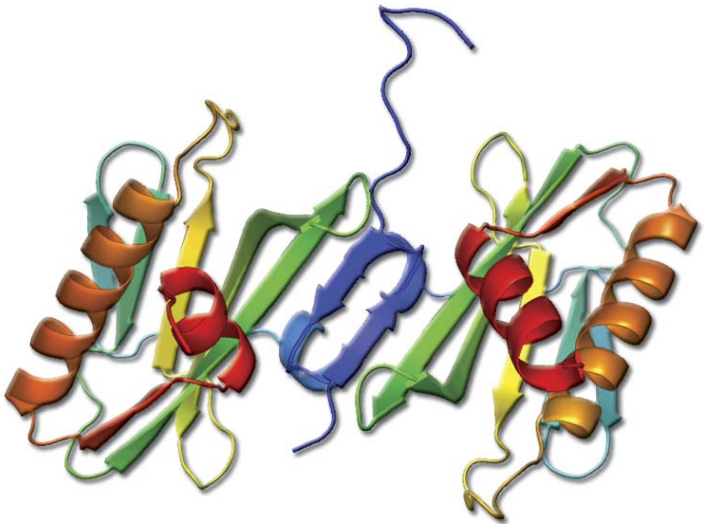

Left: Fig. 1. The x-ray structure of the effector domain of influenza virus NS1 protein. Each monomer subunit of the dimeric structure is depicted in rainbow colors from blue (N-terminus) to red (C-terminus). Right: Fig. 2. The x-ray structure of the effector domain of influenza virus NS1 protein, rotated by 90 degrees relative to Fig. 1.

The researchers from Baylor College of Medicine studied a protein—known as NS1—that had already been linked to the process that allows the H5N1 influenza virus to cripple the host's immune responses and thus become more deadly. The protein is thought to act by interfering with the double-stranded RNA activation of the host immune response, as well as blocking the mechanism by which host RNA is processed, thus destroying the cellular avenues used for fighting the virus. Until now, the exact details of how the protein carried out this dismantling of the host's immune system had been a mystery.

Because lethal H5N1 strains had been found to have mutations in the NS1 protein, this molecule has been of primary interest to the Baylor researchers. Genetic work done by the Chinese Academy of Agricultural Sciences team has definitively identified the NS1 gene as being responsible for the virulence of the lethal H5N1 strains in chickens [1]. So, a clear picture of the NS1 protein was urgently needed and has now been provided by the Baylor team.

The NS1 protein consists of two domains. One domain is known as the RNA-binding domain (RBD). The second domain

Continued on next page

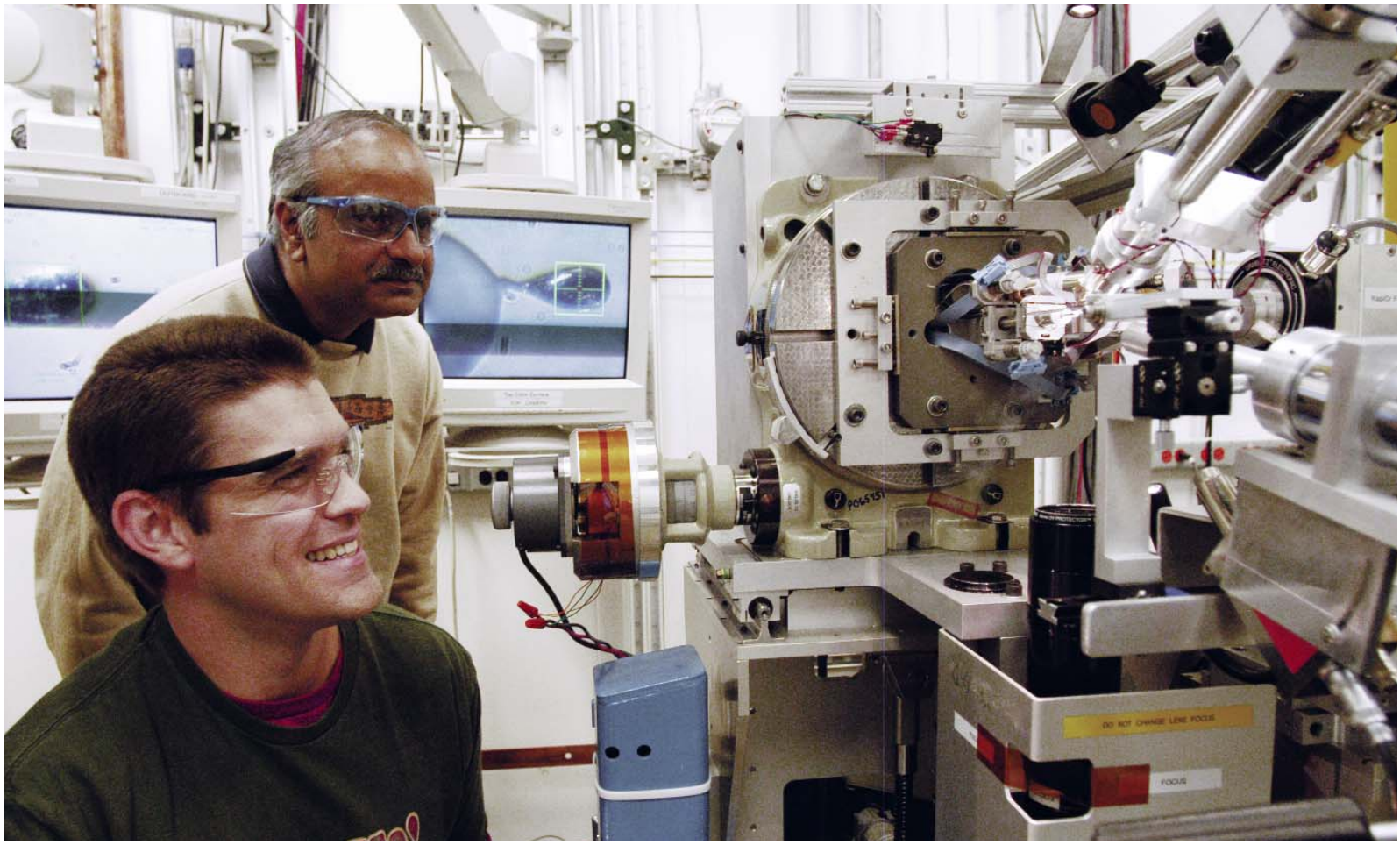

Zachary A. Bornholdt (foreground) and B. V. Venkataram Prasad in the SBC-CAT 19-ID research station.

is an effector domain that is important for proper RBD function, nuclear export, and sequestering of messenger RNA-processing proteins. It is this second domain—the effector domain—that the Baylor team found to be linked to virulence. Through careful analyses, the research team was able to determine the structure of the effector domain (Figs. 1 and 2). The structural data revealed a novel fold in the effector domain and also suggest how the H5N1 strains become more deadly in chickens.

In living cells, the NS1 effector domain most likely occurs as a dimer—i.e., with two monomeric subunits—and a fold, or cleft, that is structurally dynamic and probably linked to virulence. By analyzing the details of the structure, the Baylor team was able to propose that the known mutations in the NS1 protein lead to increased virulence by lowering the efficiency of phosphorylation of certain residues.

The team proposed a series of steps by which changes in the NS1 protein could lead to the virus having a more deadly impact on the host's immune response. Their data also allowed identification of important binding sites in the protein and made it much easier to understand how the effector domain is able to antagonize the host's interferon response. Future work can now concentrate on identifying additional functions of the effector domain and on identifying parts of the structure that would respond to antiviral drugs. The search for a way to make the bird flu virus less virulent has just become more focused.

— Mona Mort

Reference

[1] Z. Li et al., "The NS1 Gene Contributes to the Virulence of H5N1 Avian Influenza Viruses," J. Virol. **80**, 11115 (November 2006). DOI: 10.1128/JVI.00993-06

See: Zachary A. Bornholdt and B.V. Venkataram Prasad*, "X-ray structure of influenza virus NS1 effector domain," Nat. Struct. Mol. Biol. **13**, 559 (June 2006). DOI: 10.1038/nsmb1099

Author affiliation: Baylor College of Medicine

Correspondence: *vprasad@bcm.tmc.edu

This work was supported by the US National Institutes of Health (AI36040) and the Welch Foundation to B.V.V.P. and from a US National Institutes of Health virology training grant (AI07471) to Z.A.B.. Use of the Advanced Photon Source was supported by the U.S. Department of Energy, Office of Science, Office of Basic Energy Sciences, under Contract No. W-31-109-ENG-38.

Another Piece in the SARS 3-D Puzzle

The world held its breath in 2002 and 2003 as hundreds of people, primarily in Asia and North America, contracted Severe Acute Respiratory Syndrome (SARS), a never-before-seen, flu-like disease. Researchers identified the cause of the illness as a member of the coronavirus CoV family, which includes viruses that cause the common cold and a rodent form of hepatitis. SARS has not reappeared since 2004, but public health officials are keen on being prepared should it return. Scientists are making steady progress in solving the three-dimensional structures of proteins produced by the SARS virus. Cataloging the structures of these viral proteins should help in the effort to design drugs to disable them. Researchers from The Scripps Research Institute, using the GM/CA-CAT 23-ID beamline at the APS, as well as beamlines at two other U.S. Department of Energy light-source facilities, are trying to determine the structures and functions of all the virus's proteins and map their interactions with human cells. Their latest success is the structure of a small protein, nsp10, which likely plays a supporting role in the process by which the SARS virus reproduces itself.

Including nsp10, investigators have deduced the structures of part or all of 12 SARS CoV proteins, and 9 of them contain shapes that have not been observed before. To determine the structure of nsp10, the Scripps team crystallized the protein and obtained its x-ray diffraction patterns at the GM/CA-CAT beamline 23-ID at the APS (Argonne National Laboratory), the 8.2.1 beamline at the Advanced Light Source (Lawrence Berkeley National Laboratory) and the BL-11.1 beamline at the Stanford Synchrotron Radiation Laboratory (Stanford Linear Accelerator Center). Like several other SARS CoV proteins, nsp10 is folded into a shape that researchers have not observed in other protein structures. Mutations in a protein similar to nsp10 prevent the closely related rodent hepatitis virus from copying its genome, suggesting that nsp10 plays a role in the SARS CoV copying process. The protein's structure is consistent with its presumed role. Nsp10 adopts a novel oblong shape (Fig. 1) with two zinc atoms on its surface. These so-called zinc fingers are most often involved in binding to DNA or RNA—likely the latter in nsp10, because the SARS virus uses RNA for its genetic material. One side of the protein also has a positively charged patch on its surface, which, along with the zinc atoms, might help nsp10 stick to negatively charged RNA molecules during the copying process.

Previous studies have found that two other SARS CoV proteins, nsp7 and nsp8, combine to form a large cylinder-like assembly that threads RNA and is probably the core of the virus's copying machinery. Inside infected cells, nsp10 tends to associate with these proteins and others implicated in the copying process. The Scripps group suggested that nsp10 probably joins with the cylinder and other protein factors to direct RNA toward the enzyme that copies it.

These researchers have, to date, determined the partial or complete structures of six SARS CoV proteins, five of which have novel shapes. — *JR Minkel*

Continued on page 87

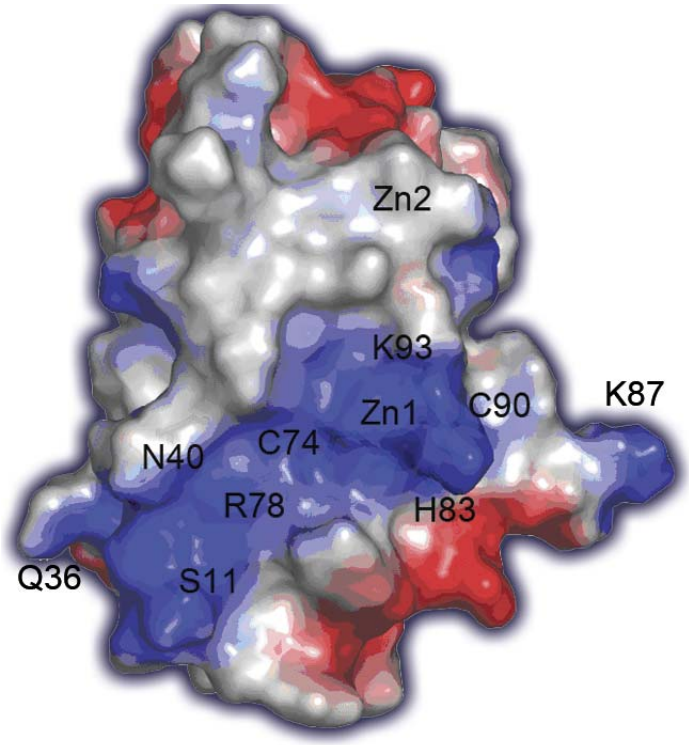

Fig. 1. The 3-D structure of nsp10, a protein that likely contributes to the ability of the deadly SARS CoV virus to copy itself.

Copyright © 2006, American Society for Microbiology. All Rights Reserved.

Proper Protein Delivery

Consider the relay race. Each runner on each relay team must be coached—pointed in the right direction and kept going in the right direction—in order to assure that the finish line is reached by the last runner in the team. Wrong turns or backtracking usually spell defeat. Similar events happen in a cell, but timing is even more critical. Molecules must end up in the right place at the right time, sometimes within nanoseconds, in order for metabolism to run well. There is a "coach"-like molecule called ubiquitin, because it seems to be everywhere and involved in lots of different relays. Ubiquitin and ubiquitin-like molecules are attached to proteins, most often on lysine residues, helping to ensure that those proteins end up in the right part of the cell. This is an important process; dire consequences can arise if it doesn't work properly and the proteins get lost. Much current research focuses on unraveling the fine details of ubiquitin's biochemistry. To that end, a research team from Sloan-Kettering Institute, using the SGX-CAT 31-ID and NE-CAT 24-ID beamlines at the APS, and National Synchrotron Light Source beamline X29A, studied a biochemical pathway for a small ubiquitin-like modifier called SUMO in order to understand how it behaves in cellular metabolism and how that behavior compares to what is known about ubiquitin. This study reveals important details about how proteins are modified with SUMO, making it easier to understand SUMO's roles in nuclear metabolism, cell-cycle control, and potential disease states caused by the absence of these important coaches.

The researchers focused on elucidating certain mechanisms in SUMO processing by determining crystal structures for SUMO precursors and SUMO-conjugated substrates in complex with a protease called SENP2 that can process SUMO precursors or cut SUMO off a substrate (Fig. 1). Using the structural data, the researchers could clearly model the steps by which the SENP2 protease interacts with SUMO and the substrate lysine, creating optimal conditions to liberate SUMO from the substrate. Since the SENP2 protease is central to this process, the team went on to study this enzyme in detail. What they found underscores how easily things can go wrong.

On the surface of the protease are amino acids that are responsible for making sure that the correct substrate is recognized—in this case SUMO attached to the substrate lysine. The researchers showed that, under certain conditions, specificity could be modified and even reversed.

To further understand the relationship between SUMO and the SENP2 protease, the research team performed mutational analysis and biochemistry. These data allowed the group to further explain why this protease is so good at releasing SUMO from substrate lysine residues, especially in comparison to other SENP2 reactions.

Using their detailed structural work, combined with biochemical analyses, the research team constructed a badly needed model for how the SENP2 protease interacts with SUMO, whether in a precursor form or when attached to a protein substrate. From this, we now have a much clearer picture of how the ubiquitin-like molecules detach from the load that they are ushering through the cell and leave it closer to the finish line. The end result of this process is that the ubiquitin-like molecules are then free to attach to the next molecule that needs guiding. *Continued on page 87*

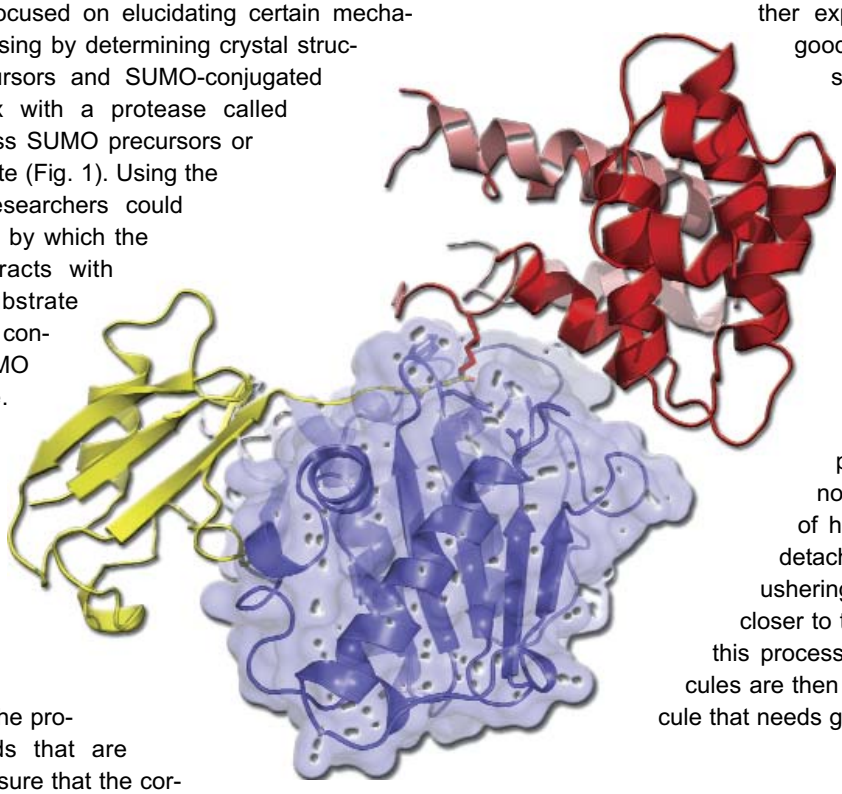

Fig. 1. Ribbon diagram representing the structure of the SENP2 protease (blue) in complex with SUMO (yellow) conjugated to RanGAP1 (red). SUMO is attached to a RanGAP1 lysine side chain within the SENP2 active site (center of the image). Graphics prepared with PYMOL (DeLano Scientific, San Carlos, CA, USA. http://www.pymol.org).

How Bacteria Succeed

Fighting bacterial infection is not easy—although it seemed so when antibiotics were first discovered—because the existing bacterial strains seemed to be rapidly eliminated by treatment with antibiotics. But then the ability of bacteria to develop resistance to commonly used antibiotics started to outpace our ability to discover new ones, resulting in the current critical situation: the existence of bacterial strains, such as some that cause tuberculosis, that have multiple drug resistance and leave the medical community wondering how to treat the infection. Most antibiotics work by interfering with a bacterium's biochemical machinery. Combining this knowledge with our increasingly sophisticated ability to design new drugs, the research community is intensely focused on understanding the particulars of bacterial biochemistry. What is especially critical is identifying the suite of molecules involved in replicating bacterial DNA, a necessary step for growth and reproduction. If bacteria can be prevented from reproducing in the host, then a bacterial infection can usually be brought under control quite quickly. Data collected by researchers from Yale University—using beamlines 19-ID (SBC-CAT) and 24-ID (NE-CAT) at the APS and Advanced Light Source beamlines 8.2.1 and 8.2.2—show the structure of a critical replication enzyme, elucidate its behavior, and point to promising ways in which to design new antibiotics. The implications of this work infuse hope into the search for treatment of multiple-drug-resistant bacterial infections.

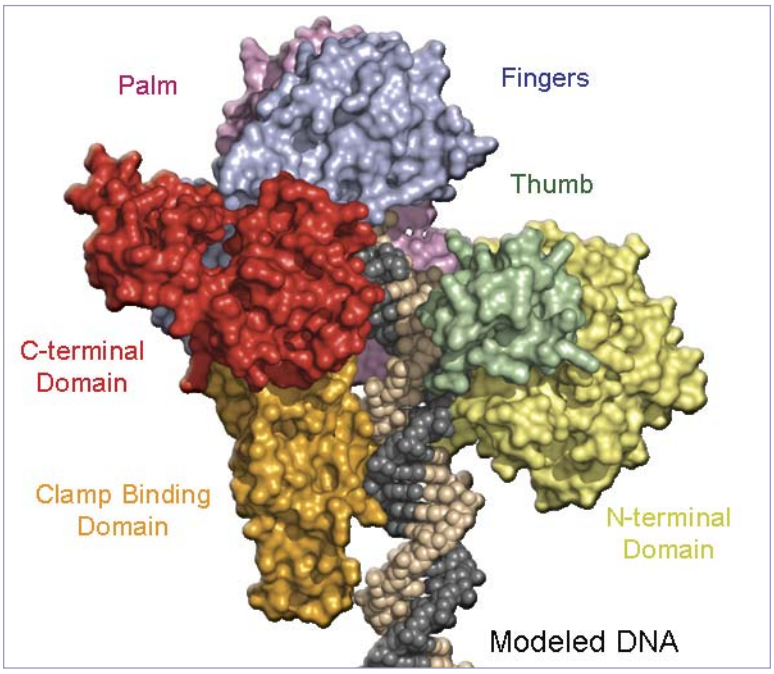

Fig. 1. DNA homology modeled onto the polymerase active site. The Clamp binding domain, N-terminal domain, and thumb have been repositioned such that they bind the modeled DNA.

In determining the crystal structure of a DNA polymerase IIIα subunit from the bacterium *Thermus aquaticus*, the researchers uncovered several previously unknown and, in some cases surprising, features of the enzyme (Fig. 1). First, the data revealed that the catalytic, or active, domain of this bacterial replicative polymerase is not related to the analogous replication enzyme in eukaryotes—organisms whose cells have a nucleus, such as humans. With respect to its structure, the bacterial enzyme belongs to an entirely different enzyme family, the βNT superfamily. That is really good news if one wants to design an antibiotic that will interfere only with the DNA replication in the bacterium trying to establish an infection and not also interfere with DNA replication of its human host. The replicase appeared to be an unusual member of its superfamily, where all of the other members are comparatively slow in terms of DNA replication. The polymerase IIIα, however, is really fast—incorporating thousands of nucleotides per binding event—making it capable of what is called high processivity, the first time this trait been shown in an enzyme from this superfamily. That is more good news for designers of antibiotics that could disable this enzyme, which is obviously a speed demon with respect to bacterial replication.

Second, the research team was able to use their data to model how the polymerase would behave in binding with DNA, which appears to interact with a domain that contains an internal binding site for attaching it to the sliding clamp. Their model agreed well with existing biochemical data on how the enzyme functions and the resulting products of that function.

Continued on next page

"SARS" continued from page 84

See: Jeremiah S. Joseph, Kumar Singh Saikatendu, Vanitha Subramanian, Benjamin W. Neuman, Alexei Brooun, Mark Griffith, Kin Moy, Maneesh K. Yadav, Jeffrey Velasquez, Michael J. Buchmeier, Raymond C. Stevens, and Peter Kuhn*, "Crystal Structure of Nonstructural Protein 10 from the Severe Acute Respiratory Syndrome Coronavirus Reveals a Novel Fold with Two Zinc-Binding Motifs," J. Virol. **80**, 7894 (August 2006). DOI: 10.1128/JVI.00467-06

Author affiliation: The Scripps Research Institute
Correspondence: *pkuhn@scripps.edu

This study was supported by National Institutes of Allergy and Infectious Disease/NIH Contract no. HHSN 266200400058C, "Functional and Structural Proteomics of the SARSCoV," to P.K. The General Medicine and Cancer Institutes Collaborative Access Team is supported by the National Cancer Institute (Y1-CO-1020) and the National Institute of General Medical Sciences (Y1-GM-1104). SSRL BL-11.1 is supported by the National Institutes of Health (NIH) National Center for Research Resources, NIH National Institutes of General Medical Sciences, Department of Energy, Office of Biological and Environmental Research, Stanford University, and The Scripps Research Institute. Use of the Advanced Photon Source was supported by the U.S. Department of Energy, Office of Science, Office of Basic Energy Sciences, under Contract No. W-31-109-ENG-38.

For more information on SARS CoV, visit the "Functional and Structural Protemics analysis of SARS-CoV related proteins" (FSPS) Web site at http://sars.scripps.edu. The goal of FSPS is to provide a comprehensive molecular characterization and cataloging of all SARS-CoV related proteins and associated functions at the viral and host levels.

"Protein" continued from page 85

When this system fails, the cellular coaches—the ubiquitin and ubiquitin-like molecules—are not able to aid in guiding the new molecules for the next relay race. It is easy to see how metabolic defects could arise from such a backup, with molecules potentially lost and unable to get to the right place at the right time for their cellular appointments.

The data collected in this study also make it much easier to see that, in the cell, protein delivery is anything but free.

— *Mona Mort*

See: David Reverter and Christopher D Lima*, "Structural basis for SENP2 protease interactions with SUMO precursors and conjugated substrates," Nat. Strct. Mol. Biol. **13** (12), 1060 (December 2006). DOI: 10.1038/nmat1593

Author affiliation: Sloan-Kettering Institute
Correspondence: *limac@mskcc.org

Use of the SGX-CAT beamline facilities was provided by SGX Pharmaceuticals, Inc., who constructed and operates the facility. Use of the NE-CAT beamline at the APS is based upon research conducted at the Northeastern Collaborative Access Team beamlines of the APS, which is supported by award RR-15301 from the National Center for Research Resources at the U.S. National Institutes of Health (NIH). Beamline X29A at the National Synchrotron Light Source is supported by the Offices of Biological and Environmental Research and of Basic Energy Sciences of the U.S. Department of Energy and the National Center for Research Resources of the NIH. D.R. and C.D.L. are supported in part by NIH grant GM65872. D.R. acknowledges support from the Charles H. Revson Foundation and C.D.L. acknowledges support from the Rita Allen Foundation. Use of the Advanced Photon Source was supported by the U.S. Department of Energy, Office of Science, Office of Basic Energy Sciences, under Contract No. W-31-109-ENG-38.

"Bacteria" continued from page 86

Third, the data create a new interpretation of biochemical evolution. The replicative polymerase studied—from a member of a group known as the eubacteria—is quite different from the replicase found in both the eukaryotes and another bacterial group known as the archaea. This finding raises extremely interesting questions: When did these enzymes emerge? What was the DNA polymerase in the last common ancestor? Did replication, and its associated enzymes, evolve independently in the two divergent lines? The researchers used their extensive data to develop fascinating hypotheses about possible ancestral enzymes, including an ancestral RNA molecule that served as an enzyme, also known as a ribozyme.

The surprisingly different structure of this bacterial replicase will require a rethinking of how bacterial and eukaryotic biochemistry are related to each other, an activity that will almost certainly lead to greater insights into how to keep bacteria from successfully infecting their human hosts. — *Mona Mort*

See: Scott Bailey, Richard A. Wing, and Thomas A. Steitz*, "The Structure of *T. aquaticus* DNA Polymerase III Is Distinct from Eukaryotic Replicative DNA Polymerases," Cell **126**, 893 (September 8, 2006). DOI: 10.1016/j.cell.2006.07.027

Author affiliation: Yale University
Correspondence: *eatherton@csb.yale.edu

This work was supported by NIH grant GM57510 to T.A.S. Use of the Advanced Photon Source was supported by the U.S. Department of Energy, Office of Science, Office of Basic Energy Sciences, under Contract No. W-31-109-ENG-38.

A New Class of Antibiotics

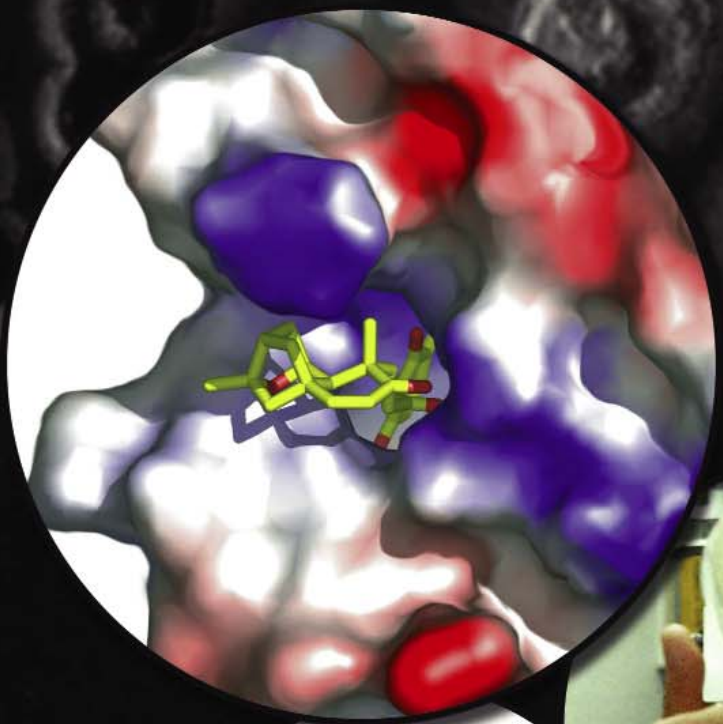

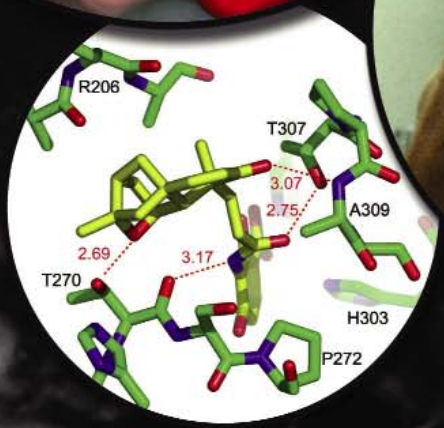

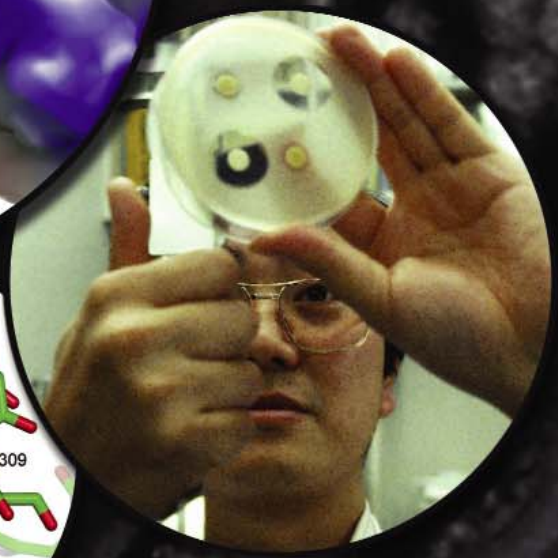

Bacteria, unlike viruses, tend to cause infections that can be treated with antibiotics, which act by throwing a wrench into the biochemical machinery. One hallmark of medical progress in the twentieth century was the successful use of antibiotics in treating bacteria-caused diseases, ranging from skin infections to pneumonia. The bacteria causing these infections, however, have proved remarkably resourceful in developing resistance, a phenomenon resulting in strains that are no longer killed by antibiotics commonly in use. Even more serious with respect to curing disease is that certain disease-causing bacteria, such as some strains causing tuberculosis, have developed multiple-resistance and are immune to available treatments. So it was welcome news when a group of Merck Research Laboratories scientists using the IMCA-CAT 17-ID beamline at the APS announced the discovery of a new class of antibiotics, known as platensimycin, which not only provides additional ways to combat bacterial disease but, most important, works in a unique way to inhibit bacterial infection, such that bacteria will most likely find it difficult to develop resistance to platensimycin.

By systematically screening 250,000 natural-product extracts, the Merck research team isolated the new antibiotic from a strain of *Streptomyces platensis* found in a soil sample collected in South Africa. Using the high-brightness x-ray beam at the 17-ID beamline, the group determined structures for platensimycin and discovered its unique method of combating bacterial infection by disrupting bacterial lipid biosynthesis. The researchers identified the antibiotic properties of platensimycin by studying its effect on *Staphylococcus aureus* in mice. Specifically, platensimycin exerts its antibiotic effect by selectively targeting an enzyme, known as FabF/B, in the biochemical pathway for synthesis of fatty acids. The investigators were able to fine-tune this knowledge of platensimycin's mode of action by using binding assays to show exactly where the platensimycin interacts with the target protein (Fig. 1). They then used x-ray crystallography to show that a conformational change must take place before platensimycin, consisting of two structural elements connected by an amide bond, can bind in such a way as to inhibit bacterial growth. Not only is the effect of platensimycin on the tested bacterial infection potent—it completely eliminated the *S. aureus* infection in mice—but it appears to act in a way that will make it difficult for bacteria to develop resistance to its inhibitory effects. Because of the complex way in which platensimycin interacts with FabF, the researchers propose that it would be unlikely that resistance could develop by mutation of the target protein.

The mode of action of platensimycin is considered to be unique in that no previously discovered antibiotics act by disrupting fatty acid synthesis. The selective mode of platensimycin's action was demonstrated by showing that it appeared to have no effect on the synthesis of DNA, RNA, protein, or the cell wall—strategies by which other antibiotics inhibit bacterial action. Platensimycin was also a strong inhibitor of important antibiotic-resistant strains tested, such as methicillin-resistant *S. aureus*, vanomycin-intermediate *S. aureus*, and vanomycin-resistant enterococci, and thus can be considered a broad-spectrum anti-bacterial agent. In addition, this new class of antibiotics appears to perform well in mice and show no observable toxicity in the treated mice.

The careful and detailed work by the researchers has identified an important new class of antibiotics and a new biochemical mechanism by which antibiotics can disrupt bacterial metabolism to inhibit their infection of mammalian hosts. Their work most certainly provides new tools for treating infections caused by bacteria showing multiple-resistance to antibiotics already in use. And, possibly even more important, the novel anti-bacterial mechanism discovered provides a new way to search for antibiotics that will be much more difficult for bacteria to resist. — *Mona Mort*

See: J. Wang*, S.M. Soisson**, K. Young, W. Shoop, S. Kodali, A. Galgoci, R. Painter, G. Parthasarathy, Y.S. Tang, R. Cummings, S. Ha, K. Dorso, M. Motyl, H. Jayasuriya, J. Ondeyka, K. Herath, C. Zhang, L. Hernandez, J. Allocco, A. Basilio, J.R. Tormo, O. Genilloud, F. Vicente, F. Pelaez, L. Colwell, S.H. Lee, B. Michael, T. Felcetto, C. Gill, L.L. Silver, J.D. Hermes, K. Bartizal, J. Barrett, D. Schmatz, J.W. Becker, D. Cully, and S.B. Singh***, "Platensimycin is a selective FabF inhibitor with potent antibiotic properties," Nature **441**, 358 (2006). DOI:10.1038/nature04784

Author affiliation: Merck Research Laboratories
Correspondence: *jun_wang2@merck.com, **stephen_soisson@merck.com, ***sheo_singh@merck.com

This work was funded by the Industrial Macromolecular Crystallography Association. Use of the IMCA-CAT beamline 17-ID at the APS was supported by the companies of the Industrial Macromolecular Crystallography Association through a contract with the Center for Advanced Radiation Sources at the University of Chicago. Use of the Advanced Photon Source was supported by the U.S. Department of Energy, Office of Science, Office of Basic Energy Sciences, under Contract No. W-31-109-ENG-38.

< Fig. 1. Background image: a culture of *Streptomyces platensis*. Superimposed, clockwise from top: platensimycin bound to its specific target; a scientist looking at antibiotic-treated pathogenic bacteria; interaction of FabF protein with the amide link and ketolide of platensimycin.

How a Deadly Virus Enters a Cell

Some viruses are simply strands of DNA or RNA and protein, while others are enveloped—they have their own membrane that must fuse with the host cell membrane to start entry. Some of the enveloped viruses, including those causing mumps and measles, belong to a family called the "paramyxoviruses." This group also contains many other human pathogens, such as the newly emergent—and deadly—Nipah and Hendra viruses. Knowing more about how these viruses get into cells is key to finding ways to combat the resulting infections. What is already known about the mechanism is elegant and involves two main players: an attachment protein, which varies among viruses and interacts with different cellular receptors, and a more conserved fusion (F) protein. The attachment protein drives and properly times F-mediated membrane fusion. Previous work on the F protein pointed to a tricky and irreversible refolding necessary for fusing the viral and host membranes, a progression making the best of jazz-fusion seem simple. For the first time, the intricate structural changes in a parainfluenza virus F protein have been visualized, thanks to painstaking work by a research team from Northwestern University using the DND-CAT 5-ID beamline at the APS and the Howard Hughes Medical Institute (HHMI) beamlines at the Advanced Light Source. Because of these new data, the search for a way to prevent viral entry is many steps ahead.

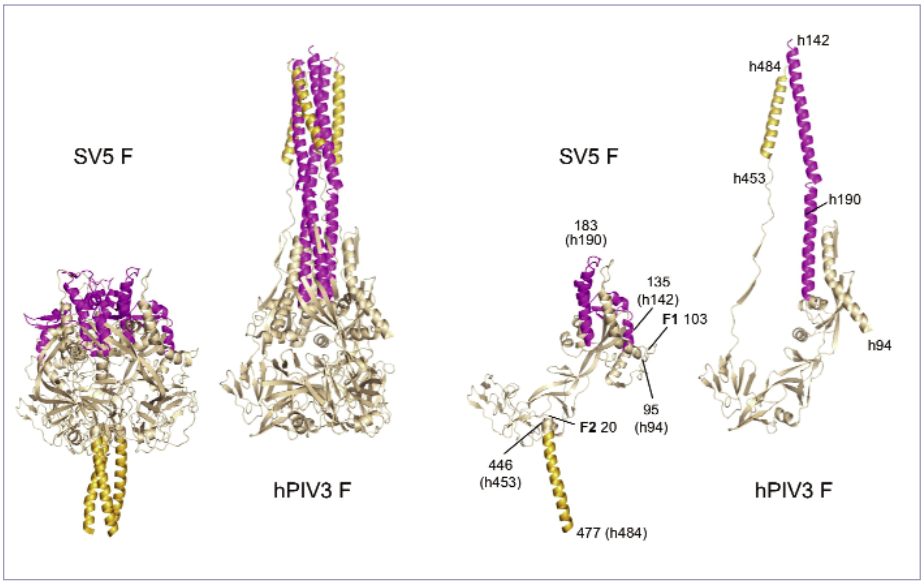

Fig. 1. Paramyxovirus F protein: structures of the prefusion and postfusion forms, shown progressing from left to right, with the prefusion SV5 F protein (shown as the biological trimeric form), the HRA region (magenta), and the HRB region (orange). The individual SV5 and hPIV3 F monomer structures are shown to the right of the trimers. The starting residues of the F1 and F2 regions present—after activating cleavage of the F protein—are labeled and key residues that change location are indicated. The numbers with the h prefix refer to the hPIV3 (postfusion) structure and are included in parentheses in the SV5 F monomer to enable comparison of the two structures.

The researchers already knew that the F protein looked markedly different before and after fusion. They wanted to know more about the exact structural changes and which of these were important to fusing the viral membrane with the host membrane. To answer these questions, the group determined the structure of the parainfluenza virus 5, known as SV5, F protein in its prefusion state, which was stabilized by adding a protein domain.

Viruses specialize in pleasing architecture, and this F protein is no exception. The F protein has a stalk formed by helical segments (called HRB) from each of three subunits, making a coiled-coil atop which rests a globular head. Within the head are three domains, two of which are rigid, with the third undergoing the main refolding as the F protein dances toward fusion. Within this third head domain is another segment (called HRA) that has the potential to form another long, three-stranded coiled-coil, but this segment is trapped in a condensed form in the head of the prefusion F protein. The investigators were able to identify a scaffold that controls the timing of changes in the HRA region so that the complex does not achieve its postfusion state before all other players are assembled. So

Continued on page 92

Breaking the Gridlock in RNA Synthesis

When the information contained in DNA is transcribed into RNA for further processing, a complex suite of associated molecules usually keeps the reaction chugging along smoothly and quickly. But, just like traffic flowing on a freeway can come to a sudden stop because of a wreck, an injury in the DNA strand can stall the reading of its message and create a backup. Because reading the DNA message in a timely manner is critical to normal metabolic functioning, elaborate and rapid repair mechanisms exist, ones that act like very efficient tow trucks, arriving to remove the cause of the blocked flow and get traffic moving again. The process is so efficient that a certain repair mechanism, known as transcription-coupled repair (TCR), specifically targets actively transcribing regions of DNA, where maintaining the flow is most important. The TCR mechanism kicks in when the transcribing enzyme, the RNA polymerase, stalls at lesions in the DNA template. With the help of the NE-CAT 8-BM and SBC-CAT 19-ID beamlines at the APS, researchers from the Rockefeller University, the University of Bristol, Harvard Medical School, and the University of Cambridge discovered important new details about the TCR process in bacteria. Their work begins to shed light on how "pile-ups" are prevented and, ultimately, how to keep DNA transcription from going awry to cause mutation and disease.

The researchers studied the transcription-repair coupling factor (TRCF) in the bacterium *Escherichia coli* because this protein, produced by the *mfd* gene, had already been shown to be critical for proper functioning of the TCR system. TRCF acts by removing RNA polymerase molecules (the machinery reading the DNA sequence and synthesizing the RNA) stalled at the site of the DNA lesion—much as a tow truck can take stalled cars away. At the same time, TRCF brings in the repair crew, the DNA excision repair machinery, to rectify the lesion in the DNA. TRCF also works in other metabolic reactions where RNA polymerase stalls at roadblocks and conflicts between transcription and DNA replication need to be dealt with. Despite such important roles, a detailed structural analysis of TRCF had been missing, until now.

Given these complex assignments, it is fitting that TRCF would have an elegant structure consisting of eight tightly packed domains. By comparing the TRCF structure to similar molecules, the investigators were able to envision how TRCF interacts with the RNA polymerase to terminate transcription and initiate excision repair. It seems that major changes in conformation have to occur in order for TRCF to perform its intricate duties. Using their carefully collected data, the group was able to develop a detailed model for how TRCF acts.

The complexity of the eight-domain TRCF structure is intriguing (Fig. 1). The researchers

Continued on page 92

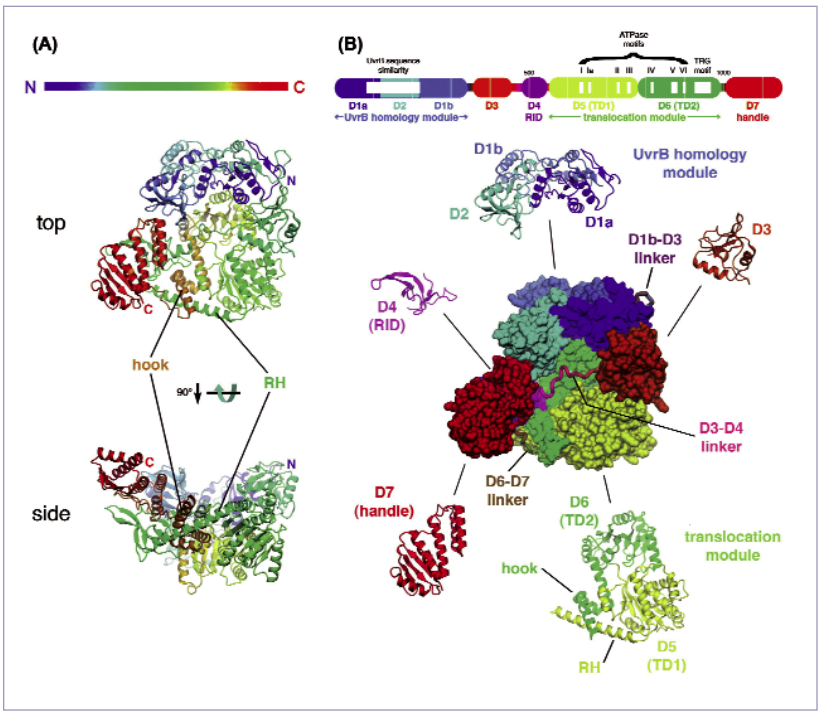

Fig. 1. Structure of *E. coli* TRCF: (A) Top and side views showing the hook and Relay Helix (RH), with color-coding as a ramp from the N-terminus (blue) to the C-terminus (red); (B) Top, schematic of TRCF domain architecture; Bottom center, top view of *E. coli* TRCF, color-coded as in the schematic above.

"Deadly Virus" continued from page 90

many changes occur in the F protein during this move from prefusion to postfusion that all of the inter-subunit contacts were found to be different.

Using their carefully collected data, the researchers constructed a five-step model, in which discrete refolding intermediates are integral to activating and driving F-mediated membrane fusion (Fig. 1). The first step involves melting the three HRB helices in the stalk to produce what the investigators call the "open-stalk" form. The research group mutated certain amino acids that confirm the importance of this intermediate. This opening of the stalk is thought to be involved in activation of the F protein. In the next step, that all-important third domain of the head region refolds and, by doing so, moves the fusion peptide toward the cell membrane of the host, eventually ending up in what is called a pre-hairpin state, with insertion of the fusion peptide into the cell membrane. Next, linkers stabilize the viral and cell membranes into the right orientation for fusion. In the postfusion state, the observed conformation is critical to membrane fusion and pore formation.

Many other interesting aspects of the fusion process emerged. Among these is that parts of the F protein could temporarily dissociate, a phenomenon observed in fusion proteins from other viruses. Also, the proposed intermediate states fit well with previous observations about how the fusion protein behaves chemically to promote fusion. Key to understanding the process is that the fold in the prefusion F protein is metastable—prone to transitioning to a more stable state—and that the folding necessary to achieve that stability actually drives fusion. Perhaps most important, however, is that the structural changes observed in the F protein are quite different from those observed in the influenza virus HA, the only other F-like viral fusion protein for which both prefusion and postfusion structures exist. This last observation suggests that fusion mechanisms cannot be generalized among viruses. Thanks to the present study, future work on fusion strategies can move forward apace. — *Mona Mort*

See: Hsien-Sheng Yin[1,2], Xiaolin Wen[2], Reay G. Paterson[2], Robert A. Lamb[1,2], and Theodore S. Jardetzky[2*], "Structure of the parainfluenza virus 5 Fprotein in its metastable, prefusion conformation," Nature **439**, 38 (January 2006). DOI:10.1038/nature04322

Author affiliations: [1]Howard Hughes Medical Institute, [2]Northwestern University
Correspondence: *tedj@northwestern.edu

Support for the Northwestern Center for Structural Biology from the R.H. Lurie Cancer Center is acknowledged. This research was supported in part by NIH research grants (to T.S.J. and R.A.L.). H.-S.Y. is an Associate and R.A.L. is an investigator of the HHMI, and T.S.J. is a Scholar of the Leukemia and Lymphoma Society of America. Use of the Advanced Photon Source was supported by the U.S. Department of Energy, Office of Science, Office of Basic Energy Sciences, under Contract No. W-31-109-ENG-38.

"Breaking the Gridlock" continued from page 91

describe the structure as resembling a tripod vessel, with legs formed by elements of three domains and one domain serving as a "handle." All of the domains meet in the concave surface of the molecule. The individual domains can be grouped according to a main function, such as RNA-polymerase Interacting Domain or Translocation-Domain, yet most are interconnected by flexible linkers, suggesting that all are acting in synergy for any given function and that large-scale conformational changes are necessary for the cycle of events.

Certain structural features make TRCF stand out. One is a long helix—dubbed the relay helix—that connects the RNA polymerase interacting domain to the translocation module. Another is that, despite intense effort by the research group, a crystal structure for the TRCF bound to nucleotides could not be produced. So, to identify the conformational changes that occur during binding, the investigators compared the translocation module of unbound TRCF to that of similar systems in other bacteria. The group was able to produce a satisfying picture, one that is consistent with their data sets and those of other research groups, about what happens when TRCF is on duty.

The graceful structure of TRCF, with its long and flexible linkers, appears to make it particularly well suited for the large-scale conformational changes that accompany its activity cycle. The reported structure and proposed mechanism for TRCF function show how it is able to, quickly and efficiently, remove the RNA polymerase stalled at the lesion and then call in the enzymes necessary to remove the lesion—quite a remarkable feat for a single protein. Future research can now concentrate on the timing of events in TRCF's functional cycle and the relative importance of various steps, leading to an even greater understanding of how to keep DNA transcription flowing and accurate. — *Mona Mort*

See: Alexandra M. Deaconescu[1], Anna L. Chambers[2,4], Abigail J. Smith[2], Bryce E. Nickels[3], Ann Hochschild[3], Nigel J. Savery[2], and Seth A. Darst[1*], "Structural Basis for Bacterial Transcription-Coupled DNA Repair," Cell **124**, 507 (February 10, 2006). DOI: 10.1016/j.cell.2005.11.045

Author affiliations: [1]The Rockefeller University, [2]University of Bristol, [3]Harvard Medical School, [4]University of Cambridge
Correspondence: *darst@rockefeller.edu

A.L.C. was supported by a studentship from the BBSRC. This work was supported by BBSRC research grant BB/C507053/1 to N.J.S. and NIH grants GM44025 to A.H. and GM073829 to S.A.D. Use of the Advanced Photon Source was supported by the U.S. Department of Energy, Office of Science, Office of Basic Energy Sciences, under Contract No. W-31-109-ENG-38.

A Bustling Hedgerow of Receptors

To find food, or to evade destruction by human immune cells, bacteria have developed a very sensitive system that detects chemicals in the environment. A bacterium responds to such stimuli by either moving toward or away from the stimuli using a built-in propeller, better known as a flagellum. Because mammalian cells like ours do nothing like this, the bacterial system is ripe as a target for antibiotic drugs. But the system is somewhat complicated, employing multiple copies of at least four different kinds of proteins, and the connection between all the protein components has so far been unclear. Researchers from Cornell University decided to determine the structure of the components as if they were all assembled in one unit. Certain proteins form complexes that make their three-dimensional structure difficult to determine, so the researchers turned to the NE-CAT 8-BM beamline at the APS. With additional biochemical experiments, the team pieced together a picture of how a nutrient tickling the sensing system of a cell at one end could get its message passed down to the flagellum, spurring the cell into self-preservation mode.

Every bacterial species has a protein network that allows it to respond to stimuli in the environment. The stimulus can be a nutrient the bacterium requires (e.g., sugars or protein building blocks), or it can be a molecule given off by animal tissue the bacterium wants to infect. Hundreds to thousands of the sensing proteins, called receptors, are clustered together on the cell surface and work cooperatively; if one of them is stimulated, dozens jump on board to help the first pass on its message. The message travels through components—called coupling proteins—to kinases proteins that switch other elements off and on, which ultimately alter the speed or direction of the flagellum. Scientists know what each of the individual components look like but do not know how they all fit together. Many cousins of bacterial species share this same sensing system, including the common intestinal bacteria *E. coli*, various pathogens, and bacteria that live in extreme environments, such as the hot-water-dwelling *Thermo-toga maritima*. Due to the stability of its proteins, *T. maritima* makes an excellent model for studying the molecular components of the process, called chemotaxis.

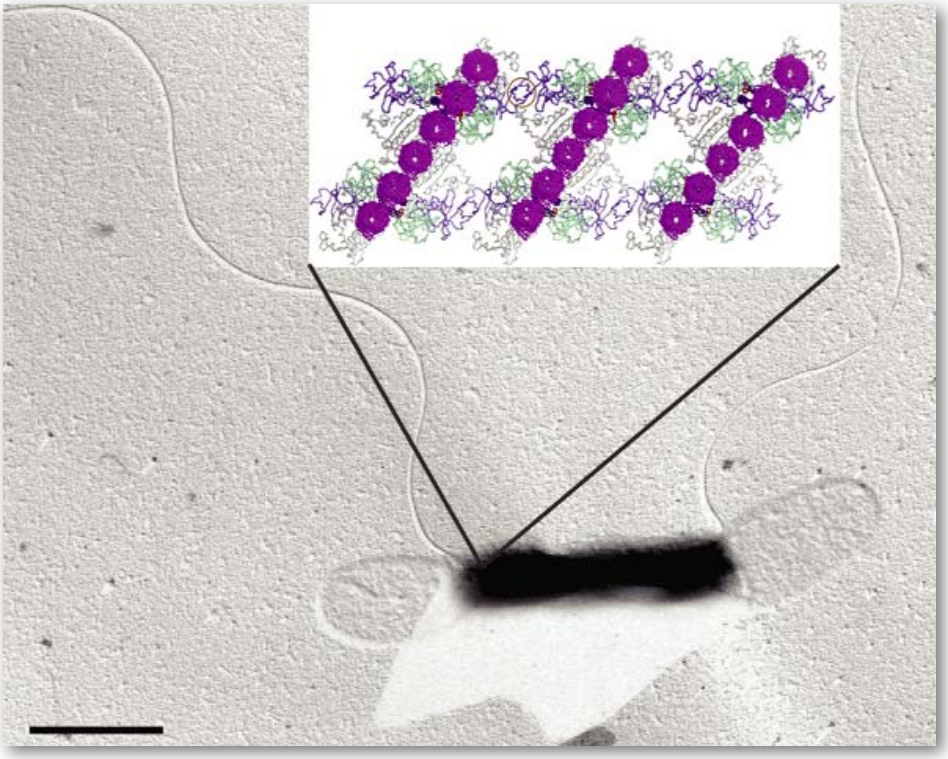

Fig. 1. Micrograph of *T. maritima* showing its flagella at the poles and a blow up of the receptor arrays (as viewed perpendicular to the membrane)—which sit in the cytoplasmic membrane—also at the poles. (Micrograph courtesy of Reinhard Rachel and Karl Stetter, University of Regensburg.)

The Cornell researchers expected the first component—the receptors—to form long helices that sit across a cell's membrane. In crystal form, these helices diffract light differently based on the direction from which the light is coming. The focused, high-brightness x-ray beams from the NE-CAT 8-BM beamline provided neat, tidy diffraction patterns that helped the researchers view the helices (Fig. 1). These receptors, they found, are packed in an arrangement that resembles a hedgerow and could, as expected, stretch across a cell membrane. This arrangement allows the proteins more contact between each other compared to the three-pack of receptor

Continued on page 95

How Cells Stick Together

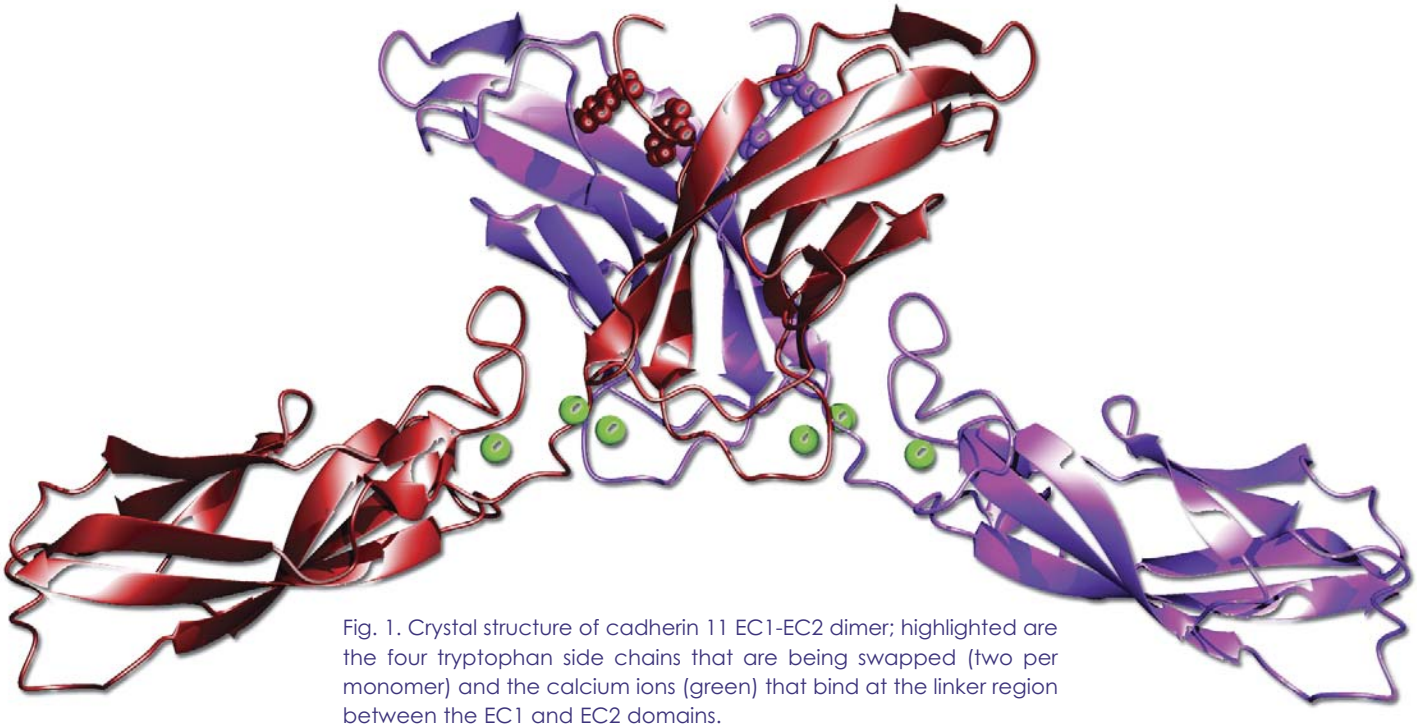

Fig. 1. Crystal structure of cadherin 11 EC1-EC2 dimer; highlighted are the four tryptophan side chains that are being swapped (two per monomer) and the calcium ions (green) that bind at the linker region between the EC1 and EC2 domains.

Cells cannot build tissues and organs until the cells find a way to stick together, and in such a way that the right cells end up in the right place at the right time. In animal cells, this adhesive specificity is achieved in part by a class of proteins called "cadherins," which lie across the cell membrane and can communicate with both the inside and outside of the cell via cadherin-cadherin interactions. There are many members of the cadherin family, from which two distinct groups emerge. The Type I cadherins, the generalists of the family, are distributed across many different tissue types. Type II cadherins tend to be specialists and are of prime importance in situations such as the developing nervous system. The type II cadherins have also proved more difficult to study, tightly shielding the secrets of their specificity from the eyes of curious investigators. Undaunted, researchers from Columbia University, the Howard Hughes Medical Institute, and University College London (with help from the SGX-CAT 31-ID beamline at the APS and beamlines X4 and X29 at the National Synchrotron Light Source) have painstakingly collected structural data on three different type II cadherins. Their work shows that a strand exchange between type II cadherin molecules, much like one that had been previously discovered in the type I cadherins, is important for determining specificity in living cells. This discovery brings us several steps closer to understanding how nervous system and other tissues assemble.

The researchers were interested in knowing more about what happens between the type II cadherin molecules on different cells that causes those cells to become bound to each other. Because of this, they focused on what is known as the ectodomain—the part of the cadherin that mediates cell-to-cell adhesion and would interact with molecules outside the cell. The group used x-ray crystallography to tease out the three-dimensional structures of five different fragments from type II cadherin ectodomains. To even more finely focus their work, they studied a specific part of the ectodomain—the N-terminal EC1 domain—because previous work on type I cadherins showed that this region was important for adhesive binding and that the individual domains yielded crystals that diffract to high resolution.

The researchers were able to use their data to construct a model for adhesion—one driven by a swapping of partner domains between cadherins, much like exchanging partners at a square dance (Fig. 1). The result of the partner exchange is that adhe-

Continued on next page

"Hedgerow of Receptors" continued from page 93

clusters proposed in *E. coli*. The tight associations within the hedgerow likely contribute to the cooperative nature of the receptors' behavior.

To elucidate the rest of the sensing conglomerate's architecture, the research team not only determined the three-dimensional structures of the coupling proteins and kinases rooted in crystals, but also used biochemical and spectroscopic techniques that allowed them to measure distances between molecules within flexible proteins in solution.

Putting all of this information together, the Cornell scientists found that duos of one coupling protein plus one kinase pair up with each other. The coupling proteins sit next to each other in these pairs and can clamp onto the tips of the receptors poking through the membrane. Because the neighboring kinases can also hang onto each other, the coupling protein-kinase groups form long chains, combining with the hedgerows of receptors to form scaffolds. When a stimulus tickles a receptor, the receptor bends or twists a little bit, causing the rest of the scaffold to also shift. In this way, a bustle in the hedgerow of receptors can amplify the level of a very small signal in the environment.

— *Mary Beckman*

See: Sang-Youn Park, Peter P. Borbat, Gabriela Gonzalez-Bonet, Jaya Bhatnagar, Abiola M. Pollard, Jack H. Freed, Alexandrine M. Bilwes, and Brian R. Crane*, "Reconstruction of the chemotaxis receptor-kinase assembly," Nat. Struct. Mol. Biol. **13**(5) 400 (May 2006). DOI: 10.1038/nsmb1085

Author affiliation: Cornell University

Correspondence: *bc69@cornell.edu

This article was the cover story in the issue of *Nature Structural & Molecular Biology*.

This work was supported by U.S. National Institutes of Health grants GM:R01066775 (to B.R.C.) and NCRR:P41-RR016292 (to J.H.F.). Use of the Advanced Photon Source was supported by the U.S. Department of Energy, Office of Science, Office of Basic Energy Sciences, under Contract No. W-31-109-ENG-38.

"Cells" continued from page 94

sive pairs of proteins, or dimers, form via the exchange of the N-terminal strands of extracellular cadherin-1 (EC1) domains presented from apposing cells. The group further refined the model by identifying how the swapped strands were anchored—using tryptophan side chains—and determining that this anchor mechanism is different than that found in type I cadherins. And, in a feature unique to the type II cadherin interface, the anchoring includes large hydrophobic regions.

The investigators were able to compare their newly described mechanism for specificity in type II cadherins with what had previously been gleaned from studying the type I cadherins. One outcome of this comparison is the identification of the EC1 domains—of both type I and type II cadherins—as the primary encoders of cell adhesive specificity, at least in the laboratory. The group further tested this hypothesis by using chimeric cadherins to perturb motor neuron segregation in chick embryos, and they found that the identity of the EC1 domain is the controlling variable in determining adhesive specificity.

By identifying the particular protein regions responsible for adhesive specificity in the type II cadherins, the researchers have learned at least some of the previously elusive adhesion secrets of this subfamily of molecules. In addition, their data reveal similarities, but also important differences, between adhesion mechanisms in the type I and type II cadherins, paving the way for a better understanding of why the subfamilies differ in terms of where they appear in tissues. For example, the fact that broadly expressed type I cadherins do not bind to their structurally different type II cousins expressed in neurons could underlie the ability of neurons to migrate through large regions of non-neural tissue to reach their targets. The current study also advances general knowledge of domain swapping, which may be driving other kinds of adhesion, such as that in the immunoglobulin proteins. Knowing more about how tissues assemble—which starts when cells find themselves in sticky situations—will also greatly interest biomedical research teams developing artificial tissues. — *Mona Mort*

See: Saurabh D. Patel[1], Carlo Ciatto[1], Chien Peter Chen[1], Fabiana Bahna[1], Manisha Rajebhosale[3], Natalie Arkus[1], Ira Schieren[2], Thomas M. Jessell[1,2], Barry Honig[1,2], Stephen R. Price[3]*, and Lawrence Shapiro[1,4]**, "Type II Cadherin Ectodomain Structures: Implications for Classical Cadherin Specificity," Science **311**, 216 (2006).
DOI: 10.1016/j.cell.2005.12.046

Author affiliations: [1]Columbia University; [2]Howard Hughes Medical Institute, Columbia University; [3]University College; [4]Edward S. Harkness Eye Institute, Columbia University

Correspondence: *ucgaspr@ucl.ac.uk, **lss8@columbia.edu

This work was supported in part by NIH grants GM-062270 (L.S.) and GM-30518 (B.H.); Wellcome Trust Grant 072914 (S.R.P.); and the RPB foundation (L.S.). T.M.J. was supported by a grant from NCI. Use of the SGX-CAT beamline facilities (ID-31) at the Advanced Photon Source was provided by SGX Pharmaceuticals, Inc., which constructed and operates the facility. Use of the Advanced Photon Source was supported by the U.S. Department of Energy, Office of Science, Office of Basic Energy Sciences, under Contract No. W-31-109-ENG-38.

Move Over Heme in 'globin

Many proteins change shape while doing their jobs. For example, hemoglobin in red blood cells must pick up oxygen in the lungs and drop it off at various locations around the body. Like a person's arms around a shopping bag, the protein has a slightly different shape when it is oxygen-laden. To determine how hemoglobin morphs in different ways, researchers take snapshots of the protein structure with and without its parcel. However, multiple steps occur between the before and after shots, and scientists have been unable to resolve the order of key events. So researchers from the University of Massachusetts Medical School and The University of Chicago used the BioCARS 14-ID beamline at the APS to gather nanosecond-time-scale data on hemoglobin molecules that were losing their baggage. They found an unexpected first step that occurs very rapidly, and they also found that water molecules take a more active role in the process.

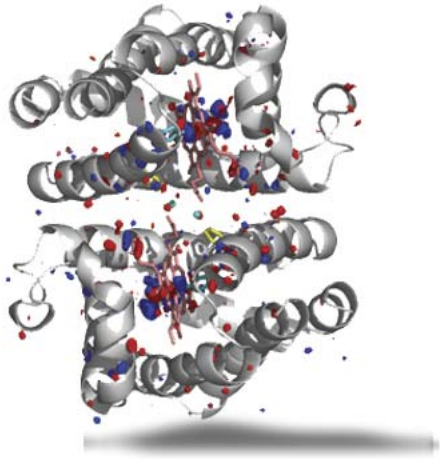

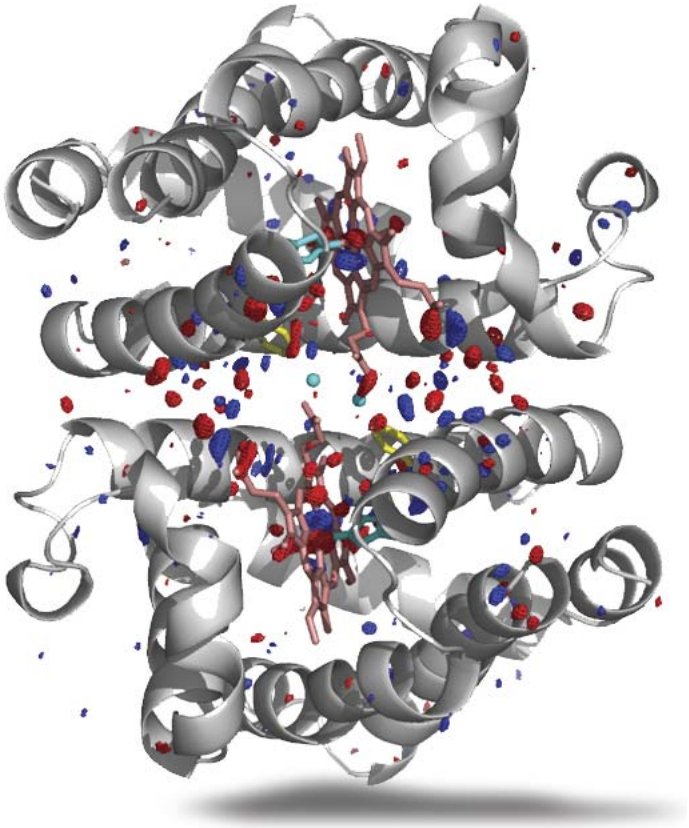

Fig. 1. A ribbon diagram of the Hbl-CO dimer (gray) with side chains for His F8 (cyan), Phe F4 (yellow), and key interface water molecules (small cyan spheres) at time delays of 5 ns (left) and 60 μs right) for the entire dimer.

Structural biologists normally want crystallized proteins to be in a static lattice framework: the more proteins in exactly the same position, the more accurate the picture of the overall protein. But often there is some “wiggle room” in crystals where different parts of the proteins can move around. To delineate the first steps that happen to hemoglobin as oxygen detaches from its mount, the research team needed to be able to take snapshots as quickly as 5 ns (5 billionths of a second) after oxygen starts to fall off and, at the same time, maintain good resolution. The BioCARS facility provides a pulsed laser to start the process and short, extremely bright x-ray pulses with which to take snapshots.

To do the experiment, the team started with crystals of hemoglobin from the mollusk *Scapharca inaequivalvis*, which is simpler than human hemoglobin. They infused the crystals, not with oxygen, but with carbon monoxide, which binds to the heme within the protein in the same way as oxygen (and is why carbon monoxide kills). They flashed the crystals with the laser and took images between 5 ns and 80 μs (Fig.1). After translating the raw data to molecular structures, the first

Continued on page 98

Insertion Mutants Hit the Right Spot

Mutations are often a mystery, making it difficult to determine just exactly what caused a protein—and the organism in which it is active—to come out different than the norm. Although single-base synthesis mistakes, or point mutations, in the coding DNA have been known to cause mutant proteins, much more dramatic effects—and evolutionary changes—usually result from insertions and deletions of base pairs into the normal coding sequence. These insertion and deletion events, nicknamed "indels," appear to be a prevalent cause of genetic differences and can be significant in effect, as in the known insertion that leads to Huntington's disease. Recently, protein engineering and design have taken advantage of the new functions created by indels to create new enzymes. Yet, the understanding of just how indels operate on protein structure is still in its infancy. A research group from the University of Iowa, with the help of the IMCA-CAT beamline 17-ID at the APS and beamline 4.2.2 at the Advanced Light Source at Lawrence Berkeley National Laboratory, has greatly enhanced the known effects of indels by reporting the behavior of insertion mutants in the important metabolic protein ubiquitin. Their work provides substantial evidence suggesting that what may be most important about an insertion mutation is where it inserts, with its specific base sequence being only second in importance. Such a discovery is of vast importance for understanding both natural and engineered mutations.

The research group had previously created and studied, using NMR chemical shifts, insertional mutants of ubiquitin to find that when different mutants—that is, those having different base sequences—were inserted into a region of the protein known as the 9-10 loop, the structural changes were minimal. When the insertions went into the region known as the 35-36 loop, however, the structural changes were quite marked, although still similar among the different types of mutants used (Fig. 1). These data led the investigators to propose what they called a "reflex response": Where you get the effect on the protein depends primarily on where you hit it with the insertion and not so much on what you hit it with. The model is especially important in understanding whether indels have been important to major structural divergence observed in the family of ubiquitin-like proteins.

In the present work, the group went on to fine-tune their understanding about what exactly happened at the 35-36 loop to create such major changes in the protein and to actually envision what happened during the reflex response. Much like when a knee is hit with a medical hammer,

Continued on page 98

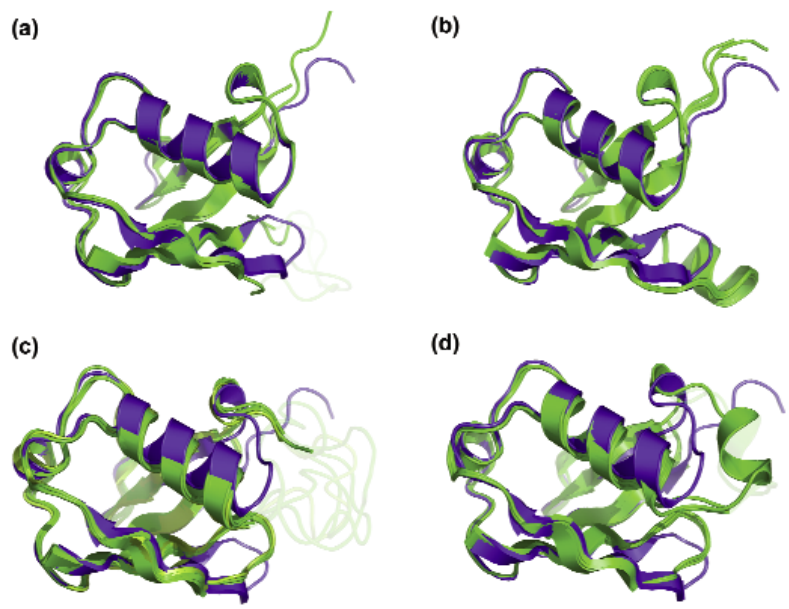

Fig. 1. Global alignments of loop insertion mutants (green) to wild type ubiquitin (blue); (a),(b): 9-10 mutants; (c),(d): 35-36 mutants.

"Heme in 'globin" continued from page 96

thing the team noticed was that the heme groups, which normally hang onto the carbon monoxide, had moved just a touch at 5 ns and remained there for a whole microsecond, instead of moving to their final resting place immediately. At around 1 μs, a particular amino acid flipped into its final spot and appeared to kick out water molecules that had been taking up space. Kicking out the water molecules allowed the heme groups to move into their final positions, suggesting that the water molecules were not just "taking up space," but were, in fact, keeping the protein from morphing too early.

Because the researchers could not keep the carbon monoxide from squeezing back into the crystal, the team could see the carbon monoxide taking up residence within the protein and the hemoglobin slowly morphing back into the shape it started in, which has a secure hold on its baggage. They had time points out to 80 μsec, but even with all that time, some of the hemoglobins loaded with carbon monoxide had not fully grasped their passengers. Hence, the researchers believe longer time points are needed to follow the reversal, which occurred more slowly than expected. — *Mary Beckman*

See: James E. Knapp[1], Reinhard Pahl[2], Vukica Srajer[2]*, and William E. Royer, Jr.[1], "Allosteric action in real time: Time-resolved crystallographic studies of a cooperative dimeric hemoglobin," Proc. Nat. Acad. Sci. **103**(20), 7649 (May 16, 2006). DOI: 10.1073pnas.0509411103

Author affiliations: [1]University of Massachusetts Medical School, [2]The University of Chicago

Correspondence: *v-srajer@uchicago.edu

This work was supported by National Institutes of Health Grant GM66756 (to W.E.R. and V.S.) and was initiated with funds from National Institutes of Health Grants DK43323 (to W.E.R.) and GM36452 (to Keith Moffat) and Postdoctoral Fellowship 9920261T from the New England affiliate of the American Heart Association (to J.E.K.). Use of BioCARS was supported by the National Institutes of Health, National Center for Research Resources, under Grant RR07707. Use of the Advanced Photon Source was supported by the U.S. Department of Energy, Office of Science, Office of Basic Energy Sciences, under Contract No. W-31-109-ENG-38.

"Insertion Mutants" continued from page 97

the helix of the ubiquitin protein bends away from the insertion site. Then, near the insertion, the hydrogen bonds that connect strands of the protein sheet lengthen and compress away from the insertion.

Using an array of data sets, including the crystal structures of four loop-insertion mutants, the researchers are now able to describe, with incredible accuracy, the effects of the insertions on the final structure of ubiquitin. Two types of structural changes in the mutants relative to wild-type ubiquitin emerged from the data. In the first, called a loop shift, the change is limited, so that on either side of the insertion region, the structure is similar to wild-type ubiquitin. The second kind of structural change is called a rigid body shift—a structural shift with one pivot point beyond which the mutant and wild-type structures diverge.

To look more closely at how specific insertions affected the protein structure, the group designed two insertions from proteins that had similar structures. With these insertions, a new protein was born, and in the insertion region, the secondary structure was the same as in the original ubiquitin molecule. The group used their data to study how well structure prediction tools can simulate the structural changes actually observed in their careful analyses. They found that the models were not able to predict the fine details of the observed structures, which is another useful piece of information for protein engineers.

The crystal structures provide strong evidence to support the reflex response and now allow future work on protein engineering to focus more on *where* in the protein changes are attempted and less on *what* is actually used to produce the change. — *Mona Mort*

See: D.M. Ferraro, D.J. Ferraro, S. Ramaswamy, and A.D. Robertson*, "Structures of Ubiquitin Insertion Mutants Support Site-specific Reflex Response to Insertions Hypothesis," J. Mol. Biol. **359**, 390-402 (2006).

Author affiliation: University of Iowa

Correspondence: *andyr@keystonesymposia.org

This article was the cover story in the issue of the *Journal of Molecular Biology.*

This work was supported by NIH grant GM46869. D.M.F. is supported by a Howard Hughes Predoctoral Fellowship, and D.J.F. is supported by a University of Iowa Center for Biocatalysis and Bioprocessing Fellowship. Use of the Molecular Biology Consortium beamline 4.2.2 at the Advanced Light Source at Lawrence Berkeley National Laboratories was made possible through the University of Iowa institutional membership in the MBC. The ALS is supported by the U.S. DOE under Contract no. DEAC03- 76SF00098. Use of the IMCA-CAT beamline 17-ID at the Advanced Photon Source was supported by the companies of the Industrial Macromolecular Crystallography Association through a contract with the Center for Advanced Radiation Sources at The University of Chicago. Use of the Advanced Photon Source was supported by the U.S. Department of Energy, Office of Science, Office of Basic Energy Sciences, under Contract no. W-31-109-ENG-38.

Keeping the Bacterial Vitamin B12 Transporter Moving

The recently discovered structure of a particular bacterial protein complex may offer researchers a new route to antibiotic candidates. In order to survive, bacteria—*E. coli*, for instance—require scarce nutrients, such as vitamin B12 and iron, that the bacteria take from their environment. Hoping to better understand the process by which bacteria ingest these nutrients, University of Virginia investigators using the SER-CAT 22-ID beamline at the APS solved the three-dimensional (3-D) structure of two proteins that cooperate to bring vitamin B12 across the cell membranes of many common bacteria. The structure might help in designing drugs that slow down bacterial growth by deactivating this nutrient transport.

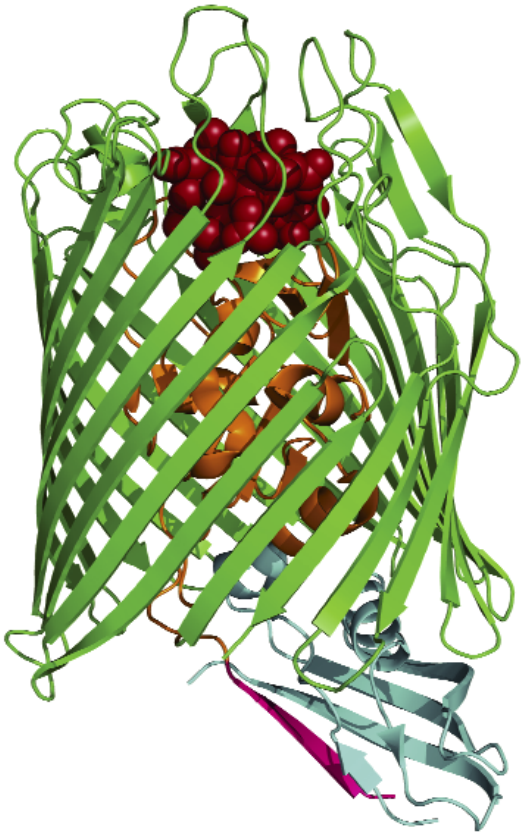

Fig. 1. Schematic diagram of the BtuB-TonB complex, which transports vitamin B12 into bacteria. A plug-like piece of protein (orange) obstructs the barrel-shaped BtuB channel (green). To open the channel, the TonB protein (cyan) pulls on another piece of BtuB (pink), allowing B12 (red spheres) to pass through.

Vitamin B12 is too big to simply wiggle through the two concentric membranes that surround the microbes. Instead, a specialized protein transporter—BtuB—creates a hole in the bacterium's outer membrane and pulls the nutrient through. Related transport proteins, using a similar mechanism, pull large iron-containing complexes across the outer membrane.

To supply energy for the transport process, another protein—TonB—tethers BtuB to a cluster of motor-like proteins on the inner membrane. It was suspected that TonB somehow tugs on BtuB to open it up and let vitamin B12 through. No experiments had as yet provided compelling evidence for this view.

Based on their x-ray crystallography work at SER-CAT, the University of Virginia researchers found that the structure of BtuB bound to one end of TonB is consistent with a pulling model . BtuB consists of a series of parallel strands rolled into a barrel shape. Obstructing the middle of this channel is a plug also made of four parallel strands and a tail that extends outside of the barrel, toward what would be the interior of a bacterial cell. This tail recognizes and sticks to the TonB fragment.

The structure of the plug suggests that an inward pulling force on the BtuB tail, called the Ton-box, would be enough to pull the plug apart, giving vitamin B12 and similar molecules a path through the channel, these researchers contend. The plug's four strands are perpendicular to the barrel that encloses them. Experiments on similar proteins have found that such a grouping of strands maintains its shape well if pulled parallel to the strands, but comes apart more easily if pulled in the perpendicular direction like an accordion, the group found. TonB is like a hand grasping and pulling the Ton-box rope, which would apply the needed perpendicular force to pull some or part of the plug from the channel.

The structure of the Ton-box may help researchers discover drugs that inactivate B12 or iron transport. Such a drug might fight infections, because bacteria that have trouble absorbing nutrients are less able to grow and divide. Experimentally interfering with the Ton-box disturbs bacterial infectiousness, suggesting that a well-designed compound might help control bacterial infections in people. — *JR Minkel*

See: David D. Shultis, Michael D. Purdy, Christian N. Banchs, and Michael C. Wiener*, "Outer Membrane Active Transport: Structure of the BtuB:TonB Complex," Science **312**, 1396 (2006). DOI: 10.1126/science.1127694

Author affiliation: University of Virginia
Correspondence: *mwiener@virginia.edu

This work supported by NIH grants DK59999 (to D.D.S., M.D.P., C.N.B., and M.C.W.) and GM00Z055 (to D.D.S.). Use of the Advanced Photon Source was supported by the U.S. Department of Energy, Office of Science, Office of Basic Energy Sciences, under Contract No. W-31-109-ENG-38.

Arsenic in the Water Supply

Quite possibly the largest environmental disaster the world has seen—affecting far more people than the accident at Chernobyl—is the arsenic contamination of ground water in Bangladesh. Some 57 million of the country's 125 million inhabitants are at risk of drinking dangerous levels of arsenic that have seeped into the nation's web of water wells, many of which were built in the 1960s and 1970s in order to protect against drinking contaminated surface water. Since the ground-well initiative, water-borne diseases have indeed decreased, but recent incidences of arsenicosis and cancer from arsenic poisoning have caused serious concern. Although the source of arsenic came to be understood, the critical question was: How did that arsenic migrate to the water supply? Researchers from Stanford University, the Massachusetts Institute of Technology, Bangladesh University, and The University of Chicago, using the GSECARS 13-ID-C beamline at the APS, have uncovered new information on the way toxins such as arsenic are released into soil and from there into water supplies.

The source of the arsenic is understood to be natural arsenic from the age-old Himalayan sediments on which Bangladesh sits, but the process of how it mobilizes into the water is still being debated. The most widely accepted explanation is that arsenic is released from aquifer sediments when microbes break down ferric (hydr)oxides. The researchers in this study, however, see no evidence for this process within the aquifer, or that ferric (hydr)oxides are present at measurable levels in the aquifer. Instead these data suggest that arsenic is released near the surface via redox cycling and is later transported to well-depth.

Sediment samples were obtained from the Munshiganj district of Bangladesh—a field site typical of the region in that it includes clay on the surface, a Holocene aquifer of gray sand, an aquitard of marine clay, and a deep burnt-orange sandy Pleistocene aquifer.

The sediments were examined at 13-ID-C using micro x-ray fluorescence (μ-XRF) elemental mapping combined with μ-x-ray absorption near-edge structure (μ-XANES) spectroscopy of the Holocene and Pleistocene aquifer sediments. the results showed arsenic-bearing grains with diameters of anywhere from 5 μm to 100 μm, in varying oxidation states. In fact, more than 60% of the arsenic was found in sulfide grains throughout the sample. As for iron, the gray Holocene layer showed a fairly even iron distribution, but with no evidence for ferric (hydr)oxides. Sediments from the orange Pleistocene aquifer, on the other hand, do contain ferric (hydr)oxides.

Spectroscopy of the surface soil showed different distributions than those found in the aquifers. Here, concentrations of solid-phase arsenic were much higher. While the aquifers had less than 3 μg/g of arsenic, the surface showed 25 μg/g, diminishing to 10 μg/g at 36-cm depth. Iron too, was more reduced deeper in the surface soil.

Continued on next page

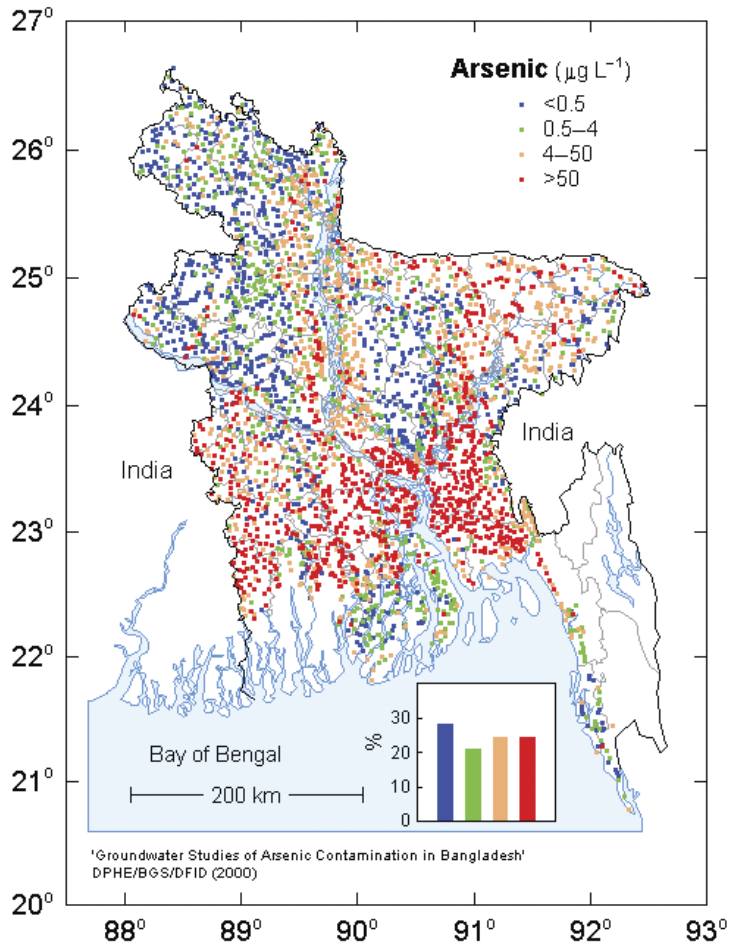

Arsenic contamination in Bangladesh. (Source and ©: Bangladesh Sustainable Development Networking Programme.)

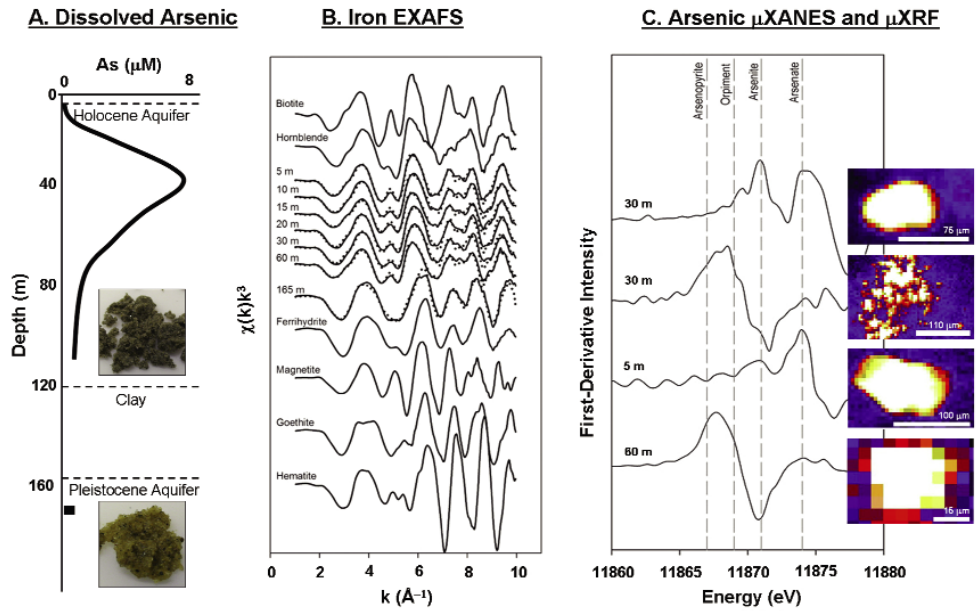

Fig. 1. (A) Dissolved arsenic peaks at 30-40-m depth in a Holocene aquifer at the field site. They are not detected in a deeper Pleistocene aquifer. (B) Iron EXAFS linear-combination fitting of aquifer sediment samples indicate that Fe mineralogy is constant with depth within the Holocene aquifer, but Fe(III) (hydr)oxides are not detected, despite the fact that they have been suggested as a source of arsenic. (C) Arsenic is found in a host of oxidation states within the solid-phase. Arsenic-bearing sulfide minerals, a previously unrecognized source of arsenic, are found throughout the sediment profile, most commonly as 10-35-μm grains, and may account for up to 60% of the total solid-phase arsenic.

In order to examine the process of arsenic release, sediments were incubated with deionized water. Approximately 15% of the total arsenic was released. Irradiating the sediments with gamma rays did not appreciably change the amount of arsenic released, suggesting that biotic activity is not a factor in the process. A third version—in which ferrihydrite-coated sand was introduced in order to examine the effects of Fe (III) on arsenic release—showed lowered amount of arsenic release, further indicating that ferric hydr(oxides) do not control arsenic retention in aquifers. Throughout all of these experiments, arsenic release was strongly correlated with phosphorous release; that was the only elemental correlation the research team found.

Given the lack of ferric (hydr)oxides in the Holocene aquifer, as well as its ability to control arsenic release in positive controls, the authors conclude that these are not contributing to arsenic mobility at well-water levels. In the lower Pleistocene aquifer, the arsenic is likely kept out of solution by adsorption to the increased level of ferric (hydr)oxides found there. Surface soils, on the other hand, undergo at least two major reduction-oxidation cycles each year—and possibly more based on irrigation and crop cycling. These surface soils contain higher arsenic concentrations than deeper sediments, which is due to annual sediment deposition that brings additional arsenic into the soil.

Based on their studies, these researchers propose an alternate scenario. At least 15% of the solid-phase arsenic is rapidly desorbed, while 60% is bound in sulfides and therefore unreactive in the strongly reducing aquifer. The arsenic released from the surface, however, binds only weakly to the silicate minerals, which dominate the aquifer sediments, so they would be easily transported to well depth.

In conclusion, the results of this paper suggest that remediation of the arsenic problem in Bangladesh requires monitoring the soil environments above the aquifers for arsenic, as well as developing a better understanding of arsenic transport.

— Karen Fox

See: Matthew L. Polizzotto[1], Charles F. Harvey[2], Guangchao Li[1], Borhan Badruzzman[3], Ashraf Ali[3], Matthew Newville[4], Steven Sutton[4], and Scott Fendorf[1]*, "Solid-phases and desorption processes of arsenic within Bangladesh sediments," Chem. Geol. **228**, 97 (2006). DOI: 10.1016/j.chemgeo.2005.11.026

Author affiliations: [1]Stanford University, [2]Massachusetts Institute of Technology, [3]Bangladesh University of Engineering and Technology, [4]The University of Chicago
Correspondence: *fendorf@stanford.edu

Portions of this research were carried out at the Stanford Synchrotron Radiation Laboratory, operated by Stanford University on behalf of the U.S. Department of Energy, Office of Basic Energy Sciences. This work was funded by the Stanford Graduate Fellowship and the National Science Foundation CRAEMS Program (Grant number CHE-0089215). Use of the Advanced Photon Source was supported by the U.S. Department of Energy, Office of Science, Office of Basic Energy Sciences, under Contract No. W-31-109-ENG-38.

Ironite: A Potentially Fertile Source of Soil Contamination

Ironite fertilizer is a common source of iron and nitrogen for lawns, gardens, and agricultural crops. The fertilizer is made from processed mine tailings left over from an inactive silver mine in Humboldt, Arizona. While the beneficial reuse of mine tailings are—by U.S. law under the Bevill Exemption—not defined as hazardous waste, there are concerns that this fertilizer could leave dangerous amounts of arsenic and lead in the ground. Previous studies by the manufacturer found that better than 95% of the arsenic was bound with iron and sulfide into the mineral arsenopyrite (FeAsS), and that this is further insulated when surrounded by pyrite (FeS). The manufacturer's study also found that most of the lead is safely bound in the mineral galena (PbS). However, researchers from the U.S. Environmental Protection Agency (EPA), utilizing the MR-CAT 10-ID and XOR/PNC 20-BM beamlines at the APS, found that by the time the fertilizer gets from the factory to the store, the arsenopyrite and the galena have decomposed, leaving arsenic bound to ferric oxides, and lead bound into anglesite. Both of these states could result in arsenic and lead leaching into the soil and being bioavailable to living creatures, human and otherwise.

To study the composition of Ironite, the EPA researchers bought bags of the fertilizer from commercial retail stores—two in Ohio and one in Florida—in order to test the composition of the fertilizers as sold to a user, not simply after recovery from the mine wastes. The researchers used x-ray absorption spectroscopy (XAS) at 20-BM and 10-ID to study the granular fertilizer both as bought and after having been crushed to less than 44 μm. Mössbauer spectra of the samples were also collected in order to study the iron chemical content. Lastly, the EPA researchers put the Ironite through aging studies to see how it degraded.

The dominant peak provided by x-ray absorption spectroscopy showed the arsenic in Ironite to be 1.57 Å from its nearest neighbor. This is indicative of the arsenic-oxygen bond distance in scorodite ($FeAsO_4 \bullet 2H_2O$), as opposed to the ~2.35-Å bond arsenic has to sulfur in arsenopyrite. A secondary, less intense peak, however, was consistent with this arsenic-sulfur bond, suggesting the Ironite has a mix of both types of bonds. The researchers' analysis shows that 60% to 70% of the arsenic is bound by oxygen in either scorodite or with iron oxides and the rest is bound in arsenopyrite (Fig. 1). Because the studies done by the manufacturers found much more arsenopyrite, the EPA researchers offer the explanation that scorodite is more stable in oxygenated environments than arsenopyrite. The original arsenopyrite likely decomposed over time once packaged for retail.

The studies performed on behalf of the manufacturer also showed that lead is found in Ironite, reporting that 82% to 91% of the lead exists in the form of galena (PbS) and 6% to 17% exists as anglesite ($PbSO_4$). However, x-ray absorption near edge structure analysis done by the EPA researchers indicates

Continued on next page

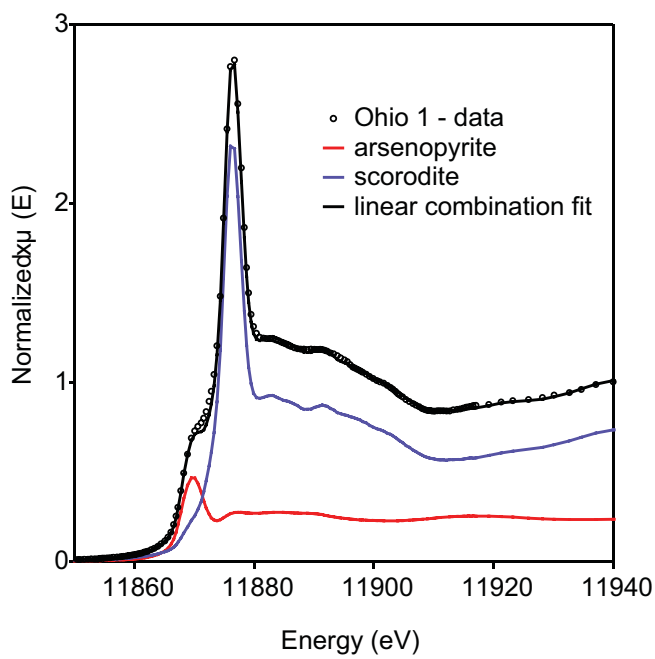

Fig. 1. Linear combination fit of an Ironite 1-0-0 sample purchased in Ohio, demonstrating an Fe-O-As-type structure similar to scorodite as the dominant As environment (60%-70%) in Ironite. Arsenopyrite, an Fe-S-As-type structure, accounts for the balance of As in Ironite.

The Ironite facility at Humboldt, AZ. The orange mountain in the background is the pile of mine waste from which Ironite is derived.

that anglesite is the dominant phase. The EPA group offers a similar explanation as for the arsenic: During storage for commercial sale, the parent material containing lead undergoes further oxidation and transformation to mineral phases that are more stable under atmospheric conditions.

Mössbauer spectroscopy was used to examine the iron chemistry that might be controlling the arsenic availability to the environment. At room temperature, there was a clear identification of pyrite, but other phases were hard to identify. Once the samples were cooled to 4.2K, however, a peak for ferrihydrite could be seen. There was not substantial evidence for scorodite, so on the basis of the high proportion of arsenic associated with iron oxides as identified with the XAS, the most probable explanation is that arsenic reacts with ferrihydrite by sorption, coprecitpitation, or both.

The EPA scientists also wanted to study how arsenopyrite ages in the environments where Ironite is used. While the manufacturer's studies show that 95% of the arsenic is in arsenopyrite, the mineral can degrade further when placed in oxygenated environments, such as on a lawn. These researchers studied Ironite after it sat in buffered water for one day and for a month. After the one-day period, both arsenopyrite and arsenic associated with ferric oxides were present. After a month, no arsenopyrite was present. Sitting in buffered water is not the equivalent of being used as a fertilizer—but this nonetheless shows that arsenopyrite is susceptible to chemical transformation in regularly watered lawns.

Having shown that the arsenic and lead in Ironite sold in stores does not remain in the same mineral state as at the factory, and that it can degrade even further once placed on a lawn, the EPA team emphasized that while the idea of using waste products from mines for beneficial products is a good one, careful consideration and scrutiny must be applied to determine if the benefits outweigh the environmental cost and risks posed by accidental ingestion and contamination of water resources. Specifically, because a January 2006 EPA regulation limits the amount of arsenic in drinking water to 10 *μg*/liter, the benefits of applying a potential source of arsenic need to be carefully evaluated. — *Karen Fox*

See: Aaron G.B. Williams, Kirk G. Scheckel*, Thabet Tolaymat, and Christopher A. Impellitteri, “Mineralogy and Characterization of Arsenic, Iron, and Lead in a Mine Waste-Derived Fertilizer,” Environ. Sci. Technol. **40**, 4874 (2006).
DOI: 10.1021/es060853c
Author affiliation: United States Environmental Protection Agency
Correspondence: *Scheckel.Kirk@epa.gov

The U.S. Environmental Protection Agency, through its Office of Research and Development, funded and managed the research described here. It has not been subject to Agency review and, therefore, does not necessarily reflect the views of the Agency. No official endorsement should be inferred. PNC-CAT facilities at the Advanced Photon Source and research at these facilities are supported by the U.S. DOE Office of Science Grant No. DEFG03-97ER45628, the University of Washington, a major facilities access grant from NSERC, Simon Fraser University. and the Advanced Photon Source. MR-CAT operations are supported by the Department of Energy and the MR-CAT member institutions. Use of the Advanced Photon Source was supported by the U.S. Department of Energy, Office of Science, Office of Basic Energy Sciences, under Contract No. W-31-109-ENG-38.

Bacterial Clues to Metallic Cleanup

Aquatic environments the world over are often contaminated with toxic metals, such as cadmium, copper, and lead, either dissolved in the water or bound to particles or bacteria. The latter determines the fate of these metals and whether or not they are bioavailable, so understanding how bacteria process metals is important from an environmental and health perspective. One such metal is manganese, an industrially important element. Layered manganese oxides are used throughout industry, in particular as the cathode in "lithium" batteries. These oxides also have potential as environmental remediation agents for removing other metals from waterways and contaminated land. The way in which certain aquatic bacteria handle this element could provide important clues as to its behavior in the environment. For instance, manganese oxide is inextricably linked to the uptake by shellfish of toxic metals such as lead and cadmium. It is also an excellent scavenger for cobalt in aquatic systems. Studies could point to new approaches to remediation as well as applications in industrial catalysis and in chemical separation technologies. One such study carried out by researchers using DND-CAT beamline 5-BM-D at the APS looked for parallels between industrial manganese oxides and the chemistry and structure of their natural counterparts.

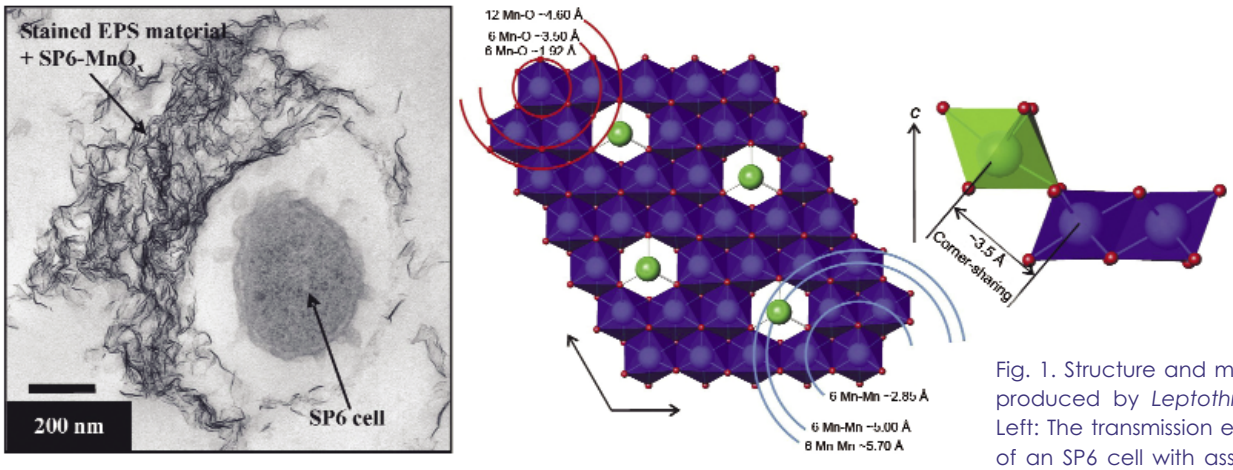

Fig. 1. Structure and morphology of MnO_x produced by *Leptothrix discophora* SP6. Left: The transmission electron micrograph of an SP6 cell with associated MnO_x illustrates extracellular formation of high surface area oxide fibrils. X-ray absorption spectroscopy reveals that SP6-MnO_x is a layered, mixed-valent Mn^{III}/Mn^{IV} oxide. Right: SP6-MnO_x layers are comprised of edge-sharing $Mn^{IV}O_6$ octahedra (blue). Mn^{III} cations (green) reside above/below Mn^{IV} layer vacancies.

The researchers from Northwestern University and the Pontificia Universidad Católica de Chile (PUC), used transmission electron microscopy, x-ray absorption spectroscopy (including full multiple-scattering analysis), and powder x-ray diffraction at the DND-CAT beamline to determine the structure of a manganese oxide from the freshwater bacterium *Leptothrix discophora* SP6, with the aim of finding parallels between industrial manganese oxides and the chemistry and structure of their natural counterparts. Their results would also settle an almost decade-old ambiguity in earlier studies of this important material.

Bacteria such as *L. discophora*, *Pseudomonas putida* strain MnB1, and spore-forming marine *Bacillus* sp. strain SG-1 are known generally as manganese oxidizers. These bacteria can convert the soluble Mn^{2+} oxidation state of the metal into its insoluble Mn^{3+}/Mn^{4+} mixed oxide state—MnO_x in water systems. The latter two bacteria produce similar MnO_x structures, but controversy surrounded the structural determination of the SP6-MnO_x produced by this freshwater microbe.

In 2003, Kim et al. used ultraviolet Raman spectroscopy to study the structure of biogenic manganese oxide produced by *L. discophora* [1, 2]. They discovered a tunnel-like structure resembling the mineral todorokite found in deep ocean-floor nodules. In contrast, Jürgensen et al. (using the PNC-CAT facility at the APS) demonstrated that SP6-MnO_x has a layered topology [3]. Obviously, these two structural forms are mutually exclusive. However, it is possible that the sample in the Kim and Stair spectroscopic experiment was simply transformed to todorokite because of the laser—perhaps via heating.

The Northwestern-PUC researchers carried out a thorough investigation to determine conclusively the detailed atomic structure of the oxide formed by the bacteria. It was this

Continued on next page

analysis and comparison to a variety of model manganese oxides that allowed the researchers to determine the vacancy (missing cations in the layers) model in a convincing way and so provide useful information about the various industrially important manganese oxides.

The team found that the manganese oxide precipitate made by the bacteria consists of tiny particles just 10 nm to 100 nm in diameter. These fiber-like particles resemble twisted sheets. Closer inspection using the x-ray studies revealed that the MnO_x is composed of sheets of edge-sharing octahedra stacked in layers. This would confirm the findings of the Jürgensen et al. study [3] as opposed to the tunnel-like structure reported by the Kim et al. study [1, 2]. The structure also hints that the bacteria have no control over the crystalline form of this mineral; it simply accumulates in this form.

Although it is not known why bacteria encrust themselves in manganese oxides, determination of biogenic oxide structures hints at their role in immobilizing metals that are otherwise mobile through aquatic environments. As a result, researchers are investigating synthetic analogs of these materials for use as metal remediation materials. — *David Bradley*

References

[1] H.-S. Kim et al., Am. Chem. Soc. **125**, 14284 (2003).
[2] (45) H.-S. Kim et al., J. Phys. Chem. B **108**, 17019 (2004).
[3] A. Jürgensen et al., Am. Mineral. **89**, 1110 (2004).

See: Ian Saratovsky[1], Peter G. Wightman[1], Pablo A. Pastén[2], Jean-François Gaillard[1]*, and Kenneth R. Poeppelmeier[1]**, "Manganese Oxides: Parallels between Abiotic and Biotic Structures," J. Am. Chem. Soc. **128**, 11188 (2006).
DOI: 10.1021/ja062097g
Author affiliations: [1]Northwestern University, [2]Pontificia Universidad Católica de Chile.
Correspondence: *jf-gaillard@northwestern.edu, **krp@northwestern.edu

This work was supported by the EMSI program of the National Science Foundation (NSF) and the U.S. Department of Energy Office of Science at the Northwestern University Institute for Environmental Catalysis. DND-CAT is supported by the E.I. Du Pont de Nemours & Co., The Dow Chemical Co., the U.S. National Science Foundation through Grant DMR-9304725, and the State of Illinois through the Department of Commerce and the Board of Higher Education Grant IBHE HECA NWU 96. Use was also made of Central Facilities supported by the MRSEC program of the NSF (Grant DMR-0076097) at the Materials Research Center of Northwestern University. P.A.P. acknowledges Proyecto Fondecyt 1040580/2004 for funding. Use of the Advanced Photon Source was supported by the U.S. Department of Energy, Office of Science, Office of Basic Energy Sciences, under Contract No. W-31-109-ENG-38.

Around the Experiment Hall

Studying the Uptake Mechanisms of Plants from Down Under

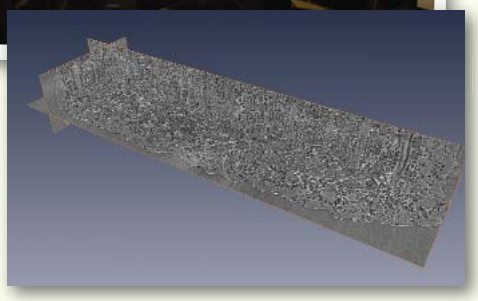

Francesco De Carlo (center, XSD) makes a point to visiting researchers Rosalie Hocking (left) and Robert Hough, both of the Australian Commonwealth Scientific and Industrial Research Organisation Division of Exploration and Mining and Division of Land & Water, during data taking in the XOR beamline 2-BM control room on the APS experiment hall floor. ● Hough: "We're collecting x-ray tomography data to look at things like the three-dimensional (3-D) microstructure of native Australian plants that grow above ore deposits and so have metals in them. For these plants, we have already collected element maps using synchrotron x-ray fluorescence at XOR/PNC sector 20 at the APS in a previous run. Those data showed that we had things like zinc in the leaf tissue and calcium oxalate in voids, so the tomography enables us to see in three dimensions how these tissues and voids are distributed, and more generally what the internal structure of leaves and twigs of Australian Acacia plants look like. ● "Here at sector 2, we are able to run many samples in a short time, so we can collect a huge amount of data in our beam-time allocation and return to Australia with heaps to work on. Hopefully, we can then bring the element maps and 3-D images together to visualize the relationships and this will answer a lot of questions we have about the metal uptake mechanisms in these plants. This has important implications for environmental background studies, bioremediation, and even mineral exploration." ● The Hough and Hocking visit to the APS was funded through the Australian Synchrotron Research Program. At right: One of the tomographic projections of an Acacia leaf obtained at the APS.

How Charged Ions Behave in Water

Water streaming through the environment is the single largest form of mineral transport through the soil. In an effort to track the movement of toxins, researchers need to know how moving water picks up ions adsorbed onto stationary minerals. Previous models of how charged ions adsorb in an aqueous environment have been fairly simple: there were thought to be two types of mechanisms. The first kind, the strong adsorption—in which the ion is directly bonded to the mineral—is known as "inner-sphere." The second, weaker adsorbed ions are named "outer sphere" and have a layer of water between the ions and the substrate. Researchers from Argonne and the University of Illinois at Chicago examined rubidium and strontium cations at one of the simplest models of a solid-liquid interface—a mica-water interface—and found evidence to contradict this simple description. In this study, the strontium adsorbed with both kinds of bonds simultaneously, leading to a new description of adsorption based on balancing the energy cost of disrupting ion and interface hydration with electrostatic attraction between the cation and the charged surface.

Experiments were conducted on the XOR/BESSRC 11-ID-D and 12-BM-B beamlines at the APS. The researchers studied samples of 0.01 M RbCl and $Sr(NO_3)_2$ at a pH of ~5.5. Laterally-averaged total and element-specific electron density profiles along the surface normal direction of the mica (001) surface were determined using high-resolution x-ray reflectivity and resonant anomalous x-ray reflectivity, respectively.

Comparison of the Rb^+ and Sr^{2+} distributions showed fundamental differences. The Rb^+ adsorbs as a single discrete layer, while the Sr^{2+} adsorbs over a broader region with two distinct heights above the mica surface. The residual interfacial hydration structures are also different: a distinct hydration layer is observed in the Rb^+ with a less-distinct hydration structure in the presence of the Sr^{2+}. However, both hydration profiles are dissimilar to that of pure deionized water, suggesting that the adsorbed cations play a critical role in altering the hydrogen bonding network near the mineral surface.

The interfacial structures for Sr^{2+} were quite distinct from those of rubidium. The Rb^+ distance from the surface is fairly even at 2.33 ± 0.10 Å. The first Sr^{2+} distance (1.26 ± 0.22 Å) corresponds to that of a classical inner-sphere—or partially hydrated—adsorption. The second adsorbed Sr^{2+} layer is at a significantly larger height (4.52 ± 0.24 Å), suggesting it is a fully hydrated ion, or a classical outer-sphere adsorption. The coexistence of

Continued on page 108

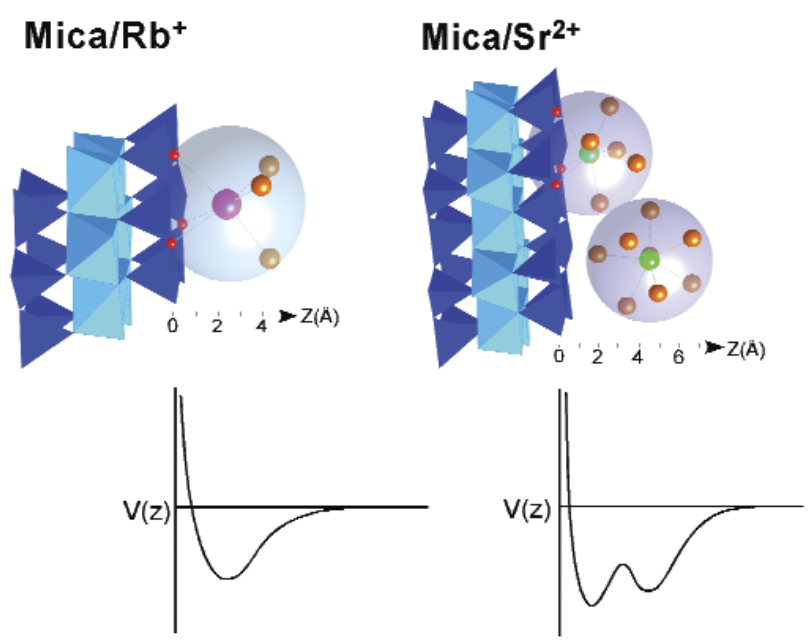

Fig. 1. Pictorial models of Rb^+ and Sr^{2+} aqueous complexes on the muscovite surface and schematic drawings of expected potential distributions as a function of height, based on measured ion adsorption profiles and known ion-hydration structures in bulk solution. These potentials should be configured by balancing ion and interface hydration energies with the electrostatic attraction between the cation and charged surface. Note that the two potential minima of Sr^{2+} are comparable and the second distinct minimum is due to strong ion hydration.

The Evolution of Uranyl into an Organic-rich Calcite

The Earth's crust contains some 4% by weight of the mineral calcite, making it one of the most common materials in the crust. While the mechanism was not understood, it has been shown that calcite ($CaCO_3$) can incorporate hexavalent uranium (U(VI)) into its chemical composition. This leads to two important effects: first, uranium bound in a calcite could be used for geological dating; second, calcite that incorporates excess uranium—perhaps from a contaminated site—will keep that uranium out of groundwater over the long term. By studying an ancient 298-million-year-old organic-rich calcite (calcrete), researchers from Argonne and SUNY Stony Brook have, for the first time, shown the mineral's chemical composition around a stable uranyl—the most common form of U(VI)—contained therein. The researchers believe that the uranyl environment may evolve over long time scales, becoming more calcite-like and even more stable. This is good news for those interested in remediation and dating techniques alike.

The researchers studied a calcrete sample that was precisely dated at 298 ± 1 millennia. The sample shows no evidence of loss of uranium over its lifetime and is believed to have been formed near a water table with some exposure to a reducing environment. Using the MR-CAT sector 10-ID beamline at the APS, the team examined the calcrete with x-ray fluorescence (XRF), microprobe x-ray absorption near-edge spectra (μXANES), and microprobe x-ray absorption fine structure (μEXAFS) data processing.

Previous laboratory studies failed to show how uranium is incorporated into calcite, suggesting that the UO^2_{2+} didn't substitute for the Ca^{2+} in the calcite's crystal structure. It was hypothesized that perhaps the linear UO^2_{2+} moiety could not substitute for the spherically shaped Ca^{2+} and in changing its symmetry from the hexagonal bipyramidal structure of aqueous uranyl triscarbonate to the square bipyramidal structure of the solid calcite, the UO^2_{2+} simply became randomly oriented in the Ca^{2+} site within the calcite.

With the use of the brilliant x-ray beams from the APS, however, the researchers in this study were able to spot the low concentration of uranium and show a different reality. The researchers found that UO^2_{2+} is indeed incorporated at the Ca^{2+} site within the calcite structure, within a well-ordered square bipyramidal geometry. Inside the crystal, one calcium and two carbonate groups are replaced with one uranium and two oxygen of the uranyl structure. The calcite showed three coordination shells of calcium atoms surrounding this uranyl at a distance of approximately 6.5 Å. The presence of the Ca signals at such a large distance attests to the well incorporated uranyl within the calcite structure.

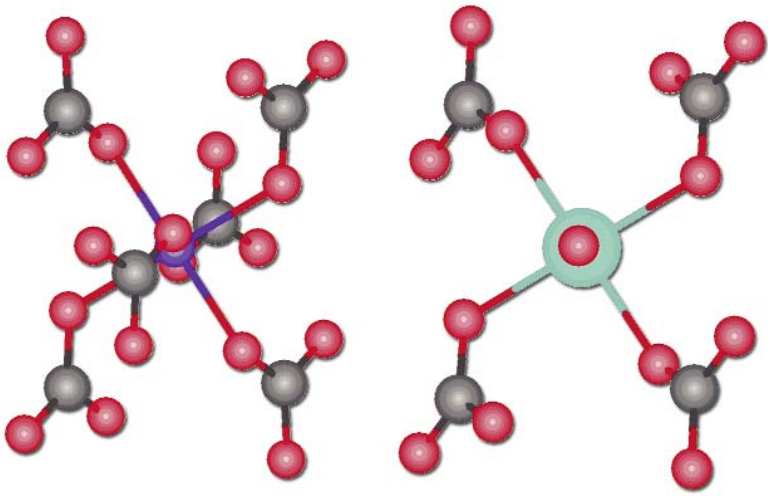

Fig. 1. Schematic of two calcites. The left diagram shows calcium (small dark blue) at the center, and the right diagram has uranyl (large light blue) at the center. Surrounding the centers are oxygen (small red) and carbon (small grey) atoms.

The mechanism of uranium incorporation is still unknown. Biological processes, organic matter, or other impurities may be necessary to incorporate the uranyl into calcite, and understanding this process is certainly not trivial. While this study shows that uranium can be incorporated into calcite under natural conditions, knowing the details of uranium uptake and its stability under different atomic environments is crucial for remediation purposes. This calcite does, however, show a path towards reliable long-term sequestration of uranium. In addition, the stability of the uranium confirms its usefulness as a geological dating technique. — *Karen Fox*

Continued on page 108

"Evolution of Uranyl" continued from page 107

See: Shelly D. Kelly[1]*, E. Troy Rasbury[2], Soma Chattopadhyay[1], A. Jeremy Kropf[1], and Kenneth M. Kemner[1], "Evidence of a Stable Uranyl Site in Ancient Organic-Rich Calcite," Environ. Sci. Tech. **40**, 2262 (2006).
DOI: 10.1021/es051970v
Author affiliations: [1]Argonne National Laboratory, [2]SUNY Stony Brook
Correspondence: *skelly@anl.gov.

This work is supported by the Environmental Remediation Science Program, Office of Biological and Environmental Research, Office of Science, U.S. Department of Energy (DOE), under contract W-31-109-Eng-38. The MR-CAT operations are supported by DOE and the MR-CAT member institutions. Use of the Advanced Photon Source was supported by the U.S. Department of Energy, Office of Science, Office of Basic Energy Sciences, under Contract No. W-31-109-ENG-38.

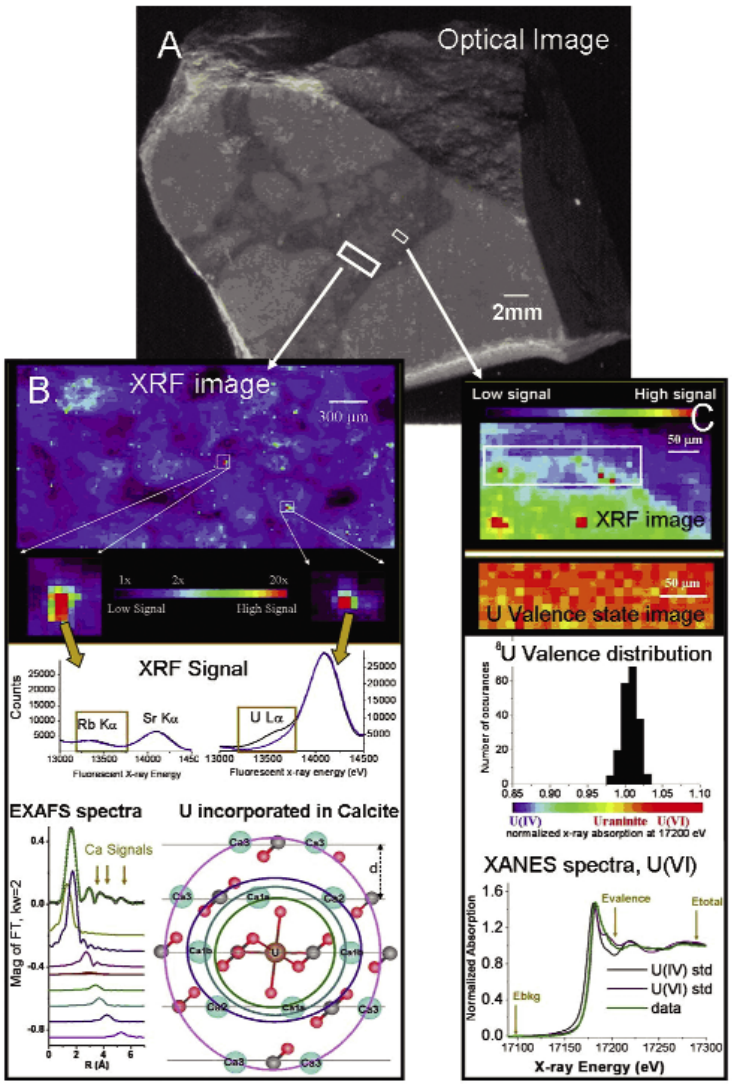

Fig. 2 (A): The centimeter-sized calcrete with dark traces representing the remains of dark organic-rich matter around lighter circular regions left from the cross sections of roots. Fig. 2 (B). Shown at the top, the U μ -XRF signal, for a spatial distribution of uranium concentration, was determined in the dark organic-rich region outlined with a large square. Within this region, a relatively enriched location was selected for μ-EXAFS measurement. The measured spectrum was determined to be consistent with full incorporation of uranium into the calcite structure, as shown by the μ-EXAFS spectra, model, model components, and molecular diagram at the bottom of the figure. Fig. 3 (C). In another region, outlined by the smaller rectangle in Figure 1a, the μ -XANES structure was imaged (shown at the top). These measurements indicate that the coordination environment of uranium in this region is similar to that where the μ-EXAFS signal was collected, as shown by the Gaussian distribution (shown in the middle) of the absorption signal at the valence state energy above the absorption edge. An example of the full XANES spectra is shown at the bottom of the figure.

"Charged Ions" continued from page 106

fully and partially hydrated Sr^{2+} provides an unprecedented description of ion adsorption at mineral-water interfaces.

The distribution of the Sr^{2+} in two different interfacial sites involves a balance between the energy needed to remove water molecules form the ion's hydration shell and the energy released by compensating the surface charge. The authors theorize that the total structure represents a dynamic equilibrium between partially and fully hydrated species of Sr^{2+}. Therefore the adsorption strengths for the inner and outer spheres must be comparable, contrary to the common assumption that the outer-sphere type is inherently weaker. Ion-hydration energies alone are not, however, able to explain the results given the electrostatic energy difference between the two adsorbed divalent cation species, since the reduction in energy is not large enough. Thus, the difference in hydration energies for Rb^{+} and Sr^{2+} can explain their different distributions, but the interfacial hydration structure must also play a role in stabilizing the distributions. Direct determination of such structures, therefore, must be incorporated into theoretical descriptions. — *Karen Fox*

See: Changyong Park[1]*, Paul A. Fenter[1], Kathryn L. Nagy[2], and Neil C. Sturchio[2], "Hydration and Distribution of Ions at the Mica-Water Interface," Phys. Rev. Lett. **97**, 016101 (7 July 2006). DOI: 10.1103/PhysRevLett.97.016101
Author affiliations: [1]Argonne National Laboratory, [2]University of Illinois at Chicago
Correspondence: *cypark@anl.gov

This work was supported by the Geosciences Research Program of the Office of Basic Energy Sciences, U.S. Department of Energy, through Contract No. W-31-109-ENG-38 to Argonne National Laboratory and DOE Grants No. FG02-03ER15381 and No. FG02-02ER15364 to the University of Illinois at Chicago. Use of the Advanced Photon Source was supported by the U.S. Department of Energy, Office of Science, Office of Basic Energy Sciences, under Contract No. W-31-109-ENG-38.

The Europium-Americium Divide

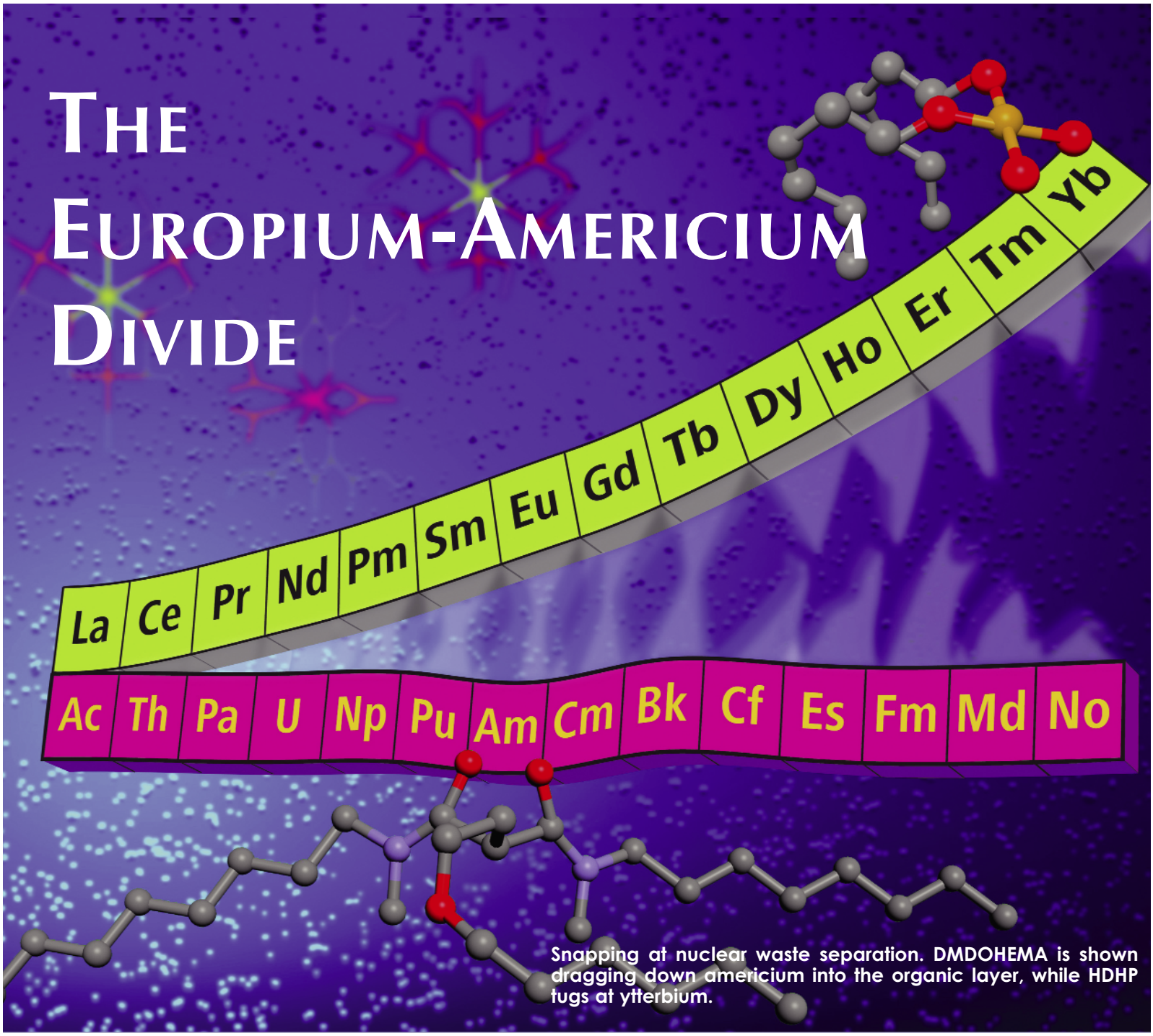

Snapping at nuclear waste separation. DMDOHEMA is shown dragging down americium into the organic layer, while HDHP tugs at ytterbium.

© The Royal Society of Chemistry 2006

Finding a safe and efficient way to separate the components of nuclear waste has been a technological problem since the advent of the nuclear power industry. Of particular difficulty is how to separate the long-lived radioactive elements, such as americium, from chemically similar non-radioactive elements, which include europium. Now, researchers from Argonne, the Commissariat à l'Energie Atomique (CEA), and the Ecole Nationale Supérieure de Chimie de Paris have used XOR/BESSRC beamline 12-BM-B to obtain detailed structural information that could improve a novel process for separating ions of these elements.

Continued on page 110

"Europium" continued from page 109

Liquid-liquid extraction—one approach for nuclear waste component separation—uses water and an organic solvent containing additives to selectively trap americium and carry it into the organic phase, leaving europium dissolved in the water. Finding the most effective additives is, however, a difficult process. The ions of these elements have the same charge and are almost the same size, which makes them almost indistinguishable, chemically speaking.

A new approach developed at CEA-Valrhô uses two molecular extractants—a diamide (*N*,*N*′-dimethyl-*N*,*N*′-dioctylhexylethoxymalonamide, DMDOHEMA) and a dialkylphosphoric acid (di-*n*-hexylphosphoric acid, HDHP). However, despite their potential for separating radioactive from non-radioactive materials, there is a dearth of structural information about how these additives interact with lanthanides and actinides. Atomic-level insights could be pivotal in understanding and improving the process.

The Franco-American research team synthesized complexes of the trivalent (3^+) actinide and lanthanide ions—neodymium, europium, ytterbium, and americium—with the two organic additives DMDOHEMA and HDHP. They then studied each individual structure at atomic detail, using x-ray absorption (EXAFS) and infrared (IR) spectroscopies.

By varying the extraction conditions and the concentrations of each additive to the process and then analyzing the complexes formed, the researchers were able to elucidate particular characteristics of each and to make several generalizations about the results. They found that the HDHP complexes with the 3^+ ions (M) resulted in the coordination of six oxygen atoms to the M ions, forming MO_6 structures. They also observed distant interactions between the M ions and either three or six phosphorus atoms from the HDHP.

In contrast, DMDOHEMA complexes with the 3^+ ions to form an MO_8 structure, in which pairs of oxygen atoms from the carbonyl (C=O) groups of two DMDOHEMA molecules—as well as oxygen atoms from three charge-balancing nitrate ions (NO_3^-)—bind to the M ions.

The EXAFS results do not provide detailed three-dimensional information about the shape of the complexes. However, by combining the EXAFS results with data on the extraction process and IR spectra, the team could work out the details of the chemistry taking place, the actual numbers of molecules involved, and the stoichiometries. This information helps improve understanding of the structural basis of the additive assisted liquid-liquid extraction.

This research suggests that the partitioning of Am(3^+) in the process is facilitated by the presence of DMDOHEMA and HDHP molecules, which allow more freedom of movement during binding to the M ions. Supramolecular organization of the M–molecular complexes also likely assists in this process. The researchers still face many challenges before they can improve the extraction process significantly; they plan to continue the x-ray research at the APS in order to determine whether or not the two extractants act independently or if aggregated species act in concert.

The researchers anticipate that their results will stimulate theoretical studies of the molecular structures by providing a benchmark against which molecular simulations of the complex liquid-liquid separations systems can be studied. Such simulations could provide new insights into how to fine-tune the extraction additives and so improve the process still further. A better separation process would be of benefit to the environment by providing a more effective means of recycling nuclear waste. — *David Bradley*

See: Benoît Gannaz[1], Mark R. Antonio[2]*, Renato Chiarizia[2], Clément Hill[1], and Gérard Cote[3], "Structural study of trivalent lanthanide and actinide complexes formed upon solvent extraction," Dalton Trans. 4553 (2006).
DOI: 10.1039/b609492a

Author affiliations: [1]CEA-Valrhô, [2]Argonne National Laboratory, [3]Université Pierre et Marie Curie-Paris 6
Correspondence: *mantonio@anl.gov

This work is supported by the U.S. DOE, BES-Chemical Sciences and Materials Sciences under contract number W-31–109-ENG-38, for the part performed at Argonne National Laboratory; and by the CEA, DRCP/SCPS, for the part performed at Marcoule. This collaboration was realized in the framework of the CEA-DOE agreement (C5096). Use of the Advanced Photon Source was supported by the U.S. Department of Energy, Office of Science, Office of Basic Energy Sciences, under Contract No. W-31-109-ENG-38.

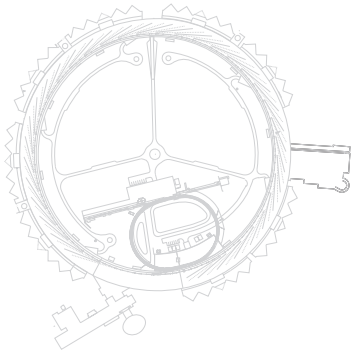

What Stardust is Made of

Stardust, NASA's comet sample return mission, forever changes the way scientists are able to study the makeup of the outer Solar System. The mission spacecraft collected samples from the Wild 2 comet and delivered them to teams of researchers from various scientific disciplines using a variety of experimental techniques. Among these are scientists utilizing synchrotron light sources around the world, including four at the national laboratories funded by the U.S. Department of Energy (DOE). At the Argonne APS, the synchrotron-based x-ray microprobe afforded by GSECARS beamline 13-ID-C was used to characterize the elemental composition of these materials from the outer reaches of the Solar System.

Until the remarkable Stardust mission, scientists had only been able to study the outer Solar System through telescopes, spectroscopes, and the camera lenses of visiting spacecraft. American and Russian spacecraft and astronauts had brought back pieces of the Moon, while meteorites gave us random samples of the asteroid belt, the Moon, and even the surface of Mars. Dust particles, collected by NASA from the Earth's atmosphere, sampled comets and asteroids, but no individual particle can be associated with a particular source. Before Stardust, scientists had never been able to get up close and personal with actual physical samples known to come from the reaches of the outer Solar System, material that could hold vital clues to the origins of the planets, our sun, and life itself.

The Stardust spacecraft changed all that by collecting particles of the Wild 2 comet and delivering them to Earth, bringing planetary scientists an unprecedented bonanza of new knowledge. Reaping that knowledge requires the work of an interdisciplinary team of researchers from hundreds of institutions, using a myriad of techniques to probe the secrets of the Stardust samples. One team focused on studying the elemental composition of a group of samples, using advanced techniques of microscopy and spectroscopy, including synchrotron-based x-ray microprobes (SXRM) at the GSECARS 13-ID-C beamline at the APS.

Stardust caught pieces of the Wild 2 comet mainly through two ingenious tools: a specially-developed silica aerogel designed to slow down and trap speeding particles without destroying them, and the aluminum-foil-covered frame holding the aerogel, in which particles left residue in tiny impact craters like microscopic meteors. The synchrotron-based x-ray microprobe was used to study the tracks left by particles in 23 sample wedges of aerogel (called "keystones") at the APS and five other synchrotron facilities (the DOE's Advanced Light Source, the National Synchrotron Light Source, the Stanford Synchrotron Radiation Laboratory; SPring-8 in Japan, and the European Synchrotron Radiation Facility in France).

Continued on page 112

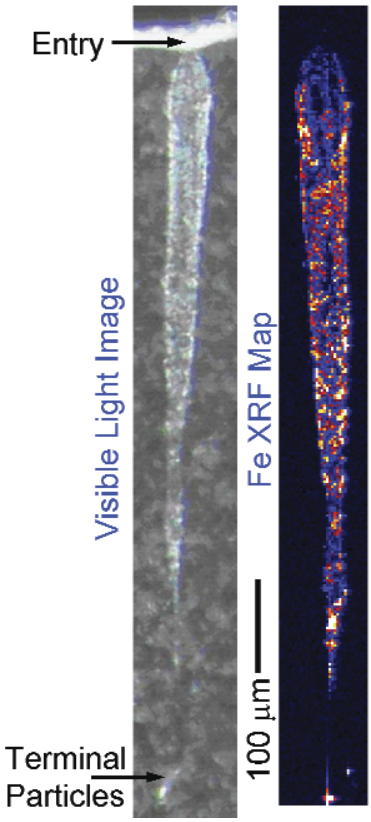

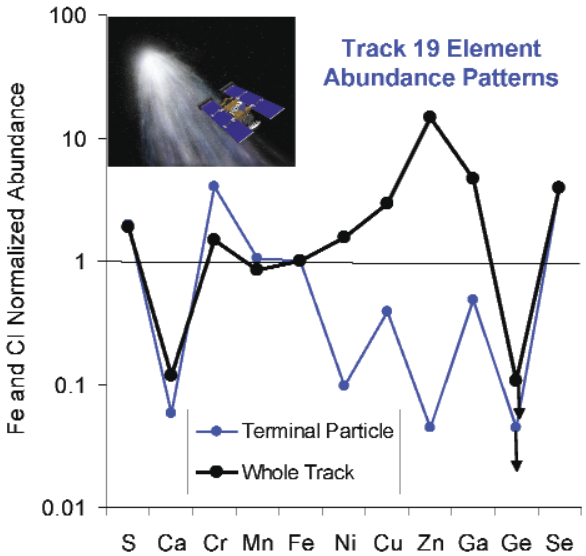

Fig. 1. Stardust Track 19 is 890 µm long. The visible light image (left; NASA-JSC) shows a carrot-like morphology with the entry hole at the top and terminal particles at the bottom. The center image is the Fe map (highest concentrations are bright) obtained at 13-ID-C (GSECARS) showing that the particle disaggregated during the capture process. The element abundance patterns (normalized to Fe and the concentration in CI meteorites) for the whole track and main terminal particle (right) show that the whole track is depleted in Ca and Ge and enriched in moderately volatile elements (Cu, Zn, Ga, Se) with the terminal particle exhibiting a composition distinct from that of the whole track. Inset: Artist's rendering of Stardust encounter with Wild 2 (NASA-JSC).

"Stardust" continued from page 111

The powerful SXRM beam can completely penetrate an entire keystone, causing fluorescence throughout the particle track that indicates the signature presence of various elements. The experimenters compared the Wild 2 samples with the composition of CI meteorites (a class of carbonaceous [C] meteorites whose type specimen is the Ivuna [I] meteorite and that are generally thought to be the most primitive), which, like comets, are believed to consist of material from the early Solar System. Most tracks contained material throughout their lengths, as the slowing particle broke up and scattered pieces of itself, so that the composition of the terminal particle at the end of the track is generally different than the composition of material throughout the entire track.

Two different basic methods were used to analyze the tracks: either a fluorescence spectrum of the whole track was collected by raster scan over an extended time, or a quick scan was performed to identify "hot spots" of elements that were then subjected to more intensive scrutiny. The first strategy gives a good picture of the distribution of abundant elements, while the second is more sensitive for finding scant amounts of trace elements.

One closely-analyzed representative track, number 19, showed iron deposited along almost its entire path with only a small amount remaining in the final particle (Fig. 1). Other detected elements in the Stardust material include calcium, chromium, gallium, selenium, nickel, potassium, sulfur, manganese, zinc, and copper. Because the aerogel material consists mainly of silicon and oxygen, these elements could not be separated from the particle tracks. Ratios between certain elements are similar to the CI composition in some cases, but lower or higher in others. The most commonly detected elements were iron (in all 23 tracks), nickel, and sulfur.

The team found that the Wild 2 particle samples are consistent with the CI meteorite composition and with spectrometry taken of Halley's comet from spacecraft in 1986. Of course, the direct measurements made of the Wild 2 physical samples provide a much clearer picture of cometary composition than the remote Halley spectroscopy results. Compared to CI meteorites, the Wild 2 samples are depleted in sulfur and iron relative to silicon, and enriched in copper, zinc, and gallium. This suggests that the CI meteorite composition may not accurately reflect the distribution of these moderately volatile elements in the early Solar System. A more accurate determination of the amounts of these elements in the Sun's photosphere might better account for this difference. — *Mark Wolverton*

See: George J. Flynn[1]*, Pierre Bleuet[2], Janet Borg[3], John P. Bradley[4], Frank E. Brenker[5], Sean Brennan[6], John Bridges[7], Don E. Brownlee[8], Emma S. Bullock[9], Manfred Burghammer[2], Benton C. Clark[10], Zu Rong Dai[4], Charles P. Daghlian[11], Zahia Djouadi[3], Sirine Fakra[12], Tristan Ferroir[13], Christine Floss[14], Ian A. Franchi[7], Zack Gainsforth[15], Jean-Paul Gallien[16], Philippe Gillet13, Patrick G. Grant[4], Giles A. Graham[4], Simon F. Green[7], Faustine Grossemy[3], Philipp R. Heck[17], Gregory F. Herzog[18], Peter Hoppe[17], Friedrich Hörz[19], Joachim Huth[17], Konstantin Ignatyev[6], Hope A. Ishii[4], Koen Janssens[20], David Joswiak[8], Anton T. Kearsley[21], Hicham Khodja[16], Antonio Lanzirotti[22], Jan Leitner[23], Laurence Lemelle[13], Hugues Leroux[24], Katharina Luening[6], Glenn J. MacPherson[9], Kuljeet K. Marhas[14], Matthew A. Marcus[12], Graciela Matrajt[8], Tomoki Nakamura[25], Keiko Nakamura-Messenger[26], Tsukasa Nakano[27], Matthew Newville[22], Dimitri A. Papanastassiou[28], Piero Pianetta[6], William Rao[29], Christian Riekel[2], Frans J.M. Rietmeijer[30], Detlef Rost[9], Craig S. Schwandt[26], Thomas H. See[26], Julie Sheffield-Parker[31], Alexandre Simionovici[13], Ilona Sitnitsky[1], Christopher J. Snead[15], Frank J. Stadermann[14], Thomas Stephan[23], Rhonda M. Stroud[32], Jean Susini[2], Yoshio Suzuki[33], Stephen R. Sutton[22], Susan Taylor[34], Nick Teslich[4], D. Troadec[24], Peter Tsou[28], Akira Tsuchiyama[35], Kentaro Uesugi[33], Bart Vekemans[20], Edward P. Vicenzi[9], Laszlo Vincze[36], Andrew J. Westphal[15], Penelope Wozniakiewicz[21], Ernst Zinner[14], and Michael E. Zolensky[19], "Elemental Compositions of Comet 81P/Wild 2 Samples Collected by Stardust," Science **314**, 1731 (2006). DOI: 10.1126/science.1136141

Author affiliations: [1]State University of New York at Plattsburgh; [2]European Synchrotron Radiation Facility; [3]Institut d'Astrophysique Spatiale; [4]Lawrence Livermore National Laboratory; [5]Johann Wolfgang Goethe-Universität; [6]Stanford Linear Accelerator Center; [7]The Open University; [8]University of Washington; [9]Smithsonian Institution; [10]Lockheed Martin; [11]Dartmouth College; [12]Advanced Light Source; [13]École Normale Supérieure de Lyon; [14]Washington University; [15]University of California, Berkeley; [16]CEA/CNRS; [17]Max Planck Institute for Chemistry; [18]Rutgers University; [19]NASA Johnson Space Center; [20]Universiteit Antwerpen; [21]The Natural History Museum, London; [22]The University of Chicago; [23]Universität Münster; [24]University Lille; [25]Kyushu University; [26]Engineering and Science Contract Group/Jacobs Sverdrup, NASA Johnson Space Center; [27]National Institute of Advanced Industrial Science and Technology; [28]Jet Propulsion Laboratory, California Institute of Technology; [29]University of Georgia; [30]University of New Mexico; [31]XRT Limited; [32]U.S. Naval Research Laboratory; [33]Japan Synchrotron Radiation Research Institute/SPring-8; [34]Engineering Research and Development Center/Cold Regions Research and Engineering Laboratory; [35]Osaka University; [36]Ghent University

Correspondence: *george.flynn@plattsburgh.edu

Four synchrotrons used in this effort are national user facilities supported in part by the U.S. Department of Energy, Office of Science, Office of Basic Energy Sciences, under contract numbers (with managing institutions in parentheses) DE-AC02-05CH11231 (Advanced Light Source, University of California), DE-AC02-06CH11357 (Advanced Photon Source, University of Chicago Argonne, LLC), DE-AC02-98CH10886 (National Synchrotron Light Source, Brookhaven Science Associates), and DE-AC03- 765F00515 (Stanford Synchrotron Radiation Laboratory, Stanford University). Experiments were performed at the BL47XU in the SPring-8 with the approval of the Japan Synchrotron Radiation Research Institute. The European Synchrotron Radiation Facility provided synchrotron radiation facilities. Stardust was the fourth flight project of NASA's Discovery Program.

Is an Iron-rich Silicate the Key to Ultra-low-velocity Zones?

Deep beneath the Earth's surface, just above its iron-rich core, lies the D" layer, one of the most poorly understood portions of our planet. The enigmatic layer was slightly demystified in 2004 and 2005 as scientists discovered a post-perovskite (ppv) transition in $MgSiO_3$, which could explain many of the intriguing seismic features observed in this region. However, one feature that could not be easily explained is the origin of 5-km- to 40-km-thick patches, known as ultra-low-velocity zones (ULVZs). As seismic waves cross these regions their velocities are depressed dramatically—the compressional wave velocities drop 5% to 10%, and the shear wave velocities drop 10% to 30%. Density increases of up to 50% may also be present. Researchers from Los Alamos National Laboratory, the Carnegie Institution of Washington, Argonne, and The University of Chicago have examined iron-rich silicate using three beamlines at the APS, and found that it has the low-velocity, high-density signature characteristic of ULVZs, thus providing an alternate explanation for the origin of these zones.

The experimenters examined a sample of $Fe_{0.4}Mg_{0.6}SiO_3$ (referred to as Fs40) at pressures of up to 170 GPa, using synchrotron x-ray diffraction (XRD) at the GSECARS 13-ID-D and the HP-CAT 16-ID-B beamlines at the APS. The samples were compressed to 130 GPa and laser-heated to 2000K, which converted the sample into well-crystallized, single-phase ppv silicate. Pressure was increased incrementally to 170 GPa and decreased down to 125 GPa, with repeated laser annealing to 2000K between each increment to release deviatoric strain. The researchers found that the density $\rho = 6.08$ g/cm^3, the bulk modulous K = 792 GPa, and the seismic bulk sound speed $V_\varphi = 11.43$ km/s at 130 GPa for this ppv composition (Fig. 1).

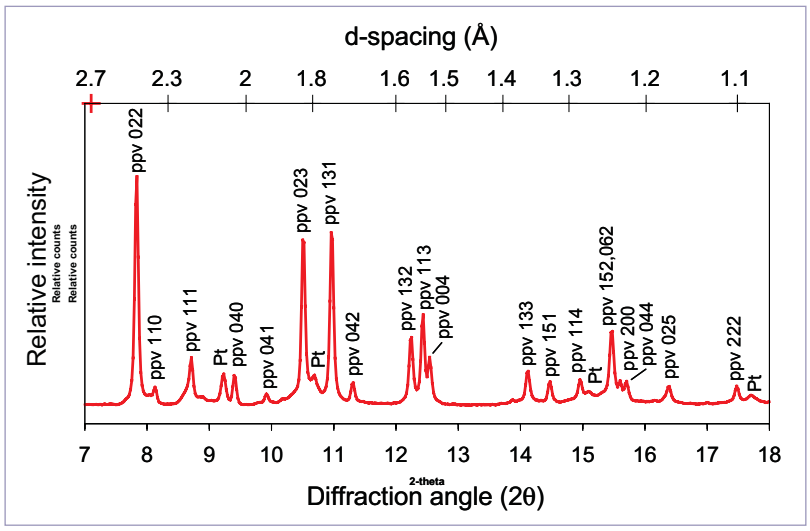

© 2006 American Association for the Advancement of Science. All Rights Reserved.

Fig. 1. X-ray diffraction pattern for Fs40 ppv at 138 GPa (λ = 0.3344 A°).

After utilizing a panoramic diamond-anvil cell in an x-ray transparent Be gasket to synthesize the Fs40 sample at 130 GPa and 2000K, the researchers confirmed the formation of post-perovskite by the use of XRD. The researchers then carried out nuclear resonant inelastic x-ray scattering measurements at room temperature on the XOR 3-ID beamline at the APS. The spectra were used to obtain the iron-related partial phonon density of states (DOS). The low-energy portion of the DOS could then be fitted to a Debye model to give the Debye velocity. In conjunction with the XRD results, this allowed for calculation of the compressional and shear wave velocities. The group determined that the compressional wave velocity across Fs40 ppv at 130 GPa and 300K was 12.72 ± 0.12 km/s and the shear wave velocity was 4.86 ± 0.03 km/s.

These room-temperature parameters are close to those in the ULVZ. Temperature correction to the core mantle boundary (CMB) conditions further reduces the velocities beyond ULVZ values. This may indicate that $FeSiO_3$ contents lower than 40%—or the addition of solid phases such as magnesiowüstite—would be needed to bring the values back into agreement. The present results indicate that the addition of iron is sufficient to explain the seismic features of the ULVZ, thus providing an alternative explanation to partial melting.

The vast reservoirs of iron and silicates at the CMB provide favorable chemical-physical conditions for the formation of iron-rich ppv silicate, which holds the key to understanding the geophysical and geochemical properties of the D" layer. Contrary to previous thinking that the mantle composition was essentially unchanged by contact with the core—i.e., the composition of the mantle silicate remains within its iron-poor solubility limit—the new scenario calls for a reaction layer of denser silicates with much higher iron content. In regions of downward or horizontal movement at the CMB, the thickness of the iron-rich layer is limited by solid reaction and diffusivity. In upwelling regions, the iron-rich layer is too heavy to rise and will pile up

Continued on page 116

Sound Velocities in the Earth's Deep Mantle

The Earth's lower mantle is thought to be made of approximately 20% ferropericlase and 80% silicate perovskite. Measuring the properties of these two materials at high pressures and temperatures is therefore crucial to understanding the geophysics and geochemistry of the deep mantle. Ferropericlase has a chemical formula of (Mg, Fe)O and is thought to contain approximately 20% ferrous iron in the lower-mantle. Under ambient conditions the ferrous iron in ferropericlase has two paired 3*d* electrons and four unpaired ones (where 3*d* electrons, in general, are the electrons that occupy the outermost shell of the iron electron cloud). This configuration is known as a "high-spin" state. At pressure conditions of 40 to 60 GPa, all six 3*d* electrons pair up, thus forming a "low-spin" state, which has very different chemical and physical properties than the former. Until recently, only the high-spin state had been studied and the low-spin characteristics were extrapolated or neglected. Now, researchers from Lawrence Livermore National Laboratory, the Carnegie Institution of Washington, Northwestern University, Argonne, and the California Institute of Technology have carried out the first successful study of lower-mantle ferropericlase at pressures up to 110 GPa to describe the seismic velocities across the electronic high-spin to low-spin transition in ferropericlase at conditions similar to that of the lower mantle.

The researchers placed a tiny sample—just 50 μm across—of polycrystalline ferropericlase [$(Mg_{0.75}, Fe_{0.25})O$], with ~95% enrichment of ^{57}Fe isotope, into a diamond anvil cell on which they conducted high-pressure nuclear resonant inelastic x-ray scattering experiments at XOR beamline 3-ID at the APS. A modified diamond cell with a beryllium gasket and boron powder was used for pressures over one megabar. They used a ruby fluorescence scale (provided by HP-CAT at APS sector 16) to determine pressures.

Thanks to the very-high-energy resolution and high photon flux of the APS beamline, the team was able to extract the partial phonon density of states from the measured energy spectra and then derive the Debye sound velocities for the sample under ultrahigh pressures. Together with the density and incompressibility results of ferropericlase that had been measured earlier [1], they derived the compressional and shear wave velocities of the ferropericlase sample across the electronic high-spin to low-spin transition. Under higher pressures between 42 GPa to 58 GPa, the researchers saw abnormal behavior on the compressional and shear velocities across the electronic spin transition. These parameters and their pressure derivatives increase significantly for the low-spin ferropericlase over that of the high-spin state.

Continued on page 116

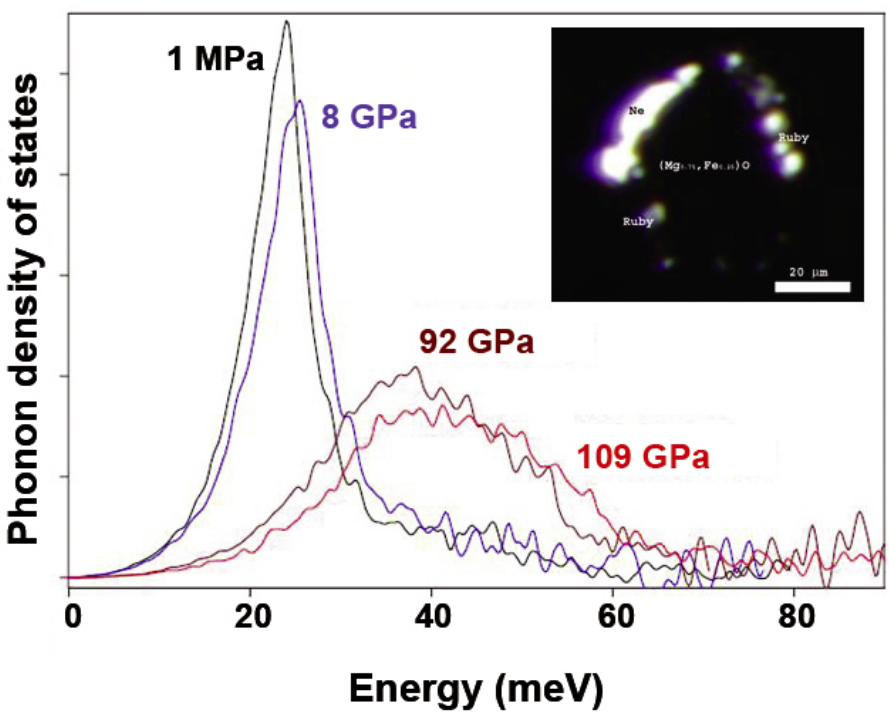

Fig. 1. Partial phonon density of states of iron in ferropericlase [$(Mg_{0.75}, Fe_{0.25})O$] at high pressures measured by nuclear resonant inelastic x-ray scattering. The samples at 1 MPa and 8 GPa were in the high-spin state and in the low-spin state at 92 GPa and 109 GPa. The initial slopes of the phonon density of states are shifted to much higher energies due to the spin transition, as well as the pressure effect. The initial slopes of the spectra are used by the researchers to derive sound velocities of the sample across the electronic spin transition. A picture of the sample at 8 GPa is shown at the upper-right corner. The opaque region at the center is the sample.

Perovskite under Pressure

One of the least understood regions of our planet is a mysterious layer—known simply as D"—that lies between the Earth's core and mantle. Seismic waves crossing this layer have anomalous properties—an effect that is inconsistent with (Mg, Fe)SiO_3 in a perovskite phase, the material thought to make up the bulk of the Earth's deep mantle. The 2004 discovery of a post-perovskite phase of the material has helped create a new paradigm. A post-perovskite layer might indeed account for this ultra-low-velocity zone. Experiments and theories have placed constraints on some physical properties of the layer, including the elastic tensor and the Clapeyron slope of the transition. Researchers from National Cheng Kung University, Princeton University, The University of Chicago, the Japan Agency for Marine-Earth Science and Technology, the Tokyo Institute of Technology and the Japan Synchrotron Radiation Research Institute—using the GSECARS 13-ID beamline at the APS, and the BL10XU beamline at SPring-8 in Japan—have obtained the first experimental studies of the equation of state of perovskite and post-perovskite phases over a broad range of pressures in order to compare them with current theories.

The researchers synthesized samples of combined perovskite and post-perovskite from an orthopyroxene sample containing 9 mol. % iron by using a laser-heated diamond anvil cell. The samples were examined with synchrotron x-ray diffraction performed at 13-ID-D and at BL10XU. The group obtained pressure-volume data at 300K by gradual decompression of the sample without additional heating.

Analysis of the data showed that the post-perovskite phase has a bulk modulus K_o of 219 GPa and an ambient pressure volume V_o of 164.9 Å^3 for bulk modulus pressure derivative, K'_o fixed at 4. This agrees fairly well with theory, and indicates that low concentrations of iron do not strongly affect the bulk modulus of the post-perovskite phase.

Examining samples combining perovskite and post-perovskite provides some challenges to obtaining high-quality diffraction patterns. On the other hand, it allows for studying the two phases under identical conditions. A direct comparison of the volumes of perovskite and post-perovskite at 83 to 106 GPa shows that the post-perovskite has a lower volume than the perovskite by 1.1%. This differs slightly from theoretical predictions, which have estimated volume changes of 1.4-1.6% at 120 GPa.

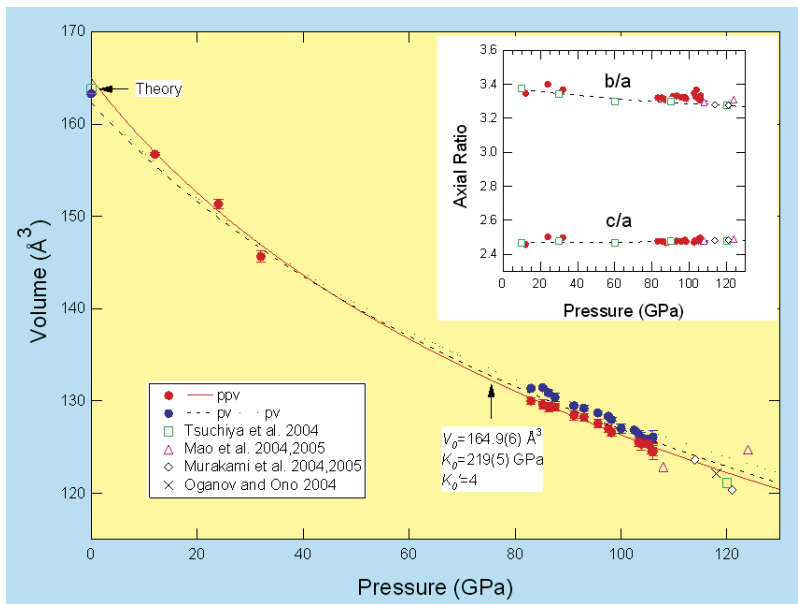

Fig. 1. The equation of state of perovskite and post-perovskite phases. The dashed and dotted curves are the experimentally determined EOS for $MgSiO_3$ perovskite and $Mg_{0.95}Fe_{0.05}SiO_3$ post-perovskite, respectively. The solid curve shows a second-order Eulerian finite strain fit (K'_0 = 4.0) to the post-perovskite phase data. Insert: The pressure dependence of the axial ratios of the post-perovskite phase.

By differentiating the pressure-volume equation of state, the bulk moduli of both phases were computed as a function of pressure. The bulk modulus of the post-perovskite phases is 575 GPa at 100-GPa pressure and 641 GPa at 120-GPa pressure. The calculated bulk modulus for perovskite was 663 GPa at 120 GPa. The bulk moduli of the two phases overlap within mutual uncertainties and this is consistent with theoretical calculations. Despite being the high-pressure phase, it is possible that post-perovskite has a lower bulk modulus than perovskite at deep mantle pressures, as this has been sometimes observed in other oxide systems. Combining the results for volume and bulk modulus indicates that at 120 GPa, the bulk sound velocity decreases by 2.3 ± 2.1%. This is compatible with theoretical predictions of a <1% velocity change, but also allows for a larger than 4% velocity change.

These results show that the post-perovskite phase can be synthesized at 109 GPa and 2400K for a starting sample with 9 mol. % $FeSiO_3$. When applied to the planet itself, this sug-

Continued on page 116

"Ultra-low-velocity Zone" continued from page 113

under plumes, resulting in the observed ULVZ. Although comprehensive studies of the equation of state, elastic anisotropy, diffusivity, rheology, magnetism, and reversible phase relation of ppv as a function of temperature and iron concentration are still needed for developing the new paradigm for this most enigmatic layer in the solid Earth, this study unearths exciting new clues about the dominating role iron-rich ppv may play in the D" layer. — *Karen Fox*

See: Wendy L. Mao[1]*, Ho-kwang Mao[2,3], Wolfgang Sturhahn[4], Jiyong Zhao[4], Vitali B. Prakapenka[5], Yue Meng[3], Jinfu Shu[2], Yingwei Fei[2], and Russell J. Hemley[1], "Iron-Rich Post-Perovskite and the Origin of Ultralow-Velocity Zones," Science **312**, 564 (28 April 2006). DOI: 10.1126/science.1123442

Author affiliations: [1]Los Alamos National Laboratory, [2]Carnegie Institution of Washington, [3]High Pressure Collaborative Access Team, [4]Argonne National Laboratory, [5]The University of Chicago
Correspondence: *wmao@lanl.gov

We thank the NSF-EAR Petrology and Geochemistry, NSF-EAR Geophysics, and NSF-EAR Instrumentation and Facility Programs for financial support. GSECARS is supported by NSF Earth Sciences (EAR-0217473), DOE Geosciences (DE-FG02-94ER14466), and the State of Illinois. HP-CAT is supported by DOE-BES, DOE-NNSA (CDAC), NSF, DOD-TACOM, and the W. M. Keck Foundation. Use of the Advanced Photon Source was supported by the U.S. Department of Energy, Office of Science, Office of Basic Energy Sciences, under Contract No. W-31-109-ENG-38.

"Sound Velocities" continued from page 114

The dramatic jump of the sound velocities across the electronic spin-pairing transition indicates that previous attempts to derive models of the lower-mantle sound velocities from high-spin ferropericlase and silicate pervoskite alone are insufficient to correctly model the lower mantle. The bulk of information about the Earth's interior is derived by using seismic waves traveling through the Earth to directly measure compressional and shear wave velocities. However, these velocities no longer correlated well with the model of the Earth's composition once the researchers incorporated into the model the characteristics of the low-spin ferropericlase. On the other hand, the change in sound velocities across the spin transition could offset the effect of adding iron to the model of the lower mantle materials. The researchers conclude that sound velocities of low-spin ferropericlase need to be considered in future geophysical models of the lower mantle. — *Karen Fox*

Reference

[1] Lin et al., Nature **436**, 375, (2005).

See: Jung-Fu Lin[1], Steven D. Jacobsen[2,3], Wolfgang Sturhahn[4], Jennifer M. Jackson[2,‡], Jiyong Zhao[4], and Choong-Shik Yoo[1], "Sound velocities of ferropericlase in the Earth's lower mantle," Geophys. Res. Lett. **33**, L22304 (2006). DOI:10.1029/2006GL028099

Author affiliations: [1]Lawrence Livermore National Laboratory, [2]Carnegie Institution of Washington, [3]Northwestern University, [4]Argonne National Laboratory. ‡Now at California Institute of Technology
Correspondence: *afu@llnl.gov

This work was supported by U.S. DOE, Basic Energy Sciences, Office of Science, under contract W-31-109-ENG-38, and the State of Illinois under HECA. This work at LLNL was performed under the auspices of the U.S. DOE by the University of California and LLNL under contract W-7405-Eng-48. J.F.L. is also supported by the Lawrence Livermore Fellowship. S.D.J. acknowledges financial support from NSF EAR-0440112, a Carnegie Fellowship and CDAC. J.M.J. acknowledges financial support from a Carnegie Fellowship. Use of the Advanced Photon Source was supported by the U.S. Department of Energy, Office of Science, Office of Basic Energy Sciences, under Contract No. W-31-109-ENG-38.

"Perovsites" continued from page 115

gests the post-perovskite phase will form some 400-550 km above the core-mantle boundary where the D" layer exists. If the D" discontinuity is indeed due to the post-perovskite phase, then the deep lower mantle would require temperatures of 3500-4000K. However, other factors and complications—such as multicomponent chemical effects, pressure scale uncertainties, Clapeyron slope uncertainties, and the effects of the transformation itself on mantle dynamics—do exist. — *Karen Fox*

See: Sean R. Shieh[1]*, Thomas S. Duffy[2], Atsushi Kubo[2], Guoyin Shen[3], Vitali B. Prakapenka[3], Nagayoshi Sata[4], Kei Hirose[5], and Yasuo Ohishi[6], "Equation of state of the postperovskite phase synthesized from a natural $(Mg,Fe)SiO_3$ orthopyroxene," Proc. Nat. Acad. Sci. U.S.A.. **103**(9), 3039 (February 28, 2006). DOI: 10.1073pnas.0506811103

Author affiliations: [1]University of Western Ontario, [2]Princeton University, [3]The University of Chicago, [4]Japan Agency for Marine-Earth Science and Technology, [5]Tokyo Institute of Technology, [6]Japan Synchrotron Radiation Research Institute
Correspondence: *sshieh@uwo.ca

This work was supported by the National Science Foundation, the Packard Foundation, the National Science Council, and the National Synchrotron Radiation Research Center. GSECARS is supported by the National Science Foundation, the Department of Energy, and the State of Illinois. Use of the Advanced Photon Source was supported by the U.S. Department of Energy, Office of Science, Office of Basic Energy Sciences, under Contract No. W-31-109-ENG-38.

Probing the Behavior of Atoms in Strong Laser Fields

Atoms in gaseous states can do fascinating things, especially when zapped with extreme electromagnetic fields from an ultrashort, intense laser pulse. One example is high-order harmonic generation (HHG), where ionized atoms produce coherent soft x radiation by recombining with laser-driven electrons. The coherent x-ray generation process is an in-phase collective response of many ion-electron recombination events in a plasma environment. To optimize HHG, and to use such phenomena for applications such as imaging molecular orbitals, one must better understand this process and how similar strong-field processes operate. In the past, electron energies and charged particle yields could only be determined for isolated atoms and details of the laser-produced plasma could only be simulated. Now, Argonne researchers have developed a synchrotron-based x-ray microprobe capable of peering into laser-produced plasmas and seeing directly the behavior of atoms in this extreme environment.

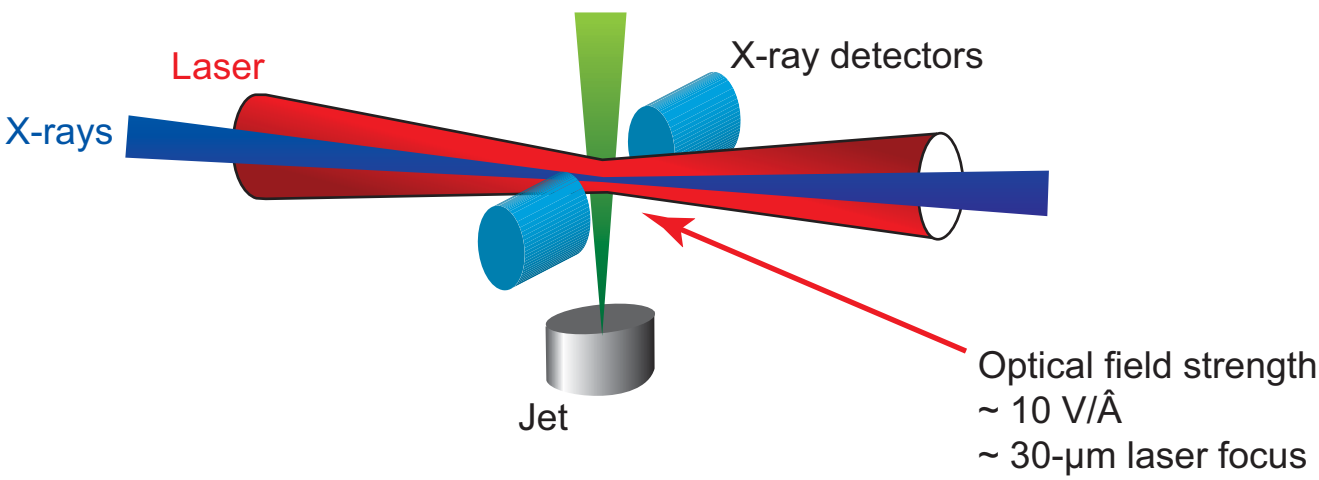

Fig. 1. Microfocused x-rays probe atoms in the focus of a high-intensity laser.

In a triple-beam arrangement, the researchers placed a micron-sized x-ray beam from the XOR 7-ID beamline at the APS within a focused optical laser beam, which intersected a third beam formed by a room-temperature jet of krypton gas. The strong optical field from the laser ionized the krypton atoms creating a localized plasma. Ionized krypton (Kr^+) has a background-free x-ray absorption signature, allowing the tunable x-rays to probe specifically the Kr^+ ions in time and space. In addition, by controlling the orientation of the laser polarization axis with respect to that of the x-rays, the researchers are able to probe the alignment direction of the empty orbital produced by the laser ionization process. The microfocus setup of the x-ray probe (Fig. 1) increases the x-ray flux density by 10^4 over standard laser/x-ray pump/probe configurations, enabling effective measurements with fewer atoms and less laser power.

X-ray spectra that demonstrate the Kr^+ signature were taken by recording $K\alpha$ emission as a function of incident x-ray energy. Because $K\alpha$ emission occurs within 0.2 fs, it is a collision-free signature of absorption. The Kr^+ spectrum shows a strong resonance at 14.313 keV because of the vacant 4p orbital created by strong-field ionization. The amplitude of this $1s \rightarrow 4p$ resonance of the Kr^+ can indicate the orbital alignment of the 4p hole, and thus shed light on the mechanism of the strong-field ionization process. The simplest model for strong field ionization assumes that the electron tunnels out along the polarization axis of the laser, leaving the 4p hole aligned in that direction. Consequently, with laser and x-ray polarization axes parallel, one expects a strong absorption resonance, and, for the perpendicular configuration, a suppressed resonance. In

Continued on page 119

Proteins Sing Optical Harmony

Chemists are using biologically inspired materials as useful tools in non-biological applications. For example, computing and communications are two applications that can benefit from modeling after nature's accomplishments. Potentially useful biological tools are bits of proteins called peptides, which can be designed and constructed easily. Researchers from Argonne and the University of Pennsylvania are investigating whether thin layers of peptides, augmented by molecules that endow the layers with optical properties, could serve as nonlinear optical materials. The researchers have taken advantage of the XOR/CMC beamline 9-ID at the APS and the X22-B beamline at the National Synchrotron Light Source to examine the structures of thin layers of peptides into which have been inserted different kinds of synthesized, optically responsive molecules. The team found they could insert molecules with nonlinear optical properties into peptide layers while maintaining the integrity of the layers themselves. This sets the foundation for tests of the materials' nonlinear optical properties, such as second harmonic generation—the conversion of light at one frequency to light at twice that frequency.

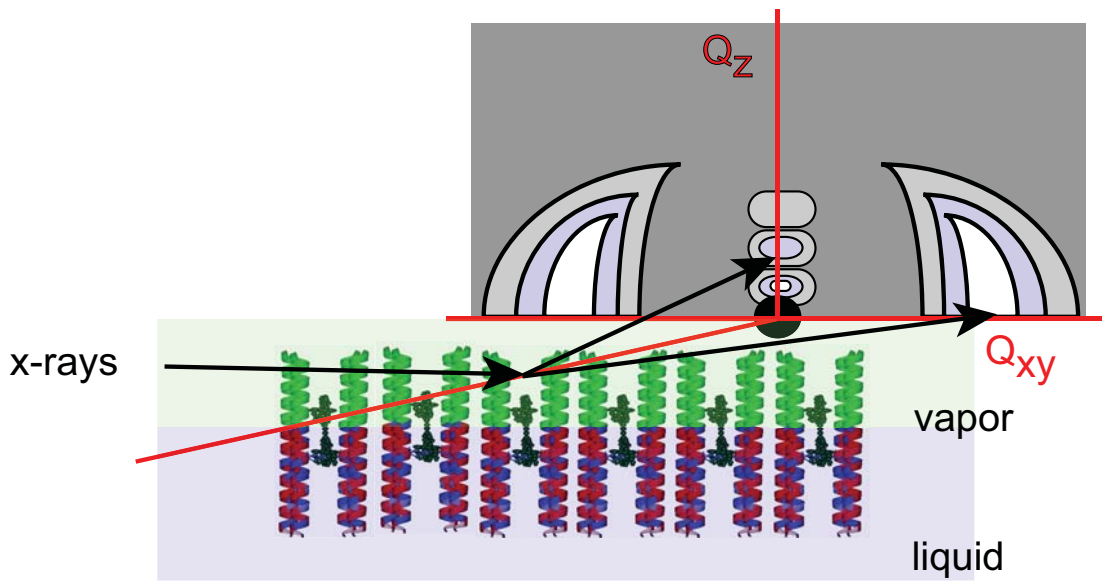

Fig. 1. Cofactors with nonlinear optical properties snuggle between peptide helices, creating a film whose structure can be determined by x-rays bouncing off the thin layer. (Illustration courtesy of J. Strzalka.)

To custom-build nonlinear optical materials, the researchers started with small peptide proteins, which they designed to form a structure called an alpha helix. Alpha helices form a nice sausage shape, and can be designed to interact with each other along their lengths. With a little surface pressure, the peptides queue up vertically in a single layer, forming a film as thick as the peptides are long. The team designed the helices to be approximately five times as long as they are wide, and with different properties at the ends: one end prefers water and the other prefers anything but. In this way, the researchers created a film with different properties on the top and bottom, a film that can bridge interfaces between unlike media. To add an optical capacity to the thin film, the team added a cofactor: a metal-containing molecule designed with non-linear optical properties. These cofactors need to be oriented along the same direction and isolated from one another in order to work properly. Groups of four peptides can bundle the cofactors within their cores, keeping the cofactors oriented and protected from each other.

After some preliminary work at Brookhaven National Laboratory to determine conditions for their experiments, the researchers tested various cofactors with their thin film at Argonne. One contained zinc and the other contained ruthe-

Continued on next page

"Behavior of Atoms" continued from page 117

the simple tunneling model, the ratio of the amplitude of the 1s → 4p resonance in the parallel:perpendicular laser/x-ray polarization configurations is predicted to be a whopping 38:1. Instead the researchers find a ratio of ~2:1. The observed ratio can be explained by models that include spin-orbit coupling, an ingredient left out of the simple, but oft-used, tunneling model.

The team's work sheds important light on the mechanism of ionization of atoms exposed to strong AC fields (1 billion V/cm). When a freed electron is driven back to its residual ion (after half an optical cycle, 2.8 fs) the presence of the laser field appears to preserve orbital alignment. The actual mechanism of ionization also strongly affects the x-ray absorption spectrum of the ion, creating stronger and weaker resonances depending on the relative polarizations of the pump and probe beams. These direct observations of orbital alignment have never before been possible and provide an important example of the value of the synchrotron-based, time-resolved x-ray microprobe technique.

Beyond probing orbital alignment in plasmas, the time-resolved x-ray microprobe technique has many other uses. By lengthening the laser pulses temporally to overlap the x-ray pulses, molecular alignment processes can be studied. The hard x-rays used here are especially well suited for experiments with laser-produced plasmas because of their ability to penetrate plasmas and produce a collision-free response. The ability to control and better understand the behavior of atoms under extreme conditions in a plasma could also allow the realization of experiments at relativistic intensities where electron trajectories are influenced by both the magnetic component of the light pulse and the electric component which dominates at lower intensities. Finally, the efficient use of laser and x-ray energy in the microprobe geometry will allow x-ray tracking of time-resolved phenomena that are initiated by infrared or ultraviolet excitations where laser pulse energy is limited.

— Mark Wolverton & Linda Young

See: L. Young*, D.A. Arms, E.M. Dufresne, R.W. Dunford, D.L. Ederer, C. Höhr, E.P. Kanter, B. Krassig, E.C. Landahl, E.R. Peterson, J. Rudati, R. Santra, and S.H. Southworth, "X-Ray Microprobe of Orbital Alignment in Strong-Field Ionized Atoms," Phys. Rev. Lett **97**, 083601 (25 August 2006).
DOI: 10.1103/PhysRevLett.97.083601
Author affiliation: Argonne National Laboratory
Correspondence: *young@anl.gov

This work was supported by the Chemical Sciences, Geosciences, and Biosciences Division of the Office of Basic Energy Sciences, Office of Science, U.S. Department of Energy, under Contract No. W-31-109-ENG-38. Use of the Advanced Photon Source was supported by the U.S. Department of Energy, Office of Science, Office of Basic Energy Sciences, under Contract No. W-31-109-ENG-38.

"Optical Harmony" continued from page 118

nium and zinc. Because their peptide film rested on a layer of water and could not be tipped at different orientations to the beam, the team used the liquid surface spectrometer at XOR/CMC sector 9, an instrument that can steer the synchrotron x-ray beam toward the surface of the thin film. In addition, an area detector allowed the team to quickly capture data and minimize the dose of damaging x-rays.

The team took snapshots of the thin layer structures with and without the cofactors. Without the cofactors, the peptide helices formed bundles of fours, with the bundles assembling into a thin layer, as expected. With the addition of the all-zinc cofactor, as much as 90% to 95% of the peptides remained in their proper orientation (Fig. 1). The ruthenium-containing cofactor is bulkier and disrupted the thin film slightly more, resulting in a thinner film. Additional experiments with the all-zinc cofactor showed that the team could customize the peptides so the cofactor would bind at different places along the length of the helix. This will allow the scientists to insert the cofactors at different depths in the thin film.

Measurements taken at the University of Pennsylvania confirmed that the peptide bundles aligned the cofactors properly within the film. The researchers now plan to test the nonlinear optical properties of the thin film, which can ultimately be transferred to solid surfaces for potential device applications.

— Mary Beckman

See: Joseph Strzalka[1], Ting Xu[1], Andrey Tronin[1], Sophia P. Wu[1], Ivan Miloradovic[1], Ivan Kuzmenko[2], Thomas Gog[2], Michael J. Therien[1], and J. Kent Blasie[1]*, "Structural Studies of Amphiphilic 4-Helix Bundle Peptides Incorporating Designed Extended Chromophores for Nonlinear Optical Biomolecular Materials," Nano Lett. **6**(11), 2395 (2006).
DOI: 10.1021/nl062092h
Author affiliations: [1]University of Pennsylvania, [2]Argonne National Laboratory
Correspondence: *jkblasie@sas.upenn.edu

This work was supported primarily by the Department of Energy grant DE-FG02-04ER46156 (A.T., M.J.T. and J.K.B.) and partially by the National Institutes of Health grants RR14812-05 (T.X.) and GM-071628 (M.J.T.), as well as National Science Foundation grants MRSEC DMR-0520020 (I.K. and T.G.) and NSEC DMR-0425780 (J.S.). The National Synchrotron Light Source at Brookhaven National Laboratory is supported by the U.S. Department of Energy. Use of the Advanced Photon Source was supported by the U.S. Department of Energy, Office of Science, Office of Basic Energy Sciences, under Contract No. W-31-109-ENG-38.

An In-depth Look into Nanocrystals

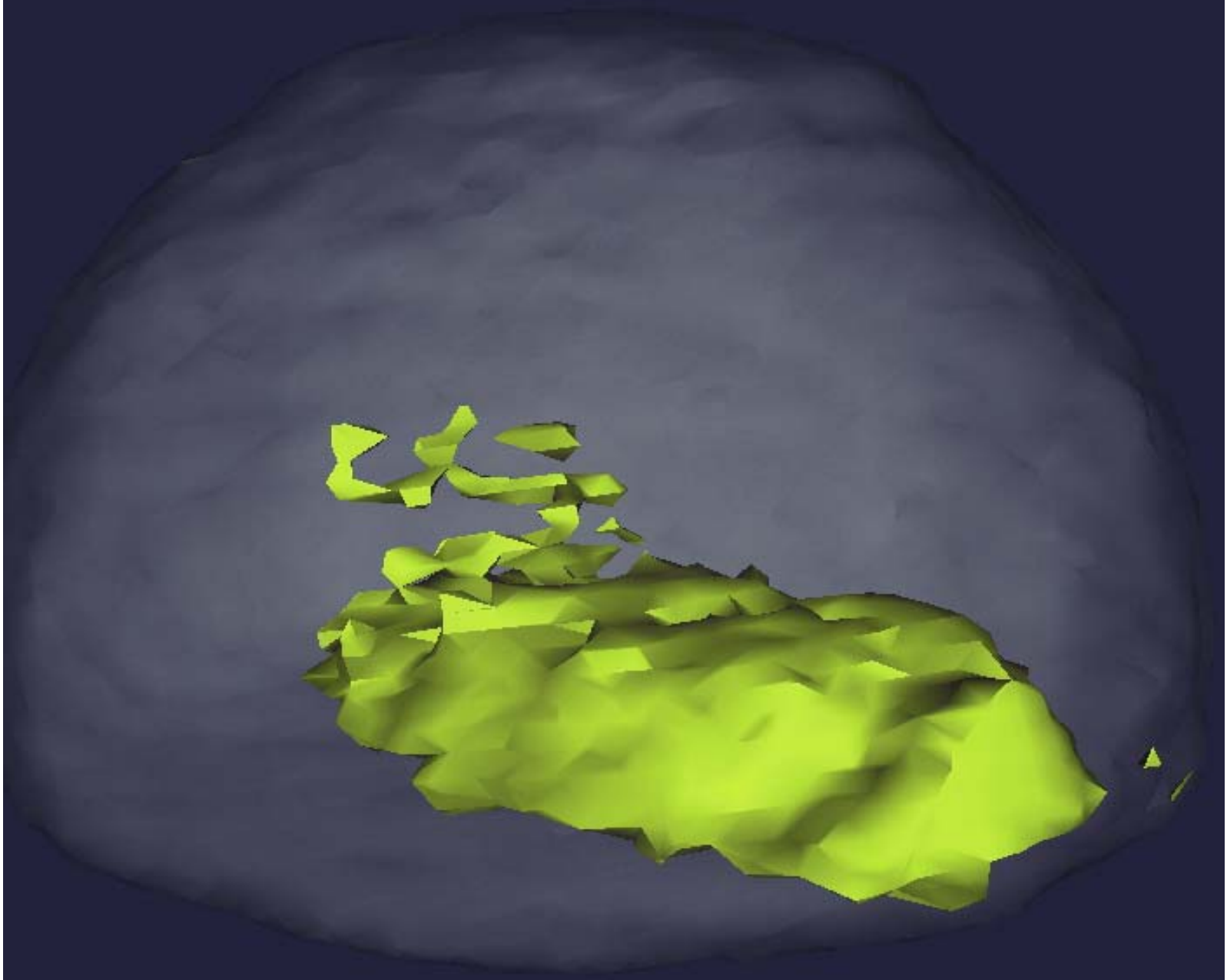

The power of ultra-bright, third-generation synchrotron radiation has revealed unprecedented images of the interior structure of lead (Pb) nanocrystals on a silica substrate. A team of researchers from the University of Illinois produced these striking three-dimensional (3-D) images at the XOR/UNI 34-ID-C beamline at the APS. The imaging technique, which relies on a novel way of inverting diffraction patterns using computational algorithms, paves the way for future exploration of materials at the atomic scale.

The researchers formed the samples under ultrahigh vacuum conditions in the vacuum chamber of beamline 34-ID-C. Evaporating Pb nanocrystals onto the wafer created a film about 20 nm thick, which was then heated to near the melting point of lead and cooled to form crystalline structures. The researchers then examined the crystals by using APS undulator x-rays at a wavelength of 1.38 Å, oversampling the diffraction patterns sufficiently that they could be phased. Real-space, three-dimensional images were produced by inverting the phased diffraction pattern data. The computational technique to phase and hence invert the diffraction pattern is based on an input-output algorithm developed by mathematicians in the 1980s.

In this experiment, the researchers have refined earlier techniques that produced real-space 3-D images of a single micrometer-sized gold crystal. X-ray diffraction imaging of an ideal crystal lattice, one with no defects, produces symmetrical patterns. Embedding a crystal on a substrate, however, was found to produce an internal strain field, registered as asymmetrical diffraction patterns at each Bragg point (Fig. 1). These defects are of principle interest in much of materials science research because they determine the inherent characteristics, and ultimate utility, of nanomaterials. The deformation of the crystal lattice is likely due to surface defects caused by mechanical forces at the point where the crystal meets the substrate.

Scanning electron microscope images of isolated crystals confirmed that the expected structure of the exterior is faceted, hemispherical, and about 200 nm in size, but the 3-D data obtained through x-ray diffraction revealed the complexity and density of the interior under strain in a quantitative way.

Although much of the crystal remained undeformed, the researchers noted a distinct, egg-shaped interior bulge in the phase image. This deformation field propagates inwards from the crystal/substrate interface, suggesting the presence of contact forces emanating from some surface defect where the lead nucleated on the substrate. This defect creates a strain field within the crystal analogous to the electric field that results from electrostatic surface charges.

Lensless imaging—such as coherent x-ray diffraction—is proving superior to traditional microscopy in many applications: it is more efficient, is less likely to damage the sample, and achieves better electromagnetic penetration of materials. The current resolution is at the 40-nanometer scale. In the future, as more powerful optic devices and coherent x-ray sources are developed, achieving 3-D images of the interior of materials at the atomic scale—using the current oversampled diffraction and inversion methods applied in this work—will be possible. The technique will also be useful when x-ray free electron lasers, which will increase the power of imaging by orders of magnitude, come on line. — *Elise LeQuire*

See: Mark A. Pfeifer[1], Garth J. Williams[1], Ivan A. Vartanyants[1], Ross Harder[1], and Ian K. Robinson[1*], "Three-dimensional mapping of a deformation field inside a nanocrystal," Nature **442** (6 July 2006). DOI: 10.1038/nature04867
Author affiliations: University College London
Correspondence: *i.robinson@ucl.ac.uk

This research was funded by the NSF Division of Materials Research and the EPSRC. The XOR/UNI facility at the APS is supported by the U.S. Department of Energy through the Frederick Seitz Materials Research Laboratory. Use of the Advanced Photon Source was supported by the U.S. Department of Energy, Office of Science, Office of Basic Energy Sciences, under Contract No. W-31-109-ENG-38.

< Fig. 1. A view of the phase isosurface of the strain distribution inside a lead nanocrystal using coherent x-ray diffraction. The strain (yellow) is superimposed on a translucent image of the nanocrystal itself (gray).

Structural Disorder of Crystalline Nanoparticles

It is well known that inorganic nanoparticles can adopt different structures than the equivalent bulk material, but obtaining detailed descriptions of nanoparticle structure remains challenging for conventional methods of analysis such as electron microscopy and x-ray diffraction. High-energy x-ray scattering, which is more sensitive to medium-range disorder than conventional diffraction approaches, is proving to be a powerful tool to explore the structure of nanoscale materials [1]. Researchers from the University of California, Berkeley (UCB), and the Chinese Academy of Sciences (CAS) used two beamlines at the APS and a third beamline at the Stanford Synchrotron Radiation Laboratory (SSRL) to study surface coating molecules on zinc-sulfide nanoparticles. This study indicates that a wide range of strain and disorder results from the different ways in which ligands interact with a surface.

The researchers used small-angle x-ray scattering (SAXS) at DND-CAT beamline 5-ID-D at the APS and beamline 1-4 at the SSRL, and wide-angle x-ray scattering at XOR/BESSRC beamline 11-1D-B at APS, to observe in real space the structural consequences of the interactions of surface coating molecules on zinc-sulfide nanoparticles (ZnS) measuring 3.2 nm to 3.5 nm in diameter. Their findings indicate that a wide range of strain and disorder results from the different ways in which ligands interact with the surface. Independent research has shown that such structural differences significantly alter the materials properties of ZnS nanoparticles [2].

In this effort, the team used real-space pair distribution function (PDF) analysis to obtain atomic-scale structural information and observe interior disorder (Fig. 1). The PDF analysis found dramatic differences in the crystallinity of a suite of ZnS nanoparticles synthesized at room temperature with methods that produced nanoparticles with different surface chemistry: hydroxylated surface in water, mercaptoethanol ligand coated surface in water, water adsorption from methanol, and pure methanol.

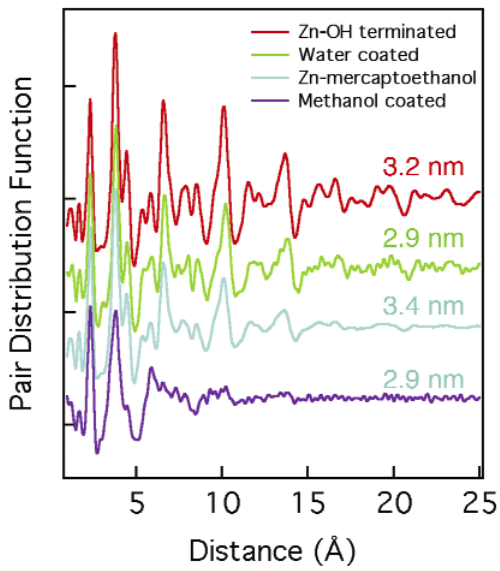

Fig. 1. Pair distribution function analysis of ZnS nanoparticles synthesized with different surface chemical environments. The synthesis methods produce nanoparticles with approximately the same mean diameters, shown next to each curve. However, the different synthesis methods produce nanoparticles that possess considerably different interior strain and disorder, identified by the rate at which the PDF intensity is truncated at larger distances.

To rule out particle size as a factor in structural disorder, the team used the transmission electron microscopy measurements obtained at the National Center for Electron Microscopy at Lawrence Berkeley National Laboratory and the SAXS data at APS to measure the size of the nanoparticles. In each medium, the size was similar, within a range of radii between 14.3 Å and 17.6 Å. These analyses confirmed that the trends in the PDF data may be interpreted as differences in structural disorder, rather than size.

Fourier transform infrared spectroscopy was used to analyze the surface chemistry and showed evidence of a relationship between the surface coating and interior structure. Stronger chemical interactions at the nanoparticle surface (covalent or electrostatic bonds) produced the most crystalline nanoparticles. In the absence of strong surface interactions, the nanoparticle surface restructures itself to a lower energy configuration, disrupting the structure of the entire particle.

The current study—focused on ZnS nanoparticles—builds upon previous research on the disorder and strain of nanoparticles by a group at the Department of Earth and Planetary Sciences at the University of California, Berkeley, and helps provide a clearer picture of the structure of nanoparticles less than 5 nm in diameter. Not only does size affect the relative crystallinity of nanoparticles, which tend to become more disordered with smaller size, surface chemistry has an effect on the structure: the stronger the surface chemical bonds, the higher the interior crystallinity. The UCB/CAS team believes that these conclusions are relevant to other inorganic nanoparticles. — *Elise LeQuire*

Continued on next page

"Structutal Disorder" continued from page 122

REFERENCES

[1] B. Gilbert, F. Huang, H. Zhang, G. A. Waychunas, and J.F. Banfield, Science **305**, 651 (2004).

[2] B. Gilbert, H. Zhang, B. Chen, M. Kunz, F. Huang, and J. F. Banfield, Phys. Rev. B **74**, 115405 (2006).

See: B. Gilbert[1]*, F. Huang[2], Z. Lin[2], C. Goodell[1], H. Zhang[1], and J.F. Banfield[1], "Surface Chemistry Controls Crystallinity of ZnS Nanoparticles," Nano Lett. **6**(4), 605 (2006).

Author affiliations: [1]University of California, Berkeley; [2]Chinese Academy of Sciences

Correspondence: bgilbert@lbl.gov

Funding for this work was provided by a grant from the Department of Energy Chemical Sciences Program ER 15218 and the National Science Foundation NIRT program EAR0123967, and by the Director, Office of Science, of the U.S. Department of Energy under Contract no. DE-AC02-05CH11231. Use of the Advanced Photon Source was supported by the U.S. Department of Energy, Office of Science, Office of Basic Energy Sciences, under Contract No. W-31-109-ENG-38.

How Quantum Size Effects Regulate Nanocrystalline Islands

The unique electrical, mechanical, and thermal properties of many nanomaterials promise a dazzling array of new commercial applications. But to realize this potential, scientists must identify robust and reproducible methods for controlling the production of nanostructures made from these materials on an atomic scale. An important step in this direction was taken by researchers from the University of Missouri–Columbia, the Georgia Institute of Technology, Iowa State University, and Kyunghee University, who studied the unexpected spontaneous behavior of nanocrystalline islands of lead deposited on epitaxial silicon substrates. This investigation clarified the role of the quantum size effect (QSE) in the nucleation, growth, and coarsening of the islands. The observations showed the existence of novel and efficient pathways to self-organization that not only operate at much lower temperature but also result in sharper size distributions than those achievable through classical Ostwald ripening.

The x-ray scattering experiments were performed in the *in situ* growth chamber at the MU-CAT 6-ID-C beamline at the APS, at a 12.4-keV x-ray energy. The Pb films were prepared *in situ* in ultrahigh vacuum using an e-beam evaporator, and the surface of the Si(111)-(7 × 7) substrate was prepared using standard techniques. Island densities were determined by measuring the splitting of the diffuse scattering lobes (Henzler rings) around the Pb(111) Bragg point. Scanning tunneling microscopy (STM) experiments were carried out using a variable-temperature STM.

The conventional nucleation, growth, and coarsening of large-scale islands have been extensively described in terms of the classical Gibbs-Thomson analysis. With large-scale islands, initial island nucleation is established by a steady-state concentration of adatoms on the surface. Once the deposition flux is turned off, the island density slowly begins to decrease due to coarsening (Ostwald ripening), whereby a critical island radius is established such that islands having larger radii slowly grow as the radii of islands having smaller radii shrink.

The experiments revealed that the nanocrystalline islands exhibit novel coarsening behavior whereby the island density does not converge to a single coarsening curve, as would be predicted by the classical Ostwald ripening picture, when the initial density is varied by using different growth fluxes. Instead, as shown in Fig. 1, the curves actually diverge at long times. Moreover, the island relaxation rates were found to be orders of magnitude faster than expected from studies on larger crystals, and the relaxation rate was observed to be proportional to the growth flux, which is not expected from the classical theory.

The results suggest the following picture for the growth of QSE nanocrystals. Initial island nucleation exhibits a weak dependence on the deposition flux, as in standard nucleation theory. The types of islands that are produced, however, depend strongly on the flux rate, and this is what leads to the breakdown of the Gibbs-Thomson effect. High flux rates generate a broader range of island heights (having a broader range of stability), presumably because of the larger adatom concentration that drives a higher chemical potential. Thus, many of the islands are unstable and decay once the deposition flux is turned off. This quickly leads to a significantly lower island density. Conversely, lower flux rates generate a narrower height

Continued on page 125

REVERSIBLE WRINKLING LAYERS OF GOLD

Imagine trying to rack up billions of billiard balls on a flat surface so that they form a regular pattern. Now, imagine that each of those balls is just a few billionths of a meter across—a nanoparticle, in other words. The task would be seemingly impossible. However, finding a method to organize gold nanoparticles into just such a two-dimensional (2-D) array on a surface could open up a range of possibilities for exploiting the unique optical, electronic and chemical properties of nanoparticles by allowing them to be manipulated more readily. Researchers from The University of Chicago and Argonne are working to uncover the secrets of the self-organization processes involved in forming such 2-D arrays. Their research is not only improving our understanding of the behavior of monolayers and how they might be formed more effectively, but could shed new light on the natural analogs in biology.

One way to produce such 2-D arrays from a solution of uniform-size nanoparticles is via the Langmuir-Blodgett (LB) technique, developed about a century ago. The idea is to spread hydrophobic nanoparticles on top of water so they float on the surface and can be squeezed to form a compact layer. Many researchers have been successful in making such monolayers and transferring them onto various solid surfaces, including glass and silicon. But a deep understanding of the structure of monolayers of gold nanoparticles on a liquid surface is lacking. The University of Chicago-Argonne team hope to uncover the secrets of this self-organization process in LB monolayers.

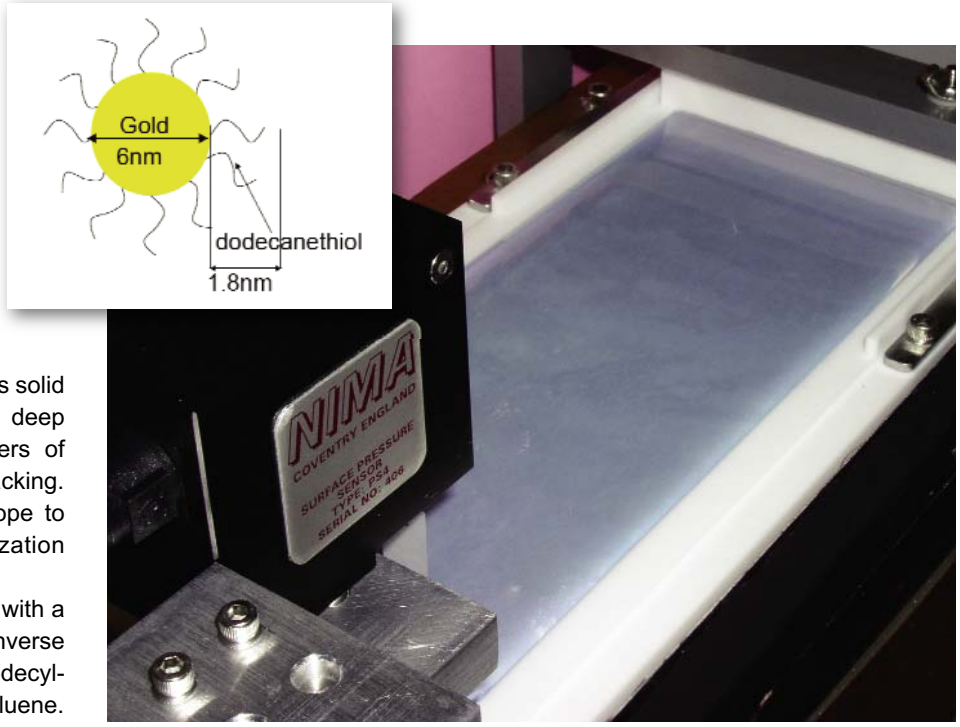

Fig. 1. Diagram of a uniform monolayer of gold nanoparticles (depicted in the inset) on the surface of pure water, prepared using the LB technique.

To make nano-particles, the team began with a gold salt dissolved in tiny water cages (inverse micelles) formed by adding a surfactant didodecyldimethylammonium bromide (DDAB) to toluene. The gold salt was then converted into gold nanoparticles using a chemical reducing agent. The researchers next swapped the DDAB coating using sulfur-containing dodecanethiol, which binds to the surface much tighter than DDAB. Next, a process of digestive ripening—in which the mixture is heated with excess thiol—was used to make the whole ensemble more uniform. Finally, the nanoparticles were given a good wash and suspended in heptane. The resulting suspension contains 10^{15} particles per ml of solvent.

The University of Chicago-Argonne team carried out *in situ* optical microscopy and x-ray scattering experiments at ChemMatCARS beamline 15-ID at the APS to investigate the formation of the nanocrystal monolayer with the LB technique. The optical microscopy experiment revealed macroscopic information about the monolayers. The x-ray scattering study, on the other hand, yielded detailed information on the small length scale, showing how the nanoparticles pack to-gether locally in the monolayer and with what symmetry. The researchers could also measure the distances between the particles in the layer and any organization perpendicular to the layer using this method.

The most interesting discovery was that the hexagonally ordered nanoparticle monolayer could fold like a piece of paper when it is squeezed hard enough. The wrinkles unfold—once the pressure is subsequently released—only in the presence of enough excess dodecanethiol in the solution to prevent neighboring particles from sticking together. In addition, the team found that squeezing the monolayer does not change the spacing between the nanoparticles, indicating the molecular coating is quite rigid. The combination of optical microscopy and x-ray scattering has proven to be crucial in understanding the complex structural evolution under different conditions.

Continued on next page

"Quantum Size Effects" continued from page 123

distribution of the more stable islands that decay slowly in time. To account for the extremely fast decay times observed at high flux rates, the researchers postulated that collective effects must be operating whereby the detachment of a single atom can trigger the highly correlated detachment of many more atoms. Although the microscopic origin of such processes still needs to be identified, the new results have tremendous implications about the self-organization in the epitaxial growth of nanocrystals.

The novel coarsening behavior of QSE nanocrystals can have important practical implications. For example, the nanocrystalline islands exhibit improved height and size distributions along with a much lower island density after deposition at high rather than low flux rates, contrary to what occurs with the large-scale islands described by the classical scaling theory of nucleation and Ostwald ripening.

These experiments also illustrate the crucial role that surface x-ray scattering plays in exploring phenomena that involve statistical distributions. Bright undulator radiation produces sufficient scattered signal to obtain statistically meaningful data during real-time *in situ* experiments and, in this case, over nearly three decades of time scale.

— Vic Comello

See: C.A. Jeffrey[1], E.H. Conrad[2], R. Feng[2], M. Hupalo[3], C. Kim[4], P.J. Ryan[5], P.F. Miceli[1], and M.C. Tringides[3], "Influence of quantum size effects on island coarsening," Phys. Rev. Lett. **96**, 106105 (2006).

Author affiliations: [1]University of Missouri–Columbia, [2]Georgia Institute of Technology, [3]Iowa State University, [4]Kyunghee University, [5]MU-CAT

Correspondence: micelip@missouri.edu

The MU-CAT beamline is supported through Ames Laboratory, and operated for the DOE by Iowa State University under Contract No. W 7405-Eng-82. Research funding was supported, in part, by Ames Laboratory (M.C.T.), Canim Scientific Group (E.H.C.), the Missouri University Research Board, the National Science Foundation DMR-0405742, and the Petroleum Research Fund No. 41792AC10 (P.F.M., C.A.J., C.K.), the Natural Sciences and Engineering Research Council (NSERC) of Canada (C.A.J.), the Center for Nanostructured Materials Technology under 21st Century Frontier R&D Programs of the Ministry of Science and Technology (No. 05K1501-02520), Korea (C.K.). Use of the Advanced Photon Source was supported by the U.S. Department of Energy, Office of Science, Office of Basic Energy Sciences, under Contract No. W-31-109-ENG-38.

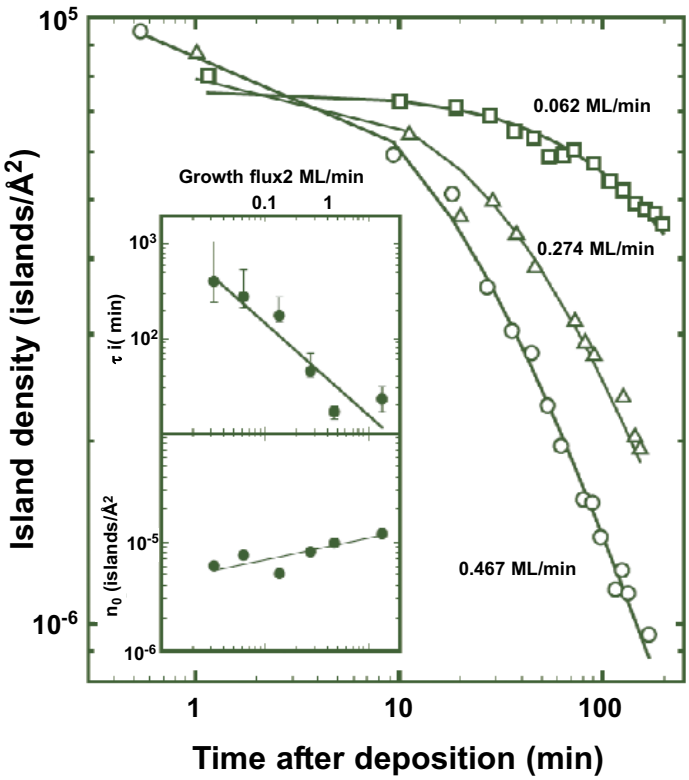

Fig. 1. The density of Pb islands was determined from x-ray diffuse scattering about the Pb(111) Bragg position as a function of time after 1.2 monolayers of Pb were deposited on Si(111)-(7 × 7) at 208K. The curves, obtained using different deposition fluxes, do not approach each other at long times, which is contrary to the predictions of classical Ostwald ripening. The solid curves are a fit of the data to $n(t)=n_0/(1+t/\tau)$, from which the initial island density n_0 and the island relaxation time τ were obtained. Both n_0 and τ are plotted in the inset. Although the initial island density changes little with flux rate, the relaxation time exhibits an unusual 1/flux dependence and it is orders of magnitude faster than expected.

© 2006 The American Physical Society

"Reversible Wrinkling" from page 124

Understanding the behavior of nanoparticle monolayers could lead to practical applications in making novel devices using the LB technique. The phenomenon of folding could improve our understanding of the behavior of thin molecular layers, such as cell membranes. Even though the chemistry is very different, the underlying physics could be similar.

— David Bradley

See: David G. Schultz[1], Xiao-Min Lin[2], Dongxu Li[1], Jeff Gebhardt[1], Mati Meron[1], P. James Viccaro[1], and Binhua Lin[1]*, "Structure, Wrinkling, and Reversibility of Langmuir Monolayers of Gold Nanoparticles," J. Phys. Chem. B **110**, 24522 (2006). DOI: 10.1021/jp063820s

Author affiliations: [1]The University of Chicago, [2]Argonne National Laboratory

Correspondence: *lin@cars.uchicago.edu.

ChemMatCARS is principally supported by the National Science Foundation and Department of Energy under Grant No. CHE0565344. This work and the APS are supported by the U.S. Department of Energy, Office of Science, Office of Basic Energy Sciences, under Contract No. W-31-109-ENG-38.

NANOSECOND DOMAIN DYNAMICS IN FERROELECTRIC OXIDES

Ferroelectric materials have an intrinsic electrical polarization that can be reversed by large electric fields. Although the steady-state properties of these materials are well understood—thanks to detailed theoretical and experimental analysis—the rapid changes that occur at nanometer scales have been difficult to capture experimentally. Manipulating the polarization of ferroelectric materials already forms the basis for non-volatile memories, and could lead to a new generation of electronic, optical, and acoustic devices. Understanding the dynamics of how this polarization switches in nanoscale structures is essential to developing these applications, as well as to sorting out the fundamental physics of ferroelectrics. Researchers from the University of Wisconsin and Argonne have adapted x-ray microscopy techniques with high spatial and temporal resolution to track polarization switching in ferroelectric thin films.

Ferroelectric switching is widely thought to occur in three steps following the application of an external field pulse. First, small regions of reversed polarization begin nucleating in response to the switching pulse. These initial domains then grow in the direction of the applied electric field and span the distance between the electrodes. Finally, the domain walls grow laterally in a direction perpendicular to the switching field. The dynamics at high applied field, however, have not been adequately visualized, owing to the very fast time scales and small length scales involved. Time-resolved microdiffraction with picosecond x-ray pulses from the APS provides a detailed picture of ferroelectric domain wall dynamics at a spatial resolution of 115 nm and a temporal resolution of less than 1 ns.

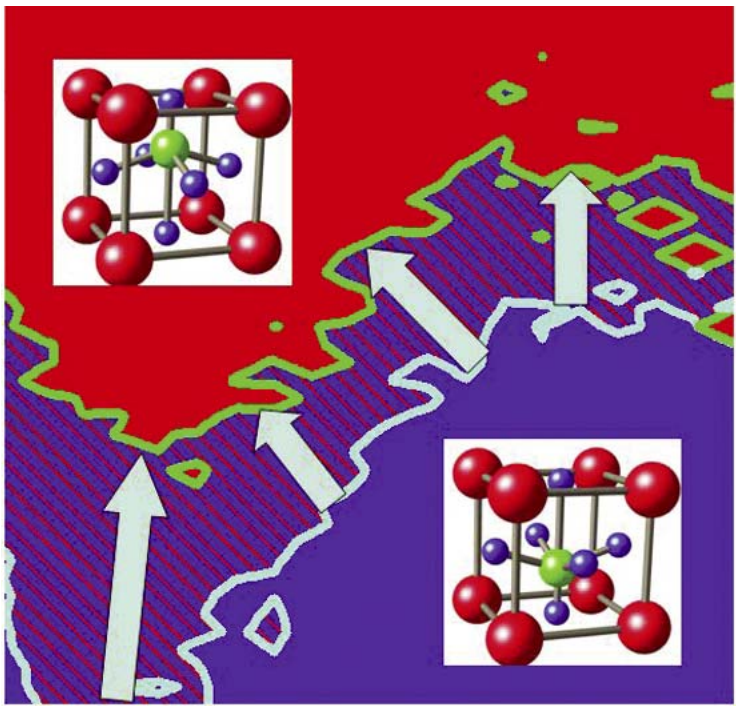

Fig. 1. Polarization switching in a 20 × 20 μm^2 area of a thin-film ferroelectric capacitor. The polarization-up and polarization-down domains are red and blue, respectively. The dashed area shows the domain boundary advancement during 100 ns; the arrows show the advancement direction. Inset diagrams show the lattice configurations in the two ferroelectric polarization states.

The ferroelectric devices studied here consisted of 400-nm-thick films of $Pb(Zr_{0.45}Ti_{0.55})$ (PZT) between conducting $SrRuO_3$ electrodes. In PZT, the remnant polarization arises from a structural effect that can be can be probed using techniques such as diffraction. The time dependence of these structural signals can be used to follow the domain walls at small scales. Specifically, the Wisconsin-Argonne group used the time-resolved signature of polarization switching in the intensity and motion in reciprocal space of the (002) and (00$\bar{2}$) x-ray Bragg reflections of PZT. These reflections correspond to opposite polarization states and have different intensities, and respond to applied electric fields with opposite signs of the piezoelectric response. The microdiffraction experiments were carried out with 10-keV x-ray pulses from the XOR 7-ID-C beamline at the APS. The x-ray pulses arrived at the ferroelectric devices in a stream of pulses with ~100-ps durations separated by 153 ns. X-rays scattered from the sample were detected with a fast avalanche photodiode. By synchronizing the electrical pulses applied to the sample to induce ferroelectric polarization reversal with the x-rays from a single circulating electron bunch, the experimenters were able to probe particular times in the polarization switching process.

An upper limit of the time resolution of the experiment was obtained using the piezoelectric effect, which is the fastest of

Continued on page 128

PEERING UNDER THE SURFACE

One of the greatest challenges of nanoscience arises out of its very nature: the difficulty in seeing what is really going on when dealing with things that are so incredibly tiny. But if scientists and engineers are to make nanotechnology applications—such as molecular electronics—a practical reality, they must develop ways of seeing at the molecular level. This problem is even more difficult when studying the structure of surfaces buried within other materials, such as at the junctions of electrodes. Techniques such as electron microscopy simply do not permit the Ångstrom resolution necessary to characterize nanostructures for molecular electronics applications. A team of researchers has used high-energy x-ray reflectivity at the XOR/CMC 9-ID beamline at the APS, in conjunction with the X22A beamline at the National Synchrotron Light Source, to obtain direct Å-resolution measurements of the molecular structure of electronic junctions buried deep in interface monolayers. These results show that high-energy x-ray reflectivity can be usd to study a variety of differing molecular layers at different surfaces.

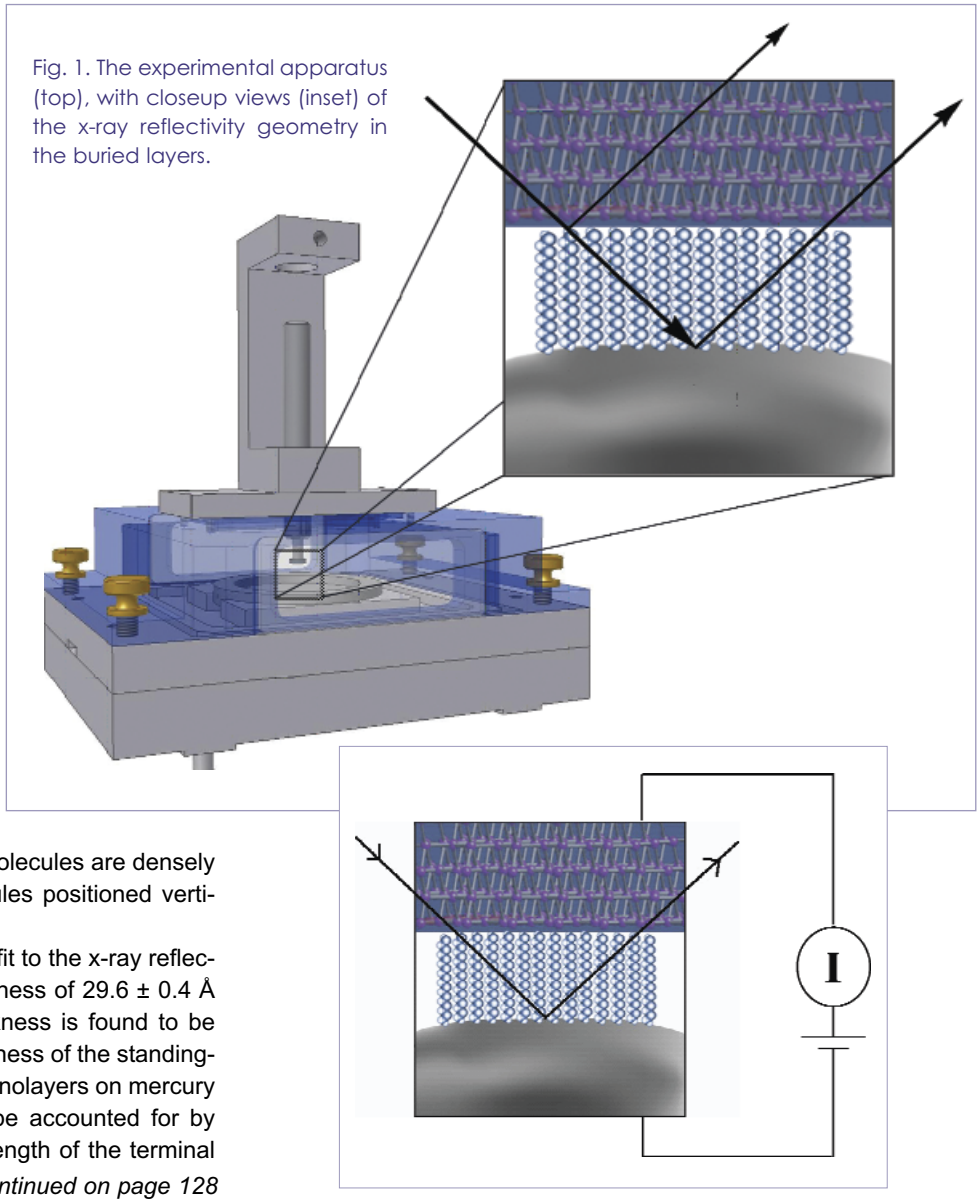

Fig. 1. The experimental apparatus (top), with closeup views (inset) of the x-ray reflectivity geometry in the buried layers.

The investigators, from Argonne National Laboratory, Columbia University, Brookhaven National Laboratory, Bar-Ilan University, and Harvard University, examined alkyl-thiol (octadecanethiol, $C_{18}SH$) and alkyl-silane (octadecyltrichlorosilane, OTS) self-assembled monolayer films, as well as a bilayer film, between a mercury droplet and a solid silicon substrate. The team chose these particular molecules because their qualities—chiefly their simple molecular structure and their electron conduction properties—are of fundamental interest to researchers in the field of molecular electronics.

When x-rays are reflected from organic layer interfaces, the x-rays reflected at different depths give rise to an interference pattern. The measured amplitude of the fringes reveals the electron densities at the buried junction, and the fringe period provides the organic film's average thickness. By analyzing the x-ray scattering data, the researchers discovered that the organic molecules are densely packed together, with most of the molecules positioned vertically.

For the Si-thiol-Hg interface, the best fit to the x-ray reflectivity was obtained with a monolayer thickness of 29.6 ± 0.4 Å corresponding to the C_{18} layer. This thickness is found to be larger than the corresponding 25.2-Å thickness of the standing-up phase of C18SH for self-assembled monolayers on mercury at the air interface. This difference can be accounted for by considering three factors: the C-H bond length of the terminal

Continued on page 128

"Domain Dynamics" continued from page 126

the structural responses of ferroelectrics to applied electric fields. With electrical pulses of a single polarity the transient piezoelectric response occurred with a risetime of 620 ps. Electrical pulses of alternating polarity lead to polarization switching. X-ray microdiffraction indicated that at the start of each pulse the lattice of the PZT contracted and shifted the Bragg reflection in reciprocal space. Several hundred nanoseconds after this shift, the Bragg peak abruptly shifted in the opposite direction, indicating the start of polarization reversal. The time at which this switching event happened at various locations in the thin-film structure corresponded to the time required for a domain wall to move from the nucleation site to that location. With these data, it is possible to construct a map of polarization switching times over the area of the film, showing how the domain walls move across the sample (Fig. 1).

The domain wall velocities obtained with this technique show that the wall motion is not near the limit set by elastic deformation. This suggests that more optimal structures and higher fields should permit faster switching. The results also demonstrate the potential of microdiffraction tools made possible by high-brightness, third-generation synchrotron sources such as APS in understanding basic phenomena of great technological interest. — *David Voss*

See: Alexei Grigoriev[1], Dal-Hyun Do[1], Dong Min Kim[1], Chang-Beom Eom[1], Bernhard Adams[2], Eric M. Dufresne[2], and Paul G. Evans[1]*, "Nanosecond Domain Wall Dynamics in Ferroelectric PbZr; TiO_3 Thin Films," Phys. Rev. Lett. **96**, 187601 (12 May 2006). DOI: 10.1103/PhysRevLett.96.187601

Author affiliations: [1]University of Wisconsin, [2]Argonne National Laboratory

Correspondence: *evans@engr.wisc.edu

This work was supported by the U.S. Department of Energy, Office of Basic Energy Sciences, under Grant No. DE-FG02-04ER46147. C. B. E. acknowledges support from NSF DMR-0313764 and ECS-0210449. Use of the Advanced Photon Source was supported by the U.S. Department of Energy, Office of Science, Office of Basic Energy Sciences, under Contract No. W-31-109-ENG-38.

"Under the Surface" continued from page 127

methyl group and the van der Waals (vdW) radii of both the terminal hydrogen atom and the silicon oxide, all of which do not contribute to the measured thickness of the films at the air interface. Taking into account these factors, the agreement clearly shows that the alkyl chains in these buried junctions are standing straight up. The electron density profile of the bilayer junction shows a near-doubling in the thickness, as expected, compared to the monolayer.

These researchers also studied the structure of the buried bilayer junction under applied potentials. The x-ray reflectivity at several sample voltages and the current-voltage dependence at several fixed q_z positions were also measured. In these measurements, no structural changes were observed when a potential of up to 1 V was applied across the junction. This finding indicates a highly stable molecular structure, something quite handy if such molecular junctions are to be eventually developed for practical uses.

In the exacting world of nanoscience, the movement and location of a single molecule can be critical, particularly if scientists are going to control what is going on in the nanoworld. By demonstrating the power and versatility of this technique, the research team has opened up a new window that will allow future nanoelectronics designers to see and know what is happening deep inside their inventions—and make molecules dance to whatever tune they call. — *Mark Wolverton*

NOTE: In June 2006, Brookhaven scientist Julian Baumert, one of the lead authors of this study, died of melanoma at the age of 31.

See: Michael Lefenfeld[1], Julian Baumert[2], Eli Sloutskin[3], Ivan Kuzmenko[4], Peter Pershan[5], Moshe Deutsch[3], Colin Nuckolls[1], and Benjamin M. Ocko[2*], "Direct structural observation of a molecular junction by high-energy x-ray reflectometry," Proc. Natl. Acad. Sci. USA **103**(8), 2541 (2006).
DOI: 10.1073pnas.0508070103

Author affiliations: [1]Columbia University, [2]Brookhaven National Laboratory, [3]Bar-Ilan University, [4]Argonne National Laboratory, [5]Harvard University

Correspondence: *ocko@bnl.gov

M.L. and C.N. acknowledge financial support from the Nanoscale Science and Engineering Initiative of the National Science Foundation under National Science Foundation Award No. CHE-0117752 and from the New York State Office of Science, Technology, and Academic Research. Work at Brookhaven National Laboratory is supported by the U.S. Department of Energy, Division of Materials Science, under Contract DE-AC02–98CH10886. Support to M.D. by the German–Israeli Foundation, Jerusalem (GIF), is gratefully acknowledged. P.P. acknowledges support from the National Science Foundation under Grant NIRT 03-03916. Use of the Advanced Photon Source was supported by the U.S. Department of Energy, Office of Science, Office of Basic Energy Sciences, under Contract No. W-31-109-ENG-38.

Research at the APS and U.S. Economic Competitiveness

Our nation's national laboratories and their national user facilities, under the auspices of the U.S. Department of Energy (DOE), are uniquely suited to meeting a variety of challenges, including the pursuit of technological advances that spur economic prosperity and national security. User facilities such as the APS, the Intense Pulsed Neutron Source, the Electron Microscopy Center, the Center for Nanoscale Materials, the Argonne Tandem-Linac Accelerator System, and the Atmospheric Radiation Measurement Climate Research Facility—all at Argonne—bring unique capabilities and talented people to bear on the missions of the DOE in advancing science and technology for the nation: increasing the storehouse of fundamental knowledge, dealing with problems whose solutions are scientific, bettering lives, and maintaining forward progress in an increasingly competitive technological and economic global arena.

The latter is made clear by looking at light-source research in terms of the gross domestic product (GDP), the primary engine for U.S. economic competitiveness. The (real) gross domestic product, according to the U.S. Bureau of Economic Analysis (BEA), is "the output of goods and services produced by labor and property located in the United States." [1]

Much of synchrotron x-ray science at the APS can be readily mapped onto the GDP. Here are some of the GDP categories compiled by the BEA and corresponding APS research:

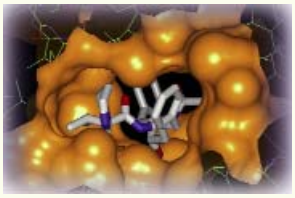

Medical care: APS x-rays played an essential role in the development of Abbott Labs' Kaletra®—the most-prescribed pharmaceutical in its class for AIDS therapy. See: www.anl.gov/Media_Center/News/2006/APS060901.html

Gasoline, fuel oil, other energy goods: The APS enabled a study of bacteria used to convert methane to methanol at room temperature, which may help improve methanol synthesis; and revealed new information on the structure of high-speed fuel injector sprays, which can help improve injector efficiency. See: R.L. Lieberman and A.C. Rosenzweig, Nature **434**, 177 (March 2005); A.G. MacPhee et al., Science **295**, 5558, 1261 (2002).

Electricity and gas: APS x-rays gave researchers the first look at the composition of the plasma arcs that produce the glow in energy-efficient halide arc lamps, an important step in improving the lamps' efficiency even more. See: J.J. Curry et al., "J. Appl. Phys. **93**(5), 2359 (1 March 2003).

Information processing equipment and software: APS studies of alloys in DVDs could help "fine tune" the alloys, advancing the state of data storage devices and remote-programmable computers. See: D. A. Baker et al., Phys. Rev. Lett. **96**, 255501 (2006).

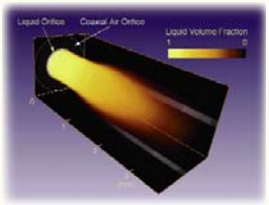

Industrial equipment: The first x-ray images of the internal structure of the flow from a high-speed industrial paint sprayer could aid in improving sprayer efficiency. See: Y.J. Wang et al., Appl. Phys. Lett. **89**, 151913 (9 October 2006) and page 42 of this report.

Structures: Studies at the APS are refining our understanding of how to make cement more durable. See: N.N. Naik et al., Cement Concrete Res. **36**, 144 (2006) and page 36 of this report.

Each day that researchers gather experiment data at the APS brings the real possibility of new information that can move our nation forward. These and other research breakthroughs are highlighted on the constantly-updated APS Website science highlights index at www.aps.anl.gov/Science/Highlights/ index.htm.

Reference

[1] www.bea.gov/newsreleases/national/gdp/gdpnewsrelease.htm

APS Beams Probe the Nanoscale

At Argonne, you can now not only characterize a nanomaterial, but also build it. That is the elegantly simple mission statement for nanoscience at the Argonne user facilities supported by the U.S. Department of Energy's Office of Basic Energy Sciences (DOS-BES). The Center for Nanoscale Materials (CNM)—one of five new BES Nanoscale Science Research Centers at DOE national laboratories—is the cornerstone for nanoscience at Argonne. The CNM joins the Argonne Intense Pulsed Neutron Source and Electron Microscopy Center facilities, as well as the many researchers from Argonne divisions who are exploring the nano-realm. The CNM adjoins the APS experiment hall, where a new hard x-ray nanoprobe at APS sector 26 is coming on line, and a plethora of nanoscience capabilities are being developed at five other sectors on the experiment hall floor (see facing page). It all starts with the sample. The CNM will allow researchers to "build" any amount of nanomaterials, and then swiftly and efficiently move those samples to one or more of the superb Argonne characterization tools best suited to the purpose at hand: an integrated approach to nanocharacterization, which also applies to researchers bringing their samples to Argonne.

APS x-rays will be a vital resource for nanoscience researchers. By dedicating certain beamlines to different nanocharacterization techniques, the APS will enable rapid-access for a minimum of 10% of available beam time at those sectors. All of these tools are nothing without the right people in place to make them work. Because they are engaged in a relatively new field of investigation, nanoscience users will come to the APS seeking answers to questions that may never have been asked before. A tried-and-true measurement technique may be right for a particular problem, but it is just as likely that something may need to be measured in some entirely new way. The beamline staff at the APS, because of their immersion in the science at hand, can create new methods of measurement that will allow users to leave with answers. Taken together, the nanoscience capabilities at Argonne follow the "Centers of Excellence" model, where excellent machines, tools, and, most crucially, people are concentrated to create an intensely creative and productive resource for the advancement of science and the national interest. *Contact: Gabrielle Long (gglong@aps.anl.gov)*

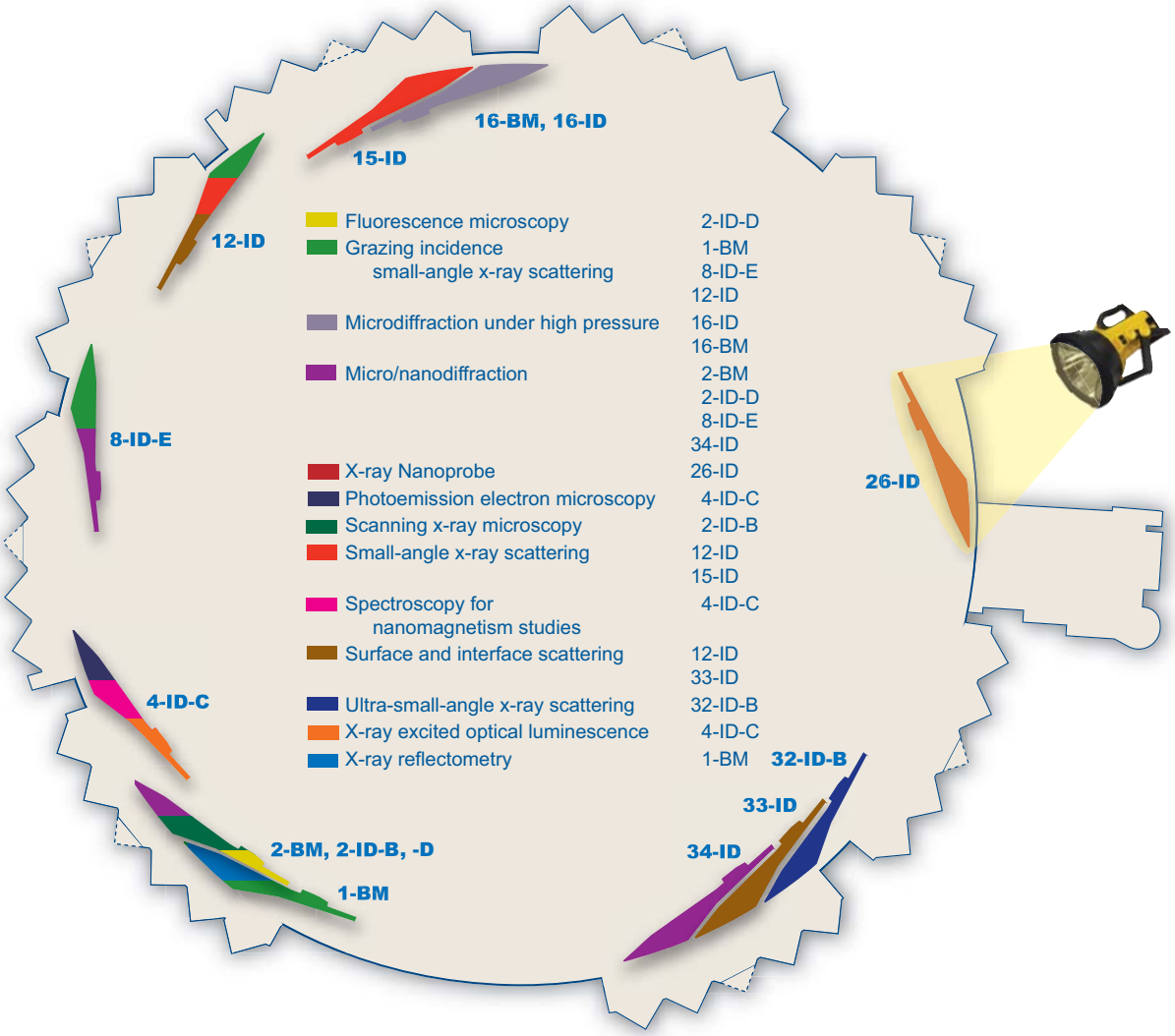

APS sectors with nanoprobe capabilities.

Grazing incidence small-angle x-ray scattering *1-BM, 8-ID-E, 12-ID* Grazing incidence small-angle scattering (GISAXS) measurements are sensitive to the surface morphology and the internal structure of films, and provide information lateral and normal to the surface on length scales from 1 to 100 nm. It is an excellent complement to such probes as atomic force microscopy and transmission electron microscopy. An increasingly important structural-characterization technique, GISAXS finds applications in studies of nanostructures and nanocomposites at surfaces and interfaces. Most significantly, it serves as a complementary method to conventional surface-sensitive tools such as scanning probe microscopy and electron microscopy, GISAXS can be used *in situ* and in real time to monitor the formation of a nanostructure or nanocomposite, which makes it especially suitable for studying the kinetics of nanoassembly processes. The structural information that can be obtained includes particle size distribution or shape, particle composition, the internal surface area per unit volume, the volume fraction, and characteristic length of ordered structures. GISAXS averages over macroscopic regions to provide statistically significant information on the nanometer scale, and provides information on particle geometry, size distributions, and spatial correlations.

X-ray reflectometry *1-BM* When x-rays strike a surface at glancing incidence they can reflect off the surface. However, if the surface is rough or covered by a film, then the x-ray reflectivity of a surface can change. X-ray reflectivity (XRR) experiments take advantage of this effect by measuring the intensity of x-rays reflected from a surface as a function of angle. Thin films on a surface can give rise to oscillations of the x-ray intensity with angle. XRR can provide information on the thickness, roughness, and density of thin films on a surface. Thus, it probes the structure of surfaces, thin films, or buried interfaces, as well as processes occurring at surfaces and interfaces such as adsorption, adhesion and interdiffusion. Applications include photosensitive films, electrochemical and catalytic interfaces, surfactant layers, polymer coatings and biological membranes. The increasing importance of hybrid materials, the properties of which are determined by their interfaces and the rapid development in the field of thin-film technology provides a strong demand for x-ray reflectometry.

Small-angle x-ray scattering *12-ID, 15-ID* • **Ultra-small-angle x-ray scattering** *32-ID-B* Small-angle x-ray scattering (SAXS) is widely used for the nanoscale structural characterization of composite materials, polymers, and nanoparticles. Areas of high current interest include protein solutions, fibers, vesicles, micelles, biopolymers, liquid crystals, polymer films and fibers, micro- (and nano-) emulsions, and quantum dots. In particular, SAXS and ultra-small-angle x-ray scattering together bridge the gap between atomic level and micrometer-level structures.

Surface and interface scattering *12-ID, 33-ID* Knowledge of nanoscale structural arrangements and composition at surfaces and buried interfaces is fundamental to understanding the function and properties of many synthetic structures and reactive interfaces found in nature. X-rays from the APS offer a unique opportunity to penetrate through overlayers to probe the structure and chemistry of surfaces and internal boundaries from the nanoscale down to the atomic level. The APS source enables *in situ* studies, permits real-time investigations to elucidate thin-film growth mechanisms, and allows molecular-scale studies of chemical interactions at internal boundaries.

Micro/nanodiffraction *2-BM, 2-ID-D, 8-ID-E, 34-ID* • **Microdiffraction under high pressure** *16-ID, 16-BM* X-ray diffraction is routinely used to investigate materials structure. With x-rays focused to a spot size of one micron or less, one can perform x-ray diffraction experiments with very high spatial resolution. X-ray microdiffraction is providing new insights in the fields of materials and environmental science. X-ray microdiffraction can measure local variations in stress, orientation, and plastic deformation between grains and within individual grains, helping us understand mechanical properties at this critical length scale. With x-ray microdiffraction, we can measure local characteristics such as texture and stress within individual devices, offering an experimental counterpart to computer simulations. X-ray microdiffraction also allows structural identification of small amounts of phases imbedded in a heterogeneous matrix.

Scanning x-ray microscopy *2-ID-B* • **Fluorescence microscopy** *2-ID-D* Scanning transmission x-ray microscopy is a popular probe that can map functional groups in cells as well as environmental samples. Very small (a few tens of nanometers) beams are created using Fresnel zone plates, enabling detailed mapping of nanoscale structures in biology, polymer science, electronic nanostructures, magnetic materials, and meteorites.

Photoemission electron microscopy *4-ID-C* In photoemission electron microscopy (PEEM), linearly or circularly polarized x rays are used for real-space imaging with simultaneous chemical and magnetic contrast. In imaging of magnetic domains, it is complementary to Kerr microscopy. PEEM is currently used to image a broad range of materials such as magnetic nanostructures, magnetic domains in epitaxial films, antiferromagnetic structures, spin transport, chemical and magnetic properties of complex materials, multiferroics, and the surface chemistry of polymer films and protein adsorbates.

Spectroscopy for nanomagnetism studies *4-ID-C* X-ray magnetic circular dichroism (XMCD) is an x-ray absorption spectroscopy technique that plays a key role in the study of nanomagnetic materials. The major strength of XMCD is its capacity to deduce orbital-projected magnetic moments both in magnitude and direction with the full benefit of the element selectivity inherent to x-ray absorption spectroscopy. It is now widely used to unravel the microscopic origin of magnetism in ferromagnetic and ferrimagnetic systems. XMCD could be recorded from paramagnetic systems subjected to a high magnetic field, and it is a remarkable element-specific magnetometry tool for heteromagnetic systems. It is unique for the study of the magnetic properties of reduced-dimensionality structures such as thin magnetic films and multilayers, magnetic quantum wires, and dots.

X-ray excited optical luminescence *4-ID-C* The x-ray excited optical luminescence technique is particularly sensitive to structures less than 10 nm in size due to quantum confinement phenomena. One can chemically map sites responsible for producing low-energy (1-eV to 6-eV) fluorescence. An intriguing application makes use of the time structure of the x-ray pulses, which enables investigations of the dynamic behavior of the states involved in the luminescence.

X-ray nanoprobe *26-ID* The Center for Nanoscale Materials nanoprobe will advance the state of the art in x-ray microscopy by providing the highest spatial resolution in the world. This unique suite of instruments will be key to the specific research areas of the CNM, and it will also be of general utility to the broader science community in studying nanomaterials and nanostructures, particularly for embedded structures. *See next page.*

The Hard X-ray Nanoprobe

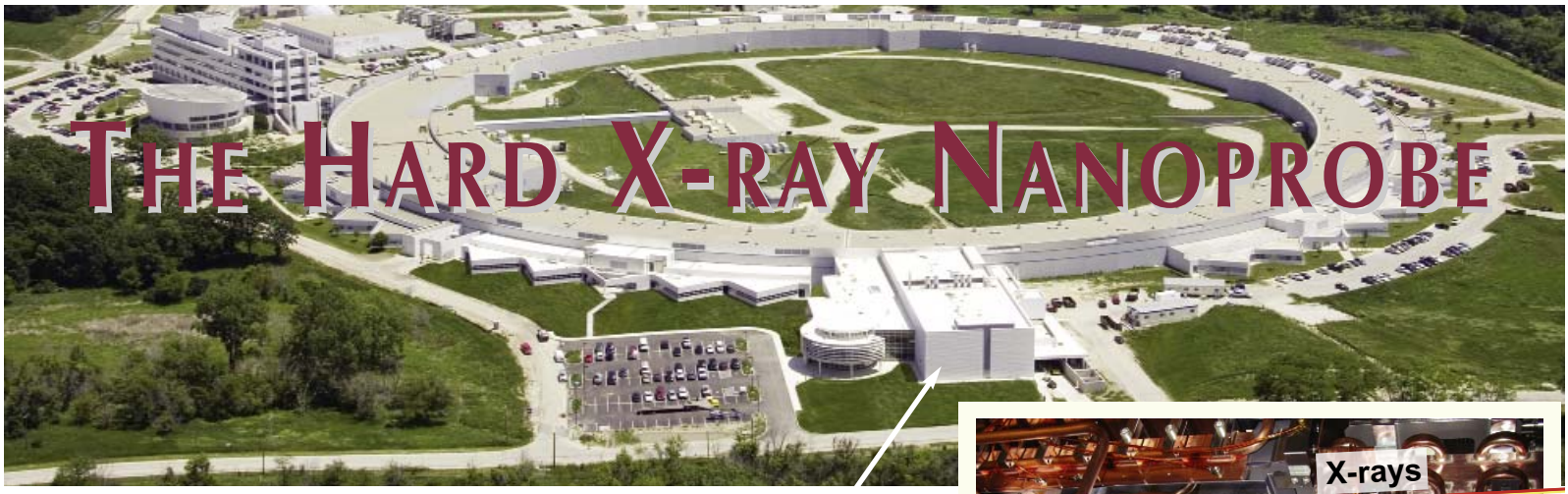

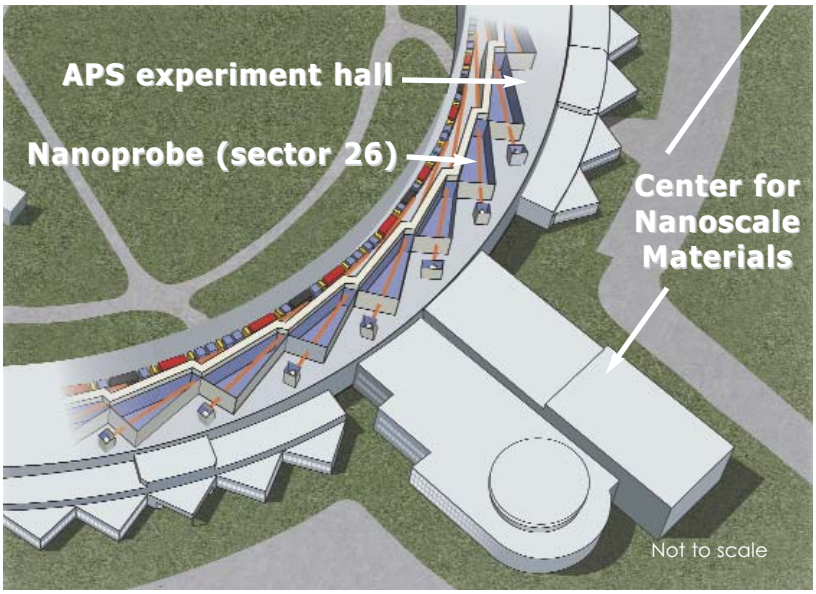

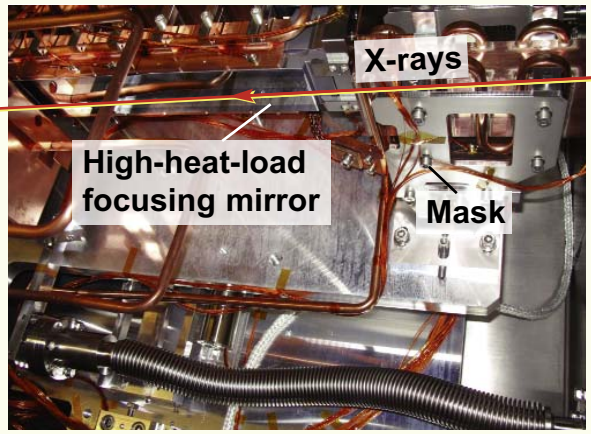

A double-mirror system serves as high-heat load components of the nanoprobe beamline. It provides reduction of total power, reduction of power density on the crystal monochromator, and harmonics filtering. It also acts as focusing components of a spatial filter. Double-mirror design allows adjustment of the grazing angle without changing the angle of the doubly reflected beam. The first component is a mechanically bent, horizontally focusing, water-cooled mirror with a length of 460 mm, shown above. X-rays from two collinear undulators enter the mirror system from the right.

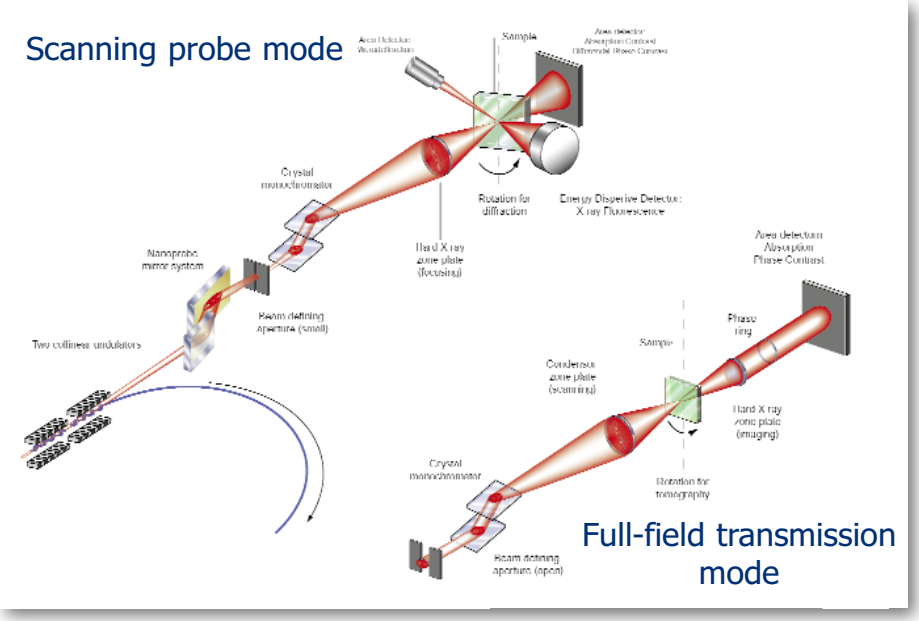

Schematic of the nanoprobe beamline showing the major techical components.

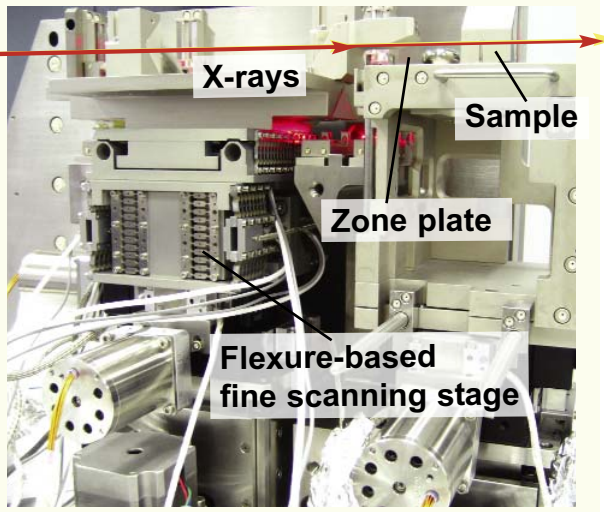

For acquisition of high-resolution data in scanning probe mode, the zone plate will be raster-scanned in x and y. To that effect, a high-resolution, flexure-based scanning stage is used to position the zone plate. Coarse motion of both zone plate and specimen will be provided by stepping motors. The photo above shows the zone plates and specimen module with related laser optics.

The Center for Nanoscale Materials (CNM, http://nano.anl.gov/) at Argonne National Laboratory is a U.S. Department of Energy user facility for nanoscience research located adjacent to the APS experiment hall on the west side of the ring. The CNM has become operational in the past year, and provides facilities for the synthesis, processing, characterization, and modeling of new generations of nanoscale materials and devices. As part of its suite of characterization tools for the nanoscience community, CNM has constructed the Hard X-ray Nanoprobe Beamline at APS sector 26 [1]. Commissioning of the Nanoprobe will begin in July 2007, and it will support full user operations in 2008.

The Hard X-ray Nanoprobe Beamline will utilize x-ray energies from 3 to 30 keV to produce the world's highest-resolution hard x-ray images. The beamline takes advantage of the high brilliance at high photon energy provided by the APS to produce diffraction-limited focal spots for scanning probe microscopy. Photon energies in the hard x-ray portion of the electromagnetic spectrum are ideally suited for imaging with contrast mechanisms such as x-ray fluorescence and x-ray diffraction. These contrast mechanisms allow researchers to characterize and quantify elemental constituents of materials with sensitivity to individual nanoparticles, and to observe atomic-scale structural properties of nanoscale materials and systems, such as crystal structure and strain. Hard x-rays also allow penetration of overlayers, environments, and fields for *in situ* studies. Using Fresnel zone plates as focusing and imaging optics, the nanoprobe will provide an initial spatial resolution of 30 nm—the size of 100 atoms. (One meter is to one nanometer as the diameter of the Earth is to a hazelnut.) It is anticipated that significantly higher spatial resolution will be reached over the lifetime of the nanoprobe as x-ray optics continue to improve. For example, a novel type of x-ray optic known as a Multilayer Laue Lens being developed by Argonne researchers [2, 3], can potentially efficiently focus hard x-rays to 5 nm or smaller.

The instrumentation at the Hard X-ray Nanoprobe Beamline provides, for the first time, a combination of scanning-probe and full-field transmission imaging. Full-field imaging will allow efficient three-dimensional visualization of complex systems and devices. Scanning probe imaging provides sensitive, quantitative analysis of elemental composition, chemical states, crystallographic phase, and strain. Using x-ray fluorescence radiation of *K* and *L* atomic states, the system will be suitable for spectroscopic studies of elements with Z >18; elemental mapping, which requires excitation energies above electron binding energies, can also be pursued for elements with smaller atomic numbers. Strain-contrast imaging will be a powerful tool to study systems such as ferroelectrics and ferroelastics. Linearly and circularly polarized x-rays will allow the study of magnetic materials. A beam chopper will allow extraction of single x-ray pulses from the APS, providing a time resolution of 100 ps that, combined with small focal sizes, will allow qualitatively new studies of dynamics at the nanoscale.

The Hard X-ray Nanoprobe Beamline will be operated jointly by CNM and APS. Access to the nanoprobe will be available to users through the coordinated proposal systems of CNM and APS.

Contact: Brian Stephenson (stephenson@anl.gov)

Hard x-ray nanoprobe capabilities

- Study of nanoscale materials and devices through a variety of contrast mechanisms to image elemental composition, chemical state, crystallographic phase, strain, and magnetism
- High penetration power (10 μm to 10 mm) for *in situ* studies
- High sensitivity to trace elements

Hard x-ray nanoprobe characterization techniques

- Fluorescence and diffraction in scanning probe mode
- Absorption and phase contrast in full-field transmission mode
- X-ray fluorescence radiation of *K* and *L* atomic states suitable for spectroscopic studies of chemical states of elements with Z >18
- Efficient elemental mapping for elements with Z >11
- Diffraction contrast imaging of crystal structure and strain
- Circularly polarized x-rays for the study of magnetic materials
- Stroboscopic time-resolved experiments using a beam chopper

References

[1] J. Maser, R. Winarski, M. Holt, D. Shu, C. Benson, B. Tieman, C. Preissner, A. Smolyanitskiy, B. Lai, S. Vogt, G. Wiemerslage, and G.B. Stephenson, *Proceedings of the 8th Int. Conf. X-ray Microscopy*, IPAP Conf. Series 7, 26 (2005).

[2] "Nanometer Linear Focusing of Hard X-rays by a Multilayer Laue Lens," *APS Science 2005*, **ANL-05/29**, 133 (2006). Also: www.aps.anl.gov/News/Annual_Report/annual_report_2005.pdf, pg. 133.

[3] H.C. Kang, J. Maser, G.B. Stephenson, C. Liu, R. Conley, A.T. Macrander, and S. Vogt, Phys. Rev. Lett. **96**, 127401 (2006).

Novel X-ray Techniques & Instrumentation

LERIX: Pinning Down the *q* in XRS

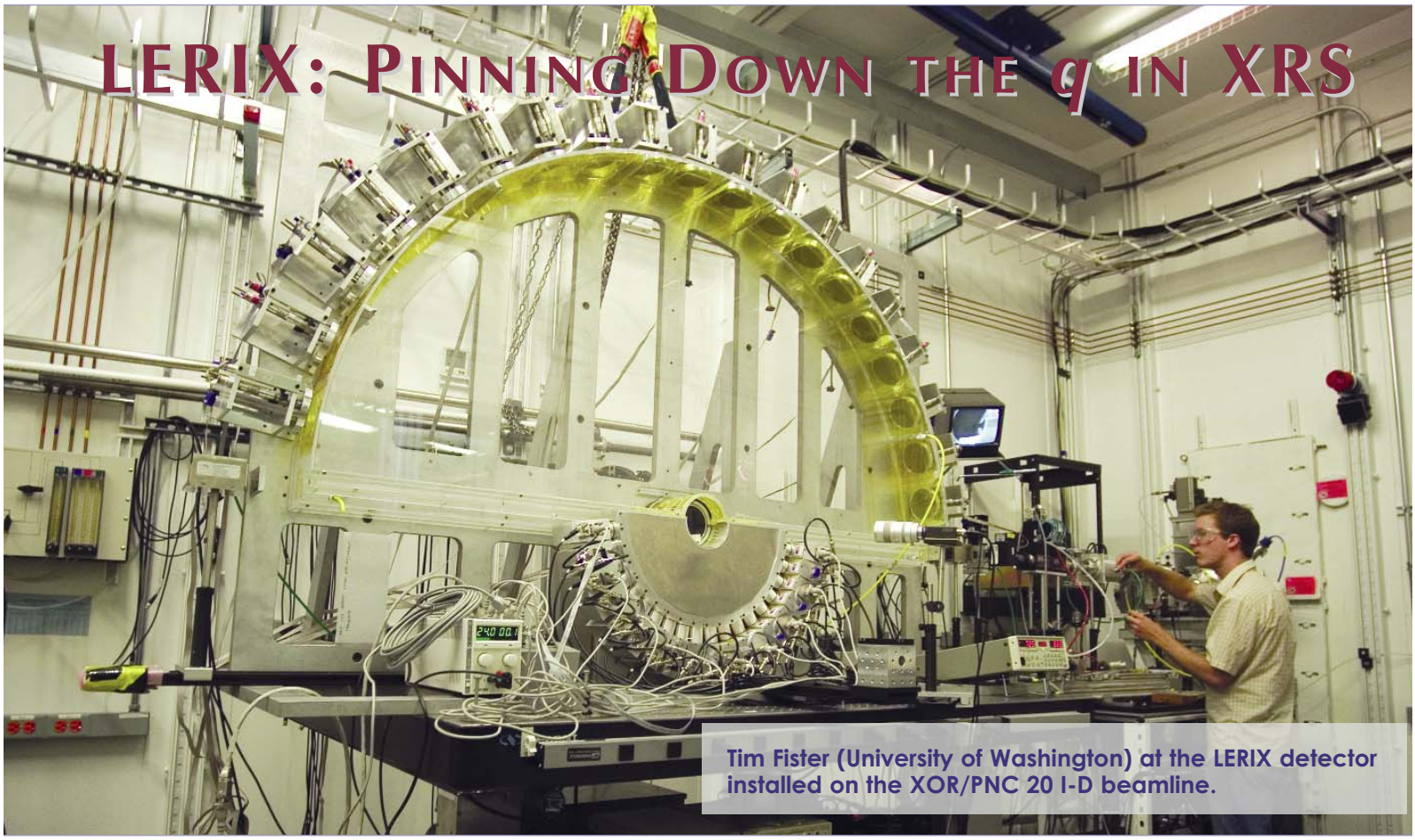

Tim Fister (University of Washington) at the LERIX detector installed on the XOR/PNC 20 I-D beamline.

Nineteen measurements are better than one—especially when using nonresonant x-ray Raman scattering (XRS) techniques to study certain low-Z elements. The problem is that XRS yields a low cross section, so obtaining measurements at differing momentum transfer *q* values is tedious and time-consuming because the instrumentation must be repeatedly retuned or realigned for the different *q* levels. Obviously, the ability to measure XRS simultaneously at many different values of *q* would be a boon for researchers using XRS and would improve counting statistics. An instrument capable of doing just that—the lower-energy-resolution inelastic scattering (LERIX) spectrometer—has been developed by a group of researchers from the University of Washington; Argonne National Laboratory; the University of California, Davis; the New Jersey Institute of Technology; and the NJ-XRSTECH Company. The LERIX detector is now available to general users of the APS.

X-ray Raman scattering encompasses a variety of inelastic x-ray scattering (IXS) techniques and IXS is one of the most useful tools available to the researcher studying condensed matter. Although XRS is especially handy for the examination of scattering from the core shells of low-Z elements and heavier elements with less tightly-bound shells, its low cross section is one reason that XRS has not been used as frequently as other, more established core shell spectroscopy methods such as x-ray absorption fine structure (XAFS) or electron energy loss spectroscopy (EELS). However, for electronic shells with low binding energy, XAFS and EELS are not very effective for studying samples in certain extreme conditions, e.g., in high-pressure chambers that soft x-rays or electron beams cannot penetrate. X-ray Raman scattering, on the other hand, utilizes high-energy, better-penetrating x-rays that can avoid such limitations.

Continued on next page

With all this in mind, the research team set out to create the LERIX instrument to make the use of XRS more practical and versatile. They designed a multielement spectrometer (Fig. 1) consisting of (originally 10 and now 19) analyzers arranged in a semicircle and mounted in an aluminum frame. An incident x-ray beam enters horizontally from one side of the base to focus on the sample enclosure at the center of the semicircle. At each end of the base is a gas ionization chamber for measuring the incident and transmitted energy of the x-ray beam. The arrangement of the analyzers in a semicircle allows the simultaneous measurement of XRS from the sample ranging from the low-q dipole limit to a high-q multipole limit near backscattering. Surrounding the sample enclosure at the center of the semicircle are 19 NaI scintillation detectors. The sample enclosure, like the area inside the semicircle between the sample and the analyzers and detectors, is filled with He to reduce air scattering. The instrument was carefully designed to minimize background signal from stray x-ray scattering. For example, with nearly 10^{13} photons/s incident on the sample, there are typically only a few-photons-per-second of stray background counts at each detector.

After previous work developing the LERIX spectrometer at the APS, the team has conducted numerous experiments to demonstrate the versatility of the instrument. These include measurements (at the XOR/PNC 20-ID beamline) of both the LiC_6 and the Li-metal oxide electrode materials in Li-ion batteries; of the isomers of a carborane molecule, which may be a novel component in future cancer therapies; and of carbon "nano-onions," which have been proposed as an important constituent of interstellar dust. Preliminary data from the first two general user groups for LERIX have also been very promising, with clean data on boron-carbide ceramics used for coating industrial tools and also on silicon-oxide glasses to be used in improved solar cell technology.

The multielement spectrometer developed by the research team promises to be a useful addition to APS capabilities, allowing high-energy, nonresonant IXS experiments with a great deal of versatility and adaptability to the needs of individual users. It opens the door to the further development of XRS as a powerful research technique for the 21st century.

— Mark Wolverton

See: T.T. Fisher[1], G.T. Seidler[1]*, L. Wharton[2], A.R. Battle[1], T.B. Ellis[1], J.O. Cross[3], A.T. Macrander[3], W.T. Elam[1], T.A. Tyson[4], and Q. Qian[5], "Multielement spectrometer for efficient measurement of the momentum transfer dependence of inelastic x-ray scattering," Rev. Sci. Instrum. **77**, 063901 (2006).
DOI: 10.1063/1.2204581
Author affiliations: [1]University of Washington; [2]University of California, Davis; [3]Argonne National Laboratory; [4]New Jersey Institute of Technology; [5]NJ-XRSTECH Company
Correspondence: *seidler@phys.washington.edu

This research was supported by the U.S. DOE Office of Science, Office of Basic Energy Sciences Contracts Nos. DE-FGE03-97ER45628 and W-31-109-ENG-38; ONR Grant No. N00014-05-1-0843; and the Summer Research Institute program at the Pacific Northwest National Laboratory. The operation of XOR/PNC is supported by DOE Basic Energy Sciences Contract No. DEFG03-97ER45629, the University of Washington, and grants from the Natural Sciences and Engineering Research Council of Canada. Use of the Advanced Photon Source was supported by the U.S. Department of Energy, Office of Science, Office of Basic Energy Sciences, under Contract No. W-31-109-ENG-38.

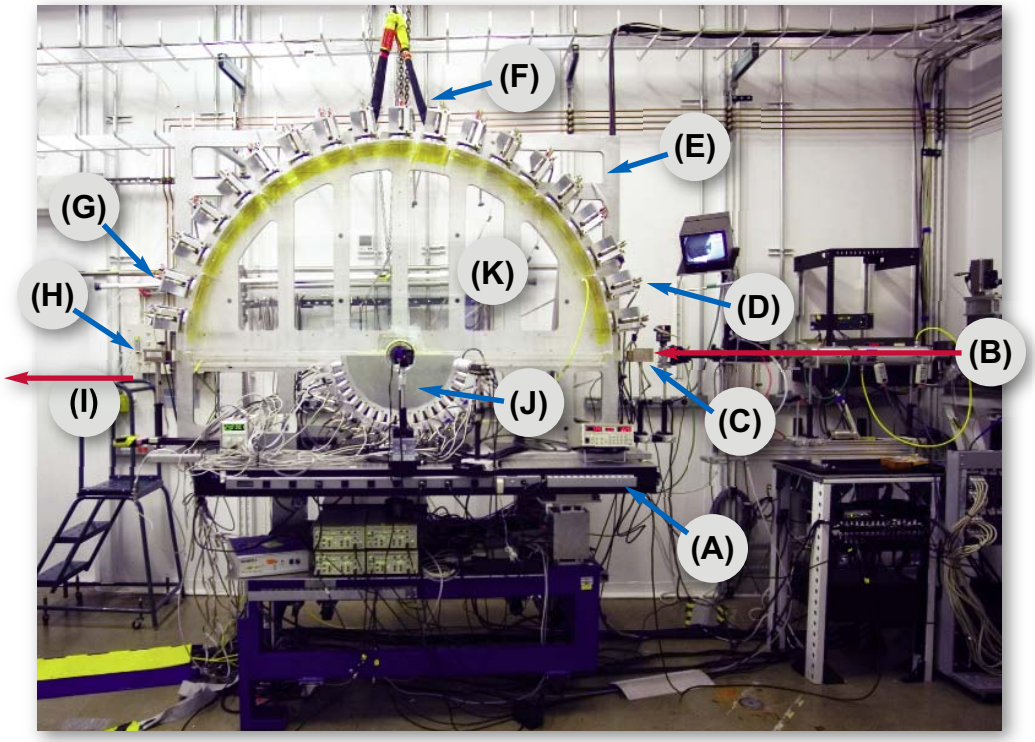

Fig. 1. Selected components of the LERIX spectrometer: (A) baseplate of the support frame; (B) incident x-ray beam; (C) gas ionization chamber for monitoring the incident intensity; (D) analyzer module for energy loss measurements at high momentum transfer, corresponding to near backscattering from the sample; (E) vertical back plate of the support frame; (F) hoist rings; (G) analyzer module for energy loss measurements at low momentum transfer, corresponding to a relatively small scattering angle from the sample; (H) gas ionization chamber for monitoring the transmitted intensity; (I) transmitted x-ray beam; (J) detector assembly; (K) helium-filled flight path. For scale, the outer radius of (K) is approximately 95 cm. The sample is located on the rotation axis of the inner, cylindrical region bounded by (J) and (K). Under usual operation, the location of the 10 analyzer modules correspond to momentum transfers ranging from 0.8 $Å^{-1}$ (G) to 10.1 $Å^{-1}$ (D) when working at an incident photon energy of ~10 keV.

Seeing the Smallest Steps

Many important things happen at interfaces: adsorption, corrosion, and catalysis, to name just a few. Understanding how such processes operate is of critical importance in many scientific areas ranging from geochemistry to physics, but observing phenomena at such tiny scales is not easy. Conventional techniques such as electron- and atomic-force microscopy and optical interferometry have inherent limitations that can compromise the resolution and quality of the observations. X-ray microscopy (XRM) has been hampered by its resolving power of about 10–20 nm. This is a problem for interfacial science, in which the reactivity depends on the topography (e.g., distinguishing subnanometer-high steps from flat terrace regions). Without the ability to make direct observations at the molecular level, interfacial scientists have been limited in many systems to broad descriptions and generalized averaging approaches that can only approximate what is really happening. Is there a better way? Can molecular-scale features be somehow imaged utilizing current microscopic methods? Researchers from Argonne and Xradia, Inc., have found a solution by developing a novel form of XRM: reflecting x-rays off a surface and using phase contrast of the reflected rays to detect monomolecular steps in the (001) surface of orthoclase. For the first time, the technique (x-ray reflection interface microscopy, or XRIM) presents the ability to observe subnanometer features that are smaller than the optical resolution of the x-ray microscope—in this case, some 300 times smaller.

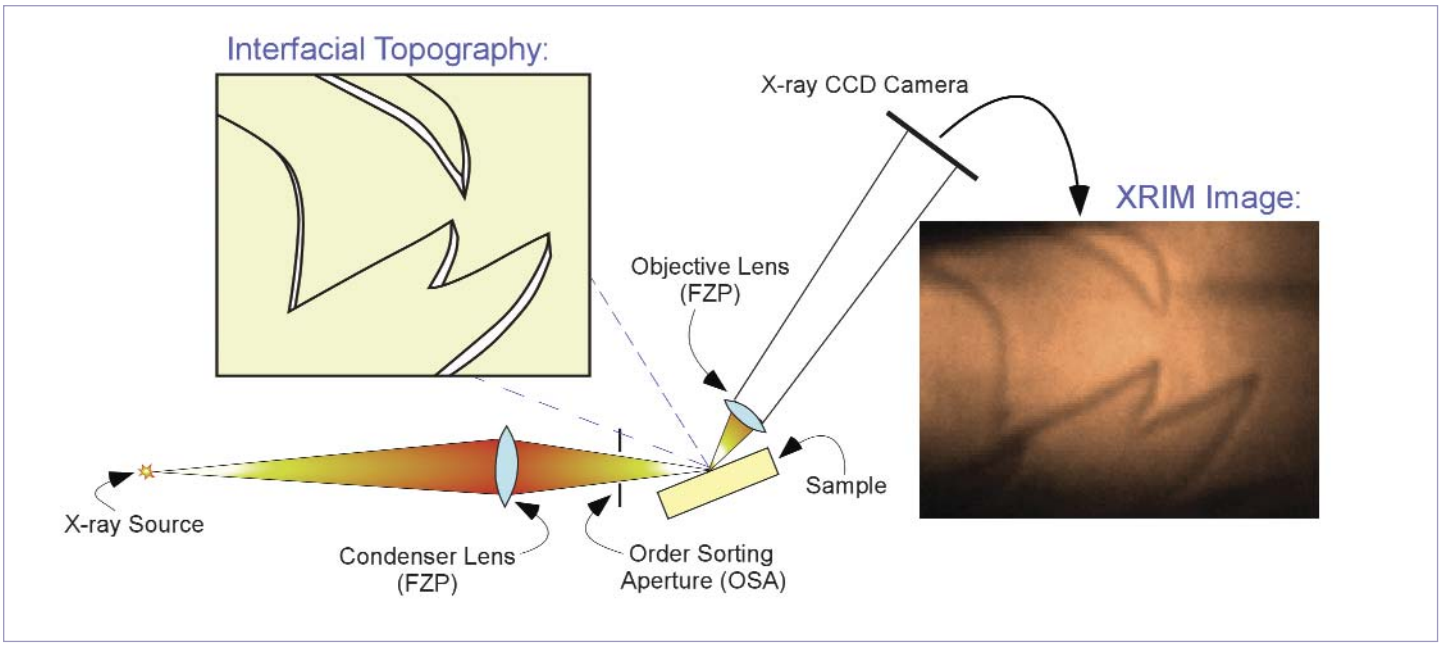

Fig. 1. X-ray reflection interface microscopy is shown schematically. A monochromatic x-ray beam from the synchrotron source is focused onto the sample using a condenser lens in the form of an FZP, and the focused beam is selected using an order sorting aperture. An objective FZP lens is then used to image the variation of the reflected x-ray intensity across the sample onto an x-ray CCD camera. Changes in the surface topography due to the presence of elementary steps (shown in the inset on the left) are observed as changes to the x-ray intensity in the magnified image (inset on the right).

All XRM work to date has been centered on getting as small a focus spot as possible—or the best resolution possible—and then looking at objects that size or bigger. The state of the art in terms of resolution is approximately 20 nm. That effectively restricts x-ray microscopy from looking at any molecular-scale phenomena, which are important for many areas of study; scientists ultimately want to be able to see the fundamental response of a material as layers are added or removed.

The research team's XRIM technique uses a monochromatic x-ray undulator beam from the XOR/BESSRC 12-ID-D beamline at the APS, focused by a condenser Fresnel zone

Continued on page 138

Simultaneous X-ray Measurements of Density and Acoustic Velocity

Understanding the composition of the Earth requires studies of the characteristics of various minerals under pressures and temperatures consistent with those at our planet's interior. One such study involves comparing the densities and seismic velocities of such materials to the known seismic velocities and densities inside the Earth. In an effort to enhance this kind of data collection by finding densities and velocities of samples simultaneously—a method that assures that the characteristics are measured at the exact same temperature and pressure—researchers from the University of Illinois at Urbana-Champaign, The University of Chicago, and the Carnegie Institution of Washington have built a Brillouin spectrometer that can interface successfully with x-ray diffraction techniques. This instrument is now installed at the GSECARS 13-BM-D beamline at the APS.

Brillouin spectroscopy is used to measure acoustic velocity by sending a laser to bounce off the vibrating atoms in a sample and then measuring the Doppler shift of the laser's scattered light. But in order to accommodate simultaneous use of x-ray diffraction to measure sample density, the researchers in this study had to modify the traditional set-up. Among many considerations, the spectrometer had to assemble and break down easily, it had to be compact, and it had to keep its laser beam safely enclosed. It was crucial that the spectrometer optics be movable, because x-ray diffraction often requires changing the placement of the sample—a tricky requirement as Brillouin spectrometers usually need a stable set-up to ensure exact knowledge of the angle between the incident laser and the reflected signal.

The team's instrument (Fig. 1) is built on two levels, with the sample sitting on the lower one, lined up with the incident x-ray beam. The laser for the Brillouin spectrometer begins its route on the top level and initially passes through several optical components to control and condition the laser beam. For safety's sake, all of these components can be controlled from outside of the enclosure. The beam then travels to the lower portion through a focusing assembly to the sample, and then the scattered signal is brought back to the top level and is analyzed by a six-pass, Sandercock-type, piezoelectrically scanning tandem Fabry-Perot interferometer. The focusing and collecting paths of the spectrometer can translate independently and thus be moved around to accommodate different placements of the sample if need be, depending on the positioning required by the incoming x-ray.

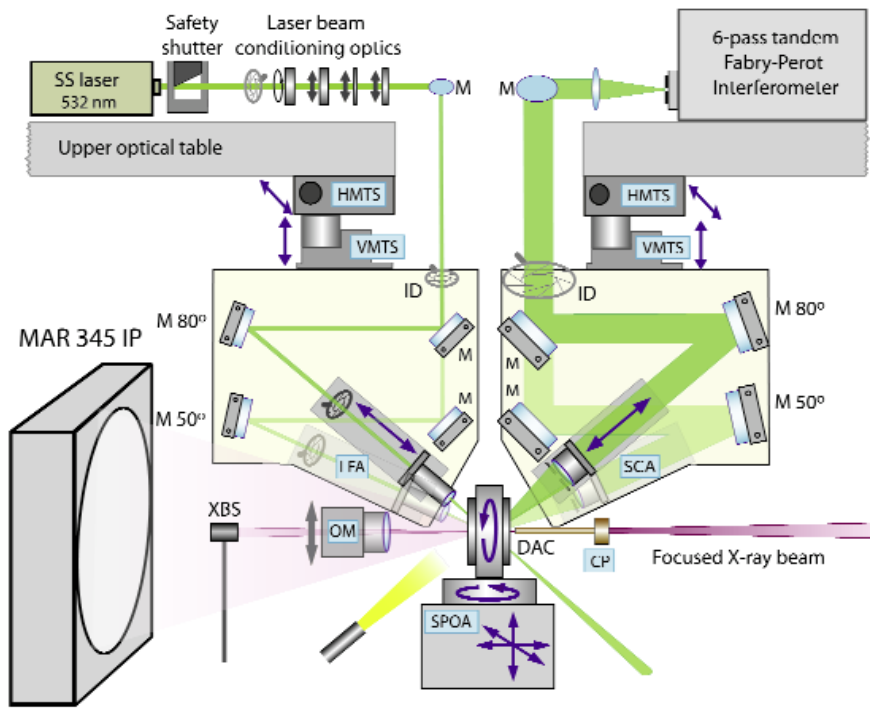

Fig. 1. Schematic diagram of the combined Brillouin–x-ray system at GSECARS. The motorized translation components (those fully controllable from outside the hatch) are labeled as HMTS (horizontal motorized translation stage), VMTS (vertical motorized translation stage), LFA (motorized laser focusing assembly), SCA (motorized signal collecting assembly), SPOA (sample positioning and orientation assembly), and OM (removable online microscope). X-ray components are MAR 345 IP (MAR imaging plate), XBS (x-ray beam stop), and CP (cleanup pinhole). Other labeled components are DAC (diamond anvil cell), M (mirror), and ID (iris diaphragm).

To test the new Brillouin spectrometer's operation, the researchers examined several typical crystal and polycrystalline samples at various pressure and temperature conditions. They found their system is ideally suited for measuring single-crystal elastic moduli of materials in a diamond anvil cell.

Continued on page 138

"Smallest Steps" continued from page 136

plate (FZP) lens onto the sample surface. Reflected x-rays are magnified by another FZP lens into a charge-coupled device (CCD) camera to obtain images in full-field imaging mode. The differences in vertical topography across the surface are indicated by changes in the reflected intensity across the image due to phase contrast, revealing the locations of individual steps. The results do not show the atomic structure of the step, but they do image the step itself. That is an important advance for interfacial science, because interfacial reactivity is often controlled by steps, which tend to be more reactive.

The XRIM technique thus enhances and expands the traditional capabilities of x-ray microscopy and changes the way forward for the XRM community by extending the reach of what can be studied at a much smaller length scale—down to molecular-scale features.

A key inspiration for the group was the insight that, even though the portion of the x-ray beam that is reflected by the interface is perhaps only a millionth of the incident beam flux, the intensity reduction of x-rays reflected from the monomolecular steps (with respect to other parts of the surface) is still sufficiently large to allow the subnanometer steps to be detected, and enough to compensate for the weak surface x-ray reflectivity. Even so, an extremely bright and strong x-ray source is needed for the technique, and the team found the APS, the brightest x-ray source in the Western Hemisphere, to be the perfect tool for their work.

Now that these researchers have proven the feasibility of the technique, the next step is to apply this technique to studies of the liquid-solid interface where there are many processes that are difficult to observe with traditional techniques. The researchers are aiming for the ability to observe interfacial reactivity under liquids. Other possible applications include probing interfacial processes that have never before been accessible to direct observation (including buried interfaces) and observing processes including ion adsorption, corrosion, catalytic reactions, particle nucleation, and the formation and switching of ferromagnetic domains.

The team is confident that the XRIM technique will prove to be a valuable addition to the imaging arsenal of interfacial chemists and physicists. They hope these first steps will carry them to the point where XRIM becomes a standard technique for probing interfaces. — *Mark Wolverton*

See: Paul Fenter[1*], Changyong Park[1], Zhan Zhang[1], and Steve Wang[2], "Observation of subnanometre-high surface topography with X-ray reflection phase-contrast microscopy," Nat. Phys. **2**, 700 (October 2006). DOI: 10.1038/nphys419

Author affiliations: [1]Argonne National Laboratory, [2]Xradia, Inc.
Correspondence: *fenter@anl.gov

This work was supported by the U.S. Department of Energy, Office of Science, Office of Basic Energy Sciences, Division of Chemical Sciences, Geosciences and Biosciences, Geosciences Research Program through contract No. W-31-109-ENG-38 to Argonne National Laboratory. XOR/BESSRC at the APS is supported by the U.S. Department of Energy, Office of Basic Energy Sciences. Use of the Advanced Photon Source was supported by the U.S. Department of Energy, Office of Science, Office of Basic Energy Sciences, under Contract No. W-31-109-ENG-38.

"Acoustic Velocity" continued from page 137

The combined Brillouin scattering and x-ray diffraction provided unambiguous identification of the orientation and phonon direction in the sample and direct measurements of single-crystal and aggregate elastic moduli of materials. The stress state of the crystal and its deformation could be assessed from analysis of the diffraction image and integrated spectra. And last, the lattice parameters could easily be determined.

The instrument's advantage on polycrystalline samples is that the angle-dispersive x-rays provide a direct measurement of lattice parameters (and therefore the density of the sample), while simultaneous Brillouin measurements provide a direct measurement of the aggregate compressional and shear velocities. From these the adiabatic bulk and shear moduli can be calculated. On the other hand, the quality and accuracy of polycrystalline Brillouin measurements depend on the elastic anisotropy of the sample: too high and the Brillouin peaks are too broad and hard to interpret. However, because the elastic anisotropy decreases with pressure for many materials, the polycrystalline Brillouin measurements at high pressures are more reliable.

In addition, the combined techniques provide much more accurate determination of pressure at high temperatures than the current standards. Indeed, one of the researchers' main purposes for combing the two instruments was to perform accurate calibration of the pressure-temperature-volume equations-of-state of materials, which can then be used as accurate pressure sensors in high-pressure, high-temperature experiments.

— *Karen Fox*

See: Stanislav Sinogeikin[1,3*], Jay Bass[1], Vitali Prakapenka[2], Dmitry Lakshtanov[1], Guoyin Shen[2,3], Carmen Sanchez-Valle[1], Mark Rivers[2], "Brillouin spectrometer interfaced with synchrotron radiation for simultaneous x-ray density and acoustic velocity measurements, " Rev. Sci. Instrum. **77**, 103905 (2006). DOI: 10.1063/1.2360884

Author affiliations: [1]University of Illinois at Urbana-Champaign, [2]GSECARS, The University of Chicago, [3]HP-CAT, Carnegie Institution of Washington
Correspondence: *ssinog@hpcat.aps.anl.gov

This research was partially supported by COMPRES, the Consortium for Materials Properties Research in Earth Sciences under NSF Cooperative Agreement EAR 01-35554. GeoSoilEnviroCARS is supported by the National Science Foundation-Earth Sciences EAR-0622171 and Department of Energy-Geosciences DE-FG02-94ER14466. Use of the Advanced Photon Source was supported by the U.S. Department of Energy, Office of Science, Office of Basic Energy Sciences, under Contract No. W-31-109-ENG-38.

A New Channel-cut Monochromator for Coherence-based Techniques

Third-generation synchrotron sources such as the APS have enabled development of coherence-based experimental tools, among them coherent x-ray diffraction and x-ray photon correlation spectroscopy (XPCS), which require monochromatic x-ray beams while being brilliance-limited. The monochromators for these techniques must preserve beam brilliance by employing highly polished diffracting faces. While there are decided advantages to the "traditional" channel-cut monochromator (TCCM) utilized on X-ray Operations and Research beamline 8-ID, there is also a disadvantage in that the crystal surface cannot be appropriately polished to avoid producing a spatially inhomogeneous beam. Researchers from the X-ray Science Division's Time Resolved Research Group, and Mechanical and Interlock Systems in the APS Experimental Support Division (AES) have developed a new channel-cut monochromator design that overcomes this problem.

X-ray Operations and Research beamline 8-ID-I, which hosts the XPCS program at the APS, requires a double-bounce germanium monochromator with the necessary brilliance preservation, stability, and longitudinal coherence for XPCS measurements in the small-angle regime. In the past, the 8-ID beamline used a TCCM because the monochromator's diffracting planes are inherently parallel, yielding a fairly simple mechanical design. Because reflecting crystal faces of the TCCM design cannot be adequately polished, the large surface roughness introduces unwanted phase modulation into the x-ray beam, producing a spatially inhomogeneous beam.

To overcome this, the Time Resolved Research Group embarked on a new "artificial" channel-cut monochromator (ACCM) design that facilitates polishing of the diffracting faces while retaining the mechanical stability provided by the TCCM. The ACCM incorporates a novel, in-vacuum, sine-bar drive mechanism for the combined pitch motion of the two crystals. Further, to develop a stable mechanism that facilitates aligning an assembly of two crystals to achieve the same performance as a single channel-cut crystal, the group developed a UHV-compatible, high-stiffness, flexure-based weak-link mechanism for fine tuning the pitch and roll of the second crystal relative to the first crystal.

Ge(111) crystals of 25 mm × 25 mm × 20 mm were polished to state-of-the-art surface finish, root mean square surface roughness of sub-angstroms, and flatness of $\lambda/25$ (λ = 638 nm). A relatively small gap of 3 mm was chosen for the ACCM so as to have a compact mechanical design, a small offset in the monochromatic beam height, and maximum angular range for a given linear travel of the sine bar. Figures 1(a) and 1(b), respectively, show the monochromatic beam produced by the TCCM and the ACCM as two-dimensional intensity maps measured using a charge-coupled-device detector (CCD).

Improvement in beam uniformity with the ACCM is evident. The intensity in Fig. 1(a) varies by more than 50% over considerably smaller length scales (~50 μm, the typical aperture size used for XPCS) with negative implications for the stability of the overall setup. With the ACCM, the variation in intensity over the beam area is less than 10%. A significant contribution to the intensity variation, the broad vertical band in Fig. 1(b), is attributed to imperfections in the side-bounce mirror in the first optics enclosure. The horizontal and vertical stripes at the edges are due to Fraunhofer diffraction from the beam-defining slits. The rocking curve measurements carried out at several energies in the range of 6-11 keV indicate that the crystals are perfect and strain-free, and that the two crystals—once aligned parallel to each other at one energy—remained parallel over the entire energy range. The error in the absolute energy, defined as the difference in the measured and calculated photon energy, was found to be less than ±2 eV over the energy range of 6-11 keV, with no measurable hysteresis. The monochromator delivers an exceptionally uniform and stable beam and improved brilliance preservation.

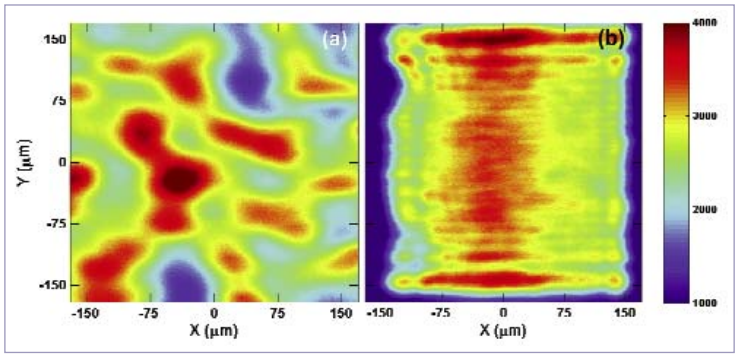

Fig. 1. Monochromatic beam imaged using a CCD detector from (a) the traditional channel-cut monochromator, and (b) the artificial channel-cut monochromator.

Contact: Suresh Narayanan (sureshn@aps.anl.gov), Alec Sandy (asandy@aps.anl.gov), Deming Shu (shud@aps.anl.gov), Michael Sprung (sprung@aps.anl.gov)

A significant portion of the construction costs of the monochromator was provided by an X-ray Operations and Research Beamline Competition Award. Use of the APS was supported by the U.S. Department of Energy, Office of Science, Office of Basic Energy Sciences, under Contract No. DE-AC02-06CH11357.

Using CXD to Determine 3-D Crystal Structure

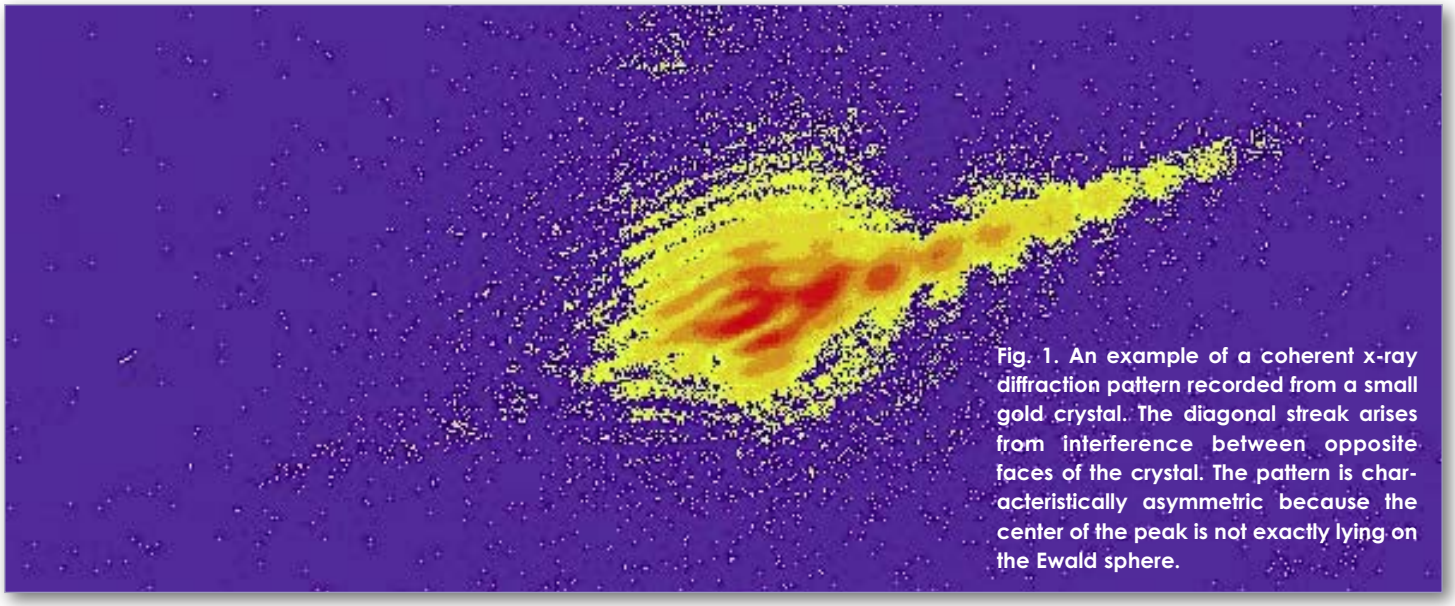

Fig. 1. An example of a coherent x-ray diffraction pattern recorded from a small gold crystal. The diagonal streak arises from interference between opposite faces of the crystal. The pattern is characteristically asymmetric because the center of the peak is not exactly lying on the Ewald sphere.

The three-dimensional (3-D) characterization of small Au crystals has been successfully resolved by the coherent x-ray diffraction (CXD) technique, which employs the direct inversion of diffraction patterns through computation methods. In an earlier paper, collaborators from the University of Illinois at Urbana-Champaign described an effective method for resolving the 3-D shape of small crystals from a CXD pattern [1]. Based on this result, the collaborators further refined their studies by describing the experimental conditions and computational methods used to recover the 3-D shape of nanocrystals of Au from diffraction data near a high-angle Bragg peak. Using the XOR/UNI beamline 33-ID-D at the APS, the collaborators performed only a small-angle scan of the sample with a two-dimensional (2-D) measurement at each angle.

In the CXD technique, the scattering from the sample of a very coherent x-ray beam is measured. Conventional x-ray diffraction (XRD) techniques only yield information about the structure that is averaged over many coherent volumes.

However, with CXD the 3-D sample shape is determined by (1) reconstructing the phase of the diffracted wave in the far field using iterative algorithms based on oversampling to obtain a general solution of the diffraction phase problem and (2) recognizing the intricate connection between the sample's electron density and the diffracted wave's amplitude.

In preparation for the experiment, the collaborators prepared a small Si wafer on which Au film was deposited while in vacuum. The film/substrate sample was centrally positioned within an atmospheric-stabilized chamber. The chamber, constructed of two cured ceramic pieces and four quartz slides containing Au film, was heated to a constant temperature of 1,050º C for 10 h. Then, the sample was cooled to a temperature of 850º C for another 10 h. Finally, the chamber's temperature was quickly dropped to room temperature.

The sample was removed from the chamber and held in place inside a closed steel cylinder containing entrance and exit apertures covered with a DuPont™ Kapton® high-performance polyimide film. A halogen light bulb was attached as a heat source. With the experiment ready to proceed, the entire apparatus was placed on the diffractometer at the XOR/UNI beamline.

The CXD pattern was collected from the sample at 950º C in a grazing-exit geometry. As the sample was heated, it separated from its substrate and formed small single crystals. As a

Continued on next page

function of the sample angle, a large number of diffraction peaks was detected, caused by the illumination of approximately 100 to 120 crystals within the beam. Nevertheless, because of large separations between reflections, the collaborators were able to individually select the pattern from a single sample grain.

A charge-coupled-device detector set at a Bragg point measured a 2-D CXD pattern (Fig. 1). This corresponds to a slice through the diffraction by a plane placed tangentially to the Ewald sphere—a geometric construction specifying the relationship between the angle of diffraction for a given reflection. The sample was then rocked in steps of 0.002 degrees, rotating the Ewald sphere through the Bragg point. The full 3-D pattern was measured by stacking the planes.

To recover the complex amplitude of the diffracted wave, an inversion procedure was used, with alternating periods of a certain number of iterations of a particular algorithm with a predetermined set of constant parameters.

Oversampling produced approximately 20 pixels for each fringe along the diagonal flare, about 10 pixels per fringe around the central maxima, and, due to estimation difficulties, more than half the total number of slices in the third direction. The collaborators feel that three distinct effects (Fig. 2) are apparent in the reconstructed images: (1) Extremely high density is found near the crystal's center, (2) very fine lines of apparent low density appear as diagonal dark stripes from top-left to bottom-right, and (3) misorientation is seen from some sections of the crystal.

This study demonstrates that solutions involving various beginning points result in almost identical results when considering data uncertainty. However, the electron density that is recovered did contain unexpected variations at the nanometer scale. This result is explained as natural deformation within the crystal. — *William Arthur Atkins*

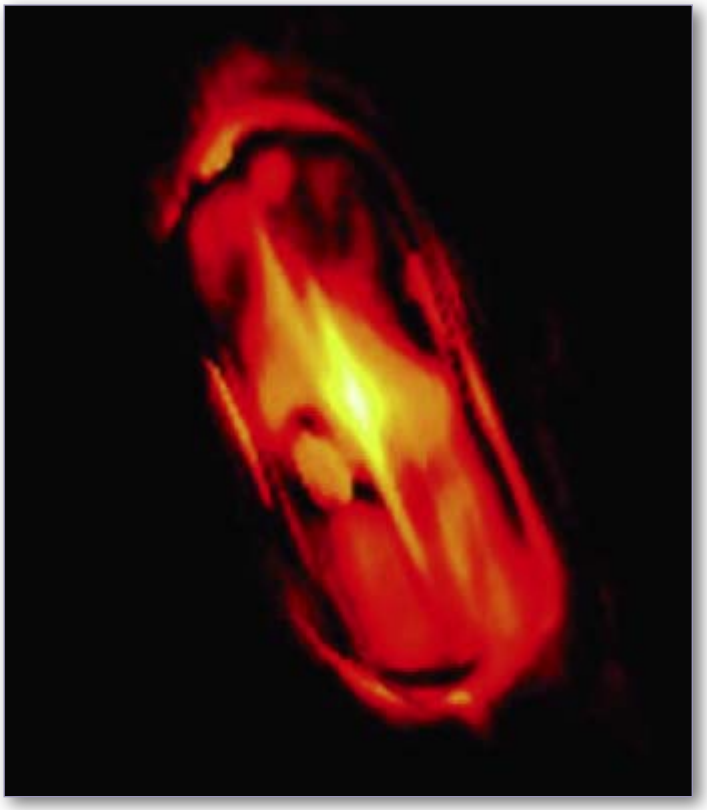

Fig. 2. One section of the 3-D reconstruction of the density of the gold crystal, showing the bright center and striped internal structure.

Author affiliation: University of Illinois at Urbana-Champaign
Correspondence: *i.robinson@ucl.ac.uk and ikr@uiuc.edu

This research was supported by the NSF under Grant No.DMR 03-08660. The XOR/UNI facility at the APS was supported by the University of Illinois at Urbana-Champaign, Materials Research Laboratory U.S. DOE Contract No. DEFG02-91ER45439, the State of Illinois-IBHE-HECA, and the NSF, the Oak Ridge National Laboratory (U.S. DOE) under contract with UT-Battelle LLC, the National Institute of Standards and Technology, U.S. Department of Commerce, and UOP LLC. Scanning electron microscope work was carried out in the Center for Microanalysis of Materials, University of Illinois. Use of the Advanced Photon Source was supported by the U.S. Department of Energy, Office of Science, Office of Basic Energy Sciences, under Contract No. W-31-109-ENG-38.

Reference

[1] G. J. Williams, M.A. Pfeifer, I.A. Vartanyants, and I.K. Robinson, Phys. Rev. Lett. **90**, 175501 (2003)

.

See: G.J. Williams, M.A. Pfeifer, I.A. Vartanyants, and I.K. Robinson*, "Internal structure in small Au crystals resolved by three-dimensional inversion of coherent x-ray diffraction," Phys. Rev. B **73**, 094112 (2006).

Ramping Up Remote Access at SER-CAT

Striving to give its users the best possible synchrotron data collection experience, and to increase the productivity of its beamlines, SER-CAT at APS sector 22 has embarked on an aggressive program in beamline automation and remote access that has significantly reduced both data collection time and user effort. As part of this approach, SER-CAT has recently made available to its users the SGXPro Crystallographers Workbench (SGXPro), a powerful cluster-based parallel workflow engine for automated structure determination developed at the University of Georgia [1]. SGXPro will allow SER-CAT users to quickly analyze their data and carry out initial phasing while still on-site, and is aimed at improving productivity by providing users with both high-quality data and initial structural results, as well as feedback to the data collection process.

SGXPro offers a user-friendly, easily extendable computational environment that incorporates transparent links to many popular crystallographic programs. It uses a pseudo-parallel workflow engine to automatically manage communication among different processes and to build sophisticated searches of algorithm, program, and/or program parameter space to increase the likelihood of a successful structure solution. This is done by providing the user with a palette of programs and techniques commonly used in x-ray structure determination, in an environment that lets the user pick programs in a mix-and-match manner (without worrying about interprogram communication and file formats) during the structure determination process. SGXPro incorporates a number of commonly used programs for (a) data quality evaluation (3DSCALE, which includes Ras analysis); (b) heavy-atom site identification (SHELXD, SOLVE); (c) initial phasing (SOLVE, ISAS); (d) electron density improvement (DM, SOLOMON, DMMULTI); (e) visualization (XFIT, COOT); (f) auto-tracing (ARP/wARP, RESOLVE, MAID); and (g) molecular replacement with BLAST assisted (AMORE and EPMR).

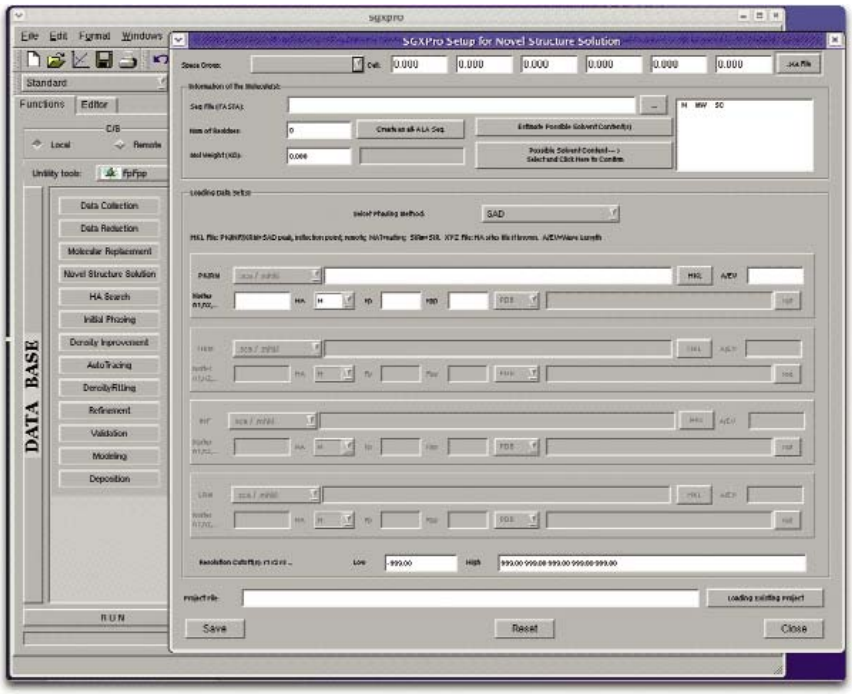

Fig. 1. The SGXPro general-user interface showing the setup page for the Novel Structure Solution workflow. Most of the required information (white space) is auto-generated from the corresponding structure factor and sequence files.

A new feature of SGXPro designed specifically for SER-CAT users, who may be strapped for time, is the Novel Structure Solution workflow (Fig. 1) for *de novo* structure determination from multiwavelength anomalous dispersion (MAD) or single-wavelength anomalous scattering (SAS) data. Here the user need only select the appropriate reflection file (SCALE-PACK format) and sequence file (FASTA format) using the browser. Alternatively, the user can generate a polyalanine chain of appropriate length if the FASTA sequence is unavailable. Based on the space group, unit cell volume, and molecular weight, an estimate of the number of molecules per crystallographic asymmetric unit and corresponding solvent content is presented to the user. The user then selects the approximate solvent content from the list provided, inputs the energy (or wavelength) of x-rays used to record the data, the type and number of anomalous scatterers to be found (or $\Delta F'$ and $\Delta F''$ values for MAD phasing) and whether SAS or MAD phasing will be employed. If MAD phasing is selected, the current version of the program allows the user to load two-to-four data sets with their corresponding energies to be used in the analysis. Once input is complete and saved, the workflow is executed using the RUN command.

Continued on next page

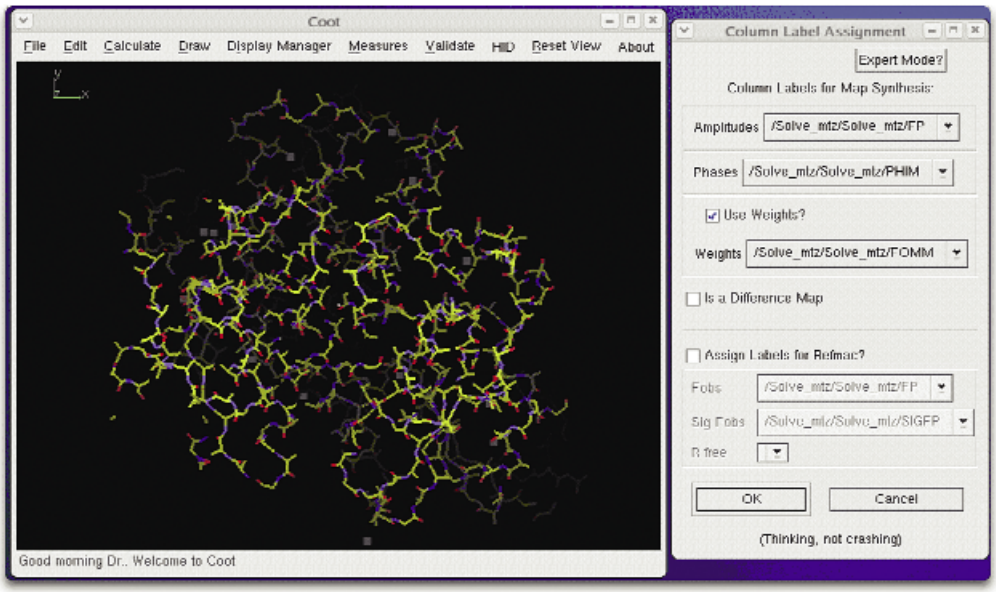

Fig. 2. Upon completion of the SGXPro Novel Structure Solution workflow, the solution having the highest probability of being correct (i.e., the solution having the largest chain traced from RESOLVE) is displayed together with the corresponding electron density map. This allows the user to confirm the quality of the phases, the resulting electron density map, and the structure.

The Novel Structure Solution workflow consists of the following tasks: (a) Identification of the anomalous scattering substructure using both a parallelized version of SHELXD [2] and SOLVE running simultaneously on the SER-CAT 32-processor Linux cluster; (b) determination of the correct hand of the anomalous scattering substructure using ISAS; (c) initial phasing using ISAS and SOLVE; (d) automated chain tracing using RESOLVE, MAID, or ARP/wARP (depending on data resolution); and (e) visualization of results using COOT (COOT will automatically choose and display the model and electron density map corresponding to the top solution, as shown in Fig. 2).

More than 20 research groups have now used SGXPro for fast and efficient structure determination. For example, during a recent trip to SER-CAT, a team from the University of Georgia headed by Dr. Lirong Chen was able to solve five structures on-site using the SGXPro Crystallographers Workbench, most in a matter of minutes using the Novel Structure Solution workflow (Table 1). *Contact: John Rose (rose@bcl4.bmb.uga.edu)*

References

[1] Z.Q. Fu, J. Rose, and B.C. Wang, "SGXPro: a parallel workflow engine enabling optimization of program performance and automation of structure determination," Acta Crystallogr. D **61**, 951 (2005).

[2] Z.Q. Fu et al., "Parallelization of SHELXD for quick heavy-atom partial structural solution on high-performance computers," J. Appl. Crystallogr., 2007 (in press).

Work supported by funds from the National Institutes of Health, the Georgia Research Alliance, and the University of Georgia Research Foundation. The Advanced Photon Source is supported by the U.S. Department of Energy, Office of Science, Office of Basic Energy Sciences, under Contract No. W-31-109-ENG-38.

Table 1. UGA structures solved using the SGXpro Crystallographers Workbench.

ORF	Size (AA)	MW (kD)	Method	Se Sites	a (Å)	b (Å)	c (Å)	Space Group	Resolution (Å)	Rsym (%)	Run time
PH0987	225	25.3	Se-SAS	1	105.85	105.85	51.87	$P6_1$	2.30	5.7	12 min
GK1651	278	31	Se-SAS	8	53.57	59.82	69.69	$P2_12_12_1$	1.52	6.1	19 min
PH0730	214	24.3	Se-SAS	4	34.71	60.97	84.43	$P2_12_12_1$	1.79	7.1	15 min
MJ0922	138	15.5	Se-SAS	4	57.21	94.69	102.04	$P2_12_12_1$	2.60	7.1	20min
AQ_1208	420	46.9	MR		75.52	87.68	152.58	$P2_12_12_1$	2.00	8.8	6hrs

TRXEOL at XOR 4-ID-C

The normal operating mode of the APS produces x-ray beams with pulse widths of 80 ps, with 153-ns gaps between pulses. Much like a strobe light, these pulses can be used to "freeze" events in time, allowing the measurement of times-of-flight of a variety of particles. If the particles are electrons, one can determine their kinetic energies; if the particles are ions, one can determine their mass; if the particles are optical photons, one can determine the lifetime of the excited state that emits the photon. It is the latter aspect that is utilized for time-resolved x-ray excited optical luminescence (TRXEOL), a technique that has been developed in the X-ray Science Division's Magnetic Materials Group at 4-ID-C. Applications of luminescent materials range from coatings for CRTs and watch dials to lasers. For coatings, one would like to have a material that has a long luminescence lifetime (phosphorescence, approximately minutes), while for lasers, the initially excited level should have a short lifetime (<nsec), while the lasing level should have a relatively long lifetime in order to achieve population inversion. The time structure of the x-ray beam from the APS permits the determination of lifetimes from <1 ns to >1 μs.

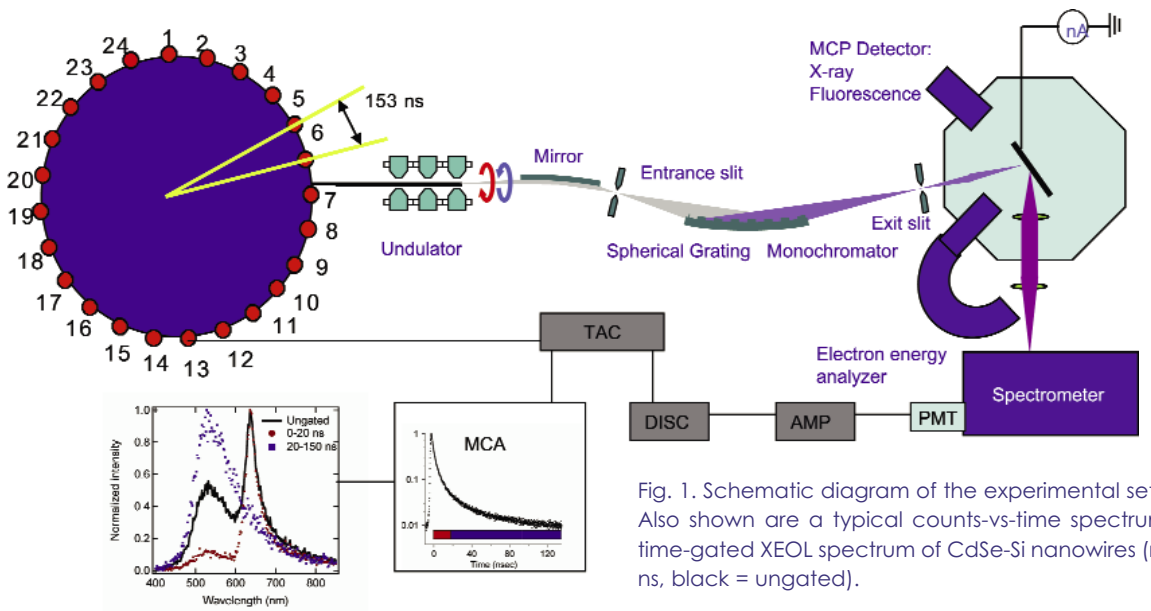

Fig. 1. Schematic diagram of the experimental setup for performing TRXEOL. Also shown are a typical counts-vs-time spectrum (decay curve) and the time-gated XEOL spectrum of CdSe-Si nanowires (red = 0-20 ns, blue = 20-150 ns, black = ungated).

X-ray absorption near edge spectroscopy (XANES) is a powerful tool for determining the atom-specific structure of a material. By performing XANES measurements, using the optical luminescence as a signal, it is possible to determine the local environment of the sites responsible for the emitted light, as well as their time response. This technique has recently been used by the author to show that the sites responsible for the defect luminescence in ZnS nanowires have a zinc-blende structure, even though the overall structure of the nanowire is wurtzite [1].

The experimental setup for TRXEOL is shown schematically in Fig. 1; a photo is shown in Fig. 2. X-rays from the APS irradiate a sample and the resulting optical luminescence is collected by an objective lens and then focused by another lens onto the entrance slit of a monochromator. After being dispersed the monochromatic light is detected by a fast photomultiplier tube (PMT). The output signal is then amplified and discriminated, and used to trigger the "Start" channel of a time-to-amplitude converter (TAC). A bunch clock signal, originating from the storage ring, is used to provide the "Stop" signal to the TAC. The output signal from the TAC is then directed into a multi-channel analyzer (MCA) operating in the pulse-height analysis mode. An example of the resulting counts-vs-time spectrum is also shown in Fig. 1.

An example of the power of TRXEOL was demonstrated in a recent study of CdSe-Si heterostructured nanowires [2]. Silicon nanowires (NWs) are important in nanotechnology because Si-based nanoelectronics are compatible with the Si-based microelectronics. Si NWs exhibit quantum confinement

Continued on next page

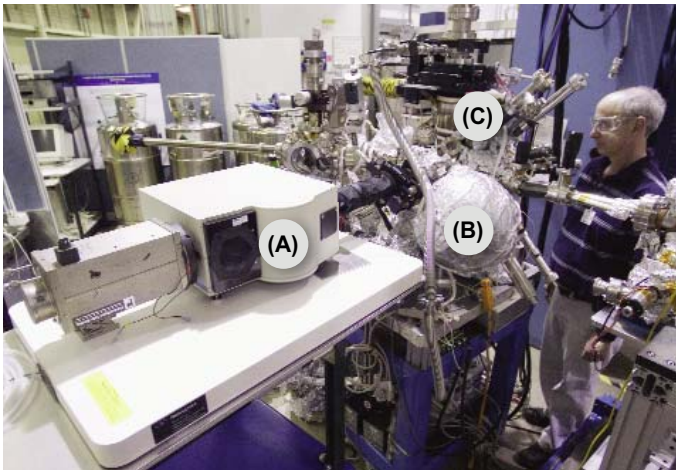

< Fig. 2. Photograph of the apparatus (with R. Rosenberg): (A) spectrometer, (B) electron energy analyzer; (C) MCP detector.

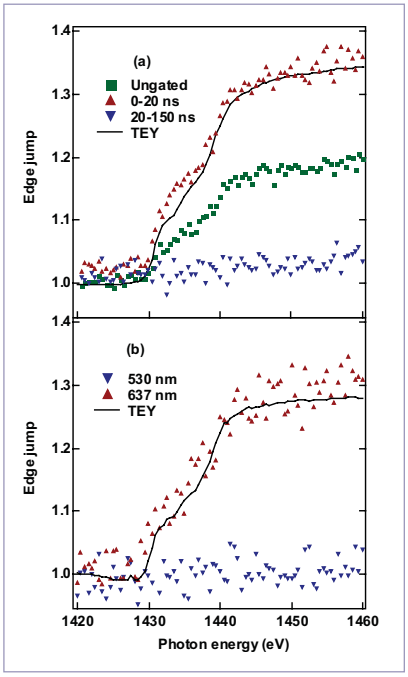

> Fig. 3. Se L_3 edge optical luminescence yield spectra: (a) spectra obtained using undispersed (0 order) luminescence but with different time gates (as indicated) and compared to the TEY spectrum; (b) spectra obtained with no time gates but dispersed luminescence (as indicated). The ordinate units are the edge jump where the pre-edge signal is normalized to one.

effects and are expected to play a key role as interconnects and functional components in future nanosized electronic and optical devices. CdSe is an important II-VI semiconductor for optoelectronics as well. With a direct band gap of 1.76 eV (704 nm), zero-dimensional CdSe quantum dots have been intensively studied and widely used for laser diodes, nanosensing, biomedical imaging, etc. Si-based one-dimensonal nano-heterostructures will be the desired building blocks for nanoscale electronics and optoelectronics.

The nanowires have a coaxial structure with a Si core encased by a CdSe sheath, with diameters of 30-80 nm and lengths of up to tens of µm. The time-gated x-ray excited optical luminescence (XEOL) spectra of the heterostructure, excited at 1000 eV, are shown in Fig. 1. The ungated (solid line, black) spectrum consists of a sharp peak at 637 nm and a broader structure centered at 530 nm. By applying different time gates it is possible to determine the relative lifetimes of the two peaks. In the fast time window (0-20 ns, dots, red) the 637-nm band is accentuated, while in the slow window (20-150 ns, squares, blue) the 530-nm peak dominates. We assign the 637-nm peak to near-edge emission from the CdSe sheath and the 530-nm peak to levels in the Si core. The broadband emission peak is similar in energy and shape to that observed in silicon nanowires, and the energy of the sharp emission band at 637 nm (1.93 eV) is close to the band gap of 1.76 eV for bulk wurtzite CdSe, except for a blue shift.

By performing x-ray absorption measurements using the various luminescence signals as probes, one is able to confirm the aforementioned assignments. Figure 3 shows the Se L_3 edge excitation spectra, which are compared to the total electron yield (TEY, the overall absorption coefficient). The data are shown in terms of the "edge jump" where the pre-edge (1420-1425-eV) signal is normalized to 1. This allows for a quantitative comparison among the various channels. Spectra shown in Fig. 3(a) were obtained using undispersed, zero-order light from the luminescence spectrometer and different time gates. The spectrum obtained using the short (0-20 ns) time gate is qualitatively and quantitatively similar to the TEY. No edge jump is observed in the long time gate spectrum while the ungated curve lies between the short and long time gate spectra. This comparison demonstrates that the short-lived luminescence emanates from the CdSe layer and the long-lived component does not.

The data obtained using ungated, monochromatic luminescence [Fig. 3(b)] further supports this assignment. The 637-nm excitation curve quantitatively matches the absorption spectrum (TEY) of the CdSe layer, while the 530-nm data show no contrast. These results are further proof of the assignments based on the time-gated excitation spectra in Fig. 3(a).

The relative life times of the states giving rise to the two bands in Fig. 2 are in contrast with typical homostructured semiconductor luminescence temporal behavior, where a sharp, short-lived, near-edge emission is found at relatively short wavelengths, and broad, long-lived, defect luminescence occurs at longer wavelengths. In homogenous systems, higher energy states have relatively short lifetimes as a result of efficient coupling to lower lying levels. The fact that such behavior is not seen in Si-CdSe nano-heterostructures indicates that there are no efficient pathways to couple the higher-lying, excited electronic levels in the Si core to the lower ones in the CdSe sheath. *Contact: Richard A. Rosenberg (rar@aps.anl.gov)*

REFERENCES

[1] R.A. Rosenberg, G.K. Shenoy, F. Heigl, S.-T. Lee, P.-S.G. Kim, X.-T. Zhou, and T.K. Sham, "Determination of the local structure of luminescent sites in ZnS nanowires using x-ray excited optical luminescence," Appl. Phys. Lett. **86**, 263115 (2005).

[2] R.A. Rosenberg, G.K. Shenoy, X.H. Sun, and T.K. Sham, "Time-resolved X-ray-Excited Optical Luminescence Characterization of One-dimensional Si-CdSe Heterostructures," Appl. Phys. Lett. **89**, 243102 (2006).

Use of the Advanced Photon Source was supported by the U.S. Department of Energy, Office of Science, Office of Basic Energy Sciences, under Contract No. W-31-109-ENG-38.

A New Tool for Structure Studies at High Pressures with a DAC

A scanning-angle energy-dispersive x-ray diffraction (SA-EDXD) technique employing an energy-dispersive solid-state detector and white synchrotron radiation has been developed for high-pressure structure studies using a diamond anvil cell (DAC). The main feature of the technique is well-defined collimation in the beam pass to the detector, which improves the signal-to-noise ratio significantly compared to routine monochromatic angle-dispersive powder diffraction. This is particularly useful and essential for low-scattering materials, as well as amorphous and liquid diffraction/scattering studies using a DAC.

The diamond anvil cell is one of the most common devices used for high-pressure structure studies. Due to the thin sample used in a DAC at high pressure, the background from the diamond and from pressure-transmitting media is often significant for routine angle-dispersive powder diffraction. Combining a solid-state point detector with a scanning diffraction angle, one can establish a good detecting collimation using only the diffraction signals from a sample (Fig. 1). A similar technique has been developed for the large-volume press for use in powder diffraction by Wang et al. (2004). A group at the HP-CAT, sector 16 at the APS, has extended the technique, making it suitable for DAC experiments by employing high-precision stages with a sphere-of-confusion that is less than 5 μm. Together with the software developed for automation control and data analysis, this technique is now available for general users. The diffraction intensity is sorted to 4,000 channels by the energy-dispersive detector. When the multichannel energy data is converted to constant-energy angle-dispersive data, only a coarse 2θ scan is required to achieve the regular angle-dispersive diffraction resolution. One example of Fe_2O_3 powder diffraction is shown in Fig. 2(a), with the intensity plotted in two dimensions as a function of dif-

Continued on page 148

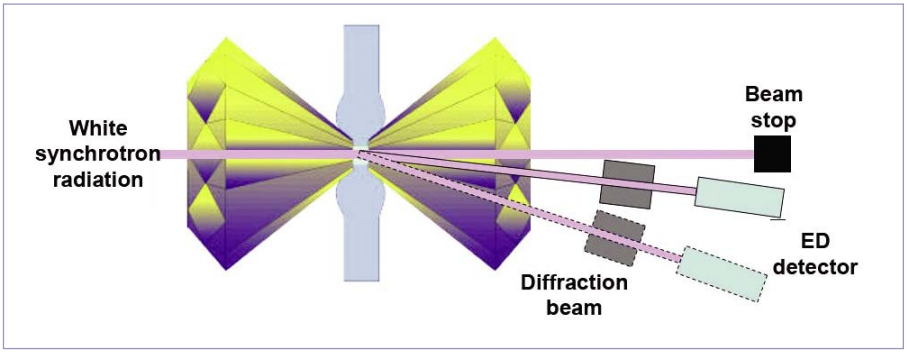

Fig. 1. Schematic of data acquisition with the SA-EDXD technique.

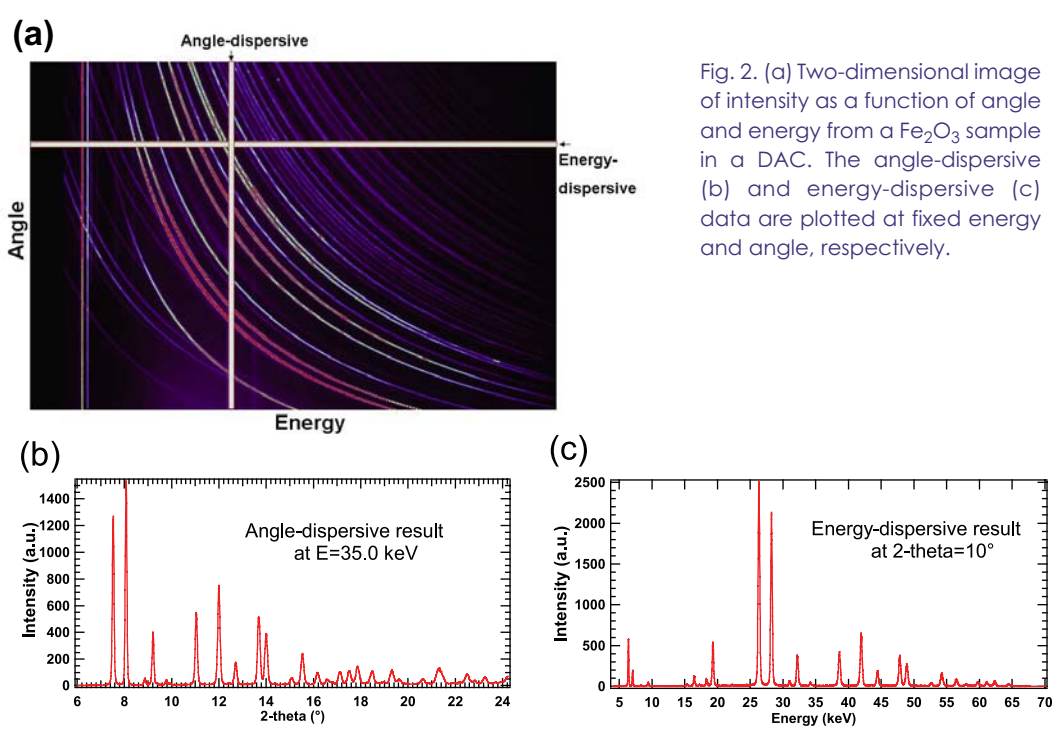

Fig. 2. (a) Two-dimensional image of intensity as a function of angle and energy from a Fe_2O_3 sample in a DAC. The angle-dispersive (b) and energy-dispersive (c) data are plotted at fixed energy and angle, respectively.

High-pressure XMCD Capability at XOR 4-ID-D

Magnetic ordering of electronic spins is intimately connected to the overlap between their electronic orbitals. Altering this overlap by the application of pressure, for example, has profound effects on the magnetic interactions, whether they are mediated by direct or indirect exchange (i.e., whether the wave-functions of spin-carrying electrons overlap directly, or indirectly through hybridization with non-magnetic ions or conduction electrons). When combined with the element- and orbital-specificity of x-ray magnetic circular dichroism (XMCD), high-pressure studies of magnetism provide a unique tool for understanding magnetic interactions at the atomic level. Members of the X-ray Science Division Magnetic Materials Group have developed a high-pressure, low-temperature, high magnetic field XMCD capability at XOR beamline 4-ID-D.

The setup, shown in Fig. 1, uses a copper-beryllium diamond-anvil cell (DAC) suitable for low-temperature measurements. The DAC features perforated diamond anvils that allow high transmission of the relatively low-energy x-rays (5-9 keV) associated with *K*-absorption edges of transition metals and *L*-absorption edges of rare-earth elements. The phase-retarding optics at 4-ID-D is optimized for delivering circularly-polarized x-rays in this energy range. In addition, the beamline's toroidal focusing mirror provides a 200-$\mu m^2 \times$ 100-μm^2 x-ray beam at the sample position. This almost matches the smallest aperture in the diamond perforation, of about 150 μm^2. The piston's motion, and hence the sample pressure, can be controlled remotely by regulating the He gas pressure in an expanding membrane, thus allowing *in situ* pressure changes at low temperature. The DAC attaches to the cold finger of an He-flow cryostat and reaches a base temperature of 9K. The cryostat is mounted on high-resolution translation stages for sample positioning with micron resolution. In addition, a rotation stage is utilized to avoid unwanted diamond diffraction that introduces glitches in the absorption spectra.

The cryostat is placed between the pole pieces of an electromagnet delivering a magnetic flux density of about 0.7 T. The DAC's size and surrounding vacuum shroud limit the magnetic field strength, while the pressure is limited by the size of the diamonds. Currently, 450-μm diamond culets are being used, reaching sample pressures of about 16 GPa. Pressure calibration is done from x-ray absorption fine struc-

Continued on page 148

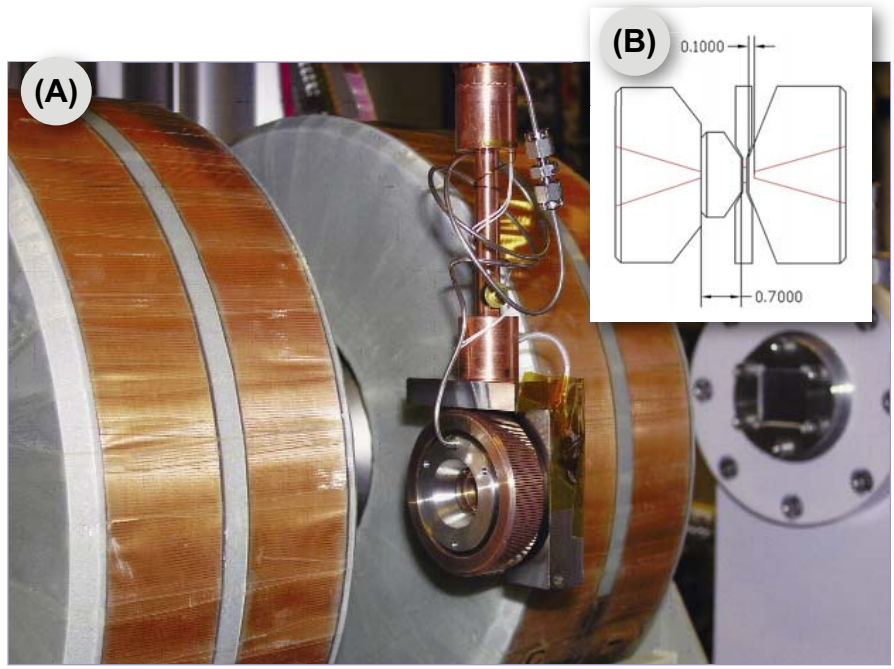

Fig. 1 (above). (A): DAC assembly at the end of the cryostat's cold-finger extension. The DAC is shown outside the magnet poles with the vacuum shroud removed. (B) Schematic of the diamond anvils. The total diamond thickness seen by the x-ray beam is 0.8 mm.

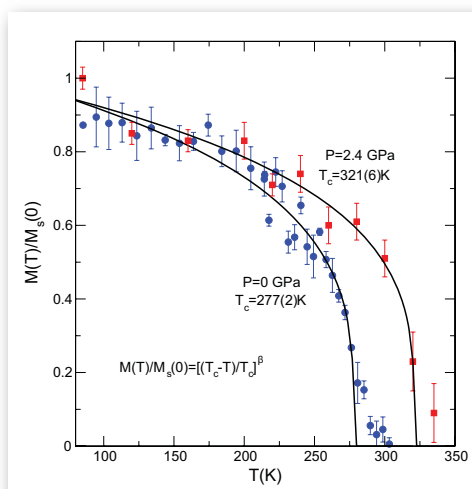

Fig. 2 (right). Pressure-induced changes in magnetic ordering temperature in a $Gd_5Si_2Ge_2$ magnetocaloric material measured with this setup.

"Structure Studies" continued from page 146

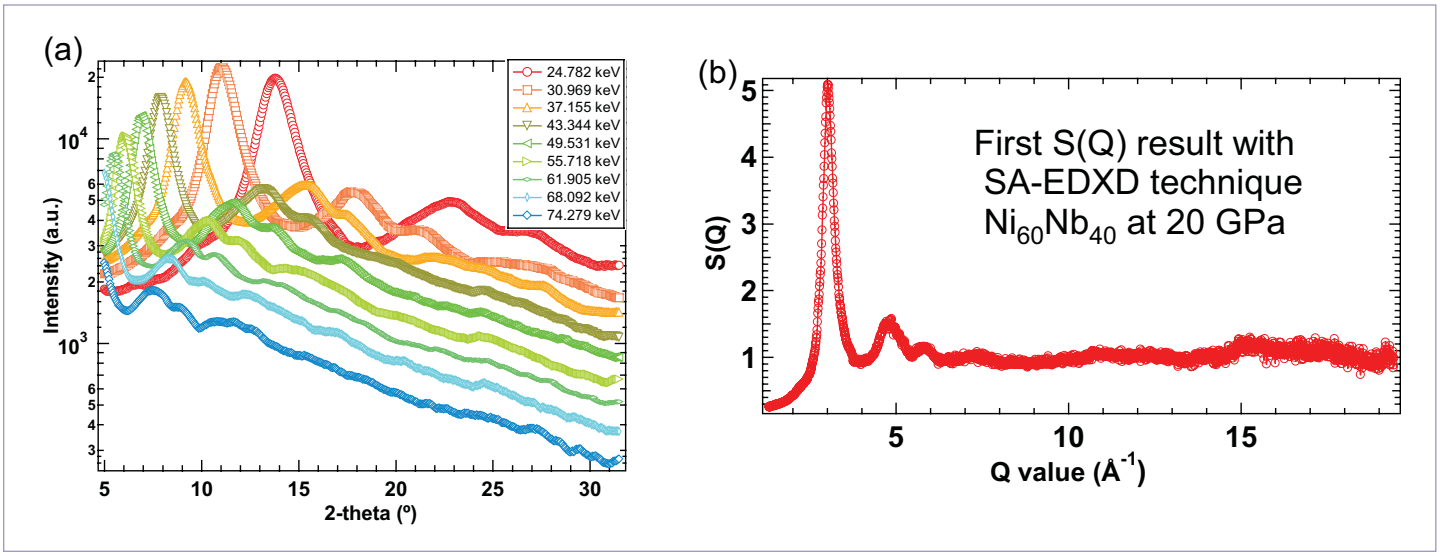

Fig. 3. Data obtained by the SA-EDXD technique for an Ni-Nb amorphous material at 20 GPa in a DAC. Nine angle-dispersive data (a), with energies from 24 keV to 74 keV, are used to obtain the full structural factor S(Q) (b). Multiple-energy data can also be used to get partial structural factors for multi-element amorphous/liquid samples (in progress).

fraction angle and energy. One can achieve an angle-dispersive diffraction pattern at certain energies [Fig. 2(b)], and energy-dispersive diffraction pattern at certain angles [Fig. 2(c)], for structure analysis and refinement.

Recently, amorphous and liquid structure studies under extreme conditions have attracted significant interest. The SA-EDXD technique provides an important new tool in this area for a number of reasons. The well-defined collimation ensures the necessary signal-to-noise ratio for weak signals from amorphous and liquid materials in a DAC. The use of white beam up to 110 keV covers a large Q-range (>20 Å^{-1}). The intensity data collected by the SA-EDXD technique are a function of energy and angle, from which one can obtain angle-dispersive data from different energies, and energy-dispersive data at different angles as well. Figure 3 is an example of a binary amorphous $Ni_{60}Nb_{40}$ sample at 20 GPa measured in a DAC. The structure factor, S(Q), can be calculated from the angle-dispersive pattern at different energies [shown in Fig. 3(a)], while each one has a different Q-range. A combined S(Q) can be obtained for a large Q-range [Fig. 3(b)]. For multi-element amorphous, Fig. 3(b) only represents a total structural factor. The work for partial structural factors is in progress.

Contact: Wenge Yang (wyang@hpcat.aps.anl.gov)

References:

W. Yang, G. Shen, Y. Wang, and H-k. Mao, Rev. Sci. Instrum. (to be submitted)

Y. Wang et al., J. App. Cryst. **37**, 947 (2004).

Y. Waseda, *The structure of non-crystalline materials, liquids and amorphous solids*. McGraw-Hill Inc. (1980).

This work is supported by the U.S. DOE-Basic Energy Sciences, DOE-National Nuclear Security Administration, NSF, DOD-TACOM, and the W.M. Keck Foundation. Use of the Advanced Photon Source was supported by the U.S. Department of Energy, Office of Science, Office of Basic Energy Sciences, under Contract No. W-31-109-ENG-38.

"XMCD" continued from page 147

ture measurements of the lattice parameter of Cu powders loaded with the sample (*in situ*) and from the energy shift of fluorescence from Ruby powders also loaded with the sample (*ex situ*).

Figure 2 shows the temperature dependence of the Gd L_3 XMCD signal taken on the magnetocaloric material $Gd_5Si_2Ge_2$ at ambient pressure and at P = 2.5 GPa. The shift to a higher magnetic transition temperature with pressure is clearly seen. For these measurements, the focused beam was further slit down to ~50 × 50 μm^2 and the sample size (gasket hole) was ~250 μm. Future work will include incorporation of a Ruby system and modified vacuum shroud for additional *in situ* pressure calibration, extension to higher pressures by reducing both the diamond culet size and the x-ray beam size with additional focusing optics, and measurements at higher magnetic fields using a smaller, screw-type DAC in a superconducting magnet.

Contact: Daniel Haskel (haskel@aps.anl.gov)

This work was supported by the U.S. Department of Energy, Office of Science, Office of Basic Energy Sciences, under Contract No. DE-AC02-06CH11357.

A Dedicated High-energy Beamline at XOR 1-ID

Upgrading XOR beamline 1-ID to a dedicated, optimized, high-energy beamline is a three-phase process. Members of the Materials Characterization Group in the X-ray Science Division have now completed Phase I, including installation of new high-energy instrumentation.

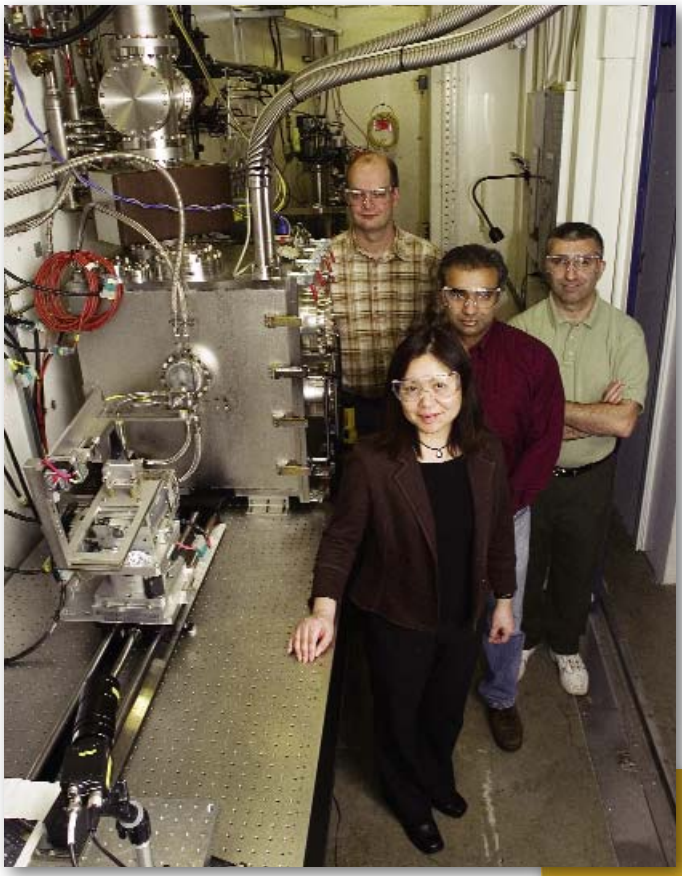

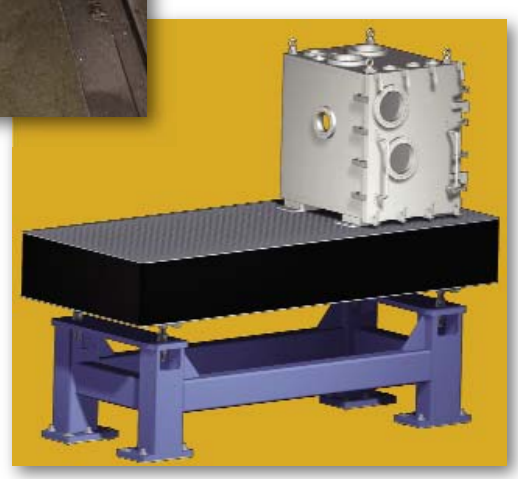

Photo above, front to back): Yifei Jaski (AES), Sarvjit Shastri, Ali Mashayekhi, and Dean Haeffner (all XSD) in the XOR 1-ID-A first-optics enclosure, next to the newly installed high-energy monochromator. At right is a rendering of the high-energy monochromator tank and support seen in the photo above.

Phase I of upgrading the 1-ID beamline to an optimized beamline dedicated to high-energy operations is now complete. Low-energy (6-40 keV) operations at 1-ID were phased out and the instrumentation for the high-energy (45-130 keV) monochromator and three-dimensional x-ray diffraction (3DXRD) microscope were upgraded. The bent double-Laue high-energy monochromator was relocated from 1-ID-B, where it had been developed as part of a high-energy x-ray optics project, to a permanent location in the 1-ID-A enclosure. As part of this move, a new vacuum chamber and support table were designed, purchased, and installed.

The 3DXRD microscope is part of a project to measure the diffraction properties of the individual single grains that make up polycrystalline materials. This is of great interest because the mechanical behavior of most structural materials is largely determined by a complex combination of the mechanical behavior of individual grains and the interaction between individual grains. Nearly all measurements of the mechanical properties of materials are made on bulk material as a whole (i.e., the aggregate of the single grains) and only average information is obtained. Following changes in materials grain-by-grain while they are exposed to physical transformations validates and extends our understanding of fundamental materials properties and has many implications for manufacturing.

Phase II of the 1-ID upgrade will see the current 1-ID-C monochromatic station replaced by two white-beam stations and associated transport. The two new stations (1-ID-D and 1-ID-E) will provide sufficient room for several dedicated instruments and improve the microfocusing performance by increasing the demagnification ratio of the focusing optics.

Phase III will be a project to put a side-bounce monochromator and monochromatic side station and transport (1-ID-F) on the 1-ID beamline. This will allow simultaneous operations for high-energy x-ray experiments and, hopefully, somewhat alleviate the very high oversubscription rate for high-energy experiments at 1-ID. Implementation of Phase II and III will be pursued when funding is available.

Contact: Dean Haeffner (haeffner@aps.anl.gov)

This work was supported by the U. S. Department of Energy, Office of Science, Office of Basic Energy Sciences, under Contract No. DE-AC02-06CH11357.

The APS User Community in 2006

During fiscal year (FY) 2006, the APS user program continued to grow, as measured by a variety of different metrics: the number of users coming to the APS to conduct research, the number of samples sent to the APS for measurement, the number of beam-time requests submitted through the General User Program (GUP), and the number of beamlines and shifts available to general users.

The upward trend in the number of APS users continued for the tenth straight year, with 3,274 individuals (861 of whom were first-time users) coming to the APS one or more times during 2006 to conduct research (Fig. 1). In addition, almost 100 individuals sent samples to the APS to be measured by beamline staff. The number of users visiting the APS multiple times also increased, with 10,830 user visits recorded during the year—a 12% increase over FY 2005 (Fig. 2). As shown in Fig. 3, the proportion of general user visits also continued to increase.

Almost 90% of this year's users came from U.S. institutions (Fig. 4), a slight increase from last year.

Approximately 46% of FY06 users conducted research in life sciences, with a similar percentage conducting research in the combined disciplines of materials science, physics, chemistry, geology, and environmental sciences (Fig. 5).

More than 70% of FY 2006 users were from colleges and universities, with the next largest groups coming from government laboratories (17%) and industry (6%) (Fig. 6). More than 25% of all users were students (Fig. 7).

Opportunities for users also increased this year, with five new beamlines becoming available to general users through the general user peer-review proposal process. At the end of 2006, 49 APS beamlines were hosting general users. The number of 8-h shifts available for general users increased from 11,009 in 2005 to 14,716 in 2006, a 33% increase, as shown in Fig. 8. Despite the increased number of available shifts, the APS continues to be oversubscribed, as underscored by Fig. 9, which shows the total number of general user beam-time requests vs. those receiving time for the past four years. Over this 4-year period, only 62% of all beam-time requests actually received time.

The end result: more than 1,000 publications again in calendar year (CY) 2006 (Fig. 10).

Contact: Susan Strasser (strasser@aps.anl.gov)

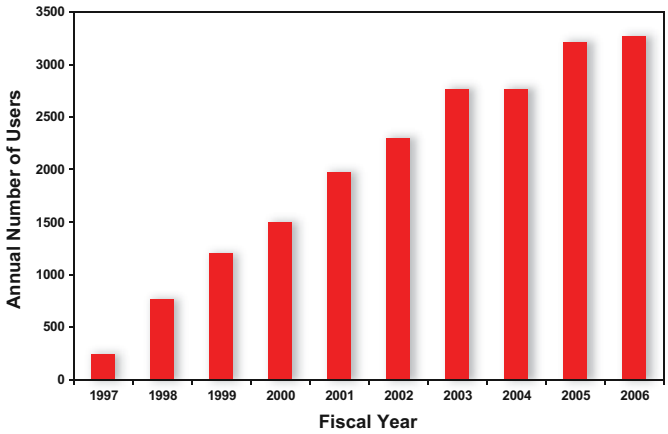

Fig. 1. APS unique user visits, by fiscal year.

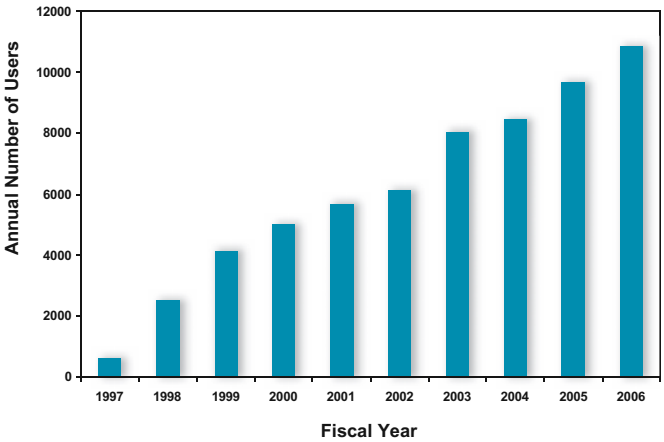

Fig. 2. Total user visits to the APS, by fiscal year.

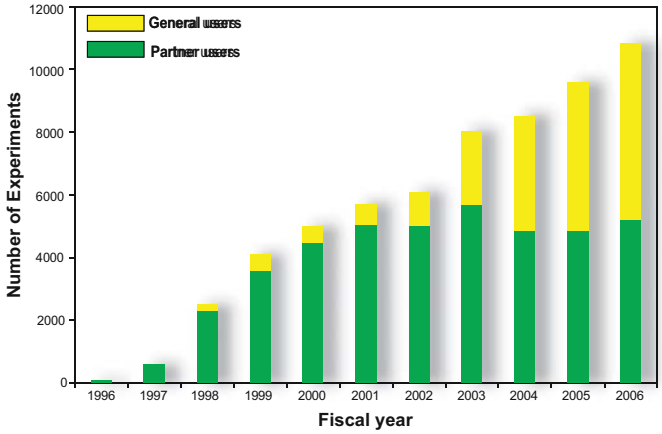

Fig. 3. Visits to the APS by user type, by fiscal year.

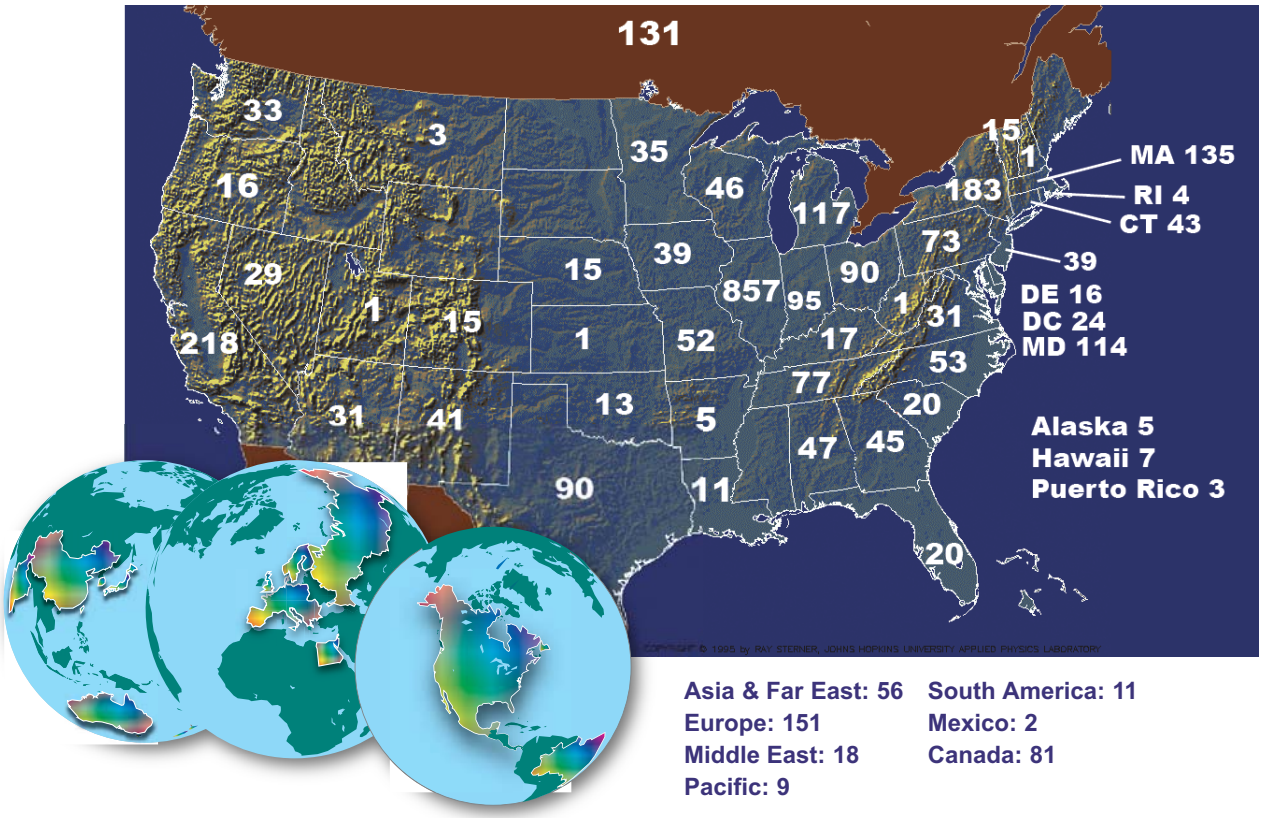

Fig. 4. Users who visited the APS at least once in FY 2006, by geographic distribution.

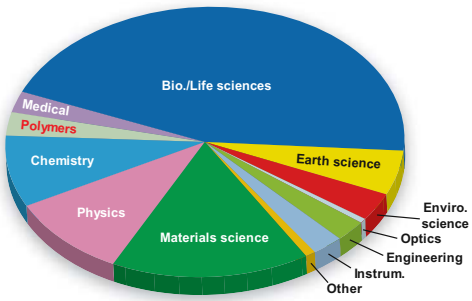

Fig. 5. APS users by research interest (FY 2006).

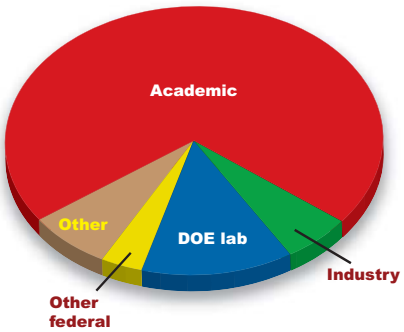

Fig. 6. APS users by institution (FY 2006).

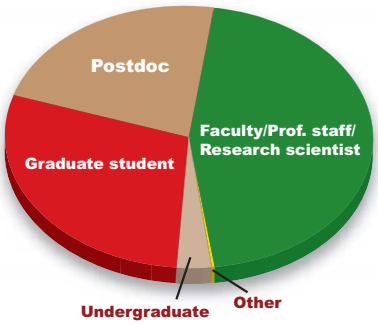

Fig. 7. APS users' employment level (FY 2006).

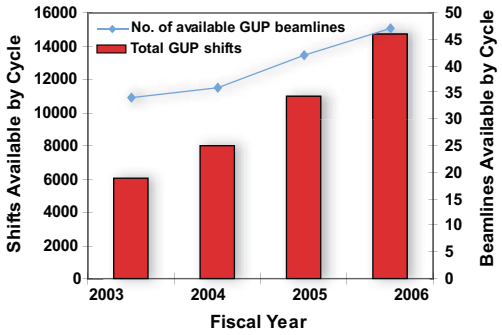

Fig. 8. GUP shifts and beamlines by cycle (FY 2006).

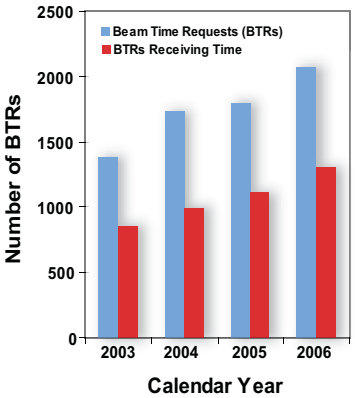

Fig. 9. GU beam time requests vs. beam time granted (FY 2006).

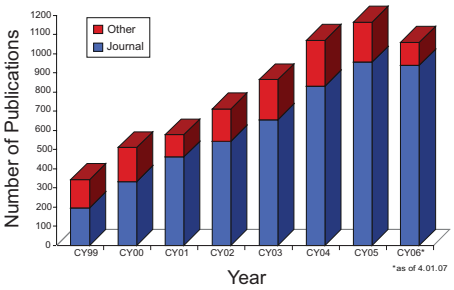

Fig. 10. APS publications in CY 2006.

All Together at the 2006 Argonne

Collaboration between the four U.S. Department of Energy, Office of Basic Energy Sciences (DOE-BES) user facilities at Argonne is increasing. In 2006, for the first time, all four facilities (APS, Center for Nanoscale Materials [CNM], Electron Microscopy Center, and Intense Pulsed Neutron Source) were involved in a week of sequential and joint user meetings.

The first two days of the combined meetings—which spanned May 1-5—focused primarily on the CNM, while the remaining three days comprised a series of plenary science sessions, poster sessions, and workshops directed to users of one or more of the Argonne DOE-BES-supported facilities. The week began with a welcome from Al Sattelberger (Argonne Associate Laboratory Director for Physical Sciences) and the "View from the Hill," courtesy of Representative Judy Biggert (R-IL 13th).

The APS portion of the meeting was opened on Wednesday, May 3, by Carol Thompson (Northern Illinois University and then-Chair, APS Users Organization), followed by Roger Klaffky (Program Manager, X-ray and Neutron User Facilities, Division of Scientific User Facilities, DOE-BES) who offered attendees the "DOE Perspective." Murray Gibson (Argonne Associate Laboratory Director for Scientific User Facilities and APS Director) then presented the traditional "Advanced Photon Source Update."

After Michael Borland (ASD) discussed the APS upgrade, the user-science talks commenced with Michelle Buchanan, Oak Ridge National Laboratory's Associate Director for Physical Sciences (and a new member of the APS Scientific Advisory Committee) on "Addressing Energy Grand Challenges through Advanced Materials." Wendy Mao, winner of the 2006 Advanced Photon Source Users Organization "Rosalind Franklin Young Investigator Award" (see sidebar, next page), delivered a plenary talk describing her use of integrated synchrotron techniques to address and solve a 50-year-old problem involving the behavior of graphite when compressed at room temperature. Amy Rosenzweig (Northwestern University) delivered a talk on "Biological Methane Oxidation," followed by Mark Sutton (McGill University) on "Using X-ray Speckle to Test Dynamical Scaling," Scott Chambers (Pacific Northwest National Laboratory) on "Synchrotron-Based Measurements of Magnetically Doped Transition Metal Oxides," and Ken Kemner (Argonne) on "From X-rays to Biogeochemistry to Beethoven."

The 11 user meeting workshops ranged from those primarily for nanoscience users to those for users of multiple facilities, such as "Texture and Strain Mapping with X-rays, Neutrons, and Electrons" and "Diffuse Scattering: Emerging Opportunities with Advanced X-ray and Neutron Sources." Further information about the workshops can be found on the Web at:

http://www.aps.anl.gov/Users/Meeting/2006/index.html

Other meeting highlights included the largest-ever congregation of suppliers (43), the largest number of poster entries (180, of which 32 were from students), and a number of social events, including a banquet ("Chicago Blues") with entertainment by the APS's own Blues Band. *Contact: Susan Strasser (strasser@aps.anl.gov)*

Clockwise from directly above: Carol Thompson (left), Wendy Mao, and Murray Gibson at the presentation of the Franklin award; a user meeting poster session in the lobby of the new CNM building; another poster session in a CNM conference room; the Hon. Judy Biggert; Roger Klaffky of DOE-BES; the APS Blues Band finds a groove.

DOE-BES User Facilities Meeting

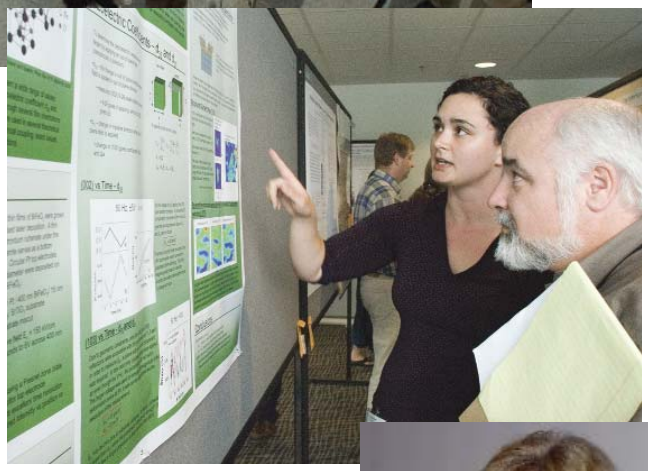

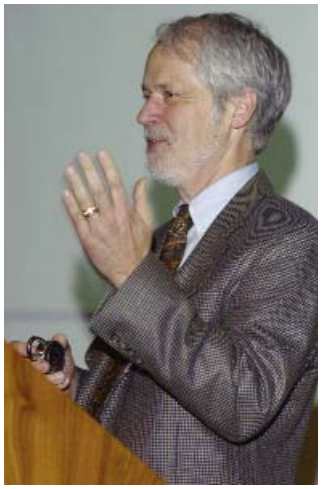

The 2006 Rosalind Franklin Young Investigator Award to Wendy Mao

Wendy Mao

Wendy L. Mao (Los Alamos National Laboratory) relieved the 2006 Rosalind Franklin Young Investigator Award presented by the APS Users Organization in recognition of an important technical or scientific accomplishment by a young investigator that depends on, or is beneficial to, the APS.

Mao received her bachelor's degree from MIT in 1998 and her Ph.D. from The University of Chicago in 2005. She has made contributions to an exceptionally broad range of topics, from the structure of graphite under pressure, to the properties of iron-rich materials at the boundary between the Earth's core and mantle, to the synthesis and characterization of a new family of hydrogen storage materials based on molecular compounds. In her work on graphite, she looked at a half-century-old problem: the behavior of graphite when it is compressed at room temperature. It turns, not into diamond, but into an unusual and unexpected phase. The structure and bonding of this phase remained stubbornly enigmatic because existing techniques could not probe electronic structure at high pressure. At the APS, Mao applied x-ray Raman scattering (XRS) spectroscopy to map the detailed changes in the carbon K-edge that give a signature of the bonding. For graphite at high pressure, XRS revealed an unusual bonding arrangement that explained the material's properties. An additional hydrostatic x-ray diffraction study identified its structure. The high photon flux of the APS made the XRS technique feasible in this case. In fact, with this application of XRS, Mao has opened a new field—investigation of the electronic structure of light elements under pressure. She later exploited the strange properties of this graphite material—its hardness is both pressure-dependent and reversible—for experimental hardware that helped her achieve new results at the APS in a different field: studies of deep-Earth minerals. In that work, she discovered an iron-rich silicate that occurs at deep-mantle conditions. The material properties of this new phase may explain the strange seismic features of the D" zone—the lower 300 kilometers of the mantle, just outside the Earth's molten core.

The Rosalind Franklin Young Investigator Award is open to senior graduate students and those whose Ph.D. was awarded no more than two years prior to nomination. Franklin pioneered the use of x-ray diffraction in analyzing complex, unorganized matter such as large biological molecules and not just single crystals. In 1951, she went to work as a research associate for John Randall at King's College. While in her early 30s, Franklin performed x-ray crystallographic studies of DNA that were a critical contribution to the solution of the molecule's structure. J.D. Bernal called her images of DNA "the most beautiful x-ray photographs of any substance ever taken." Franklin's career was cut short by her untimely death at age 37.

Tomorrow's Users

The 2006 APS XAFS Summer School

The National School for Neutron and X-ray Scattering, class of 2006.

Sixty graduate students from U.S. universities majoring in physics, chemistry, earth sciences, materials science, and related fields spent two weeks, from August 13 to the 27, 2006, at the eighth edition of the National School for Neutron and X-ray Scattering at Argonne. The 60, who were selected to participate in an intensive general background course in neutron and x-ray techniques, were given lectures by top senior scientists from academia, industry, and national laboratories, including basic tutorials on the principles of scattering theory and the characteristics of neutron and x-ray sources, as well as seminars on the application of scattering methods to a variety of scientific subjects. The school is supported each year by the U.S. Department of Energy's (DOE's) Office of Basic Energy Sciences in the DOE Office of Science.

The students also availed themselves of the opportunity to carry out four hands-on experiments at Argonne's Intense Pulsed Neutron Source (IPNS) and APS (Argonne is the only U.S. national laboratory with both a synchrotron source and a neutron source). The experiment topics (18 altogether) ranged from "Neutron Spectroscopy of Molecular Crystals" and "Neutron Powder Diffraction, Experimental: SEPD and GPPD," to "Internal Strain, Stress and Texture Measurements Using High-energy X-rays" and "Small-angle X-ray Scattering from Biomaterials."

Lectures included "Interaction of X-rays and Neutrons with Matter," S.K. Sinha (University of California, San Diego; Los Alamos National Laboratory); "Neutron Generation/ Detection," T.E. Mason (Oak Ridge National Laboratory); "Single Crystal Diffraction," T.F. Koetzle (Argonne); "X-ray Optics for Synchrotron Radiation," D.M. Mills (Argonne); "Inelastic Scattering," R. Osborn (Argonne); "Magnetic Scattering," C.F. Majkrzak (National Institute of Standards and Technology); "Extended X-ray Absroption Fine Structure (EXAFS)," E.A. Stern (University of Washington); "Small Angle Scattering (SAS)," P. Thiyagarajan (Argonne); "Understanding Materials Behavior Using Neutron Diffraction," D.W. Brown (Los Alamos National Laboratory); "Real/Reciprocal Space Complementarity," J.M. Gibson (Argonne); "Applications of Powder Diffraction Methods," J.J. Rhyne (Los Alamos National Laboratory); "Diffuse Scattering," G.E. Ice (Oak Ridge National Laboratory); "Coherent X-ray Scattering," L.B. Lurio (Northern Illinois University); "Nanoscience with X-rays and Neutrons," E.D. Isaacs (Argonne); "Imaging," S.R. Stock (Northwestern University); "Understanding Materials Behavior Using Neutron Diffraction," D.W. Brown (Los Alamos National Laboratory); "Nuclear Resonant Inelastic X-ray Scattering," W. Sturhahn (Argonne); "Spin Echo," R. Pynn (Indiana University Cyclotron Facility); and others. (See http://www.dep.anl.gov/nx/ for a complete list.)

The school, under Scientific Directors Dean Haeffner (X-ray Science Division [XSD]) and Raymond Osborn (Materials Science Division [MSD]), is a collaborative effort among several Argonne divisions: XSD, IPNS, MSD, and Educational Pro-=grams (DEP), and has support for experiments from several of the APS sectors and collaborative access teams.

In addition to Haeffner and Osborn, the Local Organizing Committee comprised Raymond Teller (IPNS); Education Division Director Harold Myron (DEP), George Crabtree (MSD), Dennis Mills (Scientific User Facilities), Experiment Coordinators Jonathan Lang (XSD) and Alexander I. Kolesnikov (IPNS), and Conference Secretary Carol Reynolds (DEP).

Contact: Dean Haeffner (haeffner@aps.anl.gov)
Raymond Osborn (rosborn@anl.gov)

The 2006 ACA Summer School in Macromolecular Crystallography

A select group of tomorrow's structural biologists were taken deep into the finer points of their chosen field by the organizers, lecturers, and support personnel who carried out the 2006 American Crystallography Association (ACA) Summer School in Macromolecular Crystallography. 2006 was the fourth year the Illinois Institute of Technology (IIT) and the APS collaborated on this two-week course designed for upper-level graduate students, postdoctoral researchers, lower-level graduate students, and industry scientists. Eighteen students attended the 2006 school. They were drawn from every part of the U.S. and from Canada, Croatia, and Poland. All applicants were accepted for admission to the ACA Summer School this year.

The 2006 school included 22 lectures by eminent crystallographers and qualified graduates of previous IIT/APS ACA Summer Schools programs, plus extensive chemistry and crystallographic lab work, and a minimum of three visits per student to macromolecular crystallographic beamlines at the APS. Students worked on crystallizing their own proteins and learned crystallization techniques using commercial proteins; they also collected diffraction data at the APS from their actual research samples and from test crystals.

Most of the first week was spent at IIT, with time divided among lectures and lab experiences. The second week was held partly at IIT and partly at the APS, where students not only collected data but engaged in training experiences shepherded by beamline staff scientists. For the first time, the APS visits included instruction in skills other than beamline and software usage: students were provided with overviews of cryo-cooling and heavy-atom derivatization techniques. The schedule and the content of the lectures, labs, and beamline visits are listed on the school Website (http://acaschool.iit.edu/). Social events were included in the school, and the students were allowed free time to visit Chicago's attractions in the evenings and during the middle Saturday of the school.

The school's location in Chicago made it easy to recruit world-class scientists to lecture and lead lab demonstrations; only two of the featured academic speakers were from outside the Chicago area, and all the local speakers spoke without compensation. Several industry scientists gave of their time to serve as integral members of the teaching team; for their employers, this school was a marketing opportunity and a chance to contribute to the scientific community.

Almost all lecturers provided notes that are also available on the Summer School Website. In addition, almost all the lectures were digitally video-recorded and the video record is now on file. It will be made available to the ACA and interested participants free of charge, and to others for a modest fee.

The organizers (Andy Howard, Carlo Segre, and Faith Kancauski, all IIT) hope that the school will continue to be an important resource for the crystallographic and biochemical communities, and that it can serve to acquaint a wider circle of scientists with the realities of macromolecular crystallography.

Sean Taylor (Yale Univ.), a 2006 ACA Summer School student, mounts a sample inside one of the SBC-CAT hutches on the APS experiment hall floor.

Faculty and support personnel for the school included: Lectures: Spencer Anderson (BioCARS), Michael Becker (GM/CA-CAT), Grant Bunker (IIT), Chuck Campana (Bruker AXS), Jim Cary (Northern Illinois University [NIU]), Chris Dankulich (Fluidigm), Bill Furey (Pittsburgh VA/University of Pittsburgh), Andy Howard (IIT), Tom Irving (IIT), Constance Jeffery (UIC), Jim Kaduk (Innovene), Gocha Khelashvili (IIT), Allan Myerson (Provost, IIT), Joseph Orgel (IIT), Jim Pflugrath (Rigaku/MSC), Narayanasami Sukumar (NE-CAT), Jeff Terry (IIT). Lab facilitation: Jim Cary (NIU), Shih-Chia Chang (IIT), David Ehle (IIT), Andy Howard (IIT), Rebecca Howard (University of California, San Francisco [UCCSF]), Sireesha Ratakonda (IIT), Pauls Reinfelds (IIT), Greg Sahli (IIT)
Administration and Technical Assistance: David Ehle (IIT), Rebecca Howard (UCSF), Sandra Howard (IIT), Faith Kancauski (IIT). Beamline science user support: Randy Alkire (SBC-CAT), Spencer Anderson (BioCARS), Michael Becker (GM/CA-CAT), Michael Bolbat (BioCARS), Norma Duke (SBC-CAT), Albert Fu (SER-CAT), Frank Rotella (SBC-CAT), Ruslan Sanishvili (GM/CA-CAT), Ward Smith (GM/CA-CAT), Narayanasami Sukumar (NE-CAT), Zdzislaw Wawrzak (DND-CAT). *Contact: Andy Howard (howard@agni.phys.iit.edu)*

The 2006 APS XAFS Summer School

The students and faculty of the 2006 APS XAFS Summer School, gathered on the front steps of the APS central lab/office building.

The second annual APS XAFS Summer School was held at Argonne from July 26-28, 2006. The school welcomed 20 participants from around the U.S. and from as far away as Israel, Germany, and Switzerland. Unlike previous x-ray absorption fine structure (XAFS) courses at the APS, which were aimed at novice practitioners and included hands-on lab work and data collection, this year's course targeted intermediate-to-advanced XAFS users and focused primarily on analysis techniques. The course was organized by Julie Cross (Argonne), Matt Newville (The University of Chicago), and Robert Gordon (Simon Fraser University), and taught by Newville, Bruce Ravel and Shelly Kelly (both Argonne), and Scott Calvin (Sarah Lawrence College).

After an introduction, by Ravel, to the data analysis programs IFEFFIT, ATHENA, and ARTEMIS, the curriculum covered advanced data modeling and analysis concepts. Newville presented a lecture on statistics in extended x-ray absorption fine structure (EXAFS) analysis. Kelly demonstrated the use of IFEFFIT and ARTEMIS to solve two complex environmental science problems. Her first example showed how to determine the cation coordination in biomineralized uranyl complexes. Her second example showed how to distinguish surface lead complexes on iron oxide substrates from co-precipitated iron/lead minerals.

Calvin demonstrated the solution to a complicated materials science question. The magnetic properties of zinc manganese ferrite nanoparticles depend strongly on the distribution of the cations among the tetrahedral and octahedral sites in the spinel structure of these nanoscale materials. By co-refining EXAFS data made at all three cation edges, Calvin showed how to determine the proportions of each cation in each site. Finally, Ravel demonstrated the use of linear combination x-ray absorption near-edge structure (XANES) analysis to determine the kinetics of a gold reduction from gold chloride mediated by cyanobacteria and monitored by XAFS, and to identify a previously unknown intermediate state in this reaction.

The students had plenty of time to work with the data analysis software and to solicit help and advice from the instructors. On the third day of the course, several students gave short presentations on their own research and discussed the ways they incorporated XAFS measurements into their research projects. These presentations prompted considerable discussion among the participants, just one factor contributing to the consensus among students and instructors alike that this year's XAFS Summer School was a huge success.

For more on the XAFS Summer School, see: http://cars9.uchicago.edu/xafs_school/index.html

Contact: Julie O. Cross (jox@aps.anl.gov)

Links

For current APS users:
www.aps.anl.gov/Users/Welcome/Current_User/index.html

For new APS users:
www.aps.anl.gov/Users/Welcome/New_User/index.html

For prospective APS users:
www.aps.anl.gov/Users/Welcome/Prospective_User/index.html

Quick links for users:
www.aps.anl.gov/Users/General_Reference/Database_Systems/index.html

To learn about the APS:
www.aps.anl.gov/About/APS_Overview/index.html

Safety and training:
www.aps.anl.gov/Safety_and_Training/index.html

Archive of APS science highlights:
www.aps.anl.gov/Science/Highlights/index.html

Back issues of *APS Science*:
www.aps.anl.gov/News/Annual_Report/index.htm

APS User News-at-a-Glance
www.aps.anl.gov/Users/Communications/User_News/index.html

Courses and summer schools:
www.lightsources.org/cms/?pid=1000510

DOE Office of Science page on experimental techniques at light source beamlines:
www.sc.doe.gov/bes/synchrotron_techniques/index.htm

Exploring the Art of Materials Science at SRMS-5

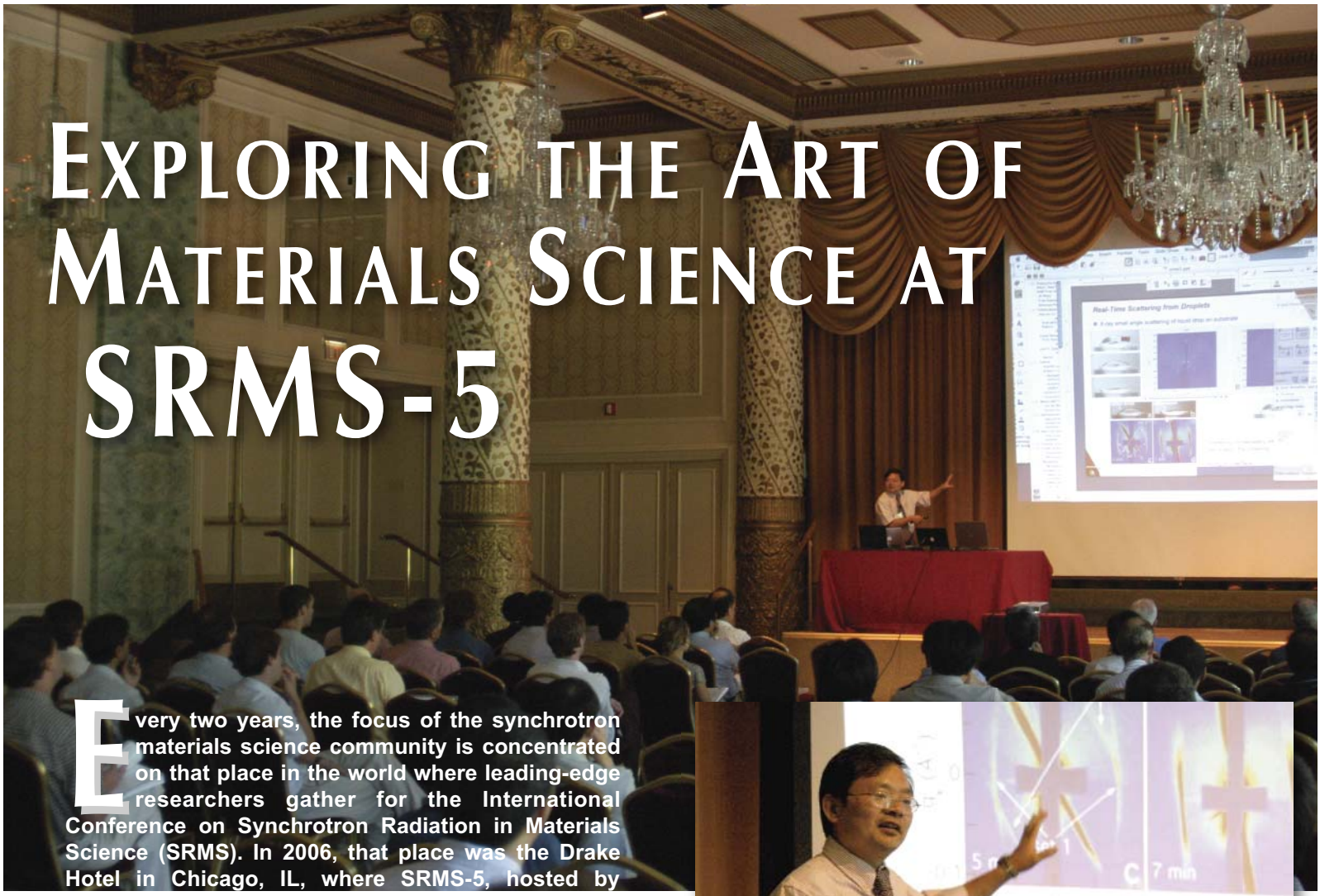

Every two years, the focus of the synchrotron materials science community is concentrated on that place in the world where leading-edge researchers gather for the International Conference on Synchrotron Radiation in Materials Science (SRMS). In 2006, that place was the Drake Hotel in Chicago, IL, where SRMS-5, hosted by Argonne and the APS, welcomed more that 250 materials scientists from 22 countries to two-and-a-half days of lectures, breakout sessions, and poster presentations. These highlighted recent breakthroughs in materials science advanced via synchrotron radiation and pointing the way to future innovation and discovery. The conference provided an overview of the latest research developments in a broad range of materials areas, including polymers and biomaterials, magnetic and superconducting materials, glasses and ceramics, engineering materials, materials under extreme conditions, complex oxides, innovative instrumentation, membranes, and thin films.

Lectures covered a spectrum of topics, while breakout sessions were typically more focused on a particular research area. The ever-popular poster presentations followed the topics of each day's breakout session and provided an opportunity for spirited exchanges of information. In all, there were 35 plenary and invited talks, 37 contributed talks, and 134 poster presentations. Full-color versions of the conference contributions can be viewed and downloaded from http://www.aps.anl.gov/SRMS5/Contributions.

A Local Organizing Committee that included representatives from Northwestern University, The University of Chicago, the Illinois Institute of Technology, Iowa State University, and the University of Illinois at Urbana-Champaign was invaluable to the success of the conference, as was the International Advisory Committee chaired by Professor Neville Greaves (University of Wales).

Above: A presentation on self-assembly of nanostructures by Jin Wang (Argonne) in the main meeting room for SRMS-5. Inset: Wang makes a point.

Just a few of the conference highlights include:

- An opening plenary lecture by J.C. Campuzano (Argonne and the University of Illinois at Chicago) on the challenge of explaining the electronic structure of high-temperature superconductors determined with angle-resolved photoemission.
- H. Dosch (Max Planck Institute for Materials Research) on the phase behavior of metallic alloys and how its relation to the physical properties of these alloys in nanoconfined geometries may be understood in terms of misfit strains.
- T.P. Russell (University of Massachusetts) and E.E. Fullerton (Hitachi Global Storage Technologies) on orienting domains in block copolymer thin films and magnetic reversal in antiferromagnetically-coupled films, respectively.
- C.S. Yoo (Lawrence Livermore National Laboratory) on understanding the exotic states of matter that can be created in extreme environments, such as nonmolecular phases in simple molecular solids occurring under high pressure and high temperature.

Continued on next page

- C.S. Nelson (Brookhaven National Laboratory) on orbital ordering in calcium ruthenates, where her x-ray resonant scattering studies showed some surprising results.
- C.G. (Kees) de Kruif (NIZO Food Research, and Utrecht University) on synchrotron methods for food science and soft-matter investigations into protein-polysaccaride correlations.
- T. Rayment (University of Birmingham) on x-ray absorption spectroscopy above, below, and at electrodes—revealing structural and electronic changes as a function of depth below the electrode surface.
- A.Q.R. Baron (SPring-8) on electron-phonon coupling in high-T_c superconductors as measured by meV-resolved inelastic x-ray scattering, especially the softening of in-plane longitudinal bond-stretching modes and their dependence on doping.
- P.M. Derlet (Paul Scherrer Institute) on the use of Green's functions and molecular dynamics to understand dislocations and lattice vibrations in small metal grains and grain boundaries.
- L. Paolasini (European Synchrotron Radiation Facility) on resonant x-ray scattering as a site- and shell-selective technique for measuring structural modifications of SmS and $CeFe_2$ under extreme conditions.

Altogether, the diverse and wide-ranging nature of the presentations and posters underscored the fact that a significant percentage of research at synchrotron user facilities continues to be in the fields of materials science and condensed matter physics. Given the growing emphasis on membranes, biomaterials, and nanostructured materials, this percentage can only continue to increase. It is worth noting that, among the research papers published in 2005 in the often-cited journals *Nature* and *Science*, 19% (*Nature*) and 27% (*Science*) reported on materials research; of these, more than 28% and 35%, respectively, made use of synchrotron radiation.

When it came time to relax, attendees boated on the Chicago River while hearing about the city's famed architecture, attended a mini-operetta on the subject of chocolate, and attended a reception amid the world-class collection of the Art Institute of Chicago, followed by a conference banquet held in the institute's famed Trading Room.

Laboratório Nacional de Luz Síncrotron in Brazil was selected by the International Organizing Committee to host the 2008 SRMS. See you in Campinas!

Contact: Gabrielle Long (gglong@aps.anl.gov)

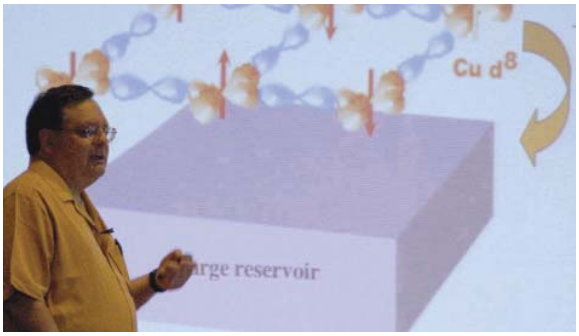

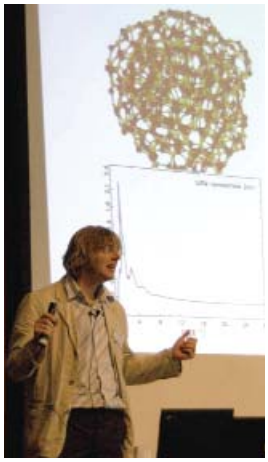

Clockwise from top: Preparing for a poster session; G.N. Greaves (center, Univ. of Wales, Chair, SRMS-5 International Advisory Committee); G.G. Long (center, Argonne, Chair, SRMS-5 Local Organizing Committee); the Art Institute of Chicago; S.J.L. Billinge (Michigan State Univ.); J.C. Campuzano (Argonne and the Univ. of Illinois at Chicago); center: H. Dosch (Max Planck Institute for Metals Research).

OPERATIONS

LIGHT SOURCE OPERATIONS IN CY 2006

In calendar year (CY) 2006, the APS operated with exceptional reliability and availability, continuing the stellar performance of the previous years. No changes were made in fill patterns this year. However, a new lattice, the Reduced Horizontal Beamsize (RHB) lattice, was introduced as a special operating mode (see next page). Accelerator R&D concentrated on short-pulse production using pulsed crab cavities and exploration of options for the APS upgrade, as discussed in other articles.

BEAM AVAILABILITY & MTBF IN CY 2006

For CY 2006, the APS scheduled 4,986 h for user operations and delivered 4,875 h, giving x-ray availability of 97.78% for the year, virtually unchanged from CY 2005. The mean time between faults (MTBF) was 93.8 h, up slightly from CY 2005 owing to fewer faults in CY 2006. Injector availability remained high at 98.2%, providing reliable beam for top-up. Table 1 shows detailed statistics for CY 2006.

The APS is clearly enjoying a period of mature, stable operation, characterized by unparalleled reliability. Indeed, the last run of 2006 was the tenth consecutive run for which the MTBF exceeded 48 h. The lowest MTBF during that 10-run period was 55.9 h, which is already very good. However, the median value was even more impressive, at 88.2 h. The lowest availability during the same period was 96.9%, with a median of 98.4%.

FILL PATTERNS

The APS ring has the flexibility to support different fill patterns and lattices for special needs. The fill patterns used in CY 2006 (Fig. 1) were the same as those used in CY 2005. (The standard average beam current for all operating modes is 100 mA.) A description of each operating mode follows:

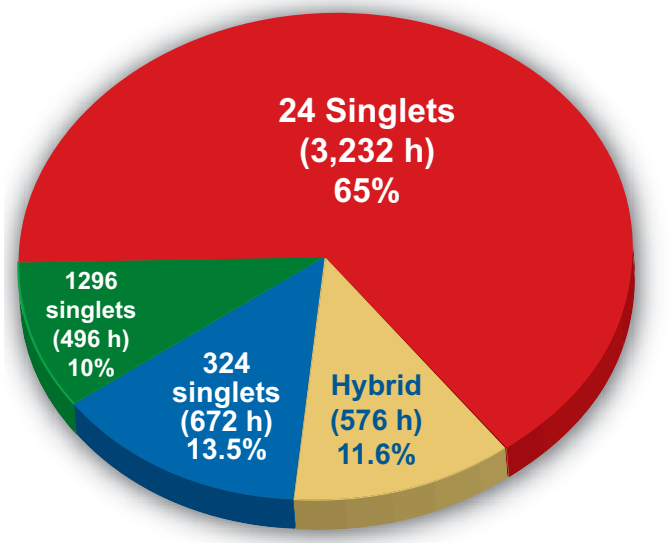

Fig. 1. Calendar year 2006 scheduled times for different APS operating modes. Total scheduled hours: 4,986.1.

- *24 uniformly spaced bunches ("24 singlets") in top-up mode, used 65.0% of the time.* 24 singlets is the most common fill pattern and features 24 equally-populated bunches separated by 154 ns. The bunch length is 40 ps rms. This bunch pattern is a good compromise between the needs of timing users, who benefit from the bunch separation, and flux-hungry users, who require 100 mA but do not have requirements

Continued on next page

Table 1. Operations statistics: CY 2005 (summary) and CY 2006 (by run and totals).

	CY 2005				CY 2006
Run number		Run 2006-1	Run 2006-2	Run 2006-3	
Start		1/31/06	5/30/06	10/3/06	
End		4/24/06	8/25/06	12/19/06	
Scheduled hours	5,024.4	1,655	1,752	1,579.1	4986.1
Beam available for users (h)	4,925.3	1,627.6	1,704.3	1,543.3	4875.2
Beam availability (%)	98.03	98.3	97.3	98.4	97.78
Total downtime (h)	99.2	27.4	47.7	35.8	110.9
Average current (mA)	100.3	100.1	100.4	99.8	100.1
Number of faults	57	13	22	17	52
Mean time between faults (h)	86.4	125.2	74.1	90.8	93.8
Mean time to recovery (h)	1.7	2.1	2.2	2.1	2.1
Injector availability (%)	97.28	98.1	98.2	98.2	98.2

Table 2. Comparison of parameters: RHB sectors vs. standard sectors.

	Horiz. Beta (m)	Horiz. Eta (m)	Horiz. Size (μm)	Horiz. Diverg. (μrad)	Vert. Beta (m)	Vert. Size (μm)	Vert. Diverg. (μrad)
Normal	19.5	0.170	286	12.0	2.9	9.0	3.1
RHB	3.2	0.078	120	29.6	5.4	12.3	2.3

for the bunch distribution. Bunch purity is very important in this mode. Recent improvements to the Particle Accumulator Ring, one of the injector systems (see "The Particle Accumulator Ring Gets Cleaner," *APS Science 2005*, ANL-05/29, p. 178), allows us to consistently maintain bunch purity at a level of a few parts in 10^7. Top-up at a 2-min interval is needed for this pattern due to the relatively short beam lifetime (about 6 h). High-current machine studies have shown that we can stably store up to 164 mA in the 24-singlets mode. Higher-order mode (HOM) dampers installed in 4 of the 16 radio frequency accelerating cavities in 2005 have raised the coupled-bunch instability threshold from about 100 mA to above 164 mA. The current limitation is not due to beam instabilities, but rather the heating of a few accelerator components, including the HOM dampers themselves. The high-current studies were conducted in anticipation of future upgrades to high-heat-load front ends, which will allow higher current.

- *324 uniformly spaced bunches in non-top-up mode, used 13.5% of the time.* Non-top-up operation, whereby the storage ring is refilled to 100 mA twice every 24 h, is mainly used to allow for injector maintenance and improvement, operator training, and injector beam time for parasitic injector study. The beam lifetime in the 324-bunch mode is such that the beam decays to about 83 mA after 12 h. With smaller bunch currents (compared with 24 singlets), the bunch length in the 324-bunch mode is 25 ps rms. High-current studies have shown stable operation up to 200 mA in this bunch pattern. In contrast with the 24-singlet case, there are no accelerator component heating issues in this mode, a result of the much smaller bunch current.

- *1 + 8 × 7 hybrid pattern in top-up mode with 16 mA in the isolated bunch, used 11.6% of the time*. In this pattern, a single 16-mA bunch is injected on one side of the ring. The remaining 84 mA of stored beam current resides in 8 groups of 7 bunches on the other side of the ring. This arrangement results in symmetrical, beam-free regions with a duration of 1.59 μsec on either side of the intense bunch. The bunch length of the 16-mA bunch is 65 ps rms and that of the remaining bunches is 32 ps rms. Top-up is essential for the hybrid pattern. Because of the short lifetime of the intense bunch, the top-up interval is 1 min when using this pattern. Roughly three out of four top-up injections go toward maintaining the current in the intense bunch.

- *1,296 uniformly spaced bunches in non-top-up mode, used 10.0% of the time*. Calendar year 2006 marks the first year in which a significant fraction of operating time was devoted to the 1,296-bunch pattern. This pattern, introduced in CY 2005, has an extremely long lifetime—on the order of 120 h—so that even with 12 h between fills, the current never decays below about 90 mA. The bunch pattern is continuous without any gaps. In other rings, an ion-clearing gap is required to prevent the trapping of positive ions in the electron beam, which can cause beam instabilities; no such effects are observed in the APS. An alternate injection scheme is employed to achieve good bunch-current uniformity. Normally, the storage ring bunches are injected one at a time. For the 1,296-bunch mode, the Particle Accumulator Ring is bypassed and a bunch train is injected from the linac directly into the booster, then into the storage ring. This is called "direct injection."

The RHB Lattice

The standard symmetric low-emittance lattice introduced in CY 2003 was utilized for almost all user operations during CY 2006. An exception was in Run 2006-03, when, for the first time, the APS delivered beam to users in the RHB lattice, which is non-symmetric. In this lattice, the rms horizontal beam size at beamlines 8-ID and 32-ID is reduced from 280 μm to 120 μm, at the expense of approximately 10% higher horizontal emittance. This was accomplished by reducing the horizontal beta function and dispersion at those insertion devices by adjusting quadrupoles in the surrounding sectors. Table 2 gives a comparison of the parameters at the RHB sectors to those in standard sectors, assuming nominal 1% coupling. This lattice was used in 24-singlets mode for 8.7% of the total time. Other periods of operation with this lattice are planned for CY 2007.

The benefits of the RHB lattice were demonstrated by the X-ray Microscopy and Imaging Group in X-ray Operations and Research, using in-line phase-contrast imaging studies (see "X-ray Imaging & Optics Development," *APS Science 2002*, ANL-03/15, p. 93.) Phase-contrast imaging relies on interference effects, and the source size contributes to geometric blurring.

In the nominal lattice, the blurring due to source size is ~0.6 μm vertically and 9.3 μm horizontally (full width half maximum). The detector resolution is 1-2 μm; thus, the source size is the limiting factor. The RHB lattice reduces the source-size-induced blurring by a factor given by the beam size ratio, in this case ~2. Figure 2 (next page) shows the source size dependence of the phase-contrast image. The low-beta image clearly has better resolution and higher contrast.

Continued on page 162

"Operations" continued from page 161

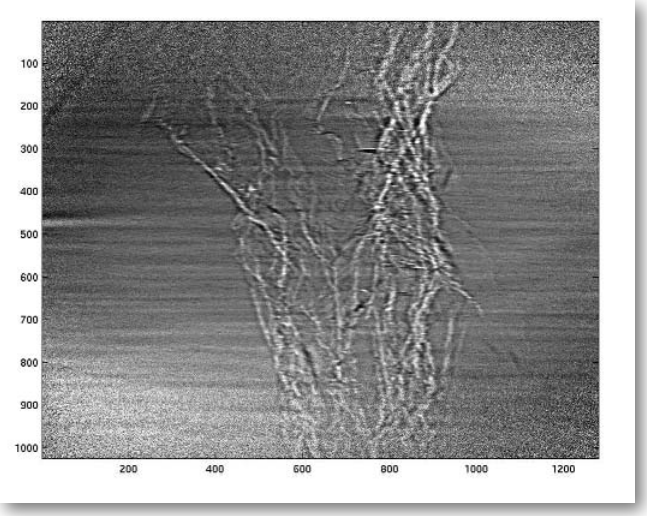

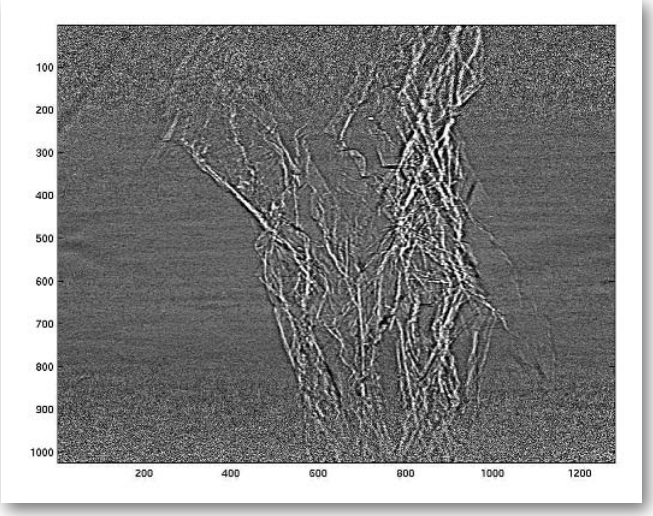

Fig. 2. Phase contrast images of an aluminum stress-crack sample, ~3 mm thick, taken with nominal beta (left) and low beta (right) (30-keV photons). Both figures show the same grey scale. (Images courtesy of Wah-Keat Lee, XSD.)

Storage Ring Parameters On Line

The APS storage ring has evolved over the years as its performance incrementally improved and as the needs of the users changed. To meet the challenge of providing accurate and timely basic beam parameters for users and accelerator physicists, a Web-based tool was developed in 2005 and fully implemented in 2006.

At the APS home page (http://www.aps.anl.gov) one can use the "Facility" pull-down menu to find "Nominal Storage Ring Parameters." This link gives access to a set of Web pages that form a living document that is periodically updated to correspond to operational and/or hardware changes. Detailed information is provided on main beam parameters, lattice, orbit stability, source parameters computed in real-time, operation modes, and hardware such as magnets and power supplies. These pages will be expanded in the future to include the injectors and any other data requested by users.

Contact: *Michael Borland (borland@aps.anl.gov)*
Katherine Harkay (harkay@aps.anl.gov)

Around the APS

The Robert R. Wilson Prize to Lee Teng

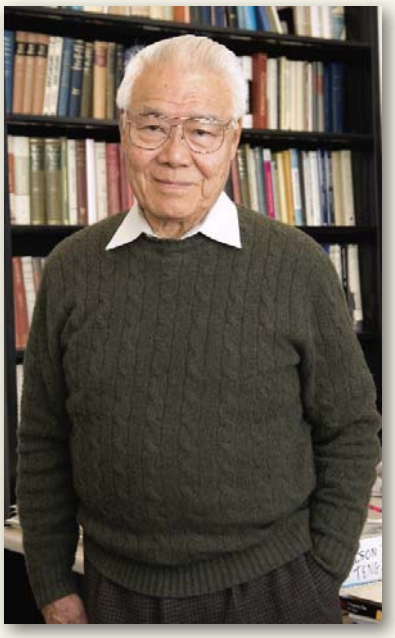

Lee Teng (ASD) was named the winner of the 2007 American Physical Society's Robert R. Wilson Prize, recognizing outstanding achievements in the physics of particle accelerators. Teng, a senior physicist at Argonne, was honored by the society "for invention of resonant extraction and transition crossing techniques critical to hadron synchrotrons and storage rings, for early and continued development of linear matrix theory of particle beams, and for leadership in the realization of a facility for radiation therapy with protons." The prize includes $5,000 and will be presented at the annual American Physical Society meeting in April in Jacksonville, FL, at a special Ceremonial Session, where Teng will deliver a talk based on the work for which he has been honored. The award is named for the late Robert R. Wilson, founding director of the Department of Energy's Fermilab in Illinois, and one of the world's leading experimental physicists and accelerator builders. • Teng came to the United States from China in 1947 to obtain his Ph.D. in physics at The University of Chicago. He was the first non-U.S. citizen hired by Argonne, where he rose to the position of Director of the Particle Accelerator Division with responsibility for the Zero Gradient Synchrotron and the associated beam transport lines and bubble chambers. In 1967, when Fermilab was established, Teng accepted an appointment (from Robert Wilson) as head of Accelerator Theory. In 1983 he took a partial leave of absence from Fermilab to serve as the first director of the Synchrotron Radiation Research Center in Taiwan. In 1989, Teng returned to Argonne to head up the accelerator physics contingent at the newly-formed 7-GeV Advanced Photon Source Project. Teng retired in 2004 and is currently serving as a special Emeritus appointee in ASD.

Design and Test of Undulators for the LCLS

The Linac Coherent Light Source (LCLS) will be the world's first x-ray free-electron laser when it becomes operational in 2009. The LCLS, a project funded by the U.S. Department of Energy (DOE), is currently under construction at the Stanford Linear Accelerator Center (SLAC) in California. Pulses of x-ray laser light from the LCLS will be many orders of magnitude brighter and several orders of magnitude shorter than presently-available x-rays from existing sources. These characteristics will enable frontier new science in areas that include discovering and probing new states of matter, understanding and following chemical reactions and biological processes in real time, imaging chemical and structural properties of materials on the nanoscale, and imaging non-crystalline biological materials at atomic resolution.

Fig. 1. The first production undulator is shown on the prototype support and motion system for the SUT.

Design and construction of the LCLS are being accomplished by a partnership of three DOE national laboratories, including SLAC as home laboratory, the APS at Argonne, and the Lawrence Livermore National Laboratory. Argonne is responsible for the design and construction of the 130-m-long insertion device undulator system, including magnets, supports, controls, vacuum, and beam diagnostics systems.

At the end of 2006, 28 undulators out of a total of 40 had been produced by two vendors and were accepted by APS. The remainder were on schedule for completion by mid-2007. At the time of this writing (early 2007), the quadrupole magnet contract has been awarded and work is progressing. The support and motion systems were put out for bid in early 2007 and under construction soon thereafter. Production of the controls, vacuum, and beam diagnostics systems will also take place during 2007.

The first production undulator is shown in Fig. 1, mounted on the prototype precision support and motion system that was constructed for the single undulator test (SUT) at the APS. The main purpose of the SUT was to verify that the support and motion system design was adequate to enable all of the physics and engineering requirements to be met. Undulators are mounted on translation stages and can be adjusted horizontally or moved 80 mm out of the beam. The girder that supports over 2000 lbs of undulator and quadrupole magnets is moved by a precision, 5-axis, camshaft-mover system. The mover system enables roll, pitch, and yaw motions for positioning the girder and its magnets with submicron accuracy. The combined system was extensively tested in the SUT during 2006 and found to meet all requirements.

A Long Term Test (LTT) facility is under construction at the APS. The purpose of the LTT facility is to test the evolving production undulator module and associated hardware. The LTT will initially be constructed using prototype components that will eventually be replaced with production components as they become available. The test area will have a full-scale, 20-ft-long, half-section mock-up of the LCLS tunnel. The undulator components will be positioned and oriented precisely as they will be in the Undulator Hall Tunnel at SLAC. It is expected that the LTT facility will remain in place through the LCLS commissioning stages.

Contact: Geoff Pile (pile@aps.anl.gov)
Marion White (mwhite@aps.anl.gov)

This work is supported by the U. S. Department of Energy, Office of Science, Office of Basic Energy Sciences, under Contract No. DE-AC02-06CH11357.

Short Pulses on a Fast Track

Occasionally in science, one finds that something "everyone knows" to be impossible is, in fact, possible. A case in point is the production of intense, short-pulse x-rays from a storage ring, a subject that is of great interest to some APS users. It is well known that making short electron bunches in a storage ring is very difficult, unless one is willing to accept very low bunch current. Proven methods of making short x-ray pulses from storage rings, such as laser slicing [1], suffer even more from low intensity, particularly in high-energy rings such as the APS.

Thus, it seemed that there was no viable way to provide short, intense x-ray pulses from the APS. That changed with a presentation by A. Zholents (Lawrence Berkeley National Labora-tory) at the APS strategic planning meeting in August 2004. The scheme [2] that Zholents proposed relies on using high-frequency transverse deflecting radio frequency (rf) cavities to impart a transverse momentum chirp to the beam. This means that particles in the head and tail of the beam are deflected in opposite directions, with the degree of deflection proportional in first order to the time offset of each particle from the bunch's time center. As illustrated in Fig. 1, a set of these so-called "crab cavities" can be used with a suitably placed undulator to create an x-ray pulse with an angle chirp, which in turn allows production of short pulses by slitting or using compression optics.

The minimum achievable x-ray pulse length is given by a simple formula [3], namely,

$$\sigma_{t,min} = \frac{E}{2\pi V h f_a}\sqrt{\sigma^2_{y',e} + \sigma^2_{y',p}}$$

where E is the beam energy, V is the crab cavity voltage, h is the ratio of the crab cavity frequency to the main rf frequency f_a, $\sigma_{y',e}$ is the vertical divergence of the electron beam when the crab cavities are unpowered, and $\sigma_{y',p}$ is the opening angle of the photons for a zero-emittance electron beam. A study [4] by APS accelerator physicists and engineers determined that V = 6 MV and h = 8 were feasible. Using f_a = 352 MHz, $\sigma_{y',e} \approx 3$ μrad, and $\sigma_{y',p} \approx 5$ μrad (for 10-keV radiation from a 2.4-m device), we get $\sigma_{t,min} \approx 0.4$ ps. This number, although just an estimate, is quite remarkable and indicates why this concept has generated so much excitement.

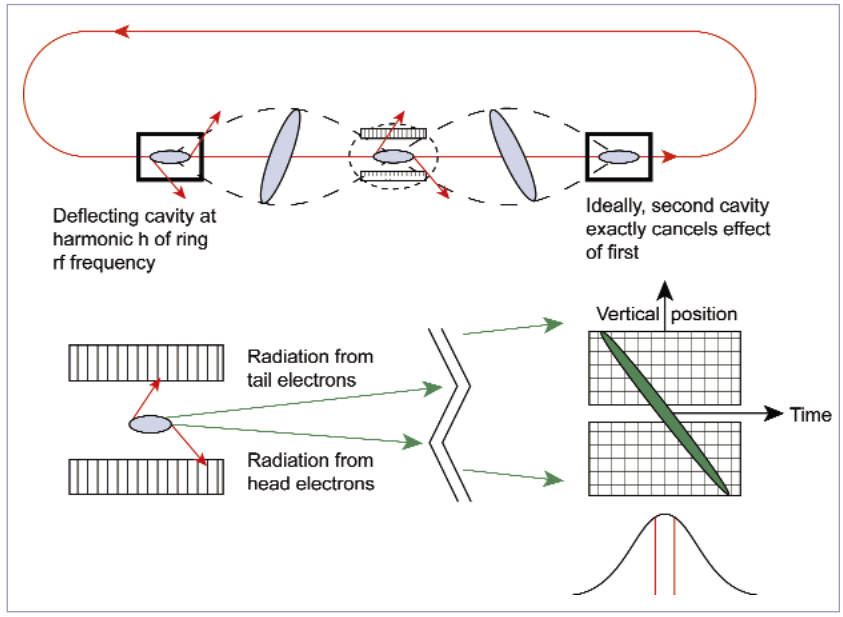

Fig. 1. Illustration of Zholents' crab cavity scheme for production of short x-ray pulses from a storage ring. This example implicitly shows the two deflecting, or crab, cavities separated by several storage ring sectors. The bunch tilt produced by the first cavity oscillates due to the focusing properties of the accelerator magnets. The oscillation is canceled by the second cavity so that other users, ideally, see no ill effects.

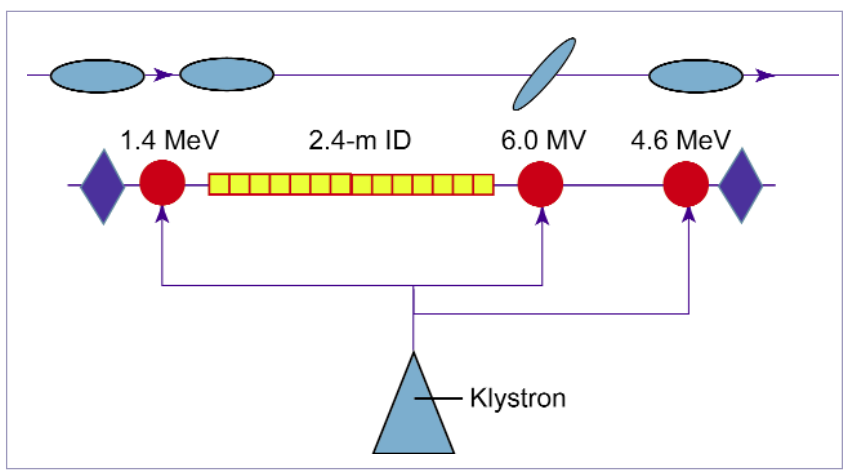

Fig. 2. Schematic of possible arrangement of pulsed crab cavities in a single straight section along with a standard 2.4-m undulator.

The concept was originally conceived to operate continuously (CW), which requires the use of superconducting technology. The advantage of superconducting crab cavities is that they provide continuous chirped pulses, so that users can take advantage of improvements in laser technology to perform experiments at higher repetition rates. Another advantage is that the CW sys-

Continued on next page

tem is compatible with all operating modes. One difficulty with this concept is that the cavities require considerable space in straight sections that might otherwise be used for insertion devices. Development time and cost are also a factor. However, no satisfactory solution to the space issue seemed forthcoming.

A compelling case was made [5] for pulsed crab cavities, which can be normal conducting. They are much smaller, about 0.5-m long each, and can deliver similar deflecting voltages [6]. With such small cavities, the entire system can be placed in a single straight section, as indicated in Fig. 2. The cavities essentially function as a very fast time-dependent, three-kicker bump, so the ratios of the cavity strengths are related to the distances between the cavities by simple geometry. With a 6-MV limit on any one cavity, the geometry constraints of a standard straight section and undulator results in a 1.4-MV limit on the first cavity, thus increasing the minimum achievable rms x-ray pulse duration to 1.7 ps. A future evolution of this concept will involve a lengthened straight section that can accommodate four cavities in a 1-2-1 arrangement with equal spacing of the first/second and third/fourth cavities. This allows for increasing the voltage of the first cavity to produce even shorter x-ray pulses or using a longer insertion device for higher flux. Disadvantages of the normal conducting option is that the chirped pulses are delivered only during a special operating mode and the repetition rate is limited to 1 kHz. However, the advantages for a near-term implementation are compelling.

Although the use of pulsed crab cavities resolves issues with space, there are several challenges that must be addressed. Perhaps chief among these is the need to design the cavities in such a way that the existing single-bunch and multi-bunch current limits are not compromised. Advanced Photon Source staff are collaborating with experts from the Stanford Linear Accelerator Center on an advanced pulsed cavity design with heavy damping of unwanted modes. Although the cavities will initially be pulsed at 120 Hz, eventually we wish to operate at 1 kHz. This presents challenges for the thermal design. Finally, the rf phase and voltage tolerances are quite demanding, which presents challenges for timing and rf control. Steady progress is being made on all of these issues, and there is good reason to be optimistic that this system for delivering short pulses will come together in the near future. Longer-term development includes the design of compression x-ray optics and superconducting crab cavities.

Contact: *M. Borland (borland@aps.anl.gov), J. Carwardine (carwar@aps.anl.gov), Y. Chae (chae@aps.anl.gov), L. Emery (emery@aps.anl.gov), K. Harkay (harkay@aps.anl.gov), A. Nassiri (nassiri@aps.anl.gov), V. Sajaev (sajaev@aps.anl.gov)*

References

[1] A. Zholents et al., Phys. Rev. Lett. **76**, 912 (1996).
[2] A. Zholents, P. Heimann, M. Zolotorev, and J. Byrd, Nucl. Instrum. Methods Phys. Res., Sect. A **425**, 385 (1999).
[3] M. Borland, Phys. Rev. ST Accel. Beams **8**, 074001 (2005).
[4] K. Harkay et al., Proc. 2005 Particle Accelerator Conference (Knoxville, Tennessee, 2005) 668.
[5] P. Anfinrud, private communication.
[6] V. Dolgashev, private communication.

Around the APS

The Fourth CW and High Average Power RF Workshop

The fourth international workshop on continuous and high average power radio frequency (rf) systems, jointly organized by Argonne's Accelerator Systems Division and Intense Pulsed Neutron Source, was held at the APS on May 1-4, 2006. These workshops bring together rf experts from synchrotron facilities to share their rf experiences, problems, and solutions. The technology under discussion ranges from high average power linac rf systems, high-power klystrons, and high-voltage power supplies to rf cavities, and power couplers and tuners. ● More than 30 participants came to the workshop from accelerator facilities in Europe and Canada including TRIUMF, DESY, ELETTRA, the European Synchrotron Radiation Facility, the Swiss Light Source, and SOLEIL, in addition to the U.S. Department of Energy facilities at Oak Ridge National Laboratory, Fermilab, the Thomas Jefferson Lab, the Stanford Linear Accelerator Center, Los Alamos National Laboratory, and of course, Argonne. Presentations and small group discussions were focused on current status and operational issues of large rf systems. A wide range of topics, including key operational issues, the development of high-power rf power sources, high-power rf systems upgrades, and exploring and developing new rf technology for future synchrotron facilities were discussed. ● To view all of the workshop presentations, go to http://www.aps.anl.gov/News/Conferences/2006/CWHAP06/index.html.

Contact: Ali Nassiri (nassiri@aps.anl.gov)

Toward 100-nrad-scale Beam Stability at the APS

Beam stability in the APS machine is, at present, quite good. But in the course of the next 3-to-5 years, it is likely that beam stability will become a limiting factor for many users' experiments. In an effort to stay on the leading edge of machine performance, a new set of beam stability goals has been developed, and critical efforts toward those goals have been initiated. The main idea behind developing these goals was to eliminate the accelerator altogether as a source of beamline instability. Specifically, the beam position noise and drift resulting in a 100-nrad pointing stability would correspond to a level of motion that would be transparent, and thus irrelevant to beamline operation. To achieve the ultimate 100-nrad-scale beam stability, a detailed understanding of the limitations and upgrade paths is necessary. These efforts are important not only for the present users, but also for facility upgrades such as the proposed energy-recovery linac

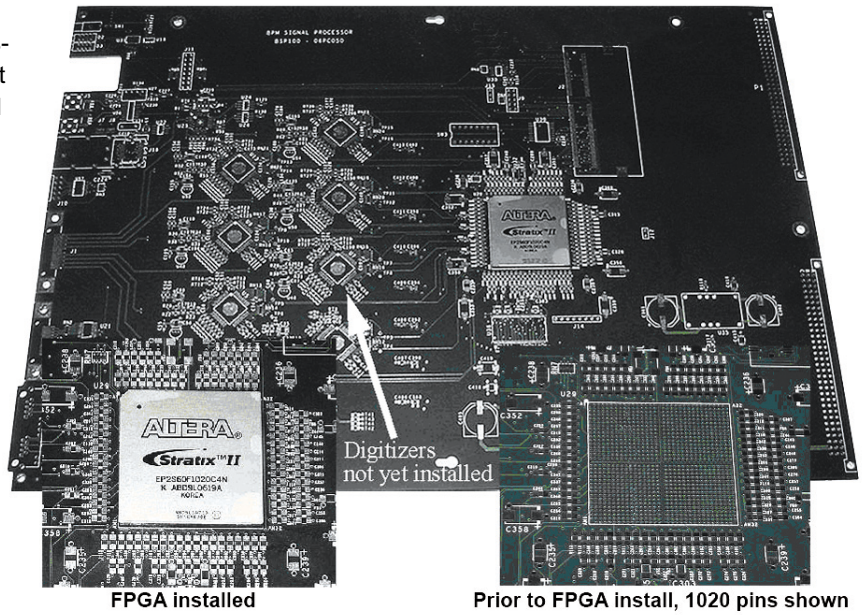

Fig. 1. Prototype broadband rf bpm data acquisition board, with eight digitizers plus FPGA. (Courtesy R. Laird, AES.)

Most critical to meeting challenging long-term stability goals is the ability to measure both particle and x-ray beam trajectories with high confidence in a frequency range from DC to several-hundred Hz. The substantial improvements needed to accomplish long-term stability goals will rely heavily on the success of several key beam trajectory measurement initiatives, along with efforts to eliminate sources of beam instability. As a result of more than 10 years of development on orbit correction, APS dynamic beam stability today is really quite good—at the level of 1.8 μm/300 nrad rms vertically in a frequency band from 0.1 to 200 Hz. The long-term goals for these measures of beam stability are 0.42 μm and 220 nrad rms, respectively.

While progress to date has been significant, certain portions of the installed orbit correction infrastructure are rapidly approaching the theoretical performance limit. Further, many system components have maintenance issues associated with a limited stock of now-unobtainable spare parts. Modern technological advances, specifically fast digiziters coupled with field-programmable gate arrays (FPGAs), provide the potential for very substantial performance enhancements in addition to vastly expanded functionality. For example, a prototype data acquisition board using this technology for the broadband radio frequency (rf) beam position monitor (bpm) system (Fig. 1) is under development in a cross-divisional collaboration among the APS Controls, Diagnostics, and Operations and Analysis groups. In addition to providing a considerable reduction in noise, new capabilities such as transient turn-by-turn orbit history, postmortem analysis, multi-turn injection trajectory measurement, and frequency band noise power measurement will be included.

The extensive use of insertion device photon bpms for closed-loop orbit correction is unique to the APS. This is due to an effort to eliminate stray radiation sources by means of a 7-year-long accelerator realignment program (the "Decker distortion," see *APS Science 2004*, ANL-05/04, p. 149), and a further several-year effort to minimize residual gap-dependent systematic errors. This has been critical to the ability to reproduce insertion device source angle and position over periods ranging from days to months at the few-microradian level.

To go to the next level, a program was started in 2005 to develop a photon bpm sensitive to hard x-rays—in contrast to the present photon bpms, which are sensitive to ultraviolet radiation present at the beam's periphery. The new detector relies on the principle of hard x-ray back fluorescence, in a fashion similar to what has been done with monochromatic beams [1]. A pre-prototype assembly for testing a variety of detector configurations has been installed in a spare monochromator vacuum tank at beamline 19-ID (SBC-CAT) and extensive studies are ongoing.

Contact: Katherine Harkay (harkay@aps.anl.gov)
Glenn A. Decker (decker@aps.anl.gov)

Reference

[1] R. Alkire, G. Rosenbaum, and G. Evans, J. Synch. Rad. **7**, 61 (2000).

High-heat-load R&D for the APS Front Ends

Glidcop®, an aluminum oxide, dispersion-strengthened copper, is a high-strength material with a thermal conductivity near that of copper. It is widely used at the APS as the x-ray beam absorbing material in most of the front-end high-heat load components. The thermal fatigue properties of Glidcop® are not well characterized and, therefore, the APS adopted conservative design criteria, allowing a maximum surface temperature of only 300° C to limit material movement due to prolonged exposure to high temperatures or high stresses. Front-end high-heat load components at the APS have been designed to withstand at least 10,000 thermal cycles during normal operation; but increasing demand for higher power densities and total power have pushed the design of beam-absorbing components to the limit.

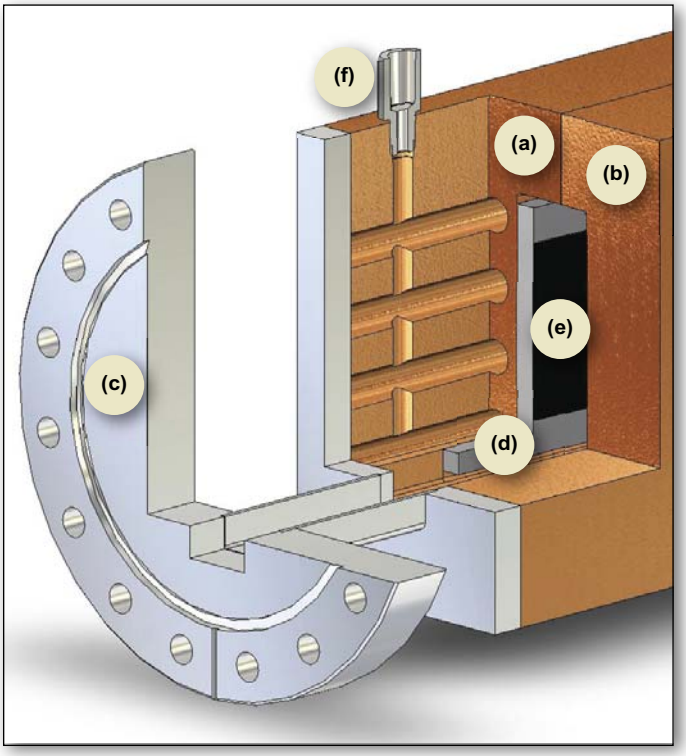

Fig. 1. Multilayered photon shutter with a CVD-diamond layer. (a): Glidcop®-cooled half; (b): Glidcop® SiC non-cooled half; (c): SS 304 vacuum flange; (d): CVD SiC substrates (500 mm x 80 mm x 6 mm); (e): CVD-diamond layer; (f): cooling-water ports.

Recent experiments conducted at XOR beamline 26-ID-A assessed the thermal fatigue properties of Glidcop® exposed to cyclic thermal loading by the APS x-ray beam. Experimentally determining the actual maximum surface temperature limit may allow revision of the design criteria for Glidcop®, increasing the expected life of existing components and allowing for operation at higher storage ring current levels. Although Glidcop® samples cracked and failed at temperatures greater than 500° C, a sample at 450° C survived 20,000 cycles with no visible signs of damage. Samples still require metallurgical evaluation, but initial results indicate that operation at levels significantly above 300° C will be possible, doubling the expected operational life while enabling the use of more powerful x-ray beams.

As a means of tolerating higher total power and power densities, a recent investigation has focused on the use of chemical vapor deposition (CVD)-diamond layers deposited onto Glidcop® to "spread" thermal loads deposited on the surfaces of front-end high-heat load components. Figure 1 shows a conceptual design for a multilayered photon shutter with CVD diamond bonded to the beam-strike surface. Although many fabrication details still need to be worked out, initial finite element analysis results are quite encouraging, indicating allowable operation at the 300-mA level with this design.

Two new high-heat-load-component designs have recently been developed, fabricated, and installed for use in the hard x-ray nanoprobe beamline at sector 26 of the APS, including an 8-mm-diameter, clear-aperture CVD-diamond window and a set of high-power white-beam slits. Unlike previous beryllium x-ray window designs, the new CVD-diamond window can withstand operation with dual inline undulators, or single undulator operation up to 200 mA. The new white-beam slit design incorporates monolithic Glidcop® slit bodies mounted to commercially available x-y drive systems, making this design very cost effective and relatively easy to fabricate. The new slit design can tolerate a peak power density of 763 W/mm^2 and allows beamline operation up to 180 mA.

Contact: Jeff Collins (collins@aps.anl.gov)

See: Y. Jaski and D. Cookson, "Design and Application of CVD Diamond Windows for X-Rays at the Advanced Photon Source," AIP Conference Proceedings **879**, 9th International Conference on Synchrotron Radiation Instrumentation, May 28-June 3, 2006, Daegu, Korea (January 2007).

C. Benson, Y. Jaski, J. Maser, T. Powers, R. Winarski, O. Schmidt, E. Rossi, and T. Grabinski, "White Beam Slits and Pink Beam Slits for the Hard X-ray Nanoprobe Beamline at the Advanced Photon Source," AIP Conference Proceedings **879**, 9th International Conference on Synchrotron Radiation Instrumentation, May 28-June 3, 2006, Daegu, Korea (January 2007).

V. Ravindranath et al., "Thermal Fatigue Life Prediction of Glidcop® Al-15," MEDSI 2006, May 24-26, 2006 Himeji, Hyogo, Japan. [Online]. http://medsi2006.spring8.or.jp/proc/31_1.pdf [January 2007].

The SmCo Insertion Device and Radiation Damage

Through 10 years of operation, most insertion devices (IDs) installed in the APS storage ring have shown minimal changes in their performance over time. In sectors with narrow-gap (5-mm beam clearance) vacuum chambers, however, the storage-ring radiation due to beam losses was significantly higher than that seen in a typical APS sector (7.5- or 8-mm beam clearance). This radiation can damage the permanent magnets of the undulator, demagnetizing them and producing a non-ideal magnetic profile (see "Radiation Effects on Insertion Devices," *APS Science 2003*, ANL-04/07, p. 154). To maintain optimum performance, the IDs in such sectors needed to be periodically removed to remagnetize the magnets and re-tune the device. At present, sector 4 is the only sector that has a narrow-gap chamber. In an effort to alleviate the radiation problem, a new device with more radiation-resistant samarium cobalt (SmCo) magnets was installed in sector 4 in January 2006 (see "A New, Blue SmCo Insertion Device," *APS Science 2005*, ANL-05/29, p. 184).

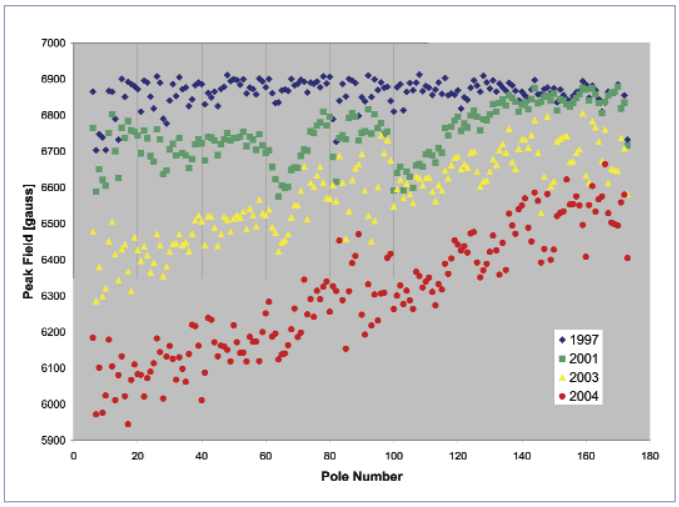

Fig. 1. Damage sequence for undulator A installed on a 5-mm vacuum chamber at the downstream end of sector 3. The beam travels from right to left relative to the graph; i.e., the beam exits the undulator at pole #1. This vacuum chamber was replaced by a 7.5-mm chamber in 2005; no further damage has been observed in the device.

The cumulative effect of beam-loss-induced radiation damage on an undulator can be seen in Fig. 1. The graph shows the magnitude of the peak magnetic field under each undulator pole vs. numerical position along the downstream undulator in sector 3. The first step in keeping this undulator operational was to redefine "parallel," which was defined as when the magnetic field was as flat as possible. This was achieved by reducing the mechanical gap at the undulator end with the weakest magnets

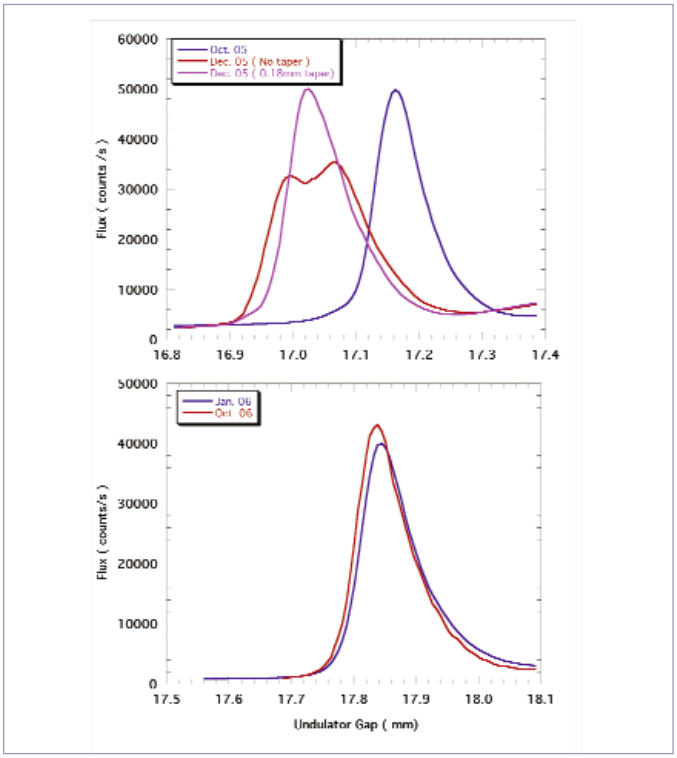

Fig. 2. Scan of the undulator gap at 35 keV for undulator A (top) showing the effects of radiation damage and SmCo (bottom) showing minimal effects.

to increase the field strength there. The taper grew to a few hundred microns difference between the ends. The peak field in the damaged device shown here is approximately linear along the undulator, but the dependence of the field on gap is exponential. Although tapering does not provide a perfect correction, it is a reasonable temporary solution. When the radiation damage exceeds a certain threshold, tapering is no longer effective and the device must be removed and remagnetized. The undulator damage seen in sector 4 was not as linear, so more tuning effort was required to flatten the field after tapering. Clearly, minimizing or avoiding radiation damage altogether is an obvious advantage.

The radiation-induced loss of magnetization is most pronounced when measuring the photon flux of higher-order undulator harmonics. Figure 2 shows the flux measured at 35 keV as the undulator gap was scanned through the fifth harmonic for both undulator A with neodymium iron boron magnets and the new undulator with SmCo magnets. After only three months in the storage ring, the flux obtained with undulator A (red curve in top panel) is significantly degraded compared to scans taken at the beginning of a run cycle (blue curve). Nearly all the flux

Continued on next page

could be recovered, however, by tapering the undulator by 0.18 mm (magenta curve). Note that the position of the harmonic is shifted to a smaller gap. The smaller gap results in the higher field strength required to achieve 35 keV.

The new SmCo device (bottom panel of Fig. 2), on the other hand, showed no significant damage even after nine months of operation in the storage ring. The flux at 35 keV for this device is ~20% smaller compared to the previous 3.3-cm device, due to the longer 3.5-cm period of the SmCo device.

Accelerator simulations demonstrated that beam losses at the undulator were largely resulting from particles being scattered from the stored beam in a process called "Touschek scattering" [1]. This motivated a strategy for protecting the sector 4 undulator from such losses by placing a scraper in a location with good selection for off-energy particles. A horizontal scraper was therefore installed at the downstream end of a straight sector that is occupied by radio frequency accelerating cavities. Radiation studies were conducted under various machine conditions using RadFET detectors positioned along the length of the sector 4 chamber. The detectors responded to beam losses from injection, Touschek scattering, and beam dumps. Inserting the scraper reduced the sector 4 radiation due to all of these sources, while at the same time not appreciably affecting the injection efficiency. The scraper has been implemented operationally.

In addition to the user synchrotron radiation output results, it would be desirable to obtain magnetic measurements of the SmCo device to compare with the pre-installation measurements. In view of the user results in Fig. 2, there was no immediate need to remove and retune the device. It will be removed during a future shutdown for re-measurement and retuning, if required.

Contact: Katherine Harkay (harkay@aps.anl.gov)
Jonathan Lang (lang@aps.anl.gov),
Liz Moog (moog@aps.anl.gov)

Reference

[1] M. Borland and L. Emery, "Touschek Lifetime and Undulator Damage in the Advanced Photon Source," Proceedings of the 2005 Particle Accelerator Conference, IEEE (2005), 3835.

Around the APS

The 2006 EPICS Collaboration Meeting

In June 2006, the APS hosted a successful meeting of the Experimental Physics and Industrial Control System (EPICS) collaboration. EPICS is a set of software tools and applications that was jointly developed by Argonne National Laboratory and Los Alamos National Laboratory to provide a software infrastructure for use in building distributed control systems to operate devices such as particle accelerators, beamlines, large experiments, major telescopes, and large industrial plants. EPICS continues to be seen as a viable and desirable control system tool kit and the last year has seen a number of new projects in both the U.S. and Asia starting to examine and use EPICS. • The collaboration meeting at the APS was attended by more than 140 people from 36 organizations spread over 11 countries. The last EPICS meeting at the APS was 28 meetings ago in 1994, when the sessions had many fewer attendees. New at the 2006 meeting were the Special Interest Group Workshops, for discussion of minority-interest topics. • Notable presentations covered the successes of the EPICS-based control systems in the construction and commissioning of the Spallation Neutron Source, the Australian Synchrotron, and the Diamond Light Source. Future developments to watch include Version 4 Java IOC; and the growing number of client application frameworks that are being worked on, the leading candidate for which appears to be the Eclipse-based Control System Suite development started at the Deutsches Elektronen Synchrotron in Hamburg, Germany, for use with the XFEL project. *Contact: Andrew Johnson (anj@aps.anl.gov)*

Savings in the Air: No-cost Improvements in Beam Stability

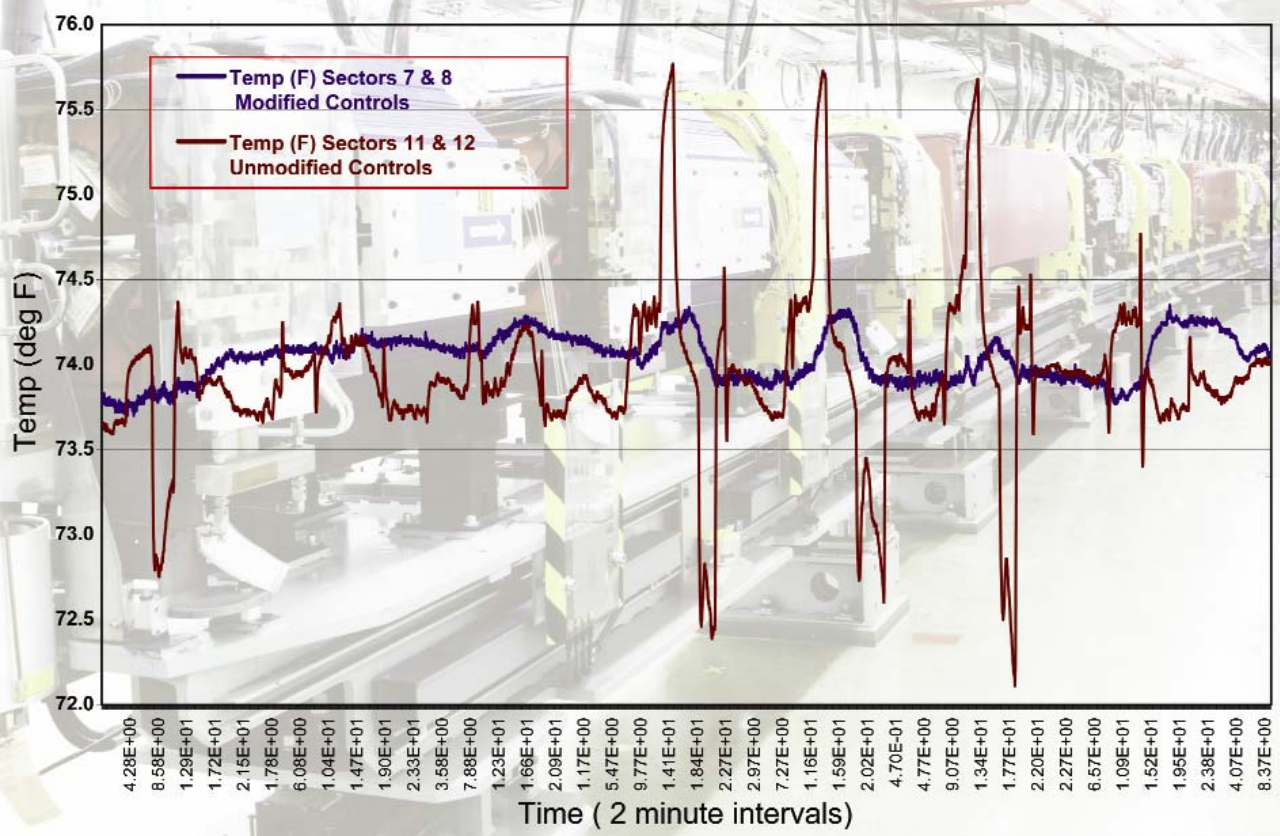

Top: Example of storage ring air-temperature fluctuations before (red) and after (blue) air conditioning upgrades. Bottom photo: AES and FMS personnel conducting an in-progress review of construction activities in preparation for commissioning of the upgraded storage ring air conditioning system. Left to right: Rick Janik (AES), Robert Brachle and Glenn Willes (both FMS), and Marvin Kirshenbaum and Andrew Stevens (both AES).

Efficient and reliable delivery of x-ray beams to APS users is dependent on many factors, not least of which is the utility infrastructure that supplies electrical power, space temperature control, and primary cooling water for the accelerator and storage ring, user beamlines, and other technical systems and components. One of the main objectives at the APS has been to enhance the orbital stability of the storage ring beam. Temperature stability in the storage ring enclosure is a factor in meeting this challenge, because fluctuations in temperature can cause dimensional changes in storage ring components that can substantially affect electron-beam orbit.

Much attention has been paid over the years to temperature control of the APS water-cooling sys-

Continued on next page

tem responsible for the heat rejection and temperature stability of magnets and vacuum chambers. But the temperature stability of the air around the water-cooled components, girders, and other non-water-cooled structural elements within the storage ring tunnel is another factor, one that has recently been addressed by an innovative air-handling system upgrade that was accomplished with no capital expenditure by Argonne or the APS, while promising to yield future cost savings for the facility.

The Conventional Facilities Group (CFG) in the APS Engineering Support Division, which has primary responsibility for conventional design and construction at the APS, along with the role of providing engineering support for monitoring the operation and performance of the utility infrastructure, initiated the upgrade to the APS storage ring air conditioning system. To finance implementation of this work, a scheme was devised to utilize waste heat from the APS. This permitted the leveraging of U.S. Department of Energy (DOE)-sanctioned "performance contracting," which allows outside contractors to finance construction with cost recovery for their efforts paid out of a guaranteed energy savings. Thus, all costs associated with the upgrade of the entire APS storage ring air conditioning system are being recovered from the cost reduction in energy usage. Johnson Controls, Inc., was selected by Argonne from a list of contractors prequalified by the DOE to, upon review and acceptance, provide the financing and construction services required to implement these changes.

The foundation for this work was a study conducted by the CFG in cooperation with the Argonne Facilities Management and Services (FMS) Maintenance Group. Originally, the storage ring tunnel space air temperature was specified to be maintained within a 2º C peak-to-peak range. As user demands on storage ring performance have increased with the development of more and more beamlines, it became apparent that a more stringent specification was required to enhance electron-beam orbital stability. Various simulations and measurements indicated that, at the very least, the tunnel air temperature variation must be constrained to a peak-to-peak range of 0.5º C.

In the years since facility construction, improvements have been made in control of the storage ring tunnel air temperatures. But without physical changes to the existing air-handling system, the level of improvement required could not be achieved. A greater reliance had been placed on utilization of colder cooling water as a means of improving temperature stabilization of storage ring magnets and vacuum chambers. This increased reliance on direct water cooling resulted in the shifting of heat rejection from the tunnel space air directly to the cooling water. The excess capacity in the air conditioning system created by this shift acted to "drive," rather than respond to, the tunnel air temperature, further limiting the existing system's ability to achieve tighter temperature control.

The aforementioned study, conducted in 2005, demonstrated that while adjustments to the temperature control loop tuning parameters could offset some of the increased gain of the cooling system, this in itself would not result in a consistent air temperature within the desired range. Further, under the original design, all air conditioning systems served the dual role of cooling and ventilating the tunnel with outdoor air. This coupling of the tunnel space temperature control to variations in the outdoor air temperature was another cause of air-temperature instability, especially during the transitional seasons when multiple switchovers between cooling and heating of outdoor air would occur within a single 24-h period. These findings led to an overall re-evaluation of the existing space cooling system and the identification of a number of changes that could be made to modify the existing system with minimum impact to its physical configuration. These changes included replacement of the existing air conditioning units' large cooling-water control valves with smaller valves, optimization of control loop tuning parameters, and decoupling of the outdoor air influence. All of these improvements, as shown in the 2005 engineering study, would produce remarkable improvements in tunnel space temperature stability.

At the time of this writing (early calendar year 2007) after completion of the initial system modifications in January 2007, the tunnel temperature is being maintained well within the tighter range of 0.5º C (a four-fold reduction in temperature variation) and initial operation indicates that a further reduction in variation can be achieved, yielding peak-to-peak temperatures of 0.2º C.

The success of this project will serve as a model for additional work at the APS, allowing the facility to implement energy recovery to reduce operating costs and finance needed facility improvements in the future.

Contact: Marvin Kirshenbaum (kirshen@ aps.anl.gov)

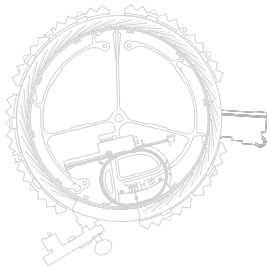

FPGAs and IOCs at the APS

Advances in semiconductor technology (faster, smaller, more precise) are being applied to challenging controls problems at the APS in order to continually improve the performance of the accelerator and beamlines. Two areas where substantial progress has been seen are the size of the processor required to run the Experimental Physics and Industrial Control System (EPICS) software used at the APS, and the use of large field-programmable gate arrays (FPGAs) for high-speed data processing. An FPGA is an integrated circuit containing an array of simple logic elements and interconnections. The functions performed by the logic blocks and the interconnections between them are set as specified by the system designer rather than by the integrated circuit manufacturer (i.e., they are "programmable").

Although the size of the typical processors running EPICS software has decreased dramatically, the performance of the units shown is comparable. The small size of the recent microcontrollers, however, allows tight integration with other high-performance integrated circuits in very small enclosures.

Another area where phenomenal performance increases have been realized is with large-scale FPGA integrated circuits. Today's high-end FPGA chips might contain hundreds of thousands of internal gates and over a thousand input/output (I/O) pins. The FPGAs used in the projects described in this article contain low-level logic elements as well as memory blocks and dedicated arithmetic blocks useful for performing digital signal processing.

The combination of these two technologies (a single-chip microcontroller module and a large FPGA, Fig. 2) is providing control system and data acquisition developers at the APS with a powerful new tool. Several projects based on this technology are in use or under development at the APS.

The first component [(A) in Fig. 2] of this combination of electronics is a commercially-available module the same size as a notebook computer memory module (about the size of a credit card), containing a single-chip microcontroller, memory, and Ethernet network interface. This module is capable of functioning as a complete EPICS input/output controller (IOC) and appears to EPICS clients as a standard IOC. The low cost (under $200) and high level of integration of this module means that EPICS IOC capability can be added to an application quickly and easily. The second component [(B) in Fig. 1] is the large FPGA chip described above.

The first production use of this technology at the APS is the Particle Accumulator Ring's radio frequency (rf) phase adjustment controller. This application began as a quick "proof of principle" test that lent itself to the rapid prototyping environment provided by the embedded IOC/FPGA combination. The prototype unit proved to operate so successfully that it was immediately put to use on a day-to-day basis. It has functioned without any problems for well over a year.

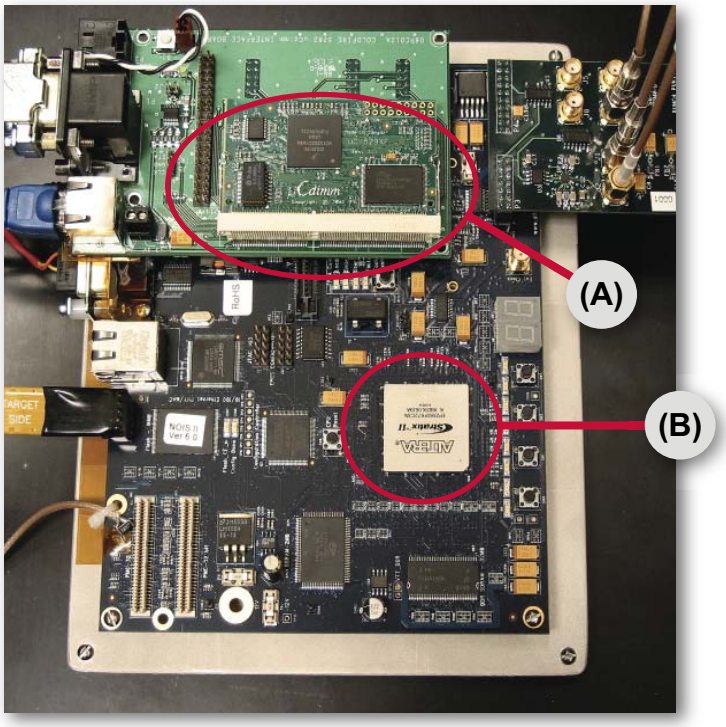

Fig. 1. Two technologies in one. An EPICS IOC (A) and a large FPGA (B).

Another project utilizing the embedded IOC/FPGA combination is the single-bunch beam stabilizer. This device measures the position of a particular bunch of electrons in the storage ring, applies a digital filter computation to the most recent 32 measurements of that bunch's position, and sends a signal to stabilize the position of the bunch on the next pass around the ring. The large number of computation blocks within the FPGA allows these operations to be performed once for every fourth bunch—i.e., every 11.26 nsec—resulting in the FPGA continuously executing 88 million I/O operations per second and over 5.8 billion multiplications and additions per second. Both of these values are far beyond what a desktop PC could perform.

Additional projects under development for the APS include a nanoprobe positioning controller, a low-level rf measurement system, a bunch-purity measurement system, a replacement for the controllers used in many magnet power supplies, and an improved beam position monitor processor. All of these projects benefit from the greatly reduced component count, low power consumption, high data throughput, and tight integration of the IOC/FPGA solution. New designs can be quickly prototyped, and the embedded IOC allows for a single-chassis, turn-key, "EPICS-compliant" instrument delivered to the customer.

Contact: Eric Norum (norume@aps.anl.gov)
Ned Arnold (nda@aps.anl.gov)

APS Safety Innovation

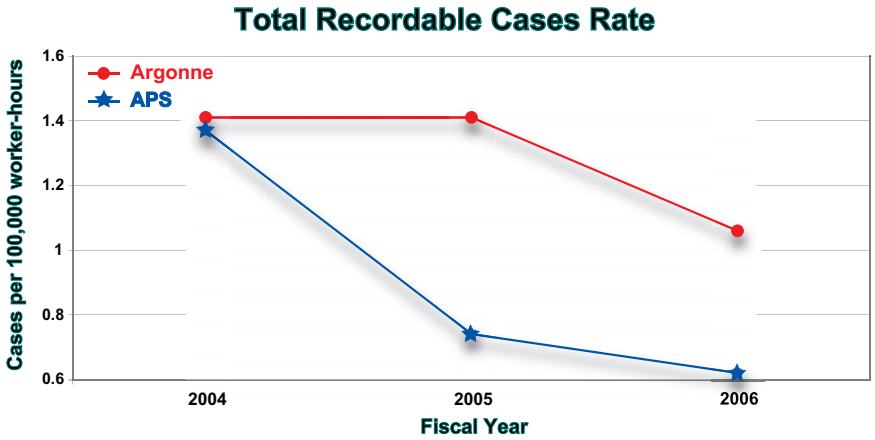

Fig. 1. Total recordable cases rate for APS employees vs. other Argonne employees (not including contractors nor APS users). The DOE-SC publishes data that includes contractors and users. This data yields different values for the three Argonne rates shown (1.5 for fiscal year [FY] 2004 and FY 2005 rather than 1.41, and 1.2 for FY 2006 rather than 1.06). This type of data is presently not readily available for the APS.

Department of Energy (DOE) requirements and expectations related to preserving the health and safety of workers and the general public, as well as protecting the environment, have steadily increased and have become more detailed. This presents a unique challenge to the APS as a large DOE user facility. Along with continued efforts to maintain a safe workplace for employees, the needs of the many and varied APS users must be balanced with the necessity of adhering to the DOE requirements and providing the safest possible working environment. The APS has striven to be innovative in addressing DOE concerns in order to not unduly inhibit user activities once they have arrived at the APS.

One example of this innovative approach is the APS Web-based Experiment Safety Assessment Form (ESAF) process. The ESAF process, which is the responsibility of the APS Engineering Support Division User ESH Support Group, ensures that proposed experimental activities with significant hazards are identified at a sufficiently early stage in order to arrange for proper mitigation before users arrive and the activities are initiated. The ESAF also must support a large number of reviews in an expeditious manner. The key to achieving both is the use of predefined hazard categories. Each hazard category identifies the minimum necessary mitigating measures that will be used, such as personal protective equipment, training, and use of formal procedures. The ESAF process requires users to provide sufficient information so that the hazard categories associated with their proposed experiment or experimental apparatus can be easily identified. This process has been finely honed over several years of use. The result is an efficient method for screening-out the numerous proposed experimental activities with negligible hazards so that the few with significant hazards receive rapid and proper attention.

The APS has taken the lead within Argonne in addressing DOE concerns over the use of electrical equipment that has not been type tested by a nationally recognized testing laboratory (e.g., Underwriters Laboratory). Manufacturers of highly specialized scientific equipment do not always expend the resources necessary to have each device type tested, especially for devices with low production runs. Also, "home built" devices that users bring to the facility may have deficiencies that have not been recognized by their constructors. The DOE requirement that contractors inspect all unlisted electrical equipment implements specific features of the Occupational Safety and Health (OSHA) Act, and of the National Electric Code. The Argonne program was piloted at the APS and specifically targeted the inspection of user-provided, unlisted electrical equipment.

Being able to identify electrical deficiencies requires multi-day, hands-on training of personnel familiar with electrical equipment. The APS arranged for selected personnel to obtain the training and to be certified as inspectors. The experience gained during the pilot program demonstrated that most inspections took 1 to 2 hours to perform, and that slightly more than 50% of devices inspected failed to pass. Users were not allowed to deploy the equipment until repairs had been completed and the device passed re-inspection. Most of the repairs were relatively minor, but occasional major rework did occur. The APS has been providing minor repair work to users at a nominal charge.

Each DOE contractor is obligated to investigate and report injuries that occur on their site. A standard method for reporting injuries developed by the Department of Labor in administering the OSHA Act—and by DOE—classifies certain injuries as "recordable," as defined by OSHA Regulation 1904.7(b)(1). The DOE Office of Science (SC) director has issued a set of goals for reducing the number of injuries occurring at SC-funded sites. The goals are based on the injury rates reported by companies performing R&D activities similar to those at the DOE-SC sites. The intent is to achieve DOE-SC injury rates within the lowest 10% of the companies used as a basis (i.e., 90% of the basis companies will have higher injury rates than DOE-SC sites).

The APS injury rates are lower than the overall Argonne injury rates. Figure 1 shows the rates for APS and Argonne for the past three years associated with the total number of OSHA recordable cases per 100,000 worker-hours. It clearly shows that both APS and Argonne rates have been decreasing in accordance with achieving the DOE-SC goals.

Contact: Tom Barkalow (barkalow@aps.anl.gov)

AES: An Efficient Division of Resources

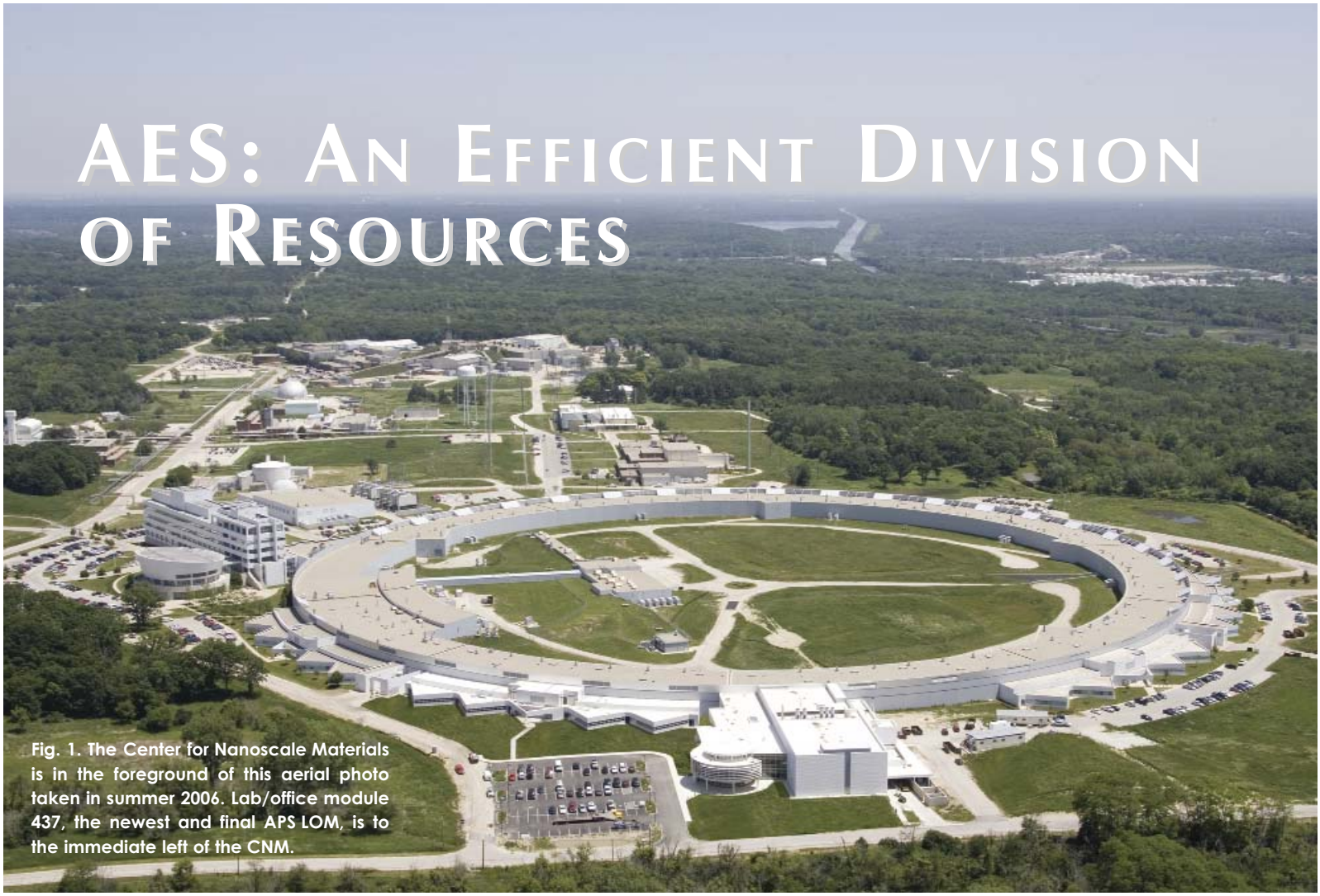

Fig. 1. The Center for Nanoscale Materials is in the foreground of this aerial photo taken in summer 2006. Lab/office module 437, the newest and final APS LOM, is to the immediate left of the CNM.

A strategic reorganization of the APS in 2006 brought clearer focus to the missions of the X-ray Science Division and the Accelerator Systems Division, and created a new third division: APS Engineering Support (AES). The AES Division efficiently and effectively serves the APS community by centralizing facility services and consolidating a wide range of support expertise from across the APS. The result is optimization of the resources allocated for facility and infrastructure design and maintenance.

During 2006, Conventional Facilities Group personnel, who reside under Computer Systems (CS) within AES, oversaw the completion of the Center for Nanoscale Materials (CNM) building adjoining the APS experiment hall, and the construction of the final lab/office module (LOM 437) next to the CNM (Fig. 1). The common areas of the 20,000-sq-ft LOM are complete and the sector support spaces are now available to be built out to meet the needs of nearby beamlines.

With the goal of providing more-efficient and better-integrated computer support services, the Information Technology, Information Solutions, Controls, and Beamline Controls and Data Acquisition groups were brought together under CS. These groups are responsible for maintaining a high-perform-

Continued on next page

Fig. 2. Christy Dannenberg (foreground) and Mary Westbrook (both AES) at the Information Technology Support Request System (SRS) center, which handles requests for computer support from APS personnel, and resident and visiting users. Since statistics were first collected in 1998, requests for computer support to the Web-based SRS have grown from approximately 1,000 per fiscal year (FY) to more than 5,500 in FY 2006, keeping pace with the increase in APS beamlines and users, while the response time per request is continually improving.

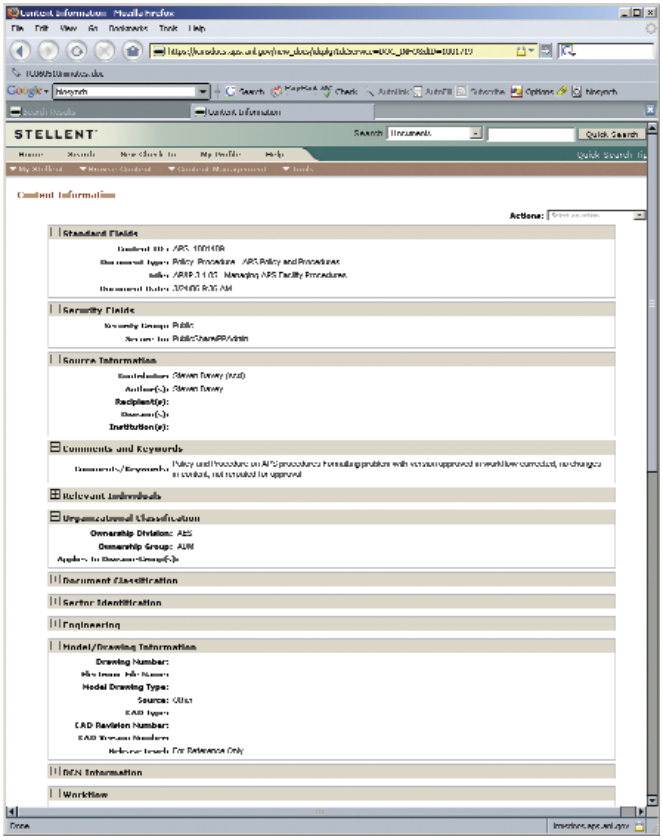

Fig. 2. A typical ICMS "Content Information" page.

ance, highly reliable computing environment (Fig. 2). In 2006, the Beamline Controls and Data Acquisition Group accelerated the implementation of a state-of-the-art computing infrastructure for a growing number of APS beamlines.

Computer Systems groups were also instrumental in the development of an electronic document management system (the Integrated Content Management System, or ICMS) for the APS (Fig. 2). This system, when fully deployed, will provide tools for efficient document management (e.g., automated workflows, revision tracking, and a base for Web content management) and ensure that technical and administrative groups have rapid access operational records and historical references.

The CS Controls Group continued as a leading contributor to the advancement of accelerator control system technology at the APS and within the global accelerator community. Their contributions included the development of high-speed controls applications such as digital radio frequency signal processing and ongoing support of the EPICS (Experimental Physics and Industrial Control System) suite of tools by maintaining critical extensions, providing EPICS release control, and maintaining the EPICS Web site.

Groups dedicated to safety; mechanical engineering, design, operations and maintenance; drafting; survey and alignment; and safety interlocks now form an integrated engineering support services organization under the umbrella of Mechanical and Interlocks Systems (MIS) within AES. These groups provide streamlined services for new projects as well as for maintaining existing facilities. For instance, MIS groups provided mechanical design support to the High Resolution Inelastic X-ray Spectrometer at sector 30, which was brought into operation in 2006 (see page 129). Mechanical and Interlocks Systems groups are supporting APS contributions to the Linac Coherent Light Source at the Stanford Linear Accelerator Center. And technical personnel from MIS helped ensure another year of outstanding x-ray source performance, with beam availability at greater than 97% of scheduled beam time.

Because the AES has been charged with responsibility for overseeing the beamline experiment safety program, the traditional role of APS floor coordinators, which once included both technical and operational support for beamline operations and safety oversight, has been changed. To better focus beamline support, technical and administrative user support services were placed in the X-ray Science Division's Beamline Technical Support Group. The AES floor coordinators are now dedicated to ensuring that a safe work environment is maintained in the beamline experimental facilities (Fig. 3). In 2006, AES was responsible for the safety of the more than 3,200 users who came to the APS more than 10,000 times, helping to continue the excellent experiment safety record at the APS.

Contact: William Ruzicka (ruzicka@aps.anl.gov)

Mark Vukonich (seated), of Bio-CAT at sector 18, and AES floor coordinator Nena Moonier demonstrate proper use of a portable biosafety cabinet, one of two recently purchased by the APS. The cabinets can be deployed around the experiment hall as needed for work involving hazardous biological material that would otherwise pose an inhalation risk for APS users and staff.

APS Data

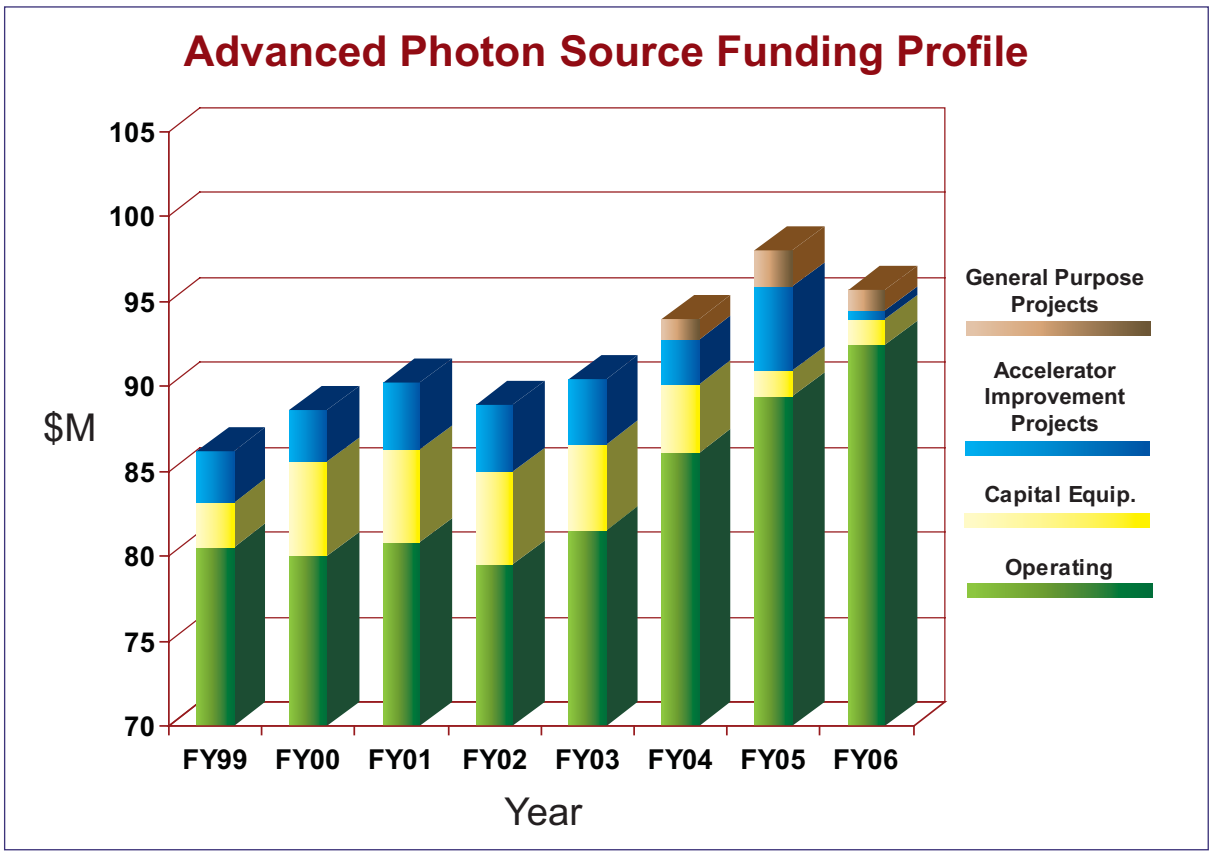
Advanced Photon Source Funding Profile
105
100
95
90
85
80
75
70
$M
FY99
FY00
FY01
FY02
FY03
FY04
FY05
FY06
Year
General Purpose Projects
Accelerator Improvement Projects
Capital Equip.
Operating

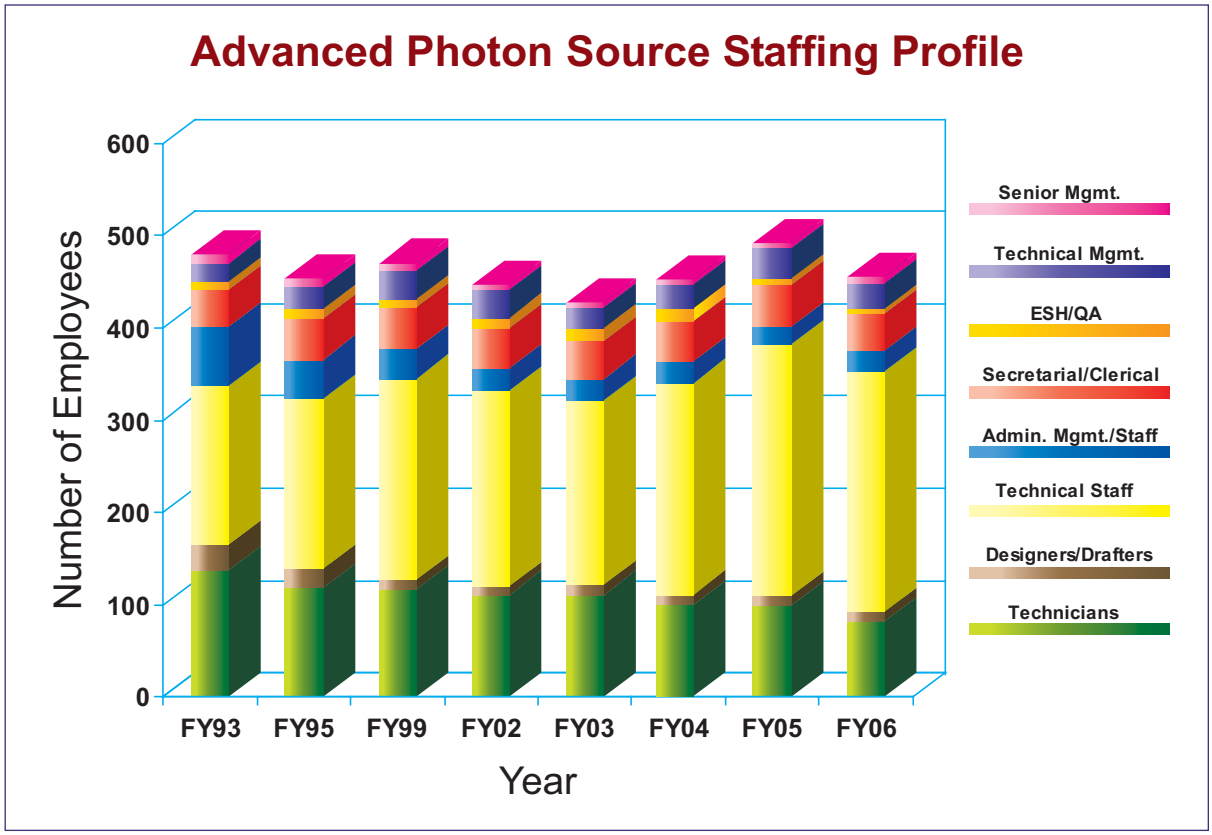
Advanced Photon Source Staffing Profile
600
500
400
300
200
100
0
Number of Employees
FY93
FY95
FY99
FY02
FY03
FY04
FY05
FY06
Year
Senior Mgmt.
Technical Mgmt.
ESH/QA
Secretarial/Clerical
Admin. Mgmt./Staff
Technical Staff
Designers/Drafters
Technicians

APS Organization Chart

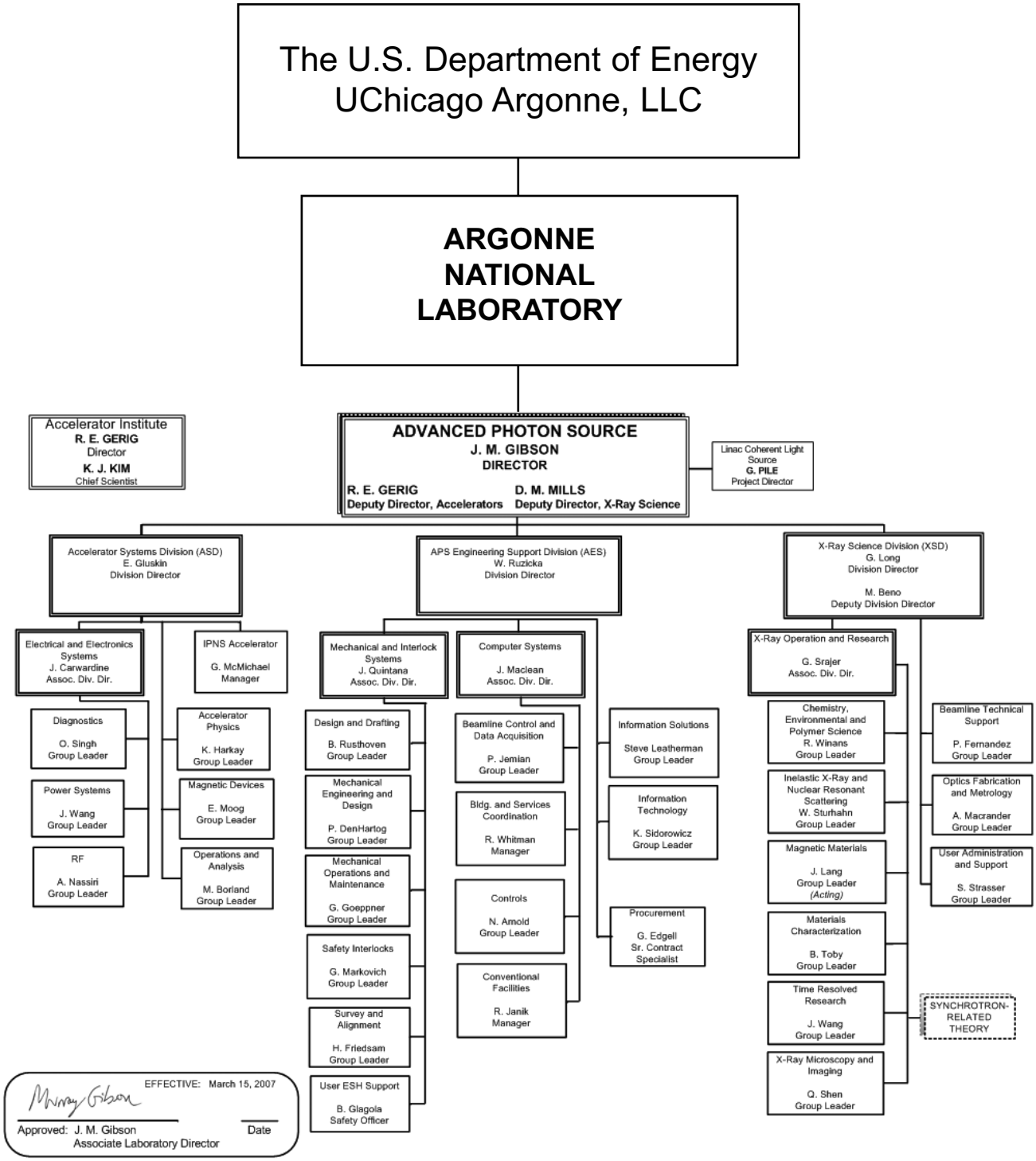

Typical APS Machine Operations Parameters

Linac

Output energy	325 MeV
Maximum energy	450 MeV
Output beam charge	1–3 nC
Normalized emittance	10–20 mm-mrad
Frequency	2.856 GHz
Modulator pulse rep rate	30 Hz
Gun rep rate (1–6 pulses, 33.3 ms apart every 0.5 s)	2–12 Hz
Beam pulse length	8–30 ns
Bunch length	1–10 ps FWHM

Particle Accumulator Ring

Nominal energy	325 MeV
Maximum energy	450 MeV
Circumference	30.66 m
Cycle time	500 ms
Fundamental rf frequency (RF1)	9.77 MHz
12th harmonic rf frequency (RF12)	117.3 MHz
RMS bunch length (after compression)	0.34 ns

Injector Synchrotron (Booster)

Nominal extraction energy	7.0 GeV
Injection energy	325 MeV
Circumference	368.0 m
Lattice structure	10 FODO cells/ quadrant
Ramping rep rate	2 Hz
Natural emittance	65 nm-rad
Radio frequency	351.930 MHz

Storage Ring System

Nominal energy	7.0 GeV
Circumference	1,104 m
Number of sectors	40
Length available for insertion device	5.0 m
Nominal circulating current, multibunch	100 mA
Natural emittance	2.8 nm-rad
RMS momentum spread	0.096%
Effective emittance	3.1 nm-rad
Vertical emittance	0.025 nm-rad
Coupling	1%
Revolution frequency	271.554 kHz
Radio frequency	351.930 MHz
Number of bunches	24 to 1296
Time between bunches	153 to 2.8 ns
RMS bunch length	25 ps to 40 ps
RMS bunch length of 16 mA in hybrid mode	65 ps

APS Source Parameters

Undulator A

Period: 3.30 cm
Length: 2.4 m
K_{max}: 2.74 (effective; at minimum gap)
Minimum gap: 10.5 mm
Tuning range: 3.0–13.0 keV (1st harmonic)
3.0–45.0 keV (1st-5th harmonic)
On-axis peak brilliance:
5.0×10^{19} ph/s/mrad^2/mm^2/0.1%bw at 7 keV
Source size and divergence at 8.0 keV:
Σ_x: 275 μm Σ_y: 9 μm
$\Sigma_{x'}$: 12.6 μrad $\Sigma_{y'}$: 6.4 μrad

2.30-cm Undulator (sector 14)

Period: 2.30 cm
Length: 2.4 m
K_{max}: 1.19 (effective; at minimum gap)
Minimum gap: 10.5 mm
Tuning range: 11.8–20.0 keV (1st harmonic)
11.8–70.0 keV (1st-5th harmonic, non-contiguous)
On-axis peak brilliance:
8.7×10^{19} ph/s/mrad^2/mm^2/0.1%bw at 12 keV
Source size and divergence at 12.0 keV:
Σ_x: 275 μm Σ_y: 9 μm
$\Sigma_{x'}$: 12.2 μrad $\Sigma_{y'}$: 5.5 μrad

2.70-cm Undulator (sectors 3 & 14)

Period: 2.70 cm
Length: 2.4 m
K_{max}: 1.78 (effective; at minimum gap)
Minimum gap: 10.5 mm
Tuning range: 6.7–16.0 keV (1st harmonic)
6.7–60.0 keV (1st-5th harmonic, non-contiguous)
On-axis peak brilliance:
7.0×10^{19} ph/s/mrad^2/mm^2/0.1%bw at 8.5 keV
Source size and divergence at 8.0 keV:
Σ_x: 275 μm Σ_y: 9 μm
$\Sigma_{x'}$: 12.6 μrad $\Sigma_{y'}$: 6.4 μrad

APS Source Parameters

3.00-cm Undulator (sector 30)

Period: 3.00 cm
Length: 2.4 m
K_{max}: 2.20 (effective; at minimum gap)
Minimum gap: 10.5 mm
Tuning range: 4.6–14.5 keV (1st harmonic)
4.6–50.0 keV (1st-5th harmonic)
On-axis peak brilliance:
5.9×10^{19} ph/s/mrad^2/mm^2/0.1%bw at 8 keV
Source size and divergence at 8.0 keV:
Σ_x: 275 μm Σ_y: 9 μm
$\Sigma_{x'}$: 12.6 μrad $\Sigma_{y'}$: 6.4 μrad

3.50-cm SmCo Undulator (sector 4)

Period: 3.50 cm
Length: 2.4 m
K_{max}: 3.08 (effective; at minimum gap)
Minimum gap: 9.5 mm
Tuning range: 2.3–12.5 keV (1st harmonic)
2.3–42.0 keV (1st-5th harmonic)
On-axis peak brilliance:
4.5×10^{19} ph/s/mrad^2/mm^2/0.1%bw at 7 keV
Source size and divergence at 8.0 keV:
Σ_x: 275 μm Σ_y: 9 μm
$\Sigma_{x'}$: 12.6 μrad $\Sigma_{y'}$: 6.4 μrad

5.50-cm Undulator (sector 2)

Period: 5.50 cm
Length: 2.4 m
K_{max}: 4.97 (effective; at minimum gap)
Minimum gap: 14.0 mm
Tuning range: 0.6–7.0 keV (1st harmonic)
0.6–25.0 keV (1st-5th harmonic)
On-axis peak brilliance:
2.0×10^{19} ph/s/mrad^2/mm^2/0.1%bw at 4 keV
Source size and divergence at 4.0 keV:
Σ_x: 275 μm Σ_y: 9 μm
$\Sigma_{x'}$: 13.9 μrad $\Sigma_{y'}$: 8.6 μrad

Circularly Polarized Undulator (sector 4)

Period: 12.8 cm
Length: 2.1 m
Circular mode:
K_{max}: 2.65 (effective; for both horizontal and vertical fields at maximum currents of 1.2 kA horizontal and 0.34 kA vertical)
B_{max}: 0.26 T (peak fields)
Tuning range: 0.5–3.0 keV (1st harmonic)
On-axis peak circular brilliance:
3.6×10^{18} ph/s/mrad^2/mm^2/0.1%bw at 1.8 keV
Linear mode:
K_{max}: 2.80 (effective; for both horizontal and vertical fields at maximum currents 1.4 kA horizontal and 0.40 kA vertical)
B_{max}: 0.29 T (peak fields)
Tuning range: 0.8–3.0 keV (1st harmonic)
0.8–10.0 keV (1st–5th harmonic)
On-axis peak linear brilliance:
2.7×10^{18} ph/s/mrad^2/mm^2/0.1%bw at 2.1 keV
Switching frequency: 0-5 Hz
Switching rise time: 20 ms
Source size and divergence at 1.5 keV:
Σ_x: 275 μm Σ_y: 9 μm
$\Sigma_{x'}$: 18.0 μrad $\Sigma_{y'}$: 14.3 μrad

APS Bending Magnet

Critical energy: 19.51 keV
Energy range: 1–100 keV
On-axis peak brilliance:
6.5×10^{15} ph/s/mrad^2/mm^2/0.1%bw at 16 keV
On-axis peak angular flux density:
9.6×10^{13} ph/s/mrad^2/0.1%bw at 16 keV
On-axis peak horizontal angular flux density:
1.6×10^{13} ph/s/mradh/0.1%bw at 6 keV
Source size and divergence at the critical energy:
Σ_x: 92 μm Σ_y: 26 μm
$\Sigma_{x'}$: 6 mrad $\Sigma_{y'}$: 47 μrad

Partner User Proposals Approved for Beam Time*

Investigators	Partner User Proposal Title (PUP number)	Beamline	Beam Time Award
T.A. Calcott, D.L. Ederer J. Freeland, G. Srajer	Soft X-ray Spectroscopy for the Study of Complex Magnetic Materials (PUP-1)	4-ID-C	10%/run for three years beginning with run 2003-3 through 2006-2
Richard Garrett	Australian Synchrotron Research Program-XOR Partnership Proposal (PUP-15)	1,3,4	Negotiated each run
S. Mochrie, A. Sandy L. Lurio, S. Narayanan	Development of Small-Angle X-ray Photon Correlation Spectroscopy for Studies of the Dynamics of Soft Matter (PUP-35)	8-ID-I	20% for three years beginning with run 2004-3 through 2007-2
L. Young, S. Southworth D. Ederer, E. Landahl E. Kanter, B. Kraessig R. Dunford	Ultrafast and Ultrasmall Laser X-ray Techniques (PUP-37)	7-ID	15% for three years beginning with run 2004-3 through 2007-2
L. Soderholm, P. Burns J. Neuefeind, M. Beno S. Skanthakumar	Short-range Order in Solution: Development of a Dedicated Beamline for Pair-distribution Functions (PDF) studies at the APS (PUP-52)	11-ID-B	20% beginning 2005-3 through 2008-2
J. Miao, M. Glimcher	Three-dimensional Imaging of Nanoscale Systems Using Coherent X-rays (PUP-53)	2-ID-B	15% beginning 2005-3 through 2008-2
S. Risbud, J Amonette I. McNulty, D. Paterson E. Stern, E.D. Crozier S. Heald, G. Seidler D. Brewe, J. Cross	Novel X-ray Spectroscopies and Microscopies for the Determination of Structure with Atomic Resolution (extension of PUP-24) (PUP-55)	20-ID	Various allocations for different programs
L. Chen, K. Attenkofer G. Jennings, D. Tiede	Developing Laser Initiated Time-resolved X-ray Facility at 11-ID-D for Photochemical Research using XAS and WAXS (PUP-56)	11-ID-D	20% beginning 2006-2 through 2007-3
A. Allen, L.E. Levine	Advanced USAXS Studies for Solution-Mediated Nanoscale Processing, Nanostructural MaterialsImaging, and High-Spatial-Resolved Gradient Microstructure Characterization (PUP-59)	32-ID	10% beginning 2007-1 through 2008-3
E. D. Crozier T.-K. Sham	Pacific Northwest Consortium Synchrotron Radiation Facility XOR Bending Magnet Partnership Proposal (PUP-60)	20-BM	10% beginning 2007-1 through 2009-3
B. Ocko, K. Blasie T. Gog, I. Kuzmenko	Partner User Proposal: Liquid Surface Scattering (LSS) at Sector 9 (PUP-61)	9-ID	15% beginning 2007-1 through 2009-3
J. Hill, Y.-J. Kim T. Gog, D. Casa	Partner User Proposal: Inelastic X-ray Scattering (IXS) at Sector 9 (PUP-62)	9-ID	15% beginning 2007-1 through 2009-3
E. Landahl et al.	Picosecond Science at the Advanced Photon Source, Partner User Proposal: Sector 7-ID (PUP-63)	7-ID	15% beginning 2007-1 through 2007-3
T.-K. Lee, J.H. Je G. Margaritondo K.S. Liang	Short Proposal for Limited Scope Partnership User at the Advanced Photon Source Phase-Contrast Hard X-ray Microscopy for Biological and In Situ Materials Science Applications at Sub 6--nm Spatial Resolution (PUP-64)	32-ID	20% of the beam time on 32-ID for 2007-2 through 2010-1
E.D. Crozier T.-K. Sham	Renewal Proposal for PUP-21, Pacific Northwest Consortium Synchrotron Radiation Facility-XOR Insertion Device Partnership User Proposal (PUP 65)	20-ID	10% for 2007-1, 20% for 2007-2, and 15% for 2007-3 through 2009-3

* As of 4.4.07.
Source: http://www.aps.anl.gov/Users/Scientific_Access/Partner_User_Information/Results/index.html
Abstracts for these proposals are at the URl above.
Completed Partner User Proposalss: http://www.aps.anl.gov/Users/Scientific_Access/Partner_User_Information/Results/completed.html
Partner user call for proposals:
www.aps.anl.gov/Users/Scientific_Access/Partner_User_Information/Call_For_Proposals/index.html
Partner user procedure: www.aps.anl.gov/Users/General_Reference/Policy_Procedures/Partner_Users/access_procedures.htm
Partner user policy: www.aps.anl.gov/Users/General_Reference/Policy_Procedures/Partner_Users/access_policy.htm

Partner users are individuals or groups whose work involves a greater degree of collaboration with the APS than is generally expected of general users.

Collaborative access teams are the most comprehensive type of partner users.

Another type is a collaborative development team, an external partner group that drives the development of a beamline that will be ultimately operated by the APS. Typically, a partner user requires access to more than 10% of the beam time on a beamline or sector for two years or more.

(Source: www.aps.anl.gov/Users/Scientific_Access/Partner_User_Information/index.html

APS Beamline Guide*

*As of 4.4.07. Source: http://beam.aps.anl.gov/pls/apsweb/beamline_display_pkg.beamline_dir

KEY: 2.3, 2.7, 3.0, 3.3, 5.5: undulator period; BM: Bending Magnet; CPU: Circularly Polarized Undulator; CU: Canted undulator; GU: General Users

Beamline	Sector	Discipline	Supported Techniques	Source	Status
1-BM-B,C	XOR	Materials science, physics, chemistry	Powder diffraction, x-ray reflectivity	BM	Operational/GU
1-ID-C	XOR	Materials science, physics, chemistry	High-energy x-ray scattering	3.3	Operational/GU
2-BM-B	XOR	Physics, life sciences	Phase-contrast imaging, tomography, microdiffraction, general diffraction	BM	Operational/GU
2-ID-B	XOR	Physics	Microfluorescence, phase-contrast imaging, coherent x-ray scattering	5.5-cm und.	Operational/GU
2-ID-D	XOR	Life sciences, materials science, enviro. science	Microfluorescence, microdiffraction, micro-x-ray absorption fine structure(XAFS)	3.3	Operational/GU
2-ID-E	XOR	Life sciences, enviroscience	Microfluorescence	3.3, 5.5	Operational/GU
3-ID-B,C,D	XOR	Physics	Nuclear resonant scattering, inelastic x-ray scattering	2.7 (x 2)	Operational/GU
4-ID-C	XOR	Physics, materials science	Photoemission electron microscopy, x-ray photoemission spectroscopy, magnetic circular dichroism (soft x-ray), x-ray magnetic linear dichroism, magnetic x-ray scattering, anomalous & resonant scattering (soft x-ray)	CPU (canted)	Operational/GU
4-ID-D	XOR	Physics	Magnetic circular dichroism (soft x-ray), anomalous & resonant scattering (hard x-ray), magnetic x-ray scattering	3.5 (canted)	Operational/GU
5-BM-C	DND-CAT	Materials science, polymer science	Tomography, powder diffraction	BM	Operational/GU
5-BM-D	DND-CAT	Materials science, polymer science	XAFS, high-energy x-ray diffraction	BM	Operational/GU
5-ID	DND-CAT	Materials science, polymer science	Macromolecular crystallography powder diffraction, small-angle x-ray scattering (SAXS), x-ray optics development/techniques, inorganic crystallography	3.3	Operational/GU
6-ID-B,C	MU-CAT	Materials science	Liquid scattering, magnetic x-ray scattering, powder diffraction, surface diffraction	3.3	Operational/GU
6-ID-D	MU-CAT	Materials science	High-energy x-ray diffraction, magnetic x-ray scattering, powder diffraction, pair-distribution function	3.3	Operational/GU
7-ID-B,C,D	XOR	Materials science, chemistry, atomic physics	Time-resolved x-ray scattering, radiography, time-resolved XAFS	3.3	Operational/GU
8-BM-B	NE-CAT	Life sciences	Macromolecular crystallography, multiwavelength anomalous dispersion	BM	Operational/GU
8-ID-E	XOR	Materials science, physics polymer science	Intensity fluctuation spectroscopy, x-ray reflectivity, x-ray photon correlation spectroscopy, grazing-incidence SAXS	3.3	Operational/GU
8-ID-I	XOR	Materials science, physics polymer science	Intensity fluctuation spectroscopy, coherent x-ray scattering, SAXS, x-ray photon correlation spectroscopy	3.3	Operational/GU
9-BM-B,C	XOR/CMC	Materials science	XAFS	BM	Operational/GU
9-ID-B,C	XOR/CMC	Materials science	Liquid scattering, SAXS, general diffraction, inelastic x-ray scattering	3.3	Operational/GU
10-BM-A	MR-CAT	Materials science	TBD	BM	Reprogramming

Continued on page 182

APS Beamline Guide (cont'd.)

10-ID-B	MR-CAT	Materials science, enviro. science, chemistry	Microfluorescence, XAFS, diffraction anomalous fine structure, microXAFS	3.3	Operational/GU
11-BM-B	XOR/BESSRC	Materials science, chemistry, physics	Powder diffraction	BM	Commissioning
11-ID-B	XOR/BESSRC	Materials science, chemistry, enviro. science	High-energy x-ray diffraction, pair distribution function	3.3	Operational/GU
11-ID-C	XOR/BESSRC	Materials science, physics, geoscience, chemistry	High-energy x-ray diffraction	3.3	Operational/GU
11-ID-D	XOR/BESSRC	Materials science, geoscience	XAFS, general diffraction	3.3	Operational/GU
12-BM-B	XOR/BESSRC	Materials science, geoscience	XAFS, powder diffraction, general diffraction	BM	Operational/GU
12-ID-B,C,D	XOR/BESSRC	Materials science, chemistry, physics	SAXS, wide-angle x-ray scattering, grazing incidence SAXS	3.3	Operational/GU
13-BM-C,D	GSECARS	Geoscience, enviro. science	Tomography, XAFS, high-pressure diamond anvil cell, high-pressure multi-anvil press	BM	Operational/GU
13-ID-C,D	GSECARS	Geoscience, enviro. science	Microfluorescence, XAFS, microdiffraction, surface diffraction, high-pressure diamond anvil cell, high-presure multi-anvil press, inelastic x-ray scatterring	3.3	Operational/GU
14-BM-C	BioCARS	Life sciences	Macromolecular crystallography, fiber diffraction large unit cell crystallography	BM	Operational/GU
14-BM-D	BioCARS	Life sciences	Macromolecular crystallography, multiwavelength anomalous dispersion	BM	Operational/GU
14-ID-B	BioCARS	Life sciences	Macromolecular crystallography, multiwavelength anomalous dispersion, time-resolved x-ray scattering, Laue crystallography	2.3 & 2.7	Operational/GU
15-ID-B,C,D	ChemMatCARS	Materials science, chemistry	Anomalous & resonant scattering (hard x-ray), small-angle & wide-angle x-ray scattering, liquid scattering, time-resolved x-ray scattering, microdiffraction	3.3	Operational/GU
16-BM-B	HP-CAT	Materials science, geoscience	Powder diffraction, single-crystal diffraction	BM	Operational/GU
16-ID-B	HP-CAT	Materials science, geoscience	Microdiffraction, powder diffraction, single-crystal diffraction, high-pressure diamond anvil cell	3.3	Operational/GU
16-ID-D	HP-CAT	Materials science, geoscience	Nuclear resonant scattering, general diffraction, inelastic x-ray scattering, x-ray Raman scattering, x-ray emission spectroscopy	3.3	Operational/GU
17-BM-B	IMCA-CAT	Life science, physics	Macromolecular crystallography, multiwavelength anomalous dispersion	BM	Operational/GU
17-ID-B	IMCA-CAT	Life sciences	Macromolecular crystallography, multiwavelength anomalous dispersion	3.3	Operational/GU
18-ID-D	Bio-CAT	Life sciences	Microfluorescence, microdiffraction, SAXS, microXAFS, fiber diffraction	3.3	Operational/GU
19-BM-D	SBC-CAT	Life sciences	Macromolecular crystallography, multiwavelength anomalous dispersion	BM	Operational/GU
19-ID-D	SBC-CAT	Life sciences	Macromolecular crystallography, multiwavelength anomalous dispersion	3.3	Operational/GU

Continued on next page

APS Beamline Guide (cont'd.)

20-BM-B	XOR/PNC	Materials science, enviro. science	Microfluorescence, XAFS, microXAFS	BM	Operational/GU
20-ID-B,C	XOR/PNC	Materials science enviro. science, chemistry	Microfluorescence, XAFS, time-resolved XAFS, microXAFS, x-ray Raman scattering, surface diffraction	3.3	Operational/GU
21-ID-D	LS-CAT	Life sciences	Macromolecular crystallography, multiwavelength anomalous dispersion	CU	Commissioning
21-ID-E	LS-CAT	Life sciences	Macromolecular crystallography, multiwavelength anomalous dispersion	CU	Construction
21-ID-F	LS-CAT	Life sciences	Macromolecular crystallography, multiwavelength anomalous dispersion		
21-ID-G	LS-CAT	Life sciences	multiwavelength anomalous dispersion multiwavelength anomalous dispersion		
22-BM-D	SER-CAT	Life sciences	Macromolecular crystallography	BM	Operational
22-ID-D	SER-CAT	Life sciences	Macromolecular crystallography, multiwavelength anomalous dispersion	3.3	Operational
23-BM-B	GM/CA-CAT	Life sciences	Macromolecular crystallography, multiwavelength anomalous dispersion	BM	Construction
23-ID-B	GM/CA-CAT	Life sciences	Macromolecular crystallography, multiwavelength anomalous dispersion	CU	Operational
23-ID-D	GM/CA-CAT	Life sciences	Macromolecular crystallography, multiwavelength anomalous dispersion	CU	Operatiional/GU
24-BM-B	NE-CAT	Life sciences	Macromolecular crystallography, multiwavelength anomalous dispersion	BM	Construction
24-ID-C	NE-CAT	Life sciences	Macromolecular crystallography, multiwavelength anomalous dispersion	CU	Operational/GU
24-ID-D	NE-CAT	Life sciences	Macromolecular crystallography, multiwavelength anomalous dispersion	3.3	Operational/GU
24-ID-E	NE-CAT	Life sciences	Macromolecular crystallography, multiwavelength anomalous dispersion	CU	Construction
26-ID-C	XOR/CNM	Nanoscience, energy science, materials science, optics development	Fluorescence, diffraction, & transmission imaging, tomography, SAXS, polarization dependent scattering	3.3	Commissioning
0 30-ID-B,C	XOR/IXS	Materials science, physics, geoscience	Medium-energy resolution inelastic x-ray scattering, high-energy-resolution inelastic x-ray scattering, nuclear inelastic x-ray scattering	3.0	Operational/GU
31-ID-D	SGX-CAT	Life sciences	Macromolecular crystallography	3.3	Operational/GU
32-ID-B	XOR	Materials science	Phase contrast imaging	3.3	Commissioning
33-BM-B,C	XOR/UNI	Materials science, physics, chemistry	Anomalous & resonant scattering (hard x-ray), diffuse x-ray scattering, powder diffraction, x-ray reflectivity, general diffraction, grazing incidence diffraction	BM	Operational/GU
33-ID-D	XOR/UNI	Materials science, physics, chemistry	Anomalous & resonant scattering (hard x-ray), diffuse x-ray scattering, x-ray reflectivity, surface diffraction, general diffraction, grazing incidence diffraction	3.3	Operational/GU
34-ID-C	XOR/UNI	Materials science, physics	Coherent x-ray scattering, microdiffraction	3.3	Operational/GU
34-ID-E	XOR/UNI	Materials science, physics	Coherent x-ray scattering & diffraction, microbeam diffraction, microprobe	3.3	Operational/GU

APS Committees (cont'd.)

APS Scientific Advisory Committee*

Jens Als-Nielsen
Professor, Københavns Universitet
Niels Bohr Institutet Ørsted Laboratoriet

Michelle V. Buchanan
Associate Laboratory Director for Physical Sciences; Director, Molecular and Cellular Systems
Oak Ridge National Laboratory

Slade G. Cargill
Fairchild Professor and Department Chair, Dept. of Materials Science and Engineering
Lehigh University

Howard M. Einspahr
Research Fellow, Bristol-Myers Squibb (retired)

Patrick D. Gallagher
Director, NIST Center for Neutron Research
National Institute of Standards and Technology

Peter Ingram
Department of Pathology
Duke University Medical Center

Miles V. Klein
Research Professor of Physics and Center for Advanced Study Professor of Physics Emeritus
University of Illinois at Urbana-Champaign

Richard Leapman
Acting Director; Chief, Supramolecular Structure and Function Resource, DBEPS, ORS, NIH
National Institutes of Health

Piero A. Pianetta
Professor (Research) of Stanford Synchrotron Radiation Laboratory (SSRL) and Electrical Engineering
Deputy Director, SSRL
Stanford Linear Accelerator Center

Michael R. Wasielewski
Professor, Department of Chemistry
Northwestern University

Glenn Waychunas
Scientist, Molecular Geochemistry and Nanogeoscience Group Leader
Lawrence Berkeley National Laboratory

Donald J. Weidner
Professor, Department of Earth and Space Sciences,
State University of New York, Stony Brook

Pierre E. Wiltzius *(Chair)*
Director, Beckman Institute for Advanced Science and Technology,
Professor, Departments of Materials Science & Engineering and Physics
University of Illinois at Urbana-Champaign

Wei Yang
Chief, Structural Biology and Cell Signaling Section
National Institutes of Health Laboratory of Molecular Biology

Source: www.aps.anl.gov/About/Committees/Scientific_Advisory_Committee/Members/index.html

APS Users Organization Steering Committee*

Simon Billinge *Michigan State University*
Keith Brister *Northwestern University*
Paul Evans *University of Wisconsin-Madison*
Millicent Firestone *Argonne National Laboratory*
Thomas Gog *Argonne National Laboratory*
Barbara Golden *Purdue University*
Tim Graber *The University of Chicago*
Gene Ice *Oak Ridge National Laboratory (Chair)*
Laurence Lurio *Northern Illinois University*
Simon Mochrie *Yale University*
Anne Mulichak *The University of Chicago*
David Reis *University of Michigan*
Ward Smith *Argonne National Laboratory*
Ex-Officio
Carol Thompson, *Northern Illinois University*

Source: http://www.aps.anl.gov/About/Committees/APS_Users_Organization/Members/index.html

Partner User Council*

Dean R. Haeffner *sector 1, Argonne National Laboratory*
Qun Shen *sector 2, Argonne National Laboratory*
Wolfgang Sturhahn *sector 3, Argonne National Laboratory*
George Srajer *sector 4, Argonne National Laboratory*
Denis T. Keane *sector 5, Northwestern University*
Douglas S. Robinson *sector 6, Iowa State University*
Roy Clarke *sector 7, University of Michigan*
Simon G.J. Mochrie *sector 8, Yale University*
J. Kent Blasie *sector 9, University of Pennsylvania*
Bruce A. Bunker *sector 10, University of Notre Dame (Chair)*
Mark A. Beno *sector 11, Argonne National Laboratory*
Randall E. Winans *sector 12, Argonne National Laboratory*
Mark L. Rivers *sector 13, The University of Chicago*
Keith Moffat *sector 14, The University of Chicago*
P. James Viccaro *sector 15, The University of Chicago*
David Mao *sector 16, Carnegie Institution of Washington*
Lisa J. Keefe *sector 17, The University of Chicago*
Thomas C. Irving *sector 18, Illinois Institute of Technology*
Andrzej Joachimiak *sector 19, Argonne National Laboratory*
Edward A. Stern *sector 20, University of Washington*
Wayne F. Anderson *sector 21, Northwestern University*
John J. Chrzas *sector 22, University of Georgia*
Robert F. Fischetti *sector 23, Argonne National Laboratory*
Malcolm Capel *sector 24, Cornell University*
G. Brian Stephenson *sector 26, Argonne National Laboratory*
John P. Hill *sector 30, Brookhaven National Laboratory*
Kevin L. D'Amico *sector 31, SGX Pharmaceuticals, Inc.*
Paul Zschack *sectors 33-34, Argonne National Laboratory*

Source: www.aps.anl.gov/About/Committees/Partner_Users_Council/Members/puc_list.htm

* As of 4.07

APS Committees (cont'd.)

Proposal Review Panels*

High Pressure
Thomas Duffy *Princeton University (Chair)*
Dion Heinz *The University of Chicago*
Kurt Leinenweber *Arizona State University*
Jie Li *University of Illinois at Urbana-Champaign*
Guoyin Shen *Carnegie Institution of Washington*
Viktor Struzhkin *Carnegie Institution of Washington*

Instrumentation
Peter Eng *The University of Chicago (Chair)*
Sarvjit Shastri *Argonne National Laboratory*
Don Walko *Argonne National Laboratory*

Imaging/Microbeam
Yong Chu *Argonne National Laboratory (Chair)*
George Cody *Carnegie Institution of Washington*
George Flynn *State University of New York, Plattsburgh*
Tatjana Paunesku *Northwestern University*
Steve Sutton *The University of Chicago*

Macromolecular Crystallography
Arnon Lavie *University of Illinois at Chicago*
Anne Mulichak *The University of Chicago*
John Rose *University of Georgia (Chair)*

Scattering/Applied Materials
Sean Brennan *Stanford Linear Accelerator Center (Chair)*
Jeff Eastman *Argonne National Laboratory*
George Fenske *Argonne National Laboratory*
Ersan Ustundag *Iowa State University*

Scattering/Condensed Matter
Peter Abbamonte *Brookhaven National Laboratory*
Tai-Chang Chiang *University of Illinois at Urbana-Champaign*
Valery Kiryukhin *Rutgers University*
Karl Ludwig *Boston University (Chair)*
Christie Nelson *Brookhaven National Laboratory*
David Vaknin *Iowa State University*

Scattering/Chemistry/Biology/ Environmental Science
Peter Burns *University of Notre Dame*
Jean-Francois Gaillard *Northwestern University*
Ursula Perez-Salas *Argonne National Laboratory*
Lois Pollack *Cornell University*
Mark Schlossman *University of Illinois at Chicago (Chair)*

Small-angle Scattering
Yvonne Akpalu *Rensselaer Polytechnic Institute*
Peter Jemian *Argonne National Laboratory (Chair)*
Joanna Krueger *University of North Carolina at Charlotte*
Byeongdu Lee *Argonne National Laboratory*
Surya K. Mallapragada *Ames Laboratory*
Hiro Tsuruta *Stanford Linear Accelerator Center*

Spectroscopy (EXAFS)
Mark Antonio *Argonne National Laboratory*
Daniel Haskel *Argonne National Laboratory (Chair)*
Jeff Kortright *Lawrence Berkeley National Laboratory*
Matt Newville *The University of Chicago*
Ingrid Pickering *University of Saskatchewan*
Bruce Ravel *Argonne National Laboratory*

Source: www.aps.anl.gov/About/Committees/Proposal_Review_Panel/index.html

Beam Time Allocation Committees*

Macromolecular Crystallography
Joseph Brunzelle *Northwestern University*
Robert Fischetti *Argonne National Laboratory (Chair)*
Vukica Srajer *The University of Chicago*

All Other Science
Carlo Segre *Illinois Institute of Technology*
Denis Keane *Northwestern University*
G. Brian Stephenson *Argonne National Laboratory*
Jonathan Tischler *Oak Ridge National Laboratory (Chair)*

Source: http://www.aps.anl.gov/About/Committees/Beam_Time_Allocation_ Committees/index.html

APS InterCAT Technical Workgroup*

Subgroups:

Top-off Subgroup: John Quintana, \
Argonne National Laboratory

Beam Stability Subgroup: Paul Zschack,
Argonne National Laboratory

Detector Subgroup: Thomas Irving,
Illinois Institute of Technology

Diagnostics Subgroup: Jonathan Lang,
Argonne National Laboratory

Source: www.aps.anl.gov/About/Committees/InterCAT_Technical_Workgroup/index.html

Safety Committees

Safety Overview Committee

Safety Committee for Design Reviews

Radiation Safety Policy & Procedures Committee

Radiation Safety Shielding Committee for Design Reviews

Chemical Safety Committee

Electrical Safety Committee

Laser Safety Committee

* As of 4.07

APS Publications 2006*

***As of 4.6.07.**

NOTE: For reasons of space, conference papers/proceedings, technical reports, and abstracts are not included here. For those records, and for an up-to-date list of all records, see the searchable, publicly available database of all APS-related scientific and technical publications from APS users and personnel at:
http://beam.aps.anl.gov/pls/apsweb/pub_v2_0006.review_start_page

Journal Articles

Carnie Abajian, Amy C. Rosenzweig, "Crystal structure of yeast Sco1," J. Biol. Inorg. Chem. 11, 459-466 (2006). DOI: 10.1007/s00775-006-0096-7

Rebecca J. Abergel, Jeffrey A. Warner, David K. Shuh, Kenneth N. Raymond, "Enterobactin protonation and iron release: Structural characterization of the salicylate coordination shift in ferric enterobactin," J. Am. Chem. Soc. 128 (27), July, 8920-8931 (2006). DOI: 10.1021/ja062046j

Nermeen W. Aboelella, Benjamin F. Gherman, Lyndal M.R. Hill, John T. York, Nicole Holm, Victor G. Young, Jr., Christopher J. Cramer, William B. Tolman, "Effects of Thioether Substituents on the O[subscript 2] Reactivity of [beta]-Diketiminate-Cu(I) Complexes: Probing the Role of the Methionine Ligand in Copper Monooxygenases," J. Am. Chem. Soc. 128 (10), 3445-3458 (2006). DOI: 10.1021/ja057745v

Kristl L. Adams, Stanislav Tsoi, Jiusheng Yan, Stephen M. Durbin, Anant K. Ramdas, William A. Cramer, Wolfgang Sturhahn, E. Ercan Alp, Charles Schulz, "Fe Vibrational Spectroscopy of Myoglobin and Cytochrome f," J. Phys. Chem. B 110 (1), 530-536 (2006). DOI: 10.1021/jp053440r

Kim K. Adkison, David G. Barrett, David N. Deaton, Robert T. Gampe, Anne M. Hassell, Stacey T. Long, Robert B. McFadyen, Aaron B. Miller, Larry R. Miller, J. Alan Payne, Lisa M. Shewchuk, Kevin J. Wells-Knecht, Derril H. Willard, Jr., Lois L. Wright, "Semicarbazone-based inhibitors of cathepsin K, are they prodrugs for aldehyde inhibitors?," Bioorg. Med. Chem. Lett. 16 (4), February, 978-983 (2006). DOI: 10.1002/chin.200620217

Johnson Agniswamy, Machal J. Nagiec, Mengyao Liu, Peter Schuck, James M. Musser, Peter D. Sun, "Crystal Structure of Group A Streptococcus Mac-1: Insight into Dimer-Mediated Specificity for Recognition of Human IgG," Structure 14, February, 225-235 (2006). DOI: 10.1016/j.str.2005.10.012

K.H. Ahn, T. Lookman, A.R. Bishop, "Model for strain-induced metal-insulator phase coexistence in colossal magnetoresistive perovskite manganites (invited)," J. Appl. Phys. 99 (8), 08A703-1-08A703-3 (2006). DOI: 10.1063/1.2162337

Victoria E. Ahn, Paul Leyko, Jean-Rene Alatti, Lu Chen, Gilbert G. Prive, "Crystal structures of saposins A and C," Protein Sci. 15, 1849-1857 (2006). DOI: 10.1110/ps.062256606

A. Abdul Ajees, G.M. Anantharamaiah, Vinod K. Mishra, M. Mahmood Hussain, H.M. Krishna Murthy, "Crystal structure of human apolipoprotein A-1: Insights into its protective effect against cardiovascular diseases," Proc. Natl. Acad. Sci. USA 103 (7), February, 2126-2131 (2006). DOI: 10.1073/pnas.0506877103

A. Abdul Ajees, K. Gunasekaran, John E. Volanakis, Sthanamv L. Narayana, Girish J. Kotwal, H.M.Krishna Murthy, "The structure of complement C3b provides insights into complement activiation and regulation," Nature 444, November, 221-225 (2006). DOI: 10.1038/nature05258

David L. Akey, Jeffrey D. Kittendorf, John W. Giraldes, Robert A. Fecik, David H. Sherman, Janet L. Smith, "Structural basis for macrolactonization by the pikromycin thioesterase," Nat. Chem. Biol. 2, 537-542 (2006). DOI: 10.1038/nchembio824

R. Al-Raoush, K. Alshibli, "Calculation of local void ratios of granular materials from three-dimensional images," Physica A 359 (1-4), February, 713-728 (2006).

Hui-wang Al, J. Nathan Henderson, S. James Remington, Robert E. Campbell, "Directed evolution of a monomeric, bright and photostable version of Clavularia cyan fluorescent protein: structural characterization and applications in fluorescence imaging," Biochem. J. 400 (3), December, 531-540 (2006). DOI: 10.1042/BJ20060874

Mehdi Ali, Kanishka Marasinghe, Robert Hart, Chris Benmore, Nathaniel Wyckoff, Richard Brow, "Normalisation and sample composition analysis of binary rare earth phosphate glasses by high energy x-ray scattering," Phys. Chem. Glasses-B 47 (2), April, 146-149 (2006).

R.W. Alkire, Michael Molitsky, F.J. Rotella, N.E.C. Duke, Patrick M. De Lurgio, John Lee, Tim Madden, "Development of a real-time timing-shutter performance monitor for protein crystallography," J. Synchrotron Rad. 13, 408-410 (2006). DOI: 10.1107/S0909049506027610

Johnjeff Alvarado, Anita Ghosh, Tyler Janovitz, Andrew Jauregui, Miriam S. Hasson, David Avram Sanders, "Origin of Exopolyphosphatase Processivity: Fusion of an ASKHA Phosphotransferase and a Cyclic Nucleotide Phosphodiesterase Homolog," Structure 14 (8), July, 1263-1272 (2006). DOI: 10.1016/j.str.2006.06.009

Kyle J. Alvine, Diego Pontoni, Oleg G. Shpyrko, Peter S. Pershan, David J. Cookson, Kyusoon Shin, Thomas P. Russell, Markus Brunnbauer, Francesco Stellacci, Oleg Gang, "Solvent Mediated Assembly of Nanoparticles Confined in Mesoporous Alumina," Phys. Rev. B 73 (9), March, 125412-1-125412-9 (2006). DOI: 10.1103/PhysRevB.73.125412

Kandi K. D. Amarasinghe, Artem G. Evidokimov, Kevin Xu, Cynthia M. Clark, Matthew B. Maier, Anil Srivastava, Anny-Odile Colson, Gina S. Gerwe, George E. Stake, Brian W. Howard, Matthew E. Pokross, Jeffrey L. Gray, Kevin G. Peters, "Design and synthesis of potent, non-peptidic inhibitors of HPTP Beta," Bioorg. Med. Chem. Lett. 16 (16), August, 4252-4256 (2006). DOI: 10.1016/j.bmcl.2006.05.074

George M. Amulele, Murli H. Manghnani, Maddury Somayazulu, "Application of radial x-ray diffraction to determine the hydrostatic equation of state and strength of TiB[subscript]2 up to 60 GPa," J. Appl. Phys. 99 (2), January, 023522-1-023522-6 (2006).

B.J. Anderson, V. Gopalakrishnan, S. Ramakrishnan, C.F. Zukoski, "Scattering for mixtures of hard spheres: Comparison of total scattering intensities with model," Phys. Rev. E 73 (3), March, 031407-1-031407-13 (2006).

Thomas E. Angelini, Ramin Golestanian, Robert H. Coridan, John C. Butler, Alexandre Beraud, Michael Krisch, Harald Sinn, Kenneth S. Schweizer, Gerard C.L. Wong, "Counterions between charged polymers exhibit liquid-like organization and dynamics," Proc. Natl. Acad. Sci. USA 103 (21), May, 7962-7967 (2006). DOI: 10.1073/pnas.0601435103

Brent A. Appleton, Justin Brooks, Arianna Loregian, David J. Filman, Donald M. Coen, James M. Hogle, "Crystal Structure of the Cytomegalovirus DNA Polymerase Subunit UL44 in Complex with the C Terminus from the Catalytic Subunit: Differences in Structure and Function Relative to Unliganded UL44," J. Biol. Chem. 281 (8), February, 5224-5232 (2006).

Y. Arai, A. Lanzirotti, S.R. Sutton, M. Newville, J. Dyer, D.L. Sparks, "Spatial and Temporal Variability of Arsenic Solid-State Speciation in Historically Lead Arsenate Contaminated Soils," Environ. Sci. Technol. 40 (3), February, 673-678 (2006). DOI: 10.1021/es051266e

D.A. Arena, E. Vescovo, C.-C. Kao, Y. Guan, W.E. Bailey, "Weakly coupled motion of individual layers in ferromagnetic resonance," Phys. Rev. B 74 (6), August, 064409-1-064409-7 (2006). DOI: 10.1103/PhysRevB.74.064409

B.D. Arhatari, A.G. Peele, K.A. Nugent, F. De Carlo, "Quality of the reconstruction in x-ray phase contrast tomography," Rev. Sci. Instrum. 77, 063709-1-063709-6 (2006). DOI: 10.1063/1.2214667

Palaniappa Arjunan, Martin Sax, Andrew Brunskill, Krishnamoorthy Chandrasekhar, Natalia Nemeria, Sheng Zhang, Frank Jordan, William Furey, "A Thiamin-bound, Pre-decarboxylation Reaction Intermediate Analogue in the Pyruvate Dehydrogenase E1 Subunit Induces Large Scale Disorder-to-Order Transformations in the Enzyme and Reveals Novel Structural Features in the Covalently Bound Adduct," J. Biol. Chem. 281 (22), June, 15296-15303 (2006).

Nathan N. Aronson, Jr, Brian A. Halloran, Mikhail F. Alexeyev, Xioayin E. Zhou, Yujun Wang, Edward J. Meehan, Liqing Chen, "Mutation of a Conserved Tryptophan in the Chitin-Binding Cleft of Serratia marcescens Chitinase A Enhances Transglycosylation," Biosci. Biotech. Bioch. 70 (1), January, 243-251 (2006).

Ernest Asante-Appiah, Sangita Patel, Caroline Desponts, Jillian M. Taylor, Cheuk Lau, Claude Dufresne, Michel Therien, Rick Friesen, Joseph W. Becker, Yves Leblanc, Brian P. Kennedy, Giovanna Scapin, "Conformation-assisted Inhibition of Protein-tyrosine Phosphatase-1B Elicits Inhibitor Selectivity over T-cell Protein-tyrosine Phosphatase," J. Biol. Chem. 281 (12), March, 8010-8015 (2006). DOI: 10.1074/jbc.M511827200

George V. Avvakumov, John R. Walker, Sheng Xue, Patrick J. Finerty Jr., Farrell Mackenzie, Elena M. Newman, Sirano Dhe-Paganon, "Amino-terminal dimerization, NRDP1-rhodanese interaction, and inhibited catalytic domain conformation of the ubiquitin-specific protease 8 (USP8)," J. Biol. Chem. 281 (49), December, 38061-38070 (2006). DOI: 10.1074/jbc.M606704200

S.S. Babu, E.D. Specht, M.L. Santella, G.E. Ice, S.A. David, "In-Situ Observations of Oxidation and Phase Stability in Cast Nickel-Based Intermetallic Alloys," Metall. Mater. Trans. A 37A (1), January, 195-205 (2006).

Helen K. Baca, Carlee Ashley, Eric Carnes, Deanna Lopez, Jeb Flemming, Darren Dunphy, Seema Singh, Zhu Chen, Nanguo Liu, Hongyou Fan, Gabriel P. Lopez, Susan M. Brozik, Margaret Werner-Washburne, C. Jeffrey Brinker, "Cell-Directed Assembly of Lipid-Silica Nanostructures Providing Extended Cell Viability," Science 313, July, 337-341 (2006). DOI: 10.1126/science.1126590

Scott Bailey, Richard A. Wing, Thomas A. Steitz, "The Structure of T. aquaticus DNA Polymerase III Is Distinct from Eukaryotic Replicative DNA Polymerases," Cell 126 (5), September, 893-904 (2006). DOI: 10.1016/j.cell.2006.07.027

D.A. Baker, M.A. Paesler, G. Lucovsky, S.C. Agarwal, P.C. Taylor, "Application of Bond Constraint Theory to the Switchable Optical Memory Material Ge[subscript 2]Sb[subscript 2]Te[subscript 5]," Phys. Rev. Lett. 96 (25), July, 255501-1-255501-3 (2006). DOI: 10.1103/PhysRevLett.96.255501

D.A. Baker, M.A. Paesler, G. Lucovsky, P.C. Taylor, "EXAFS study of amorphous Ge[subscript 2]Sb[subscript 2]Te[subscript 5]," J. Non-Cryst. Solids 352 (9-20), June, 1621-1623 (2006).

Dorian K. Balch, David C. Dunand, "Load partitioning in aluminum syntactic foams containing ceramic microspheres," Acta Mater. 54 (6), April, 1501-1511 (2006).

R. Bandyopadhyay, D. Liang, J.L. Harden, R.L. Leheny, "Slow dynamics, aging, and glassy rheology in soft and living matter," Solid State Commun. 139 (11), September, 589-598 (2006). DOI: http://dx.doi.org/10.1016/j.ssc.2006.06.023

Anirban Banerjee, Webster L. Santos, Gregory L. Verdine, "Structure of a DNA glycosylase searching for lesions," Science 311 (5764), February, 1153-1157 (2006). DOI: 10.1126/science.112028

Duhee Bang, Alexey V. Gribenko, Valentina Tereshko, Anthony A. Kossiakoff, Stephen B. Kent, George I. Makhatadze, "Dissecting the energetics of protein [alpha]-helix C-cap termination through chemical protein synthesis," Nat. Chem. Biol. 2, 139-143 (2006). DOI: 10.1038/nchembio766

Joona Bang, Sumeet Jain, Zhibo Li, Timothy P. Lodge, Jan Skov Pedersen, Ellina Kesselman, Yeshayahu Talmon, "Sphere, Cylinder, and Vesicle Nanoaggregates in Poly(styrene-b-isoprene) Diblock Copolymer Solutions," Macromolecules 39 (3), February, 1199-1208 (2006). DOI: 10.1021/ma052023+

Oleg M. Barabash, Rozaliya I. Barabash, Stan A. David, Gene E. Ice, "Residual Stresses, Thermomechanical Behavior and Interfaces in the Weld Joint of Ni-based Superalloys," Adv. Eng. Mater. 8 (3), 202-205 (2006). DOI: 10.1002/adem.200500239

R.I. Barabash, O.M. Barabash, G.E. Ice, C. Roder, S. Figge, S. Einfeldt, D. Hommel, T.M. Katona, J.S. Speck, S.P. DenBaars, R.F. Davis, "Characterization of crystallographic properties and defects via X-ray microdiffraction in GaN (0001) layers," Phys. Status Solidi. a. 203 (1), 142-148 (2006). DOI: 10.1002/pssa.200563503

R.I. Barabash, G.E. Ice, W. Liu, C. Roder, S. Figge, S. Einfeldt, D. Hommel, T.M. Katona, J.S. Speck, S.P. DenBaars, R.F. Davis, "Mapping Misorientation and Crystallographic Tilt in GaN Layers Via Polychromatic Microdiffraction," Phys. Status Solidi. b. 243 (7), 1508-1513 (2006). DOI: 10.1002/pssb.200565442

R.I. Barabash, C. Roder, G. E. Ice, S. Einfeldt, J. D. Budai, O. M. Barabash, S. Figge, D. Hommel, "Spatially Resolved Distribution of Dislocations and Crystallographic Tilts in GaN Layers Grown on Si(111) Substrates by Maskless Cantilever Epitaxy," J. Appl. Phys. 100 (5), September, 053103-053103-11 (2006). DOI: 10.1063/1.2234807

Simon R. Bare, George E. Mickelson, Frank S. Modica, Andrzej Z. Ringwelski, N. Yang, "Simple flow through reaction cells for in situ transmission and fluorescence x-ray-absorption spectroscopy of heterogeneous catalysts," Rev. Sci. Instrum. 77, 023105-1-023105-6 (2006). DOI: 10.1063/1.2168685

Cyril Barinka, Graham Parry, Jennifer Callahan, David E. Shaw, Alice Kuo, Khalil Bdeir, Douglas B. Cines, Andrew Mazar, Jacek Lubkowski, "Structural Basis of Interaction between Urokinase-type Plasminogen Activator and its Receptor," J. Mol. Biol. 363 (2), October, 482-495 (2006). DOI: 10.1016/j.jmb.2006.08.063

A.S. Barnard, Y. Xiao, Z. Cai, "Modelling the shape and orientation of ZnO nanobelts," Chem. Phys. Lett. 419 (4-6), February, 313-316 (2006). DOI: 10.1016/j.cplett.2005.12.003

Peter J. Barnard, Louise E. Wedlock, Murray V. Baker, Susan J. Berners-Price, David A. Joyce, Brian W. Skelton, James H. Steer, "Luminescence Studies of the Intracellular Distribution of a Dinuclear Gold(I) N-Heterocyclic Carbene Complex," Angew. Chem. Int. Ed. 45 (36), September, 5966-5970 (2006). DOI: 10.1002/anie.200601526

David G. Barrett, John G. Catalano, David N. Deaton, Anne M. Hassell, Stacey T. Long, Aaron B. Miller, Larry R. Miller, John A. Ray, Vicente Samano, Lisa M. Shewchuk, Kevin J. Wells-Knecht, Derril H. Willard Jr., Lois L. Wright, "Novel, potent P[superscript 2]–P[superscript 3] pyrrolidine derivatives of ketoamide-based cathepsin K inhibitors," Bioorg. Med. Chem. Lett. 16 (6), March, 1735-1739 (2006). DOI: 10.1016/j.bmcl.2005.11.101

William A. Barton, Dorothea Tzvetkova-Robev, Edward P. Miranda, Momchil V. Kolev, Kanagalaghatta R. Rajashankar, Juha P. Himanen, Dimitar B. Nikolov, "Crystal structures of the Tie2 receptor ectodomain and the angiopoietin-2-Tie2 complex," Nat. Struct. Mol. Biol. 13 (6), June, 524-532 (2006). DOI: 1038/nsmb1101

A. Baruth, D.J. Keavney, J.D. Burton, K. Janicka, E.Y. Tsymbal, L. Yuan, S.H. Liou, S. Adenwalla, "Origin of the interlayer exchange coupling in [Co/Pt]/NiO/[Co/Pt] multilayers studied with XAS, XMCD, and micromagnetic modeling," Phys. Rev. B 74, 054419-1-054419-13 (2006). DOI: 10.1103/PhysRevB.74.054419

Vinod K. Batra, William A. Beard, David D. Schock, Joshep M. Krahn, Lars C. Pedersen, Saumel H. Wilson, "Magnesium-Induced Assembly of a Complete DNA Polymerase Catalytic Complex," Structure 14, April, 757-766 (2006). DOI: 10.1016/j.str.2006.01.011

Timothy H. Bayburt, Yelena V. Grinkova, Stephen G. Sligar, "Assembly of single bacteriorhodopsin trimers in bilayer nanodiscs," Arch. Biochem. Biophys. 450, 215-222 (2006). DOI: 10.1016/j.abb.2006.03.013

Douglas G. Beak, Nicholas T. Basta, Kirk G. Scheckel, Samuel J. Traina, "Bioaccessibility of Arsenic(V) Bound to Ferrihydrtie Using a Simulated Gastrointestinal System," Environ. Sci. Technol. 40 (4), February, 1364-1370 (2006). DOI: 10.1021/es0516413

Douglas G. Beak, Nicholas T. Basta, Kirk G. Scheckel, Samuel J. Traina, "Bioaccessibility of Lead Sequestered to Corundum and Ferrihydrite in a Simulated Gastrointestinal System," J. Environ. Qual. 35, December, 2075-2083 (2006). DOI: 10.2134/jeq2005.0467

Lluis Bellsolell, Park F. Cho-Park, Francis Poulin, Nahum Sonenber, Stephen K. Burley, "Two Structurally Atypical HEAT Domains in the C-Terminal Portion of Human eIF4G Support Binding to eIF4A and Mnk1," Structure 14, May, 913-923 (2006). DOI: 10.1016/j.str.2006.03.012

J. V. Bernier, M. P. Miller, "A direct method for the determination of the mean orientation-dependent elastic strains and stresses in polycrystalline materials from strain pole figures," J. Appl. Crystallogr. 39, June, 358-368 (2006). DOI: doi:10.1107/S0021889806009873

J. V. Bernier, M. P. Miller, D. E. Boyce, "A novel optimization-based pole-figure inversion method: comparison with WIMV and maximum entropy methods," J. Appl. Crystallogr. 39, October, 697-713 (2006). DOI: doi:10.1107/S002188980602468X

Andrew J. Berry, Alistair C. Hack, John A. Mavrogenes, Matthew Newville, Stephen R. Sutton, "A XANES study of Cu speciation in high-temperature brines using synthetic ß uid inclusions," Am. Mineral. 91 (11-12), November, 1773-1782 (2006).

Pradip K. Bhowmik, Haesook Han, Ivan K. Ndedeltchev, James J. Cebe, Shin-Woong Kang, Satyendra Kumar, "Synthesis and characterization of ionic liquids: viologen bis{tetrakis[3,5-bis(trifluoromethyl)phenyl]borate} salts," Liq. Cryst. 33 (8), August, 891-906 (2006). DOI: 10.1080/02678290600871598

Wen Bian, Hong Wang, Ian McCullough, Gerald Stubbs, "WCEN: a computer program for initial processing of fiber diffraction patterns," J. Appl. Crystallogr. 39 (5), October, 752-756 (2006). DOI: 10.1107/S0021889806025386

Patrick Bilder, Sandra Lightle, Graeme Bainbridge, Jeffrey Ohren, Barry Finzel, Fang Sun, Susan Holley, Loola Al-Kassim, Cindy Spessard, Michael Melnick, Marcia Newcomer, Grover L. Waldrop, "The Structure of the Carboxyltransferase Component of Acetyl-CoA Carboxylase Reveals a Zinc-Binding Motif Unique to the Bacterial Enzyme," Biochemistry-US 45 (6), February, 1712-1722 (2006). DOI: 10.1021/bi0520479

Osman Bilsel, C. Robert Matthews, "Molecular dimensions and their distributions in early folding intermediates," Curr. Opin. Struct. Biol. 16 (1), February, 86-93 (2006). DOI: 10.1016/j.sbi.2006.01.007

Eduard Bitto, Craig A. Bingman, Gary E. Wesenberg, Jason G. McCoy, George N. Phillips, Jr., "Structure of Pyrimidine 5'-Nucleotidase Type 1: Insight into Mechanism of Action and Inhibition During Lead Poisoning," J. Biol. Chem. 281 (29), July, 20521-20529 (2006). DOI: 10.1074/jbc.M602000200

D.R. Black, J.C. Woicik, M. Erdtmann, T.A. Langdo, "Imaging defects in strained-silicon thin films by glancing-incidence x-ray topography," Appl. Phys. Lett. 88, 224102-1-224102-3 (2006). DOI: 10.1063/1.2209411

Karen M. Boeshans, Fang Liu, Guihong Peng, William Idler, Shyh-Ing Jang, Lyuben Marekov, Lindsay Black, Bijan Ahvazi, "Purification, crystallization and preliminary X-ray diffraction analysis of the phage T4 vertex protein gp24 and its mutant forms," Protein Expres. Purif. 49, 235-243 (2006). DOI: 10.1016/j.pep.2006.05.021

Karen M. Boeshans, Ronald Wolf, Christopher Voscopoulos, William Gillette, Dominic Esposito, Timothy C. Mueser, Stuart H. Yuspa, Bijan Ahvazi, "Purification, crystallization and preliminary X-ray diffraction of human S100A15," Acta Crystallogr. F 62, 467-470 (2006). DOI: 10.1107/S1744309106012838

M. Borland, "A Super-Bright Storage Ring Alternative to an Energy Recovery Linac," Nucl. Instrum. Methods A 557 (1), February, 230-235 (2006). DOI: 10.1016/j.nima.2005.10.076

Michael Borland, "Evaluation of the Possibility of Upgrading the Advanced Photon Source to an Energy Recovery Linac," Nucl. Instrum. Methods A 557 (1), February, 224-229 (2006). DOI: 10.1016/j.nima.2005.10.075

Zachary A. Bornholdt, B.V. Venkataram Prasad, "X-ray structure of influenza virus NS1 effector domain," Nat. Struct. Mol. Biol. 13 (6), June, 559-560 (2006). DOI: 10.1038/nsmb1099

Emma Borrego-Diaz, Frederic Kerff, Sung Haeng Lee, Francois Ferron, Yu Li, Roberto Dominguez, "Crystal structure of the actin-binding domain of [alpha]-actinin 1: Evaluating two competing actin-binding models," J. Struct. Biol. 155 (2), August, 230-238 (2006). DOI: 10.1016/j.jsb.2006.01.013

Jurgen Bosch, Stewart Turley, Thomas M. Daly, Stephen M. Bogh, Michelle L. Villasmil, Claudia Roach, Na Zhou, Joanne M. Morrisey, Akhil B. Vaidya, Lawrence W. Bergman, Wim G.J. Hol, "Structure of the MTIP–MyoA complex, a key component of the malaria parasite invasion motor," Proc. Natl. Acad. Sci. USA 103 (13), March, 4852-4857 (2006). DOI: 10.1073/pnas.0510907103

Maria Victoria Botuyan, Joseph Lee, Irene M. Ward, Ja-Eun Kim, James R. Thompson, Junjie Chen, Georges Mer, "Structural Basis for the Methylation State-Specific Recognition of Histone H4-K20 by 53BP1 and Crb2 in DNA Repair," Cell 127 (7), December, 1361-1373 (2006). DOI: 10.1016/j.cell.2006.10.043

Christina R. Bourne, M.G. Finn, Adam Zlotnick, "Global structural changes in hepatitis B virus capsids induced by the assembly effector HAP1," J. Virol. 80 (22), November, 11055-11061 (2006). DOI: 10.1128/JVI.00933-06

Sébastien Boutet, Ian K. Robinson, "Radiation driven collapse of protein crystals," J. Synchrotron Rad. 13 (1), January, 1-7 (2006). DOI: 10.1107/S0909049505038811

Brian R. Bowman, Carmen M. Moure, Bhakti M. Kirtane, Robert L. Welschhans, Kaoru Tominaga, Olivia M. Pereira-Smith, Florante A. Quiocho, "Multipurpose MRG Domain Involved in Cell Senescence and Proliferation Exhibits Cell Senescence and Proliferation Exhibits," Structure 14, January, 151-158 (2006). DOI: 10.1016/j.str.2005.08.019

Brian R. Bowman, Robert L. Welschhans, Hariharan Jayaram, Nigel D. Stow, Valerie G. Preston, Florante A. Quiocho, "Structural Characterization of the UL25 DNA-Packaging Protein from Herpes Simplex Virus Type 1," J. Virol. 80 (5), March, 2309-2317 (2006). DOI: 10.1128/JVI.80.5.2309-2317.2006

Randall Bramley, Kenneth Chiu, Tharaka Devadithya, Nisha Gupta, Charles Hart, John C. Huffman, Kianosh Huffman, Yu Ma, Donald F. McMullen, "Instrument Monitoring, Data Sharing, and Archiving Using Common Instrument Middleware Architecture (CIMA)," J. Chem. Inf. Model. 46 (3), 1017-1025 (2006). DOI: 10.1021/ci050368l

Sylvia Braselmann, Vanessa Taylor, Haoran Zhao, Su Wang, Catherine Sylvain, Muhammad Balloum, Kunbin Qu, Ellen Herlaar, Angela Lau, Chi Young, Brian R. Wong, Scott Lovell, Thomas Sun, Gary Park, Ankush Argade, Stipo Jurcevic, Polly Pine, Rajinder Singh, Elliott B. Grossbard, Donald G. Payan, Esteban S. Masuda, "R406, an Orally Available Syk Kinase Inhibitor Blocks Fc Receptor Signaling and Reduces Immune Complex-Mediated Inflammation," J. Pharmacol. Exp. Ther. 319, August, 998-1008 (2006). DOI: 10.1124/jpet.106.109058

Chad A. Brautigam, R. Max Wynn, Jacinta L. Chuang, Mischa Machius, Diana R. Tomchick, David T. Chuang, "Structural Insight into Interactions between Dihydrolipoamide Dehydrogenase (E3) and E3 Binding Protein of Human Pyruvate Dehydrogenase Complex," Structure 14, March, 611-621 (2006). DOI: 10.1016/j.str.2006.01.001

Tom J. Brett, Valerie Legendre-Guillemin, Peter S. McPherson, Daved H. Fremont, "Structural definition of the F-actin–binding THATCH domain from HIP1R," Nat. Struct. Mol. Biol. 13 (2), February, 121-130 (2006).

A.H. Brothers, D.C. Dunand, "Density-graded cellular aluminum," Adv. Eng. Mater. 8 (9), September, 805-809 (2006). DOI: 10.1002/adem.200600074

Michael I. Bruce, Natasha N. Zaitseva, Brian W. Skelton, "Some complexes containing Pt-C[subscript 5]-Co[subscript 3] fragments: Molecular structure of trans-Pt{C[triple bond]CC[triple bond]C-[mu subscript 3]-C[Co[subscript 3]([mu]-dppm)(CO)[subscript 6](PPh[subscript 3])]}[subscript 2](PPh[subscript3])[subscript 2] determined using synchrotron radiation," J. Organomet. Chem. 691 (4), February, 759-764 (2006).

Todd A. Brugel, Jennifer A. Maier, Michael P. Clark, Mark Sabat, Adam Golebiowski, Roger G. Bookland, Matthew J. Laufersweiler, Steven K. Laughlin, John C. VanRens, Biswanath De, Lily C. Hsieh, Marlene J. Mekel, Michael J. Janusz, "Development of N-2,4-pyrimidine-N-phenyl-N'-phenyl ureas as inhibitors of tumor necrosis factor alpha (TNF-[alpha]) synthesis. Part 1," Bioorg. Med. Chem. Lett. 16 (13), July, 3510-3513 (2006). DOI: 10.1016/j.bmcl.2006.03.095

M.L. Brusseau, S. Peng, G. Schnaar, M.S. Costanza-Robinson, "Relationships among air-water interfacial area, capillary pressure, and water saturation for a sandy porous medium," Water Resour. Res. 42 (W0350), March, W03501-W03505 (2006). DOI: 10.1029/2005WR004058

Craig L. Bukll, Tetsuya Kawashima, Paul F. McMillan, Denis Machon, Olga Shebanova, Dominik Daisenberger, Emmanuel Soignard, E. Takayama-Muromachi, Laurent C. Chapon, "Crystal structure and high-pressure properties of [gamma]-Mo[subscript 2]N determined by neutron powder diffraction and X-ray diffraction," J. Solid State Chem. 179, 1762-1767 (2006). DOI: 10.1016/j.jssc.2006.03.011

T. Buonassisi, A.A. Istratov, M.D. Pickett, M. Heuer, J.P. Kalejs, G. Hahn, M.A. Marcus, B. Lai, Z. Cai, S.M. Heald, T.F. Ciszek, R.F. Clark, D.W. Cunningham, A.M. Gabor, R. Jonczyk, S. Narayanan, E. Sauar, E.R. Weber, "Chemical natures and distributions of metal impurities in multicrystalline silicon materials," Prog. Photovolt. Res. Appl. 14 (8), 513-531 (2006). DOI: 10.1002/pip.690

T. Buonassisi, A.A. Istratov, M.D. Pickett, J.-P. Rakotoniaina, O. Breitenstein, M.A. Marcus, S.M. Heald, E.R. Weber, "Transition metals in photovoltaic-grade ingot-cast multicrystalline silicon: Assessing the role of impurities in silicon nitride crucible lining material," J. Cryst. Growth 287, 402-407 (2006). DOI: 10.1016/j.jcrysgro.2005.11.053

Andrew Burchat, David W. Borhani, David J. Calderwood, Gavin C. Hirst, Biqin Li, Robert F. Stachlewitz, "Discovery of A-770041, a src-family selective orally active lck inhibitor that prevents organ allograft rejection," Bioorg. Med. Chem. Lett. 16 (1), January, 118-122 (2006). DOI: 10.1016/j.bmcl.2005.09.039

Peta-Gaye Burnett, Christopher J. Daughney, Derek Peak, "Cd adsorption onto Anoxybacillus flavithermus: Surface complexation modeling and spectroscopic investigations," Geochim. Cosmochim. Acta 70 (21), November, 5253-5269 (2006). DOI: 10.1016/j.gca.2006.08.002

C.A. Burns, G. Vanko, H. Sinn, A. Alatas, E.E. Alp, A. Said, "Excitations of lithium ammonia complexes studied by inelastic x-ray scattering," J. Chem. Phys. 124, 024720-1-024720-7 (2006).

Eveline Bus, Jeffrey T. Miller, A. Jeremy Kropf, Roel Prins, Jeroen A. van Bokhoven, "Analysis of in situ EXAFS data of supported metal catalysts using the third and fourth cumulant," Phys. Chem. Chem. Phys. 8, 3248-3258 (2006). DOI: 10.1039/b605248g

Wei Bu, Philip J. Ryan, David Vaknin, "Ion distributions at charged aqueous surfaces by near-resonance X-ray spectroscopy," J. Synchrotron Rad. 13 (6), October, 459-463 (2006). DOI: 10.1107/S0909049506038635

W. Bu, D. Vaknin, A. Travesset, "How Accurate Is Poisson-Boltzmann Theory for Monovalent Ions near Highly Charged Interfaces?," Langmuir 22, 5673-5681 (2006). DOI: 10.1021/la053400e

E. Bychkov, M. Miloshova, D.L. Price, C.J. Benmore, A. Lorriaux, "Short, intermediate and mesoscopic range order in sulfur-rich binary glasses," J. Non-Cryst. Solids 352, 63-70 (2006). DOI: 10.1016/j.jnoncrysol.2005.11.002

A. Cady, D. Haskel, J.C. Lang, Z. Islam, G. Srajer, A. Ankudinov, G. Subìas, J. Garcìa, "Site-specific magnetization reversal studies of magnetite," Phys. Rev. B 73, April, 144416-1-144416-5 (2006). DOI: 10.1103/PhysRevB.73.144416

Mark B. Cannon, S. James Remington, "Re-engineering redox-sensitive green fluorescent protein for improved response rate," Protein Sci. 15, 45-57 (2006). DOI: 10.1110/ps.051734306

Christopher J. Carrell, Leslie A. Bush, F. Scott Mathews, Enrico Di Cera, "High resolution crystal structures of free thrombin in the presence of K[superscript +] reveal the molecular basis of monovalent cation selectivity and an inactive slow form," Biophys. Chem. 121 (3), June, 177-184 (2006). DOI: 10.1016/j.bpc.2005.12.008

P.D. Carr, F. Conlan, S. Ford, D.L. Ollis, I.G. Young, "An improved resolution structure of the human [beta] common receptor involved in IL-3, IL-5 and GM-CSF signalling which gives better definition of the high-affinity binding epitope," Acta Crystallogr. F 62, 509-513 (2006). DOI: 10.1107/S1744309106016812

J.P. Castellan, B.D. Gaulin, H.A. Dabkowska, A. Nabialek, G. Gu, X. Liu, Z. Islam, "Two- and three-dimensional incommensurate modulation in optimally-doped Bi[subscript 2]Sr[subscript 2]CaCu[subscript 2]O[subscript 8]+[delta]," Phys. Rev. B 73, 174505-1-174505-8 (2006). DOI: 10.1103/PhysRevB.73.174505

J.G. Catalano, J.P. McKinley, J.M. Zachara, S.M. Heald, S.C. Smith, G.E. Brown, Jr., "Changes in uranium speciation through a depth sequence of contaminated Hanford sediments," Environ. Sci. Technol. 40 (8), April, 2517-2524 (2006). DOI: 10.1021/es0520969

J.G. Catalano, C. Park, Z. Zhang, P. Fenter, "Termination and Water Adsorption at the [alpha]-Al[subscript 2]O[subscript3] (012)-Aqueous Solution Interface," Langmuir 22 (10), April, 4668-4673 (2006). DOI: 10.1021/la060177s

Jeffrey G. Catalano, Zhan Zhang, Paul Fenter, Michael J. Bedzyk, "Inner-sphere adsorption geometry of Se(IV) at the hematite 100)–water interface," J. Colloid Interf. Sci. 297 (2), 665-671 (2006). DOI: 10.1016/j.jcis.2005.11.026

Derek F. J. Ceccarelli, Hyun Kyu Song, Florence Poy, Michael D. Schaller, Michael J. Eck, "Crystal Structure of the FERM Domain of Focal Adhesion Kinase," J. Biol. Chem. 281 (1), January, 252-259 (2006). DOI: 10.1074/jbc.M509188200

J. Chakhalian, J.W. Freeland, G. Srajer, J. Strempfer, G. Khaliullin, J.C. Cezar, T. Charlton, R. Dalgliesh, C. Bernhard, G. Cristiani, H.-U. Habermeier, B. Keimer, "Magnetism at the interface between ferromagnetic and superconducting oxides," Nature Phys. 2, April, 244-248 (2006). DOI: 10.1038/nphys272

Chung-I Chang, Yogarany Chelliah, Dominika Borek, Dominique Mengin-Lecreulx, Johann Deisenhofer, "Structure of Tracheal Cytotoxin in Complex with a Heterodimeric Pattern-Recognition Receptor," Science 311, March, 1761-1764 (2006). DOI: 10.1126/science.1123056

Mitchell C.Y. Chan, Satoshi Karasawa, Hideaki Mizuno, Ivan Bosanac, Dona Ho, Gilbert G. Prive, Atsushi Miyawaki, Mitsuhiko Ikur, "Structural Characterization of a Blue Chromoprotein and Its Yellow Mutant from the Sea Anemone Cnidopus Japonicus," J. Biol. Chem. 281 (49), December, 37813-37819 (2006).

Esther Y.H. Chao, Jon L. Collins, Stephanie Gaillard, Aaron B. Miller, Liping Wang, Lisa A. Orband-Miller, Robert T. Nolte, Donald P. McDonnell, Timothy M. Willson, William J. Zuercher, "Structure-guided synthesis of tamoxifen analogs with improved selectivity for the orphan ERR[subscript gamma]," Bioorg. Med. Chem. Lett. 16 (4), February, 821-824 (2006). DOI: 10.1016/j.bmcl.2005.11.030

Karena W. Chapman, Peter J. Chupas, Cameron J. Kepert, "Compositional Dependence of Negative Thermal Expansion in the Prussian Blue Analogues M[superscript II]Pt[superscript IV](CN)[subscript 6] (M = Mn, Fe, Co, Ni, Cu, Zn, Cd)," J. Am. Chem. Soc. 128 (21), May, 7009-7014 (2006). DOI: 10.1021/ja060916r

Karena W. Chapman, Peter J. Chupas, Evan R. Maxey, James W. Richardson, "Direct observation of adsorbed H[subscript 2]-framework interactions in the Prussian Blue analogue Mn[superscript II][subscript 3][Co[superscript III](CN)[subscript 6]][subscript 2]: The relative importance of accessible coordination sites and van der Waals interactions," Chem. Comm. 38, October, 4013-4015 (2006). DOI: 10.1039/b607250j

Santanu Chaudhuri, Peter Chupas, Benjamin J. Morgan, Paul A. Madden, Clare P. Grey, "An atomistic MD simulation and pair-distribution-function study of disorder and reactivity of [alpha]-AlF[subscript 3] nanoparticles," Phys. Chem. Chem. Phys. 8, 5045-5055 (2006). DOI: 10.1039/b604750e

Melina Cheah, Paul J. Saines, Brendan J. Kennedy, "The Jahn–Teller distortion and cation ordering in the perovskite Sr[subscript 2]MnSbO[subscript 6]," J. Solid State Chem. 179, 1775-1781 (2006). DOI: 10.1016/j.jssc.2006.03.013

Celia C. H. Chen, Ying Han, Weiling Niu, Anna N. Kulakova, Andrew Howard, John P. Quinn, Debra Dunaway-Mariano, Osnat Herzberg, "Structure and Kinetics of Phosphonopyruvate Hydrolase from Voriovorax sp. Pal2: New Insight into the Divergence of Catalysis within the PEP Mutase/Isocitrate Lyase Superfamily," Biochemistry-US 45 (38), September, 11491-11504 (2006). DOI: 10.1021/bi061208l

Chen Chen, Ajay K. Saxena, William N. Simcoke, David N. Garboczi, Peter L. Pedersen, Young H. Ko, "Mitochondrial ATP Synthase: Crystal Structure of the Catalytic F[subscript 1] Unit in a Vanadate-Induced Transition-Like State and Implications for Mechanism," J. Biol. Chem. 281 (19), 13777-13783 (2006). DOI: 10.1074/jbc.M513369200

Hao Cheng, Kai Zhang, Joseph A. Libera, Monica Olvera de la Cruz, Michael J. Bedzyk, "Polynucleotide Adsorption to Negatively Charged Surfaces in Divalent Salt Solutions," Biophys. J. 90 (4), February, 1164-1174 (2006). DOI: 10.1529/biophysj.105.070649

G. Chen, J. Johnson, R. Weber, R. Nishikawa, S. Schweizer, P. Newman, D. MacFarlane, "Fluorozirconate-based nanophase glass ceramics for high-resolution medical X-ray imaging," J. Non-Cryst. Solids 352 (6-7), May, 610-614 (2006). DOI: 10.1016/j.jnoncrysol.2005.11.048

Gang Chen, Jacqueline Johnson, John Woodford, Stefan Schweizer, "Insights into phase formation in fluorochlorozirconate glass-ceramic storage phosphors," Appl. Phys. Lett. 88 (19), May, 191915-1-191515-7 (2006). DOI: 10.1063/1.2202688

Gang Chen, Dileep Singh, Osman Erylimaz, Jules Routbort, Bennett C. Larson, Wenjun Liu, "Depth-resolved residual strain in MoN/Mo nanocrystalline films," Appl. Phys. Lett. 89, October, 172104-1-172104-3 (2006). DOI: 10.1063/1.2364131

J.M. Chen, R.S. Liu, J.M. Lee, K.T. Lu, T.J. Yang, M.J. Kramer, R.W. McCallum, "High-resolution XANES study of Eu(Ba[subscript 1-x]R[subscript x])[subscript 2]Cu[subscript 3]O[subscript 7+delta](R = Eu, Pr)," New J. Phys. 8, September, 215-224 (2006). DOI: 10.1088/1367-2630/8/9/215

Kevin G. Chen, Julio C. Valencia, Barry Lai, Guofeng Zhang, Jill K. Paterson, Francois Rouzaud, Werner Berens, Stephen M. Wincovitch, Susan H. Garfield, Richard D. Leapman, Vincent J. Hearing, Michael M. Gottesman, "Melanosomal sequestration of cytotoxic drugs contributes to the intractability of malignant melanomas," Proc. Natl. Acad. Sci. USA 103 (26), 9903-9907 (2006). DOI: 10.1073/pnas.0600213103

Liqing Chen, Yujun Wang, David Wells, Diana Toh, Hunt Harold, Jing Zhou, Enrico DiGiammarino, Edward J. Meehan, "Structure of the SH3 domain of human osteoclast-stimulating factor at atomic resolution," Acta Crystallogr. F 62, 844-848 (2006). DOI: 10.1107/s1744309106030004

Peng R. Chen, Taeok Bae, Wade A. Williams, Erica M. Duguid, Phoebe A. Rice, Olaf Schneewind, Chuan He, "An oxidation-sensing mechanism is used by the global regulator MgrA in Staphylococcus aureus," Nat. Chem. Biol. 2, 591-595 (2006). DOI: 10.1038/nchembio820

Yu Chen, George Minasov, Tomer A. Roth, Fabio Prati, Brian K. Shoichet, "The Deacylation Mechanism of AmpC [beta]-Lactamase at Ultrahigh Resolution," J. Am. Chem. Soc. 128 (9), 2970-2976 (2006). DOI: 10.1021/ja056806m

Yong Chen, Yuting Yang, Feng Wang, Ke Wan, Kenichi Yamane, Yi Zhang, Ming Lei, "Crystal structure of human histone lysine-specific demethylase 1 (LSD1)," Proc. Natl. Acad. Sci. USA 103 (38), September, 13956-13961 (2006). DOI: 10.1073/pnas.0606381103

Zhi-wei Chen, Alshaimaa Hassan-Abdulah, Gouhua Zhao, Marilyn Schuman Jorn, F. Scott Mathews, "Heterotetrameric Sarcosine Oxidase: Structure of a Diflavin Metalloenzyme at 1.85 Å Resolution," J. Mol. Biol. 360 (5), 1000-1018 (2006). DOI: 10.1016/j.jmb.2006.05.067

G.N. Chesnut, D. Schiferl, B.D. Streetman, W.W. Anderson, "Diamond-anvil cell for radial x-ray diffraction," J. Phys. Condens. Matter 18, S1083-S1090 (2006). DOI: 10.1088/0953-8984/18/25/S15

Ya-Huei (Cathy) Chin, David L. King, Hyun-Seog Roh, Yong Wang, Steven M. Heald, "Structure and reactivity investigations on supported bimetallic Au–Ni catalysts used for hydrocarbon steam reforming," J. Catal. 244 (2), December, 153-162 (2006). DOI: 10.1016/j.jcat.2006.08.016

Malcolm H. Chisholm, Judith C. Gallucci, Hongfeng Yin, "Polymerization Special Feature: Cyclic esters and cyclodepsipeptides derived from lactide and 2,5-morpholinediones," Proc. Natl. Acad. Sci. USA 103 (42), October, 15315-15320 (2006). DOI: 10.1073/pnas.0602662103

Sung Yeun Choi, Byeongdu Lee, Daniel B. Carew, Marc Mamak, Frank C. Peiris, Scott Speakman, Naveen Chopra, Geoffrey A. Ozin, "3D hexagonal (R-3meso) mesostructured nanocrystalline titania thin films: synthesis and characterization," Adv. Funct. Mater. 16 (13), July, 1731-1738 (2006). DOI: 10.1002/adfm.200500507

Sunkyung Choi, Peggy A. O'Day, Nelson A. Rivera, Karl T. Mueller, Murthy A. Vairavamurthy, Supapan Seraphin, Jon Chorover, "Strontium Speciation during Reaction of Kaolinite with Simulated Tank-Waste Leachate: Bulk and Microfocused EXAFS Analysis," Environ. Sci. Technol. 40 (8), 2608-2614 (2006). DOI: 10.1021/es051869q

Y. Choi, D. Haskel, A. Cady, J.C. Lang, D.R. Lee, G. Srajer, J.S. Jiang, S.D. Bader, "Twisted magnetization states near the compensation temperature of Fe/Gd multilayers: Anisotropy and surface-termination effects," Phys. Rev. B 73 (17), 174401-1-174401-10 (2006). DOI: 10.1103/PhysRevB.73.174401

Y. Choi, D.R. Lee, J.W. Freeland, G. Srajer, V. Metluchko, "Layer-resolved study of magnetic interaction effects in heterostructure dot arrays," Appl. Phys. Lett. 88 (11), 112502-1-112502-3 (2006). DOI: 10.1063/1.2179116

Jill E. Chrencik, Alexei Brooun, Michelle L. Kraus, Michael I. Recht, Anand R. Kolatkar, Gye Won Han, Jan Marcus Seifert, Hans Widmer, Manfred Auer, Peter Kuhn, "Structural and Biophysical Characterization of the EphB4•EphrinB2 Protein-Protein Interaction and Receptor Specificity," J. Biol. Chem. 281 (38), September, 28185-28192 (2006). DOI: 10.1074/jbc.M605766200

B. Chung, S. Ramakrishnan, R. Bandyopadhyay, D. Liang, C.F. Zukoski, J.L. Harden, R.L. Leheny, "Microscopic Dynamics of Recovery in Sheared Depletion Gels," Phys. Rev. Lett. 96 (22), June, 228301-1-228301-4 (2006). DOI: 10.1103/PhysRevLett.96.228301

Inna Y. Churbanova, Andrey Tronin, Joseph Strzalka, Thomas Gog, Ivan Kuzmenko, Jonas S. Johansson, J. Kent Blasie, "Monolayers of a Model Anesthetic-Binding Membrane Protein: Formation, Characterization, and Halothane-Binding Affinity," Biophys. J. 90, May, 3255-3266 (2006). DOI: 10.1529/biophysj.105.072348

Ewa M. Ciszak, Anna Makal, Young S. Hong, Ananthalakshmy K. Vettaikkorumakankauv, Lioubov G. Korotchkina, Mulchand S. Patel, "How Dihydrolipoamide Dehydrogenase-binding Protein Binds Dihydrolipoamide Dehydrogenase in the Human Pyruvate Dehydrogenase Complex," J. Biol. Chem. 281, January, 648-655 (2006). DOI: 10.1074/jbc.M507850200

Craig S. Clements, Lars Kjer-Nielsen, Lyudmila Kostenko, James McCluskey, Jamie Rossjohn, "The production, purification and crystallization of a soluble form of the nonclassical MHC HLA-G: the essential role of cobalt," Acta Crystallogr. F 62 (1), January, 70-73 (2006). DOI: 10.1107/S1744309105041473

Sara E. Cnudde, Mary Prorok, Francis J. Castellino, James H. Geiger, "X-ray Crystallographic Structure of the Angiogenesis Inhibitor, Angiostatin, Bound to a Peptide from the Group A Streptococcal Surface Protein PAM," Biochemistry-US 45 (37), September, 11052-11060 (2006). DOI: 10.1021/bi060914j

Christopher L. Colbert, Qiong Wu, Paul J.A. Erbel, Kevin H. Gardner, Johann Deisenhofer, "Mechanism of substrate specificity in Bacillus subtilis ResA, a thioredoxin-like protein involved in cytochrome c maturation," Proc. Natl. Acad. Sci. USA 103 (12), March, 4410-4415 (2006). DOI: 10.1073/pnas.0600552103

Joanna Collingwood, Jon Dobson, "Mapping and characterization of iron compounds in Alzheimer's tissue," J. Alzheimers Dis. 10 (2-3), November, 215-222 (2006).

Linda Columbus, Jan Lipfert, Heath Klock, Ian Millett, Sebastian Doniach, Scott A. Lesley, "Expression, purification, and characterization of Thermotoga maritima membrane proteins for structure determination," Protein Sci. 15, May, 961-975 (2006). DOI: 10.1110/ps.051874706

Kenneth M. Comess, Jonathan D. Trumbull, Chang Park, Zehan Chen, Russell A. Judge, Martin J. Voorbach, Michael Coen, Lan Gao, Hua Tang, Peter Kovar, Xueheng Cheng, Mark E. Schurdak, Haiying Zhang, Tom Sowin, David J. Burns, "Kinase Drug Discovery by Affinity Selection/Mass Spectrometry (ASMS): Application to DNA Damage Checkpoint Kinase Chk1," J. Biomol. Screen. 11 (7), September, 755-764 (2006). DOI: 10.1177/1087057106289972

David Cookson, Nigel Kirby, Robert Knott, Myungae Lee, David Schultz, "Strategies for data collection and calibration with a pinhole-geometry SAXS instrument on a synchrotron beamline," J. Synchrotron Rad. 13 (6), November, 440-444 (2006). DOI: 10.1107/S0909049506030184

Michael S. Cosgrove, Katherine Bever, Jose L. Avalos, Shabazz Muhammad, Xiangbin Zhang, Cynthia Wolberger, "The Structural Basis of Sirtuin Substrate Affinity," Biochemistry-US 45 (24), May, 7511-7521 (2006). DOI: 10.1021/bi0526332

Jean-Francois Couture, Evys Collazo, Glenn Hauk, Raymond C. Trievel, "Structural basis for the methylation site specificity of SET7/9," Nat. Struct. Mol. Biol. 13 (2), February, 140-146 (2006). DOI: 10.1038/nsmb1045

Jean-Francois Couture, Glenn Hauk, Mark J. Thompson, G. Michael Blackburn, Raymond C. Trievel, "Catalytic Roles for Carbon-Oxygen Hydrogen Bonding in SET Domain Lysine Methyltransferases," J. Biol. Chem. 281 (28), July, 19280-19287 (2006). DOI: 10.1074/jbc.M602257200

William A. Cramer, Huamin Zhang, "Consequences of the structure of the cytochrome b[subscript 6]f complex for its charge transfer pathways," Biochim. Biophys. Acta 1757, 339-345 (2006). DOI: 10.1016/j.bbabio.2006.04.020

William A. Cramer, Huamin Zhang, Jiusheng Yan, Genji Kurisu, Janet L. Smith, "Transmembrane Traffic in the Cytochrome b[subscript 6]f Complex," Annu. Rev. Biochem. 75, 769-790 (2006). DOI: 10.1146/annurev.biochem.75.103004.142756

Jonathan C. Crowhurst, Alexander F. Goncharov, Babak Sadigh, Cheryl L. Evans, Peter G. Morrall, James L. Ferreira, A. J. Nelson, "Synthesis and Characterization of the Nitrides of Platinum and Iridium," Science 311, March, 1275-1278 (2006). DOI: 10.1126/science.1121813

Jun Cui, Yong S. Chu, Olugbenga O. Famodu, Yasubumi Furuya, Jae. Hattrick-Simpers, Richard D. James, Alfred Ludwig, Sigurd Thienhaus, Manfred Wuttig, Zhiyong Zhang, Ichiro Takeuchi, "Combinatorial search of thermoelastic shape-memory alloys with extremely small hysteresis width," Nat. Mater. 5, April, 286-290 (2006). DOI: 10.1038/nmat1593

J. Cui, Q. Huang, B.H. Toby, "Magnetic structure refinement with neutron powder diffraction data using GSAS: A tutorial," Powder Diffr. 21 (1), March, 71-79 (2006). DOI: 10.1154/1.2179805

Dimitrie Culcer, C. Lechner, R. Winkler, "Spin precession and alternating spin polarization in spin-3/2 hole systems," Phys. Rev. Lett. 97 (10), September, 106601-1-106601-3 (2006). DOI: 10.1103/PhysRevLett.97.106601

K.A. Culligan, D. Wildenschild, B.S.B. Christensen, W.G. Gray, M.L. Rivers, "Pore-scale Characteristics of Multiphase Flow in Porous Media: a Synchrotron-based CMT Comparison of Air-Water and Oil-Water Experiments," Adv. Water Resour. 29 (2), February, 227-238 (2006). DOI: 10.1016/j.advwatres.2005.03.021

Matthew J. Cuneo, Anita Changela, Joshua J. Warren, Lorena S. Beese, Homme W. Hillinga, "The Crystal Structure of a Thermophilic Glucose Binding Protein Reveals Adaptations that Interconvert Mono and Di-saccharide Binding Sites," J. Mol. Biol. 362, June, 259-270 (2006). DOI: 10.1016/j.jmb.2006.06.084

Liem X. Dang, Gregory K. Schenter, Vassiliki-Alexandra Glezakou, John L. Fulton, "Molecular Simulation Analysis and X-ray Absorption Measurement of Ca[superscript 2+], K[superscript +] and C[superscript -] Ions in Solution," J. Phys. Chem. B 110, 23644-23654 (2006). DOI: 10.1021/jp064661f

J.E. Daniels, J.L. Jones, T.R .Finlayson, "Characterization of domain structures from diffraction profiles in tetragonal ferroelastic ceramics," J. Phys. D 39, 5294-5299 (2006). DOI: 10.1088/0022-3727/39/24/029

Gautam Dantas, Alexander L. Watters, Bradley Lunde, Ziad Eletr, Nancy Isern, Jan Lipfert, Sebastian Doniach, Brian Kuhlman, Barry L. Stoddard, Gabriele Varani, David Baker, "Mistranslation of a Computationally Designed Protein Yields an Exceptionally Stable Homodimer: Implications for Protein Engineering and Evolution," J. Mol. Biol. 362 (5), October, 1004-1024 (2006). DOI: 10.1016/j-jmb.2006.07.092

Chittaranjan Das, Quyen Q. Hoang, Cheryl A. Kreinbring, Sarah J. Luchansky, Robin K. Meray, Soumya S. Ray, Peter T. Lansbury, Dagmar Ringe, Gregory A. Petsko, "Structural basis for conformational plasticity of the Parkinson's disease-associated ubiquitin hydrolase UCH-L1," Proc. Natl. Acad. Sci. USA 103 (12), March, 4675-4680 (2006). DOI: 10.1073/pnas.0510403103

Aniket Datar, Kaushik Balakrishnan, Xiaomei Yang, Xiaobing Zuo, Jialing Huang, Randy Oitker, Max Yen, Jincai Zhao, David M. Tiede, Ling Zang, "Linearly Polarized Emission of an Organic Semiconductor Nanobelt," J. Phys. Chem. B 110 (25), June, 12327-12332 (2006). DOI: 10.1021/jp061739j

Sacha De Carlo, Baoyu Chen, Timothy R. Hoover, Elena Kondrashkina, Eva Nogales, B. Tracy Nixon, "The structural basis for regulated assembly and function of the transcriptional activator NtrC," Gene Dev. 20, June, 1485-1495 (2006). DOI: 10.1101/gad.1418306

Martin D. de Jonge, Chanh Q. Tran, Christopher T. Chantler, Zwi Barnea, "Improved techniques for measuring x-ray mass attenuation coefficients," Opt. Eng. 45 (4), April, 046501-1-046501-8 (2006).

Alexandra M. Deaconescu, Anna L. Chambers, Abigail J. Smith, Bryce E. Nickels, Ann Hochschild, Nigel J. Savery, Seth A. Darst, "Structural Basis for Bacterial Transcription-Coupled DNA Repair," Cell 124 (3), February, 507-520 (2006). DOI: 10.1016/j.cell.2005.11.045

Aniruddha Deb, Uwe Bergmann, Stephen P. Cramer, Elton J. Cairns, "Local structure of LiNi[subscript 0.5]Mn[subscript 0.5]O[subscript 2] cathode material probed by in situ x-ray absorption spectroscopy," J. Appl. Phys. 99 (6), March, 063701-1-063701-10 (2006). DOI: 10.1063/1.2179198

G. Decker, M. Borland, D. Horan, A. Lumpkin, N. Sereno, B. Yang, S. Krinsky, "Transient Bunch Compression using Pulsed Phase Modulation in High-Energy Electron Storage Rings," Phys. Rev. Spec. Top., Accel. Beams 9, December, 120702 (2006).

Valentina F. Degtyareva, Olga Degtyareva, Ho-kwang Mao, Russell J. Hemley, "High-pressure behavior of CdSb: Compound decomposition, phase formation, and amorphization," Phys. Rev. B 73 (21), 214108-1-214108-8 (2006). DOI: 10.1103/PhysRevB.73.214108

Ranjit K. Deka, Chad A. Brautigam, Xiaofeng F. Yang, Jon S. Blevins, Mischa Machius, Diana R. Tomchick, Michael V. Norgard, "The PnrA (Tp0319; TmpC) Lipoprotein Represents a New Family of Bacterial Purine Nucleoside Receptor Encoded within an ATP-binding Cassette (ABC)-like Operon in Treponema pallidum," J. Biol. Chem. 281 (12), March, 8072-8081 (2006). DOI: 10.1074/jbc.M511405200

Alexey Dementiev, Jozsef Dobo, Peter G.W. Gettins, "Active Site Distortion is Sufficient for Proteinase Inhibition by Serpins: Structure of the Covalent Complex of [subscript alpha 1]-Proteinase Inhibitor with Porcine Pancreatic Elastase," J. Biol. Chem. 281 (6), February, 3452-3457 (2006). DOI: 10.1074/jbc.M510564200

Zygmunt S. Derewenda, Peter G. Vekilov, "Entropy and surface engineering in protein crystallization," Acta Crystallogr. D 62, January, 116-124 (2006). DOI: 10.1107/S0907444905035237

P. DeSanto, Jr., D.J. Buttrey, R.K. Grasselli, W.D. Pyrz, C.G. Lugmair, A.F. Volpe, Jr., T. Vogt, B.H. Toby, "Comparison of MoVTaTeO and MoVNbTeO M1 crystal chemistry," Top. Catal. 38 (1-3), July, 31-40 (2006). DOI: 10.1007/s11244-006-0068-8

William Desmarais, David L. Bienvenue, Krzysztof P. Bzymek, Gregory A. Petsko, Dagmar Ringe, Richard C. Holz, "The high-resolution structures of the neutral and the low pH crystals of aminopeptidase from Aeromonas proteolytica," J. Biol. Inorg. Chem. 11, 398-408 (2006). DOI: 10.1007/s00775-006-0093-x

M.D. Determan, L. Guo, P. Thiyagarajan, S.K. Mallapragada, "Supramolecular self-assembly of multiblock copolymers in aqueous solution," Langmuir 22 (4), February, 1469-1473 (2006). DOI: 10.1021/la0527691

B.B. Dhal, A.G. Peele, P.J. McMahon, F. De Carlo, K.A. Nugent, "Bending magnet source: A radiation source for X-ray phase contrast tomography," Radiat. Phys. Chem. 75 (11), November, 2004-2007 (2006).

Nancy L. Dietz, Chieh-Tsung Lo, Byeongdu Lee, Randall E. Winans, P. Thiyagarajan, "Self-assembly of diblock copolymers/Au nanoparticle nanocomposites in thin films," Microsc. Microanal. 12 (2), November, 606 CDROM (2006). DOI: 10.1017/S1431927606067936

Haitao Ding, Todd J. Green, Shanyun Lu, Ming Luo, "Crystal Structure of the Oligomerization Domain of the Phosphoprotein of Vesicular Stomatitis Virus," J. Virol. 80 (6), March, 2808-2814 (2006). DOI: 10.1128/JVI.80.6.2808-2814.2006

Y. Ding, P. Chow, H.-K. Mao, Y. Ren, C.T. Prewitt, "Determining thermal diffuse scattering of vanadium with x-ray transmission scattering," Appl. Phys. Lett. 88 (6), February, 061903-1-061903-3 (2006). DOI: 10.1063/1.2170142

Yang Ding, Yang Ren, Paul Chow, Jianzhong Zhang, Sven C. Vogel, Bjoern Winkler, Jian Xu, Yusheng Zhao, Ho-kwang Mao, "Pressure-induced long-range magnetic ordering in cobalt oxide," Phys. Rev. B 74 (14), 144101-1-144101-4 (2006). DOI: 10.1103/PhysRevB.74.144101

A. Umran Dogan, Y. zzettin Baris, Meral Dogan, Salih Emri, Ian Steele, Amira G. Elmishad, Michele Carbone, "Genetic Predisposition to Fiber Carcinogenesis Causes a Mesothelioma Epidemic in Turkey," Cancer Res. 66 (10), May, 5063-5068 (2006).

Daniel B. Drazkowski, Andre Lee, Timothy S. Haddad, David J. Cookson, "Chemical Substituent Effects on Morphological Transitions in Styrene-Butadiene-Styrene Triblock Copolymer Grafted with Polyhedral Oligomeric Silsesquioxanes," Macromolecules 39 (5), February, 1854-1863 (2006). DOI: 10.1021/ma0518813

Charles Dumont, Yoshitaka Matsumura, Seung Joong Kim, Jinsong Li, Elena Kondrashkina, Hiroshi Kihara, Martin Gruebele, "Solvent-tuning the collapse and helix formation time scales of [lambda][superscript*][subscript 6-85]," Protein Sci. 15, November, 2596-2604 (2006). DOI: 10.1110/ps.062257406

R.W. Dunford, E.P. Kanter, B. Kraessig, S.H. Southworth, L. Young, P.H. Mokler, Th. Stoehlker, S. Cheng, "Two-photon decay in gold atoms," Phys. Rev. A 74 (1), July, 012504-1-012504-11 (2006). DOI: 10.1103/PhysRevA.74.012504

R.W. Dunford, E.P. Kanter, B. Kraessig, S.H. Southworth, L. Young, P.H. Mokler, Th. Stoehlker, S. Cheng, A.G. Kochur, I.D. Petrov, "Coster-Kronig transition probability f₂₃ in gold atoms," Phys. Rev. A 74 (6), December, 062502-1-062502-6 (2006). DOI: 10.1103/PhysRevA.74.062502

John S. Edmonds, Masatoshi Morita, Peter Turner, Brian W. Skelton, Allan H. White, "Aerial oxidation of the glucocorticoid side-chain under pH control," Steroids 71 (1), January, 34-41 (2006).

Scott D. Edmondson, Anthony Mastracchio, Robert J. Mathvink, Jiafang He, Bart Harper, You-Jung Park, Maria Beconi, Jerry DiSalvo, George J. Eiermann, Huaibing He, Barbara Leting, Joseph F. Leone, Dorothy A. Levorse, Kathryn Lyons, Reshma A. Patel, Sangita B. Patel, Aleksandr Petrov, Giovanna Scapin, Jackie Shang, Ranabir Sinha Roy, Aaron Smith, Joseph K. Wu, Shiyao Xu, Bing Zhu, Nancy A. Thornberry, Anne E. Weber, "(2S,3S)-3-Amino-4-(3,3-difluoropyrrolidin-1-yl)-N,N-dimethyl-4-oxo-2-(4-[1,2,4]triazolo[1,5-a]-pyridin-6-ylphenyl)butanamide: a selective alpha-amino amide dipeptidyl peptidase IV inhibitor for the treatment of type 2 diabetes.," J. Med. Chem. 49 (12), 3614-3627 (2006). DOI: 10.1021/jm060015t

William F. Edmonds, Zhibo Li, Marc A. Hillmyer, Timothy P. Lodge, "Disk Micelles from Nonionic Coil-Coil Diblock Copolymers," Macromolecules 39 (13), June, 4526-4530 (2006). DOI: 10.1021/ma060633j

Martin Egli, Pradeep S. Pallan, Rekha Pattanayek, Christopher J. Wilds, Paolo Lubini, George Minasov, Max Dobler, Christian J. Leumann, Albert Eschenmoser, "Crystal structure of homo-DNA and nature's choice of pentose over hexose in the genetic system," J. Am. Chem. Soc. 128 (33), August, 10847-10856 (2006). DOI: 10.1021/ja062548x

Maria Elberry, Kunhung Xiao, Lothar Esser, Di Xia, Linda Yu, Chang-An Yu, "Generation, characterization and crystallization of a highly active and stable cytochrome bc[subscript 1] complex mutant from Rhodobacter sphaeroides," BBA-Bioenergetics 1757 (7), July, 835-840 (2006). DOI: 10.1016/j.bbabio.2006.05.031

J.W. Elmer, T.A. Palmer, E.D. Specht, "Direct observations of rapid diffusion of Cu in Au thin films using in situ x-ray diffraction," J. Vac. Sci. Technol. A 24 (4), June, 978-987 (2006). DOI: 10.1116/1.2204926

Thomas H. Epps, III, Frank S. Bates, "Effect of Molecular Weight on Network Formation in Linear ABC Triblock Copolymers," Macromolecules 39 (7), April, 2676-2682 (2006). DOI: 10.1021/ma052132o

D. Errandonea, J. Pellicer-Porres, F.J. Manjon, A. Segura, Ch. Ferrer-Roca, R.S. Kumar, O. Tschauner, J. Lopez-Solano, P. Rodriguez-Hernandez, S. Radescu, A. Mujica, A. Munoz, G. Aquilanti, "Determination of the high-pressure crystal structure of BaWO[subscript 4] and PbWO[subscript 4]," Phys. Rev. B 73 (22), 224103-1-224103-15 (2006). DOI: 10.1103/PhysRevB.73.224103

Lothar Esser, Xing Gong, Shaoqing Yang, Linda Yu, Chang-An Yu, Di Xia, "Surface-modulated motion switch: Capture and release of iron-sulfur protein in the cytochrome bc[subscript 1] complex," Proc. Natl. Acad. Sci. USA 103 (5), August, 13045-13050 (2006). DOI: 10.1073/pnas.0601149103

W.J. Evans, M.J. Lipp, C.-S. Yoo, H. Cynn, J.L. Herberg, R.S. Maxwell, M.F. Nicol, "Pressure-Induced Polymerization of Carbon Monoxide: Disproportionation and Synthesis of an Energetic Lactonic Polymer," Chem. Mater. 18 (10), 2520-2531 (2006). DOI: 10.1021/cm0524446

Artem G. Evdokimov, Matthew E. Pokross, Nikolay S. Egorov, Andrey G. Zaraisky, Ilya V. Yampolsky, Ekaterina M. Merzlyak, Andrey N. Shkoporov, Ian Sander, Konstantin A. Lukyanov, Dmitriy M. Chudakov, "Structural basis for the fast maturation of Arthropoda green fluorescent protein," EMBO reports 7, October, 1006-1012 (2006). DOI: 10.1038/sj.embor.7400787

Artem G. Evdokimov, Matthew Pokross, Richard Walter, Marlene Mekel, Brooke Cox, Chuiying Li, Randy Bechard, Frank Genbauffe, Ryan Andrews, Conrad Diven, Brian Howard, Vinit Rastogi, Jeffrey Gray, Matthew Maier, Kevin G. Peters, "Engineering the catalytic domain of human protein tyrosine phosphatase [beta] for structure-based drug discovery," Acta Crystallogr. D 62, December, 1435-1445 (2006). DOI: 10.1107/S0907444906037784

Guennadi Evmenenko, Haiding Mo, Sumit Kewalramani, Pulak Dutta, "Conformational rearrangements in interfacial region of polydimethylsiloxane melt films," Polymer 47, 878-882 (2006). DOI: 10.1016/j.polymer.2005.12.010

Christopher R. Faehnle, Xuying Liu, Alexander Pavlovsky, Ronald E. Viola, "The initial step in the archaeal aspartate biosynthetic pathway catalyzed by a monofunctional aspartokinase," Acta Crystallogr. F 62 (10), October, 962-966 (2006). DOI: 10.1107/S1744309106038279

P. Falus, M.A. Borthwick, S. Narayanan, A.R. Sandy, S.G.J. Mochrie, "Crossover from Stretched to Compressed Exponential Relaxations in a Polymer-Based Sponge Phase," Phys. Rev. Lett. 97 (2), August, 066102-1-066102-4 (2006). DOI: 10.1103/PhysRevLett.97.066102

P. Falus, L.B. Lurio, S.G.J. Mochrie, "Optimizing the signal-to-noise ratio for X-ray photon correlation spectroscopy," J. Synchrotron Rad. 13 (3), May, 253-259 (2006). DOI: 10.1107/S0909049506006789

Bin Fang, Peter I . Boross, Jozsef Tozser, Irene T. Weber, "Structural and Kinetic Analysis of Caspase-3 Reveals Role for S5 Binding Site in Substrate Recognition," J. Mol. Biol. 360 (3), June, 654-666 (2006). DOI: 10.1016/j.jmb.2006.05.041

G.J. Fan, L.F. Fu, Y.D. Wang, Y. Ren, H. Choo, P.K. Liaw, G.Y. Wang, N.D. Browning, "Uniaxial tensile plastic deformation of a bulk nanocrystalline alloy studied by a high-energy x-ray diffraction technique," Appl. Phys. Lett. 89 (10), September, 101918-1-101918-3 (2006). DOI: 10.1063/1.2348783

G.J. Fan, Y.D. Wang, L.F. Fu, H. Choo, P.K. Liaw, Y. Ren, N.D. Bowning, "Orientation-dependent grain growth in a bulk nanocrystalline alloy during the uniaxial compressive deformation," Appl. Phys. Lett. 88 (17), April, 171914-1-171914-3 (2006).

Gerrie P. Farman, John S. Walker, Pieter P. de Tombe, Thomas C. Irving, "Impact of osmotic compression on sarcomere structure and myofilament calcium sensitivity of isolated rat myocardium," Amer. J. Physiol. Heart. Circ. Physiol. 291, H1847-H1855 (2006). DOI: 10.1152/ajpheart.01237.2005

T.G. Fawcett, J. Faber, F. Needham, S.N. Kabekkodu, C.R. Hubbard, J.A. Kaduk, "Developments in formulation analyses by powder diffraction analysis," Powder Diffr. 21 (2), June, 105-110 (2006). DOI: 10.1154/1.2204958

Alena Fedarovich, Joshua Tomberg, Robert A. Nicholas, Christopher Davies, "Structure of the N-terminal domain of human CEACAM1: binding target of the opacity proteins during invasion of Neisseria miningitidis and N. gonorrhoeae," Acta Crystallogr. D 62, 971-979 (2006). DOI: 10.1107/S907444906020737

Brett Feeney, Cristina Pop, Paul Swartz, Carla Mattos, A. Clay Clark, "Role of Loop Bundle Hydrogen Bonds in the Maturation and Activity of (Pro)caspase-3," Biochemistry-US 45 (44), November, 13249-13263 (2006). DOI: 10.1021/bi0611964

Debbie S. Feeney, John W. Crawford, Tim Daniell, Paul D. Hallett, Naoise Nunan, Karl Ritz, Mark Rivers, Iain M. Young, "Three-dimensional microorganization of the soil-root-microbe system," Microbial Ecol. 52 (1), July, 151-158 (2006). DOI: 10.1007/s00248-006-9062-8

Richard L. Felts, Thomas J. Reilly, John J. Tanner, "Structure of Francisella tularensis AcpA: Prototype of a unique superfamily of acid phosphatases and phospholipases C," J. Biol. Chem. 281 (40), October, 30289-30298 (2006). DOI: 10.1074/jbc.M606391200

P. Fenter, J. G. Catalano, C. Park, Z. Zhang, "On the use of CCD area detectors for high-resolution specular X-ray reflectivity," J. Synchrotron Rad. 13 (4), July, 293-303 (2006). DOI: 10.1107/S0909049506018000

Paul Fenter, Changyong Park, Zhan Zhang, Steve Wang, "Observation of Subnanometre-high Surface Topography with X-ray Reflection Phase Contrast Microscopy," Nature Phys. 2 (10), October, 700-704 (2006). DOI: 10.1038/nphys419

Magali Ferrandon, Theodore Krause, "Role of the oxide support on the performance of Rh catalysts for the autothermal reforming of gasoline and gasoline surrogates to hydrogen," Appl. Catal. A-Gen. 311, September, 135-145 (2006). DOI: 10.1016/j.apcata.2006.06.014

D.M. Ferraro, D.J. Ferraro, S. Ramaswamy, A.D. Robertson, "Structures of Ubiquitin Insertion Mutants Support Site-specific Reflex Response to Insertion Hypothesis," J. Mol. Biol. 359, 390-402 (2006). DOI: 10.1016/j.jmb.2006.03.047

Daniel J. Ferraro, Adam L. Okerlund, Jonathan C. Mowers, S. Ramaswamy, "Structural Basis for Regioselectivity and Stereoselectivity of Product Formation by Naphthalene 1,2-Dioxygenase," J. Bacteriol. 188 (19), October, 6986-6994 (2006). DOI: 10.1128/JB.00707-06

Frederico M. Ferreira, Guillermo Mendoza-Hernandez, Maria Castaneda-Bueno, Ricardo Aparicio, Hannes Fischer, Mario L. Calcagno, Glaucius Oliva, "Structural Analysis of N-acetylglucosamine-6-phosphate Deacetylase Apoenzyme from Escherichia coli," J. Mol. Biol. 359, 308-321 (2006). DOI: 10.1016/j.jmb.2006.03.024

T.T. Fister, G.T. Seidler, C. Hamner, J.O. Cross, J.A. Soininen, J.J. Rehr, "Background proportional enhancement of the extended fine structure in nonresonant inelastic x-ray scattering," Phys. Rev. B 74, 214117-1-214117-7 (2006). DOI: 10.1103/PhysRevB.74.214117

T.T. Fister, G.T. Seidler, L. Wharton, A.R. Battle, T.B. Ellis, J.O. Cross, A.T. Macrander, W.T. Elam, T.A. Tyson, Q. Qian, "Multielement spectrometer for efficient measurement of the momentum transfer dependence of inelastic x-ray scattering," Rev. Sci. Instrum. 77 (6), 063901-1-063901-7 (2006). DOI: 10.1063/1.2204581

Mary X. Fitzgerald, Jeannie R. Rojas, John M. Kim, Gunter B. Kohlhaw, Ronen Marmorstein, "Structure of a Leu3-DNA Complex: Recognition of Everted CGG Half-Sites by a Zn[subscript 2]Cys[subscript 6] Binuclear Cluster Protein," Structure 14 (4), April, 725-735 (2006). DOI: 10/1016/j.str.2005.11.025

George J. Flynn, Pierre Bleuet, Janet Borg, John P. Bradley, Frank E. Brenker, Sean Brennan, John Bridges, Don E. Brownlee, Emma S. Bullock, Manfred Burghammer, Benton C. Clark, Zu Rong Dai, Charles P. Daghlian, Zahia Djouadi, Sirine Fakra, Tristan Ferroir, Christine Floss, Ian A. Franchi, Zack Gainsforth, Jean-Paul Gallien, Philippe Gillet, Patrick G. Grant, Giles A. Graham, Simon F. Green, Faustine Grossemy, Philipp R. Heck, Gregory F. Herzog, Peter Hoppe, Friedrich Horz, Joachim Huth, Konstantin Ignatyev, Hope A. Ishii, Koen Janssens, David Joswiak, Anton T. Kearsley, Hicham Khodja, Antonio Lanzirotti, Jan Leitner, Laurence Lemelle, Hugues Leroux, Katharina Luening, Glenn J. MacPherson, Kuljeet K. Marhas, Matthew A. Marcus, Graciela Matrajt, Tomoki Nakamura, Keiko Nakamura-Messenger, Tsukasa Nakano, Matthew Newville, Dimitri A. Papanastassiou, Piero Pianetta, William Rao, Christian Riekel, Frans J.M. Rietmeijer, Detlef Rost, Craig S. Schwandt, Thomas H. See, Julie Sheffield-Parker, Alexandre Simionovici, Ilona Sitnitsky, Christopher J. Snead, Frank J. Stadermann, Thomas Stephan, Rhonda M. Stroud, Jean Susini, Yoshio Suzuki, Stephen R. Sutton, Susan Taylor, Nick Teslich, D. Troadec, Peter Tsou, Akira Tsuchiyama, Kentaro Uesugi, Bart Vekemans, Edward P. Vicenzi, Laszlo Vincze, Andrew J. Westphal, Penelope Wozniakiewicz, Ernst Zinner, Michael E. Zolensky, "Elemental Compositions of Comet 81P/Wild 2 Samples Collected by Stardust," Science 314, December, 1731-1735 (2006). DOI: 10.1126/science.1136141

Pamela J. Focia, Joseph Gawronski-Salernoa, John S. Coon, V., Douglas M. Freymann, "Structure of a GDP:AlF[subscript 4] Complex of the SRP GTPases Ffh and FtsY, and Identification of a Peripheral Nucleotide Interaction Site," J. Mol. Biol. 360, 631-643 (2006). DOI: 10.1016/j.jmb.2006.05.031

D.D. Fong, A.M. Kolpak, J.A. Eastman, S.K. Streiffer, P.H. Fuoss, G.B. Stephenson, Carol Thompson, D.M. Kim, K.J. Choi, C.B. Eom, I. Grinberg, A.M. Rappe, "Stabilization of Monodomain Polarization in Ultrathin PbTiO[subscript 3] Films," Phys. Rev. Lett. 96 (12), March, 127601-1-127601-4 (2006). DOI: 10.1103/PhysRevLett.96.127601

Robert G. Ford, Richard T. Wilkin, Gina Hernandez, "Arsenic cycling within the water column of a small lake receiving contaminated ground-water discharge," Chem. Geol. 228 (1-3), April, 137-155 (2006). DOI: 10.1016/j.chemgeo.2005.11.021

Mark E. Fraley, Robert M. Garbaccio, Kenneth L. Arrington, William F. Hoffman, Edward S. Tasber, Paul J. Coleman, Carolyn A. Buser, Eileen S. Walsh, Kelly Hamilton, Christine Fernandes, Michael D. Schaber, Robert B. Lobell, Weikang Tao, Victoria J. South, Youwei Yan, Lawrence C. Kuo, Thomayant Prueksaritanont, Cathy Shu, Maricel Torrent, David C. Heimbrook, Nancy E. Kohl, Hans E. Huber, George D. Hartman, "Kinesin spindle protein (KSP) inhibitors. Part 2: The design, synthesis, and characterization of 2,4-diaryl-2,5-dihydropyrrole inhibitors of the mitotic kinesin KSP," Bioorg. Med. Chem. Lett. 16 (7), April, 1775-1779 (2006). DOI: 10.1016/j.bmcl.2006.01.030

M.R. Frank, C.E. Runge, H.P. Scott, S.J. Maglio, J. Olson, V.B. Prakapenka, G. Shen, "Experimental study of the NaCl–H[subscript 2]O system up to 28 GPa: Implications for ice-rich planetary bodies," Phys. Earth Planet. In. 155, 152-162 (2006). DOI: 10.1016/j.pepi.2005.12.001

Marie E. Fraser, Koto Hayakawa, Millicent S. Hume, David G. Ryan, Edward R. Brownie, "Interactions of GTP with the ATP-grasp Domain of GTP-specific Succinyl-CoA Synthetase," J. Biol. Chem. 281 (16), April, 11058-11065 (2006). DOI: 10.1074/jbc.M511785200

J.T. Fredrich, A.A. DiGiovanni, D.R. Noble, "Predicting macroscopic transport properties using microscopic image data," J. Geophys. Res. 111, March, B03201-1-B03201-14 (2006). DOI: 10.1029/2005JB003774

A.I. Frenkel, D.M. Pease, J.I. Budnick, P. Metcalf, E.A. Stern, P. Shanthakumar, T. Huang, "Strain-Induced Bond Buckling and Its Role in Insulating Properties of Cr-Doped V[subscript 2]O[subscript 3]," Phys. Rev. Lett. 97, November, 195502-1-195502-4 (2006). DOI: 10.1103/PhysRevLett.97.195502

Timothy A. Fritz, Jayalakshmi Raman, Lawrence A. Tabak, "Dynamic Association between the Catalytic and Lectin Domains of Human UDP-GalNAc:Polypeptide (alpha)-N-Acetylgalactosaminyltransferase-2," J. Biol. Chem. 281, March, 8613-8619 (2006). DOI: 10.1074/jbc.M513590200

John L. Fulton, Yongsheng Chen, Steve M. Heald, Mahalingam Balasubramanian, "Hydration and contact ion pairing of Ca[superscript 2+] with Cl[superscript –] in supercritical aqueous solution," J. Chem. Phys. 125, 094507-1-094507-10 (2006). DOI: 10.1063/1.2346548

Zhuji Fu, Sheng Chen, Michael R. Baldwin, Grant E. Boldt, Adam Crawford, Kim D. Janda, Joseph T. Barbieri, Jung-Ja P. Kim, "Light Chain of Botulinum Neurotoxin Serotype A: Structural Resolution of a Catalytic Intermediate," Biochemistry-US 45 (29), 8903-8911 (2006). DOI: 10.1021/bi060786z

Zhuji Fu, Jennifer A. Runquist, Farhad Forouhar, Munif Hussain, John F. Hunt, Henry M. Miziorko, Jung-Ja P. Kim, "Crystal Structure of Human 3-Hydroxy-3-methyl-glutaryl-CoA Lyase: Insights Into Catalysis and the Molecular Basis for Hydroxymethylglutaric Aciduria," J. Biol. Chem. 281 (11), March, 7526-7532 (2006). DOI: 10.1074/jbc.M506880200

Jianhua Gan, Yijun Gu, Yue Li, Honggao Yan, Xinhua Ji, "Crystal Structure of Mycobacterium tuberculosis Shikimate Kinase in Complex with Shikimic Acid and an ATP Analogue," Biochemistry-US 45, June, 8539-8545 (2006). DOI: 10.1021/bi0606290 S0006-2960(06)00629-5

Jianhua Gan, Joseph E. Tropea, Brian P. Austin, Donald L. Court, David S. Waugh, Xinhua Ji, "Structural Insight into the Mechanism of Double-Stranded RNA Processing by Ribonuclease III," Cell 124, January, 355-364 (2006). DOI: 10.1016/j.cell.2005.11.034

Lu Gan, Jeffrey A. Speir, James F. Conway, Gabriel Lander, Naiqian Cheng, Brian A. Firek, Roger W. Hendrix, Robert L. Duda, Lars Liljas, John E. Johnson, "Capsid Conformational Sampling in HK97 Maturation Visualized by X-Ray Crystallography and Cryo-EM," Structure 14 (11), November, 1655-1665 (2006). DOI: 10.1016/j.str.2006.09.006

Benoit Gannaz, Mark R. Antonio, Renato Chiarizia, Clement Hill, Gerard Cote, "Structural study of trivalent lanthanide and actinide complexes formed upon solvent extraction," Dalton T. 38, October, 4553-4562 (2006). DOI: 10.1039/b609492a

Miguel Garcia-Diaz, Katarzyna Bebenek, Joseph M. Krahn, Lars C. Pedersen, Thomas A. Kunkel, "Structural Analysis of Strand Misalignment during the DNA Synthesis by a Human DNA Polymerase," Cell 124 (2), January, 331-342 (2006). DOI: 10.1016/j.cell.2005.10.039

Milen Gateshki, Valeri Petkov, Taeghwan Hyeon, Jin Joo, Markus Niederberger, Yang Ren, "Interplay between the local structural disorder and the length of structual coherence in stabilizing the cubic phase in nanocrystalline ZrO[subcript 2]," Solid State Commun. 138 (6), May, 279-284 (2006). DOI: 10.1016/j.ssc.2006.03.013

James L. Gattis, A. Valance Washington, Maia M. Chisholm, Laura Quigley, Agnieszka Szyk, Daniel W. McVicar, Jacek Lubkowski, "The Structure of the Extracellular Domain of Triggering Receptor Expressed on Myeloid Cells Like Transcript-1 and Evidence for a Naturally Occurring Soluble Fragment," J. Biol. Chem. 281 (19), May, 13396-13403 (2006). DOI: 10.1074/jbc.M600489200

A.G. Gavriliuk, V.V. Struzhkin, I.S. Lyubutin, M.I. Eremets, I.A. Trojan, V.V. Artemov, "Equation of State and High Pressure Irreversible Amorphization in Y[subscript 3] Fe[subscript 5]O[subscript 12]," Pisma Zh ETF 83 (1), January, 41-45 (2006).

Cory J. Gerdts, Valentina Tereshko, Maneesh K. Yadav, Irina Dementieva, Frank Collart, Andrzej Joachimiak, Raymond C. Stevens, Peter Kuhn, Anthony Kossiakoff, Rustem F. Ismagilov, "Time-Controlled Microfluidic Seeding in nL-Volume Droplets To Separate Nucleation and Growth Stages of Protein Crystallization," Angew. Chem. Int. Ed. 45 (48), December, 8156-8160 (2006). DOI: 10.1002/anie.200602946

H. Giefers, S. Koval, G. Wortmann, W. Sturhahn, E.E. Alp, M.Y. Hu, "Phonon density of states of Sn in textured SnO under high pressure: Comparison of nuclear inelastic x-ray scattering spectra to a shell model," Phys. Rev. B 74, 094303-1-094303-12 (2006). DOI: 10.1103/PhysRevB.74.094303

Hubertus Giefers, Malcolm Nicol, "Equations of state of several iron–tin intermetallic compounds," J. Phys. Chem. Solids 67, 2027-2032 (2006). DOI: 10.1016/j.jpcs.2006.05.056

Hubertus Giefers, Malcolm Nicol, "High pressure X-ray diffraction study of all Fe-Sn intermetallic compounds and one Fe-Sn solid solution," J. Alloy Comp. 422, 132-144 (2006). DOI: 10.1016/j.jallcom.2005.11.061

Hubertus Giefers, Michael Pravica, Hanns-Peter Liermann, Wenge Yang, "Radiation-induced decomposition of PETN and TATB under pressure," Chem. Phys. Lett. 429, 304-309 (2006). DOI: 10.1016/j.cplett.2006.07.092

Benjamin Gilbert, Feng Huang, Zhang Lin, Carmen Goodell, Hengzhong Zhang, Jillian F. Banfield, "Surface Chemistry Controls Crystallinity of ZnS Nanoparticles," Nano Lett. 6 (4), April, 605-610 (2006). DOI: 10.1021/nl052201c

B. Gilbert, H. Zhang, B. Chen, M. Kunz, F. Huang, J.F. Banfield, "Compressibility of zinc sulfide nanoparticles," Phys. Rev. B 74 (11), September, 115405-1-115405-7 (2006). DOI: 10.1103/PhysRevB.74.115405

Marie-Alda Gilles-Gonzalez, Ana Isabel Caceres, Eduardo Henrique Silva Sousa, Diana R. Tomchick, Chad Brautigam, Constancio Gonzalez, Mischa Machius, "A Proximal Arginine R206 Participates in Switching of the Bradyrhizobium japonicum FixL Oxygen Sensor," J. Mol. Biol. 360 (1), June, 80-89 (2006). DOI: 10.1016/j.jmb.2006.04.054

Asta Gindulyte, Anat Bashan, Ilana Agmon, Lou Massa, Ada Yonath, Jerome Karle, "The transition state for formation of the peptide bond in the ribosome," Proc. Natl. Acad. Sci. USA 103 (36), September, 13327-13332 (2006). DOI: 10.1073/pnas.0606027103

John W. Giraldes, David L. Akey, Jeffrey D. Kittendorf, David H. Sherman, Janet L. Smith, Robert A. Fecik, "Structural and mechanistic insights into polyketide macrolactonization from polyketide-based affinity labels," Nat. Chem. Biol. 2 (10), October, 531-536 (2006). DOI: 10.1038/nchembio822

David Glesne, Stefan Vogt, Jorg Maser, Daniel Legnini, Eliezer Huberman, "Regulatory properties and cellular redistribution of zinc during macrophage differentiation of human leukemia cells," J. Struct. Biol. 155, 2-11 (2006). DOI: 10.1016/j.jsb.2005.09.012

David A. Glesne, Wen Zhang, Suneeta Mandava, Lyann Ursos, Margaret E. Buell, Lee Makowski, Diane J. Rodi, "Subtractive Transcriptomics: Establishing Polarity Drives In vitro Human Endothelial Morphogenesis," Cancer Res. 66, 4030-4040 (2006).

Vassiliki-Alexandra Glezakou, Yongsheng Chen, John L. Fulton, Gregory K. Schenter, Liem X. Dang, "Electronic structure, statistical mechanical simulations, and EXAFS spectroscopy of aqueous potassium," Ther. Chem. Acc. 115, 86-99 (2006). DOI: 10.1007/s00214-005-0054-4

Michael H. Godsey, Stephan Ort, Elisabetta Sabini, Manfred Konrad, Arnon Lavie, "Structural Basis for the Preference of UTP over ATP in Human Deoxycytidine Kinase: Illuminating the Role of Main-Chain Reorganization," Biochemistry-US 45 (2), March, 452-461 (2006). DOI: 10.1021/bi0518646

Siew Wei Goh, Alan N. Buckley, Robert N. Lamb, "Copper(II) sulfide?," Miner. Eng. 19 (2), February, 204-208 (2006).

Siew Wei Goh, Alan N. Buckley, Robert N. Lamb, Richard A. Rosenberg, Damian Moran, "The oxidation states of copper and iron in mineral sulfides, and the oxides formed on initial exposure of chalcopyrite and bornite to air," Geochim. Cosmochim. Acta 70, 2210-2228 (2006). DOI: 10.1016/j.gca.2006.02.007

Pavel A. Golubkov, William H. Johnson Jr., RobertM. Czerwinski, Maria D. Person, Susan C. Wang, Christian P. Whitman, Marvin L. Hackert, "Inactivation of the phenylpyruvate tautomerase activity of macrophage migration inhibitory factor by 2-oxo-4-phenyl-3-butynoate," Bioorg. Chem. 34 (4), August, 183-199 (2006). DOI: 10/1016/j.bioorg.2006.05.001

Kristie D. Goodwin, Mark A. Lewis, Farial A. Tanious, Richard R. Tidwell, W. David Wilson, Millie M. Georgiadis, Eric C. Long, "A high-throughput, high-resolution strategy for the study of site-selective DNA binding agents: Analysis of a 'Highly twisted' benzimidazole-diamidine," J. Am. Chem. Soc. 128, 7846-7854 (2006). DOI: 10.1021/ja0600936

Vijay Gopalakrishnan, Charles F. Zukoski, "Viscosity of Hard-Sphere Suspensions: Can We Go Lower?," Ind. Eng. Chem. Res. 45 (21), October, 6906-6914 (2006). DOI: 10.1021/ie051255u

Gayathri Gopalan, Zengyoong He, Kevin P. Battaile, Sheng Luan, Kunchithapadam Swaminathan, "Structural Comparisons of Oxidized and Reduced FKBP13 from Arabidopsis thaliana," Proteins 65 (4), December, 789-795 (2006). DOI: 10.1002/prot.21108

R.A. Gordon, E.D. Crozier, "In-plane structural anisotropy of ultrathin Fe films on GaAs(001)-4×6: X-ray absorption fine-structure spectroscopy measurements," Phys. Rev. B 74 (16), October, 165405-1-165405-6 (2006). DOI: 10.1103/PhysRevB.74.165405

Marina Gorelik, Vladimir V. Lunin, Tatiana Skarina, Alexei Savchenko, "Structural characterization of GntR/HutC family signaling domain," Protein Sci. 15, 1506-1511 (2006). DOI: 10.1110/ps.062146906

Zenon Grabarek, "Structural Basis for Diversity of the EF-hand Calcium-binding Proteins," J. Mol. Biol. 359, 509-525 (2006). DOI: 10.1016/j.jmb.2006.03.066

M.L. Green, A.J. Allen, X. Li, J. Wang, J. Ilavsky, A. Delabie, R.L. Puurunen, B. Brijs, "Nucleation of atomic-layer-deposited HfO[subscript 2] films, and evolution of their microstructure, studied by grazing incidence small angle x-ray scattering using synchrotron radiation," Appl. Phys. Lett. 88 (3), January, 032907-1-032907-3 (2006). DOI: 10.1063/1.2164417

Todd J. Green, Ming Luo, "Resolution improvement of X-ray diffraction data of crystals of a vesicular stomatitis virus nucleocapsid protein oligomer complexed with RNA," Acta Crystallogr. D 62 (5), May, 498-504 (2006). DOI: 10.1107/S0907444906006809

Todd J. Green, Xin Zhang, Gail W. Wertz, Ming Luo, "Structure of the Vesicular Stomatitis Virus Nucleoprotein-RNA Complex," Science 313, July, 357-360 (2006). DOI: 10.1126/science.1126953

Eugene Gregoryanz, Chrystele Sanloup, Roberto Bini, Jorg Kreutz, Hans J. Jodl, Maddury Somayazulu, Ho-kwang Mao, Russell J. Hemley, "On the [epsilon]-[zeta] transition of nitrogen," J. Chem. Phys. 124 (11), 116102-1-116102-2 (2006).

Jolanta Grembecka, Tomasz Cierpicki, Yancho Devedjiev, Urszula Derewenda, Beom Sik Kang, John H. Bushweller, Zygmunt S. Derewenda, "The Binding of the PDZ Tandem of Syntenin to Target Proteins," Biochemistry-US 45 (11), August, 3674-3683 (2006). DOI: 10.1021/bi052225y

Alexei Grigoriev, Dal-Hyun Do, Dong Min Kim, Chang-Beom Eom, Bernhard Adams, Eric M. Dufresne, Paul G. Evans, "Nanosecond Domain Wall Dynamics in Ferroelectric Pb(Zr, Ti)O[subscript3] Thin Films," Phys. Rev. Lett. 96, May, 187601-1-187601-4 (2006). DOI: 10.1103/PhysRevLett.96.187601

Alexei Grigoriev, Dal-Hyun Do, Dong Min Kim, Chang-Beom Eom, Paul G. Evans, Bernhard Adams, Eric M. Dufresne, "Subnanosecond piezoelectric x-ray switch," Appl. Phys. Lett. 89, July, 021109-1-021109-3 (2006). DOI: 10.1063/1.2219342

Alexei Grigoriev, Dal-Hyun Do, Dong Min Kim, Chang-Beom Eom, Paul G. Evans, Bernhard W. Adams, Eric M. Dufresne, "Nanosecond structural visualization of the reproducibility of polarization switching in ferroelectrics," Integr. Ferroelectr. 85, November, 165-173 (2006). DOI: 10.1080/10584580601085842

Dan Grilley, Ana Maria Soto, David E. Draper, "Mg[superscript 2+]–RNA interaction free energies and their relationship to the folding of RNA tertiary structures," Proc. Natl. Acad. Sci. USA 103 (38), September, 14003-14008 (2006). DOI: 10.1073/pnas.0606409103

David A. Grossie, William A. Feld, Giselle Sandi, Zdzislaw Wawrzak, "Di-[mu]-acetone-[kappa superscript 2]O:O-bisI (acetone-kO)-aqualithium(I)] di-[mu]-acetone-k[superscript 2]O:O-bis-[diaqualithium(I)] tetrakis{[phthalocyanphthalocyaninato(2-)-k[superscript 4]N,N',N",N"']lithiate (I)}," Acta Crystallogr. E 62 (4), April, m827-m829 (2006). DOI: 10.1107/S1600536806008488

Guilherme A.R. Gualda, "Crystal Size Distributions Derived from 3D Datasets: Sample Size Versus Uncertainties," J. Petrol. 47 (6), 1245-1254 (2006). DOI: 10.1093/petrology/egl010

Guilherme A.R. Gualda, Mark Rivers, "Quantitative 3D petrography using x-ray tomography: Application to Bishop Tuff pumice clasts," J. Volcanol. Geoth. Res. 154 (1-2), June, 48-62 (2006). DOI: 10.1016/j.jvolgeores.2005.09.019

Y. Guana, W.E. Bailey, C.-C. Kao, E. Vescovo, D.A. Arena, "Comparison of time-resolved x-ray magnetic circular dichroism measurements in reflection and transmission for layer-specific precessional dynamics measurements," J. Appl. Phys. 99, 08J305-1-08J305-3 (2006). DOI: 10.1063/1.2167632

Camilo Guaqueta, Lori K. Sanders, Gerard C.L. Wong, Erik Luijten, "The Effect of Salt on Self-Assembled Actin-Lysozyme Complexes," Biophys. J. 90, June, 4630-4638 (2006). DOI: 10.1529/biophysj.105.078253

K. Yu. Guslienko, X.F. Han, D.J. Keavney, R. Divan, S.D. Bader, "Magnetic Vortex Core Dynamics in Cylindrical Ferromagnetic Dots," Phys. Rev. Lett. 96 (6), February, 067205-1-067205-4 (2006). DOI: 10.1103/PhysRevLett.96.067205

Y. Guyodo, S.K. Banerjee, R.L. Penn, D. Burleson, T.S. Berquo, T. Seda, P. Solheid, "Magnetic properties of synthetic six-line ferrihydrite nanoparticles," Phys. Earth Planet. In. 154, 222-233 (2006). DOI: 10.1016/j.pepi.2005.05.009

Matthew D. Hall, Rebecca A. Alderden, Mei Zhang, Philip J. Beale, Zhonghou Cai, Barry Lai, Anton P.J. Stampfl, Trevor W. Hambley, "The fate of platinum(II) and platinum(IV) anti-cancer agents in cancer cells and tumours," J. Struct. Biol. 155, 38-44 (2006). DOI: 10.1016/j.jsb.2006.01.011

Michal Hammel, Kasra X. Ramyar, Charles T. Spencer, Brian V. Geisbrecht, "Crystallization and X-ray diffraction analysis of the complement component-3 (C3) inhibitory domain of Efb from Staphylococcus aureus," Acta Crystallogr. F 62, 285-288 (2006). DOI: 10.1107/S1744309106005926

Byung Woo Han, Craig A. Bingman, Donna K. Mahnke, Ryan M. Bannen, Sebastian Y. Bednarek, Richard L. Sabina, George N. Phillips Jr., "Membrane Association, Mechanism of Action, and Structure of Arabidopsis Embryonic Factor 1 (FAC1)," J. Biol. Chem. 281 (21), May, 14939-14947 (2006). DOI: 10.1074/jbc.M513009200

Byung Woo Han, Craig A. Bingman, Gary E. Wesenberg, George N. Phillips, Jr., "Crystal structure of Homo sapiens thialysine N[epsilon]-acetyltransferase (HsSSAT2) in complex with acetyl coenzyme A," Proteins 64 (1), June, 288-293 (2006). DOI: 10.1002/prot.20967

J. Han, Y. Jin, C.S. Willson, "Virus retention and transport in chemically heterogeneous porous media under saturated and unsaturated flow conditions," Environ. Sci. Technol. 40 (5), 1547-1555 (2006). DOI: 10.1021/es051351m

Tracey Hanley, David Sutton, David Cookson, Edward Kosior, Robert Knot, "Molecular Morphology of Petaloid Bases of PET Bottles: A Small-Angle X-ray Scattering Study," J. Appl. Polym. Sci. 99 (6), 3328-3335 (2006). DOI: 10.1002/app.22757

S.W. Han, "X-ray absorption fine structure and nanostructures," Int. J. Nanotech. 3 (2/3), 396-413 (2006).

S.-W. Han, C.H. Booth, E.D. Bauer, P.H. Huang, Y.Y. Chen, J.M. Lawrence, "Lattice Disorder and Size-Induced Kondo Behavior in CeAl[subscript 2] and CePt[subscript 2+x]," Phys. Rev. Lett. 97, September, 097204-1-097204-4 (2006). DOI: 10.1103/PhysRevLett.97.097204

S.W. Han, S.H. Kang, "Sensitivity of Zn[subscript 1-x]Cd[subscript x]Te to tera-hertz signals enhanced by structural orderings," Sol. St. Phen. 111, 25-30 (2006).

S.-W. Han, H.-J. Yoo, SungJin An, Jinjyoung Yoo, Gyu-Chul Yi, "Local structure around Ga in ultrafine GaN/ZnO coaxial nanorod heterostructures," Appl. Phys. Lett. 88, March, 111910-1-111910-3 (2006).

J. K. Harper, D. M. Grant, Y. G. Zhang, P. L. Lee, R. B. Von Dreele, "Characterizing challenging microcrystalline solids with solid-state NMR shift tensor and synchrotron X-ray powder diffraction data: Structural analysis of ambuic acid," J. Am. Chem. Soc. 128 (5), February, 1547-1552 (2006). DOI: 10.1021/ja055570j

R.T. Hart, Q. Mei, C.J. Benmore, J.C. Neuefeind, J.F.C. Turner, M. Dolgos, B. Tomberli, P.A. Egelstaff, "Isotope quantum effects in water around the freezing point," J. Chem. Phys. 124, April, 134505-1-134505-8 (2006). DOI: 10.1063/1.2181974

H. Hashizume, K. Ishiji, J. C. Lang, D. Haskel, G. Srajer, J. Minar, H. Ebert, "Observation of x-ray magnetic circular dichroism at the Ru K edge in Co-Ru alloys," Phys. Rev. B 73, 224416-1-224416-5 (2006). DOI: 10.1103/PhysRevB.73.224416

J. Hass, R. Feng, T. Li, X. Li, Z. Zong, W.A. de Heer, P.N. First, E.H. Conrad, C.A. Jeffrey, C. Berger, "Highly ordered graphene for two dimensional electronics," Appl. Phys. Lett. 89 (14), October, 143106-1-143106-3 (2006). DOI: 10.1063/1.2358299

Bing He, Robert T. Gampe, Jr., Andrew T. Hnat, Jonathan L. Faggart, John T. Minges, Frank S. French, Elizabeth M. Wilson, "Probing the Functional Link between Androgen Receptor Coactivator and Ligand-binding Sites in Prostate Cancer and Androgen Insensitivity," J. Biol. Chem. 281 (10), March, 6648-6663 (2006). DOI: 10.1074/jbc.M511738200

Lizbeth Hedstrom, Lu Gan, "IMP dehydrogenase: structural schizophrenia and an unusual base," Curr. Opin. Chem. Biol. 10 (5), October, 520-525 (2006). DOI: 10.1016/j.cbpa.2006.08.005

Peter Hedstrom, Jon Almer, Ulrich Lienert, Magnus Oden, "Evolution of Residual Strains in Metastable Austenitic Stainless Steels and the Accompanying Strain Induced Martensitic Transformation," Mater. Sci. Forum 524-525, 821-826 (2006).

Georg Heimel, Kerstin Hummer, Claudia Ambrosch-Draxl, Withoon Chunwachirasiri, Michael J. Winokur, Michael Hanfland, "Phase transition and electronic properties of fluorene: A joint experimental and theoretical high-pressure study," Phys. Rev. B 73, January, 024109-1-024109-13 (2006). DOI: 10.1103/PhysRevB.73.024109

E.E. Heldwein, H. Lou, F.C. Bender, G.H. Cohen, R.J. Eisenberg, S.C. Harrison, "Crystal Structure of Glycoprotein B from Herpes Simplex Virus 1," Science 313 (5784), July, 217-220 (2006). DOI: 10.1126/science.1126548

Juan D. Henao, Tiziana Caputo, Jeff H. Yang, Mayfair C. Kung, Harold H. Kung, "In Situ Transient FTIR and XANES Studies of the Evolution of Surface Species in CO Oxidation on Au/TiO[subscript 2]," J. Phys. Chem. B 110, 8689-8700 (2006). DOI: 10.1021/jp0568733

Sarah C. Hennebry, Ruby H.P. Law, Samantha J. Richardson, Ashley M. Buckle, James C. Whisstock, "The Crystal Structure of the Transthyretin-like Protein from Salmonella dublin, a Prokaryote 5-Hydroxyisourate Hydrolase," J. Mol. Biol. 359, 1389-1399 (2006). DOI: 10.1016/j.jmb.2006.04.057

Tao He, Jiazhong Chen, H. David Rosenfeld, M.A. Subramanian, "Thermoelectric Properties of Indium-Filled Skutterudites," Chem. Mater. 18 (3), 759-762 (2006). DOI: 10.1021/cm052055b

G.M. Hettiarachchi, K.G. Scheckel, J.A. Ryan, S.R. Sutton, M. Newville, "[mu]-XANES and [mu]-XRF investigations of metal binding mechanisms in biosolids," J. Environ. Qual. 35, 342-351 (2006). DOI: 10.2134/jeq2004.0259

A.H. Heuer, A. Reddy, D.B. Hovis, B. Veal, A. Paulikas, A. Vlad, M. Ruhle, "The effect of surface orientation on oxidation-induced growth strains in single crystal NiAl: An in situ synchrotron study," Scripta Mater. 54, 1907-1912 (2006). DOI: 10.1016/j.scriptamat.2006.02.021

Matthias Heuer, Tonio Buonassisi, Matthew A. Marcus, Andrei A. Istratov, Matthew D. Pickett, Tomohiro Shibata, Eicke R. Weber, "Complex intermetallic phase in multicrystalline silicon doped with transition metals," Phys. Rev. B 73, 235204-1-235204-5 (2006). DOI: 10.1103/PhysRevB.73.235204

Hilary L. Hoare, Lucy C. Sullivan, Gabriella Pietra, Craig S. Clements, Eleanor J. Lee, Lauren K. Ely, Travis Beddoe, Michela Falco, Lars Kjer-Nielsen, Hugh H. Reid, James McCluskey, Lorenzo Moretta, Jamie Rossjohn, Andrew G. Brooks, "Structural basis for a major histocompatibility complex class Ib–restricted T cell response," Nat. Immunol. 7 (3), February, 256-264 (2006). DOI: 10.1038/ni1312

Kevin G. Hoff, Jose L. Avalos, Kristin Sens, Cynthia Wolberger, "Insights into the Sirtuin Mechanism from Ternary Complexes Containing NAD[superscript +] and Acetylated Peptide," Structure 14 (8), August, 1231-1240 (2006). DOI: 10.1016/j.str.2006.06.006

E. Holbig, L. Dubrovinsky, G. Steinle-Neumann, V. Prakapenka, V. Swamy, "Compression behavior of Zr-doped nanoanatase," Z. Naturforsch. Pt. B 61b, 1577-1585 (2006). DOI: 0932-0776/06/1200-1577

C.M. Holl, J.R. Smyth, M.H. Manghnani, G.M. Amulele, M. Sekar, D.J. Frost, V.B. Prakapenka, G. Shen, "crystal structure and compression of an iron-bearing Phase A to 33 GPa," Phys. Chem. Miner. 33 (3), 192-199 (2006). DOI: 10.1007/s00269-006-0073-2

Daniel D. Holsworth, Cuiman Cai, Xue-Min Cheng, Wayne L. Cody, Dennis M. Downing, Noe Erasga, Chitase Lee, Noel A. Powell, Jeremy J. Edmunds, Michael Stier, Mehran Jalaie, Erli Zhang, Pat McConnell, Michael J. Ryan, John Bryant, Tingsheng Li, Aparna Kasani, Eric Hall, Rajendra Subedi, Mohammad Rahim, Samarendra Maiti, "Ketopiperazine-based renin inhibitors: Optimization of the “C” ring," Bioorg. Med. Chem. Lett. 16 (9), May, 2500-2504 (2006). DOI: 10.1016/j.bmcl.2006.01.084

Bum Soo Hong, Mi Kyung Yun, Yong-Mei Zhan, Shigeru Chohnan, Charles O. Rock, Stephen W. White, Suzanne Jackowski, Hee-Won Park, Roberta Leonardi, "Prokaryotic Type II and Type III Pantothenate Kinases: The Same Monomer Fold Creates Dimers with Distinct Catalytic Properties," Structure 14 (8), August, 1251-1261 (2006). DOI: 10.1016/j.str.2006.06.008

Jill S. Hontz, Maria T. Villar-Lecumberri, Lawrence A. Dreyfus, Marilyn D. Yoder, "Crystallization of Escherichia coli CdtB, the biologically active subunit of cytolethal distending toxin," Acta Crystallogr. F 62 (3), March, 192-195 (2006). DOI: 10.1107/S1744309106002454

Jill S. Hontz, Maria T. Villar-Lecumberri, Belinda M. Potter, Marilyn D. Yoder, Lawrence A. Dreyfus, John H. Laity, "Differences in Crystal and Solution Structures of the Cytolethal Distending Toxin B Subunit: Relevance to Nuclear Translocation and Functional Activation," J. Biol. Chem. 281 (35), October, 25365-25372 (2006). DOI: 10.1074/jbc.M603727200

Corey R. Hopkins, Steven V. O'Neil, Michael C. Laufersweiler, Yili Wang, Matthew Pokross, Marlene Mekel, Artem Evdokimov, Richard Walter, Maria Kontoyianni, Maria E. Petrey, Georgios Sabatakos, Jeff T. Roesgen, Eloise Richardson, Thomas P. Demuth, Jr., "Design and synthesis of novel N-sulfonyl-2-indole carboxamides as potent PPAR-[gamma] binding agents with potential application to the treatment of osteoporosis," Bioorg. Med. Chem. Lett. 16 (21), November, 5659-5663 (2006). DOI: 10.1016/j.bmcl.2006.08.003

Geoff P. Horsman, Jiyuan Ke, Shaodong Dai, Stephen Y.K. Seah, Jeffrey T. Bolin, Lindsay D. Eltis, "Kinetic and Structural Insight into the Mechanism of BphD, a C-C Bond Hydrolase from the Biphenyl Degradation Pathway," Biochemistry-US 45 (37), August, 11071-11086 (2006). DOI: 10.1021/bi0611098

John R. Horton, Kirsten Liebert, Miklos Bekes, Albert Jeltsch, Xiaodong Cheng, "Structure and Substrate Recognition of the Escherichia coli DNA Adenine Methyltransferase," J. Mol. Biol. 358 (2), April, 559-570 (2006). DOI: 10.1016/j.jmb.2006.02.028

John R. Horton, Xing Zhang, Robert Maunus, Zhe Yang, Geoffrey G. Wilson, Richard J. Roberts, Xiaodong Cheng, "DNA nicking by HinP1I endonuclease: bending, base flipping and minor groove expansion," Nucleic Acids Res. 34 (3), February, 939-948 (2006). DOI: 10.1093/nar/gkj484

L. A. Hough, M. F. Islam, B. Hammouda, A. G. Yodh, P. A. Heiney, "Structure of Semidilute Single-Wall Carbon Nanotube Suspensions and Gels," Nano Lett. 6 (2), February, 313-317 (2006). DOI: 10.1021/nl051871f

P.Y. Hou, A.P. Paulikas, B.W. Veal., "Strains in thermally growing alumina films measured in-situ synchrotron X-rays," Mater. Sci. Forum 522-523, 433-440 (2006).

Colin M. House, Nancy C. Hancock, Andreas Moller, Brett A. Cromer, Victor Fedorov, David D.L. Bowtell, Michael W. Parker, Galina Polekhina, "Elucidation of the Substrate Binding Site of Siah Ubiquitin Ligase," Structure 14 (4), April, 695-701 (2006). DOI: 10.1016/j.str.2005.12.013

D.B. Hovis, A. Reddy, A.H. Heuer, "X-ray elastic constants for [alpha]-Al[subscript 2]O[subscript 3]," Appl. Phys. Lett. 88 (13), March, 131910-1-131910-3 (2006). DOI: 10.1063/1.2189071

William C. Ho, Cheng Luo, Kehao Zhao, Xiaomei Chai, Mary X. Fitzgerald, Ronen Marmorstein, "High-resolution structure of the p53 core domain: implications for binding small-molecule stabilizing compounds," Acta Crystallogr. D 62, December, 1484-1493 (2006). DOI: 10.1107/S090744490603890X

Pavel Hrma, John D. Vienna, Benjamin K. Wilson, Trevor J. Plaisted, Steve M. Heald, "Chromium phase behavior in a multi-component borosilicate glass melt," J. Non-Cryst. Solids 352, May, 2114-2122 (2006). DOI: 10.1016/j.jnoncrysol.2006.02.051

Robert W. Hsieh, Shyamala S. Rajan, Sanjay K. Sharma, Yuee Guo, Eugene R. DeSombre, Milan Mrksich, Geoffrey L. Greene, "Identification of Ligands with Bicyclic Scaffolds Provides Insights into Mechanisms of Estrogen Receptor Subtype Selectivity," J. Biol. Chem. 281 (26), June, 17909-17919 (2006). DOI: 10.1074/jbc.M513684200

Qing Huai, Andrew P. Mazar, Alice Kuo, Graham C. Parry, David E. Shaw, Jennifer Callahan, Yongdong Li, Cai Yuan, Chuanbing Bian, Liqing Chen, Bruce Furie, Barbara C. Furie, Douglas B. Cines, Mingdong Huang, "Structure of Human Urokinase Plasminogen Activator in Complex with Its Receptor," Science 311, February, 656-659 (2006). DOI: 10.1126/science.1121143

Jin Huang, Ayyappan Subbiah, David Pyle, Adam Rowland, Brentley Smith, Abraham Clearfield, "Globular Porous Nanoparticle Tin(IV) Phenylphosphonates and Mixed Methyl Phenylphosphonates," Chem. Mater. 18 (22), October, 5213-5222 (2006). DOI: 10.1021/cm061333j

Yihua Huang, Richard Baxter, Barbara S. Smith, Carrie L. Partch, Christopher L. Colbert, Johann Deisenhofer, "Crystal structure of cryptochrome 3 from Arabidopsis thaliana and its implications for photolyase activity," Proc. Natl. Acad. Sci. USA 103 (47), November, 17701 -17706 (2006). DOI: 10.1073/pnas.0608554103

T.C. Hufnagel, R.T. Ott, J. Almer, "Structural aspects of elastic deformation in a metallic glass," Phys. Rev. B 73 (6), February, 064204-1-064204-8 (2006). DOI: 10.1103/PhysRevB.73.064204

Robert V. Hull, Liang Li, Yangchuan Xing, Charles C. Chusuei, "Pt Nanoparticle Binding on Functionalized Multiwalled Carbon Nanotubes," Chem. Mater. 18 (7), April, 1780-1788 (2006). DOI: 10.1021/cm0518978

A. Huq, P.W. Stephens, "Crystal Structure of Rb[subscript 4]C[subscript 60] under pressure: X-ray diffraction experiments," Phys. Rev. B 74 (7), August, 075424-1-075424-4 (2006). DOI: 10.1103/PhysRevB.74.075424

X. Hu, Z. Jiang, S. Narayanan, X. Jiao, A.R. Sandy, S.K. Sinha, L.B. Lurio, J. Lal, "Observation of a low-viscosity interface between immiscible polymer layers," Phys. Rev. E 74 (01), July, 010602-1-010602-4 (2006). DOI: http://dx.doi.org/10.1103/PhysRevE.74.010602

Hugh Huxley, Massimo Reconditi, Alex Stewart, Tom Irving, "X-ray Interference Studies of Crossbridge Action in Muscle Contraction: Evidence from Quick Releases," J. Mol. Biol. 363 (4), November, 743-761 (2006). DOI: 10.1016/j.jmb.2006.08.075

Hugh Huxley, Massimo Reconditi, Alex Stewart, Tom Irving, "X-ray Interference Studies of Crossbridge Action in Muscle Contraction: Evidence from Muscles During Steady Shortening," J. Mol. Biol. 363 (4), November, 762-772 (2006). DOI: 10.1016/j.jmb.2006.08.055

G.E. Ice, J.W.L. Pang, R.I. Barabash, Y. Puzyrev, "Characterization of three-dimensional crystallographic distributions using polychromatic X-ray microdiffraction," Scripta Mater. 55, April, 57-62 (2006). DOI: 10.1016/j.scriptamat.2006.02.046

Eugene S. Ilton, Steve M. Heald, Steven C. Smith, David Elbert, Chongxuan Liu, "Reduction of Uranyl in the Interlayer Region of Low Iron Micas under Anoxic and Aerobic Conditions," Environ. Sci. Technol. 40 (16), July, 5003-5009 (2006). DOI: 10.1021/es0522478 S0013-936X(05)02247-9

Fumie Imabayashi, Sanjukta Aich, Lata Prasad, Louis T.J. Delbaere, "Substrate-Free Structure of a Monomeric NADP Isocitrate Dehydrogenase: An Open Conformation Phylogenetic Relationship of Isocitrate Dehydrogenase," Proteins 63 (1), January, 100-112 (2006). DOI: 10.1002/prot.20867

C.A. Impellitteri, K.G. Scheckel, "The distribution, solid-phase speciation, and desorption/dissolution of As in waste iron-based drinking water treatment residuals," Chemosphere 64 (6), September, 875-880 (2006). DOI: 10.1016/j.chemosphere.2006.02.001

Eric D. Isaacs, "Microscopy: X-ray nanovision," Nature 442, 35 (2006). DOI: 10.1038/442035a

A.F. Isakovic, P.G. Evans, J. Kmetko, K. Cicak, Z. Cai, B. Lai, R.E. Thorne, "Shear Modulus and Plasticity of a Driven Charge Density Wave," Phys. Rev. Lett. 96 (4), 046401-1-046401-4 (2006). DOI: 10.1103/PhysRevLett.96.046401

Zahirul Islam, D. Haskel, J.C. Lang, G. Srajer, Y. Lee, B.N. Harmon, A.I. Goldman, D.L. Schlagel, T.A. Lograsso, "An X-ray study of non-zero nickel moment in a ferromagnetic shape-memory alloy," J. Magn. Magn. Mater. 303, 20-25 (2006). DOI: 10.1016/j.jmmm.2005.10.245

Tina Izard, Guy Tran Van Nhieu, Philippe R. J. Bois, "Shigella applies molecular mimicry to subvert vinculin and invade host cells," J. Cell Biol. 175 (3), November, 465-475 (2006). DOI: 10.1083/jcb.200605091

Terrence Jach, Alex S. Bakulin, Stephen M. Durbin, Joseph Pedulla, Albert Macrander, "Variable Magnification With Kirkpatrick-Baez Optics for Synchrotron X-Ray Microscopy," J. Res. Natl. Inst. Stan. 111 (3), 219-225 (2006).

Colin J. Jackson, Paul D. Carr, Hye-Kyung Kim, Jian-Wei Liu, David L. Ollis, "The purification, crystallization and preliminary diffraction of a glycerophosphodiesterase from Enterobacter aerogenes," Acta Crystallogr. F 62, 659-661 (2006). DOI: 10.1107/S1744309106020021

S.G. Jackson, Y. Zhang, X. Bao, K. Zhang, R. Summerfield, R.J. Haslam, M.S. Junop, "Structure of the carboxy-terminal PH domain of pleckstrin at 2.1 Å," Acta Crystallogr. D 62 (3), March, 324-330 (2006). DOI: 10.1107/S0907444905043179

Marc Jacobs, Koto Hayakawa, Lora Swenson, Steven Bellon, Mark Fleming, Paul Taslimi, John Doran, "The Structure of Dimeric ROCK I Reveals the Mechanism for Ligand Selectivity," J. Biol. Chem. 281 (1), January, 260-268 (2006). DOI: 10.1074/jbc.M508847200

Gaurav Jain, Mahalingam Balasubramanian, Jun John Xu, "Structural Studies of Lithium Intercalation in a Nanocrystalline [alpha]-Fe[subscript 2]O[subscript 3] Compound," Chem. Mater. 18 (2), January, 423-434 (2006). DOI: 10.1021/cm052014f

Sumeet Jain, Xiaobo Gong, L.E. Scriven, Frank S. Bates, "Disordered Network State in Hydrated Block-Copolymer Surfactants," Phys. Rev. Lett. 96, April, 138304-1-138304-4 (2006). DOI: 10.1103/PhysRevLett.96.138304

Bo Jakobsen, Henning F. Poulsen, Ulrich Lienert, Jonathan Almer, Sarvjit D. Shastri, Henning O. Sørensen, Carsten Gundlach, Wolfgang Pantleon, "Formation and Subdivision of Deformation Structures During Plastic Deformation," Science 312 (5775), May, 889-892 (2006). DOI: 10.1126/science.1124141

Michael James, Liliana Morales, Kia Wallwork, Maxim Avdeev, Ray Withers, Darren Goossens, "Structure and magnetism in rare earth strontium-doped cobaltates," Physica B 385-386, 199-201 (2006). DOI: 10.1016/j.physb.2006.05.244

Veronica J. James, "Reply to the letter of Rogers et al. entitled 'Reproducibility of cancer diagnosis using hair'," Int. J. Cancer 118 (4), February, 1061-1062 (2006). DOI: 10.1002/ijc.21457

Veronica J. James, "A place for fiber diffraction in the detection of breast cancer?," Cancer Detect. Prev. 30 (3), June, 233-238 (2006). DOI: 10.1016/j.cdp.2006.04.001

Srinivas Janaswamy, Rengaswami Chandrasekaran, "Sodium [iota]-Carrageenan: A Paradigm of Polymorphism and Pseudopolymorphism," Macromolecules 39 (9), 3345-3349 (2006). DOI: 10.1021/ma060024b

Mariusz Jaskólski, Mi Li, Gary Laco, Alla Gustchina, Alexander Wlodawer, "Molecular replacement with pseudosymmetry and model dissimilarity: a case study," Acta Crystallogr. D 62 (2), February, 208-215 (2006). DOI: 10.1107/S0907444905040655

Hariharan Jayaram, Hui Fan, Brian R. Bowman, Amy Ooi, Jyothi Jayaram, Ellen W. Collisson, Julien Lescar, B.V. Venkataram Prasad, "X-Ray Structures of the N- and C-Terminal Domains of a Coronavirus Nucleocapsid Protein: Implications for Nucleocapsid Formation," J. Virol. 80 (13), July, 6612-6620 (2006). DOI: 10.1128/JVI.00157-06

Robert Jedrzejczak, Miroslawa Dauter, Zbigniew Dauter, Marcin Olszewski, Anna Dtugotecka, Jozef Kur, "Structure of the single-stranded DNA-binding protein SSB from Thermus aquaticus," Acta Crystallogr. D 62, 1407-1412 (2006). DOI: 10.1107/S0907444906036031

Robert Jedrzejczak, Zbigniew Dauter, Miroslawa Dauter, Rafal Piatek, Beata Zalewska, Marta Mroz, Katarzyna Bury, Bogdan Nowicki, Jozef Kur, "Structure of DraD invasin from uropathogenic Escherichia coli: a dimer with swapped [beta]-tails," Acta Crystallogr. D 62, 157-164 (2006). DOI: 10.1107/S0907444905036747

C.A. Jeffrey, E.H. Conrad, R. Feng, M. Hupalo, C. Kim, P. Ryan, P.F. Miceli, M.C. Tringides, "Influence of Quantum Size Effects on Island Coarsening," Phys. Rev. Lett. 96 (10), March, 106105-1-106105-4 (2006). DOI: 10.1103/PhysRevLett.96.106105

Jermaine L. Jenkins, John J. Tanner, "High-resolution structure of human D-glyceraldehyde-3-phosphate dehydrogenase," Acta Crystallogr. D 62 (3), March, 290-301 (2006). DOI: 10.1107/S0907444905042289

Won Bae Jeon, Simon T.M. Allard, Craig A. Bingman, Eduard Bitto, Byung Woo Han, Gary E. Wesenberg, George N. Phillips, Jr., "X-ray Crystal Structures of the Conserved Hypothetical Proteins From Arabidopsis thaliana Gene Loci At5g11950 and At2g37210," Proteins 65, December, 1051-1054 (2006). DOI: 10.1002/prot.21166

Mark R. Jezyk, Jason T. Snyder, Svetlana Gershberg, David K. Worthylake, T. Kendall Harden, John Sondek, "Crystal structure of Rac1 bound to its effector phospholipase C-[beta]2," Nat. Struct. Mol. Biol. 13 (12), December, 1135-1140 (2006).

F. Jiang, R.-V. Wang, A. Munkholm, S.K. Streiffer, G.B. Stephenson, P. H. Fuoss, K. Latifi, Carol Thompson, "Indium adsorption on GaN under metal-organic chemical vapor deposition conditions," Appl. Phys. Lett. 89 (16), October, 161915-1-161915-3 (2006). DOI: 10.1063/1.2364060

Jianyong Jin, Dennis W. Smith, Jr., Sybille Glasser, Dvora Perahia, Stephen H. Foulger, John Ballato, Shin Woong Kang, Satyendra Kumar, "Liquid Crystalline Perfluorocyclobutyl Aryl Ether Polymers Containing Oligophenylene Mesogens," Macromolecules 39 (14), July, 4646-4649 (2006). DOI: 10.1021/ma060501q

Xiangshu Jin, Jason Touhey, Rachelle Gaudet, "Structure of the N-terminal Ankyrin Repeat Domain of the TRPV2 Ion Channel," J. Biol. Chem. 281 (35), September, 25006-25010 (2006). DOI: 10.1074/jbc.C600153200

B. Johannessen, P. Kluth, D.J. Cookson, G.J. Foran, M.C. Ridgway, "Size-dependent structural disorder in nanocrystalline Cu probed by synchrotron-based X-ray techniques," Nucl. Instrum. Methods B 246, 45-49 (2006). DOI: 10.1016/j.nimb.2005.12.015

B. Johannessen, P. Kluth, C.J. Glover, S.M. Kluth, G.J. Foran, D.J. Cookson, D.J. Llewellyn, M.C. Ridgway, "Structural stability of Cu nanocrystals in SiO[subscript 2] exposed to high-energy ion irradiation," Nucl. Instrum. Methods B 250 (1-2), September, 210-214 (2006). DOI: 10.1016/j.nimb.2006.04.112

J.A. Johnson, S. Schweizer, B. Henke, G. Chen, J. Woodford, P.J. Newman, D.R. MacFarlane, "Eu-activated fluorochlorozirconate glass-ceramic scintillators," J. Appl. Phys. 100 (3), August, 034701-1-034701-5 (2006). DOI: 10.1063/1.2225765

Ronald L. Jones, Tengjiao Hu, Christopher L. Soles, Eric K. Lin, Ronald M. Reano, Stella W. Pang, Diego M. Casa, "Real-Time Shape Evolution of Nanoimprinted Polymer Structures during Thermal Annealing," Nano Lett. 6 (8), July, 1723-1728 (2006). DOI: 10.1021/nl061086i

Ronald L. Jones, Christopher L. Soles, Eric K. Lin, Walter Hu, Ronald M. Reano, Stella W. Pang, Steven J. Weigand, Denis T. Keane, John P. Quintana, "Pattern fidelity in nanoimprinted films using critical dimension small angle x-ray scattering," J. Microlith. Microfab. 5 (1), 013001-1-013001-7 (2006).

Jeremiah S. Joseph, Kumar Singh Saikatendu, Vanitha Subramanian, Benjamin W. Neuman, Alexei Brooun, Mark Griffith, Kin Moy, Maneesh K. Yadav, Jeffrey Velasquez, Michael J. Buchmeier, Raymond C. Stevens, Peter Kuhn, "Crystal Structure of Nonstructural Protein 10 from the Severe Acute Respiratory Syndrome Coronavirus Reveals a Novel Fold with Two Zinc-Binding Motifs," J. Virol. 80 (16), August, 7894-7901 (2006). DOI: 10.1128/JVI.00467-06

Hemant K. Joshi, Christopher Etzkorn, Lorentz Chatwell, Jurate Bitinaite, Nancy C. Horton, "Alteration of Sequence Specificity of the Type II Restriction Endonuclease HincII through an Indirect Readout Mechanism," J. Biol. Chem. 281 (33), August, 23852-23869 (2006). DOI: 10.1074/jbc.M512339200

Ratnakar Josyula, Zhongmin Jin, Zhengqing Fu, Bingdong Sha, "Crystal Structure of Yeast Mitochondrial Peripheral Membrane Protein Tim44p C-terminal Domain," J. Mol. Biol. 359, June, 798-804 (2006). DOI: 10.1016/j.jmb.2006.04.020

Ratnakar Josyula, Zhongmin Jin, Deborah McCombs, Lawrence DeLucas, Bingdong Sha, "Preliminary crystallographic studies of yeast mitochondrial peripheral membrane protein Tim44p," Acta Crystallogr. F 62 (2), February, 172-174 (2006). DOI: 10.1107/S1744309106002053

Andrew C. Jupe, Angus P. Wilkinson, "Sample cell for powder x-ray diffraction at up to 500 bars and 200 °C," Rev. Sci. Instrum. 77 (11), 113901-1-113901-4 (2006). DOI: 10.1063/1.2364134

Venkataraman Kabaleeswaran, Neeti Puri, John E. Walker, Andrew G.W. Leslie, David M. Mueller, "Novel features of the rotary catalytic mechanism revealed in the structure of yeast F1 ATPase," EMBO J. 25 (22), November, 5433-5442 (2006). DOI: 10.1038/sj.emboj.7601410

Satwik Kamtekar, Andrea J. Berman, Jimin Wang, Jose M. Lazaro, Miguel de Vega, Luis Blanco, Margarita Salas, Thomas A. Steitz, "The [phi]29 DNA polymerase:protein-primer structure suggests a model for the initiation to elongation transition," EMBO J. 25, 1335-1343 (2006). DOI: 10.1038/sj.emboj.7601027

Satwik Kamtekar, Roger S. Ho, Melanie J. Cocco, Weikai Li, Sandra V.C.T. Wenwieser, Martin R. Boocock, Nigel D. Grindley, Thomas A. Steitz, "Implications of structures of synaptic tetramers of [gamma delta] resolvase for the mechanism of recombination," Proc. Natl. Acad. Sci. USA 103 (28), July, 10642-10647 (2006). DOI: 10.1073/pnas.0604062103

Shankar Prasad Kanaujia, Chellamuthu Vasuki Ranjani, Jeyaraman Jeyakanthan, Seiki Baba, Lirong Chen, Zhi-Jie Liu, Bi-Cheng Wang, Masami Nishida, Akio Ebihara, Akeo Shinkai, Seiki Kuramitsu, Yoshitsugu Shiro, Kanagaraj Sekar, Shigeyuki Yokoyama, "Crystallization and preliminary crystallographic analysis of molybdenum-cofactor biosynthesis protein C from Thermus thermophilus," Acta Crystallogr. F 63 (1), December, 27-29 (2006). DOI: 10.1107/S1744309106052560

H.C. Kang, J. Maser, G.B. Stephenson, C. Liu, R. Conley, A.T. Macrander, S. Vogt, "Nanometer linear focusing of hard x-rays by a multilayer laue lens," Phys. Rev. Lett. 96, March, 127401-1-127401-4 (2006). DOI: 10.1103/PhysRevLett.96.127401

J.M. Kang, K.J. Beers, "Synthesis and characterization of PCL-b-PEO-b-PCL-based nanostructured and porous hydrogels," Biomacromolecules 7 (2), February, 453-458 (2006). DOI: 10.1021/bm050637g

Joo H. Kang, Laurent D. Menard, Ralph G. Nuzzo, Anatoly I. Frenkel, "Unusual Non-Bulk Properties in Nanoscale Materials: Thermal Metal-Metal Bond Contraction of [gamma]-Alumina-Supported Pt Catalysts," J. Am. Chem. Soc. 128, 12068-12069 (2006). DOI: 10.1021/ja064207

E.P. Kanter, I. Ahmad, R.W. Dunford, D.S. Gemmell, B. Krässig, S.H. Southworth, L. Young, "Double K-shell photoionization of silver," Phys. Rev. A 73 (2), 022708-1-022708-11 (2006). DOI: 10.1103/PhysRevA.73.022708

E.P. Kanter, R.W. Dunford, B. Kraessig, S.H. Southworth, L. Young, "Double K-photoionization of heavy atoms," Radiat. Phys. Chem. 75 (11), November, 1529-1533 (2006). DOI: 10.1016/j.radphyschem.2005.12.044

E.P. Kanter, R.W. Dunford, B. Kraessig, S.H. Southworth, L. Young, "Higher-order processes in X-ray photoionization of atoms," Radiat. Phys. Chem. 75 (12), December, 2174-2181 (2006). DOI: 10.1016/j.radphyschem.2005.05.003

J.M. Karner, S.R. Sutton, J.J. Papike, C.K. Shearer, J.H. Jones, M. Newville, "Application of a new vanadium valence oxybarometer to basaltic glasses from the Earth, Moon, and Mars," Am. Mineral. 91, 270-277 (2006).

T.C. Kaspar, T. Droubay, D.E. McCready, P. Nachimuthu, S.M. Heald, C.M. Wang, A.S. Lea, V. Shutthanandan, S.A. Chambers, M.F. Toney, "Magnetic properties of epitaxial Co-doped anatase TiO[subscript 2] thin films with excellent structural quality," J. Vac. Sci. Technol. B 24 (4), June, 2012-2017 (2006). DOI: 10.1116/1.2216723

T.C. Kaspar, T. Droubay, V. Shutthanandan, S.M. Heald, C.M. Wang, D.E. McCready, S. Thevuthasan, J.D. Bryan, D.R. Gamelin, A.J. Kellock, M.F. Toney, X. Hong, C.H. Ahn, S.A. Chambers, "Ferromagnetism and structure of epitaxial Cr-doped anatase TiO[subscript 2] thin films," Phys. Rev. B 73 (15), April, 155327-1-155327-12 (2006). DOI: 10.1103/PhysRevB.73.155327

Masato Kato, R. Max Wynn, Jacinta L. Chuang, Chad A. Brautigam, Myra Custorio, David T. Chuang, "A synchronized substrate-gating mechanism revealed by cubic-core structure of the bovine branched-chain alpha-ketoacid dehydrogenase complex," EMBO J. 25 (24), December, 5983-5994 (2006). DOI: 10.1038/sj.emboj.7601444

Amy K. Katz, Xinmin Li, H.L. Carrell, B. Leif Hanson, Paul Langan, Leighton Coates, Benno P. Schoenborn, Jenny P. Glusker, Gerard J. Bunick, "Locating active-site hydrogen atoms in D-xylose isomerase: Time-of-flight neutron diffraction," Proc. Natl. Acad. Sci. USA 103 (22), May, 8342-8347 (2006). DOI: 10.1073/pnas.0602598103

A. Kazimirov, A.A. Sirenko, D.H. Bilderback, Z.-H. Cai, B. Lai, R. Huang, A. Ougazzaden, "Synchrotron high angular resolution microdiffraction analysis of selective area grown optoelectronic waveguide arrays," J. Phys. D 39, March, 1422-1426 (2006). DOI: 10.1088/0022-3727/39/7/013

Lukasz Kedzierski, Robyn L. Malby, Brian J. Smith, Matthew A. Perugini, Anthony N. Hodder, Thomas Ilg, Peter M. Colman, Emanuela Handman, "Structure of Leishmania mexicana Phosphomannomutase Highlights Similarities with Human Isoforms," J. Mol. Biol. 363 (1), October, 215-227 (2006). DOI: 10.1016/j.jmb.2006.08.023

S.D. Kelly, E.T. Rasbury, S. Chattopadhyay, A.J. Kropf, K.M. Kemner, "Evidence of a Stable uranyl site in Ancient Organic-Rich Calcite," Environ. Sci. Technol. 40, April, 2262-2268 (2006). DOI: 10.1021/es051970v

Ivan M. Kempson, William M. Skinner, "Advanced analysis of metal distributions in human hair," Environ. Sci. Technol. 40 (10), May, 3423-3428 (2006). DOI: 10.1021/es052158v

Amy Kendall, Gerald Stubbs, "Oriented sols for fiber diffraction from limited quantities or hazardous materials," J. Appl. Crystallogr. 39, February, 39-41 (2006). DOI: 10.1107/S0021889805033455

V. Khanna, E.W. Cochran, A. Hexemer, G.E. Stein, G.H. Fredrickson, E.J. Kramer, X. Li, J. Wang, S.F. Hahn, "Effect of Chain Architecture and Surface Energies on the Ordering Behavior of Lamellar and Cylinder Forming Block Copolymers," Macromolecules 39 (26), December, 9346-9356 (2006). DOI: 10.1021/ma0609228

Uriah J. Kilgore, Xiaofan Yang, John Tomaszewski, John C. Huffman, Daniel J. Mindiola, "Activation of Atmospheric Nitrogen and Azobenzene N=N Bond Cleavage by a Transient Nb(III) Complex," Inorg. Chem. 45 (26), December, 10712-10721 (2006). DOI: 10.1021/ic061642b

Chang-Yong Kim, Jeffrey W. Elam, Michael J. Pellin, Dipak K. Goswami, Steven T. Christensen, Mark C. Hersam, Peter C. Stair, Michael J. Bedzyk, "Imaging of atomic layer deposited (ALD) tungsten monolayers on [alpha]-TiO[subscript 2](110) by X-ray standing wave fourier inversion," J. Phys. Chem. B 110 (25), June, 12616-12620 (2006). DOI: 10.1021/jp061391s

Eun Young Kim, Nils Schrader, Birthe Smolinsky, Cecile Bedet, Christian Vannier, Gunter Schwarz, Hermann Schindelin, "Deciphering the structural framework of glycine receptor anchoring by gephyrin," EMBO J. 25, 1385-1395 (2006). DOI: 10.1038/sj.emboj.7601029

H.J. Kim, C.D. Malliakas, A.T. Tomic, S.H. Tessmer, M.G. Kanatzidis, S.J.L. Billinge, "Local atomic structure and discommensurations in the charge density wave of CeTe[subscript 3]," Phys. Rev. Lett. 96 (22), June, 226401-1-226401-4 (2006). DOI: 10.1103/PhysRevLett.96.226401

Pilho Kim, Yong-Mei Zhang, Gautham Shenoy, Quynh-Anh Nguyen, Helena I. Boshoff, Ujjini H. Manjunatha, Michael B. Goodwin, John Lonsdale, Allen C. Price, Darcie J. Miller, Ken Duncan, Stephen W. White, Charles O. Rock, Clifton E. Barry, III, Cynthia S. Dowd, "Structure-Activity Relationships at the 5-Position of Thiolactomycin: An Intact (5R)-Isoprene Unit is Required for Activity against the Condensing Enzymes from Mycobacterium tuberculosis and Eshcherichia coli," J. Med. Chem. 49 (2), January, 159-171 (2006). DOI: 10.1021/jm050825p

Sook-Kyung Kim, Sathyavelu K. Reddy, Bryant C. Nelson, Gregory B. Vasquez, Andrew Davis, Andrew J. Howard, Sean Patterson, Gary L. Gilliland, Jane E. Ladner, Prasad T. Reddy, "Biochemical and Structural Characterization of the Secreted Chorismate Mutase (Rv1885c) from Mycobacterium tuberculosis H[subscript 37]R[subscript v]: an *AroQ Enzyme Not Regulated by the Aromatic Amino Acids," J. Bacteriol. 188 (24), December, 8638-8648 (2006). DOI: 10.1128/JB.00441-06

Youngchang Kim, Natalia Maltseva, Irina Dementieva, Frank Collart, Denise Holzle, Andrzej Joachimiak, "Crystal structure of hypothetical protein YfiH from Shigella flexneri at 2 Å resolution," Structure 63 (4), 1097-1101 (2006). DOI: 10.1002/prot.20589

Nigel Kirby, David Cookson, Craig Buckley, Eliza Bovell, Tim St. Pierree, "Iron K-edge anomalous small-angle X-ray scattering at 15-ID-D at the Advanced Photon Source," J. Appl. Crystallogr. 40, November, s1-s6 (2006). DOI: 10.1107/S0021889806046309

Kevin R. Kittilstved, Dana A. Schwartz, Allan C. Tuan, Steve M. Heald, Scott A. Chambers, Daniel R. Gamelin, "Direct Kinetic Correlation of Carriers and Ferromagnetism in Co[superscript 2+]:ZnO," Phys. Rev. Lett. 97, 037203-1-037203-4 (2006). DOI: 10.1103/PhysRevLett.97.037203

Lars Kjer-Nielsen, Natalie A. Borg, Daniel G. Pellicci, Travis Beddoe, Lyudmila Kostenko, Craig S. Clements, Nicholas A. Williamson, Mark J. Smyth, Gurdyal S. Besra, Hugh H. Reid, Mandvi Bharadwaj, Dale I. Godfrey, Jamie Rossjohn, James McCluskey, "A structural basis for selection and cross-species reactivity of the semi-invariant NKT cell receptor in CD1d/glycolipid recognition," J. Exp. Med. 203 (3), 661-673 (2006). DOI: 10.1084/jem.20051777

Sean R. Klopfenstein, Artem G. Evdokimov, Anny-Odile Colson, Neil T. Fairweather, Jeffrey J. Neuman, Matthew B. Maier, Jeffrey L. Gray, Gina S. Gerwe, George E. Stake, Brian W. Howard, Julie A. Farmer, Matthew E. Pokross, Thomas R. Downs, Bhavani Kasibhatla, Kevin G. Peters, "1,2,3,4-Tetrahydroisoquinolinyl sulfamic acids as phosphatase PTP1B inhibitors," Bioorg. Med. Chem. Lett. 16 (6), March, 1574-1578 (2006). DOI: 10.1016/j.bmcl.2005.12.051

P. Kluth, B. Johannessen, D.J. Cookson, G.J. Foran, M.C. Ridgway, "SAXS and EXAFS studies of ion beam synthesized Au nanocrystals," Nucl. Instrum. Methods B 246, 30-34 (2006). DOI: 10.1016/j.nimb.2005.12.014

P. Kluth, B. Johannessen, G.J. Foran, D.J. Cookson, S.M. Kluth, M.C. Ridgway, "Disorder and cluster formation during ion irradiation of Au nanoparticles in SiO[subscript 2]," Phys. Rev. B 74, 014202-1-014202-9 (2006). DOI: 10.1103/PhysRevB.74.014202

P. Kluth, B. Johannessen, S.M. Kluth, G.J. Foran, D.J. Cookson, M.C. Ridgway, "Structure and morphology of ion irradiated Au nanocrystals in SiO[subscript 2]," Nucl. Instrum. Methods B 250 (1-2), September, 215-219 (2006). DOI: 10.1016/j.nimb.2006.04.113

James E. Knapp, Reinhard Pahl, Vukica Srajer, William E. Royer Jr., "Allosteric action in real time: Time-resolved crystallographic studies of a cooperative dimeric hemoglobin," Proc. Natl. Acad. Sci. USA 103 (20), May, 7649-7654 (2006). DOI: 10.1073/pnas.0509411103

Benjamin D. Kocar, Mitchell J. Herbal, Katherine J. Tufano, Scott Fendorf, "Contrasting Effects of Dissimilatory Iron(III) and Arsenic(V) Reduction on Arsenic Retention and Transport," Environ. Sci. Technol. 40 (21), 6715-6721 (2006). DOI: 10.1021/es061540k

Venkat R. Koganti, Darren Dunphy, Vignesh Gowrishankar, Michael D. McGehee, Xuefa Li, Jin Wang, Stephen E. Rankin, "Generalized Coating Route to Silica and Titania Films with Orthogonally Tilted Cylindrical Nanopore Arrays," Nano Lett. 6 (11), September, 2567-2570 (2006). DOI: 10.1021/nl061992v

Jeffrey T. Kohrt, Kevin J. Filipski, Wayne L. Cody, Christopher F. Bigge, Frances La, Kathleen Welch, Tawny Dahring, John W. Bryant, Daniele Leonard, Gary Bolton, Lakshmi Narasimhan, Erli Zhang, J. Thomas Peterson, Staci Haarer, Vaishali Sahasrabudhe, Nancy Janiczek, Shrilakshmi Desiraju, Mostofa Hena, Charles Fiakpui, Neerja Saraswat, Raman Sharma, Shaoyi Sun, Samarendra N. Maiti, Robert Leadley, Jeremy J. Edmunds, "The discovery of glycine and related amino acid-based factor Xa inhibitors," Bioorgan. Med. Chem. 14, 4379-4392 (2006). DOI: 10.1016/j.bmc.2006.02.040

Jeffrey T. Kohrt, Kevin J. Filipski, Wayne L. Cody, Cuiman Cai, Danette A. Dudley, Chad A. Van Huis, J. Adam Willardsen, Lakshmi S. Narasimhan, Erli Zhang, Stephen T. Rapundalo, Kamlai Saiya-Cork, Robert J. Leadley, Jeremy J. Edmunds, "The discovery of fluoropyridine-based inhibitors of the factor VIIa/TF complex—Part 2," Bioorg. Med. Chem. Lett. 16 (4), 1060-1064 (2006).

Takashi Komesu, G. D. Waddill, J.G. Tobin, "Spin-polarized electron energy loss spectroscopy on Fe(100) thin films grown on Ag(100)," J. Phys. Condens. Matter 18, 8829-8836 (2006). DOI: 10.1088/0953-8984/18/39/013

Chong Min Koo, Marc A. Hillmyer, Frank S. Bates, "Structure and Properties of Semicrystalline-Rubbery Multiblock Copolymers," Macromolecules 39 (2), January, 667-677 (2006). DOI: 10.1021/ma051098a

Nicole M. Koropatkin, Himadri B. Pakrasi, Thomas J. Smith, "Atomic structure of a nitrate-binding protein crucial for photosynthetic productivity," Proc. Natl. Acad. Sci. USA 103 (26), June, 9820-9825 (2006). DOI: 10.1073/pnas.602517103

Michael S. Kostelansky, Ji Sun, Sangho Lee, Jaewon Kim, Rodolfo Ghirlando, Aitor Hierro, Scott D. Emr, James H. Hurley, "Structural and Functional Organization of the ESCRT-I Trafficking Complex," Cell 125 (1), April, 113-126 (2006). DOI: 10.1016/j.cell.2006.01.049

Andrey Y. Kovalevsky, Fengling Liu, Sofiya Leshchendo, Arun K. Ghosh, John M. Louis, Robert W. Harrison, Irene T. Weber, "Ultra-high Resolution Crystal Structure of HIV-1 Protease Mutant Reveals Two Binding Sites for Clinical Inhibitor TMC114," J. Mol. Biol. 363, August, 161-173 (2006). DOI: 10.1016/j.jmb.2006.08.007

Andrey Yu Kovalevsky, Younfeng Tie, Fengling Liu, Peter I. Boross, Yuan-Fang Wang, Sofiya Leshchenko, Arun K. Ghosh, Robert W. Harrison, Irene T. Weber, "Effectiveness of Nonpeptide Clinical Inhibitor TMC-114 on HIV-1 Protease with Highly Drug Resistant Mutations D30N, I50V, and L90M," J. Med. Chem. 49, February, 1379-1387 (2006). DOI: 10.1021/jm050943c

Rumiana Koynova, Li Wang, Robert C. MacDonald, "An intracellular lamellar–nonlamellar phase transition rationalizes the superior performance of some cationic lipid transfection agents," Proc. Natl. Acad. Sci. USA 103 (39), 14373-14378 (2006). DOI: 10.1073/pnas.0603085103

Julia Kraineva, Chiara Nicolini, Pappannan Thiyagarajan, Elena Kondrashkina, Roland Winter, "Incorporation of [alpha]-chymotrypsin into the 3D channels of bicontinuous cubic lipid mesophases," BBA- Proteins Proteo. 1764 (3), March, 424-433 (2006). DOI: 10.1016/j.bbapap.2005.11.004

Daniel A. Kraut, Paul A. Sigala, Brandon Pybus, Corey W. Liu, Dagmar Ringe, Gregory A. Petsko, Daniel Herschlag, "Testing Electrostatic Complementarity in Enzyme Catalysis: Hydrogen Bonding in the Ketosteroid Isomerase Oxyanion Hole," PLoS Biol. 4 (4, e99), April, 0501-0519 (2006). DOI: 10.1371/journal.pbio.0040099

E. Kravtsov, D. Haskel, A. Cady, A. Yang, C. Vittoria, X. Zuo, V.G. Harris, "Site-specific local structure of Mn in artificial manganese ferrite films," Phys. Rev. B 74, 104114-1-104114-8 (2006). DOI: 10.1103/PhysRevB.74.104114

Barry Kreutz, Douglas M. Yau, Mark R. Nance, Shihori Tanabe, John J. G. Tesmer, Tohru Kozasa, "A New Approach to Producing Functional GR Subunits Yields the Activated and Deactivated Structures of GR[alpha][subscript 12/13] Proteins," Biochemistry-US 45 (1), 167-174 (2006). DOI: 10.1021/bi051729t

S. Krinsky, Y. Li, "Statistical analysis of the chaotic optical field from a self-amplified spontaneous-emission free-electron laser," Phys. Rev. E 73, 066501-1-066501-13 (2006). DOI: 10.1103/PhysRevE.73.066501

K.M. Krupka, H.T. Shaef, B.W. Arey, S.M. Heald, W.J. Deutsch, M.J. Lindberg, K.J. Cantrell, "Residual Waste from Hanford Tanks 241-C-203 and 241-C-204. 1. Solids Characterization," Environ. Sci. Technol. 40, 3749-3754 (2006). DOI: 10.1021/es051155f

Jan Kubelka, Thang K. Chiu, David R. Davies, William A. Eaton, James Hofrichter, "Sub-microsecond Protein Folding," J. Mol. Biol. 359, 546-553 (2006). DOI: 10.1016/j.jmb.2006.03.034

Atsushi Kubo, Boris Kiefer, Guoyin Shen, Vitali B. Prakapenka, Robert J. Cava, Thomas S. Duffy, "Stability and equation of state of the post-perovskite phase in MgGeO[subscript 3] to 2 Mbar," Geophys. Res. Lett. 33, L12S12-1-L12S12-4 (2006). DOI: 10.1029/2006GL025686

D.A. Kukuruznyak, J.G. Moyer, N.T. Nguyen, E.A. Stern, F.S. Ohuchi, "Relationship between electronic and crystal structure in Cu–Ni–Co–Mn–O spinels Part A: Temperature-induced structural transformation," J. Electron. Spectrosc. 150, February, 275-281 (2006). DOI: 10.1016/j.elspec.2005.06.009

Anand Kulkarni, Allen Goland, Herbert Herman, Andrew J. Allen, Tabbetha Dobbins, Francesco De Carlo, Jan Ilavsky, Gabrielle G. Long, Stacy Fang, Paul Lawton, "Advanced neutron and X-ray techniques for insights into the microstructure of EB-PVD thermal barrier coatings," Mat. Sci. Eng. A 426, 43-52 (2006). DOI: 10.1016/j.msea.2006.03.070

Ravhi S. Kumar, Andrew L. Cornelius, Malcolm F. Nicol, Kinson C. Kam, Anthony K. Cheetham, Jason S. Gardner, "Pressure-induced structural transitions in Tb-pyrochlore oxides," Appl. Phys. Lett. 88, 031903-1-031903-3 (2006). DOI: 10.1063/1.2165212

Ravhi S. Kumar, D. Prabhakaran, Andrew Boothroyd, Malcolm F. Nicol, Andrew Cornelius, "High-pressure structure of LaSr[subscript 2]Mn[subscript 2]O[subscript 7] bilayer manganite," J. Phys. Chem. Solids 67, 2046-2050 (2006). DOI: 10.1016/j.jpcs.2006.05.029

Vinit Kumar, Kwang-Je Kim, "Analysis of Smith-Purcell Free-Electron Lasers," Phys. Rev. E 73 (2), February, 026501-1-026501-15 (2006). DOI: 10.1103/PhysRevE.73.026501

Jennifer Kung, Baosheng Li, Robert C. Liebermann, "Ultrasonic observations of elasticity changes across phase transformations in MgSiO[subscript 3] pyroxenes," J. Phys. Chem. Solids 67 (9-10), 2051-2055 (2006). DOI: 10.1016/j.jpcs.2006.05.028

Mitsuo Kuratani, Hiroaki Sakai, Masahiro Takahashi, Tatsuo Yanagisawa, Takatsugu Kobayashi, Kazutaka Murayama, Lirong Chen, Zhi-Jie Liu, Bi-Cheng Wang, Chizu Kuroishi, Seiki Kuramitsu, Takaho Terada, Yoshitaka Bessho, Mikako Shirouzu, Shun-ichi Sekine, Shigeyuki Yokoyama, "Crystal Structures of Tyrosyl-tRNA Synthetases from Archaea," J. Mol. Biol. 355, 395-408 (2006). DOI: 10.1016/j.jmb.2005.10.073

Deborah A. Kuzmanovic, Ilya Elashvili, Charles Wick, Catherine O'Connell, Susan Krueger, "Quantification of RNA in bacteriophage MS2-like viruses in solution by small-angle X-ray scattering," Radiat. Phys. Chem. 75 (3), March, 359-368 (2006). DOI: 10.1016/j.radphyschem.2005.11.005

Konstantin Kuznedelov, Valerie Lamour, Georgia Patikoglou, Mark Chlenov, Seth A. Darst, Konstantin Severinov, "Recombinant Thermus aquaticus RNA Polymerase for Structural Studies," J. Mol. Biol. 359 (1), May, 110-121 (2006). DOI: 10.1016/j.jmb.2006.03.009

L.W. Kwok, I. Shcherbakova, J.S. Lamb, H.Y. Park, K. Andresen, H. Smith, M. Brenowitz, L. Pollack, "Concordant Exploration of the Kinetics of RNA Folding from Global and Local Perspectives," J. Mol. Biol. 355 (2), January, 282-293 (2006). DOI: 10.1016/j.jmb.2005.10.070

Debdutta Lahiri, "Distortion induced by Zn in La[subscript 1.85]Sr[subscript 0.15]CuO[subscript 4] superconductor: An XAFS study," Physica C 436 (1), April, 32-37 (2006). DOI: 10.1016/j.physc.2006.01.003

Debdutta Lahiri, V. Subramanian, Bruce A. Bunker, Prashant V. Kamat, "Probing photochemical transformations at TiO[subscript 2]/Pt and TiO[subscript 2]/Ir interfaces using x-ray absorption spectroscopy," J. Chem. Phys. 124 (20), 204720-1-204720-7 (2006). DOI: 10.1063/1.2198193

Chunqiu Lai, Rebecca J. Gum, Melissa Daly, Elizabeth H. Fry, Charles Hutchins, Celerino Abad-Zapatero, Thomas W. von Geldern, "Benzoxazole benzenesulfonamides as allosteric inhibitors of fructose-1,6-bisphosphatase," Bioorg. Med. Chem. Lett. 16 (7), April, 1807-1810 (2006). DOI: 10.1016/j.bmcl.2006.01.014

David C. Lamb, Youngchang Kim, Liudmilla V. Yermalitskaya, Valery N. Yermalitsky, Galina I. Lepesheva, Steven L. Kelly, Michael R. Waterman, Larissa M. Podust, "A Second FMN Binding Site in Yeast NADPH-Cytochrome P450 Reductase Suggests a Mechanism of Electron Transfer by Diflavin Reductases," Structure 14, January, 51-61 (2006). DOI: 10.1016/j.str.2005.09.015

Jason S. Lamoureux, J.N. Mark Glover, "Principles of Protein-DNA Recognition Revealed in the Structural Analysis of Ndt80-MSE DNA Complexes," Structure 14, March, 555-565 (2006). DOI: 10.1016/j.str.2005.11.017

Phoebe J. Lam, James K.B. Bishop, Cara C. Henning, Matthew A. Marcus, Glenn A. Waychunas, Inez Y. Fung, "Wintertime phytoplankton bloom in the subartic Pacific supported by continental margin iron," Global Biogeochem. Cy. 20, GB1006-GB1017 (2006). DOI: 10.1029/2005GB002557

Patrick J. LaRiviere, David Billmire, Phillip Vargas, Mark Rivers, Stephen R. Sutton, "Penalized-likelihood image reconstruction for x-ray fluorescence computed tomography," Opt. Eng. 45 (7), July, 077005-1-077005-10 (2006). DOI: 0091-3286/2006

Michael V. Lasker, Santosh M. Kuruvilla, Mark M. Gajjar, Anubhav Kapoor, Satish K. Nair, "Metal Ion–Mediated Reduction in Surface Entropy Improves Diffraction Quality of Crystals of the IRAK-4 Death Domain," J. Biomol. Tech. 17 (2), April, 114-121 (2006).

Cheryl Lau, Ronit Bitton, Havazelet Bianco-Peled, David G. Schultz, David J. Cookson, ShaneT. Grosser, James W. Schneider, "Morphological Characterization of Self-Assembled Peptide Nucleic Acid Amphiphiles," J. Phys. Chem. B 110, 9027-9033 (2006). DOI: 10.1021/jp057049h

A. Lazicki, C.-S. Yoo, W.J. Evans, W.E. Pickett, "Pressure-induced antifluorite-to-anticotunnite phase transition in lithium oxide," Phys. Rev. B 73 (18), 184120-1-184120-7 (2006). DOI: 10.1103/PhysRevB.73.184120

V. Lebedev, V. Nagaslaev, A. Valishev, V. Sajaev, "Measurement and Correction of Linear Optics and Coupling at Tevatron Complex," Nucl. Instrum. Methods A 558, 299-302 (2006).

Byeongdu Lee, Chieh-Tsung Lo, Soenke Seifert, RandallE. Winans, "Silver behenate as a calibration standard of grazing-incidence small-angle X-ray scattering," J. Appl. Crystallogr. 39 (5), October, 749-751 (2006). DOI: 10.1107/S0021889806031244

Chingwei V. Lee, Sarah G. Hymowitz, Heidi J. Wallweber, Nathaniel C. Gordon, Karen L. Billeci, Siao-Ping Tsai, Deanne M. Compaan, Jian Ping Yin, Qian Gong, Robert F. Kelley, Laura E. DeForge, Flavius Martin, Melissa A. Starovasnik, Germaine Fuh, "Synthetic anti-BR3 antibodies that mimic BAFF binding and target both human and murine B cells," Blood 108 (9), November, 3103-3111 (2006). DOI: 10.1182/blood-2006-03-011031

D.R. Lee, A. Hagman, Xuefa Li, S. Narayanan, Jin Wang, K.R. Shull, "Perturbation to the resonance modes by gold nanoparticles in a thin-film-based x-ray waveguide," Appl. Phys. Lett. 88, April, 153101-1-153101-3 (2006). DOI: 10.1063/1.2191091

Jihun Lee, Vikash Kumar Dubey, Thayumanasamy Somasundaram, Michael Blaber, "Conversion of Type I 4:6 to 3:5 [beta]-Turn Types in Human Acidic Fibroblast Growth Factor: Effects upon Structure, Stability, Folding, and Mitogenic Function," Proteins 62 (3), February, 686-697 (2006). DOI: 10.1002/prot.20808

Jae Young Lee, Wei Yang, "UvrD Helicase Unwinds DNA One Base Pair at a Time by a Two-Part Power Stroke," Cell 127 (7), December, 1349-1360 (2006). DOI: 10.1016/j.cell.2006.10.049

M.H. Lee, R.T. Ott, M.F. Besser, M.J. Kramer, D.J. Sordelet, "Compositional dependence on phase selection during devitrification of amorphous Zr–Pt alloys," Scripta Mater. 55 (6), 505-508 (2006). DOI: 10.1016/j.scriptamat.2006.05.039

Raphael C. Lee, Florin Despa, L. Guo, Pravin Betala, Anne Kuo, P. Thiyagarajan, "Surfactant Copolymers Prevent Aggregation of Heat Denatured Lysozyme," Ann. Biomed. Eng. 34 (7), June, 1190-1200 (2006). DOI: 10.1007/s10439-006-9139-z

Michael Lefenfeld, Julian Baumert, Eli Sloutskin, Ivan Kuzmenko, Peter Pershan, Moshe Deutsch, Colin Nuckolls, Benjamin M. Ocko, "Direct structural observation of a molecular junction by high-energy x-ray reflectometry," Proc. Natl. Acad. Sci. USA 103 (8), February, 2541-2545 (2006). DOI: 10.1073/pnas.0508070103

Christopher Lehmann, Tadhg P. Begley, Steven E. Ealick, "Structure of the Escherichia coli ThiS-ThiF complex, a key component of the sulfur transfer system in thiamin biosynthesis," Biochemistry-US 45 (1), December, 11-19 (2006). DOI: 10.1021/bi051502y

Matthias Lehmann, Shin-Woong Kang, Christiane Kohn, Sonke Haseloh, Ute Kolb, Dieter Schollmeyer, Qing Bing Wang, Satyendra Kumar, "Shape-persistent V-shaped mesogens—formation of nematic phases with bixaial order," J. Mater. Chem. 16, 4326-4334 (2006). DOI: 10.1039/b605718g

Petr G. Leiman, Mikhail M. Shneider, Vadim V. Mesyanzhinov, Michael G. Rossmann, "Evolution of Bacteriophage Tails: Structure of T4 Gene Product 10," J. Mol. Biol. 358 (3), May, 912-921 (2006). DOI: 10.1016/j.jmb.2006.02.058

Maggy F. Lengke, Bruce Ravel, Michael E. Fleet, Gregory Wanger, Robert A. Gordon, Gordon Southam, "Mechanisms of Gold Bioaccumulation by Filamentous Cyanobacteria from Gold(III)–Chloride Complex," Environ. Sci. Technol. 40 (20), 6304-6309 (2006). DOI: 10.1021/es061040r

Lyle E. Levine, Bennett C. Larson, Wenge Yang, Michael E. Kassner, Jonathan Z. Tischler, Michael A. Delos-Reyes, Richard J. Fields, Wenjun Liu, "X-ray microbeam measurements of individual dislocation cell elastic strains in deformed single-crystal copper," Nat. Mater. 5, August, 619-622 (2006). DOI: 10.1038/nmat1698

Igor Levin, Eric Cockayne, Michael W. Lufaso, Joseph C. Woicik, James E. Maslar, "Local Structures and Raman Spectra in the Ca(Zr,Ti)O[subscript 3] Perovskite Solid Solutions," Chem. Mater. 18 (3), February, 854-860 (2006). DOI: 10.1021/cm0523438

D. Lexa, A.J. Kropf, "Thermal, Structural, and Radiological Properties of Irradiated Graphite from the ASTRA Research Reactor – Implications for Disposal," J. Nucl. Mater. 348, 122-132 (2006). DOI: 10.1016/j.jnucmat.2005.09.010

B. Li, H.D. Brody, D.R. Black, H.E. Burdette, C. Rau, "A compact design of a temperature gradient furnace for synchrotron microradiography," Meas. Sci. Technol. 17, 1883-1887 (2006). DOI: 10.1088/0957-0233/17/7/029

B. Li, H.D. Brody, D.R. Black, H.E. Burdette, C. Rau, "Real time observation of dendritic solidification in alloys by synchrotron microradiography," J. Phys. D 39, 4450-4456 (2006). DOI: 10.1088/0022-3727/39/20/023

Bo Li, John Paul J. Yu, Joseph S. Brunzelle, Gert N. Moll, Wilfred A. van der Donk, Satish K. Nair, "Structure and Mechanism of the Lantibiotic Cyclase Involved in Nisin Biosynthesis," Science 311, March, 1464-1467 (2006). DOI: 10.1126/science.1121422

Chunhua Li, Hyunjung Kim, Jun Jiang, Clive Li, Tadanori Koga, Laurence Lurio, Steve Schwarz, Suresh Narayanan, Heeju Lee, Young Joo Lee, Zhang Jiang, Sunil Sinha, M.H. Rafailovich, J.C. Sokolov, "The effect of surface interactions on the viscosity of polymer thin films," Europhys. Lett. 73 (6), 899-905 (2006). DOI: 10.1209/epl/i2005-10475-5

D. Li, B. H. O'Connor, I.-M. Low, A. Van Riessen, B. H. Toby, "Mineralogy of Al-Substituted Goethites," Powder Diffr. 21 (4), December, 289-299 (2006). DOI: 10.1154/1.2358358

Hanns-Peter Liermann, Robert T. Downs, Hexiong Yang, "Site disorder revealed through Raman spectra from oriented single crystals: A case study on karooite (MgTi[subscript 2]O[subscript 5])," Am. Mineral. 91 (5-6), May, 790-793 (2006). DOI: 10.2138/am.2006.2027

Feng Li, Sanjay Sarkhel, Christopher J. Wilds, Zdzislaw Wawrzak, Thazha P. Prakash, Muthiah Manoharan, Martin Egli, "2'-Fluoroarabino- and Arabinonucleic Acid Show Different Conformations, Resulting in Deviating RNA Affinities and Processing of Their Heteroduplexes with RNA by RNase H," Biochemistry-US 45 (13), 4141-4152 (2006). DOI: 10.1021/bi052322r

Haitao Li, Serge Ilin, Wooikoon Wang, Elizabeth M. Duncan, Joanna Wysocka, C. David Allis, Dinshaw J. Patel, "Molecular basis for site-specific read-out of histone H3K4me3 by the BPTF PHD finger of NURF," Nature 442, 91-95 (2006). DOI: 10.1021/bi051502y S0006-2960(05)01502-3

J. Li, W. Sturhahn, J.M. Jackson, V.V. Struzhkin, J.F. Lin, J. Zhao, H.K. Mao, G. Shen, "Pressure effect on the electronic structure of iron in (Mg,Fe)(Si,Al)O[subscript 3] perovskite: a combined synchrotron Mössbauer and X-ray emission spectroscopy study up to 100 GPa," Phys. Chem. Miner. 33 (8-9), November, 575-585 (2006). DOI: 10.1007/s00269-006-0105-y

J. Li, D. Vaknin, S.L. Bud'ko, P.C. Canfield, D. Pal, M.R. Eskildsen, Z. Islam, V.G. Kogan, "Magnetic-field-induced orientation of superconducting MgB[subscript 2] crystallites determined by x-ray diffraction," Phys. Rev. B 74, 064502-1-064502-4 (2006). DOI: 10.1103/PhysRevB.74.06450

Jingzhi Li, Yunkun Wu, Xinguo Qian, Bingdong Sha, "Crystal structure of yeast Sis1 peptide-binding fragment and Hsp70 Ssa1 C-terminal complex," Biochem. J. 398, September, 353-360 (2006). DOI: 10.1042/BJ20060618

Liang Li, Debarshi Mustafi, Qiang Fu, Valentina Tereshko, Delai L. Chen, Joshua D. Tice, Rustem F. Ismagilov, "Nanoliter microfluidic hybrid method for simultaneous screening and optimization validated with crystallization of membrane proteins," Proc. Natl. Acad. Sci. USA 103 (51), December, 19243-19248 (2006). DOI: 10.1073/pnas.0607502103

Wayne Lilyestrom, Michael G. Klein, Rongguang Zhang, Andrzej Joachimiak, Xiaojiang S. Chen, "Crystal structure of SV40 large T-antigen bound to p53: interplay between a viral oncoprotein and a cellular tumor suppressor," Gene Dev. 20, 2373-2382 (2006). DOI: 10.1101/gad.1456306

B. Lings, J. S. Wark, M.F. DeCamp, D.A. Reis, S. Fahy, "Simulations of time-resolved x-ray diffraction in Laue geometry," J. Phys. Condens. Matter 18, 9231-9244 (2006). DOI: 10.1088/0953-8984/18/40/009

Jung-Fu Lin, Alexander G. Gavriliuk, Viktor V. Struzhkin, Steven D. Jacobsen, Wolfgang Sturhahn, Michael Y. Hu, Paul Chow, Choong-Shik Yoo, "Pressure-induced electronic spin transition of iron in magnesiowustite-(Mg,Fe)O," Phys. Rev. B 73, 113107-1-113107-4 (2006). DOI: 10.1103/PhysRevB.73.113107

Jung-Fu Lin, Steven D. Jacobsen, Wolfgang Sturhahn, Jennifer M. Jackson, Jiyong Zhao, Choong-Shik Yoo, "Sound velocities of ferropericlase in the Earth's lower mantle," Geophys. Res. Lett. 33, November, L22304-1-L22304-5 (2006). DOI: 10.1029/2006GL028099

Jan Lipfert, Ian S. Millett, Sonke Seifert, Sebastian Doniach, "Sample holder for small-angle x-ray scattering static and flow cell measurements," Rev. Sci. Instrum. 77 (4), 046108-1-046108-3 (2006). DOI: 10.1063/1.2194484

Kristina E. Lipinska-Kalita, Michael Pravica, Gino Mariotto, Patricia E. Kalita, Yoshimichi Ohki, "Core/shell ZrTiO[subscript 4]/LiAlSi[subscript 2]O[subscript 6] nanocrystals: A synchrotron X-ray diffraction study of high-pressure compression," J. Phys. Chem. Solids 67, 2072-2076 (2006). DOI: 10.1016/j.jpcs.2006.05.053

Harry J. Lipkin, Philip D. Mannheim, "Bounds on localized modes in the crystal impurity problem," Phys. Rev. B 73 (17), 174105-1-174105-11 (2006). DOI: 10.1103/PhysRevB.73.174105

Qing' An Li, K.E. Gray, S. Nyborg Ancona, H. Zheng, S. Rosenkranz, R. Osborn, J.F. Mitchell, "First-Order Metal-Insulator Transitions in Manganites: Are They Universal?," Phys. Rev. Lett. 96, February, 087201-1-087201-4 (2006). DOI: 10.1103/PhysRevLett.96.087201

Qun Li, Keith W. Woods, Sheela Thomas, Gui-Dong Zhu, Garrick Packard, John Fisher, Tongmei Li, Jianchun Gong, Jurgen Dinges, Xiaohong Song, Jason Abrams, Yan Luo, Eric F. Johnson, Yan Shi, Xuesong Liu, Vered Klinghofer, RonDes Jong, Tilman Oltersdorf, Vincent S. Stoll, Clarissa G. Jakob, Saul H. Rosenberg, Vincent L. Giranda, "Synthesis and structure–activity relationship of 3,4'-bispyridinylethylenes: Discovery of a potent 3-isoquinolinylpyridine inhibitor of protein kinase B (PKB/Akt) for the treatment of cancer," Bioorg. Med. Chem. Lett. 16 (7), April, 1759-2052 (2006). DOI: 10.1016/j.bmcl.2005.12.065

Chian Liu, R. Conley, A.T. Macrander, J. Maser, H.C. Kang, G.B. Stephenson, "A multilayer nanostructure for linear zone-plate applications," Thin Solid Films 515 (2), October, 654-657 (2006). DOI: 10.1016/j.tsf.2005.12.233

Fengling Liu, Andrey Y. Kovalevsky, John M. Louis, Peter I. Boross, Yuan-Fang Wang, Robert W. Harrison, Irene T. Weber, "Mechanism of Drug Resistance Revealed by the Crystal Structure of the Unliganded JHIV-1 Protease with F53L Mutation," J. Mol. Biol. 358 (5), May, 1191-1199 (2006). DOI: 10.1016/j.jmb.2006.02.076

Gang Liu, Sudeep Debnath, Kristian W. Paul, Weiqiang Han, Douglas B. Hausner, Hazel-Ann Hosein, F. Marc Michel, John B. Parise, Donald L. Sparks, Daniel R. Strongin, "Characterization and Surface Reactivity of Ferrihydrite Nanoparticles Assembled in Ferritin," Langmuir 22 (22), 9313-9321 (2006). DOI: 10.1021/la0602214

Guijian Liu, Weidong Huang, Robert D. Moir, Charles R. Vanderburg, Barry Lai, Zicheng Peng, Rudolph E. Tanzi, Jack T. Rogers, Xudong Huang, "Metal exposure and Alzheimer's pathogenesis," J. Struct. Biol. 155, 45-51 (2006). DOI: 10.1016/j.jsb.2005.12.011

Haozhe Liu, John S. Tse, Ho-kwang Mao, "Stability of rocksalt phase of zinc oxide under strong compression: Synchrotron x-ray diffraction experiments and first-principles calculation studies," J. Appl. Phys. 100 (9), 093509-1-093509-5 (2006). DOI: 10.1063/1.2357644

Jing-Yuan Liu, David E. Timm, Thomas D. Hurley, "Pyrithiamine as a Substrate for Thiamine Pyrophosphokinase," J. Biol. Chem. 281 (10), March, 6601-6607 (2006). DOI: 10.1074/jbc.M510951200

Quansheng Liu, Jaclyn C. Greimann, Christopher D. Lima, "Reconstitution, Activities, and Structure of the Eukaryotic RNA Exosome," Cell 127 (6), December, 1223-1237 (2006). DOI: 10.1016/j.cell.2006.10.037

Xin Liu, Adrienne Clements, Kehao Zhao, Ronen Marmorstein, "Structure of the Human Papillomavirus E7 Oncoprotein and Its Mechanism for Inactivation of the Retinoblastoma Tumor Suppressor," J. Biol. Chem. 281 (1), 578-586 (2006). DOI: 10.1074/jbc.M508455200

Xinqi Liu, Yanan Zhu, Shaodong Dai, Janice White, Fred Peyerl, John W. Kappler, Philippa Marrack, "Bcl-xl does not have to bind Bax to protect T cells from death," J. Exp. Med. 203 (13), December, 2953-2961 (2006). DOI: 10.1084/jem.20061151

Zhi-Jie Liu, Galina A Stepanyuk, Eugene S . Vysotski, John Lee, Svetlana V. Markova, Natalia P. Malikova, Bi-Cheng Wang, "Crystal structure of obelin after Ca[superscript 2+]-triggered bioluminescence suggests neutral coelenteramide as the primary excited state," Proc. Natl. Acad. Sci. USA 103 (8), February, 2570-2575 (2006). DOI: 10.1073/pnas.0511142103

F. Livet, F. Bley, F. Ehrburger-Dolle, I. Morfin, E. Geissler, M. Sutton, "X-ray intensity fluctuation spectroscopy by heterodyne detection," J. Synchrotron Rad. 13 (6), November, 453-458 (2006). DOI: 10.1107/S0909049506030044

Y. Li, "Electro-optical sampling at near-zero optical bias," Appl. Phys. Lett. 88, June, 251108-1 -251108-3 (2006). DOI: http://dx.doi.org/10.1063/1.2214143

Y. Li, W. Guo, K. Harkay, W. Liu, "Storage-Ring-Based, Ultrashort Positron Beam Source," Appl. Phys. Lett. 89, July, 021113-1-021113-3 (2006). DOI: 10.1063/1.2221503

Yong-Fu Li, Steven Poole, Fatima Rasulova, Lothar Esser, Stephen J. Savarino, Di Xia, "Crystallization and preliminary X-ray diffraction analysis of CfaE, the adhesive subunit of the CFA/I fimbriae from human enterotoxigenic Escherichia coli," Acta Crystallogr. F 62, 121-124 (2006). DOI: 10.1107/S1744309105043198

Chieh-Tsung Lo, Byeongdu Lee, Randall E. Winans, P. Thiyagarajan, "Effect of Dispersion of Inorganic Nanoparticles on the Phase Behavior of Block Copolymers in a Selective Solvent," Macromolecules 39 (19), September, 6318-6320 (2006). DOI: 10.1021/ma060879o

E. Lombi, K.G. Scheckel, R.D. Armstrong, S. Forrester, J.N. Cutler, D. Paterson, "Speciation and Distribution of Phosphorus in a Fertilized Soil: A Synchrotron-Based Investigation," Soil Sci. Soc. Am. J. 70, 2038-2048 (2006). DOI: 10.2136/sssaj2006.0051

Kenton L. Longenecker, Kent D. Stewart, David J. Madar, Clarissa G. Jakob, Elizabeth H. Fry, Sherwin Wilk, Chun W. Lin, Stephen J. Ballaron, Michael A. Stashko, Thomas H. Lubben, Hong Yong, Daisy Pireh, Zhonghua Pei, Fatima Basha, Paul E. Wiedeman, Thomas W. von Geldern, James M. Trevillyan, Vincent S. Stoll, "Crystal Structures of DPP-IV (CD26) from Rat Kidney Exhibit Flexible Accommodation of Peptidase-Selective Inhibitors," Biochemistry-US 45 (24), June, 7474-7482 (2006). DOI: 10.1021/bi060184f

Meizhen Lou, Thomas P.J. Garrett, Neil M. McKern, Peter A. Hoyne, V. Chandana Epa, John D. Bentley, George O. Lovrecz, Leah J. Cosgrove, Maurice J. Frenkel, Colin W. Ward, "The first three domains of the insulin receptor differ structurally from the insulin-like growth factor 1 receptor in the regions governing ligand specificity," Proc. Natl. Acad. Sci. USA 103 (33), August, 12429-12434 (2006). DOI: 10.1073/pnas.0605395103

George T. Lountos, Rongrong Jiang, William B. Welborn, Tracey L. Thaler, Andreas S. Bommarius, Allen M. Orville, "The Crystal Structure of NAD(P)H Oxidase from Lactobacillus sanfranciscensis: Insights into the Conversion of O[subscript 2] into Two Water Molecules by the Flavoenzyme," Biochemistry-US 45, August, 9648-9659 (2006). DOI: 10.1021/bi060692p

Jeffrey J. Lovelace, Gloria E.O. Borgstahl, "Ripple: a program to collect and analyze digital topographic sequences," J. Appl. Crystallogr. 39, 466-467 (2006). DOI: 10.1107/S0021889806014956

Jeffrey J. Lovelace, Cameron R. Murphy, Reinhard Pahl, Keith Brister, Gloria E.O. Borgstahl, "Tracking reflections through cryogenic cooling with topography," J. Appl. Crystallogr. 39 (3), June, 425-432 (2006). DOI: 10.1107/S0021889806012763

Jeff Zhiqiang Lu, Tamaki Fujiwara, Hitoshi Komatsuzawa, Motoyuki Sugai, Joshua Sakon, "Cell Wall-targeting Domain of Glycylglycine Endopeptidase Distinguishes among Peptidoglycan Cross-bridges," J. Biol. Chem. 281 (1), January, 549-558 (2006). DOI: 10.1074/jbc.M509691200

L. Lu, J.N. Hancock, G. Chabot-Couture, K. Ishii, O.P. Vajk, G. Yu, J. Mizuki, D. Casa, T. Gog, M. Greven, "Incident energy and polarization-dependent resonant inelastic x-ray scattering study of La[subscript 2]CuO[subscript 4]," Phys. Rev. B 74, 224509-1-224509-9 (2006). DOI: 10.1103/PhysRevB.74.224509

Miao Lu, Tongpil Min, David Eliezer, Hao Wu, "Native Chemical Ligation in Covalent Caspase Inhibition by p35," Chem. Biol. 13 (2), February, 117-122 (2006). DOI: 10.1016/j.chembiol.2005.12.007

A.H. Lumpkin, "Nonintercepting Diagnostics for Transverse Beam Parameters: from Rings to ERLs," Nucl. Instrum. Methods 557 (1), February, 318-323 (2006).

Vladimir V. Lunin, Elena Dobrovetsky, Galina Khutoreskaya, Rongguang Zhang, Andrzej Joachimiak, Declan A. Doyle, Alexey Bochkarev, Michael E. Maguire, Aled M. Edwards, Christopher M. Koth, "Crystal structure of the CorA Mg[superscript 2+] transporter," Nature 440 (6), April, 833-837 (2006). DOI: 10.1038/nature04642

Guangming Luo, Sarka Malkova, Sai Venkatesh Pingali, David G. Schultz, Binhua Lin, Mati Meron, Ilan Benjamin, Petr Vanysek, Mark L. Schlossman, "Structure of the Interface between Two Polar Liquids: Nitrobenzene and Water," J. Phys. Chem. B 110 (10), 4527-4530 (2006). DOI: 10.1021/jp057103u

Guangming Luo, Sarka Malkova, Jaesung Yoon, David G. Schultz, Binhua Lin, Mati Meron, Ilan Benjamin, Petr Vanysek, Mark L. Schlossman, "Ion Distributions near a Liquid-Liquid Interface," Science 311 (5758), January, 216-218 (2006). DOI: 10.1126/science.1120392

Guangming Luo, Sarka Malkova, Jaesung Yoon, David G. Schultz, Binhua Lin, Mati Meron, Ilan Benjamin, Petr Vanysek, Mark L. Schlossman, "Ion distributions at the nitrobenzene–water interface electrified by a common ion," J. Electroanal. Chem. 593 (1-2), August, 142-158 (2006). DOI: 10.1016/j.jelechem.2006.03.051

Peng Lu, Yun Li, Amanda Gorman, Young-In Chi, "Crystallization of hepatocyte nuclear factor 1[beta] in complex with DNA," Acta Crystallogr. F 62, 525-529 (2006). DOI: 10.1107/S1744309106015168

I.S. Lyubutin, A.G. Gavriliuk, V.V. Struzhkin, S.G. Ovchinnikov, S.A. Kharlamova, L.N. Bezmaternykh, M. Hu, P. Chow, "Pressure-Induced Electron Spin Transition in the Paramagnetic Phase of the GdFe[subscript 3](BO[subscript 3])[subscript 4] Heisenberg Magnet," JETP Lett. 84 (9), 518-523 (2006). DOI: 10.1134/S0021364006210119

Mischa Machius, R. Max Wynn, Jacinta L. Chuang, Jun Li, Ronald Kluger, Daria Yu, Diana R. Tomchick, Chad A. Brautigam, David T. Chuang, "A Versatile Conformational Switch Regulates Reactivity in Human Branched-Chain [alpha]-Ketoacid Dehydrogenase," Structure 14, February, 287-298 (2006). DOI: 10.1016/j.str.2005.10.009

B.R. Maddox, A. Lazicki, C.S. Yoo, V. Iota, M. Chen, A.K. McMahan, M.Y. Hu, P. Chow, R.T. Scalettar, W.E. Pickett, "4f Delocalization in Gd: Inelastic X-Ray Scattering at Ultrahigh Pressure," Phys. Rev. Lett. 96, June, 215701-1-215701-4 (2006). DOI: 10.1103/PhysRevLett.96.215701

B.R. Maddox, C.S. Yoo, Deepa Kasinathan, W.E. Pickett, R.T. Scalettar, "High-pressure structure of half-metallic CrO[subscript 2]," Phys. Rev. B 73, April, 144111-1-144111-9 (2006). DOI: 10.1103/PhysRevB.73.144111

Jennifer A. Maier, Todd A. Brugel, Michael P. Clark, Mark Sabat, Adam Golebiowski, Roger G. Bookland, Matthew J. Laufersweiler, Steven K. Laughlin, John C. VanRens, Biswanath De, Lily C. Hsieh, Kimberly K. Brown, Karen Juergens, Richard. L. Walter, Michael J. Janusz, "Development of N-2,4-pyrimidine-N-phenyl-N'-alkyl ureas as orally active inhibitors of tumor necrosis factor alpha (TNF-a) synthesis. Part 2," Bioorg. Med. Chem. Lett. 16, May, 3514-3518 (2006).

John K. Ma, Christopher J. Carrell, F. Scott Mathews, Victor L. Davidson, "Site-Directed Mutagenesis of Proline 52 To Glycine in Amicyanin Converts a True Electron Transfer Reaction into One that Is Conformationally Gated," Biochemistry-US 45 (27), 8284-8293 (2006). DOI: 10.1021/bi0605134

Koki Makabe, Dan McElheny, Valentia Tereshko, Aaron Hilyard, Grzegorz Gawlak, Shude Yan, Akiko Koide, Shohei Koide, "Atomic structures of peptide self-assembly mimics," Proc. Natl. Acad. Sci. USA 103 (47), November, 17753-17758 (2006). DOI: 10.1073/pnas.0606690103

Koki Makabe, Valentina Tereshko, Grzegorz Gawlak, Shude Yan, Shohei Koide, "Atomic-resolution crystal structure of Borrelia burgdorferi outer surface protein A via surface engineering," Protein Sci. 15, 1907-1914 (2006). DOI: 10.1110/ps.062246706

Mohamed Makha, Colin L. Raston, Alexandre N. Sobolev, Leonard J. Barbour, Peter Turner, "Endo- versus exo-cavity interplay of p-benzylcalix[4]arene with spheroidal molecules," Cryst. Eng. Comm. 8 (4), 306-308 (2006). DOI: 10.1039/b600550k

Mohamed Makha, Colin L. Raston, Alexandre N. Sobolev, Peter Turner, "Exclusive Endo-Cavity Interplay of t-Bu-calix[6]arene with C[subscript 70]," Cryst. Growth Des. 6 (1), November, 224-228 (2006).

Zulfiqar A. Malik, Brian F. Tack, "Structure of human MIP-3[alpha] chemokine," Acta Crystallogr. F 62 (7), July, 631-634 (2006). DOI: 10.1107/S1744309106006890

M.E. Manley, M. Yethiraj, H. Sinn, H.M. Volz, A. Alatas, J.C. Lashley, W.L. Hults, G.H. Lander, J.L. Smith, "Formation of a New Dynamical Mode in [alpha]-Uranium Observed by Inelastic X-Ray and Neutron Scattering," Phys. Rev. Lett. 96, March, 125501-1-125501-4 (2006). DOI: 10.1103/PhysRevLett.96.125501

Philip D. Mannheim, "Arbitrary force-constant changes in the crystal impurity problem," Phys. Rev. B 73, 184103-1-184103-8 (2006). DOI: 10.1103/PhysRevB.73.184103

Bouchaib Manoun, R.P. Gulve, S.K. Saxena, S. Gupta, M.W. Barsoum, C.S. Zha, "Compression behavior of M[subscript 2]AlC (M=Ti, V, Cr, Nb, and Ta) phases to above 50 GPa," Phys. Rev. B 73, 024110-1-024110-7 (2006). DOI: 10.1103/PhysRevB.73.02411

Bouchaib Manoun, S.K. Saxena, T. El-Raghy, M.W. Barsoum, "High-pressure x-ray diffraction study of Ta[subscript 4]AlC[subscript 3]," Appl. Phys. Lett. 88, 201902-1-201902-3 (2006). DOI: 10.1063/1.2202387

Bouchaib Manoun, F.X. Zhanga, S.K. Saxena, T. El-Raghy, M.W. Barsoum, "X-ray high-pressure study of Ti[subscript 2]AlN and Ti[subscript 2]AlC," J. Phys. Chem. Solids 67, 2091-2094 (2006). DOI: 10.1016/j.jpcs.2006.05.051

Ho-kwang Mao, James Badro, Jinfu Shu, Russell J. Hemley, Anil K. Singh, "Strength, anisotropy, and preferred orientation of solid argon at high pressures," J. Phys. Condens. Matter 18, S963-S968 (2006). DOI: 10.1088/0953-8984/18/25/S04

Wendy L. Mao, Andrew J. Campbell, Dion L. Heinz, Guoyin Shen, "Phase relations of Fe–Ni alloys at high pressure and temperature," Phys. Earth Planet. In. 155 (1-2), April, 146-151 (2006). DOI: 10.1016/j.pepi.2005.11.002

Wendy L. Mao, Ho-kwang Mao, "Ultrahigh-pressure experiment with a motor-driven diamond anvil cell," J. Phys. Condens. Matter 18, S1069-S1073 (2006). DOI: 10.1088/0953-8984/18/25/S13

W.L. Mao, H.-K. Mao, Y. Meng, P.J. Eng, M.Y. Hu, P. Chow, Y.Q. Cai, J. Shu, R.J. Hemley, "X-ray–Induced Dissociation of H[subscript 2]O and Formation of an O[subscript 2]–H[subscript 2] Alloy at High Pressure," Science 314 (10), 636-638 (2006). DOI: 10.1126/science.1132884

W.L. Mao, H.-K. Mao, V.B. Prakapenka, J. Shu, R.J. Hemley, "The effect of pressure on the structure and volume of ferromagnesian post-perovskite," Geophys. Res. Lett. 33, L12S02-L12S06 (2006).

Wendy L. Mao, Ho-kwang Mao, Wolfgang Sturhahn, Jiyong Zhao, Vitali B. Prakapenka, Yue Meng, Jinfu Shu, Yingwei Fei, Russell J. Hemley, "Iron-Rich Post-Perovskite and the Origin of Ultralow-Velocity Zones," Science 312, April, 564-565 (2006). DOI: 10.1126/science.1123442

Qing Ma, R. Divan, D.C. Mancini, R.A. Rosenberg, J.P. Quintana, D.T. Keane, "X-ray induced, substrate-carrier mediated deposition of metal on GaAs," Appl. Phys. Lett. 89 (8), August, 083114-1-083114-3 (2006). DOI: 10.1063/1.2336592

Zara Marland, Travis Beddoe, Leyla Zaker-Tabrizi, Isabelle S. Lucet, Rajini Brammananth, James C. Whisstock, Matthew C.J. Wilce, Ross L. Coppel, Paul K. Crellin, Jamie Rossjohn, "Hijacking of a Substrate-binding Protein Scaffold for use in Mycobacterial Cell Wall Biosynthesis," J. Mol. Biol. 359 (4), June, 983-997 (2006). DOI: 10.1016/j.mb.2006.04.012

Matthew J. Marshall, Alexander S. Beliaev, Alice C. Dohnalkova, David W. Kennedy, Liang Shi, Zheming Wang, Maximl. Boyanov, Barry Lai, Kenneth M. Kemner, Jeffrey S. McLean, Samantha B. Reed, David E. Culley, Vanessa L. Bailey, Cody J. Simonson, Daad A. Saffarini, Margaret F. Romine, John M. Zachara, James K. Fredrickson, "c-Type Cytochrome-Dependent Formation of U(IV) Nanoparticles by Shewanella oneidensis," PLoS Biol. 4 (8), 1324-1333 (2006). DOI: 10.1371/journal.pbio.0040268

C. David Martin, Wilson A. Crichton, Haozhe Liu, Vitali Prakapenka, Jiuhua Chen, John B. Parise, "Phase transitions and compressibility of NaMgF[subscript 3] (Neighborite) in perovskite- and post perovskite-related structures," Geophys. Res. Lett. 33, June, L11305-1-L11305-4 (2006). DOI: doi:10.1029/2006GL026150, 2006

Charles David Martin, Wilson A. Crichton, Haozhe Liu, Vitali B. Prakapenka, Jiuhua Chen, John B. Parise, "Rietveld structure refinement of perovskite and post-perovskite phases of NaMgF[subscript 3] (Neighborite) at high pressures," Am. Mineral. 91 (10), October, 1703-1706 (2006). DOI: 10.2138/am.2006.2308

Dariusz Martynowski, Yvonne Eyobo, Tingfeng Li, Kun Yang, Aimin Liu, Hong Zhang, "Crystal Structure of [alpha]-Amino-[beta]-carboxymuconate-[epsilon]-semialdehyde Decarboxylase: Insight into the Active Site and Catalytic Mechanism of a Novel Decarboxylation Reaction," Biochemistry-US 45 (35), 10412-10421 (2006). DOI: 10.1021/bi060903q

Mark L. Mayer, "Glutamate receptors at atomic resolution," Nature 440 (23), March, 456-462 (2006).

Mark L. Mayer, Alokesh Ghosal, Nigel P. Dolman, David E. Jane, "Crystal Structures of the Kainate Receptor GluR5 Ligand Binding Core Dimer with Novel GluR5-Selective Antagonists," J. Neurosci. 26 (1), March, 2852-2861 (2006).

R.W. McCallum, L.H. Lewis, M.J. Kramer, K.W. Dennis, "Magnetic aspects of the ferromagnetic 'bulk metallic glass' alloy system Nd-Fe-Al," J. Magn. Magn. Mater. 299 (2), April, 265-280 (2006). DOI: 10.1016/j.jmmm.2005.04.013

Jennifer A. McCourt, Siew Siew Pang, Jack King-Scott, Luke W. Guddat, Ronald G. Duggleby, "Herbicide-binding sites revealed in the structure of plant acetohydroxyacid synthase," Proc. Natl. Acad. Sci. USA 103 (3), January, 569-573 (2006). DOI: 10.1073/pnas.0508701103

Jason G. McCoy, Abolfazl Arabshahi, Eduard Bitto, Craig A. Bingman, Frank J. Ruzicka, Perry A. Frey, George N. Phillips Jr., "Structure and Mechanism of an ADP-Glucose Phosphorylase from Arabidopsis thaliana," Biochemistry-US 45 (10), February, 3154-3162 (2006). DOI: 10.1021/bi052232m

Jason G. McCoy, Lucas J. Bailey, Eduard Bitto, Craig A. Bingman, David J. Aceti, Brian G. Fox, George N. Phillips Jr., "Structure and mechanism of mouse cysteine dioxygenase," Proc. Natl. Acad. Sci. USA 103 (9), February, 3084-3089 (2006). DOI: 10.1073/pnas.0509262103

J.G. McCoy, C.A. Bingman, E. Bitto, M.M. Holdorf, C.A. Makaroff, G. N. Phillips Jr., "Structure of an ETHE1-like protein from Arabidopsis thaliana," Acta Crystallogr. D D62, 964-970 (2006). DOI: 10.1107/S0907444906020592

Sheena McGowan, Ashley M. Buckle, James A. Irving, Poh Chee Ong, Tanya A. Bashtannyk-Puhalovich, Wan-Ting Kan, Kate N. Henderson, Yaroslava A. Bulynko, Evgenya Y. Popova, A. Ian Smith, Stephen P. Bottomley, Jamie Rossjohn, Sergei A. Grigoryev, Robert N. Pike, James C. Whisstock, "X-ray crystal structure of MENT: evidence for functional loop–sheet polymers in chromatin condensation," EMBO J. 25 (13), July, 3144-3155 (2006). DOI: 10.1038/sj.emboj.7601201

Neil M. McKern, Michael C. Lawrence, Victor A. Streltsov, Mei-Zhen Lou, Timothy E. Adams, George O. Lovrecz, Thomas C. Elleman, Kim M. Richards, John D. Bentley, Patricia A. Pilling, Peter A. Hoyne, Kellie A. Cartledge, Tam M. Pham, Jennifer L. Lewis, Sonia E. Sankovich, Violet Stoichevska, Elizabeth Da Silva, Christine P. Robinson, Maurice J. Frenkel, Lindsay G. Sparrow, Ross T. Fernley, V. Chandana Epa, Colin W. Ward, "Structure of the insulin receptor ectodomain reveals a folded-over conformation," Nature 443 (13), September, 218-221 (2006). DOI: 10.1038/nature05106

James P. McKinley, John M. Zachara, Chongxuan Liu, Steven C. Heald, Brenda I. Prenitzer, Brian W. Kempshall, "Microscale controls on the fate of contaminant uranium in the vadose zone, Hanford Site, Washington," Geochim. Cosmochim. Acta 70, 1873-1887 (2006).

Jason S. McLellan, Shenqin Yao, Xiaoyan Zheng, Brian V. Geisbrecht, Rodolfo Ghirlando, Philip A. Beachy, Daniel J. Leahy, "Structure of a heparin-dependent complex of Hedgehog and Ihog," Proc. Natl. Acad. Sci. USA 103 (46), November, 17208-17213 (2006). DOI: 10.1073/pnas.0606738103

Reagan McRae, Barry Lai, Stefan Vogt, Christoph J. Fahrni, "Correlative microXRF and optical immunofluorescence microscopy of adherent cells labeled with ultrasmall gold particles," J. Struct. Biol. 115, January, 22-29 (2006). DOI: 10.1016/j.jsb.2005.09.013

Q. Mei, C.J. Benmore, R.T. Hart, E. Bychkov, P.S. Salmon, C.D. Martin, F.M. Michel, S.M. Antao, P.J. Chupas, P.L. Lee, S.D. Shastri, J.B. Parise, K. Leinenweber, S. Amin, J.L. Yarger, "Topological changes in glassy GeSe[subscript 2] at pressures up to 9.3 GPa determined by high energy x-ray and neutron diffraction measurements," Phys. Rev. B 74 (1), July, 014203-1-014203-10 (2006). DOI: 10.1103/PhysRevB.74.014203

Q. Mei, C.J. Benmore, S. Sampath, J.K.R. Weber, K. Leinenweber, S. Amind, Paul Johnston, J.L. Yarger, "The structure of permanently densified CaAl[subscript 2]O[subscript 4] glass," J. Phys. Chem. Solids 67 (9-10), 2106-2110 (2006). DOI: 10.1016/j.jpcs.2006.05.018

Q. Mei, J.E. Siewenie, C.J. Benmore, P. Ghalsasi, J.L. Yarger, "Orientational Correlations in the Glacial State of Triphenyl Phosphite," J. Phys. Chem. B 110 (20), May, 9747-9750 (2006). DOI: 10.1021/jp060692z

Laurnet D. Menard, Fengting Xu, Ralph G. Nuzzo, Judith C. Yang, "Preparation of TiO[subscript 2]-Supported Au Nanoparticle Catalysts from a Au[subscript 13] Cluster Precursor: Ligand Removal Using Ozone Exposure versus a Rapid Thermal Treatment," J. Catal. 243 (1), October, 64-73 (2006). DOI: 10.1016/j.jcat.2006.07.006

Laurent D. Menard, Huiping Xu, Shang-Peng Gao, Ray D. Twesten, Amanda S. Harper, Yang Song, Gangli Wang, Alicia D. Douglas, Judith C. Yang, Anatoly I. Frenkel, Royce W. Murray, Ralph G. Nuzzo, "Metal Core Bonding Motifs of Monodisperse Icosahedral Au[subscript 13] and Larger Au Monolayer-Protected Clusters As Revealed by X-ray Absorption Spectroscopy and Transmission Electron Microscopy," J. Phys. Chem. B 110, 14564-14573 (2006). DOI: 10.1021/jp060740f

Y. Meng, G. Shen, H-k. Mao, "Double-sided laser heating system at HPCAT for in situ x-ray diffraction at high pressures and high temperatures," J. Phys. Condens. Matter 18, S1097-S1103 (2006). DOI: 10.1088/0953-8984/18/25/S17

Yue Meng, Robert B. Von Dreele, Brian H. Toby, Paul Chow, Michael Y. Hu, Guoyin Shen, Ho-kwang Mao, "Hard x-ray radiation induced dissociation of N[subscript 2] and O[subscript 2] molecules and the formation of ionic nitrogen oxide phases under pressure," Phys. Rev. B 74, 214107-1-214107-5 (2006). DOI: 10.1103/PhysRevB.74.214107

Zhaohui Meng, Zhiyong Lou, Zhe Liu, Ming Li, Xiaodong Zhao, Mark Bartlam, Zihe Rao, "Crystal Structure of Human Pyrroline-5-carboxylate Reductase," J. Mol. Biol. 359, 1364-1377 (2006). DOI: 10.1016/j.jmb.2006.04.053

Andreas Menzel, Kee-Chul Chang, Vladimir Komanicky, Hoydoo You, Yong S. Chu, Yuriy V. Tolmachev, John J. Rehr, "Resonance Anomalous Surface X-ray Scattering," Radiat. Phys. Chem. 75 (11), November, 1651-1660 (2006). DOI: 10.1016/j.radphyschem.2005.07.038

A. Menzel, Y.V. Tolmachev, K.-C. Chang, V. Komanicky, Y.S. Chu, J.J. Rehr, H. You, "Polarization-dependent resonant anomalous surface X-ray scattering of CO/Pt(111)," Europhys. Lett. 74 (6), June, 1032-1038 (2006). DOI: 10.1209/epl/i2006-10050-8

Sébastien Merkel, Atsushi Kubo, Lowell Miyagi, Sergio Speziale, Thomas S. Duffy, Ho-kwang Mao, Hans-Rudolf Wenk, "Plastic Deformation of MgGeO[subscript 3] Post-Perovskite at Lower Mantle Pressures," Science 311, February, 644-646 (2006).

Mandy M. Michalsen, Bernard A. Goodman, Shelly D. Kelly, Kenneth M. Kemner, James P. McKinley, Joseph W. Stucki, Jonathan D. Istok, "Uranium and Technetium Bio-Immobilization in Intermediate-Scale Physical Models of an In Situ Bio-Barrier," Environ. Sci. Technol. 40 (22), November, 7048-7053 (2006). DOI: 10.1021/es060420+

F.M. Michel, M.A.A. Schoonen, X.V. Zhang, S.T. Martin, J.B. Parise, "Hydrothermal Synthesis of Pure r-Phase Manganese(II) Sulfide without the Use of Organic Reagents," Chem. Mater. 18 (7), 1726-1736 (2006).

Jonathan Mikolosko, Kostyantyn Bobyk, Helen I. Zgurskaya, Partho Ghosh, "Conformational Flexibility in the Multidrug Efflux System Protein AcrA," Structure 14 (3), March, 577-587 (2006).

John J. Miles, Natalie A. Borg, Rebekah M. Brennan, Fleur E. Tynan, Lars Kjer-Nielsen, Sharon L. Silins, Melissa J. Bell, Jacqueline M. Burrows, James McCluskey, Jamie Rossjohn, Scott R. Burrows, "TCR[alpha] Genes Direct MHC Restriction in the Potent Human T Cell Response to a Class I-Bound Viral Epitope," J. Immunol. 177 (10), October, 6804-6814 (2006).

C.E. Miller, J. Majewski, T.L. Kuhl, "Characterization of single biological membranes at the solid–liquid interface by X-ray reflectivity," Colloid Surface 284-285, January, 434-439 (2006). DOI: 10.1016/j.colsurfa.2005.11.059

Darcie J. Miller, Yong-Mei Zhang, Charles O. Rock, Stephen W. White, "Structure of RhlG, an Essential [beta]-Ketoacyl Reductase in the Rhamnolipid Biosynthetic Pathway of Pseudomonas aeruginosa," J. Biol. Chem. 281 (26), June, 18025-18032 (2006).

Edward B. Miller, Brittney Gurda-Whitaker, Lakshmanan Govindasamy, Robert McKenna, Sergei Zolotukhin, Nicholas Muzyczka, Mavis Agbandje-McKenna, "Production, purification and preliminary X-ray crystallographic studies of adeno-associated virus serotype 1," Acta Crystallogr. F 52, 1271-1274 (2006). DOI: 10.1107/S1744309106048184

John F. Miller, C. Webster Andrews, Michael Brieger, Eric S. Furfine, Michael R. Hale, Mary H. Hanlon, Richard J. Hazen, Istvan Kaldor, Ed W. McLean, David Reynolds, Douglas M. Sammond, Andrew Spaltenstein, Roger Tung, Elizabeth M. Turner, Robert X. Xu, Ronald G. Sherrill, "Ultra-potent P1 modified arylsulfonamide HIV protease inhibitors: The discovery of GW0385," Bioorg. Med. Chem. Lett. 16 (7), April, 1788-1794 (2006). DOI: 10.1016/j.bmcl.2006.01.035

J.T. Miller, A.J. Kropf, Y. Zha, J.R. Regalbuto, L. Delannoy, C. Louis, E. Bus, J.A. van Bokhoven, "The effect of gold particle size on Au–Au bond length and reactivity toward oxygen in supported catalysts," J. Catal. 240, 222-234 (2006). DOI: 10.1016/j.jcat.2006.04.004

L.M. Miller, Q. Wang, T.P. Telivala, R.J. Smith, A. Lanzirotti, J. Miklossy, "Synchrotron-based infrared and X-ray imaging shows focalized accumulation of Cu and Zn co-localized with [beta]-amyloid deposits in Alzheimer's disease," J. Struct. Biol. 155 (1), July, 30-37 (2006).

L.-C. Ming, Y.-H. Kim, T. Uchida, Y. Wang, M. Rivers, "In situ X-ray diffraction study of phase transitions of FeTiO[subscript3] at high pressures and temperatures using a large-volume press and synchrotron radiation," Am. Mineral. 91, 120-126 (2006).

L.C. Ming, P. Zinin, Y. Meng, X.R. Liu, S.M. Hong, Y. Xie, "A cubic phase of C[subscript 3]N[subscript 4] synthesized in the diamond-anvil cell," J. Appl. Phys. 99 (3), 033520-1-033520-6 (2006).

Luke A. Moe, Craig A. Bingman, Gary E. Wesenberg, George N. Phillips, Jr., Brian G. Fox, "Structure of T4moC, the Rieske-type ferredoxin component of toluene 4-monooxygenase," Acta Crystallogr. D 62, 476-482 (2006). DOI: 10.1107/S0907444906006056

Haiding Mo, Guennadi Evmenenko, Sumit Kewalramani, Kyungil Kim, Steven N. Ehrlich, Pulak Dutta, "Observation of Surface Layering in a Nonmetallic Liquid," Phys. Rev. Lett. 96 (9), April, 096107-1-096107-4 (2006).

Jacqueline Montalibet, Kathryn Skorey, Dan McKay, Giovanna Scapin, Ernest Asante-Appiah, Brian P. Kennedy, "Residues Distant from the Active Site Influence Protein-tyrosine Phosphatase 1B Inhibitor Binding," J. Biol. Chem. 281 (8), February, 5258-5266 (2006). DOI: 10.1074/jbc.M511546200

Mariya Morar, Ruchi Anand, Aaron A. Hoskins, JoAnne Stubbe, Steven E. Ealick, "Complexed Structures of Formylglycinamide Ribonucleotide Amidotransferase from Thermotoga maritima Describe a Novel ATP Binding Protein Superfamily," Biochemistry-US 45 (50), November, 14880-14895 (2006). DOI: 10.1021/bi061591u

Lidia Mosyak, Andrew Wood, Brian Dwyer, Madhavan Buddha, Mark Johnson, Ann Aulabaugh, Xiaotian Zhong, Eleonora Presman, Susan Benard, Kerry Kelleher, James Wilhelm, Mark L. Stahl, Ron Kriz, Ying Gao, Zixuan Cao, Huai-Ping Ling, Menelas N. Pangalos, Frank S. Walsh, William S. Somers, "The Structure of the Lingo-1 Ectodomain, a Module Implicated in Central Nervous System Repair Inhibition," J. Biol. Chem. 281 (47), November, 36378-36390 (2006). DOI: 10.1074/jbc.M607314200

Joseph D. Mougous, Marianne E. Cuff, Stefan Raunser, Aimee Shen, Min Zhou, Casey A. Gifford, Andrew L. Goodman, Grazyna Joachimiak, Claudia L. Ordonez, Stephen Lory, Thomas Walz, Andrzej Joachimiak, John J. Mekalanos, "A Virulence Locus of Pseudomonas aeruginosa Encodes a Protein Secretion Apparatus," Science 312, June, 1526-1530 (2006). DOI: 10.1126/science.1128393

Carmen M. Moure, Brian R. Bowman, Paul D. Gershon, Florante A. Quiocho, "Crystal Structures of the Vaccinia Virus Polyadenylate Polymerase Heterodimer: Insights into ATP Selectivity and Processivity," Mol. Cell 22, May, 339-349 (2006). DOI: 10.1016/j.molcel.2006.03.015

Steven W. Muchmore, Richard A. Smith, Andrew O. Stewart, Marlon D. Cowart, Arthur Gomtsyan, Mark A. Matulenko, Haixia Yu, Jean M. Severin, Shripad S. Bhagwat, Chih-Hung Lee, Elizabeth A. Kowaluk, Michael F. Jarvis, Clarissa L. Jakob, "Crystal structures of human adenosine kinase inhibitor complexes reveal two distinct binding modes," J. Med. Chem. 49 (23), November, 6726-6731 (2006). DOI: 10.1021/jm060189a

Suchetana Mukhopadhyay, Wei Zhang, Stefan Gabler, Paul R. Chipman, Ellen G. Strauss, James H. Strauss, Timothy S. Baker, Richard J. Kuhn, Michael G. Rossmann, "Mapping the Structure and Function of the E1 and E2 Glycoproteins in Alphaviruses," Structure 14, January, 63-73 (2006). DOI: 10.1016/j.str.2005.07.025

Tanya A. Murphy, Lucy E. Catto, Stephen E. Halford, Andrea T. Hadfield, Wladek Minor, Timothy R. Walsh, James Spencer, "Crystal Structure of Pseudomonas aeruginosa SPM-1 Provides Insights into Variable Zinc Affinity of Metallo-[beta]-lactamases," J. Mol. Biol. 357, 890-903 (2006). DOI: 10.1016/j.jmb.2006.01.003

Bhushan Nagar, Oliver Hantschel, Markus Seeliger, Jason M. Davies, William I. Weis, Giulio Superti-Furga, John Kuriyan, "Organization of the SH3-SH2 Unit in Active and Inactive Forms of the c-Abl Tyrosine Kinase," Mol. Cell 21, March, 1-12 (2006).

Akanksha Nagpal, Michael P. Valley, Paul F. Fitzpatrick, Allen M. Orville, "Crystal Structures of Nitroalkane Oxidase: Insights into the Reaction Mechanism from a Covalent Complex of the Flavoenzyme Trapped during Turnover," Biochemistry-US 45 (4), January, 1138-1150 (2006). DOI: 10.1021/bi051966w

N.N. Naik, A.C. Jupe, S.R. Stock, A.P. Wilkinson, P.L. Lee, K.E. Kurtis, "Sulfate attack monitored by microCT and EDXRD: Influence of cement type, water-to-cement ratio, and aggregate," Cement Concrete Res. 36, 144-159 (2006).

Sajo P. Naik, Toshiyuki Yokoi, Wei Fan, Yukichi Sasaki, Ta-chen Wei, Hugh W. Hillhouse, Tatsuya Okubo, "Versatile Fabrication of Distorted Cubic Mesoporous Silica Film Using CTAB Together with a Hydrophobic Organic Additive," J. Phys. Chem. B 110 (20), April, 9751-9754 (2006). DOI: 10.1021/jp060869p

Deepak T Nair, Robert E Johnson, Louise Prakash, Satya Prakash, Aneel K Aggarwal, "Hoogsteen base pair formation promotes synthesis opposite the 1,N[superscript 6]-ethenodeoxyadenosine lesion by human DNA polymerase [iota]," Nat. Struct. Mol. Biol. 13 (7), July, 619-625 (2006). DOI: 10.1038/nsmb1118

Deepak T. Nair, Robert E. Johnson, Louise Prakash, Satya Prakash, Aneel K. Aggarwal, "An Incoming Nucleotide Imposes an anti to syn Conformational Change on the Templating Purine in the Human DNA Polymerase-[iota] Active Site," Structure 14 (4), April, 749-755 (2006).

Jayakrishnan Nandakumar, Stewart Shuman, Christopher D. Lima, "RNA Ligase Structures Reveal the Basis for RNA Specificity and Conformational Changes that Drive Ligation Forward," Cell 127 (1), October, 71-84 (2006). DOI: 10.1016/j.cell.2006.08.038

Narayana Narayana, "High-resolution structure of a plasmid-encoded dihydrofolate reductase: pentagonal network of water molecules in the D[subscript 2]-symmetric active site," Acta Crystallogr. D 62 (7), July, 695-706 (2006). DOI: 10.1107/S0907444906014764

R.A. Narayanan, P. Thiyagarajan, S. Lewis, A. Bansal, L.S. Schadler, L.B. Lurio, "Dynamics and Internal Stress at the Nanoscale Related to Unique Thermomechanical Behavior in Polymer Nanocomposites," Phys. Rev. Lett. 97 (07), August, 075505-1-075505-4 (2006). DOI: 10.1103/PhysRevLett.97.075505

Vinod Nayak, Kehao Zhao, Anastasia Wyce, Marc F. Schwartz, Wan-Sheng Lo, Shelley L. Berger, Ronen Marmorstein, "Structure and Dimerization of the Kinase Domain from Yeast Snf1, a Member of the Snf1/AMPK Protein Family," Structure 14 (3), March, 477-485 (2006).

Frances Neville, Marjolaine Cahuzac, Oleg Konovalov, Yuji Ishitsuka, Ka Yee C. Lee, Ivan Kuzmenko, Girish M. Kale, David Gidalevitz, "Lipid Headgroup Discrimination by Antimicrobial Peptide LL-37: Insight into Mechanism of Action," Biophys. J. 90 (4), February, 1275-1287 (2006). DOI: 10.1529/biophysj.105.067595

B.D. Newbury, M.R. Notis, B. Stephenson, G.S. Cargill, III, G.B. Stephenson, "The Astrolabe Craftsmen of Lahore and Early Brass Metallurgy," Ann. Sci. 63 (2), April, 201-213 (2006). DOI: 10.1080/00033790600583162

P.S. Nico, M.V. Ruby, Y.W. Lowney, S.E. Holms, "Chemical Speciation and Bioaccessibility of Arsenic and Chromium in Chromated Copper Arsenate-Treated Wood and Soils," Environ. Sci. Technol. 40, 402-408 (2006).

Stanley Nithianantham, Minghua Xu, Nan Wu, Yiping W. Hanb, and Menachem Shoham, "Crystallization and preliminary X-ray data of the FadA adhesin from Fusobacterium nucleatum," Acta Crystallogr. F 62(12), December, 1215-1217 (2006). DOI: 10.1107/S1744309106045593

B. Nocek, M. Cuff, E. Evdokimova, A. Edwards, A. Joachimiak, A. Savchenko, "1.6 Å Crystal structure of a PA2721 protein from pseudomonas aeruginosa - A potential drug-resistance protein," Proteins 63 (4), 1102-1105 (2006). DOI: 10.1002/prot.20659

M. Cristina Nonato, Joanne Widom, Jon Clardy, "Human methionine aminopeptidase type 2 in complex with L- and D-methionine," Bioorg. Med. Chem. Lett. 16 (10), May, 2580-2583 (2006). DOI: 10.1016/j.bmcl.2006.02.047

Naoise Nunan, Karl Ritz, Mark Rivers, Debbie S. Feeney, Iain M. Young, "Investigating microbial micro-habitat structure using X-ray computed tomography," Geoderma 133, October, 398-407 (2006). DOI: 10.1016/j.geoderma.2005.08.004

Grant E. Nybakken, Christopher A. Nelson, Beverly R. Chen, Michael S. Diamond, Daved H. Fremont, "Crystal Structure of the West Nile Virus Envelope Glycoprotein," J. Virol. 80 (23), December, 11467-11474 (2006). DOI: 10.1128/JVI.01125-06

Jennifer L. Nyman, Terence L. Marsh, Matthew A. Ginder-Vogel, Margaret Gentile, Scott Fendorf, Craig Criddle, "Heterogeneous response to biostimulation for U(VI) reduction in replicated sediment microcosms," Biodegradation 17 (4), July, 303-316 (2006). DOI: 10.1007/s10532-005-9000-3

N.J. O'Driscoll, S.D. Siciliano, D. Peak, R. Carignan, D.R.S. Lean, "The influence of forestry activity on the structure of dissolved organic matter in lakes: Implications for mercury photoreactions," Sci. Total Environ. 366 (2-3), August, 880-893 (2006). DOI: 10.1016/j.scitotenv.2005.09.067

Josiah Obiero, Sara A. Bonderoff, Meghan M. Goertzen, David A.R. Sanders, "Expression, purification, crystallization and preliminary X-ray crystallographic studies of Deinococcus radiodurans thioredoxin reductase," Acta Crystallogr. F 62 (8), 757-760 (2006). DOI: 10.1107/S1744309106024845

Wendy F. Ochoa, Anju Chatterji, Tianwei Lin, John E. Johnson, "Generation and Structural Analysis of Reactive Empty Particles Derived from an Icosahedral Virus," Chem. Biol. 13 (7), July, 771-778 (2006). DOI: 10.1016/j.chembiol.2006.05.014

Christopher G. Oliveri, Nathan C. Gianneschi, Son Binh T. Nguyen, Chad A. Mirkin, Charlotte L. Stern, Zdzislaw Wawrzak, Maren Pink, "Supramolecular Allosteric Cofacial Porphyrin Complexes," J. Am. Chem. Soc. 128, 16286-16296 (2006). DOI: 10.1021/ja0661010

Joseph P.R.O. Orgel, Thomas C. Irving, Andrew Miller, Tim J. Wess, "Microfibrillar structure of type I collagen in situ," Proc. Natl. Acad. Sci. USA 103 (24), June, 9001-9005 (2006). DOI: 10.1073/pnas.0502718103

Jerzy Osipiuk, Natalia Maltseva, Irina Dementieva, Shonda Clancy, Frank Collart, Andrzej Joachimiak, "Structure of YidB protein from Shigella flexneri shows a new fold with homeodomain motif," Proteins 65 (2), November, 509-513 (2006). DOI: 10.1002/prot.21054

R.T. Otta, M.J. Kramer, M.F. Besser, D.J. Sordelet, "High-energy X-ray measurements of structural anisotropy and excess free volume in a homogenously deformed Zr-based metallic glass," Acta Mater. 54, 2463-2471 (2006).

R.T. Ott, M.J. Kramer, M.F. Besser, T.C. Hufnagel, D.J. Sordelet, "Quasicrystal formation in Zr-Cu-Ni-Al-Ta metallic glasses and composites," Philos. Mag. 86, 299-307 (2006).

Aaron I. Packman, Andrea Marion, Mattia Zaramella, Cheng Chen, Jean-François Gaillard, Denis T. Keane, "Development of Layered Sediment Structure and its Effects on Pore Water Transport and Hyporheic Exchange," Virology 6 (5-6), December, 433-442 (2006). DOI: 10.1007/s11267-006-9057-y

Pius S. Padayatti, Anjaneyulu Sheri, Monica A. Totir, Marion S. Helfand, Marianne P. Carey, Vernon E. Anderson, Paul R. Carey, Christopher R. Bethel, Robert A. Bonomo, John D. Buynak, Focco van den Akker, "Rational Design of a [beta]-Lactamase Inhibitor Achieved via Stabilization of the trans-Enamine Intermediate: 1.28 Å Crystal Structure of wt SHV-1 Complex with a Penam Sulfone," J. Am. Chem. Soc. 128 (40), October, 13235-13242 (2006). DOI: 10.1021/ja063715w

Gianluca Paglia, Emil S. Bozin, Simon J.L. Billinge, "Fine-Scale Nanostructure in [gamma]-Al[subscript 2]O[subscript 3]," Chem. Mater. 18 (14), July, 3242-3248 (2006). DOI: 10.1021/cm060277j

G. Paglia, E.S. Bozin, D. Vengust, D. Mihailovic, S.J.L. Billinge, "Accurate structure analysis of Mo[subscript 6]S[subscript y]I[subscript z] nanowires from atomic pair distribution function (PDF) analysis," Chem. Mater. 18 (1), January, 100-108 (2006).

John E. Pak, Pascal Arnoux, Sihong Zhou, Prashanth Sivarajah, Malathy Satkunarajah, Xuekun Xing, James M. Rini, "X-ray crystal structure of leukocyte type core 2 [beta]1,6-N-acetylglucosaminyltransferase: Evidence for a convergence of metal ion independent glycosyltransferase mechanism," J. Biol. Chem. 281 (36), October, 26693-26701 (2006). DOI: 10.1074/jbc.M603534200

Pradeep S. Pallan, Peter von Matt, Christopher J. Wilds, Karl-Heinz Altmann, Martin Egli, "RNA-Binding Affinities and Crystal Structure of Oligonucleotides Containing Five-Atom Amide-Based Backbone Structures," Biochemistry-US 45, 8048-8057 (2006). DOI: 10.1021/bi060354o

Bradley M. Palmer, Stefan Vogt, Zengyi Chen, Richard R. Lachapelle, Martin M. LeWinter, "Intracellular distributions of essential elements in cardiomyocytes," J. Struct. Biol. 155, 12-21 (2006). DOI: 10.1016/j.jsb.2005.11.017

Baocheng Pan, Ke Shi, Muttaiya Sundaralingam, "Crystal Structure of an RNA Quadruplex Containing Inosine Tetrad: Implications for the Roles of NH[subscript 2] Group in Purine Tetrads," J. Mol. Biol. 363 (2), October, 451-459 (2006). DOI: 10.1016/j.jmb.2006.08.022

Baocheng Pan, Ke Shi, Muttaiya Sundaralingam, "Base-tetrad swapping results in dimerization of RNA quadruplexes: Implications for formation of the i-motif RNA octaplex," Proc. Natl. Acad. Sci. USA 103 (9), 3130-3134 (2006). DOI: 10.1073/pnas.0507730103

Guirong Pan, Dale W. Schaefer, Jan Ilavsky, "Morphology and water barrier properties of organosilane films: The effect of curing temperature," J. Colloid Interf. Sci. 302 (1), October, 287-293 (2006). DOI: 10.1016/j.jcis.2006.06.031

A.B. Papandrew, M.S. Lucas, R. Stevens, I. Halevy, B. Fultz, M.Y. Hu, P. Chow, R.E. Cohen, M. Somayazulu, "Absence of Magnetism in Hcp Iron-Nickel at 11 K," Phys. Rev. Lett. 97, 087202-1-087202-4 (2006). DOI: 10.1103/PhysRevLett.97.087202

Changyong Park, Paul A. Fenter, Kathryn L. Nagy, Neil C. Sturchio, "Hydration and Distribution of Ions at the Mica-Water Interface," Phys. Rev. Lett. 97, June, 016101-1-016101-4 (2006). DOI: 10.1103/PhysRevLett.97.016101

Hyunsoo Park, David M. Moureau, John B. Parise, "Hydrothermal Synthesis and Structural Characterization of Novel Zn-Triazole-Benzenedicarboxylate Frameworks," Chem. Mater. 18 (2), 525-531 (2006).

Hyun Ho Park, Hansel Emory Tookes, Hao Wua, "Crystallization and preliminary X-ray crystallographic studies of Drep-3, a DFF-related protein from Drosophila melanogaster," Acta Crystallogr. F 62 (6), June, 597-599 (2006).

Sang-Youn Park, Peter P. Borbat, Gabrje,a Gonzalez-Bonet, Jaya Bhatnagar, Abiola M. Pollard, Jack H. Freed, Alexandrine M. Bilwes, Brian R. Crane, "Reconstruction of the chemotaxis receptor-kinase assembly," Nat. Struct. Mol. Biol. 13 (5), 400-407 (2006). DOI: 10.1038/nsmb1085

S.-H. Park, H. Boysen, J.B. Parise, "Structural disorder of a new zeolite-like lithosilicate, K[subscript 2.6]Li[subscript 5.4][Li[subscript 4]Si[subscript 16]O[subscript 38]] 4.3H[subscript 2]0," Acta Crystallogr. B 62 (1), February, 42-51 (2006).

Natasha Pashkova, Yui Jin, S. Ramaswamy, Lois S. Weisman, "Structural basis for myosin V discrimination between distinct cargoes," EMBO J. 25, 693-700 (2006). DOI: 10.1038/sj.emboj.7600965

Nicola Pasquato, Rodolfo Berni, Claudia Folli, Silvia Folloni, Michele Cianci, Sergio Pantano, John R. Helliwell, Giuseppe Zanotti, "Crystal Structure of Peach Pru p 3, the Prototypic Member of the Family of Plant Non-specific Lipid Transfer Protein Pan-allergens," J. Mol. Biol. 356 (3), February, 684-694 (2006). DOI: 10.1016/j.jmb.2005.11.063

A.J. Patel, S. Narayanan, A. Sandy, S.G.J. Mochrie, B.A. Garetz, H. Watanabe, N.P. Balsara, "Relationship between Structural and Stress Relaxation in a Block-Copolymer Melt," Phys. Rev. Lett. 96 (25), June, 257801-1-257801-4 (2006). DOI: 10.1103/PhysRevLett.96.257801

Asmita Patel, Stewart Shuman, Alfonso Mondragon, "Crystal Structure of a Bacterial Type IB DNA Topoisomerase Reveals a Preassembled Active Site in the Absence of DNA," J. Biol. Chem. 281 (9), March, 6030-6037 (2006). DOI: 10.1074/jbc.M512332200

Saurabh D. Patel, Carlo Ciatto, Chien Peter Chen, Fabiana Bahna, Manisha Rajebhosale, Natalie Arkus, Ira Schieren, Thomas M. Jessell, Barry Honig, Stephen R. Price, Lawrence Shapiro, "Type II Cadherin Ectodomain Structures: Implications for Classical Cadherin Specificity," Cell 124, March, 1255-1268 (2006). DOI: 10.1016/j.cell.2005.12.046

Rekha Pattanayek, Dewight R. Williams, Sabuj Pattanayek, Yao Xu, Tetsuya Mori, Carl H. Johnson, Phoebe L. Stewart, Martin Egli, "Analysis of KaiA-DaiC protein interactions in the cyano-bacterial circadian clock using hybrid structural methods," EMBO J. 25, 2017-2028 (2006). DOI: 10.1038/sj.emboj.7601086

M.V. Pattarkine, J.J. Tanner, C.A. Bottoms, Y.-H. Lee, J.D. Wall, "Desulfovibrio desulfuricans G20 Tetraheme Cytochrome Structure at 1.5 Å and Cytochrome Interaction with Metal Complexes," J. Mol. Biol. 358, 1314-1327 (2006). DOI: 10.1016/j.jmb.2006.03.010

Tatjana Paunesku, Stefan Vogt, Jorg Maser, Barry Lai, Gayle Woloschak, "X-Ray Fluorescence Microprobe Imaging in Biology and Medicine," J. Cell. Biochem. 99, 1489-1502 (2006). DOI: 10.1002/jcb.21047

Peter D. Pawelek, Nathalie Croteau, Christopher Ng-Thow-Hing, Cezar M. Khursigara, Natalia Moiseeva, Marc Allaire, James W. Coulton, "Structure of TonB in Complex with FhuA, E. coli Outer Membrane Receptor," Science 312, June, 1399-1402 (2006). DOI: 10.1126/science.1128057

Jian Payandeh, Masahiro Fujihashi, Wanda Gillon, Emil F. Pai, "The Crystal Structure of (S)-3-O-geranylgeranylglycerol-phosphate-synthase from Archaeoglobus fulgidus Reveals an Ancient Fold for an Ancient Enzyme," J. Biol. Chem. 281 (9), March, 6070-6078 (2006). DOI: 10.1074/jbc.M509377200

Jian Payandeh, Emil F. Pai, "Crystallization and preliminary X-ray diffraction analysis of the magnesium transporter CorA," Acta Crystallogr. F 62 (2), February, 148-152 (2006). DOI: 10.1107/S1744309106000996

Derek Peak, "Adsorption mechanisms of selenium oxyanions at the aluminum oxide/water interface," J. Colloid Interf. Sci. 303 (2), November, 337-345 (2006). DOI: 10.1016/j.jcis.2006.08.014

Derek Peak, U.K. Saha, P.M. Huang, "Selenite Adsorption Mechanisms on Pure and Coated Montmorillonite: An EXAFS and XANES Spectroscopic Study," Soil Sci. Soc. Am. J. 70, 192-203 (2006).

Zhonghua Pei, Xiaofeng Li, Kenton Longenecker, Thomas W. von Geldern, Paul E. Wiedeman, Thomas H. Lubben, Bradley A. Zinker, Kent Stewart, Stephen J. Ballaron, Michael A. Stashko, Amanda K. Mika, David W.A. Beno, Michelle Long, Heidi Wells, Anita J. Kempf-Grote, David J. Madar, Todd S. McDermott, Lakshmi Bhagavatula, Michael G. Fickes, Daisy Pireh, Larry R. Solomon, Marc R. Lake, Rohinton Edalji, Elizabeth H. Fry, Hing L. Sham, James M. Trevillyan, "Discovery, Structure-Activity Relationship, and Pharmacological Evaluation of (5-Substituted-pyrrolidinyl-2-carbonyl)-2-cyanopyrrolidines as Potent Dipeptidyl Peptidase IV Inhibitors," J. Med. Chem. 49, 3520-3535 (2006). DOI: 10.1021/jm051283e

V. Petkov, M. Gateshki, M. Niederberger, Y. Ren, "Atomic-Scale Structure of Nanocrystalline BaxSr[subscript 1-x]TiO[subscript 3] (x = 1, 0.5, 0) by X-ray Diffraction and the Atomic Pair Distribution Function Technique," Chem. Mater. 18 (3), February, 814-821 (2006).

Tatiana Petrova, Stephan Ginell, Andre Mitschler, Isabelle Hazemann, Thomas Schneider, Alexandra Cousido, Vladimir Y. Lunin, Andrzej Joachimiak, Alberto Podjarny, "Ultrahigh-resolution study of protein atomic displacement parameters at cryotemperatures obtained with a helium cryostat," Acta Crystallogr. D 62 (12), December, 1535-1544 (2006). DOI: 10.1107/S0907444906041035

Mark A. Pfeifer, Garth J. Williams, Ivan A. Vartanyants, Ross Harder, Ian K. Robinson, "Three-dimensional mapping of a deformation field inside a nanocrystal," Nature 442, June, 63-66 (2006). DOI: 10.1038/nature04867

Jason Phan, Brian P. Austin, David S. Waugh, "Crystal structure of the Yersinia type III secretion protein YscE," Protein Sci. 14, February, 2759-2763 (2006).

Agustin O. Pineda, Zhi-Wei Chen, Alaji Bah, Laura C. Garvey, F. Scott Mathews, Enrico Di Cera, "Crystal structure of thrombin in a self-inhibited conformation," J. Biol. Chem. 281 (43), September, 32922-32928 (2006). DOI: 10.1074/jbc.M605530200

P. Piot, Y.-E Sun, K.-J. Kim, "Photoinjector Generation of a Flat Electron Beam with Transverse Emittance Ratio of 100," Phys. Rev. Spec. Top., Accel. Beams 9 (3), March, 031001 (2006).

J. Pittler, W. Bu, D. Vaknin, A. Travesset, D.J. McGillivray, M. Losche, "Charge Inversion at Minute Electrolyte Concentrations," Phys. Rev. Lett. 97, August, 046102-1-046102-4 (2006).

Boaz Pokroy, Andrew N. Fitch, Peter L. Lee, John P. Quintana, El'ad N. Caspi, Emil Zolotoyabko, "Anisotropic lattice distortions in the mollusk-made aragonite: A widespread phenomenon," J. Struct. Biol. 153 (2), February, 145-150 (2006).

Matthew L. Polizzotto, Charles F. Harvey, Guangchao Li, Borhan Badruzzman, Ashraf Ali, Matthew Newville, Steven Sutton, Scott Fendorf, "Solid-phases and des-orption processes of arsenic within Bangladesh sediments," Chem. Geol. 228 (1-3), April, 97-111 (2006).

Ailsa J. Powell, Zhi-Jie Liu, Robert A. Nicholas, Christopher Davies, "Crystal Structures of the Lytic Transglycosylase MltA from N. gonorrhoeae and E. coli: Insights into Interdomain Movements and Substrate Binding," J. Mol. Biol. 359, May, 122-136 (2006). DOI: 10.1016/j.jmb.2006.03.023

B.A. Powell, M.C. Duff, D.I. Kaplan, R.A. Fjeld, M. Newville, D.B. Hunter, P.M. Bertsch, J.T. Coates, P. Eng, M.L. Rivers, S.M. Serkiz, S.R. Sutton, I.R. Triay, D.T. Vaniman, "Plutonium oxidation and subsequent reduction by Mn(IV) minerals in Yucca Mountain tuff," Environ. Sci. Technol. 40 (11), 3508-3514 (2006). DOI: 10.1021/es052353+

Noel A. Powell, Emma H. Clay, Daniel D. Holsworth, John W. Bryant, Michael J. Ryan, Mehran Jalaie, Erli Zhang, Jeremy J. Edmunds, "Equipotent activity in both enantiomers of a series of ketopiperazine-based renin inhibitors," Bioorg. Med. Chem. Lett. 15 (9), May, 2371-2374 (2006). DOI: 10.1016/j.bmcl.2005.02.085

Rachel A. Powers, Christopher L. Rife, Anthony L. Schilmiller, Gregg A. Howe, R. Michael Garavito, "Structure determination and analysis of acyl-CoA oxidase (ACX1) from tomato," Acta Crystallogr. D 62, 683-686 (2006). DOI: 10.1107/S0907444906014107

Adele Poynor, Liang Hong, Ian K. Robinson, Steve Granick, Zhan Zhang, Paul A. Fenter, "How Water Meets a Hydrophobic Surface," Phys. Rev. Lett. 97 (26), December, 266101-1-266101-4 (2006). DOI: 10.1103/PhysRevLett.97.266101

Ponraj Prabakaran, Jianhua Gan, Yang Feng, Zhongyu Zhu, Vidita Choudhry, Xiaodong Xiao, Xinhua Ji, Dimiter S. Dimitrov, "Structure of Severe Acute Respiratory Syndrome Coronavirus Receptor-binding Domain Complexed with Neutralizing Antibody," J. Biol. Chem. 281 (23), June, 15829-15836 (2006).

Michael Pravica, Krystyna Lipinska-Kalita, Zachary Quinea, Edward Romano, Yongrong Shen, Malcolm F. Nicol, Walter J. Pravica, "Studies of phase transitions in PETN at high pressures," J. Phys. Chem. Solids 67, 2159-2163 (2006). DOI: 10.1016/j.jpcs.2006.05.049

Michael Pravica, Zachary Quine, Edward Romano, "X-ray diffraction study of elemental thulium at pressures up to 86 GPa," Phys. Rev. B 74, 104107-1-104107-4 (2006). DOI: 10.1103/PhysRevB.74.104107

Jie Qin, Geqing Chai, John M. Brewer, Leslie L. Lovelace, Lukasz Lebioda, "Fluoride Inhibition of Inolase: Crystal Structure and Thermodynamics," Biochemistry-US 45 (3), March, 793-800 (2006).

Jie Qin, Roshan Perera, Leslie L. Lovelace, John H. Dawson, Lukasz Lebioda, "Structures of Thiolate- and Carboxylate-Ligated Ferric H93G Myoglobin: Models for Cytochrome P450 and for Oxyanion-Bound Heme Proteins," Biochemistry-US 45 (10), March, 3170-3177 (2006). DOI: 10.1021/bi052171s

Ling Qin, Carrie Hiser, Anne Mulichak, R. Michael Garavito, Shelagh Ferguson-Miller, "Identification of conserved lipid/detergent-binding sites in a high-resolution structure of the membrane protein cytochrome c oxidase," Proc. Natl. Acad. Sci. USA 103 (44), October, 16117-16122 (2006). DOI: 10.1073/pnas.0606149103

Yang Qiu, Valentina Tereshko, Youngchang Kim, Rongguang Zhang, Frank Collart, Mohammed Yousef, Anthony Kossiakoff, Andrzej Joachimiak, "The crystal structure of Aq_328 from the hyperthermophilic bacteria Aquifex aeolicus shows an ancestral histone fold," Proteins 62 (1), 8-16 (2006).

H.M. Quiney, A.G. Peele, Z. Cai, D. Paterson, K.A. Nugent, "Diffractive imaging of highly focused X-ray fields," Nature Phys. 2, February, 101-104 (2006).

Selva Vennila Raju, Shrinivas R. Kulkarni, Surendra K. Saxena, Hans-Peter Liermann, Stanislav V. Sinogeikin, "Compression behavior of nanosized nickel and molybdenum," Appl. Phys. Lett. 89, 261901-1-261901-3 (2006). DOI: 10.1063/1.2422886

S. Ramakrishnan, C.F. Zukoski, "Microstructure and Rheology of Thermoreversible Nanoparticles Gels," Langmuir 22 (18), 7833-7842 (2006). DOI: 10.1021/la060168j S0743-7463(06)00168-5

Ursula D. Ramirez, Douglas M. Freymann, "Analysis of protein hydration in ultrahigh-resolution structures of the SRP GTPase Ffh," Acta Crystallogr. D 62 (12), December, 1520-1534 (2006). DOI: 10.1107/S0907444906040807

Yijian Rao, Chuanbing Bian, Cai Yuan, Yongdong Li, Liqing Chen, Xiaoming Ye, Zixiang Huang, Mingdong Huang, "An open conformation of switch I revealed by Sar1-GDP crystal structure at low Mg[superscript 2+]," Biochem. Biophys. Res. Commun. 348, 908-915 (2006). DOI: 10.1016/j.bbrc.2006.07.148

Rumana Rashid, Bo Liang, Daniel L. Baker, Osama A. Youssef, Yang He, Kathleen Phipps, Rebecca M. Terns, Michael P. Terns, Hong Li, "Crystal Structure of a Cbf5-Nop10-Gar1 Complex and Implications in RNA-Guided Pseudouridylation and Dyskeratosis Congenita," Mol. Cell 21, January, 249-260 (2006).

Kiira Ratia, Kumar Singh Saikatendu, Bernard D. Santarsiero, Naina Barretto, Susan C. Baker, Raymond C. Stevens, Andrew D. Mesecar, "Severe acute respiratory syndrome coronavirus papain-like protease: Structure of a viral deubiquitinating enzyme," Proc. Natl. Acad. Sci. USA 103 (15), April, 5717-5722 (2006).

C. Rau, I.K. Robinson, C.-P. Richter, "Visualizing Soft Tissue in the Mammalian Cochlea With Coherent Hard X-Rays," Microsc. Res. Techniq. 69 (8), September, 660-665 (2006). DOI: 10.1002/jemt

Olga Rechkoblit, Lucy Malinina, Yuan Cheng, Vitaly Kuryavyi, Suse Broyde, Nicholas E. Geacintov, Dinshaw J. Patel, "Stepwise Translocation of Dpo4 Polymerase during Error-Free Bypass of an oxoG Lesion," PLoS Biol. 4 (1), January, 0025-0042 (2006). DOI: 10.1371/journal.pbio.0040011

Massimo Reconditi, "Recent improvements in small angle x-ray diffraction for the study of muscle physiology," Rep. Prog. Phys. 69, 2709-2759 (2006). DOI: 10.1088/0034-4885/69/10/R01

Catherine Regni, Andrew M. Schramm, Lesa J. Beamer, "The Reaction of Phosphohexomutase from Pseudomonas aeruginosa, Structural Insights Into a Simple Processive Enzyme," J. Biol. Chem. 281 (22), June, 15564-15571 (2006). DOI: 10.1074/jbc.M600590200

Catherine Regni, Grant S. Shackelford, Lesa J. Beamer, "Complexes of the enzyme phosphomannomutase/phosphoglucomutase with a slow substrate and an inhibitor," Acta Crystallogr. F 62, 722-726 (2006). DOI: 10.1107/S1744309106025887

Jingshan Ren, Charles E. Nichols, Anna Stamp, Phillip P. Chamberlain, Robert Ferris, Kurt L. Weaver, Steven A. Short, David K. Stammers, "Structural insights into mechanisms of non-nucleoside drug resistance for HIV-1 reverse transcriptases mutated at codons 101 or 138," FEBS J. 273, September, 3850-3860 (2006). DOI: 10.1111/j.1742-4658.2006.05392.x

Arturo Flores Renteria, "Influence of geometrical and spatial characteristics of the porosity on the thermal conductivity of EB-PVD TBCs," J. Therm. Spray Techn. 15 (1), March, 29-30 (2006).

David Reverter, Christopher D. Lima, "Structural basis for SENP[subscript 2] protease interactions with SUMO precursors and conjugated substrates," Nat. Struct. Mol. Biol. 13 (12), December, 1060-1068 (2006). DOI: 10.1038/nsmb1168

Francisca E. Reyes-Turcu, John R. Horton, James E. Mullally, Annie Heroux, Xiaodong Cheng, Keith D. Wilkinson, "The Ubiquitin Binding Domain ZnF UBP Recognizes the C-Terminal Diglycine Motif of Unanchored Ubiquitin," Cell 124 (6), March, 1197-1208 (2006).

Andrew G. Richter, Rodney Guico, Ken Shull, Jin Wang, "Thickness and Interfacial Roughness Changes in Polymer Thin Films during X-Irradiation," Macromolecules 39, 1545-1553 (2006). DOI: 10.1021/ma050060v

Moira K. Ridley, Vincent A. Hackley, Michael L. Machesky, "Characterization and Surface-Reactivity of Nanocrystalline Anatase in Aqueous Solutions," Langmuir 22 (26), December, 10972-10982 (2006). DOI: 10.1021/la061774h

K. Righter, S.R. Sutton, M. Newville, L. Le, C.S. Schwandt, H. Uchida, B. Lavina, R.T. Downs, "An experimental study of the oxidation state of vanadium in spinel and basaltic melt with implications for the origin of planetary basalt," Am. Mineral. 91 (10), 1643-1656 (2006). DOI: 10.2138/am.2006.2111

Syed Alipayam Rizvi, Valentina Tereshko, Anthony A. Kossiakoff, Sergey A. Kozmin, "Structure of Bistramide A-Actin Complex at a 1.35 Å Resolution," J. Am. Chem. Soc. 128 (12), April, 3882-3883 (2006). DOI: 10.1021/ja058319c S0002-7863(05)08319-8

Istvan Robel, G. Girishkumar, Bruce A. Bunker, Prashant V. Kamat, K. Vinodgopal, "Structural changes and catalytic activity of platinum nanoparticles supported on C[subscript 60] and carbon nanotube films during the operation of direct methanol fuel cells," Appl. Phys. Lett. 88, February, 073113-1-073113-3 (2006).

Sue A. Roberts, David C. Hyatt, Jerry E. Honts, Liming Changchien, Gladys F. Maley, Frank Maley, William R. Montfort, "Structure of the Y94F mutant of Escherichia coli thymidylate synthase," Acta Crystallogr. F 62 (9), September, 840-843 (2006). DOI: 10.1107/S1744309106029691

John W. Rodgers, Qingxian Zhou, Todd . Green, John N. Barr, Ming Luo, "Purification, crystallization and preliminary X-ray crystallographic analysis of the nucleocapsid protein of Bunyamwera virus," Acta Crystallogr. F 62 (4), April, 361-364 (2006). DOI: 10.1107/S1744309106006397

P. Rodriguez-Hernandez, J. Lopez-Solano, S. Radescu, A. Mujica, A. Munoz, D. Errandonea, J. Pellicer-Porres, A. Segura, Ch. Ferrer-Roca, F.J. Manjon, R.S. Kumar, O. Tschauner, G. Aquilanti, "Theoretical and experimental study of CaWO[subscript 4] and SrWO[subscript 4] under pressure," J. Phys. Chem. Solids 67, 2164-2171 (2006). DOI: 10.1016/j.jpcs.2006.05.011

Gerd Rosenbaum, Randy W. Alkire, Gwyndaf Evans, Frank J. Rotella, Krzystof Lazarski, Rong-Guang Zhang, Stephan L. Ginell, Norma Duke, Istvan Naday, Jack Lazarz, Michael J. Molitsky, Lisa Keefe, John Gonczy, Larry Rock, Ruslan Sanishvili, Martin A. Walsh, Westbrook Edwin, Andrzej Joachimiak, "The Structural Biology Center 19ID undulator beamline: facility specifications and protein crystallographic results," J. Synchrotron Rad. 13 (1), January, 30-45 (2006).

R.A. Rosenberg, G.K. Shenoy, X.H. Sun, T.K. Sham, "Time-resolved x-ray-excited optical luminescence characterization of one-dimensional Si–CdSe heterostructures," Appl. Phys. Lett. 89 (24), 243102-1-243102-3 (2006). DOI: 10.1063/1.2402262

R.A. Rosenberg, G.K. Shenoy, L.-C. Tien, D. Norton, S. Pearton, X.H. Sun, T.K. Sham, "Anisotropic x-ray absorption effects in the optical luminescence yield of ZnO nanostructures," Appl. Phys. Lett. 89, 093118-1-093118-3 (2006). DOI: 10.1063/1.2245440

Edward F. Rosloniec, Robert A. Ivey III, Karen B. Whittington, Andrew H. Kang, Hee-Won Park, "Crystallographic Structure of a Rheumatoid Arthritis MHC Susceptibvility Allele, HLA-DRI (DRB1*0101), Complexed with the Immunodominant Determinant of Human Type II Collagen," J. Immunol. 177, September, 3884-3892 (2006).

Ashaki A. Rouff, Evert J. Elzinga, Richard J. Reeder, Nicholas S. Fisher, "The Effect of Aging and pH on Pb(II) Sorption Processes at the Calcite-Water Interface," Environ. Sci. Technol. 40 (6), March, 1792-1798 (2006). DOI: 10.1021/es051523f

William E. Royer, Jr., Hitesh Sharma, Kristen Strand, James E. Knapp, Balaji Bhyravbhatla, "Lumbricus Erythrocruorin at 3.5 Å Resolution: Architecture of a Megadalton Respiratory Complex," Structure 14 (7), July, 1167-1177 (2006). DOI: 10.1016/j.str.2006.05.011

Megan L. Ruegg, Amish J. Patel, Suresh Narayanan, Alec R. Sandy, Simon G.J. Mochrie, Hiroshi Watanabe, Nitash P. Balsara, "Condensed Exponential Correlation Functions in Multicomponent Polymer Blends Measured by X-ray Photon Correlation Spectroscopy," Macromolecules 39 (25), November, 8822-8831 (2006). DOI: 10.1021/ma061183y

Jeremy L. Ruggles, Garry J. Foran, Hajime Tanida, Hirohisa Nagatani, Yukari Jimura, Iwao Watanabe, Ian R. Gentle, "Interfacial Behavior of Tetrapyridylporphyrin Monolayer Arrays," Langmuir 22 (2), December, 681-686 (2006). DOI: 10.1021/la051474k

C.E. Runge, A. Kubo, B. Kiefer, Y. Meng, V.B. Prakapenka, G. Shen, R.J. Cava, T.S. Duffy, "Equation of state of MgGeO[subscript 3] perovskite to 65 GPa: comparison with the post-perovskite phase," Phys. Chem. Miner. 33 (10), 699-709 (2006). DOI: 10.1007/s00269-006-0116-8

A.J. Ruthenburg, W. Wang, D.M. Graybosch, H. Li, C.D. Allis, D.J. Patel, G.L. Verdine, "Histone H3 recognition and presentation by the WDR5 module of the MLL1 complex," Nat. Struct. Mol. Biol. 13 (8), 704-712 (2006).

P. Ryan, R.A. Rosenberg, D.J. Keavney, J.W. Freeland, J.C. Woicik, "Surface order dependent magnetic thin film growth: Fe on GaN(0 0 0 1)," Surf. Sci. 600 (5), March, 48-53 (2006).

Beth M. Rybak, Maryna Ornatska, Kathryn N. Bergman, Kirsten L. Genson, Vladimir V. Tsukruk, "Formation of Silver Nanoparticles at the Air-Water Interface Mediated by a Monolayer of Functionalized Hyperbranched Molecules," Langmuir 22 (3), January, 1027-1037 (2006). DOI: 10.1021/la0525269

Mark Sabat, John C. VanRens, Michael P. Clark, Todd A. Brugel, Jennifer Maier, Roger G. Bookland, Matthew J. Laufersweiler, Steven K. Laughlin, Adam Golebiowski, Biswanath De, Lily C. Hsieh, Richard L. Walter, Marlene J. Mekel, Michael J. Janusz, "The Development of novel C-2, C-8, and N-9 trisubstituted purines as inhibitors of TNF-[alpha] production," Bioorg. Med. Chem. Lett. 16 (16), August, 4360-4365 (2006). DOI: 10.1016/j.bmcl.2006.05.050

B. Sahoo, W.A. Adeagbo, F. Stromberg, W. Keune, E. Schuster, R. Peters, P. Entel, A. Luttjohann, A. Gondorf, W. Sturhahn, J. Zhao, T.S. Toellner, E.E. Alp, "Electronic Transport and Atomic Vibrational Properties of Semiconducting Mg[subscript 2][superscript 119]Sn Thin Film," Phase Transit. 79 (9-10), 839-852 (2006).

B. Sahoo, W. Keune, E. Schuster, W. Sturhahn, T. S. Toellner, E. E. Alp, "Amorphous Fe-Mg alloy thin films: magnetic properties and atomic vibrational dynamics," Hyperfine Interact. 168 (1-3), February, 1185-1190 (2006). DOI: 10.1007/s10751-006-9421-3

A.H. Said, H. Sinn, A. Alatas, C.A. Burns, D.L. Price, M.-L. Saboungi, W. Schirmacher, "Collective excitations in an early molten transition metal," Phys. Rev. B 74, 172202-1-172202-4 (2006). DOI: 10.1103/PhysRevB.74.172202

Kumar Singh Saikatendu, Xuejun Zhang, Lisa Kinch, Matthew Leybourne, Nick V. Grishin, Hong Zhang, "Structure of a conserved hypothetical protein SA1388 from S. aureus reveals a capped hexameric toroid with two PII domain lids and a dinuclear metal center," BMC Biology 6 (27), December, Open Access (2006). DOI: 10.1186/1472-6807-6-27

Parthasarathy Sampathkumar, Stewart Turley, Carol Hopkins Sibley, Wim G.J. Hol, "NADP[superscript +] Expels both the Co-factor and a Substrate Analog from the Mycobacterium tuberculosis ThyX Active Site: Opportunities for Anti-bacterial Drug Design," J. Mol. Biol. 360, 1-6 (2006). DOI: 10.1016/j.jmb.2006.04.061

E.C. Samulon, Z. Islam, S.E. Sebastian, P.B. Brooks, M.K. McCourt Jr., J. Ilavsky, I.R. Fisher, "Low-temperature structural phase transition and incommensurate lattice modulation in the spin-gap compound BaCuSi[subscript 2]O[subscript 6]," Phys. Rev. B 73, March, 100407-1-100407-4 (2006). DOI: 10.1103/PhysRevB.73.100407

Javier Santillan, Sang-Heon Shim, Guoyin Shen, Vitali B. Prakapenka, "High-pressure phase transition in Mn[subscript 2]O[subscript 3]: Application for the crystal structure and preferred orientation of the CaIrO[subscript 3] type," Geophys. Res. Lett. 33, L15307-L15312 (2006). DOI: 10.1029/2006GL026423

Ian Saratovksy, Peter G. Wightman, Pablo A. Pasten, Jean-Francois Gaillard, Kenneth R. Poeppelmeier, "Manganese Oxides: Parallels between Abiotic and Biotic Structures," J. Am. Chem. Soc. 128 (34), August, 11188-11198 (2006). DOI: 10.1021/ja062097g

P. Sarin, W. Yoon, K. Jurkschat, P. Zschack, W.M. Krivan, "Quadrupole lamp furnace for high temperature (up to 2050 K) synchrotron powder x-ray diffraction studies in air in reflection geometry," Rev. Sci. Instrum. 77, September, 093906-1-093906-9 (2006). DOI: 10.1063/1.2349600

Neuza Satomi Sato, Naomi Hirabayashi, Ilana Agmon, Ada Yonath, Tsutomu Suzuki, "Comprehensive genetic selection revealed essential bases in the peptidyl-transferase center," Proc. Natl. Acad. Sci. USA 103 (42), October, 15386-15391 (2006). DOI: 10.1073/pnas.0605970103

P. Satori, T. Buslaps, V. Honkimaki, N. Hiraoka, U. Lienert, "Crystal Spectrometers for Compton Scattering Studies," Z. Phys. Chem. 220, 831-847 (2006). DOI: 10.1524/zpch.2006.220. 831

Ajay K. Saxena, Kavita Singh, Hua-Poo Su, Michael M. Klein, Anthony W. Stowers, Allan J. Saul, Carole A. Long, David N. Garboczi, "The essential mosquito-stage P25 and P28 proteins from Plasmodium form tile-like triangular prisms," Nat. Struct. Mol. Biol. 13 (1), January, 90-91 (2006). DOI: 10.1038/nsmb1024

Matthew H. Sazinsky, Sorabh Agarwal, Jose M. Arguello, Amy C. Rosenzweig, "Structure of the actuator domain from the Archaeoglobus fulgidus Cu[superscript +]-ATPase," Biochemistry-US 45 (33), August, 9949-9955 (2006). DOI: 10.1021/bi0610045

Matthew H. Sazinsky, Pete W. Dunten, Michael S. McCormick, Alberto DiDonato, Stephen J. Lippard, "X-ray Structure of a Hydroxylase-Regulatory Protein Complex from a Hydrocarbon-Oxidizing Multicomponent Monooxygenase, Pseudomonas sp. OX1 Phenol Hydroxylase," Biochemistry-US 45 (51), November, 15392-15404 (2006). DOI: 10.1021/bi0618969

Matthew H. Sazinsky, Atin K. Mandal, Jose M. Argüello, Amy C. Rosenzweig, "Structure of the ATP Binding Domain from the Archaeoglobus fulgidus Cu[superscript +]-ATPase," J. Biol. Chem. 281 (16), April, 11161-11166 (2006).

A.M. Scheidegger, D. Grolimund, C.R. Cheeseman, R.D. Rogers, "Micro-spectroscopic investigations of highly heterogeneous waste repository materials," J. Geochem. Explor. 88 (1-3), 59-63 (2006).

Michel L. Schlegel, Kathryn L. Nagy, Paul Fenter, Likwan Cheng, Neil C. Sturchio, Steven D. Jacobsen, "Cation sorption on the muscovite (0 0 1) surface in chloride solutions using high-resolution X-ray reflectivity," Geochim. Cosmochim. Acta 70 (14), July, 3549-3565 (2006). DOI: 10.1016/j.qca.2006.04.011

Marius Schmidt, Angela Krasselt, Wolfgang Reuter, "Local protein flexibility as a prerequisite for reversible chromophore isomerization in [alpha]-phycoerythrocyanin," Biochim. Biophys. Acta 1764 (1), January, 55-62 (2006). DOI: 10.1016/j.bbapap.2005.10.022

Margaret A. Schmitt, SooHyuk Choi, Ilia A. Guzei, Samuel H. Gellman, "New Helical Foldamers: Heterogeneous Backbones with 1:2 and 2:1 [alpha]:[superscript beta]-Amino Acid Residue Patterns," J. Am. Chem. Soc. 128 (14), February, 4538-4539 (2006).

G. Schnaar, M.L. Brusseau, "Characterizing Pore-Scale Configuration of Organic Immiscible Liquid in Multiphase Systems With Synchrotron X-Ray Microtomography," Vadose Zone J. 5, May, 641-648 (2006). DOI: 10.2136/vzj2005.0063

Florian D. Schubot, Joseph E. Tropea, David S. Waugh, "Structure of the POZ domain of human LRF, a master regulator of oncogenesis," Biochem. Biophys. Res. Commun. 351, November, 1-6 (2006). DOI: 10.1016/j.bbrc.2006.09.167

David G. Schultz, Xiao-Min Lin, Dongxu Li, Jeff Gebhardt, Mati Meron, P. James Viccaro, Binhua Lin, "Structure, Wrinkling, and Reversibility of Langmuir Monolayers of Gold Nanoparticles," J. Phys. Chem. B 110 (48), November, 24522-24529 (2006). DOI: 10.1021/jp063820s

Christopher T. Seagle, Andrew J. Campbell, Dion L. Heinz, Guoyin Shen, Vitali B. Prakapenka, "Thermal equation of state of Fe[subscript 3]S and implications for sulfur in Earth's core," J. Geophys. Res. 111, June, B06209-1-B06209-7 (2006). DOI: 10.1029/2005JB004091

Erika N. Segraves, Maksymilian Chruszcz, Michael L. Neidig, Viola Ruddat, Jing Zhou, Aaron T. Wecksler, Wladek Minor, Edward I. Solomon, Theodore R. Holman, "Kinetic, Spectroscopic, and Structural Investigations of the Soybean Lipoxygenase-1 First-Coordination Sphere Mutant, Asn694Gly," Biochemistry-US 45 (34), August, 10233-10242 (2006). DOI: 10.1021/bi060577e

Anna I. Selezneva, Giorgio Cavigiolio, Elizabeth C. Theil, William E. Walden, Karl Volz, "Crystallization and preliminary X-ray diffraction analysis of iron regulatory protein 1 in complex with ferritin IRE RNA," Acta Crystallogr. F 62 (3), March, 1-4 (2006). DOI: 10.1107/S1744309106004192

T.K. Sham, P.-S.G. Kim, P. Zhang, "Electronic structure of molecular-capped gold nanoparticles from X-ray spectroscopy studies: Implications for coulomb blockade, luminescence and non-Fermi behavior," Solid State Commun. 138, 553-557 (2006). DOI: 10.1016/j.ssc.2006.03.021

P. Shanthakumar, M. Balasubramanian, D.M. Pease, A.I. Frenkel, D.M. Potrepka, V. Kraizman, J.I. Budnick, W.A. Hines, "X-ray study of the ferroelectric [Ba[subscript 0.6]Sr[subscript 0.4]] [(YTa)[subscript 0.03]Ti[subscript 0.94]]O[subscript 3]," Phys. Rev. B 74, 174103-1-174103-10 (2006). DOI: 10.1103/PhysRevB.74.174103

O. Shebanova, E. Soignard, P.F. Mcmillan, "Compressibilities and phonon spectra of high-hardness transition metal-nitride materials," High Pressure Res. 26 (2), June, 87-97 (2006). DOI: 10.1080/08957950600765186

H.W. Sheng, E. Ma, H.Z. Lui, J. Wen, "Pressure tunes atomic packing in metallic glass," Appl. Phys. Lett. 88, April, 171906 -1-171906 -3 (2006). DOI: 10.1063/1.2197315

Yuequan Shen, Andrzej Joachimiak, Marsha Rich Rosner, Wei-Jen Tang, "Structures of human insulin-degrading enzyme reveal a new substrate recognition mechanism," Nature 443, October, 870-874 (2006). DOI: 10.1038/nature05143

David H. Sherman, Shengying Li, Liudmila V. Yermalitskaya, Youngchang Kim, Jarrod A. Smith, Michael R. Waterman, Larissa M. Podust, "The Structural Basis for Substrate Anchoring, Active Site Selectivity, and Product Formation by P450 PikC from Streptomyces venezuelae," J. Biol. Chem. 281 (36), September, 26289-26297 (2006). DOI: 10.1074/jbc.M605478200

Dashuang Shi, Ljubica Caldovic, Zhongmin Jin, Xiaolin Yu, Qiuhao Qu, Lauren Roth, Hiroki Morizono, Yetrib Hathout, Norma M. Allewell, Mendel Tuchman, "Expression, crystallization and preliminary crystallographic studies of a novel bifunctional N-acetylglutamate synthase/kinase from Xanthomonas campestris homologous to vertebrate N-acetylglutamate synthase," Acta Crystallogr. F 62 (12), December, 1218-1222 (2006). DOI: 10.1107/S1744309106044101

S.R. Shieh, T.S. Duffy, A. Kubo, G. Shen, V.B. Prakapenka, N. Sata, K. Hirose, Y. Ohishi, "Equation of state of the postperovskite phase synthesized from a natural (Mg,Fe)SiO[subscript 3] orthopyroxene," Proc. Natl. Acad. Sci. USA 103 (9), 3039-3043 (2006). DOI: 10.1073/pnas.0506811103

S.R. Shieh, A. Kubo, T.S. Duffy, V.B. Prakapenka, G. Shen, "High-pressure phases in SnO[subscript 2] to 117 GPa," Phys. Rev. B 73 (1), January, 014105-1-014105-7 (2006). DOI: 10.1103/PhysRevB.73.014105

Hang Shi, Raul Rojas, Juan S. Bonifacino, James H. Hurley, "The retromer subunit Vps26 has an arrestin fold and binds Vps35 through its C-terminal domain," Nat. Struct. Mol. Biol. 13 (6), June, 540-548 (2006). DOI: 10.1038/nsmb1103

Ning Shi, Sheng Ye, Amer Alam, Liping Chen, Youxing Jiang, "Atomic structure of a Na[superscript +]- and K[superscript +]-conducting channel," Nature 440, March, 570-574 (2006). DOI: 10.1038/nature04508

Wuxian Shi, Howard Robinson, Michael Sullivan, Don Abel, John Toomey, Lonny E. Berman, Don Lynch, Gerd Rosenbaum, George Rakowsky, Larry Rock, Bill Nolan, Grace Shea-McCarthy, Dieter Schneider, Erik Johnson, Robert M. Sweet, Mark R. Chance, "Beamline X29: a novel undulator source for X-ray crystallography," J. Synchrotron Rad. 13 (5), September, 365-372 (2006). DOI: 10.1107/S0909049506027853

Alexander K. Showalter, Brandon J. Lamarche, Marina Bakhtina, Mei-I Su, Kuo-Hsiang Tang, Ming-Daw Tsai, "Mechanistic Comparison of High-Fidelity and Error-Prone DNA Polymerases and Ligases Involved in DNA Repair," Chem. Rev. 106 (2), February, 340-360 (2006). DOI: 10.1021/cr040487k

Boris G. Shpeizer, Vladimir I. Bakhmutov, Abraham Clearfield, "Supermicroporous alumina–silica zinc oxides," Micropor. Mesopor. Mat. 90, 81-86 (2006). DOI: 10.1016/j.micromeso.2005.10.023

Oleg G. Shpyrko, Alexei Yu. Grigoriev, Christoph Steimer, Peter S. Pershan, Binhua Lin, Mati Meron, Tim Graber, Jeff Gebhardt, Ben Ocko, Moshe Deutsch, "Erratum: Anomalous layering at the liquid Sn surface [Phys. Rev. B 70, 224206 (2004)]," Phys. Rev. B 73 (1), January, 019901(E) (2006).

Oleg G. Shpyrko, Reinhard Streitel, V.S.K. Balagurusamy, Alexei Y. Grigoriev, Moshe Deutsch, Benjamin M. Ocko, Mati Meron, Binhua Lin, Peter S. Pershan, "Surface Crystallization in a Liquid AuSi Alloy," Science 313, July, 77-80 (2006). DOI: 10.1126/science.1128314

R.D. Shull, V. Provenzano, A.J. Shapiro, A. Fu, M.W. Lufaso, J. Karapetrova, G. Kletetschka, V. Mikula, "The effects of small metal additions (Co, Cu, Ga, Mn, Al, Bi, Sn) on the magnetocaloric properties of the Gd[subscript 5]Ge[subscript 2]Si[subscript 2] alloy," J. Appl. Phys. 99, 08K908-1-08K908-3 (2006). DOI: 10.1063/1.2173632

David D. Shultis, Michael D. Purdy, Christian N. Banchs, Michael C. Wiener, "Outer Membrane Active Transport: Structure of the BtuB:TonB Complex," Science 312, June, 1396-1399 (2006). DOI: 10.1126/science.1127694

D.D. Shultis, M.D. Purdy, C.N. Banchs, M.C. Wiener, "Crystallization and preliminary X-ray crystallographic analysis of the Escherichia coli outer membrane cobalamin transporter BtuB in complex with the carboxy-terminal domain of TonB," Acta Crystallogr. F 62, July, 638-641 (2006). DOI: 10.1107/S1744309106018240

V. Shutthanandan, S. Thevuthasan, T.C. Droubay, S.M. Heald, M.H. Engelhard, D.E. McCready, S.A. Chambers, P. Nachimuthu, B.S. Mun, "Synthesis of Room-Temperature Ferromagnetic Cr-doped TiO[subscript 2](110) Rutile Single Crystals using Ion Implantation," Nucl. Instrum. Methods B 242 (1-2), January, 198-200 (2006).

Xiaokun Shu, Nathan C. Shaner, Corinne A. Yarbrough, Roger Y. Tsien, S. James Remington, "Novel Chromophores and Buried Charges Control Color in mFruits," Biochemistry-US 45 (32), August, 9639-9647 (2006). DOI: 10.1021/bi060773l

Yu.V. Shvyd'ko, M. Lerche, U. Kuetgens, H.D. Ruter, A. Alatas, Z. Zhao, "X-Ray Bragg Diffraction in Asymmetric Backscattering Geometry," Phys. Rev. Lett. 97 (23), 235502-1-235502-4 (2006). DOI: 10.1103/PhysRevLett.97.235502

Kathleen S. Simis, Alessandro Bistolfi, Anuj Bellare, Lisa A. Pruitt, "The combined effects of crosslinking and high crystallinity on the microstructural and mechanical properties of ultra high molecular weight polyethylene," Biomaterials 27, 1688-1694 (2006).

Paul A. Sims, Ann L. Menefee, Todd M. Larsen, Steven O. Mansoorabadi, George H. Reed, "Structure and Catalytic Properties of an Engineered Heterodimer of Enolase Composed of One Active and One Inactive Subunit," J. Mol. Biol. 355, 422-431 (2006). DOI: 10.1016/j.jmb.2005.10.050

A.K. Singh, A. Jaina, H.P. Liermann, S.K. Saxena, "Strength of iron under pressure up to 55 GPa from X-ray diffraction line-width analysis," J. Phys. Chem. Solids 67, 2197-2202 (2006). DOI: 10.1016/j.jpcs.2006.06.003

A.K. Singh, H.P. Liermann, S.K. Saxena, H.-k. Mao, Usha Devi S., "Nonhydrostatic compression of gold powder to 60 GPa in a diamond anvil cell: estimation of compressive strength from x-ray diffraction data," J. Phys. Condens. Matter 18, S969-S978 (2006). DOI: 0.1088/0953-8984/18/25/S05

Stanislav Sinogeikin, Jay Bass, Vitali Prakapenka, Dmitry Lakshtanov, Guoyin Shen, Carmen Sanchez-Valle, Mark Rivers, "Brillouin spectrometer interfaced with synchrotron radiation for simultaneous x-ray density and acoustic velocity measurements," Rev. Sci. Instrum. 77, October, 103905-1-103905-11 (2006). DOI: 10.1063/1.2360884

A.A. Sirenko, A. Kazimirov, A. Ougazzaden, S.M. O'Malley, D.H. Bilderback, Z.-H. Cai, B. Lai, R. Huang, V.K. Gupta, M. Chien, S.N.G. Chu, "Strain relaxation and surface migration effects in InGaAlAs and InGaAsP selective-area-grown ridge waveguides," Appl. Phys. Lett. 88, 081111-1-081111-3 (2006). DOI: 10.1063/1.2177634

Amos B. Smith III, Adam K. Charnley, Hironori Harada, Jason J. Beiger, Louis-David Cantin, Craig S. Kenesky, Ralph Hirschmann, Sanjeev Munshi, David B. Olsen, Mark W. Stahlhut, William A. Schleif, Lawrence C. Kuo, "Design, synthesis, and biological evaluation of monopyrrolinone-based HIV-1 protease inhibitors possessing augmented P2' side chains," Bioorg. Med. Chem. Lett. 16 (4), February, 859-863 (2006). DOI: 10.1016/j.bmcl.2005.11.011

Brian J. Smith, Trevor Huyton, Robbie P. Joosten, Jennifer L. McKimm-Breschkin, Jian-Guo Zhang, Cindy S. Luo, Mei-Zhen Lou, Nikolaos E. Labrou, Thomas P.J. Garrett, "Structure of a calcium-deficient form of influenza virus neuraminidase: implications for substrate binding," Acta Crystallogr. D 62 (9), September, 947-952 (2006). DOI: 10.1107/S0907444906020063

Michael A. Smith, Raul F. Lobo, "The local and surface structure of ordered mesoporous carbons from nitrogen sorption, NEXAFS and synchrotron radiation studies," Micropor. Mesopor. Mat. 92 (1-3), June, 81-93 (2006). DOI: 10.1016/j.micromeso.2005.09.006

Natasha Smith, Adrian E. Roitberg, Eva Rivera, Andrew Howard, Marcia J. Holden, Martin Mayhew, Salita Kaistha, D.T. Gallagher, "Structural analysis of ligand binding and catalysis in chorismate lyase," Arch. Biochem. Biophys. 445 (1), January, 72-80 (2006). DOI: :10.1016/j.abb.2005.10.02

William E. Smith, Charles F. Zukoski, "Aggregation and gelation kinetics of fumed silica–ethanol suspensions," J. Colloid Interf. Sci. 304 (2), December, 359-369 (2006). DOI: 10.1016/j.jcis.2006.09.016

Feng Song, Zhihao Zhuang, Lorenzo Finci, Debra Dunaway-Mariano, Ryan Kniewel, John A. Buglino, Veronica Solorzano, Jin Wu, Christopher D. Lima, "Structure, Function, and Mechanism of the Phenylacetate Pathway Hot Dog-fold Thioesterase PaaI," J. Biol. Chem. 281 (16), April, 11028-11038 (2006).

S.M. Malathy Sony, K. Saraboji, N. Sukumar, M.N. Ponnuswamy, "Role of amino acid properties to determine backbone [tau](N–C[alpha]–C′) stretching angle in peptides and proteins," Biophys. Chem. 120 (1), March, 24-31 (2006). DOI: 10.1016/j.bpc.2005.07.012

Jeffrey A. Speir, Brian Bothner, Chunxu Qu, Deborah A. Willits, Mark J. Young, John E. Johnson, "Enhanced Local Symmetry Interactions Globally Stabilize a Mutant Virus Capsid that Maintains Infectivity and Capsid Dynamics," J. Virol. 80 (7), April, 3582-3591 (2006). DOI: 10.1128/JVI.80.7.3582-3591.2006

S. Speziale, I. Lonardelli, L. Miyagi, J. Pehl, C.E. Tommaseo, H.-R. Wenk, "Deformation experiments in the diamond-anvil cell: texture in copper to 30 GPa," J. Phys. Condens. Matter 18, S1007-S1020 (2006). DOI: 10.1088/0953-8984/18/25/S08

John M. Squire, Tanya Bekyarova, Gerrie Farman, David Gore, Ganeshalingam Rajkumar, Carlo Knupp, Carmen Lucaveche, Mary C. Reedy, Michael K. Reedy, Thomas C. Irving, "The Myosin Filament Superlattice in the Flight Muscles of Flies: A-band Lattice Optimisation for Stretch-activation?," J. Mol. Biol. 361 (5), September, 823-838 (2006). DOI: 10.1016/j.jmb.2006.06.072

G. Srajer, L.H. Lewis, S.D. Bader, A.J. Epstein, C.S. Fadley, E.E. Fullerton, A. Hoffmann, J.B. Kortright, Kannan M. Krishnan, S.A. Majetich, T.S. Rahman, C.A. Ross, M.B. Salamon, I.K. Schuller, T.C. Schulthess, J.Z. Sun, "Advances in nanomagnetism via X-ray techniques," J. Magn. Magn. Mater. 307 (1), December, 1-31 (2006). DOI: 10.1016/j.jmmm.2006.06.033

Geoffrey F. Stamper, Kenton L. Longenecker, Elizabeth H. Fry, Clarissa G. Jakob, Alan S. Florjancic, Yu-Gui Gu, David D. Anderson, Curt S. Cooper, Tianyuan Zhang, Richard F. Clark, Yingna Cia, Candace L. Black-Schaefer, J. Owen McCall, Claude G. Lerner, Philip J. Hajduk, Bruce A. Beutel, Vincent S. Stoll, "Structure-based Optimization of MurF Inhibitors," Chem. Biol. Drug Des. 67 (1), January, 58-65 (2006). DOI: 10.111/j.1747-0285.2005.00317

Valeriia Starovoitova, Timo E. Budarz, Graeme R.A. Wyllie, W. Robert Scheidt, Wolfgang Sturhahn, E. Ercan Alp, E. W. Prohofsky, Stephen M. Durbin, "Vibrational Spectroscopy and Normal-Mode Analysis of Fe(II) Octaethylporphyrin," J. Phys. Chem. B 110 (26), 13277-13282 (2006). DOI: 10.1021/jp060345p

Calvin N. Steussy, Aaron D. Robison, Alison M. Tetrick, Jeffrey T. Knight, Victor W. Rodwell, Cynthia V. Stauffacher, Autumn L. Sutherlin, "A Structural Limitation on Enzyme Activity: The Case of HMG-CoA Synthase," Biochemistry-US 45 (48), 14407-14414 (2006). DOI: 10.1021/bi061505q

S. Stoupin, E-H. Chung, S. Chattopadhyay, C.U. Segre, E.S. Smotkin, "Pt and Ru X-ray Absorption Spectroscopy of PtRu Anode Catalysts in Operating Direct Methanol Fuel Cells," J. Phys. Chem. B 110 (20), April, 9932-9938 (2006). DOI: 10.1021/jp057047x S1520-6106(05)07047-1

James C. Stroud, Yongqing Wu, Darren L. Bates, Aidong Han, Katja Nowick, Svante Paabo, Harry Tong, Lin Chen, "Structure of the Forkhead Domain of FOXP2 Bound to DNA," Structure 14 (1), January, 159-166 (2006). DOI: 10.1016/j.str.2005.10.005

Viktor V. Struzhkin, Ho-kwang Mao, Jung-Fu Lin, Russell J. Hemley, John S. Tse, Yanming Ma, Michael Y. Hu, Paul Chow, Chi-Chang Kao, "Valence Band X-Ray Emission Spectra of Compressed Germanium," Phys. Rev. Lett. 96 (13), 137402-1-137402-4 (2006).

Joseph Strzalka, Ting Xu, Andrey Tronin, Sophia P. Wu, Ivan Miloradovic, Ivan Kuzmenko, Thomas Gog, Michael J. Therien, J. Kent Blasie, "Structural Studies of Amphiphilic 4-Helix Bundle Peptides Incorporating Designed Extended Chromophores for Nonlinear Optical Biomolecular Materials," Nano Lett. 6 (11), 2395-2405 (2006). DOI: 10.1021/nl062092h

A.N. Styka, Y. Ren, O. Yu. Gorbenko, N.A. Babushkina, D.E. Brown, "Examining the Oxygen Isotope and Magnetic Field Effect in Phase Separation in Sm[sub0.5]Sr[sub0.5]MnO[sub3]," J. Appl. Phys. 100 (10), November, 103520-1-103520-5 (2006). DOI: 0021-8979/2006/1009(10)/103520/5

Dan Su, Zhiyong Lou, Fei Sun, Yujia Zhai, Haitao Yang, Rongguang Zhang, Andrzej Joachimiak, Xuejun C. Zhang, Mark Bartlam, Zihe Rao, "Dodecamer Structure of Severe Acute Respiratory Syndrome Coronavirus Nonstructural Protein nsp10," J. Virol. 80 (16), August, 7902-7908 (2006).

Hua-Poo Su, David Yin-wei Lin, David N. Garboczi, "The Structure of G4, the Poxvirus Disulfilde Oxidoreductase Essential for Virus Maturation and Infectivity," J. Virol. 80 (15), August, 7706-7713 (2006). DOI: 10.1128/JVI.00521-06

Narayanasami Sukumar, Zhi-wei Chen, Davide Ferrari, Angelo Merli, Gian Luigi Rossi, Henry D. Bellamy, Andrei Chistoserdov, Victor L. Davidson, F. Scott Mathews, "Crystal Structure of an Electron Transfer Complex between Aromatic Amine Dehydrogenase and Azurin from Alcaligenes faecalis," Biochemistry-US 45 (45), October, 13500-13510 (2006). DOI: 10.1021/bi0612972

C.J. Sun, G.M. Chow, S.-W. Han, J.P. Wang, Y.K. Hwu, J.H. Je, "Investigation of phase miscibility of CoCrPt thin films using anomalous x-ray scattering and extended x-ray absorption fine structure," Appl. Phys. Lett. 88, March, 122508-1-122508-3 (2006).

Siyang Sun, Linda Geng, Yousif Shamoo, "Structure and enzymatic properties of a chimeric bacteriophage RB69 DNA polymerase and single-stranded DNA binding protein with increased processivity," Proteins 65 (1), October, 231-238 (2006). DOI: 10.1002/prot.21088

Tao Sun, Zixiao Pan, Vinayak P. Dravid, Zhaoyu Wang, Min-Feng Yu, Jin Wang, "Nanopatterning of multiferroic BiFeO[subscript 3] using 'soft' electron beam lithography," Appl. Phys. Lett. 89, 163117-1-163117-3 (2006). DOI: 10.1063/1.2364117

Warren Sun, Sasha Singh, Rongguang Zhang, Joanne L. Turnbull, Dinesh Christendat, "Crystal Structure of Prephenate Dehydrogenase from Aquifex aeolicus: Insights into the Catalytic Mechanism," J. Biol. Chem. 281 (18), May, 12919-12928 (2006). DOI: 10.1074/jbc.M511986200

X.H. Sun, C. Didychuk, T.K. Sham, N.B. Wong, "Germanium nanowires: synthesis, morphology and local structure studies," Nanotechnology 17 (12), June, 2925-2930 (2006). DOI: 10.1088/0957-4484/17/12/017

R.M. Suter, D. Hennessy, C. Xiao, U. Lienert, "Forward modeling method for microstructure reconstruction using x-ray diffraction microscopy: Single-crystal verification," Rev. Sci. Instrum. 77, 123905-1-123905-12 (2006). DOI: 10.1063/1.2400017

Anna-Karin E. Svensson, Osman Bilsel, Elena Kondrashkina, Jill A. Zitzewitz, C. Robert Matthews, "Mapping the Folding Free Energy Surface for Metal-free Human Cu,Zn Superoxide Dismutase," J. Mol. Biol. 364, December, 1084-1102 (2006). DOI: 10.1016/j.jmb.2006.09.005

V. Swamy, A. Kuznetsov, L.S. Dubrovinsky, P.F. Millan, V.B. Prakapenka, G. Shen, B.C. Muddle, "Size-dependent pressure-induced amorphization in nanoscale TiO[subscript 2]," Phys. Rev. Lett. 96, April, 135702-1-135702-4 (2006).

Michael K. Swan, Deepak Bastia, Christopher Davies, "Crystal structure of [pi] initiator protein–iteron complex of plasmid R6K: Implications for initiation of plasmid DNA replication," Proc. Natl. Acad. Sci. USA 103 (49), December, 18481-18486 (2006). DOI: 10.1073/pnas.0609046103

Agnieszka Szyk, Zhibin Wu, Kenneth Tucker, De Yang, Wuyuan Lu, Jacek Lubkowski, "Crystal structures of human [alpha]-defensins HNP4, HD5, and HD6," Protein Sci. 15, 2749-2760 (2006). DOI: 10.1110/ps.062336606.

Shunsuke Tanaka, Michael P. Tate, Norikazu Nishiyama, Korekazu Ueyama, Hugh W. Hillhouse, "Structure of Mesoporous Silica Thin Films Prepared by Contacting PEO[subscript 106]-PPO[subscript 70]-PEO[subscript 106] Films with Vaporized TEOS," Chem. Mater. 18 (23), October, 5461-5466 (2006). DOI: 10.1021/cm0614463

Bhupesh Taneja, Asmita Patel, Alexei Slesarev, Alfonso Mondragon, "Structure of the N-terminal fragment of topoisomerase V reveals a new family of topoisomerases," EMBO J. 25, 398-408 (2006). DOI: 10.1038/sj.emboj.7600922

Jinghua Tang, Jennifer M. Johnson, Kelly A. Dryden, Mark J. Young, Adam Zlotnick, John E. Johnson, "The role of subunit hinges and molecular 'switches' in the control of viral capsid polymorphism," J. Struct. Biol. 154 (1), March, 59-67 (2006). DOI: 10.1016/j.jsb.2005.10.013

Kemin Tan, Mark Duquette, Jin-huan Liu, Rongguang Zhang, Andrzej Joachimiak, Jia-huai Wang, Jack Lawler, "The Structures of the Thrombospondin-1 N-Terminal Domain and Its Complex with a Synthetic Pentameric Heparin," Structure 14, January, 33-42 (2006). DOI: 10.1016/j.str.2005.09.017

Franz X. Tanner, K.A. Feigl, S.A. Ciatti, Christopher F. Powell, S.-K. Cheong, J. Liu, Jin Wang, "The Structure of High-Velocity Dense Sprays in the Near-Nozzle Region," Atomization Spray 16 (5), 579-598 (2006). DOI: 10.1615/AtomizSpr.v16.i5

Zenobia F. Taraporewala, Xiaofang Jiang, Rodrigo Vasquez-Del Carpio, Hariharan Jayaram, B.V. Venkataram Prasad, John T. Patton, "Structure-Function Analysis of Rotavirus NSP2 Octamer by Using a Novel Complementation System," J. Virol. 80 (16), August, 7984-7994 (2006). DOI: 10.1128/JVI.00172-0

Michael P. Tate, Vikrant N. Urade, Jonathon D. Kowalski, Ta-chen Wei, Benjamin D. Hamilton, Brian W. Eggiman, Hugh W. Hillhouse, "Simulation and Interpretation of 2D Diffraction Patterns from Self-Assembled Nanostructured Films at Arbitrary Angles of Incidence: From Grazing Incidence (Above the Critical Angle) to Transmission Perpendicular to the Substrate," J. Phys. Chem. B 110 (20), May, 9882-9892 (2006). DOI: 10.1021/jp0566008

D.J. Taylor, J.A. Speir, V. Reddy, G. Cingolani, F.M. Pringle, L.A. Ball, J.E. Johnson, "Preliminary x-ray characterization of authentic providence virus and attempts to express its coat protein gene in recombinant baculovirus," Arch. Virol. 151 (1), January, 155-165 (2006). DOI: 10.1007/s00705-005-0637-3

R. Tedesco, A. Shaw, R. Bambal, D. Chai, N. Concha, M. Darcy, D. Dhanak, D. Fitch, A. Gates, W. Gerhardt, D. Halegoua, C. Han, G. Hofmann, V. Johnston, A. Kaura, N. Liu, R. Keenan, J. Lin-Goerke, R. Sarisky, K. Wiggall, M. Zimmerman, K. Duffy, "3-(1,1-Dioxo-2H-(1,2,4)-benzothiadiazin-3-yl)-4-hydroxy-2(1H)-quinolinones, Potent Inhibitors of Hepatitis C Virus RNA-Dependent RNA Polymerase," J. Med. Chem. 49 (3), 971-983 (2006). DOI: 10.1021/jm050855s

Ramiro Tellez-Sanz, Eleonora Cesareo, Marzia Nuccetelli, Ana M. Aguilera, Carmen Barón, Lorien J. Parker, Julian J. Adams, Craig J. Morton, Mario Lo Bello, Michael W. Parker, Luis Garcia-Fuentes, "Calorimetric and structural studies of the nitric oxide carrier S-nitrosoglutathione bound to human glutathione transferase P1-1," Protein Sci. 15, 1093-1105 (2006). DOI: 10.1110/ps.052055206

Boris G. Tencho, Robert C. MacDonald, David P. Siegel, "Cubic Phases in Phosphatidylcholine-Cholesterol Mixtures: Cholesterol as Membrane 'Fusogen'," Biophys. J. 91, October, 2508-2516 (2006). DOI: 10.1529/biophysj.106.083766

Boris Tenchov, Erin M. Vescio, G. Dennis Sprott, Mark L. Zeidel, John C. Mathai, "Salt Tolerance of Archaeal Extremely Halophilic Lipid Membranes," J. Biol. Chem. 281 (15), April, 10016-10023 (2006). DOI: 10.1074/jbc.M600369200

L.C. Teng, "Advanced Particle Acceleration Concepts," High Energy Phys. Nucl. 30 (I), 1-5 (2006).

Marianna Teplova, Yu-Ren Yuan, Anh Tuan Phan, Lucy Malinina, Serge Ilin, Alexei Teplov, Dinshaw J. Patel, "Structural Basis for Recognition and Sequestration of UUU[subscript OH] 3' Temini of Nascent RNA Polymerase III Transcripts by La, a Rheumatic Disease Autoantigen," Mol. Cell 21 (1), January, 75-85 (2006). DOI: 10.1016/j.molcel.2005.10.027

Alexey Teplyakov, Kap Lim, Peng-Peng Zhu, Geeta Kapadia, Celia C.H. Chen, Jennifer Schwartz, Andrew Howard, Prasad T. Reddy, Alan Peterkofsky, Osnat Herzberg, "Structure of phosphorylated enzyme I, the phosphoenolpyruvate:sugar phosphotransferase system sugar translocation signal protein," Proc. Natl. Acad. Sci. USA 103 (44), October, 16218-16223 (2006). DOI: 10.1073/pnas.0607587103

Alexander Y. Terekhov, Brent J. Heuser, Maria A. Okuniewski, Robert S. Averback, Soenke Seifert, Pete R. Jemian, "Small-angle X-ray scattering measurements of helium-bubble formation in borosilicate glass," J. Appl. Crystallogr. 39 (5), October, 647-651 (2006). DOI: 10.1107/S0021889806025672

M.R. Terner, P. Hedstrom, J. Almer, J. Ilavsky, M. Oden, "Residual stress evolution during decomposition of Ti[subscript1- x]Al[subscript x]N coatings using high-energy x-rays," Mater. Sci. Forum 524-525, 619-624 (2006). DOI: 164.54.85.63-20/09/06,22:43:55

Kimberly L. Terry, Patrick J. Casey, Lorena S. Beese, "Conversion of Protein Farnesyltransferase to a Geranylgeranyltransferase," Biochemistry-US 45 (32), July, 9746-9755 (2006). DOI: 10.1021/bi060295e

Karsten E. Thompson, Clinton S. Willson, Wenli Zhang, "Quantitative computer reconstruction of particulate materials from microtomography images," Powder Technol. 163, 169-182 (2006). DOI: 10.1016/j.powtec.2005.12.016

Geng Tian, Song Xiang, Robert Noiva, William J. Lennarz, Hermann Schindelin, "The Crystal Structure of Yeast Protein Disulfide Isomerase Suggests Cooperativity between Its Active Sites," Cell 124, January, 61-73 (2006). DOI: 10.1016/j.cell.2005.10.044

Vijay R. Tirumala, Gerard T. Caneba, Derrick C. Mancini, H.H. Wang, "Microfabrication by X-ray-Induced Polymerization Above the Lower Critical Solution Temperature," J. Appl. Polym. Sci. 102 (1), October, 429-435 (2006). DOI: 10.1002/app.24073

V.R. Tirumala, J. Ilavsky, M. Ilavsky, "Effect of chemical structure on the volume-phase transition in neutral and weakly charged poly(N-alkyl(meth)acrylamide) hydrogels studied by ultrasmall-angle x-ray scattering," J. Chem. Phys. 124 (23), June, 34911-34911 (2006). DOI: 10.1063/1.2205364

J.Z. Tischler, Gyula Eres, B.C. Larson, Christopher M. Rouleau, P. Zschack, Douglas H. Lowndes, "Nonequilibrium Interlayer Transport in Pulsed Laser Deposition," Phys. Rev. Lett. 96, 226104-1-226104-4 (2006). DOI: 10.1103/PhysRevLett.96.226104

Brian H. Toby, "R factors in Rietveld analysis: How good is good enough?," Powder Diffr. 21 (1), March, 67-70 (2006). DOI: 10.1154/1.2179804

T.S. Toellner, A. Alatas, A. Said, D. Shu, W. Sturhahn, J. Zhao, "A cryogenically stabilized meV-monochromator for hard X-rays," J. Synchrotron Rad. 13 (2), March, 211-215 (2006).

T.S. Toellner, M.Y. Hu, G. Bortel, W. Sturhahn, D. Shu, "Four-reflection 'nested' meV-monochromators for 20–30 keV," Nucl. Instrum. Methods A 557 (2), February, 670-675 (2006).

Caterina E. Tommaseo, Jim Devine, Sebastien Merkel, Sergio Spezial, Hans-Rudolf Wenk, "Texture development and elastic stresses in magnesiowustite at high pressure," Phys. Chem. Miner. 33, 84-97 (2006). DOI: 10.1007/s00269-005-0054-x

Thomas P. Trainor, Alexis S. Templeton, Peter J. Eng, "Structure and reactivity of environmental interfaces: Application of grazing angle X-ray spectroscopy and long-period X-ray standing waves," J. Electron. Spectrosc. 150, 66-85 (2006). DOI: 10.1016/j.elspec.2005.04.011

Chanh Q. Tran, Adrian P. Mancuso, Bipin B. Dhal, Keith A. Nugen, Andrew G. Peele, Zhonghou Cai, David Paterson, "Phase-space reconstruction of focused x-ray fields," J. Opt. Soc. Am. A 23 (7), 1779-1786 (2006).

Oliver Tschauner, Daniel Errandonea, George Serghiou, "Possible superlattice formation in high-temperature treated carbonaceous MgB[subscript 2] at elevated pressure," Physica B 371 (1), January, 88-94 (2006).

Oliver Tschauner, Sheng-Nian Luo, Paul D. Asimow, Thomas J. Ahrens, "Recovery of stishovite-structure at ambient conditions out of shock-generated amorphous silica," Am. Mineral. 91, 1857-1862 (2006). DOI: 10.2138/am.2006.2015

F. Tsui, L. He, D. Lorang, A. Fuller, Y.S. Chu, A. Tkachuk, S. Vogt, "Structure and magnetism of Co[subscript a(1-x)]Mn[subscript ax]Ge[subscript b] epitaxial films," Appl. Surf. Sci. 252, 2512-2517 (2006). DOI: 10.1016/j.apsusc.2005.03.238

C.A. Tulk, C.J. Benmore, D.D. Klug, J. Neuefeind, "Comment on 'Nature of the polyamorphic transition in ice under pressure'," Phys. Rev. Lett. 96 (14), April, 149601-149601 (2006). DOI: 10.1103/PhysRevLett.96.149601

C.A. Tulk, R. Hart, D.D. Klug, C.J. Benmore, J. Neuefeind, "Adding a Length Scale to the Polyamorphic Ice Debate," Phys. Rev. Lett. 97, September, 115503-1-115503-4 (2006). DOI: 10.1103/PhysRevLett.97.115503

Robert C. Tyler, Eduard Bitto, Christopher E. Berndsen, Craig A. Bingman, Shanteri Singh, Min S. Lee, Gary E. Wesenberg, John M. Denu, George N. Phillips, Jr., John L. Markley, "Structure of Arabidopsis thaliana At1g77540 Protein, a Minimal Acetyltransferase from the COG2388 Family," Biochemistry-US 45 (48), November, 14325-14336 (2006). DOI: 10.1021/bi0612059

Soheila Vaezeslami, Erika Mathes, Chrysoula Vasileiou, Babak Borhan, James H. Geiger, "The Structure of Apo-wild-type Cellular Retinoic Acid Binding Protein II at 1.4 Å and its Relationship to Ligand Binding and Nuclear Translocation," J. Mol. Biol. 363 (3), October, 687-701 (2006). DOI: 10.1016/j.jmb.2006.08.059

Frederic H. Vaillancourt, Jeffrey T. Bolin, Lindsay D. Ellis, "The Ins and Outs of Ring-Cleaving Dioxygenases," Crit. Rev. Biochem. Mol. 41 (4), 241-267 (2006). DOI: 10.1080/10409230600817422

V. Vaithyanathan, J. Lettieri, W. Tian, A. Sharan, A. Vasudevarao, Y.L. Li, A. Kochhar, H. Ma, J. Levy, P. Zschack, J.C. Woicik, L.Q. Chen, V. Gopalan, D.G. Schlom, "c-axis oriented epitaxial BaTiO[subscript 3] films on (001) Si," J. Appl. Phys. 100, 024108-1-024108-9 (2006). DOI: 10.1063/1.2203208

S. Vajda, R.E. Winans, J.W. Elam, B. Lee, M.J. Pellin, S. Seifert, G.Y. Tikhonov, N.A. Tomczyk, "Supported gold clusters and cluster-cased nanomaterials: characterization, stability and growth studies by in situ GISAXS under vacuum conditions and in the presence of hydrogen," Top. Catal. 39 (3-4), October, 161-166 (2006). DOI: 10.1007/s11244-006-0052-3

Ryan M. Van Wagoner, Jon Clardy, "FeeM, an N-Acyl Amino Acid Synthase from an Uncultured Soil Microbe: Structure, Mechanism, and Acyl Carrier Protein Binding," Structure 14, September, 1425-1435 (2006). DOI: 10.1016/j.str.2006.07.005

Dushyant B. Varshney, Satyendra Kumar, Evgenyi Y. Shalaev, Shin-Woong Kang, Larry A. Gatlin, Raj Suryanarayanan, "Solute Crystallization in Frozen Systems–Use of Synchrotron Radiation to Improve Sensitivity," Pharmaceut. Res. 23 (10), August, 2368-2374 (2006). DOI: 10.1007/s11095-006-9051-0

Marina N. Vassylyeva, Vladimir Svetlov, Sergiy Klyuyev, Yancho D. Devedjiev, Irina Artsimovitch, Dmitry G. Vassylyev, "Crystallization and preliminary crystallographic analysis of the transcriptional regulator RfaH from Escherichia coli and its complex with ops DNA," Acta Crystallogr. F 62 (10), October, 1027-1030 (2006). DOI: 10.1107/S174430910603658X

Boyd W. Veal, Arvydas P. Paulikas, Peggy Y. Hou, "Tensile stress and creep in thermally grown oxide," Nat. Mater. 5, May, 349-351 (2006). DOI: 10.1038/nmat1626

Michelvan Veenendaal, "Polarization Dependence of L- and M-Edge Resonant Inelastic X-Ray Scattering in Transition-Metal Compounds," Phys. Rev. Lett. 96, March, 117404-1-117404-4 (2006). DOI: 10.1103/PhysRevLett.96.117404

J. Viamontes, S. Narayanan, A.R. Sandy, J.X. Tang, "Orientational order parameter of the nematic liquid crystalline phase of F-actin," Phys. Rev. E 73 (6), June, 061901-1-061901-10 (2006). DOI: 10.1103/PhysRevE.73.061901

J.P. Vivian, C. Porter, J.A. Wilce, M.C.J. Wilce, "Crystallization and preliminary X-ray diffraction analysis of the Bacillus subtilis replication termination protein in complex with the 37-base-pair TerI-binding site," Acta Crystallogr. F 62 (11), November, 1104-1107 (2006). DOI: 10.1107/S1744309106039108

R.B. Von Dreele, "A rapidly filled capillary mount for both dry powder and polycrystalline slurry samples," J. Appl. Crystallogr. 39, 124-126 (2006).

R.B. Von Dreele, P.L. Lee, Y. Zhang, "Protein polycrystallography," Z. Kristallogr. 23 Supp., 3-8 (2006).

Thomas W. von Geldern, Chunqiu Lai, Rebecca J. Gum, Melissa Daly, Chaohong Sun, Elizabeth H. Fry, Celerino Abad-Zapatero, "Benzoxazole benzenesulfonamides are novel allosteric inhibitors of fructose-1,6-bisphosphatase with a distinct binding mode," Bioorg. Med. Chem. Lett. 16 (7), April, 1811-1815 (2006). DOI: 10.1016/j.bmcl.2006.01.015

Jenny B. Waern, Peter Turner, Margaret M. Harding, "Synthesis and Hydrolysis of Thiol Derivatives of Molybdocene Dichloride Incorporating Electron-Withdrawing Substituents," Organometallics 25 (14), June, 3417-3421 (2006). DOI: 10.1021/om060133e

William E. Walden, Anna I. Selezneva, Jerome Dupuy, Anne Volbeda, Juan C. Fontecilla-Camps, Elizabeth C. Theil, Karl Volz, "Structure of the Dual Function Iron Regulatory Protein 1 Complexed with Ferritin IRE-RNA," Science 314, December, 1903-1908 (2006). DOI: 10.1126/science.1133116

John R. Walker, Svetlana Altamentova, Alexandra Ezersky, Graciela Lorca, Tatiana Skarina, Marina Kudritska, Linda J. Ball, Alexey Bochkarev, Alexei Savchenko, "Structural and Biochemical Study of Effector Molecule Recognition by the E. coli Glyoxylate and Allantoin Utilization Regulatory Protein AllR," J. Mol. Biol. 358 (3), May, 810-828 (2006). DOI: 10.1016/j.jmb.2006.02.034

Jeremy Wally, Peter J. Halbrooks, Clemens Vonrhein, Mark A. Rould, Stephen J . Everse, Anne B. Mason, Susan K. Buchanan, "The Crystal Structure of Iron-free Human Serum Transferrin Provides Insight into Inter-lobe Communication and Receptor Binding," J. Biol. Chem. 281 (34), August, 24934-24944 (2006). DOI: 10.1074/jbc.M604592200

Scott T.R. Walsh, Anthony A. Kossiakoff, "Crystal Structure and Site 1 Binding Energetics of Human Placental Lactogen," J. Mol. Biol. 358 (3), May, 773-784 (2006). DOI: 10.1016/j.jmb.2006.02.038

C.-x. Wang, "Hamiltonian analysis of transverse beam dynamics in high-brightness photoinjectors," Phys. Rev. E 74, October, 046502 (2006).

C.-x. Wang, "Comment on the Invariant-Envelope Solution in rf Photoinjectors," Nucl. Instrum. Methods A 557, 94-97 (2006).

Feng Wang, Craig Cassidy, James C. Sacchettini, "Crystal Structure and Activity Studies of the Mycobacterium tuberculosis [beta]-Lactamase Reveal Its Critical Role in Resistance to [beta]-Lactam Antibiotics," Antimicrob. Agents Ch. 50 (8), August, 2762-2771 (2006). DOI: 10.1128/AAC.00320-06

J.W. Wang, M. Dauter, Z. Dauter, "What can be done with a good crystal and an accurate beamline?," Acta Crystallogr. D 62, December, 1475-1483 (2006). DOI: 10.1107/S0907444906038534

Jia-Yu Wang, Julie M. Leiston-Belanger, James D. Sievert, Thomas P. Russell, "Grain Rotation in Ion-Complexed Symmetric Diblock Copolymer Thin Films under an Electric Field," Macromolecules 39 (24), November, 8487-8491 (2006). DOI: 10.1021/ma0614287

J. Wang, S. Soisson, K. Young, W. Shoop, S. Kodali, A. Galgoci, R. Painter, G. Parthasarathy, Y. Tang, R. Cummings, S. Ha, K. Dorso, M. Motyl, H. Jayasuriya, J. Ondeyka, K. Herath, C. Zhang, L. Hernandez, J. Allocco, A. Basilio, J. Tormo, O. Genilloud, F. Vicente, F. Pelaez, L. Colwell, S. Lee, B. Michael, T. Felcetto, C. Gill, L. Silver, J. Hermes, K. Bartizal, J. Barrett, D. Schmatz, J. Becker, D. Cully, S. Singh, "Platensimycin is a selective FabF inhibitor with potent antibiotic properties," Nature 441, May, 358-361 (2006). DOI: 10.1038/nature04784

Li Wang, Rumiana Koynova, Harsh R. Parikh, Robert C. MacDonald, "Transfection Activity of Binary Mixtures of Cationic O-Substituted Phosphatidylcholine Derivatives: The Hydrophobic Core Strongly Modulates Physical Properties and DNA Delivery Efficacy," Biophys. J. 91 (10), November, 3692-3706 (2006). DOI: 10.1529/biophysj.106.092700

Liping Wang, William J. Zuercher, Thomas G. Consler, Millard H. Lambert, Aaron B. Miller, Lisa A. Orband-Miller, David D. McKee, Timothy M. Willson, Robert T. Nolte, "X-ray Crystal Structures of the Estrogen-related Receptor-[gamma] Ligand Binding Domain in Three Functional States Reveal the Molecular Basis of Small Molecule Regulation," J. Biol. Chem. 281 (49), December, 37773-37781 (2006). DOI: 10.1074/jbc.M608410200

Tao Wang, Xiangbin Zhang, Poonam Bheda, Javier R. Revollo, Shin-ichiro Imai, Cynthia Wolberger, "Structure of Nampt/PBEF/visfatin, a mammalian NAD[superscript +]biosynthetic enzyme," Nat. Struct. Mol. Biol. 13 (7), July, 661-662 (2006). DOI: 10.1038/nsmb1114

Weiru Wang, Adhirai Marimuthu, James Tsai, Abhinav Kumar, Heike I. Krupka, Chao Zhang, Ben Powell, Yoshihisa Suzuki, Hoa Nguyen, Maryam Tabrizizad, Catherine Luu, Brian L. West, "Structural characterization of autoinhibited c-Met kinase produced by coexpression in bacteria with phosphatase," Proc. Natl. Acad. Sci. USA 103 (10), March, 3563-3568 (2006).

Yong Wang, Nickolay Y. Chirgadze, Stephen L. Briggs, Sohaib Khan, Elwood V. Jensen, Thomas P. Burris, "A second binding site for hydroxytamoxifen within the coactivator-binding groove of estrogen receptor [beta]," Proc. Natl. Acad. Sci. USA 103 (26), June, 9908-9911 (2006). DOI: 10.1073/pnas.0510596103

Y.J. Wang, Kyoung-Su Im, K. Fezzaa, W.K. Lee, Jin Wang, P. Micheli, C. Laub, "Quantitative x-ray phase-contrast imaging of air-assisted water sprays with high Weber numbers," Appl. Phys. Lett. 89, October, 151913-1-151913-3 (2006). DOI: 10.1063/1.2358322

Y.-D. Wang, Y. Ren, H. Li, H. Choo, M.L. Benson, D.W. Brown, P.K. Liaw, L. Zuo, G. Wang, D.E. Brown, E.E. Alp, "Tracing Memory in Polycrystalline Ferromagnetic Shape-Memory Alloys," Adv. Mater. 18 (18), September, 2392-2396 (2006). DOI: 10:1002/adma.200600480

Joshua J. Warren, Lawrence J. Forsberg, Lorena S. Beese, "The structural basis for the mutagenicity of O[superscript 6]-methyl-guanine lesions," Proc. Natl. Acad. Sci. USA 103 (52), December, 19701-19706 (2006). DOI: 10.1073/pnas.0609580103

Michael R. Wasielewski, "Energy, Charge, and Spin Transport in Molecules and Self-Assembled Nanostructures Inspired by Photosynthesis," J. Org. Chem. 71 (14), July, 5051-5066 (2006). DOI: 10.1021/jo060225d

Chaille T. Webb, Michael A. Gorman, Michael Lazarou, Michael T. Ryan, Jacqueline M. Gulbis, "Crystal Structure of the Mitochondrial Chaperone TIM9•10 Reveals a Six-Bladed [alpha]-Propeller," Mol. Cell 21 (1), January, 123-133 (2006). DOI: 10.1016/j.molcel.2005.11.010

Zhiyi Wei, Yanyan Xue, Hang Xu, Weimin Gong, "Crystal Structure of the C-terminal Domain of S. cerevisiae eIF5," J. Mol. Biol. 359, May, 1-9 (2006). DOI: 10.1016/j.jmb.2006.03.037

D.M. Wellman, S.V. Mattigod, K.E. Parker, S.M. Heald, C.M. Wang, G.E. Fryxell, "Synthesis of organically templated nanoporous tin (II/IV) phosphate for radionuclide and metal sequestration," Inorg. Chem. 45 (6), 2382-2384 (2006).

H.-R. Wenk, I. Lonardelli, S. Merkel, L. Miyagi, J. Pehl, S. Speziale, C. E. Tommaseo, "Deformation textures produced in diamond anvil experiments, analysed in radial diffraction geometry," J. Phys. Condens. Matter 18, S933-S947 (2006). DOI: 10.1088/0953-8984/18/25/S02

Michelle Werner, Peter Nico, Bing Guo, Ian Kennedy, Cort Anastasio, "Laboratory Study of Simulated Atmospheric Transformations of Chromium in Ultrafine Combustion Aerosol Particles," Aerosol. Sci. Tech. 40 (7), 545-556 (2006). DOI: 10.1080/02786820600714353

Matthew C. Weston, Christoph Gertler, Mark L. Mayer, Christian Rosenmund, "Interdomain Interactions in AMPA and Kainate Receptors Regulate Affinity for Glutamate," J. Neurosci. 26 (29), July, 7650-7658 (2006). DOI: 10.1523/JNEUROSCI.1519-06.2006

Matthew C. Weston, Peter Schuck, Alokesh Ghosal, Christian Rosenmund, Mark L. Mayer, "Conformational restriction blocks glutamate receptor desensitization," Nat. Struct. Mol. Biol. 13 (12), December, 1120-1127 (2006). DOI: 10.1038/nsmb1178

C.M. Weyant, K.T. Faber, J.D. Almer, J.V. Guiheen, "Residual Stress and Microstructural Evolution in Environmental Barrier Coatings of Tantalum Oxide Alloyed with Aluminum Oxide and Lanthanum Oxide," J. Am. Ceram. Soc. 89 (3), 971-978 (2006). DOI: 10.1111/j.1551-2916.2005.00830.x

William R. Wikoff, James F. Conway, Jinghua Tang, Kelly K. Lee, Lu Gan, Naiqian Cheng, Robert L. Duda, Roger W. Hendrix, Alasdair C. Steven, John E. Johnson, "Time-resolved molecular dynamics of bacteriophage HK97 capsid maturation interpreted by electron cryo-microscopy and X-ray crystallography," J. Struct. Biol. 153 (3), March, 300-306 (2006). DOI: 10.1016/j.jsb.2005.11.009

R.R. Wilkening, R.W. Ratcliffe, E.C. Tynebor, K.J. Wildonger, A.K. Fried, M.L. Hammond, R.T. Mosley, P.M.D. Fitzgerald, N. Sharma, B.M. McKeever, S. Nilsson, M. Carlquist, A. Thorsell, L. Locco, R. Katz, K. Frisch, E.T. Birzin, H.A. Wilkinson, S. Mitra, S. Cai, E.C. Hayes, J.M. Schaeffer, S.P. Rohrer, "The discovery of tetrahydrofluorenones as a new class of estrogen receptor [beta]-subtype selective ligands," Bioorgan. Med. Chem. 16 (13), July, 3489-3494 (2006). DOI: 10.1016/j.bmcl.2006.03.098

Richard T. Wilkin, Robert G. Ford, "Arsenic solid-phase partitioning in reducing sediments of a contaminated wetland," Chem. Geol. 228 (1-3), April, 156-174 (2006).

H.-C. Wille, Yu.V. Shvyd'ko, E.E. Alp, H.D. Rüter, O. Leupold, I. Sergueev, R. Rüffer, A. Barla, J.P. Sanchez, "Nuclear resonant forward scattering of synchrotron radiation from [superscript 121]Sb at 37.13 keV," Europhys. Lett. 74, February, 170-176 (2006). DOI: 10.1209/epl/i2005-10494-2

Trevor M. Willey, Tonyvan Buuren, Jonathan R.I. Lee, George E. Overturf, John H. Kinney, Jeff Handly, Brandon L. Weeks, Jan Ilavsky, "Changes in Pore Size Distribution upon Thermal Cycling of TATB-based Explosives Measured by Ultra-Small Angle X-Ray Scattering," Propell. Explos. Pyrot. 31 (6), 466-471 (2006). DOI: 10.1002/prep.200600063

A.G.B. Williams, K.G. Scheckel, T. Tolaymat, C.A. Impellitteri, "Mineralogy and characterization of arsenic, iron, and lead in a mine waste-derived fertilizer," Environ. Sci. Technol. 40 (16), July, 4874-4879 (2006). DOI: 10.1021/es060853c

G.J. Williams, M.A. Pfeifer, I.A. Vartanyants, I.K. Robinson, "Internal structure in small Au crystals resolved by three-dimensional inversion of coherent x-ray diffraction," Phys. Rev. B 73, 094112-1-094112-8 (2006). DOI: 10.1103/PhysRevB.73.094112

G.J. Williams, H.M. Quiney, B.B. Dhal, C.Q. Tran, K.A. Nugent, A.G. Peele, D. Paterson, M.D. de Jonge, "Fresnel Coherent Diffractive Imaging," Phys. Rev. Lett. 97, July, 025506-1-025506-4 (2006). DOI: 10.1103/PhysRevLett.97.025506

Pascal G. Wilmann, Jion Battad, Jan Petersen, Matthew C.J. Wilce, Sophie Dove, Rodney J. Devenish, Mark Prescott, Jamie Rossjohn, "The 2.1 Å Crystal Structure of copGFP, a Representative Member of the Copepod Clade Within the Green Fluorescent Protein Superfamily," J. Mol. Biol. 359, 890-900 (2006). DOI: 10.1016/j.jmb.2006.04.002

Jeffrey J. Wilson, Rhett A. Kovall, "Crystal Structure of the CSL-Notch-Mastermind Ternary Complex Bound to DNA," Cell 124, March, 985-996 (2006). DOI: 10.1016/j.cell.2006.01.035

Randall E. Winans, Tony Clemens, Sonke Seifert, "In situ SAXS studies on the effects of reactive solvents and gases on coal structure," American Chemical Society, Division of Fuel Chemistry 51 (1), 165-166 (2006).

Randall E. Winans, Stefan Vajda, Gregory E. Ballentine, Jeffrey W. Elam, Byeongdu Lee, Michael J. Pellin, Sonke Seifert, George Y. Tikhonov, Nancy A. Tomczyk, "Reactivity of supported platinum nanoclusters studied by in situ GISAXS: clusters stability under hydrogen," Top. Catal. 39 (3-4), October, 145-149 (2006). DOI: 10.1007/s11244-006-0050-5

Sofia Winell, Hans Annersten, Vitali Prakapenka, "The high-pressure phase transformation and breakdown of MgFe[subscript 2]O[subscript 4]," Am. Mineral. 91, 560-567 (2006). DOI: 10.2138/am.2006.1946

Paul K. Witting, Hugh H. Harris, Benjamin S. Rayner, Jade B. Aitken, Carolyn T. Dillon, Roland Stocker, Barry Lai, Zhonghou Cai, Peter A. Lay, "The Endothelium-Derived Hyperpolarizing Factor, H[subscript 2]O[subscript 2], Promotes Metal-Ion Efflux in Aortic Endothelial Cells: Elemental Mapping by a Hard X-ray Microprobe," Biochemistry-US 45, 12500-12509 (2006). DOI: 10.1021/bi0604375

J.C. Woicik, H. Li, P. Zschack, E. Karapetrova, P. Ryan, C.R. Ashman, C.S. Hellberg, "Anomalous lattice expansion of coherently strained SrTiO[subscript 3] thin films grown on Si(001) by kinetically controlled sequential deposition," Phys. Rev. B 73 (2), 024112-1-024112-5 (2006). DOI: 10.1103/PhysRevB.73.024112

D. Wu, O. Ugurlu, L.S. Chumbley, M.J. Kramer, T.A. Lograsso, "Synthesis and characterization of hexagonal Cd[subscript 51]Yb[subscript 14] single crystals," Philos. Mag. 86 (3-5), January, 381-387 (2006).

Beth A. Wurzburg, Svetlana S. Tarchevskaya, Theodore S. Jardetzky, "Structural Changes in the Lectin Domain of CD23, the Low-Affinity IgE Receptor, upon Calcium Binding," Structure 14, June, 1049-1058 (2006). DOI: 10.1016/j.str.2006.03.017

W.-M. Wu, J. Carely, T. Gentry, M.A. Ginder-Vogel, M. Fienen, T. Mehlhorn, H. Yan, S. Caroll, M.N. Pace, J. Nyman, J. Luo, M.E. Gentile, M.W. Fields, R.F. Hickey, B. Gu, D. Watson, O.A. Cirpka, J. Zhou, S. Fendorf, P.K. Kitanidis, P.M. Jardine, C.S. Criddle, "Pilot-Scale in Situ Bioremedation of Uranium in a Highly Contaminated Aquifer. 2. Reduction of U(VI) and Geochemical Control of U(VI) Bioavailability," Environ. Sci. Technol. 40 (12), 3986-3995 (2006). DOI: 10.1021/es051960u

Yunkun Wu, Bingdong Sha, "Crystal Structure of yeast mitochondrial outer membrane translocon member Tom70p," Nat. Struct. Mol. Biol. 13 (7), June, 589-593 (2006). DOI: 10.1038/nsmb1106

Xianghui Xiao, Martin D. de Jonge, Yuncheng Zhong, Yong S. Chu, Qun Shen, "Crystal optics as guard apertures for coherent x-ray diffraction imaging," Opt. Lett. 31 (21), November, 3194-3196 (2006).

Yuming Xiao, Karl Fisher, Matt C. Smith, William E. Newton, David A. Case, Simon J. George, Hongxin Wang, Wolfgang Sturhahn, Ercan E. Alp, Jiyong Zhao, Yoshitaka Yoda, Stephen P. Cramer, "How Nitrogenase Shakes - Initial Information about P-Cluster and FeMo-cofactor Normal Modes from Nuclear Resonance Vibrational Spectroscopy (NRVS)," J. Am. Chem. Soc. 128 (23), May, 7608-7612 (2006). DOI: 10.1021/ja0603655

Yuming Xiao, Markos Koutmos, David A. Case, Dimitri Coucouvanis, Hongxin Wang, Stephen P. Cramer, "Dynamics of an [Fe[subscript 4]S[subscript 4](SPh)[subscript 4]][superscript 2–] cluster explored via IR, Raman, and nuclear resonance vibrational spectroscopy (NRVS)-analysis using [superscript 36]S substitution, DFT calculations, and empirical force fields," Dalton T. 18, 2192-2201 (2006). DOI: 10.1039/b513331a

Song Xue, Kate Calvin, Hong Li, "RNA Recognition and Cleavage by a Splicing Endonuclease," Science 312, April, 906-910 (2006). DOI: 10.1126/science.1126629

Guoqiang Xu, Mahesh Narayan, Igor Kurinov, Daniel R. Ripoll, Ervin Welker, Mey Khalili, Steven E. Ealick, Harold A. Scheraga, "A Localized Specific Interaction Alters the Unfolding Pathways of Structural Homologues," J. Am. Chem. Soc. 128 (4), January, 1204-1213 (2006). DOI: 10.1021/ja055313e

Hai Xu, Catherine Faber, Tomoaki Uchiki, James W. Fairman, Joseph Racca, Chris Dealwis, "Structures of eukaryotic ribonucleotide reductase I provide insights into dNTP regulation," Proc. Natl. Acad. Sci. USA 103 (11), March, 4022-4027 (2006). DOI: 10.1073/pnas.0600443103

Hai Xu, Catherine Faber, Tomoaki Uchiki, Joseph Racca, Chris Dealwis, "Structures of eukaryotic ribonucleotide reductase I define gemcitabine diphosphate binding and subunit assembly," Proc. Natl. Acad. Sci. USA 103 (11), March, 4028-4033 (2006). DOI: 10.1073/pnas.0600440103

M. Xu, Y. Ye, J.R. Morris, D.J. Sordelet, M.J. Kramer, "Influence of Pd on formation of amorphous and quasicrystal phases in rapidly quenched Zr[subscript 2]Cu[subscript (1-x)]Pd[subscript x]," Philos. Mag. 86 (3-5), January, 389-395 (2006).

Xiaoling Xu, Yujia Zhai, Fei Sun, Zhiyong Lou, Dan Su, Yuanyuan Xu, Rongguang Zhang, Andrzej Joachimiak, Xuejun C. Zhang, Mark Bartlam, Zihe Rao, "New Antiviral Target Revealed by the Hexameric Structure of Mouse Hepatitis Virus Nonstructural Protein nsp15," J. Virol. 80 (16), August, 7909-7917 (2006). DOI: 10.1128/JVI.00525-06

Taro Yamada, Junichi Komoto, Keitarou Saiki, Kiyoshi Konishi, Fusao Takusagawa, "Variation of loop sequence alters stability of cytolethal distending toxin (CDT): Crystal structure of CDT from Actinobacillus actinomycetemcomitans," Protein Sci. 15, 362-372 (2006). DOI: 10.1110/ps.051790506

D.S. Yamashita, R.W. Marquis, R. Xie, S.D. Nidamarthy, H. Oh, J.U. Jeong, K.F. Erhard, K.W. Ward, T.J. Roethke, B.R. Smith, H-Y. Cheng, X. Geng, F. Lin, P.H. Offen, B. Wang, N. Nevins, M.S. Head, R.C. Haltiwanger, A. Sarjeant, L.M. Liable-Sands, B. Zhoa, W.W. Smith, C.A. Janson, E. Goa, T. Tomaszek, M. McQueney, I.E. James, C.J. Gress, D.L. Zembryki, M.W. Lark, D.F. Veber, "Structure Activity Relationships of 5-, 6-, and 7-Methyl-Substituted Azepan-3-one Cathepsin K Inhibitors," J. Med. Chem. 49, 1597-1612 (2006). DOI: 10.1021/jm050915u

B. Yang, H. Friedsam, "High-Resolution Accelerator Alignment Using X-ray Optics," Phys. Rev. Spec. Top., Accel. Beams 9 (3), March, 030701 (2006).

Kun Yang, Yvonne Eyobo, Leisl A. Brand, Dariusz Martynowski, Diana Tomchick, Erick Strauss, Hong Zhang, "Crystal Structure of a Type III Pantothenate Kinase: Insight into the Mechanism of an Essential Coenzyme A Biosynthetic Enzyme Universally Distributed in Bacteria," J. Bacteriol. 188 (15), 5532-5540 (2006). DOI: 10.1128/JB.00469-06

Maojun Yang, Christian B. Gocke, Xuelian Luo, Dominika Borek, Diana R. Tomchick, Mischa Machius, Zbyszek Otwinowski, Hongtao Yu, "Structural Basis for CoREST-Dependent Demethylation of Nucleosomes by the Human LSD1 Histone Demethylase," Mol. Cell 23 (3), August, 377-387 (2006). DOI: 10.1016/j.molcel.2006.07.012

Mingyan Yang, Katsunori Horii, Andrew B. Herr, Terence L. Kirley, "Calcium-Dependent Dimerization of Human Soluble Calcium Activated Nucleotidase: Characterization of the Dimer Interface," J. Biol. Chem. 281 (38), July, 28307-28317 (2006). DOI: 10.1074/jbc.M604413200

Jiusheng Yan, Genji Kurisu, William A. Cramer, "Intraprotein transfer of the quinone analogue inhibitor 2,5-dibromo-3-methyl-6-isopropyl-p-benzoquinone in the cytochrome b[subscript 6]f complex," Proc. Natl. Acad. Sci. USA 103 (1), January, 69-74 (2006). DOI: 10.1073/pnas.0504909102

F. Ye, Y. Ren, Q. Huang, J.A. Fernandez-Baca, P.C. Dai, J.W. Lynn, T. Kimura, "Spontaneous spin-lattice coupling in the geometrically frustrated triangular lattice antiferromagnet CuFeO[subscript 2]," Phys. Rev. B 73 (22), June, 220404-1-220404-4 (2006). DOI: 10.1103/PhysRevB.73.220404

J.M. Yi, Y.S. Chu, T.S. Argunova, J.H. Je, "Analytic determination of the three-dimensional distribution of dislocations using synchrotron X-ray topography," J. Appl. Crystallogr. 39 (1), February, 106-108 (2006).

J.M. Yi, J.H. Je, Y.S. Chu, Y. Zhong, Y. Hwu, G. Margaritondo, "Bright-field imaging of lattice distortions using x rays," Appl. Phys. Lett. 89, 074103-1-074103-2 (2006). DOI: 10.1063/1.2337528

H. Yim, M.S. Kent, D.Y. Sasaki, B.D. Polizzotti, K.L. Kiick, J. Majewski, S. Satija, "Rearrangement of Lipid Ordered Phases Upon Protein Adsorption Due to Multiple Site Binding," Phys. Rev. Lett. 96, May, 198101-1-198101-4 (2006). DOI: 10.1103/PhysRevLett.96.198101

Hsien-Sheng Yin, Xiaolin Wen, Reay G. Paterson, Robert A. Lamb, Theodore S. Jardetzky, "Structure of the parainfluenza virus 5 F protein in its metastable, pre-fusion conformation," Nature 439 (5), January, 38-44 (2006). DOI: 10.1038/nature04322

Y.Z. Yoo, O. Chmaissem, S. Kolesnik, A. Ullah, L.B. Lurio, D.E. Brown, J. Brady, B. Dabrowski, C.W. Kimball, M. Haji-Sheikh, A.P. Genis, "Diverse effects of two-dimensional and step flow growth mode induced microstructures on the magnetic anisotropies of SrRuO[subscript3] thin films," Appl. Phys. Lett. 89 (24), December, 124104-1-124104-3 (2006). DOI: 10.1063/1.2356328

Young K. Yoo, Qizhen Xue, Yong S. Chu, Shifa Xu, Ude Hangen, Hyung-Chul Lee, Wolfgang Stein, Xiao-Dong Xiang, "Identification of amorphous phases in the Fe–Ni–Co ternary alloy system using continuous phase diagram material chips," Intermetallics 14 (3), March, 241-247 (2006).

Yukihiro Yoshimura, Sarah T. Stewart, Maddury Somayazulu, Ho-kwang Mao, Russell J. Hemley, "High-pressure x-ray diffraction and Raman spectroscopy of ice VIII," J. Chem. Phys. 124, January, 024502-1-024502-7 (2006).

Buhyun Youn, Sung-Jin Kim, Syed G. A. Moinuddin, Choonseok Lee, Diana L. Bedgar, Athena R. Harper, Laurence B. Davin, Norman G. Lewis, ChulHee Kang, "Mechanistic and Structural Studies of Apoform, Binary, and Ternary Complexes of the Arabidopsis Alkenal Double Bond Reductase At5g16970," J. Biol. Chem. 281 (52), December, 40076-40088 (2006). DOI: 10.1074/jbc.M605900200

Andrea F. Young, Chrystele Sanloup, Eugene Gregoryanz, Sandro Scandolo, Russell J. Hemley, Ho-kwang Mao, "Synthesis of Novel Transition Metal Nitrides IrN[subscript 2] and OsN[subscript 2]," Phys. Rev. Lett. 96 (15), April, 155501-1-155501-4 (2006).

L. Young, D.A. Arms, E.M. Dufresne, R.W. Dunford, D.L. Ederer, C. Hohr, E.P. Kanter, B. Krassig, E.C. Landahl, E.R. Peterson, J. Rudati, R. Santra, S.H. Southworth, "X-Ray Microprobe of Orbital Alignment in Strong-Field Ionized Atoms," Phys. Rev. Lett. 97, August, 083601-1-083601-4 (2006). DOI: 10.1103/PhysRevLett.97.083601

L. Young, R.W. Dunford, C. Hoehr, E.P. Kanter, B. Kraessig, E.R. Peterson, S.H. Southworth, D.L. Ederer, J. Rudati, D.A. Arms, E.M. Dufresne, E.C. Landahl, "X-ray microprobes of optical strong-field processes," Radiat. Phys. Chem. 75 (11), November, 1799-1807 (2006). DOI: 10.1016/j.radphyschem.2005.12.049

Lester W. Young, Neil D. Westcott, Klaus Attenkofer, Martin J.T. Reaney, "A high-throughput determination of metal concentrations in whole intact Arabidopsis thaliana seeds using synchrotron-based X-ray fluorescence spectroscopy," J. Synchrotron Rad. 13, 304-313 (2006). DOI: 10.1107/s0909049506019571

M.L. Young, F. Casadio, S. Schnepp, J. Almer, D.R. Haeffner, D.C. Dunand, "Synchrotron X-ray diffraction and imaging of ancient Chinese bronzes," Appl. Phys. A 83 (2), May, 163-168 (2006).

Hua Yuan, Spencer Anderson, Shinji Masuda, Vladimira Dragnea, Keith Moffat, Carl Bauer, "Crystal Structures of the Synechocystis Photoreceptor Slr1694 Reveal Distinct Structural States Related to Signaling," Biochemistry-US 45 (42), 12687-12694 (2006). DOI: 10.1021/bi061435n

I-Mei Yu, Michael L. Oldham, Jingqiang Zhang, Jue Chen, "Crystal Structure of the Severe Acute Respiratory Syndrome (SARS) Coronavirus Nucleocapsid Protein Dimerization Domain Reveals Evolutionary Linkage between Corona- and Arteriviridae," J. Biol. Chem. 281 (25), June, 17134-17139 (2006). DOI: DOI 10.1074/jbc.M602107200

A.A. Yunus, C.D. Lima, "Lysine activation and functional analysis of E2-mediated conjugation in the SUMO pathway," Nat. Struct. Mol. Biol. 13 (6), June, 491-499 (2006). DOI: 10.1038/nsmb1104

S.-W. Yu, T. Komesu, B.W. Chung, G.D. Waddill, S.A. Morton, J.G. Tobin, "f-electron correlations in nonmagnetic Ce studied by means of spin-resolved resonant photoemission," Phys. Rev. B 73, February, 075116-1-075116-8 (2006). DOI: 10.1103/PhysRevB.73.075116

Adam P.R. Zabell, Alfred D. Schroff, Jr., Bornadata Evans Bain, Robert L. Van Etten, Olaf Wiest, Cynthia V. Stauffacher, "Crystal Structure of the Human B-form Low Molecular Weight Phosphotyrosyl Phosphatase at 1.6-Å Resolution," J. Biol. Chem. 281 (10), March, 6520-6527 (2006).

Hong Zang, Adriana Irimia, Jeong-Yun Choi, Karen C. Angel, Lioudmila V. Loukachevitch, Martin Egli, F. Peter Guengerich, "Efficient and High Fidelity Incorporation of dCTP Opposite 7,8-Dihydro-8-oxodeoxyguanosine by Sulfolobus solfataricus DNA Polymerase Dpo4," J. Biol. Chem. 281 (4), January, 2358-2372 (2006). DOI: 10.1074/jbc.M510889200

Fairuz Zein, Yan Zhang, You-Na Kang, Kristin Burns, Tadhg P. Begley, Steven E. Ealick, "Structural Insights into the Mechanism of the PLP Synthase Holoenzyme from Thermotoga maritima," Biochemistry-US 45 (49), November, 14609-14620 (2006). DOI: 10.1021/bi061464y

Corinne E. Zeitler, Mary K. Estes, B.V. Venkataram Prasad, "X-Ray Crystallographic Structure of the Norwalk Virus Protease at 1.5-Å Resolution," J. Virol. 80 (10), May, 5050-5058 (2006).

Jian Zhang, Frank E. Frerman, Jung-Ja P. Kim, "Structure of electron transfer flavoprotein-ubiquinone oxidoreductase and electron transfer to the mitochondrial ubiquinone pool," Proc. Natl. Acad. Sci. USA 103 (44), October, 16212-16217 (2006). DOI: 10.1073/pnas.0604567103

Q. Zhang, G.H. Rao, Q. Huang, X.M. Feng, Z.W. Ouyang, G.Y. Liu, B.H. Toby, J.K. Liang, "Selective substitution of vanadium for molybdenum in Sr[subscript 2](Fe[subscript 1-x]] V[subscript x])MoO[subscript 6] double perovskites," J. Solid State Chem. 179 (8), August, 2458-2465 (2006). DOI: 10.1016/j.jssc.2006.05.001

R. Zhang, G. Joachimiak, S. Jiang, A. Cipriani, F. Collart, A. Joachimiak, "Structure of Phage Protein BC1872 from Bacillus cereus, a Singleton With New Fold," Proteins 64 (1), 280-283 (2006). DOI: 10.1002/prot.20910

Rongguang Zhang, Tatiana Skarina, Elena Evdokimova, Aled Edwards, Alexei Savchenko, Roman Laskowski, Marianne E. Cuff, Andrzej Joachimiak, "Structure of SAICAR synthase from Thermotoga maritima at 2.2 Å reveals an unusual covalent dimer," Acta Crystallogr. F 62, 335-339 (2006). DOI: 10.1107/S1744309106009651

Yan Zhang, Mahmoud H. el Kouni, Steven E. Ealick, "Structure of Toxoplasma gondii adenosine kinase in complex with an ATP analog at 1.1 Å resolution," Acta Crystallogr. D 62 (2), February, 140-145 (2006).

Yong-Mei Zhang, Jason Hurlbert, Stephen W. White, Charles O. Rock, "Roles of the Active Site Water, Histidine 303, and Phenylalanine 396 in the Catalytic Mechanism of the Elongation Condensing Enzyme of Streptococcus pneumoniae," J. Biol. Chem. 281 (25), June, 17390-17399 (2006). DOI: 10.1074/jbc.M513199200

Yan Zhang, Marina Porcelli, Giovanna Cacciapuoti, Steven E. Ealick, "The Crystal Structure of 5´-Deoxy-5´-methylthioadenosine Phosphorylase II from Sulfolobus solfataricus, a Thermophilic Enzyme Stabilized by Intramolecular Disulfide Bonds," J. Mol. Biol. 357, 252-262 (2006). DOI: 10.1016/j.jmb.2005.12.040

Yan Zhang, John A. Secrist III, Steven E. Ealick, "The structure of human deoxycytidine kinase in complex with clofarabine reveals key interactions for prodrug activation," Acta Crystallogr. D 62 (2), February, 133-139 (2006).

Z. Zhang, P. Fenter, L. Cheng, N.C. Sturchio, M.J. Bedzyk, M.L. Machesky, L.M. Anovitz, D.J. Wesolowski, "Zn[superscript2+] and Sr[superscript2+] adsorption at the TiO[subscript2] (110)-electrolyte interface: Influence of ionic strength, coverage and anions," J. Colloid Interf. Sci. 295 (1), March, 50-64 (2006).

Zhan Zhang, Paul Fenter, Shelly D. Kelly, Jeffery G. Catalano, Andrei V. Bandura, James D. Kubicki, Jorge O. Sofo, David J. Wesolowski, Michael L. Machesky, Neil C. Sturchio, Michael J. Bedzyk, "Structure of hydrated Zn[superscript 2+] at the rutile TiO[subscript 2] (110)-aqueous solution interface: Comparison of X-ray standing wave, X-ray absorption spectroscopy, and density functional theory results," Geochim. Cosmochim. Acta 70 (16), August, 4039-4056 (2006). DOI: 10.1016/j.gca.2006.06.325

Bin Zhao, Michael R. Waterman, Emre M. Isin, Munirathinam Sundaramoorthy, Larissa M. Podust, "Ligand-Assisted Inhibition in Cytochrome P450 158A2 from Streptomyces coelicolor A3(2)," Biochemistry-US 45 (24), May, 7493-7500 (2006). DOI: 10.1021/bi060193o S0006-2960(06)00193-0

Xiangbo Zhao, Hong Yu, Shengwei Yu, Feng Wang, James C. Sacchettini, Richard S. Magliozzo, "Hydrogen Peroxide-Mediated Isoniazid Activation Catalyzed by Mycobacterium tuberculosis Catalase-Peroxidase (KatG) and Its S315T Mutant," Biochemistry-US 45 (13), March, 4131-4140 (2006). DOI: 10.1021/bi051967o S0006-2960(05)01967-7

Jiahai Zhou, Chuan Yin Liu, Sung Hoon Back, Robert L. Clark, Daniel Peisach, Zhaohui Xu, Randal J. Kaufman, "The crystal structure of human IRE1 luminal domain reveals a conserved dimerization interface required for activation of the unfolded protein response," Proc. Natl. Acad. Sci. USA 103 (39), September, 14343-14348 (2006). DOI: 10.1073/pnas.0606480103

Ning Zhou, Timothy P. Lodge, Frank S. Bates, "Influence of Conformational Asymmetry on the Phase Behavior of Ternary Homopolymer/Block Copolymer Blends around the Bicontinuous Microemulsion Channel," J. Phys. Chem. B 110 (9), March, 3979-3989 (2006). DOI: 10.1021/jp055704f

Tianjun Zhou, Liguang Sun, John Humphreys, Elizabeth J. Goldsmith, "Docking Interactions Induce Exposure of Activation Loop in the MAP Kinase ERK2," Structure 14, June, 1011-1019 (2006). DOI: 10.1016/j.str.2006.04.006

Jochen Zimmer, Weikai Li Li, Tom A. Rapoport, "A Novel Dimer Interface and Conformational Changes Revealed by an X-ray Structure of B. subtilis SecA," J. Mol. Biol. 364 (3), December, 259-265 (2006). DOI: 10.1016/j.jmb.2006.08.044

P.V. Zinin, L.C. Ming, I. Kudryashov, N. Konishi, M.H. Manghnan, S.K. Sharma, "Pressure- and temperature-induced phase transition in the B–C system," J. Appl. Phys. 100, 013516-1-013516-6 (2006). DOI: 10.1063/1.2209170

Natasza E. Ziolkowska, Barry R. O'Keefe, Toshiyuki Mori, Charles Zhu, Barbara Giomarelli, James B. McMahon, Alexander Wlodawer, Fakhrieh Vojdani, Palmer Kenneth, "Domain-Swapped Structure of the Potent Antiviral Protein Griffithsin and Its Mode of Carbohydrate Binding," Structure 14 (7), July, 1127-1135 (2006). DOI: 10.1016/j.str.2006.05.017

Natasza E. Ziolkowska, Alexander Wlodawer, "Structural studies of algal lectins with anti-HIV activity," Acta. Biochim. Pol. 53 (4), November, 617-626 (2006).

E. Zolotoyabko, B. Pokroy, T. Cohen-Hyams, J.P. Quintana, "Depth-resolved strain measurements in thin films by energy-variable X-ray diffraction," Nucl. Instrum. Methods B 246, 244-248 (2006). DOI: 10.1016/j.nimb.2005.12.031

Olena V. Zribi, Hee Kyung, Ramin Golestanian, Tanniemola B. Liverpool, Gerard C.L. Wong, "Condensation of DNA-actin polyelectrolyte mixtures driven by ions of different valences," Phys. Rev. E 73, 031911-1-031911-10 (2006). DOI: 10.1103/PhysRevE.73.031911

Xiaobing Zuo, Guanglei Cui, Kenneth M. Merz, Ligang Zhang, Frederick D. Lewis, David M. Tiede, "X-ray diffraction 'fingerprinting' of DNA structure in solution for quantitative evaluation of molecular dynamics simulation," Proc. Natl. Acad. Sci. USA 103 (10), March, 3534-3539 (2006).

Yuhong Zuo, Helen A. Vincent, Jianwei Zhang, Yong Wang, Murray P. Deutscher, Arun Malhotra, "Structural Basis for Processivity and Single-Strand Specificity of RNase II," Mol. Cell 24 (1), October, 149-156 (2006). DOI: 10.1016/j.molcel.2006.09.004

Dissertations

Diana Arsenieva, "Rabbit and trypanosomal phosphoglucose isomerase crystal structures with and without ligands," Ph.D., University of Illinois at Chicago, 2006.

Duhee Bang, "Proteins Made by Improved Chemical Methods Unveil the Molecular Basis of Protein Structure," Ph.D., The University of Chicago, 2006.

James Robert Bayrer, "The doublesex transcription factor: structural and functional studies of a sex-determining factor," Ph.D., Case Western Reserve University, 2006.

Christopher G. Bunick, "Designing Sequence to Control Protein Function in an EF-Hand Protein-," Ph.D., Vanderbilt, 2006.

Michael Determan, "Synthesis and characterization of stimuli responsive block copolymers, self-assembly behavior and applications," Ph.D., Iowa State University, 2006.

Dal-Hyun Do, "Investigation of Ferroelectricity and Piezoelectricicty in Ferroelectric Thin Film Capacitors," Ph.D., University of Wisconsin, 2006.

Z. Feng, "Experimental and Theoretical Investigation of the Coherent X-Ray Propogation and Diffraction," Masters, McGill University, 2006.

Lu Gan, "Conformational and Covalent Control of Bacteriophage HK97 Capsid," Ph.D., Scripps Research Institute, 2006.

Robert G. Garces, "Structural analysis of three proteins affecting global transcription levels: using X-ray crystallography to elucidate function of non-enzyme proteins," Ph.D., University of Toronto, 2006.

V. Gopalakrishnan, "Linking Single Particle Dynamics to Macroscopic Phenomena in Colloidal Gels," Ph.D., University of Illinois at Urbana-Champaign, 2006.

K. Hassani, "X-ray Microdiffraction Techniques to Study the Microstructure of Materials," Ph.D., McGill University, 2006.

Angela Hoffort, "Structural studies of M-DNA," Masters, University of Saskatchewan, 2006.

Robert W. Hsieh, "Discovery and Characterization of Novel Estrogen Receptor Agonist Ligands and Development of Biochips for Nuclear Receptor Drug Discovery," Ph.D., The University of Chicago, 2006.

Erik C.B. Johnson, "Tools for the Total Chemical Synthesis of Integral Membrane Proteins," Ph.D., The University of Chicago, 2006.

Geoffrey K.-W. Kong, "Structural studies of Alzheimer's disease amyloid precursor protein," Ph.D., University of Melbourne, 2006.

Simone Lam, "XAFS and XEOL Studies of Organic Light Emitting Materials," Masters, University of Western Ontario, 2006.

Soo Heyong Lee, "Time-Resolved X-ray Measurements of Energy Relaxation in Ultrafast Laser Excited Semiconductors," Ph.D., University of Michigan, 2006.

He Lin, "Local Structure Study of New Thermoelectric Materials," Ph.D., Michigan State University, 2006.

Jing-Yuan Liu, "Structure and function of mouse thiamin pyrophosphokinase," Ph.D., Indiana University, 2006.

Ping Liu, "Structural, Kinetic and Mutational Analysis of Two Bacterial Carboxylesterases," Ph.D., Georgia State University, 2006.

Li Lu, "Resonant inelastic x-ray scattering study of two lamellar copper," Ph.D., Stanford University, 2006.

Brian Maddox, "Pressure-Induced Electronic Phase Transitions in Transition Metal Oxides and Rare Earth Metals," Ph.D., University of Califorina, Davis, 2006.

D.H. McNear, "The plant-soil interface: Nickel bioavailability and the mechanisms of plant hyperaccumulation," Ph.D., University of Delaware, 2006.

Kalam Abul Mir, "Extraction and speciation of arsenic in plants," Ph.D., Queen's University, 2006.

Bhoopesh Mishra, "Molecular Binding Mechanisms of Aqueous Cd and Pb to Siderophores, Bacteria and Mineral Surfaces," Ph.D., University of Notre Dame, 2006.

E.B. Mock, "Synthesis, Microstructure, and Mechanics of Charged Stabilized Anisotropic Nanoparticles," Masters, University of Illinois at Urbana-Champaign, 2006.

Brett J. Moldovan, "Fate and Transport of Arsenic in Uranium Mine Tailings: Rabbit Lake Mine, Saskatchewan, Canada," Ph.D., University of Saskatchewan, 2006.

Sergiy Peleshanko, "Amphiphilic Branched Block Copolymers as Responsive Materials," Ph.D., Iowa State University, 2006.

I. Saratovsky, "Investigation of Environmental Catalyst Local Structures by X-ray Absorption Spectroscopy," Ph.D., Northwestern University , 2006.

W.E. Smith, "Gelation Kinetics of Fumed Silica-Alcohol Suspensions," Ph.D., University of Illinois at Urbana-Champaign, 2006.

Prashant Srivastava, "Competative Adsorption - Desorption of Cd, Cu, Pb, and Zn on Kaolinite," Ph.D., University of Sydney, 2006.

Yunfeng Tie, "Crystallographic Analysis and Kinetic Studies of HIV-1 Protease and Drug-resistant Mutants," Ph.D., Georgia State University, 2006.

Igor Vasconselos, "X-Ray Absorption Fine Structure Spectroscopy and Molecular Dynamics Modeling Studies of Ion Adsorption to Kaolinite Clay Surfaces," Ph.D., University of Notre Dame, 2006.

Mina Wang, "Structural and functional correlates of two distinctive enzymes: phosphofructokinase and the neuropeptide processing enzyme EC3.4.24.15," Ph.D., Rosalind Franklin Medical School, 2006.

Reiko Yajima, "Insight into Ribozyme Structure and Function Using Conformationally Restricted RNA: Applications to X-ray Crystallography," Ph.D., Pennsylvania State University, 2006.

Books

S.C. Feil, G. Polekhina, J. Tang, M.W. Parker, "Membrane Insertion of Pore-forming Protein Toxins," Recent Research Developments on Bacterial and Plant Toxins, D. Gillet, L. Johannes, eds., Research Signpost, 2006, 149 - 182.

Jung-Fu Lin, Eric Schwegler, Choong-Shik Yoo, "Phase Diagram and Physical Properties of H[subscript 2]O at High Pressures and temperatures: Applications to Planetary Interiors," Earth's Deep Water Cycle, AGU Geophysical Monograph Series, Steven D. Jacobsen, Suzan van der Lee, eds., AGU, 2006, 159 - 170.

G. Polekhina, S.C. Feil, J. Tang, J. Rossjohn, K.S. Giddings, R.K. Tweten, M.W. Parker, "Comparative Three-dimensional Structure of Cholesterol-dependent Cytolysins," The Comprehensive Sourcebook of Bacterial Protein Toxins, 3rd Edition, J.E. Alouf, J.H. Freer, eds., Elsevier, 2006, 659 - 670.

R.B. Von Dreele, "Neutron Rietveld Refinement," Reviews in Mineralogy & Geochemistry, H.-R. Wenk, eds., Mineralogical Society of America, 2006, 81 - 98.

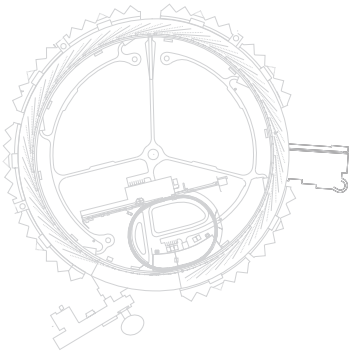

Acknowledgments

APS Science Editorial Board:
Mark A. Beno (ANL-XSD), Rodney Gerig (ANL-SUF), J. Murray Gibson (ANL-SUF), Efim Gluskin (ANL-ASD), Gabrielle G. Long (ANL-XSD), Dennis M. Mills, (ANL-SUF), William G. Ruzicka ANL-(AES), George Srajer (ANL-XSD)

The research highlights in this report were written by:
William Arthur Atkins (waarc@grics.net)
Mary Beckman (mbeckman@nasw.org)
David Bradley (david@sciencebase.com)
Yvonne Carts-Powell (yvonnecp@verizon.net)
Vic Comello (ANL-TSD), vcomello@anl.gov)
Karen Fox (kfox@nasw.org)
Elise LeQuire (cygnete@mindspring.com)
JR Minkel (jrminkel@gmail.com)
Mona A. Mort (mamort@nasw.org)
Luis Nasser (luis.nasser@gmail.com)
David Voss (dvoss@nasw.org)
Mark Wolverton (exetermw@earthlink.net)

Mechanical editing: Mary Fitzpatrick (ANLTSD), Floyd Bennett (ANL-TSD),
Kevin Brown (ANL-TSD)
Photography: Wes Agresta and George Joch (ANL-MED)
Project coordination, publication design, photography: Richard Fenner (ANL-SUFr

Our thanks to the corresponding authors who assisted in the preparation of the research highlights, to the users and APS personnel who wrote articles for the report, and our apologies to anyone inadvertently left off this list. Your contributions are appreciated.